MANITOBA

INVEST. BUILD. GROW

REPORT OF ACTIVITIES 2017

Manitoba Geological Survey

Manitoba

MINISTER, Hon. Blaine Pedersen
Room 358 Legislative Building, 450 Broadway
Winnipeg MB R3C 0V8
204-945-0067 Fax: 204-945-4882

A/DEPUTY MINISTER, Dave Dyson
Room 352 Legislative Building, 450 Broadway
Winnipeg MB R3C 0V8
204-945-5600 Fax: 204-948-2203

360 - 1395 Ellice Avenue, Winnipeg MB R3G 3P2
minesinfo@gov.mb.ca
Toll free (in North America) **1-800-223-5215**
manitoba.ca/minerals

A/ASSISTANT DEPUTY MINISTER, Jim Crone
204-945-4317 Fax: 204-945-1406

MANITOBA GEOLOGICAL SURVEY

Fax: 204-945-1406

Director	Chris Beaumont-Smith	204-945-6505
Mineral Deposits	Scott Anderson	204-945-6561
Precambrian Geoscience	Christian Böhm	204-945-6549
Sedimentary Geoscience	Michelle Nicolas	204-945-6571
Geoscience Information Services		
	Paul Lenton	204-945-6553
Incentives Coordinator	Linda Rogoski	204-945-6586

Core Storage, 10 Midland Street, Winnipeg;
Core Shed, Univ. of Manitoba; Rock Storage Facility,
Perimeter Hwy. at Brady Rd.
Colin Epp 204-945-6550
Fax: 204-948-2164

CORPORATE SERVICES

Fax: 204-945-8427

A/Manager, Marketing and Communications		
	Craig Steffano	204-945-0726
Outreach	Susan Michaels	204-945-6584
Mineral Resources Library/Publication Sales		
	Tomaz Booth	204-945-6569
Marketing Coordinator	Mark Zaluski	204-945-6288

Corporate Policy and Planning Coordinator
Bryan Spencer 204-945-5325

ABORIGINAL CONSULTATION UNIT

Aboriginal Consultation Coordinator
Garry Courchene 204-945-6563
Fax: 204-945-1406

MINES BRANCH

Fax: 204-948-2578

Director	Chris Beaumont-Smith	204-945-6505
Chief Mining Engineer	Omkar Beruar	204-945-6517
A/Mining Recorder - Mining		
	Linda Rogoski	204-945-6586
A/Mining Recorder - Quarrying		
	Lisa Combot	204-945-6531
Land Management	Tim Davis	204-945-6525

Assessment and Exploration
Jim Payne 204-945-6535

Flin Flon Recording Office:
201-143 Main Street, Flin Flon MB R8A 1K2
Claims Inspector Dale Wride 204-687-1635
Fax: 204-687-1634

PETROLEUM BRANCH

Fax: 204-945-0586

A/Director	Amy Jordan	204-945-7392
Petroleum Geologist	Pamela Fulton-Regula	204-945-6506
Chief Petroleum Engineer; Registrar		
	Peter Mraz	204-945-6576

Waskada Office:
Box 220, 23 Railway Avenue, Waskada MB R0M 2E0
Lorne Barsness 204-673-2472
Fax: 204-673-2767

Virden Office:
227 King Street West, Virden MB R0M 2C0
Allan Gervin 204-748-4261
Fax: 204-748-2208

Engineering and Inspection
Lorne Barsness 204-673-2472

Digital Information Services
Christine Steele 204-748-4264

Visit the Resource Development website Staff Directory at manitoba.ca/minerals for email addresses.

REPORT OF ACTIVITIES
2017

Manitoba Growth, Enterprise and Trade
Manitoba Geological Survey

Manitoba

Published by:
Manitoba Growth, Enterprise and Trade
Manitoba Geological Survey
360–1395 Ellice Avenue
Winnipeg, Manitoba
R3G 3P2 Canada

Telephone: 1-800-223-5215 (General Enquiry)
204-945-6569 (Publication Sales)
Fax: 204-945-8427
E-mail: minesinfo@gov.mb.ca
Website: manitoba.ca/minerals

ISBN No.: 978-0-7711-1587-5

The materials in this publication are available to download free of charge at manitoba.ca/minerals

Front cover photo: MGS geologist Xue-Ming (Eric) Yang and field assistant Jordan Watts collect geological data from an outcrop in the footwall of the Burnt Timber gold deposit in the Lynn Lake greenstone belt (GS2017-11, this volume).

REPORT OF ACTIVITIES 2017

A message from the Minister:

As Minister of Growth, Enterprise and Trade, I appreciate the opportunity to present the comprehensive professional geoscience research, findings and data you will find within the Manitoba Geological Survey's *Report of Activities*.

This year's edition contains 18 reports and features the latest scientific data on key investigations into our province's mineral resources. These uniquely Manitoban geoscience results are a part of laying a robust framework to spark investments in the exploration and development of our province's remarkable resource potential.

In 2017, geoscience efforts and endeavours led by a team of dedicated geologists resulted in a wide range of extraordinary findings, including a detailed geological framework for diamond occurrences at Knee Lake. Working collaboratively with industry and the University of Manitoba, survey geologists may also have identified Manitoba's first occurrence of kimberlite – the principal worldwide host for primary diamond deposits.

Geoscience information contained in this report underscores the significance of minerals, oil and gas – representing Manitoba's second largest primary resources industry – to our economic prosperity. As you review the report, please also take time to access our geoscience information, including databases, maps, reports, web pages and publications, available for free download at the Survey's website: Manitoba.ca/minerals.

Manitoba's distinctive mineral heritage is a given. The potential to develop our rich resources responsibly and sustainably is in our hands. Advancing into the 21st century, there's *always* more to explore.

Blaine Pedersen

Honourable Blaine Pedersen
Minister of Growth, Enterprise and Trade

In Memoriam: Peter Theyer

by J.M. Pacey

Dr. Peter Theyer passed away on July 7, 2017 at his Winnipeg home after a brave and courageous battle with ALS.

Peter was born in Kirchheim unter Teck, Germany in 1943 and graduated from the University of Vienna, Austria, where he pursued his doctoral degree in Geological Science. His career as a gifted geoscientist took him to many locations over the years including the Dominican Republic where he discovered what eventually became an open-pit mine, as described in his own words:

I was the geologist in charge of doing the mineral resources of a swath of land that Falconbridge leased from the Dominican Republic. The agreement was, once you start pouring nickel, you start paying one dollar per hectare per year. The second year 2 dollars, then 3 dollars. It's a very standard kind of thing, so you don't monopolize an area.

An American consulting geologist did an assessment of hundreds and hundreds of creeks flowing down from the central mountain. It's kind of like a spine going down. He did the analysis of the mineral sediment in the creeks. Hundreds of creeks. I looked at the map and nothing! Nothing, nothing, nothing! So, what the heck am I going to do? I don't trust other people. I thought, "Peter, check it out yourself." That's the way I always operate. I want to see for myself, no matter how hard it may be—it's hot as hell and humid—but I'm going to hike along these creeks. After maybe two or three days, I'm walking again through one of the creeks and…nothing. I always had a dog with me. It was nice because trees provided shade and you're walking in cold water.

I looked down to see red flakes in the sediment which meant there were oxides. Usually these are oxides of iron or manganese or something that might be valuable. I look on the map from the consulting geologist and there is nothing! I thought, "Sir you are full of s___! You have never taken a sample. It's impossible. The least that you have in there is iron. Why isn't there anything on the map?"

I kept walking and thinking, "Does this make any sense at all? Somebody is lying here." Of course, I took samples and then walked around a curve in the stream and…it was beautiful. There was a waterfall about two metres high. As a geologist, you immediately wonder, "Why do you have a waterfall here?" There must be something hard underneath different from where the water goes gently down. There must be a hard spot. It's like any other waterfall. There's a cause for it.

I took my hammer and bashed it against the rock to get fresh rock and it was bright yellow, which means sulphides. For a geologist, that is "WOW!" It's absolutely excellent! It turned out to be an open pit for copper, gold and zinc that I found. Which, for an economic geologist, is a very exceptional achievement—a big, big, big deal!

Peter was transferred to Manitoba where he initially worked for Falconbridge, later joining the Manitoba Geological Survey (MGS) in 1976 as an economic and mineral deposits geologist working in all areas of the province. His expertise was in mafic-ultramafic intrusions and associated magmatic nickel-copper-chrome-PGE deposit types, namely in the Bird River, Flin Flon, Lynn Lake, Thompson and Fox River belts. He also contributed to the Geoscience Data Compilation for southeastern Manitoba, and authored over ninety reports and

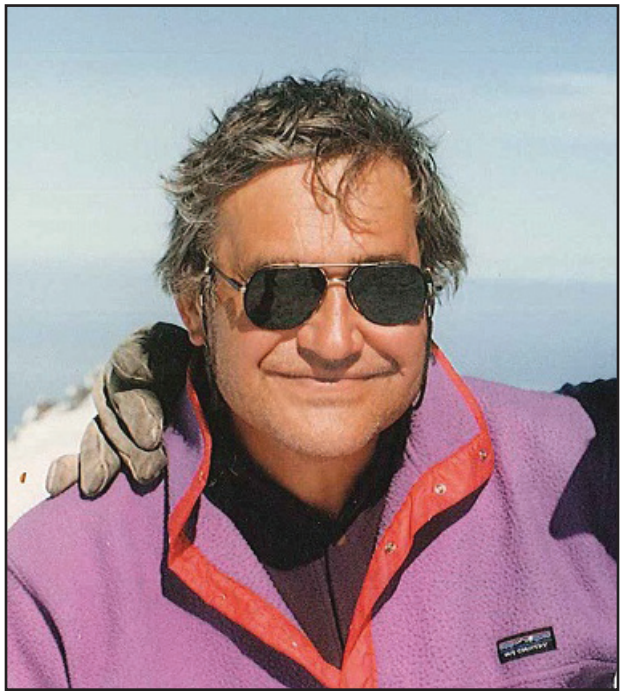

maps during his tenure at the MGS. He raised his family and settled in Manitoba for the rest of his life.

In 1993, Peter returned to the north to open and manage the MGS regional office in Thompson where some 30 years earlier he had launched his career exploring the Thompson belt. He was instrumental in initiating new co-operative projects, many of which included research collaboration from universities in Manitoba and throughout Canada. Peter discovered an undocumented soapstone occurrence near Thompson. He also developed detailed petrographic methods for studying komatiites, and was involved with the mineral potential assessment for the multi-year and multi-disciplinary endangered spaces program for the province.

After retiring from the MGS in 2006, not content to sit idle, Peter joined Wildcat Exploration where he continued to fuel his passion for geoscience in exploration and mentorship of young geologists.

His many interests beyond geology included a lifelong passion caring for dogs, reading and mountain climbing. Once again, in Peter's own words, a tale of a mountaineering adventure in Montana with his colleagues and friends Paul Gilbert and Dave McRitchie.

I always felt most alive coming up a mountain. At the edge of Avalanche Lake, we saw a small, rapidly flowing creek emerge under a metre-thick ice cover, flowing into the lake over a bed of very large boulders. Dave suggested exploring the narrow gap between the lake and the overlying ice by squeezing under the ice over the boulders. I reluctantly agreed to follow him because he was well experienced in exploring caves, as Manitoba leader of a caving club.

We crawled approximately 10 metres over wet boulders trying not to fall into the creek or to get too wet from dripping ice. The light in the cave gradually changed to a bluish green mixed with

a beam of sunlight coming in through a huge melt hole in the ice far above us. We stood in a huge, cathedral-shaped gap, carved out of the ice by the rushing stream that was leaping approximately 30 to 40 metres and along the way, broke into many individual diaphanous falls, somehow like bridal veils.

Dave and I gaped at this awesome spectacle until the wet and cold drove us back into the sun. We both were stunned and speechless by what we had just seen so that we hardly noticed that we hadn't said a word for several minutes. We just knew that we had been in the presence of something truly majestic and extraordinary.

In recent years during Peter's retirement, he continued his love for editing and achieved the twelfth position of proofreaders for Project Gutenberg, proofreading out-of-copyright books to be available as e-books. In his years with the project, Peter proofread 27,545 pages!

He also volunteered his time and expertise with the Winnipeg Humane Society, as well as with all things mechanical for anyone who asked. With boundless energy and generous with his time, Peter often offered himself, and visited and stayed loyal to his long-time friends despite his illness. He was truly an inspiration to the end.

Peter will be missed by friends and colleagues. His passionate and sometimes unorthodox approach to mapping and understanding the geology of Manitoba lives on. We remain saddened by the loss of a colourful, energetic and enthusiastic member of the geological community. Peter is survived by his two children, Nathalia Theyer-McComb of Vancouver, and Nicholas (Debra) Theyer of Lake Geneva, Wisconsin; three grandchildren Luke, Benjamin and Matthew; his two brothers, Hans of Frankfurt, Germany, and Fritz of Washington, DC.

Left to right: Paul Gilbert, Peter Theyer, unknown, and Dave McRitchie in Roscoe, Montana.

Foreword

On behalf of the Manitoba Geological Survey (MGS), it is my privilege to present the *Report of Activities 2017*—the annual peer-reviewed volume of geoscience project results by the MGS and our partners.

The MGS mandate has evolved considerably since its inception in 1928. Early efforts to document Manitoba's geology have expanded alongside the growth of the mining and petroleum industries to assist Manitoba in realizing its vast mineral potential by providing comprehensive, authoritative and accessible geoscience information, and also to meet the ever-changing needs of the exploration industry and geoscientific community. In addition to providing geoscience data to the mineral resource development sectors, the MGS now provides information in support of Indigenous and municipal land-use planning, environmental assessment and protected area assessments.

The research reported on in this year's *Report of Activities* details project areas that cover Manitoba geography from the Hudson Bay coast to our southern border. The nature of the geoscience spans regional mapping in frontier regions to detailed mineral deposit studies in established camps—from traditional commodities such as base metals and gold to emerging commodities such as lithium and diamonds. This variety speaks to the great diversity and potential of Manitoba's mineral resources, a feature that was reinforced in the recommendations of the Look North Task Force, a northern communities stakeholder group advising the government on the development of its northern economic development strategy.

The sustainability of mineral resource development requires successful petroleum and mineral exploration in order to maintain the reserve base. The MGS recognizes this as a priority, and in this context, the work of the MGS and its partners must balance geoscience support for active mineral exploration in established camps with the acquisition of fundamental geoscience in frontier and emerging districts. This approach works to improve the discovery rates in established districts to assist in new and continuing exploration initiatives, while at the same time building the geoscience infrastructure critical to reducing mineral exploration risk and informing private sector investment decision making in more remote regions.

This year's volume includes research results generated through a number of collaborations within the academic and geological survey communities. Leveraging expertise and resources is an important facet of MGS research programming, and these partnerships help to expand the scope of our research and also address the broader objective of providing opportunities to train the next generation of geoscientists to support the minerals sector in Manitoba.

The past year has seen considerable change within the organization of the Manitoba government. The Manitoba Geological Survey now resides within the Resource Development Division of the Department of Growth, Enterprise and Trade. The internal structure of the MGS has also changed, with the restructuring of geoscientific staff into three sections: Precambrian Geoscience, Mineral Deposits and Sedimentary Geoscience. These changes were accompanied by a number of staff retirements: Jim Bamburak retired after more than 41 years as an industrial and specialty minerals geologist, Viorel Varga retired from the Midland Lab and Rock Storage facility after 33 years of service, Maureen McFarlane retired from the Geoscience Information Services section after 32 years of service and Shirley Holgate retired as Convention Coordinator after 44 years of service. Linda Murphy departed the MGS to pursue opportunities in the private sector after serving as both a project geologist and Aboriginal Issues Policy Analyst.

The production of the *Report of Activities* is not possible without the dedicated efforts of geologists, cartographers and GIS specialists, lab technicians, expediters, storekeepers and administrative and Corporate Services staff. Bob Davie and his team from RnD Technical provided outstanding professional technical editing services, and Craig Steffano managed report production and publication layout. I sincerely thank everyone of the MGS team for their valuable contributions.

Chris Beaumont-Smith
Director, Manitoba Geological Survey

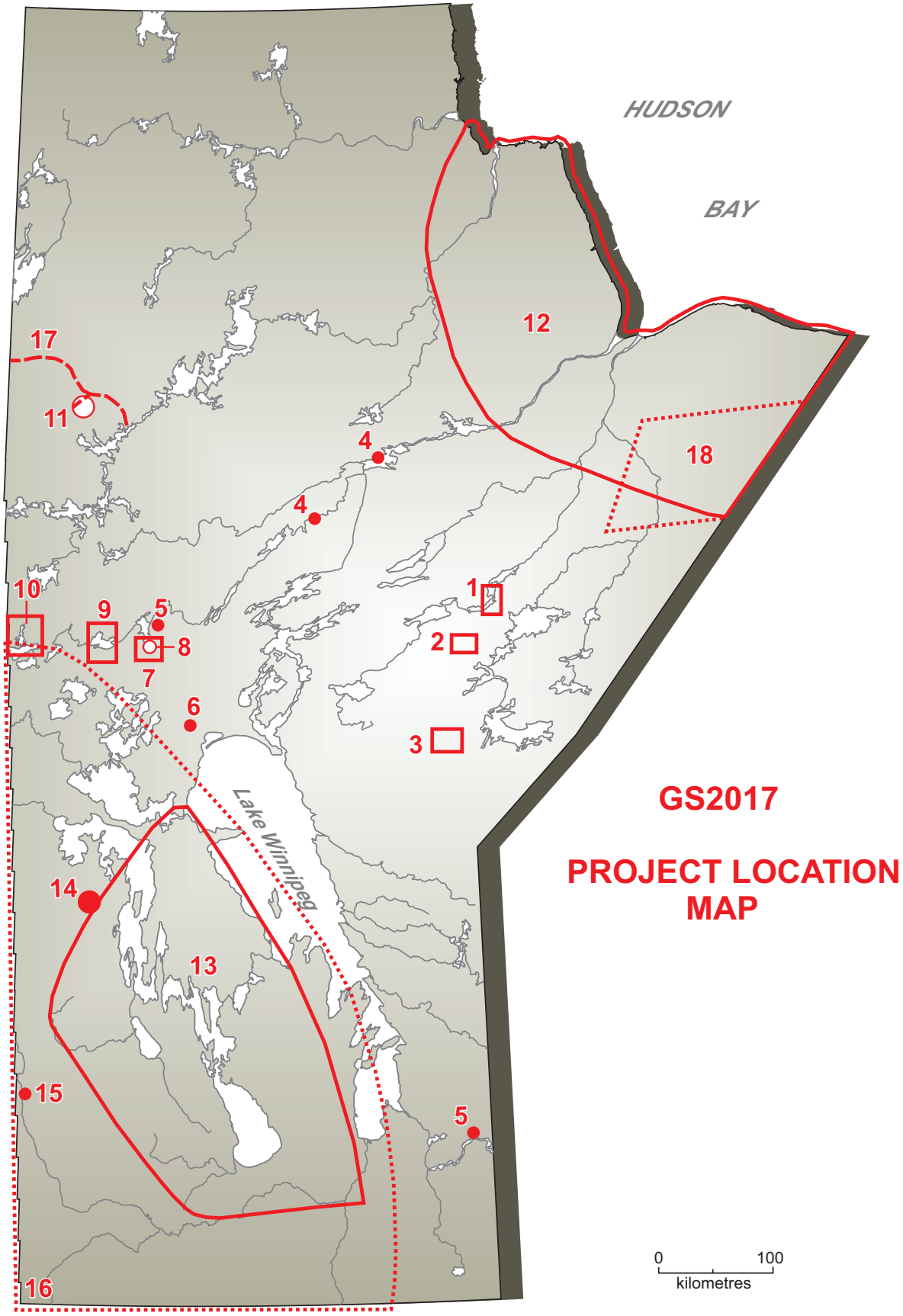
HUDSON
BAY
Lake Winnipeg
GS2017
PROJECT LOCATION MAP
0
100
kilometres

Table of Contents

PRECAMBRIAN

PHANEROZOIC

QUATERNARY

PUBLICATIONS

GS2017-1

Detailed stratigraphic and structural mapping of the Oxford Lake–Knee Lake greenstone belt at southern and central Knee Lake, Manitoba (parts of NTS 53L15, 53M2)

by S.D. Anderson

In Brief:

- Detailed mapping provides a new stratigraphic and structural framework for mineral exploration
- Imbrication of different volcanic assemblages is attributed to thrust faulting prior to regional isoclinal folding
- Diamonds and orogenic gold are hosted by fault-bounded panels within a structural collage at southern Knee Lake

Citation:
Anderson, S.D. 2017: Detailed stratigraphic and structural mapping of the Oxford Lake–Knee Lake greenstone belt at southern and central Knee Lake, Manitoba (parts of NTS 53L15, 53M2); *in* Report of Activities 2017, Manitoba Growth, Enterprise and Trade, Manitoba Geological Survey, p. 1–11.

Summary

In 2017, the Manitoba Geological Survey (MGS) continued its study of the Oxford Lake–Knee Lake greenstone belt by completing new detailed bedrock mapping at southern and central Knee Lake with the objective of better understanding the stratigraphic and structural architecture of the belt, and its tectonic evolution and mineral resource potential. Building on results of MGS mapping in 2015 and 2016, salient results of the 2017 mapping are as follows: 1) definition of a structural collage at southern Knee Lake, including a fault-bounded panel that is interpreted to belong to the ca. 2.83 Ga Hayes River group (HRG), but is imbricated with panels belonging to the ca. 2.72 Ga Oxford Lake group (OLG); 2) delineation of a distinctive unit of effusive volcanic rocks, consisting of porphyritic basalt–andesite flows of shoshonitic–calcalkalic (i.e., OLG) affinity, within rocks previously assigned to the HRG at central Knee Lake, possibly indicating the location of a major thrust fault, along which these units were imbricated prior to regional shortening and isoclinal folding; 3) enhanced understanding of stratigraphic and structural complexities that control or modify several types of mineralization in the belt, including the recently discovered diamondiferous volcanic conglomerates at southern Knee Lake; and 4) identification of favourable exploration potential for orogenic gold mineralization within the structural collage at southern Knee Lake, including zones that contain quartz-feldspar porphyry (QFP) dikes, ankerite (±silica, sericite) alteration and quartz-tourmaline veins. These results represent important progress toward a comprehensive geological synthesis of the Oxford Lake–Knee Lake belt and an up-to-date assessment of its economic potential.

Introduction

In 2012, the MGS began a renewed study of the Oxford Lake–Knee Lake greenstone belt to provide a better understanding of its stratigraphy, structure, tectonic evolution and metallogeny. As the largest contiguous belt of supracrustal rocks in the northwestern Superior province, the Oxford Lake–Knee Lake belt is critical to unlocking the resource potential of the region, which is highly prospective for a variety of commodities, including gold, rare metals, nickel and diamonds, yet remains underexplored. New bedrock mapping and thematic studies, augmented by structural, lithogeochemical, Sm-Nd isotopic, U-Pb geochronological and high-resolution aeromagnetic datasets, are being used to upgrade existing maps, with the goal of a comprehensive regional synthesis and compilation for the belt.

This renewed study expands on previous investigations in the Oxford Lake–Knee Lake belt (most recently summarized in Anderson, 2017), which have indicated considerable scope for additional work to resolve outstanding questions. Shoreline mapping for the present study took place at Oxford Lake in 2012 and 2013 (Anderson et al., 2012a–c, 2013a–d) and continued at Knee Lake in 2015 and 2016 (Figure GS2017-1-1; Anderson et al., 2015a, b, 2016; Anderson, 2016a, b). Discoveries of carbonatite dikes enriched in rare metals at Oxford Lake (Anderson et al., 2012c; Reimer, 2014) and Knee Lake (Anderson, 2016a, b; Donak, 2016), and volcanic conglomerate containing diamonds at southern Knee Lake (Anderson, 2017), are direct results of this work that have stimulated renewed exploration interest in the belt. Building on these results, the goal of the 2017 fieldwork was to unravel complex stratigraphic and structural relationships identified by previous work in two key areas of the belt at southern and central Knee Lake. New shoreline mapping at a scale of 1:10 000 was augmented by data from whole-rock geochemical analyses and industry high-resolution aeromagnetic surveys to improve understanding of both areas.

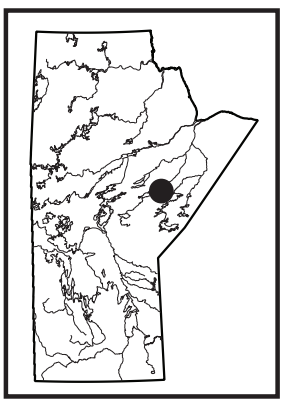

Regional setting

The Oxford Lake–Knee Lake greenstone belt is situated in the western portion of the Oxford–Stull domain of the western Superior province (Stott et al., 2010). This domain consists of ca. 2.9–2.7

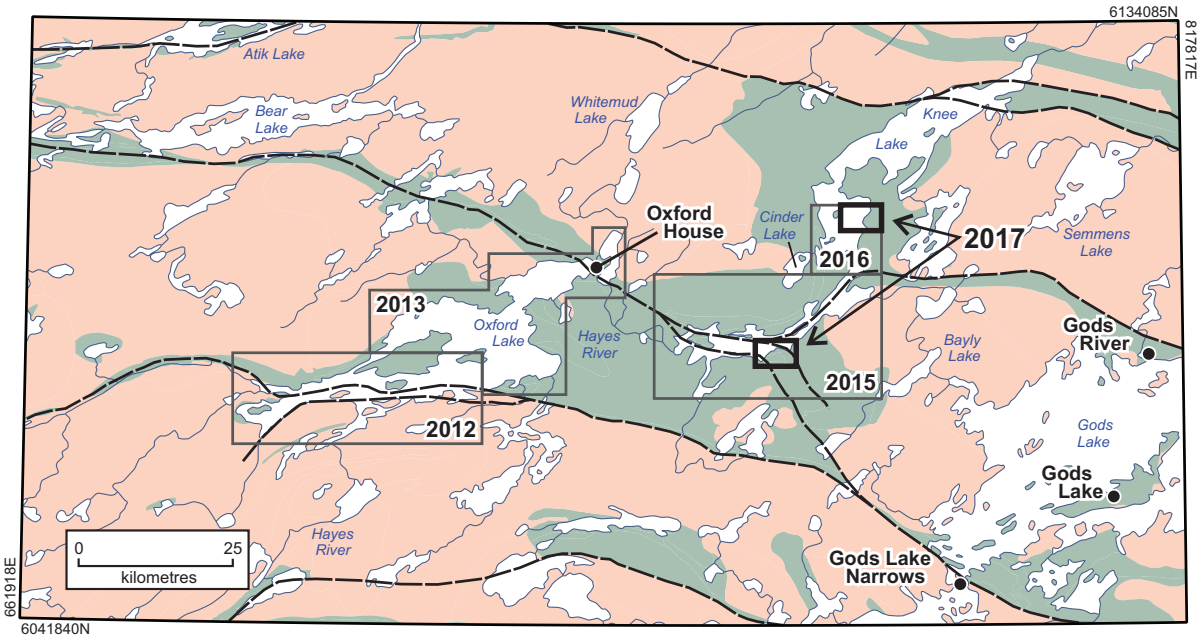

Figure GS2017-1-1: *Regional geological setting of the Oxford Lake–Knee Lake greenstone belt, showing the locations of study areas. Supracrustal rocks are indicated by green fill, whereas granitoid rocks are indicated by pink fill. Dashed black lines indicate major faults.*

Ga volcanic and plutonic rocks with mostly juvenile isotopic signatures and Nd model ages less than 3.0 Ga, thought to represent a tectonic collage of oceanic and continental-margin affinity bounded by older protocratons to the north and south (Skulski et al., 2000; Percival et al., 2006). Fault-bounded crustal blocks in the western Superior province are thought to have been juxtaposed by ca. 2.72 Ga, during a major episode of collisional orogenesis that culminated with the amalgamation of the western Superior province (Skulski et al., 2000; Lin et al., 2006; Percival et al., 2006).

Stratigraphic context

The Oxford Lake–Knee Lake belt is the largest contiguous greenstone belt in the Oxford–Stull domain and has historically been subdivided into two principal stratigraphic units: the older Hayes River group (HRG) and younger Oxford Lake group (OLG). More recent work has demonstrated that this stratigraphic scheme is oversimplified; however, it is mostly retained here for the purpose of continuity with previous reports, although recent and ongoing investigations will necessarily lead to substantial revisions. Greenschist-facies metamorphic assemblages and ductile deformation fabrics characterize rocks through most of the study area. However, primary features are generally well preserved, allowing the rocks to be described in terms of protoliths.

The classical HRG consists of monotonous successions of tholeiitic basalt flows and subvolcanic ultramafic–mafic sills, with minor calcalkalic intermediate–felsic volcanic, volcaniclastic and turbiditic sedimentary rocks, and iron formation (Gilbert, 1985; Hubregtse, 1985; Syme et al. 1997, 1998; Anderson et al., 2013d, 2015b; Anderson, 2016b). The base of the HRG is typically defined by granitoid rocks across structural or intrusive contacts, whereas the top is defined by faults or an unconformity. The type sections at central Oxford Lake and southern Knee Lake approach 10 km in thickness and define homoclinal panels (Anderson et al., 2013d, 2015b), representing either a primary stratigraphic succession (Gilbert, 1985; Hubregtse, 1985) or a tectonic collage (Syme et al., 1999). Elsewhere (e.g., central Knee Lake), the structural geometry of the HRG is far more complex, characterized by macroscopic isoclinal folds and faults, including concordant structures along which structural panels of various ages may have been imbricated, as described herein. Results of U-Pb zircon dating of felsic volcanic rocks in the HRG at Knee Lake indicate that volcanism spanned roughly 10 m.y., between ca. 2835 and 2825 Ma (Corkery et al., 2000).

The classical OLG overlies the HRG and is generally much more heterogeneous, comprising diverse volcanic, volcaniclastic and sedimentary rocks that were deposited in subaerial to basinal marine settings. The OLG has been subdivided for mapping purposes into volcanic and sedimentary subgroups, although subsequent work has demonstrated that the stratigraphy of these rocks is considerably more complex. Coherent flows and coarse fragmental deposits consisting of basalt, andesite, dacite and rhyolite of shoshonitic–calcalkalic affinity (Hubregtse, 1978, 1985; Brooks et al., 1982; Gilbert, 1985) are interstratified with coarse volcanic sedimentary rocks interpreted as debris- and grain-flow deposits in subaqueous fans sourced from nearby subaerial or shallow-marine volcanoes (Syme et al., 1997; Anderson et al., 2013d, 2015b). At southern Knee Lake, the OLG includes ultramafic (lamprophyric), basaltic

andesite (shoshonitic) and andesitic–dacitic (calcalkalic) facies associations (Figure GS2017-1-2; Anderson et al., 2015a, b). Local stratigraphic interlayering indicates that this volcanism was broadly coeval, perhaps within a volcanic field composed of multiple eruptive centres. Results of U-Pb zircon dating indicate that volcanism spanned roughly 20 m.y., between ca. 2725 and 2705 Ma (Corkery et al., 2000; Lin et al., 2006). Distal facies of the OLG comprise thick successions of submarine-fan conglomerate, sandstone, greywacke-mudstone turbidite and iron formation, with minor basalt flows; rounded cobbles of tonalite, granodiorite and gabbro in these conglomerates indicate a more diverse provenance. Type sections of the OLG at eastern Oxford Lake and southern Knee Lake have minimum stratigraphic thicknesses of 2 km; however, the OLG is everywhere characterized by structural complexities that obscure stratigraphic relationships. Hypabyssal porphyry intrusions of shoshonitic basaltic-andesite in the underlying HRG confirm it as the local basement during deposition of the OLG.

New mapping and structural analysis at southern and central Knee Lake indicate that fluvial-alluvial sandstone and conglomerate previously included in the OLG were deposited in younger basins, which are bounded at the base by angular unconformities and at the top by faults, interpreted to represent thrusts, and are thus broadly synorogenic (Anderson, 2016b). These rocks contain large-scale trough crossbeds, channel-fills and pebble–cobble lag deposits characteristic of fluvial-alluvial sequences and form homoclinal panels that range up to 800 m in thickness. Abundant clasts of vein quartz and granitoid rocks indicate that deposition was coeval with regional uplift and erosion; U-Pb dating of detrital zircons indicates maximum depositional ages of ca. 2710 Ma (Corkery et al., 2000).

Structural context

Map patterns, mesoscopic deformation structures and overprinting relationships indicate that supracrustal rocks of the Oxford Lake–Knee Lake belt have been affected by at least five generations (G_1 to G_5) of deformation structures, as summarized briefly below based on recent mapping at Knee Lake (Anderson et al., 2015b; Anderson, 2016b, 2017).

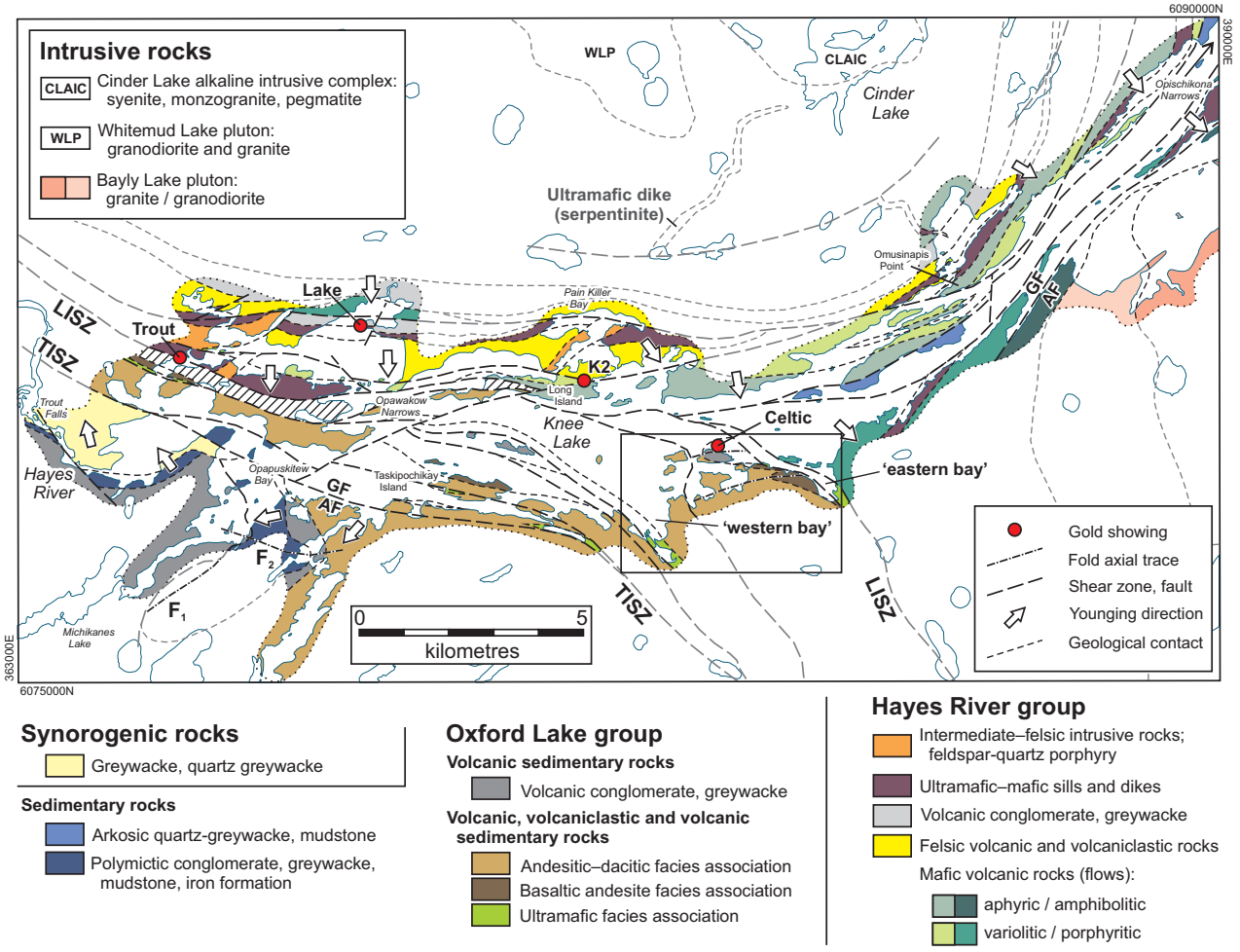

Figure GS2017-1-2: *Simplified geology of southern Knee Lake (Anderson et al., 2015a), including named gold showings and geographic features. Geology outside the 2015 mapping limit (dotted line) is simplified from Gilbert (1985) and aeromagnetic data. Hachure pattern indicates undivided tectonite of the LISZ. Abbreviations: AF and GF indicate structural boundaries between amphibolite facies and greenschist facies rocks; LISZ, Long Island shear zone; TISZ, Taskipochikay Island shear zone. Location of Figure GS2017-1-3 is outlined.*

Isoclinal F_1 folds in bedded sedimentary rocks of the OLG are the earliest ductile deformation structures observed; macroscopic F_1 folds are also inferred from bedding-cleavage relationships and aeromagnetic patterns, particularly in the area southwest of Knee Lake (Figure GS2017-1-2). The F_1 folds are overprinted by upright, open to isoclinal F_2 folds that plunge steeply and are parasitic to macroscopic F_2 folds that control map patterns within major structural panels. These folds are associated with a penetrative S_2 foliation that trends northeast to east-southeast and includes a prominent S_2 shape fabric defined by flattened primary features and a downdip stretching lineation–the main fabrics observed in most outcrops outside of later shear zones.

Macroscopic F_2 folds do not carry across the basal unconformities of the synorogenic, fluvial-alluvial sedimentary basins at Knee Lake, including the thick sequence of cross-bedded greywacke exposed at Trout Falls (Figure GS2017-1-2), which is taken to indicate that the F_2 folds are older. The faulted upper contacts of these basins, and an internal shape fabric and locally penetrative foliation, are tentatively assigned to the G_3 generation of deformation structures, and are interpreted to record structural inversion of these basins and renewed shortening during regional collisional orogenesis (Anderson, 2016b).

At southern Knee Lake, macroscopic F_2 folds are disrupted by subvertical ductile shear zones that bound major and minor structural panels, the principal examples being the Long Island shear zone (LISZ) and Taskipochikay Island shear zone (TISZ; Figure GS2017-1-2), which mostly delimit the Southern Knee Lake shear zone of Lin et al. (1998). These shear zones vary in trend from northeast to southeast; at present it is unknown whether they represent a single generation of structure, but they are assigned here to the G_4 generation on the basis of similar style and kinematics of fabrics. The shear zones contain a penetrative, commonly mylonitic, S_4 foliation. Elongate clasts define an L_4 stretching lineation that plunges shallowly and is locally subhorizontal in the cores of major G_4 shear zones. Shear-sense indicators and open to isoclinal Z-folds that overprint the S_4 foliation are interpreted to record progressive dextral shear. Systematic spatial variations in the style and orientation of deformation fabrics at southern Knee Lake indicate that deformation was strongly partitioned, possibly due to deformation-path partitioning within a kinematic regime of G_4 dextral transpression (Lin et al., 1998; Lin and Jiang, 2001) or due to overprinting by deformation structures of different generations (i.e., overprinting of G_2 fabrics by G_4 fabrics).

Later (G_5) structures include concordant to discordant, brittle-ductile or brittle faults, some of which are associated with narrow (<1 m) zones of cataclasite. A possible major structure of this type, which is defined by sharply truncated magnetic lineaments in the central portion of southern Knee Lake, trends east-northeast from Opapuskitew Bay to just south of Omusinapis Point (Figure GS2017-1-2).

Southern Knee Lake

As described in recent studies (Syme et al., 1997; Anderson et al., 2015b), each of the principal components of the Oxford Lake–Knee Lake belt is exposed in shoreline outcrop at southern Knee Lake. The HRG and OLG wrap broadly around the margins of the Bayly Lake and Whitemud Lake plutons, the latter of which includes the Cinder Lake alkaline intrusive complex (Figure GS2017-1-2). The HRG is mostly exposed along the northern and eastern shorelines of southern Knee Lake and defines homoclinal panels that are intruded inland by granitoid plutons. Internal map patterns are disrupted by shear zones and faults; those of the OLG, which is mostly exposed on the southern shoreline and adjacent islands, are further complicated by isoclinal folds. The LISZ separates the HRG on the north from the OLG on the south, whereas the TISZ coincides with an abrupt southward change from greenschist- to amphibolite-facies metamorphism in the OLG. Bedrock mapping in 2017 was focused on a complex series of structural panels bounded by the LISZ and the TISZ in the southeastern portion of southern Knee Lake, to unravel stratigraphic and structural relationships, and provide better context for occurrences of gold and diamonds in this area.

Results from the 2017 field season

Detailed bedrock mapping at 1:10 000 scale in 2017 indicates that the area bounded by the LISZ and TISZ in the southeastern portion of southern Knee Lake includes nine lithostructural panels, defined on the basis of lithology, structural style and/or metamorphic grade (Figure GS2017-1-3). Gilbert (1985) and Syme et al. (1997) identified three major panels in this area that correspond, from northeast to southwest, respectively, to the HRG and the volcanic and sedimentary subgroups of the OLG. Well-preserved sedimentary structures such as cross-bedding, scours and load casts provide unambiguous younging directions that, in several locations, indicate 'back-to-back' relationships between adjacent panels (e.g., panels 1, 2, 3), which is interpreted to indicate that they are fault-bounded. Direct evidence of faulted contacts, in the form of mapped tectonite and mylonite, is observed on both margins of panels 5 and 8, as well as the southern margin of panel 1 (corresponding to the LISZ). Panel 5 is intruded by abundant dikes of QFP and basalt that are not observed in adjacent panels, suggesting that the contacts are not simply fault-modified (as is demonstrably the case for the contact between panels 7 and 8; Anderson, 2017), but entirely structural (see below). Panels 2–7 are characterized by greenschist-facies metamorphic assemblages, whereas panels 1 and 9 contain amphibolite-facies assemblages and are intruded beyond the limits of Figure GS2017-1-3 by granitoid rocks and local pegmatite, consistent with the presence of major, possibly crustal-scale structures in these locations (i.e., the LISZ and TISZ). Brief descriptions of the lithological characteristics of each panel are provided in Figure GS2017-1-3; more detailed descriptions for all but panel 5 can be found in Syme et al. (1997) and Anderson et al. (2015b), and are not repeated here. Panels 2 and 7 contain primitive alkaline rocks of the

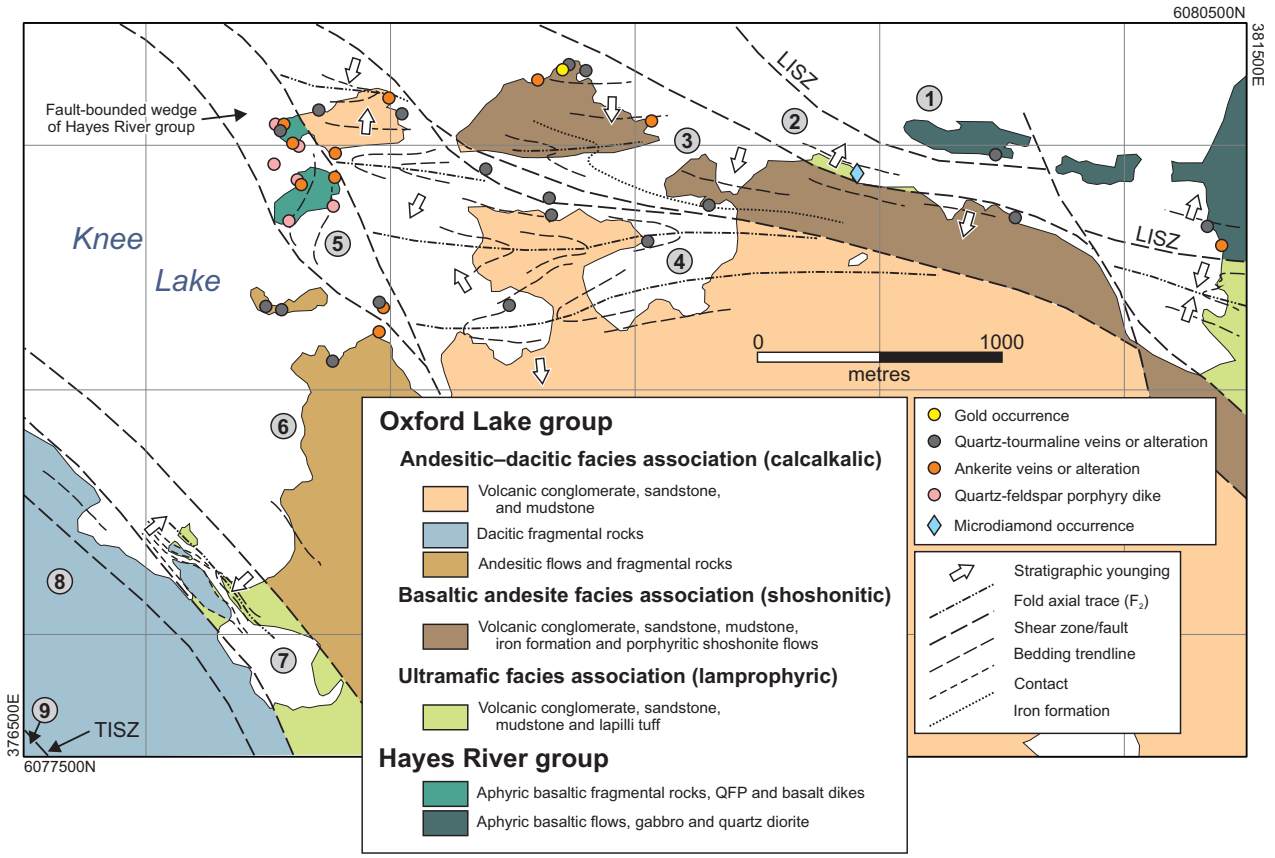

Figure GS2017-1-3: *Simplified geology of the southeastern portion of southern Knee Lake. Numbers (1–9) indicate the major litho-structural panels described in the text. Abbreviations: LISZ, Long Island shear zone; QFP, quartz-feldspar porphyry; TISZ, Taskipochikay Island shear zone. Note microdiamond and gold occurrences in panels 2 and 3, respectively.*

ultramafic facies association, which are locally diamondiferous (Anderson, 2017).

Panel 5 is particularly interesting in that it shares a number of characteristics with mafic volcanic rocks of the HRG exposed along the northern shoreline of southern Knee Lake and is distinct from all surrounding components of the OLG at southern Knee Lake. In particular, this panel consists of breccia, tuff breccia and lapilli tuff of basaltic composition, with minor interlayers of bedded tuff and rare, massive to vaguely pillowed, basalt flows. The coarse fragmental rocks are monolithic, crudely stratified and contain matrix-supported, unsorted clasts that are typically angular, and commonly distinctly cuspate, suggestive of coarse hyaloclastite (Figure GS2017-1-4a). The clasts consist of dark green, aphyric to sparsely plagioclase-phyric basalt in a matrix of similar composition; whole-rock geochemical analyses are pending. Dikes of pale pink-green QFP are ubiquitous and range up to more than 10 m in thickness; they contain conspicuous feldspar (20–25%) and lesser quartz (2–3%) phenocrysts (<5 mm) in an aphanitic, siliceous groundmass. The felsic dikes are cut by dikes of dark green, fine-grained, aphyric basalt (Figure GS2017-1-4b) that range up to 50 cm in thickness and are sparsely amygdaloidal, with thick (~5 cm) chilled margins. As noted above, neither the QFP nor the basalt dikes are observed outside of panel 5. Most of the outcrops within this panel are characterized by a penetrative L>S fabric that includes a down-dip stretching lineation (L_2); this fabric appears to be overprinted by penetrative mylonitic fabrics along both margins of the panel, possibly corresponding to G_4 shear zones.

Based on these features, panel 5 is interpreted to represent a structural slice of the HRG that has been imbricated with the OLG, either during early thrust faulting (G_1 or G_2; see below) or later transcurrent shearing (G_4). Such features support the contention of Syme et al. (1999) that much of the belt constitutes an imbricate tectonic collage, rather than a relatively intact, though deformed, stratigraphic succession. As discussed below, panel 5 also represents an excellent target for gold exploration.

Central Knee Lake

Stratigraphic and structural aspects of the central Knee Lake area have been addressed by Syme et al. (1998) and Anderson (2016b). As described by Anderson (2016b), unusually low water levels in 2016 facilitated a much improved understanding of the geology in south-central Knee Lake, including the delineation of three northwest-trending structural panels, interpreted to be separated by thrust faults (Figure GS2017-1-5).

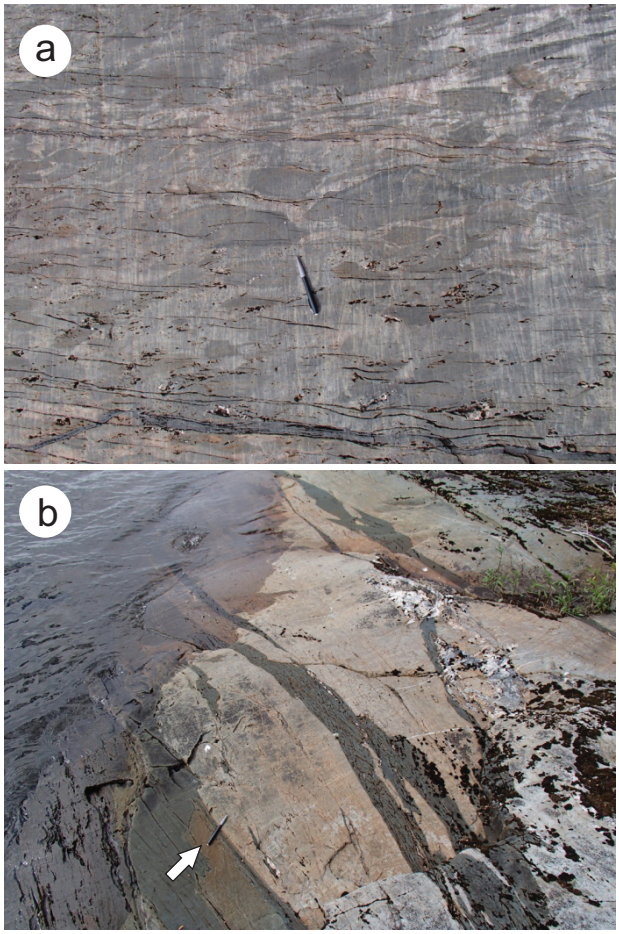

Figure GS2017-1-4: *Outcrop photographs of characteristic rock types in panel 5 of the structural collage at southern Knee Lake:* ***a)*** *tuff breccia, showing angular cuspate clasts of aphyric basalt;* ***b)*** *thick quartz-feldspar porphyry dike (pale pink) intruded by irregular dikes of aphyric basalt; arrow indicates pencil for scale.*

The 'southwest' panel includes an east-younging homocline of the HRG that is intruded at its base, beyond the limits of the map area, by the Whitemud Lake pluton and Cinder Lake alkaline intrusive complex. The HRG is overlain to the east by tightly folded marine sedimentary and volcanic rocks thought to belong to the OLG (an interpretation supported by U-Pb ages of detrital zircons, which indicate an abundance of Neoarchean detritus in the greywacke turbidites; S.D. Anderson, unpublished data, 2017). Both are overlain by a homocline of fluvial-alluvial conglomerate and sandstone across a prominent angular unconformity; gabbro intrusions and early isoclinal folds in the marine sequence do not continue upward into the fluvial-alluvial sequence, demonstrating both the presence and angular nature of the unconformity in this location. In the 'central' panel, tightly folded rocks of the HRG are overlain to the northeast by another homocline of fluvial-alluvial sedimentary rocks, comparable to that in the southwest panel, but considerably thinner and possibly less continuous.

Reconnaissance mapping in 2016 indicated that the northeast panel is similarly complex, but consists entirely of HRG rocks, interpreted to define a tight to isoclinal, northwest-facing, anticline–syncline fold pair (Anderson, 2016b). One outcrop located in the central portion of the panel was found to consist of a series of subvolcanic sills or massive flows characterized by carbonate amygdules, vague fragmental textures, thick chilled margins and abundant plagioclase as coarse tabular phenocrysts (~30%; 2–10 mm) in a dark grey biotitic groundmass–similar in most respects to shoshonite flows within the OLG. Results of a subsequent whole-rock geochemical analysis of a representative sill/flow indicate that it is andesitic, with strongly enriched K_2O (4.3 wt. %), light rare-earth and large-ion lithophile elements (chondrite-normalized La/Yb = 19.4; 1107 ppm Ba; 106 ppm Rb; 428 ppm Sr), and relatively depleted Nb (3.8 ppm). The chemistry of this rock is thus comparable to modern and ancient shoshonite, including that in the OLG (e.g., Brooks et al., 1982; Anderson, 2016a), suggesting that the northeast panel may contain previously unrecognized rocks belonging to the OLG. Hence, follow-up mapping in central Knee Lake during the 2017 field season was focused on the northeast panel, with an eye to establishing the distribution of shoshonitic rocks, documenting their field characteristics and resolving contact relationships.

Results from the 2017 field season

Figure GS2017-1-6 presents a revised interpretation of the bedrock geology in the northeast structural panel at central Knee Lake based on mapping during the 2017 field season as well as a compilation of previous work by Syme et al. (1998) and high-resolution aeromagnetic data. Map patterns and younging criteria are interpreted to indicate the presence of a macroscopic isoclinal F_2 syncline that has been disrupted by late (G_4 and G_5) faults, the most obvious of which is the highly-discordant structure that passes through the cluster of islands in the central portion of the mapped area. The geometry of the macroscopic syncline is best defined by a distinctive package of porphyritic volcanic rocks characterized by coarse, crowded phenocrysts of plagioclase. This package clearly includes lava flows (as opposed to subvolcanic intrusions cutting the HRG; see below) that have been identified on the basis of field characteristics in eight locations on both limbs of the macroscopic fold closure. Whole-rock geochemical data indicate that these flows include both alkaline (shoshonitic) and subalkaline (high-K calcalkalic) compositions, similar to the chemical diversity exhibited by the OLG at the type localities at southern Knee Lake and eastern Oxford Lake (Brooks et al., 1982; Anderson, 2016a).

The HRG in the northeast panel is typical of exposures elsewhere–it consists mostly of aphyric tholeiitic basalt and basaltic andesite flows, which are generally pillowed, but also include minor massive flows and flow breccia. Lenticular map units can be defined at various scales on the basis of variole content. Pillow cusps and shelves provide unambiguous younging directions in most locations. Minor intervals of interbedded felsic volcanic sandstone and mudstone with turbidite bedforms are

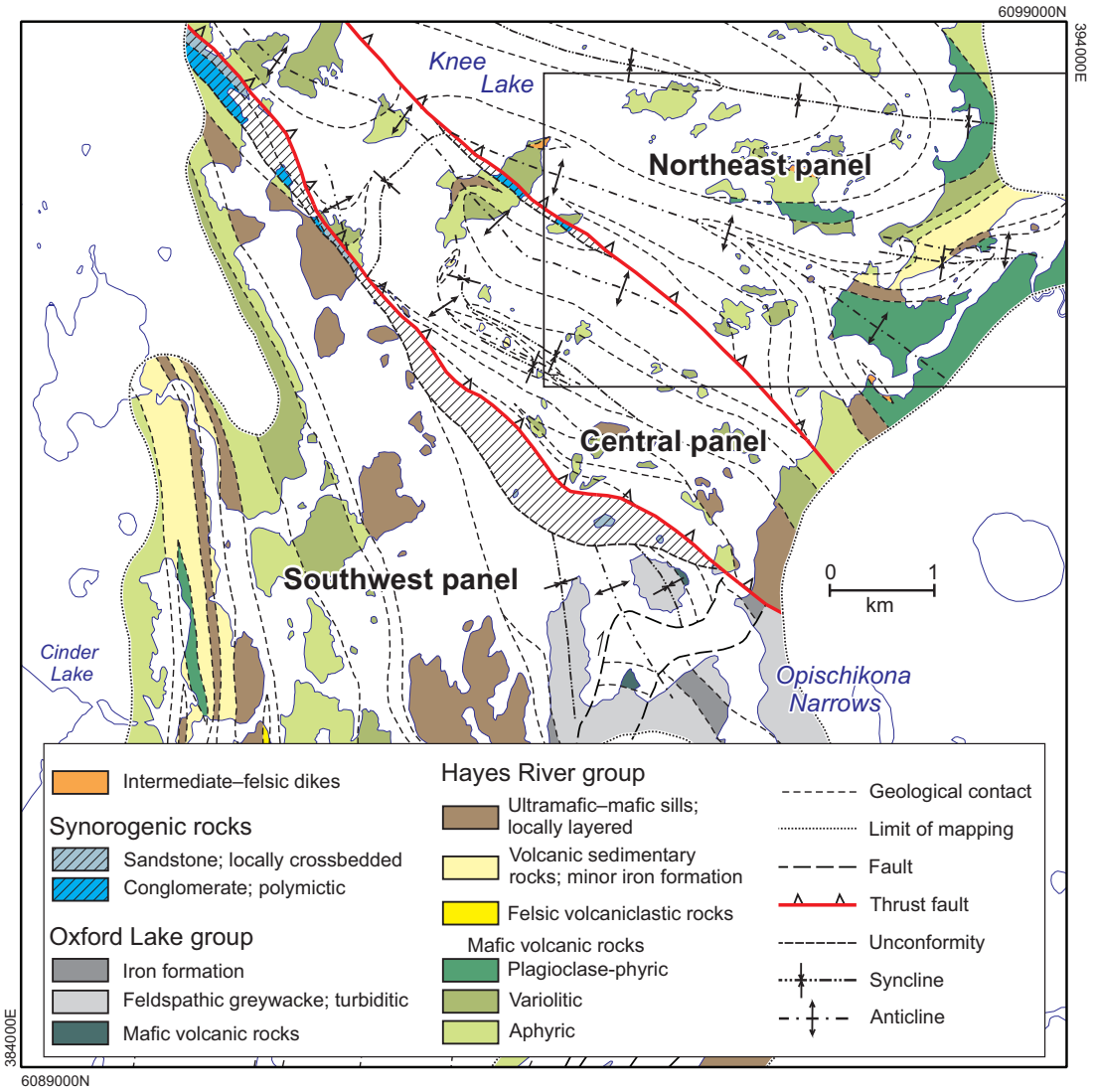

Figure GS2017-1-5: *Simplified geology of the south-central Knee Lake area (Anderson et al., 2016). Hachured pattern indicates the extent of the fluvial-alluvial sedimentary rocks that unconformably overlie the Hayes River group and Oxford Lake group. Location of Figure GS2017-1-6, which provides a revised interpretation of the geology and structure of the northeast panel based on new results from the 2017 field season, is outlined.*

interstratified with the basalts and locally provide useful marker horizons. Thick gabbro sills within the HRG are mesocratic and fine to medium grained, and contain prominent magmatic layering or evidence of in situ differentiation in some locations. All of these rocks are intruded by dikes and sills of QFP.

The shoshonitic–calcalkalic porphyry flows in the northeast panel consist of basalt, basaltic andesite and minor andesite characterized by coarse, crowded phenocrysts of plagioclase (25–50%; 2–10 mm) in a fine-grained groundmass of actinolite, chlorite and biotite. Although typically pillowed, some outcrops are massive, whereas others contain thin layers of pillow-fragment or amoeboid-pillow breccia (Figure GS2017-1-7a). The pillows tend to be very large and bulbous, with thick dark grey selvages and minor (<10%) interpillow hyaloclastite. Plagioclase phenocrysts are coarser and more abundant in pillow cores, and locally show a concentric flow alignment parallel to the pillow selvage (Figure GS2017-1-7b). Most of these flows also contain irregular carbonate (±quartz) amygdules that range up to several centimetres across. The flows are interstratified with crudely bedded sections of coarse, plagioclase-crystal–rich volcanic sandstone (Figure GS2017-1-7c), likely representing reworked hyaloclastite, and poorly exposed intervals of interbedded volcanic conglomerate and sandstone, with minor layers of banded oxide- and sulphide-facies iron formation. The best exposures of these rocks occur on the large island in central Knee Lake, where they define a section approximately 500 m in thickness, and also in the large bay in the eastern portion of the map area, where pillowed flows are particularly well exposed. Sills of fine- to medium-grained gabbro intrude these rocks, but the QFP dikes observed in the HRG are apparently lacking. At southern Knee Lake, dikes and sills of felsic porphyry are also

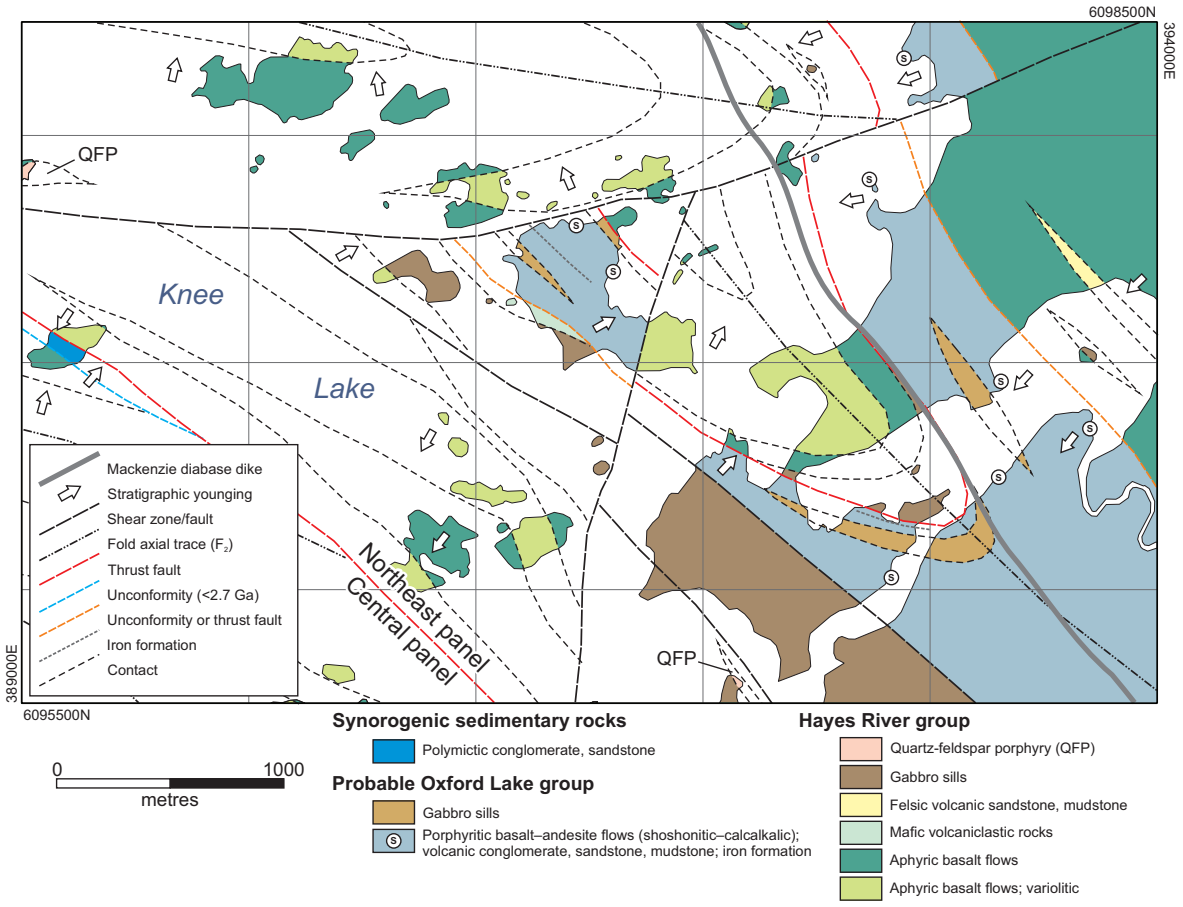

Figure GS2017-1-6: *Revised geology of the eastern portion of central Knee Lake, corresponding to the northeast structural panel of Anderson (2016b), showing the locations of porphyritic flows of shoshonitic–calcalkalic affinity (S). The Mackenzie dike is inferred from high-resolution aeromagnetic data.*

absent from the OLG, but are abundant and extensive in the HRG. This is taken to indicate that they predate the OLG, or perhaps represent subvolcanic feeders to OLG volcanic rocks.

Shoshonitic volcanism of equivalent age to the HRG has not been documented elsewhere in the northwestern Superior province, nor are there any documented occurrences of shoshonite flows within the HRG (Gilbert, 1985; Hubregtse, 1978, 1985). Moreover, the major and trace-element characteristics of the shoshonitic–calcalkalic flows in the northeast panel at central Knee Lake are closely comparable to representative examples of shoshonite flows and subvolcanic sills from the type localities at Oxford Lake and southern Knee Lake (Figure GS2017-1-8). For these reasons, the map unit containing shoshonitic flows at central Knee Lake is interpreted to represent a structural slice of the OLG (basaltic-andesite facies association of Anderson et al., 2015b) that was tectonically interleaved with the HRG, comparable but opposite to the relationship previously described at southern Knee Lake (i.e., slice of HRG within OLG; Figure GS2017-1-3). The lower contact may represent an unconformity or possibly an early (pre-F_2) thrust (Figure GS2017-1-6), but is nowhere exposed. The upper contact is almost certainly structural; it is exposed on the large island in Knee Lake, where a 1–2 m thick chloritic mylonite separates pillowed basalt flows in the hangingwall, interpreted to belong to the HRG, from a gabbro sill that intrudes shoshonitic volcanic rocks in the footwall. This contact is provisionally interpreted as an early thrust fault that formed prior to regional shortening and macroscopic folding (F_2), and is thus assigned to the G_1 generation of deformation structures. The recognition of such features is critical to resolving the stratigraphic and structural architecture of the Oxford Lake–Knee Lake belt, and provides key constraints to achieving a more thorough understanding of its tectonic and metallogenic evolution.

Economic considerations

Based on what is presently known about its geology, coupled with results of previous exploration, the Knee Lake area has potential for a number of mineral-deposit types, including volcanogenic Cu-Zn-Pb-Au-Ag, magmatic Ni-Cu-platinum group elements, intrusion-related rare metals, orogenic Au, and diamonds. Results from this study provide an improved understanding of stratigraphy and structure, which will help to inform exploration strategies. In particular, this report sheds considerable new light on the structural complexities that may be encountered in attempting to trace mineralization controlled or modified by structure; the newly discovered diamondiferous

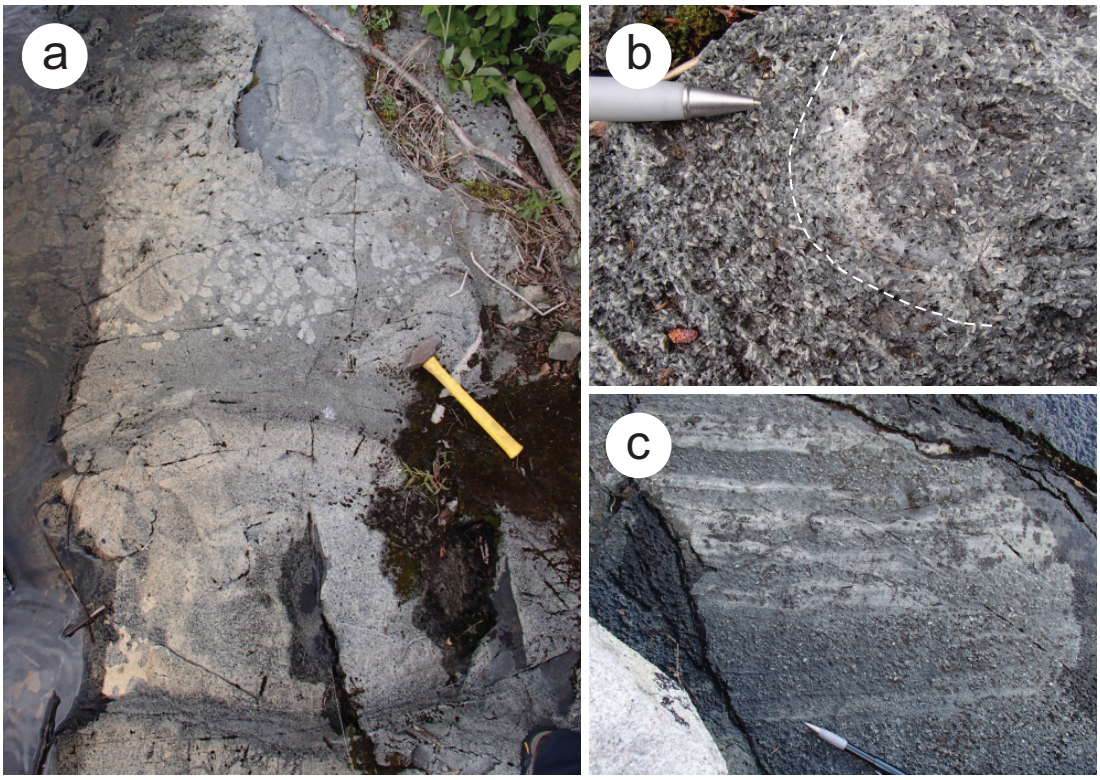

Figure GS2017-1-7: *Outcrop photographs of shoshonitic–calcalkalic volcanic rocks in the northeast structural panel of central Knee Lake:* ***a)*** *contact between pillowed flow of high-K calcalkalic basalt (bottom) and overlying breccia composed of amoeboid pillows and pillow fragments (top);* ***b)*** *detail of pillow core showing concentric flow alignment (indicated by dashed line) of plagioclase phenocrysts;* ***c)*** *bedded volcanic sandstone containing coarse plagioclase crystals, interpreted to represent reworked hyaloclastite.*

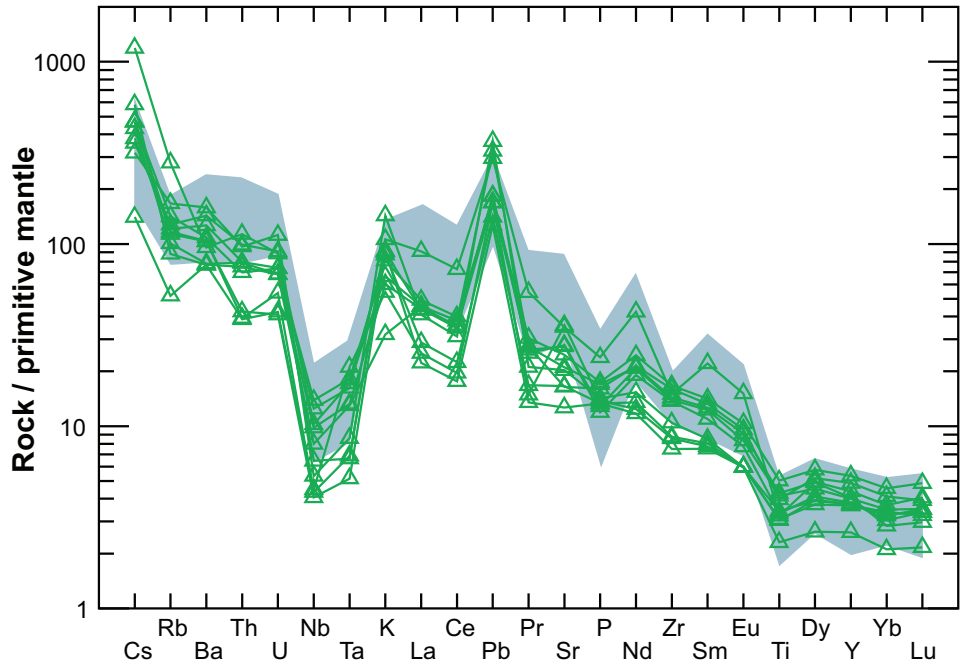

Figure GS2017-1-8: *Primitive-mantle–normalized extended-element plot illustrating geochemical similarities between shoshonitic–calcalkalic flows from central Knee Lake (green triangles; n = 10) and shoshonitic rocks from the type localities at Oxford Lake and southern Knee Lake (shaded field; n = 11). Normalizing values from Sun and McDonough (1989).*

conglomerates at southern Knee Lake (Anderson, 2017) are a notable example, as their present distribution is controlled by complex structural modifications within the imbricate structural collage described in this report.

The Oxford Lake–Knee Lake belt in general, and Knee Lake in particular, shares significant similarities with major Archean gold districts elsewhere in the Superior province, including Timmins and Kirkland Lake in Ontario, and Rice Lake in Manitoba. Commonalities include: chemically-favourable tholeiitic basalt, iron formation and gabbro; early faults and folds; synorogenic clastic basins; alkaline intrusions and volcanic rocks, including lamprophyre dikes; thick-skinned thrusts; and late strike-slip faults. Of particular note is the structural geometry of the synorogenic clastic basins, which are bounded by a footwall unconformity and hangingwall thrust fault, and are thus comparable in many respects to 'Timiskaming-type' sedimentary basins in the Kirkland Lake and Timmins districts in the Abitibi belt. Such basins are thought to offer a first-order guide to the most favourable portions of these gold metallotects, with major deposits often located in the immediate footwall, beneath the basal unconformity. This spatial coincidence is thought to reflect the fundamental role of crustal-scale faults in controlling the development of synorogenic clastic basins, channeling the large-scale hydrothermal systems required to produce orogenic gold deposits, and ultimately facilitating their preservation (Bleeker, 2015).

In the present case, and by analogy with these districts, chemically favourable rocks (mafic flows and iron formation) in the immediate footwall of these basins are logical exploration targets (Anderson, 2016b). Also of interest from the 2017 field season is the fault-bounded panel of basaltic rocks (panel 5; Figure GS2017-1-3) in the structural collage at southern Knee Lake, which is heavily intruded by felsic porphyry dikes and is thus interpreted as a structural slice of the HRG interleaved with panels belonging to the OLG. Panel 5 contains semipervasive ankerite (±silica, sericite) alteration and abundant quartz-tourmaline veins controlled by the competency contrast between porphyry dikes and their basaltic hostrocks (Figure GS2017-1-9a); both of these features are favourable indicators of orogenic gold potential. Similar alteration and veins (with haloes of acicular arsenopyrite) are associated with the 'Celtic' gold occurrence at the northern tip of the large island within panel 3 (Figure GS2017-1-3); grab samples collected by MGS in 2016 returned 2.3 and 2.6 ppm gold. Fault-fill and extensional quartz-tourmaline veins are widespread in other panels within the structural collage, but are particularly abundant along the faulted contact between panels 3 and 4 (Figure GS2017-1-3), where they commonly range up to 50 cm in thickness (Figure GS2017-1-9b). Although none of these veins are known to be auriferous, there was no evidence in the field to suggest that they have been systematically sampled.

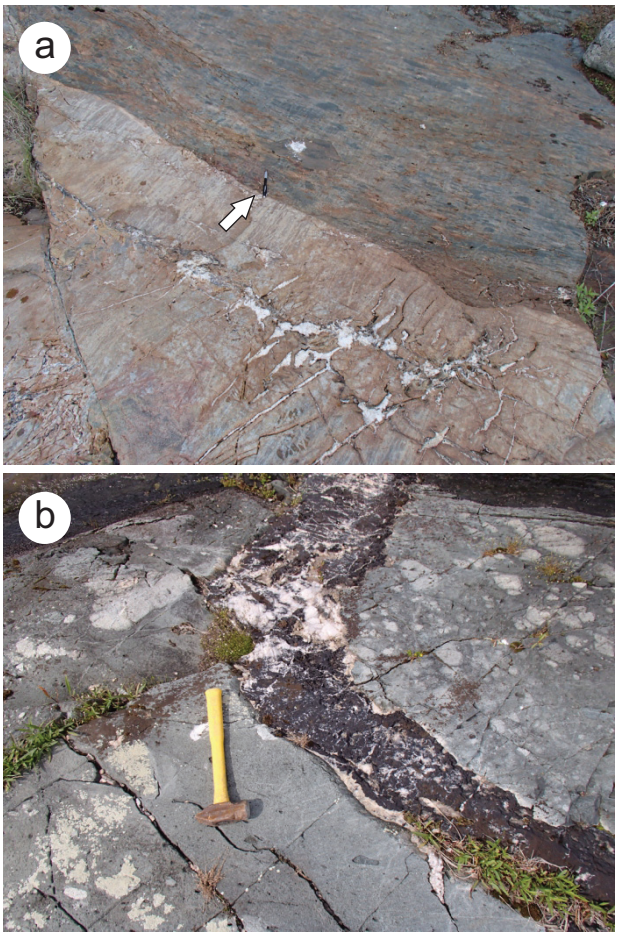

Figure GS2017-1-9: *Outcrop photographs of veins and alteration in the 2017 mapping area at southern Knee Lake:* ***a)*** *quartz-tourmaline veins and ankerite alteration in a quartz-feldspar porphyry dike (bottom) cutting basaltic lapilli tuff (top) in panel 5 (arrow indicates pencil for scale);* ***b)*** *tourmaline-quartz-carbonate±pyrite vein cutting volcanic conglomerate at the southern margin of panel 3.*

Acknowledgments

The author thanks J. Deyholos, D. Downie and M. Stocking (University of Manitoba) for cheerful and capable assistance in the field at Knee Lake; E. Anderson and N. Brandson (MGS) for efficient expediting services; P. Lenton, L. Chackowsky, M. Pacey and B. Lenton (MGS) for digital cartographic, GIS and drafting expertise; H. Crane for ongoing liaison with the Bunibonibee Cree Nation; Wings Over Kississing for air support; and M. Rinne and C. Böhm for reviewing drafts of this report.

References

Anderson, S.D. 2016a: Alkaline rocks at Oxford Lake and Knee Lake, northwestern Superior province, Manitoba (NTS 53L13, 14, 15): preliminary results of new bedrock mapping and lithogeochemistry; *in* Report of Activities 2016, Manitoba Growth, Enterprise and Trade, Manitoba Geological Survey, p. 16–27.

Anderson, S.D. 2016b: Preliminary results of bedrock mapping at central Knee Lake, northwestern Superior province, Manitoba (parts of NTS 53L15, 53M2); *in* Report of Activities 2016, Manitoba Growth, Enterprise and Trade, Manitoba Geological Survey, p. 1–15.

Anderson, S.D. 2017: Preliminary geology of the diamond occurrence at southern Knee Lake, Oxford Lake–Knee Lake greenstone belt, Manitoba (NTS 53L15); Manitoba Growth, Enterprise and Trade, Manitoba Geological Survey, Open File Report OF2017-3, 27 p.

Anderson, S.D., Kremer, P.D. and Martins, T. 2012a: Geology and structure of southwest Oxford Lake (east part), Manitoba (parts of NTS 53L12, 13); Manitoba Innovation, Energy and Mines, Manitoba Geological Survey, Preliminary Map PMAP2012-2, 1:20 000 scale.

Anderson, S.D., Kremer, P.D. and Martins, T. 2012b: Geology and structure of southwest Oxford Lake (west part), Manitoba (parts of NTS 53L12, 13, 63I9, 16); Manitoba Innovation, Energy and Mines, Manitoba Geological Survey, Preliminary Map PMAP2012-1, 1:20 000 scale.

Anderson, S.D., Kremer, P.D. and Martins, T. 2012c: Preliminary results of bedrock mapping at Oxford Lake, northwestern Superior Province, Manitoba (parts of NTS 53L12, 13, 63I9, 16); *in* Report of Activities 2012, Manitoba Innovation, Energy and Mines, Manitoba Geological Survey, p. 6–22.

Anderson, S.D., Kremer, P.D. and Martins, T. 2013a: Geology and structure of northeastern Oxford Lake, Manitoba (parts of NTS 53L13, 14): sheet 1; Manitoba Mineral Resources, Manitoba Geological Survey, Preliminary Map PMAP2013-1, 1:20 000 scale.

Anderson, S.D., Kremer, P.D. and Martins, T. 2013b: Geology and structure of northeastern Oxford Lake, Manitoba (parts of NTS 53L13, 14): sheet 2; Manitoba Mineral Resources, Manitoba Geological Survey, Preliminary Map PMAP2013-2, 1:20 000 scale.

Anderson, S.D., Kremer, P.D. and Martins, T. 2013c: Geology and structure of northeastern Oxford Lake, Manitoba (parts of NTS 53L13, 14): sheet 3; Manitoba Mineral Resources, Manitoba Geological Survey, Preliminary Map PMAP2013-3, 1:20 000 scale.

Anderson, S.D., Kremer, P.D. and Martins, T. 2013d: Preliminary results of bedrock mapping at Oxford Lake, northwestern Superior province, Manitoba (parts of NTS 53L13, 14); *in* Report of Activities 2013, Manitoba Mineral Resources, Manitoba Geological Survey, p. 7–22.

Anderson, S.D., Syme, E.C. and Corkery, M.T. 2016: Bedrock geology of south-central Knee Lake, Manitoba (parts of NTS 53L15, 53M2); Manitoba Growth, Enterprise and Trade, Manitoba Geological Survey, Preliminary Map PMAP2016-1, 1:15 000 scale.

Anderson, S.D., Syme, E.C., Corkery, M.T., Bailes, A.H. and Lin, S. 2015a: Bedrock geology of the southern Knee Lake area, Manitoba (parts of NTS 53L14, 15); Manitoba Mineral Resources, Manitoba Geological Survey, Preliminary Map PMAP2015-1, 1:20 000 scale.

Anderson, S.D., Syme, E.C., Corkery, M.T., Bailes, A.H. and Lin, S. 2015b: Preliminary results of bedrock mapping at southern Knee Lake, northwestern Superior province, Manitoba (parts of NTS 53L14, 15); *in* Report of Activities 2015, Manitoba Mineral Resources, Manitoba Geological Survey, p. 9–23.

Bleeker, W. 2015: Synorogenic gold mineralization in granite-greenstone terranes: the deep connection between extension, major faults, synorogenic clastic basins, magmatism, thrust inversion, and long-term preservation; *in* Targeted Geoscience Initiative 4: Contributions to the Understanding of Precambrian Lode Gold Deposits and Implications for Exploration, B. Dubé and P. Mercier-Langevin (ed.), Geological Survey of Canada, Open File 7852, p. 25–47.

Brooks, C., Ludden, J., Pigeon, Y. and Hubregtse, J.J.M.W. 1982: Volcanism of shoshonite to high-K andesite affinity in an Archean arc environment, Oxford Lake, Manitoba; Canadian Journal of Earth Sciences, v. 19, p. 55–67.

Corkery, M.T., Cameron, H.D.M., Lin, S., Skulski, T., Whalen, J.B. and Stern, R.A. 2000: Geological investigations in the Knee Lake belt (parts of NTS 53L); *in* Report of Activities 2000, Manitoba Industry, Trade and Mines, Manitoba Geological Survey, p. 129–136.

Donak, T.B. 2016: Carbonate dikes at Knee Lake, Oxford Lake–Knee Lake greenstone belt, northwestern Superior Province, Manitoba; B.Sc. (Major) Technical Report, University of Manitoba, Winnipeg, Manitoba, 47 p.

Gilbert, H.P. 1985: Geology of the Knee Lake–Gods Lake area; Manitoba Energy and Mines, Geological Services, Geological Report GR83-1B, 76 p.

Hubregtse, J.J.M.W. 1978: Chemistry of cyclic subalkaline and younger shoshonitic volcanism in the Knee Lake–Oxford Lake greenstone belt, northeastern Manitoba; Manitoba Department of Mines, Resources and Environmental Management, Mineral Resources Division, Geological Paper 78/2, 18 p.

Hubregtse, J.J.M.W. 1985: Geology of the Oxford Lake–Carrot River area; Manitoba Energy and Mines, Geological Services, Geological Report GR83-1A, 73 p.

Lin, S. and Jiang, D. 2001: Using along-strike variation in strain and kinematics to define the movement direction of curved transpressional shear zones: an example from northwestern Superior Province, Manitoba; Geology, v. 29, p. 767–770.

Lin, S., Davis, D.W., Rotenberg, E., Corkery, M.T. and Bailes, A.H. 2006: Geological evolution of the northwestern Superior Province: clues from geology, kinematics, and geochronology in the Gods Lake Narrows area, Oxford–Stull terrane, Manitoba; Canadian Journal of Earth Sciences, v. 43, p. 749–765.

Lin, S., Jiang, D., Syme, E.C., Corkery, M.T. and Bailes, A.H. 1998: Structural study in the southern Knee Lake area, northwestern Superior Province, Manitoba (part of NTS 53L/15); *in* Report of Activities, 1998, Manitoba Energy and Mines, Geological Services, p. 96–102.

Percival, J.A., Sanborn-Barrie, M., Skulski, T., Stott, G.M., Helmstaedt, H. and White, D.J. 2006: Tectonic evolution of the western Superior Province from NATMAP and LITHOPROBE studies; Canadian Journal of Earth Sciences, v. 43, p. 1085–1117.

Reimer, E.R. 2014: Petrography, mineralogy and geochemistry of carbonate rocks at Oxford Lake, Oxford Lake–Knee Lake greenstone belt, northwestern Superior Province, Manitoba; B.Sc. (Honours) thesis, University of Manitoba, Winnipeg, Manitoba, 112 p.

Skulski, T., Corkery, M.T., Stone, D., Whalen, J.B. and Stern, R.A. 2000: Geological and geochronological investigations in the Stull Lake–Edmund Lake greenstone belt and granitoid rocks of the northwestern Superior Province; *in* Report of Activities 2000, Manitoba Industry, Trade and Mines, Manitoba Geological Survey, p. 117–128.

Stott, G.M., Corkery, M.T., Percival, J.A., Simard, M. and Goutier, J. 2010: A revised terrane subdivision of the Superior Province; *in* Summary of Field Work and Other Activities 2010, Ontario Geological Survey, Open File Report 6260, p. 20-1–20-10.

Sun, S-s. and McDonough, W.F. 1989: Chemical and isotopic systematics of oceanic basalts: implications for mantle composition and processes; *in* Magmatism in the Ocean Basins, A.D. Saunders and M.J. Norry (ed.), Geological Society of London, Special Publications, v. 42, p. 313–345.

Syme, E.C., Corkery, M.T., Bailes, A.H., Lin, S., Cameron, H.D.M. and Prouse, D. 1997: Geological investigations in the Knee Lake area, northwestern Superior Province (parts of NTS 53L/15 and 53L/14); *in* Report of Activities, 1997, Manitoba Energy and Mines, Geological Services, p. 37–46.

Syme, E.C., Corkery, M.T., Bailes, A.H., Lin, S., Skulski, T. and Stern, R.A. 1999: Towards a new tectonostratigraphy for the Knee Lake greenstone belt, Sachigo subprovince, Manitoba. In Western Superior Transect 5th Annual Workshop; R.M. Harrap and H.H. Helmstaedt (eds.); Lithoprobe Secretariat; The University of British Columbia, Vancouver, BC; Lithoprobe Report 70, p. 124–131.

Syme, E.C., Corkery, M.T., Lin, S., Skulski, T. and Jiang, D. 1998: Geological investigations in the Knee Lake area, northern Superior Province (parts of NTS 53L/15 and 53M/2); *in* Report of Activities, 1998, Manitoba Energy and Mines, Geological Services, p. 88–95.

GS2017-2

Reconnaissance work at Reekie Lake in the Munro Lake greenstone belt, Superior province, central Manitoba (part of NTS 63L11)

by C.G. Couëslan

In Brief:

- Scheelite mineralization was investigated as a potential analog to the Monument Bay Au-W deposit
- A crustal-scale fault defines the contact between supra-crustal and plutonic rocks
- Disseminated scheelite is associated with pervasive calcsilicate alteration and elevated Cu, Mo, Hg and Au

Citation:
Couëslan, C.G. 2017: Reconnaissance work at Reekie Lake in the Munro Lake greenstone belt, Superior province, central Manitoba (part of NTS 63L11); *in* Report of Activities 2017, Manitoba Growth, Enterprise and Trade, Manitoba Geological Survey, p. 12–18.

Summary

A one-week reconnaissance was conducted in the Reekie Lake area in July 2017 to assess the potential for a 1:50 000 scale mapping project and evaluate reports of disseminated scheelite mineralization. Reekie Lake is located along the southern margin of the Munro Lake belt, where granodioritic rocks of the Bayly Lake complex are in sheared contact with volcanogenic rocks of the Hayes River group along a splay of the Stull-Wunnummin fault. Hayes River group rocks along the northern shore of Reekie Lake consist largely of pillowed and massive basalt, and gabbro intrusions. The southern shore is underlain by protomylonitic granodiorite–tonalite of the Bayly Lake complex and mafic sandstone of the Hayes River group. The sandstone contains minor beds of felsic and intermediate tuff, feldspathic wacke, conglomerate and gabbro. Peridotite is exposed in an isolated cluster of low reefs at the east end of the lake. All units display a strong S_1 foliation.

Several generations of quartz veins and a population of quartz-carbonate veins are present at Reekie Lake. At the west end of the lake, a pervasive zone of calcsilicate alteration is associated with disseminated scheelite and chalcopyrite mineralization that has yielded elevated values of Cu, Mo, W, Hg and Au. The alteration could be part of a larger zone of intense carbonate alteration reported to occur along the fault zone that defines the south margin of the greenstone belt.

Introduction

Reekie Lake is located approximately 40 km south of Oxford House and 45 km west of Gods Lake Narrows. It lies along the southern margin of the Munro Lake greenstone belt. The first recorded exploration in the area was by Gods Lake Gold Mines Ltd. from 1935 to 1945 (Barry, 1962). Airborne electromagnetic surveys were conducted over the area by Inco Ltd. in 1958 (Assessment Files 90005 and 93901, Manitoba Growth, Enterprise and Trade, Winnipeg), followed by ground surveys and diamond-drilling by Falconbridge Nickel Mines Ltd. in 1968 (Assessment File 92005), which identified several ultramafic bodies on Vivian and Reekie lakes. McGregor and Petak (1977) investigated sparsely disseminated scheelite and base-metal mineralization in skarn alteration at the west end of Reekie Lake. Noranda Exploration Company Ltd. conducted reconnaissance and detailed mapping, and rock and humus sampling in the Reekie Lake area during the summers of 1990 and 1991, and recognized the presence of a 6.8 km long zone of intense carbonate alteration along the southern margin of the greenstone belt (Assessment File 93901). Gold mineralization was identified in carbonate-altered peridotite at the eastern end of Reekie Lake and in quartz-carbonate–altered intermediate to felsic tuff 700 m north of the western end of the lake. Greater than 10% of the samples collected by Noranda yielded Au values of >100 ppb.

This report summarizes the preliminary results of a one-week reconnaissance, in July of 2017, of the Reekie Lake area. The reconnaissance was undertaken to evaluate the potential for a 1:50 000 scale mapping project of the Munro Lake belt, which was last mapped in 1972 (Elbers and Gilbert, 1972), and to evaluate the disseminated scheelite mineralization for Au potential and possible similarities to Au-W mineralization in the Monument Bay deposit (Yamana Gold Inc.), approximately 140 km to the east along strike (McCracken and Thibault, 2014).

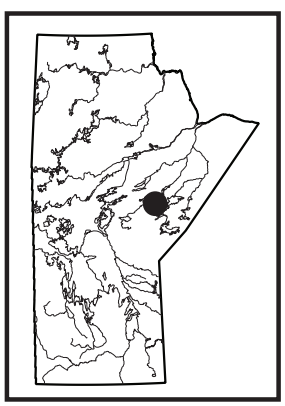

Geology of the Munro Lake belt

The Munro Lake greenstone belt is located in the Island Lake domain of the North Caribou terrane (Figure GS2017-2-1; Stott et al., 2010). The main portion of the belt stretches from Colen Lakes in the west to Touchwood Lake in the east. It is approximately 29 km long with a maximum width of 6.5 km. The belt is bordered to the north and south by tonalitic to granodioritic rocks of the Bayly Lake complex. The western end of the belt is truncated by a porphyritic granite pluton north of Colen Lakes. The eastern end of the belt narrows considerably (to approximately 200 m)

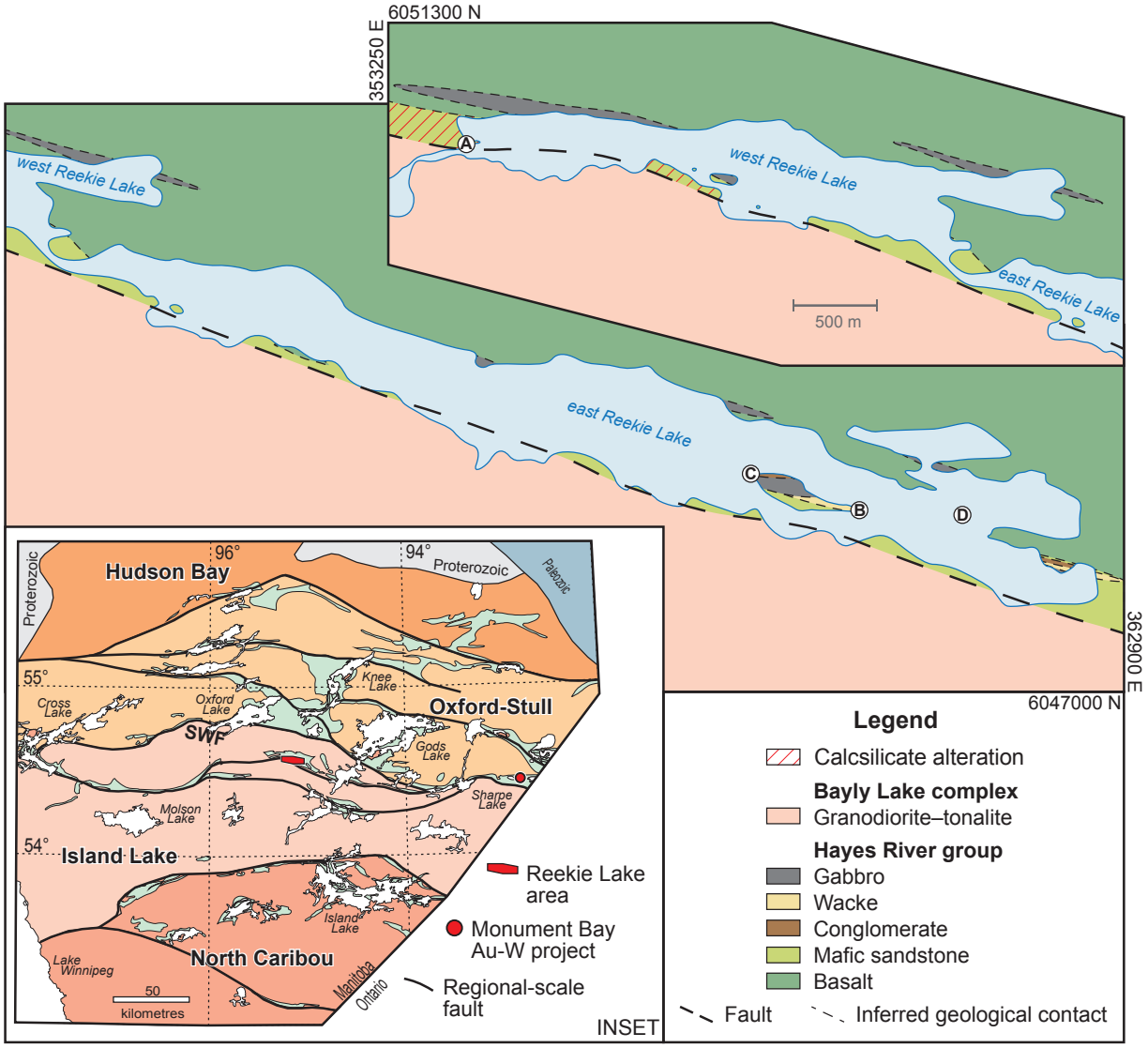

Figure GS2017-2-1: *Simplified geology of the Reekie Lake area. The east and west basins of Reekie Lake are referred to as 'east' and 'west' Reekie Lake for ease of reference. The limits of calcsilicate alteration are from McGregor and Petak (1977). Inset map is modified from Anderson et al. (2013). Abbreviation: SWF, Stull-Wunnummin fault. Co-ordinates are in NAD 83, zone 15.*

at Touchwood Lake and appears to coalesce with the Webber Lake belt at Sharpe Lake to form part of the Stull–Kistigan lakes belt, which hosts the Monument Bay deposit (Marten, 1992; Corkery et al., 1999; McCracken and Thibault, 2014). The contact between the Bayly Lake complex and supracrustal rocks at the southern margin of the belt coincides with a crustal-scale shear zone, which appears to be a splay of the Stull-Wunnummin fault.

The Munro Lake belt was mapped and described by Barry (1961), Elbers and Gilbert (1972) and Marten (1992). It is underlain by rocks of the Hayes River group, which consists of interlayered basalt, andesite, dacite, tuff and volcanogenic sediments, and related mafic intrusions. In the Munro and Reekie lakes area, the belt is divided into northern, central and southern suites of volcanic rocks (each <2.5 km wide), separated by two intervening suites of sedimentary rocks (each <1.8 km wide). The sedimentary rocks consist largely of greywacke and argillite with narrow beds of polymictic conglomerate. The overall geometry of the belt is considered to be a syncline, with the sedimentary rocks overlying an older suite of volcanic rocks, and a younger suite of volcanic rocks situated at the core of the structure. All rocks in the belt exhibit a moderate to strong S_1 foliation. Later F_2 folding resulted in the present synclinal structure. No axial-planar S_2 was developed (Elbers and Gilbert, 1972). Rocks in the Munro Lake belt are characterized by metamorphic assemblages of lower- to middle-amphibolite facies.

Reekie Lake geology

Reekie Lake occurs along the southern margin of the Munro Lake belt, where largely mafic to andesitic volcanic rocks

of the Hayes River group are in sheared contact with tonalitic to granodioritic rocks of the Bayly Lake complex along a splay of the Stull-Wunnummin fault (Figure GS2017-2-1). All units described have been metamorphosed to amphibolite-facies conditions; however, the 'meta' prefix has been omitted for brevity. Due to high strain, it is generally not possible to define the nature of contacts between units. The east and west basins of Reekie Lake are referred to as 'east' and 'west' Reekie Lake, respectively, for ease of reference (following McGregor and Petak, 1977).

Bayly Lake complex

A large granodiorite–tonalite intrusion, exposed along the southern shore of Reekie Lake, marks the southern boundary of the Munro Lake belt. The intrusion varies from grey to white to pinkish grey, and is medium to coarse grained and protomylonitic (Figure GS2017-2-2). Although dominantly granodiorite, it commonly grades into tonalite with <10% K-feldspar. Biotite is the most abundant mafic mineral at 5–10%. Potassium feldspar and plagioclase form porphyroclasts/augen <2 cm across, which are locally asymmetric, consistent with dextral shear. Attenuated mafic enclaves <5 cm thick can be continuous over several metres. The granodiorite is intruded by granitic pegmatite dikes that vary from transposed and protomylonitic to crosscutting and lower strain with a quartz fabric that is subparallel to the mylonitic foliation. Trains of coarse K-feldspar augen could represent sheared and disrupted pegmatite dikes. The contact between the granodiorite and the supracrustal rocks to the north was not observed and underlies either low ground or the lake; it is assumed to be a structural contact. The attenuated mafic enclaves could be interpreted as xenoliths of supracrustal rocks, suggesting an intrusive contact; however, no granodiorite or tonalite dikes were observed to intrude the supracrustal rocks. The mafic enclaves could also represent tectonically entrained material, xenoliths of mafic rock unrelated to the supracrustal rocks, or mafic autoliths. Hence, the age of the granodiorite relative to the supracrustal rocks is uncertain.

Figure GS2017-2-2: *Sheared tonalite of the Bayly Lake complex.*

Hayes River group

Basalt

Basalt and gabbro are the dominant rock types along the north shores of Reekie Lake. The basalt weathers dark grey-green to buff and is dark green to black on fresh surfaces. It is fine to medium grained and strongly foliated to mylonitic, and varies from relatively homogeneous to discontinuously banded. Veinlets of carbonate are common and most apparent on fresh surfaces. Recognizable pillows are rare and strongly attenuated (20:1 elongation); however, local plagioclase-rich layers (<1 cm thick) with hornblende-rich margins likely represent transposed pillow selvages (Figure GS2017-2-3a). Local pods of epidosite <20 cm thick are present in the pillowed flows, and sparse pods of carbonate could represent interpillow material. Epidote lenses <2 mm wide and quartz lenses <4 mm wide locally make up 7–10% of the unit and likely represent attenuated amygdules (Figure GS2017-2-3a). Outcrops of high-strain, fine-grained amphibolite are common, and may represent either tectonized basalt or gabbro. Gabbro intrusions, ranging from several centimetres to tens of metres, are common within the basalt.

Mafic sandstone and associated rocks

Mafic sandstone is the dominant supracrustal rock exposed along the south shoreline of Reekie Lake. It is green-grey, fine to medium grained and typically pebbly and poorly sorted (Figure GS2017-2-3b). It is usually strongly foliated and crudely layered; however, fine-grained, laminated and apparently well-sorted layers are locally present. The sand matrix appears basaltic in composition and contains <15% basaltic to pyroxenitic pebbles <5 cm across. Sparse intermediate pebbles are present, along with rare felsic pebbles and plagioclase clasts <1 cm thick (Figure GS2017-2-3b). Clasts are typically elongate (>7:1) and locally boudinaged. Local lenses of quartz <5 mm thick are likely attenuated quartz veins. Local crystal-rich beds <5 m thick contain 20–30% rounded to blocky plagioclase grains (<3 mm; Figure GS2017-2-3c). Discrete grains of hornblende up to 2 mm can be present in minor amounts. Because of the high strain, it is uncertain if the rounding of grains is primary or tectonic. The mafic sandstone contains local layers of felsic and intermediate tuff <4 m thick, and intrusions of gabbro <5 m thick. Sparse layers of feldspathic wacke <1 m thick can also be present. A 3 m wide silicate-facies iron formation occurs at a contact between mafic sandstone and felsic tuff at west Reekie Lake (Figure GS2017-2-1, location A). Beds of tuff and wacke appear to become more common toward the contact with granodiorite–tonalite.

The felsic tuff varies from buff to creamy white on weathered surfaces and is light grey when fresh (Figure GS2017-2-3d). It is fine grained, strongly foliated to mylonitic, and laminated to layered at a scale of <2 cm. Bands of this siliceous rock occasionally contain discrete plagioclase grains (<2 mm) as either phenocrysts or clasts. These grains can constitute up to 7% of the rock. Local light and dark lenses could be attenuated lapilli (Figure GS2017-2-3d), suggesting interstratified lapilli tuff beds. This unit is interpreted as a felsic tuff, but it could also represent a fine-

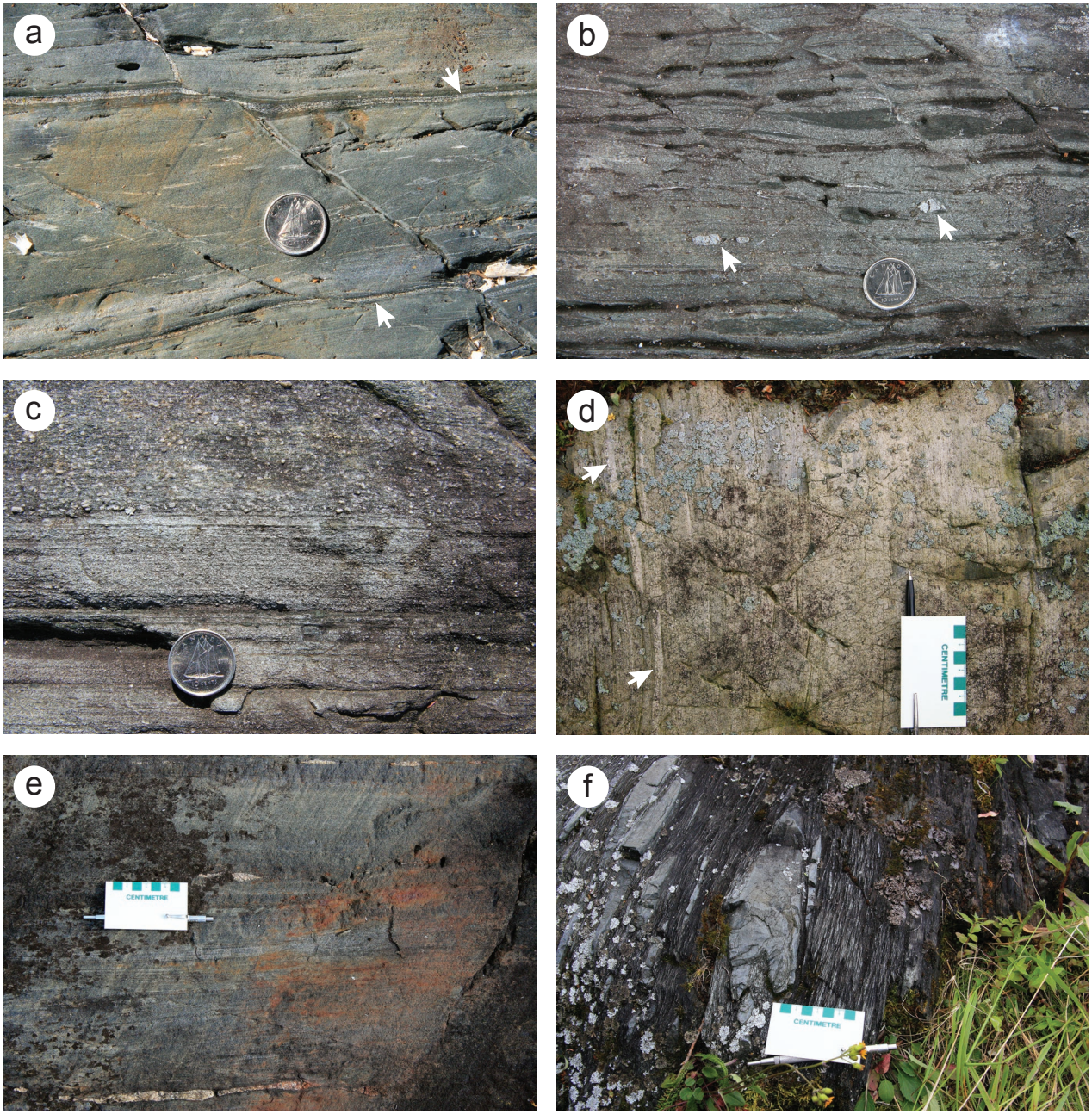

Figure GS2017-2-3: *Outcrop photographs of Hayes River group rocks at Reekie Lake:* ***a)*** *pillowed, amygdaloidal basalt; attenuated amygdules are present above and to either side of coin, and arrows indicate attenuated pillow selvages;* ***b)*** *mafic, pebbly sandstone, arrows indicating coarse plagioclase clasts;* ***c)*** *crystal-rich bed in mafic sandstone (top of image);* ***d)*** *felsic tuff with possible attenuated lapilli (arrows);* ***e)*** *locally sulphidic feldspathic wacke;* ***f)*** *altered conglomerate from location D (Figure GS2017-2-1), with an attenuated and folded pebble immediately above and left of scale card.*

grained felsic sandstone or arkosic arenite. The intermediate tuff is similar to the previously described felsic tuff but is grey to buff on the weathered surface with a less siliceous appearance and no readily apparent phenocrysts or clasts.

The feldspathic wacke is typically light grey, fine grained, strongly foliated and layered to laminated (Figure GS2017-2-3e). Beds (<15 cm thick) vary from massive to internally laminated. Local beds contain granules and pebbles <2 cm across. The pebbles are dominantly intermediate with sparse mafic clasts. Locally graded beds along the south shore of east Reekie Lake fine toward the south. At location B (Figure GS2017-2-1), the wacke is sulphidic and locally contains up to 15% pyrrhotite (Figure GS2017-2-3e). Conglomerate is locally associated with the feldspathic wacke and may grade into pebbly sand beds. Outcrops of conglomerate are highly strained (pebble elongation up to 30:1) and locally altered. At location C (Figure

GS2017-2-1), the conglomerate is light green, strongly foliated to mylonitic, and poorly sorted (Figure GS2017-2-3f). Pebbles are <15 cm thick and dominantly intermediate with lesser felsic and quartz clasts. The pebbles are supported by an altered phyllonitic matrix.

Gabbro

Gabbro to diabase intrusions, ranging from tens of centimetres to tens of metres wide, intrude all of the previously described units. The gabbro is dark green to grey-green on weathered surfaces and dark grey on fresh surfaces. It is medium to coarse grained and foliated to strongly foliated. Although generally homogeneous at outcrop scale, local intrusions contain plagioclase-rich layers <3 cm thick. Some intrusions are porphyritic, with 10–15% plagioclase phenocrysts (<3 mm) or glomerocrysts (<5 mm). Local pyroxenitic enclaves are <3 cm thick. Rare intrusions contain coarse-grained pods, which could represent fractionated segregations.

Peridotite

Outcrops of serpentinized peridotite occur as a cluster of low reefs at location D (Figure GS2017-2-1). The peridotite is light green to white, medium grained, foliated and strongly magnetic, and contains local carbonate veins up to 2 cm wide. The relationship between the peridotite and other rocks is unknown because of the isolated nature of these outcrops; however, a narrow band (<35 cm thick) of ultramafic schist, possibly representing sheared and altered peridotite, occurs along strike to the east within an outcrop of basalt.

Structure

The main penetrative fabric at Reekie Lake is the S_1 foliation, which is defined by attenuated bedding and primary layering. The S_1 foliation strikes west-northwest and is subvertical to steeply north dipping. The foliation is intense and appears mylonitic in many outcrops, with kinematic indicators suggesting dextral and possibly normal shear. This fabric appears to be related to a dextral shear zone that occurs at the contact between the supracrustal rocks and the granodiorite–tonalite to the south. Pebbles in the conglomerate at location C define a gently west-plunging stretching lineation. Local pebbles are also folded about an axis of the same orientation (Figure GS2017-2-3f). Local east-southeast-striking dextral S_2 shear bands with subvertical to steeply south-dipping orientations occur throughout the area. Sparse, conjugate, sinistral S_2 shear bands were also observed and generally strike southwest with steep northwest dips (Figure GS2017-2-4a). Hornblende

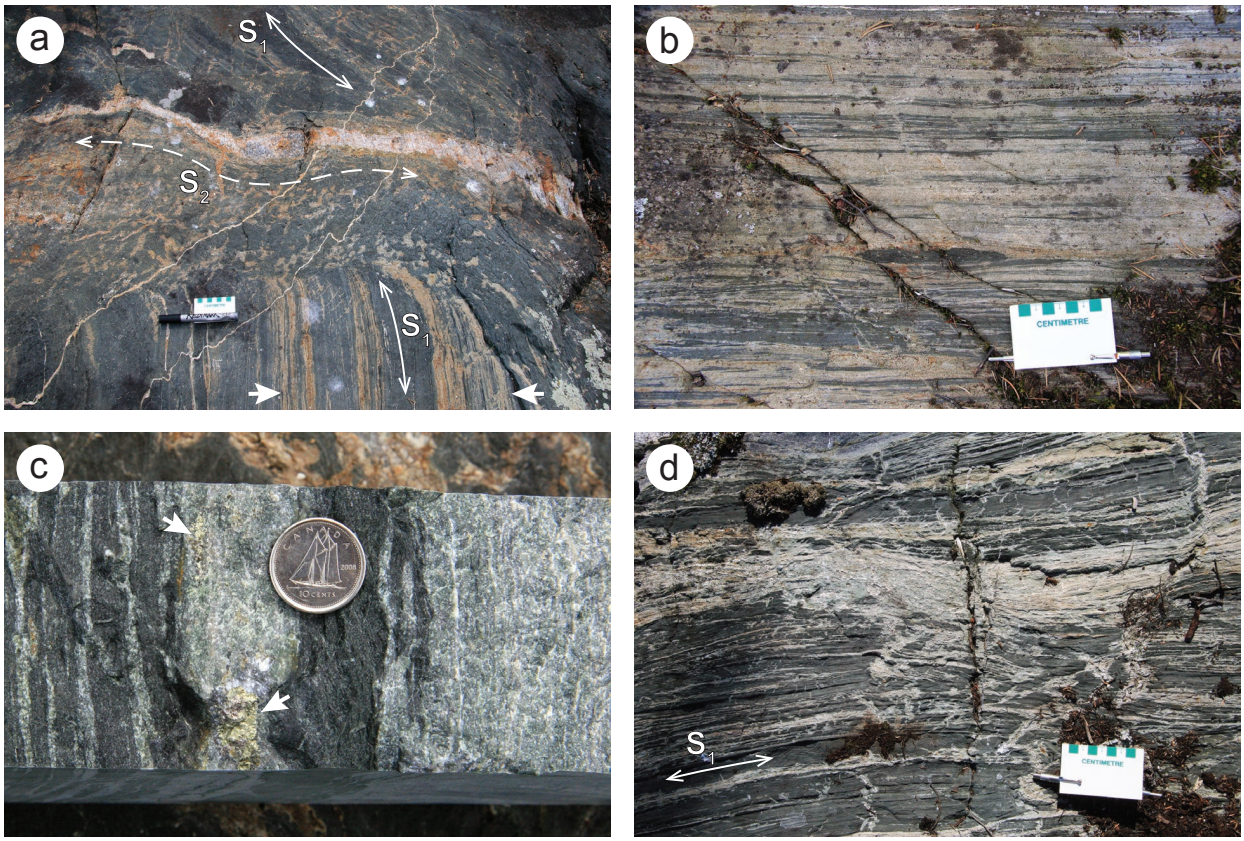

Figure GS2017-2-4: *Outcrop photographs of veins, alteration and structures from location A (Figure GS2017-2-1) at west Reekie Lake:* ***a)*** *sinistral S_2 shear structure with subparallel quartz vein transecting the S_1 regional foliation; calcsilicate alteration (arrows) appears to be largely controlled by the S_1 fabric;* ***b)*** *pervasive calcsilicate alteration of mafic sandstone along the S_1 foliation;* ***c)*** *blebs of chalcopyrite±pyrrhotite (arrows) hosted in calcsilicate alteration; photo is from the bottom of a saw-cut slab;* ***d)*** *possible fracture-controlled veins with haloes of calcsilicate alteration; the veins crosscut the S_1 fabric.*

typically defines both S_1 and S_2 fabrics, suggesting that amphibolite-facies conditions prevailed during D_1 and D_2. An S_3 foliation was observed in a weakly foliated pegmatite dike intruding protomylonitic tonalite. This later foliation is subparallel to S_1, and it is possible that the dike merely intruded late during D_1 deformation. Alternatively, it could be axial planar to the regional synclinal structure, which would make it an F_3 structure.

Veins and alteration

Homogeneous white quartz veins <60 cm thick are ubiquitous in the Reekie Lake area and likely represent several generations of vein emplacement. The most abundant suite of veins is parallel to subparallel to S_1 and characterized by pinch-and-swell structures, and likely formed prior to or during D_1 deformation. Occasional quartz veins occur within S_2 shear structures, contain ductile deformation fabrics and may have been emplaced during or subsequent to D_2 deformation (Figure GS2017-2-4a). The latest quartz veins crosscut all fabrics and were emplaced along brittle fractures. Quartz-carbonate veins occur locally within the basalt and gabbro, and are typically subparallel to S_1. The veins are typically <15 cm thick and appear foliated to weakly foliated. The carbonate typically appears to be dominated by Fe carbonate. The quartz-carbonate veins are interpreted to be relatively late in the deformational history.

Pervasive calcsilicate alteration, with local lenses of quartz and carbonate <3 mm wide, forms a 90 m by 1400 m zone at west Reekie Lake (Figure GS2017-2-1, location A) that is hosted in mafic sandstone. The alteration occurs as light green, fine- to medium-grained, diffuse bands <15 cm thick that parallel the strong S_1 foliation and make up <30% of outcrops (Figure GS2017-2-4a, b). Trace amounts of scheelite occur as finely disseminated grains and local lenses <2 mm thick, and chalcopyrite±pyrrhotite form blebs <2 cm across (Figure GS2017-2-4c). The strong structural control suggests that the alteration occurred prior to, or during, D_1; however, the alteration locally occurs as haloes to discordant fracture-controlled veins (Figure GS2017-2-4d), which suggests a protracted event.

Economic considerations

A zone of disseminated scheelite and chalcopyrite mineralization was reported by McGregor and Petak (1977) at west Reekie Lake (Figure GS2017-2-1, location A). The mineralization was described as hosted in carbonate-quartz skarn alteration. Although the zone was evaluated for W and base metals, its potential for precious metals was not tested. The zone of alteration occurs along a splay of the Stull-Wunnummin fault, which is similar to the setting of the Monument Bay Au-W deposit roughly 140 km to the east (Figure GS2017-2-1). At Monument Bay, Au mineralization is associated with coarse-grained scheelite in discrete vein systems hosted in felsic intrusive and intermediate volcanic rocks along a splay of the Stull-Wunnummin fault (McCracken and Thibault, 2014).

The style of mineralization at Reekie Lake varies considerably from that at Monument Bay. At Reekie Lake, the mineralization occurs within a zone of pervasive calcsilicate alteration, hosted in mafic sandstone with local layers of felsic tuff and silicate-facies iron formation. Although previously described as carbonate-quartz skarn mineralization, little carbonate is present, although it is possible that decarbonation occurred during regional metamorphism. The alteration appears to occur along strike with a 6.8 km long zone of intense carbonate alteration described by Noranda geologists (Assessment File 93901).

The alteration is unlikely to be skarn related to the granodiorite–tonalite of the Bayly Lake complex to the south, as previously suggested by McGregor and Petak (1977). The granodiorite has a strong S_1 protomylonitic fabric, whereas the calcsilicate alteration is characterized by local discordant veins that crosscut the S_1 fabric. Although no economic mineralization was identified, all samples from this zone yielded elevated assay values: two samples of altered mafic sandstone yielded up to 630 ppm Cu, 32 ppm Mo and 100 ppb Hg; a sample of altered felsic tuff yielded 262 ppm W and 1010 ppb Hg; and a sample of iron formation yielded 205 ppb Au (Couëslan, unpublished data). An occurrence of scheelite was also reported by Noranda at location C in east Reekie Lake (Figure GS2017-2-1; Assessment File 93901), which suggests similar mineralization over a strike length of 7.5 km.

Reefs of serpentinized peridotite and the presence of unexposed ultramafic rocks (Assessment File 92005) suggest there is at least notional potential for magmatic nickel-sulphide deposits in the Reekie Lake area. A potential source for crustal sulphide was identified in a band of sulphidic wacke (location B, Figure GS2017-2-1) west of the peridotite reefs; however, drilling by Falconbridge in the late 1960s failed to intersect sulphide mineralization in any of the targets.

Acknowledgments

The author thanks M. Stocking for providing enthusiastic field assistance, as well as E. Anderson for thorough logistical support. Air support was provided by Wings Over Kississing. M. Rinne and S. Anderson provided reviews for earlier drafts of the report.

References

Barry, G.S. 1962: Geology of the Munro Lake area (53L/11, east half); Manitoba Mines and Natural Resources, Mines Branch, Publication 61-1, 27 p. plus 1 map at 1:63 360 scale.

Corkery, M.T., Lin, S., Bailes, A.H. and Syme, E.C. 1999: Geological investigations in the Gods Lake Narrows area (parts of NTS 53L/9 and 53L/10); *in* Report of Activities 1999, Manitoba Industry, Trade and Mines, Manitoba Geological Survey, p. 76–80.

Elbers, F.J. and Gilbert, H.P. 1972: Munro Lake area (53L-11); *in* Summary of Geological Field Work 1972, Manitoba Mines, Resources, and Environmental Management, Mines Branch, Geological Paper 3/72, p. 39–40.

Marten, B. 1992: Geology of the Gods Lake, Munro Lake, Webber Lake area, Manitoba; Manitoba Energy and Mines, Geological Services, Geological Report GR83-1D, 24 p., plus 6 maps at 1:50 000 scale.

McCracken, T. and Thibault, D. 2014: Technical report and updated resource estimate on the Monument Bay project; NI 43-101 report prepared for Mega Precious Metals Inc., 123 p.

McGregor, C. and Petak, H.W. 1977: Reekie Lake (53L/11 SW and SE); *in* Report of Field Activities 1976, Manitoba Department of Mines, Resources and Environmental Management, Mineral Resources Division, Exploration Operations Branch, p. 62–63.

Stott, G.M., Corkery, M.T., Percival, J.A., Simard, M. and Goutier, J. 2010: A revised terrane subdivision of the Superior province; *in* Summary of Field Work and Other Activities 2010, Ontario Geological Survey, Open File Report 6260, p. 20-1–20-10.

GS2017-3

Preliminary results of bedrock mapping at Bigstone Lake and Knight Lake, northwestern Superior province, Manitoba (parts of NTS 53E11, 12, 13, 14)

by M.L. Rinne

In Brief:

- Correlative stratigraphic units identified at Knight Lake and Bigstone Lake
- High-grade, vein-hosted gold mineralization is controlled by late shears in mafic rocks
- Results point to untested structural targets for shear-hosted gold east of Bigstone Lake

Citation:
Rinne, M.L. 2017: Preliminary results of bedrock mapping at Bigstone Lake and Knight Lake, northwestern Superior province, Manitoba (parts of NTS 53E11, 12, 13, 14); *in* Report of Activities 2017, Manitoba Growth, Enterprise and Trade, Manitoba Geological Survey, p. 19–29.

Summary

The Manitoba Geological Survey (MGS) resumed 1:20 000 scale bedrock mapping of the Bigstone Lake greenstone belt, continuing eastward into Knight Lake. Building on previous work, results from the 2017 field season included: 1) recognition of a corridor of late dextral shear zones separating the western and eastern parts of the greenstone belt; 2) delineation of correlative stratigraphic units at Knight Lake and Bigstone Lake; 3) constraints on the relative timing of late-shear deformation events; and 4) documentation of a series of quartz-calcite-sulphide±gold veins associated with the late-shear deformation. Visible gold was found in the youngest vein set, identified on the basis of crosscutting relationships, representing one of three currently known gold occurrences that are distributed across 1.5 km of dominantly mafic and carbonate±sericite-altered rocks east of Bigstone Lake. These findings highlight the potential for more widespread gold mineralization in the Bigstone Lake greenstone belt.

Introduction

Precambrian rocks mapped in 2017 form part of the Bigstone Lake greenstone belt (BLGB), a deformed package of Archean supracrustal rocks that extends approximately 50 km along strike (Figure GS2017-3-1). Despite demonstrated potential for several mineralization styles–with known occurrences of zinc, copper and gold at surface, and in drillcore–detailed exploration work in the BLGB was last undertaken between 1986 and 1989 (Assessment Files 94359, 94022, Manitoba Growth, Enterprise and Trade, Winnipeg).

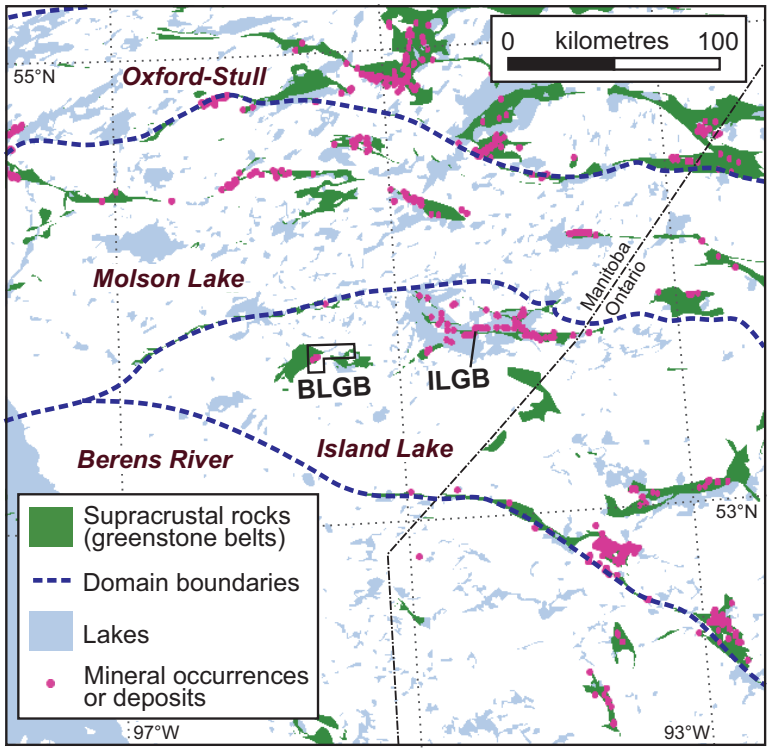

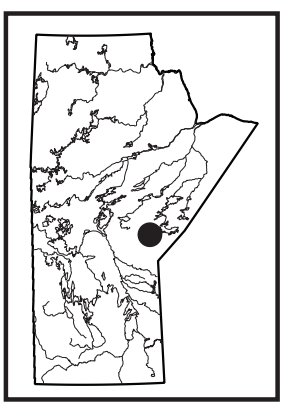

Figure GS2017-3-1: *Simplified geological domains of the northwestern Superior province, showing the locations of greenstone belts and the 2017 mapping area (outlined). Domain names are in italics and are labeled as shown in Pilkington and Thomas (2001). Mineral occurrences shown are mostly Au, Cu, Ni, Ag or Zn; occurrences shown in the Island Lake greenstone belt include two known gold deposits. Abbreviations: BLGB, Bigstone Lake greenstone belt; ILGB, Island Lake greenstone belt.*

Fieldwork completed in 2017 marks the second year of a mapping project that aims to

- document the supracrustal rocks of the Bigstone, Wass and Knight lakes areas primarily through shoreline mapping, supplemented by geochemical and geochronological analyses;
- investigate regional stratigraphic and structural relationships; and
- provide a modern assessment of mineral potential in the area, including volcanogenic massive sulphide (VMS), magmatic Ni-Cu-PGE and lode-gold styles of mineralization.

Previous mapping and exploration work undertaken in the study area was described by Rinne et al. (2016b). This summer, 1:20 000 scale shoreline mapping was carried out over 24 days in the eastern part of Bigstone Lake and the northern part of Knight Lake. Five inland traverses were completed in the eastern part of Bigstone Lake, mostly along topographic lineaments in the vicinity of known gold occurrences. One inland traverse was carried out off the southwestern end of Bigstone Lake in order to investigate a gossanous outcrop visible in satellite imagery. The field season was cut short by a wildfire at Knight Lake.

Regional geology

The BLGB forms part of the Island Lake domain of the northwestern Superior province (Figure GS2017-3-1) and may have been contiguous with supracrustal rocks of the Island Lake greenstone belt, now separated from the BLGB by younger granitoid plutons. Major stratigraphic units of both the Island Lake and Bigstone Lake greenstone belts are divided by most workers into the older Hayes River group, dominated by mafic arc-derived flows and intrusions, and the younger Island Lake group, comprising sedimentary and subordinate volcanic units atop a basal conglomerate (Herd et al., 1987; Stevenson and Turek, 1992). The supracrustal units are generally thought to have been emplaced ca. 2.9–2.7 Ga, although ages are currently better constrained in the Island Lake belt (Neale, 1985; Turek et al., 1986; Herd et al., 1987; Stevenson and Turek, 1992; Parks et al., 2014).

Local geology

Units mapped during the 2017 field season are described in this section from oldest to youngest interpreted age. The ordering of units described in this section corresponds mostly to units shown on PMAP2016-4 (Rinne et al., 2016a), with the exception of the fine-grained gabbro to melagabbro unit (assigned to a lower stratigraphic position), the exclusion of three units not seen in the 2017 mapping area (pyroxenite, ultramafic lapilli tuff and tonalite), and the addition of two units that were not documented in the 2016 mapping area (namely medium-grained gabbro and intermediate volcanic units). All of the rocks have been metamorphosed to upper-greenschist to lower-amphibolite facies; the 'meta' prefix is omitted for brevity.

Lower stratigraphic sequence (Hayes River group)

Rocks of the lower sequence occupy the outermost (north and south) supracrustal portions of both the Bigstone Lake, and the Knight and Wass lakes areas (Figure GS2017-3-2), reflecting a belt-scale syncline. Assigned to the informal Hayes River group, the lower sequence is dominated by mafic to ultramafic flows and intrusions, with subsidiary felsic volcanic and sedimentary units.

Lower mafic volcanic flows

Mafic flows of the lower sequence comprise aphyric, variolitic pillowed basalt and less abundant massive, plagioclase-phyric basalt. The rocks are grey-green to dark grey-green on fresh surfaces and grey-green to lighter grey on most weathered surfaces. Most of the lower basalt outcrops mapped in 2017 were highly strained; where preserved, pillows are typically <40 cm thick and elongated at ~10:1 aspect ratios parallel to the S_3 foliation. Massive, plagioclase-phyric basalt outcrops contain sparse plagioclase phenocrysts <0.5 mm long and, in several locations, are transitional to the fine-grained gabbro described below. Rare interflow greywacke, mudstone and oxide-facies iron formation form a minor component of the lower mafic volcanic unit, typically forming beds <50 cm thick (Rinne et al., 2016b).

Fine- to medium-grained gabbro to melagabbro

Mappable units of massive, fine- to medium-grained gabbro to melagabbro are widespread at several stratigraphic levels throughout the lower stratigraphic sequence (Rinne et al., 2016b; Figure GS2017-3-2). In 2017, gabbro was documented in highly strained outcrops along Wapatinasing Narrows (Figure GS2017-3-2; location f) and the northeastern part of Knight Lake (location i). The gabbro is grey-green on fresh and weathered surfaces, and contains approximately equal parts plagioclase and (chlorite- and actinolite-replaced) pyroxene crystals 1–2 mm long, along with trace amounts of finely disseminated pyrite in a few locations. Although most of the gabbro mapped in 2017 is mafic in composition, gabbro outcrops documented in 2016 were noted to contain gradations from mafic to ultramafic compositions (Rinne et al., 2016b). Medium-grained melagabbro identified inland from the southwestern corner of Bigstone Lake (west of Figure GS2017-3-2) has gradational contacts with komatiitic basalt (Figure GS2017-3-3a) and may thus represent a thick mafic–ultramafic flow. Elsewhere, contacts with adjacent rocks were not observed.

Lower felsic volcanic and volcaniclastic rocks

Felsic volcanic units occur throughout the lower mafic stratigraphy at Bigstone, Knight and Wass lakes (Figure GS2017-3-2; Neale, 1985; Rinne et al., 2016b). Among felsic outcrops described in 2017, most occur at Knight Lake and consist of felsic ash to lapilli tuff, with light grey-beige weathered surfaces and grey fresh surfaces. These rocks contain 50–80% subrounded cream-coloured fragments 0.5–1 mm long (rarely up to 1 cm), along with 1–5% subrounded quartz fragments 1–4 mm

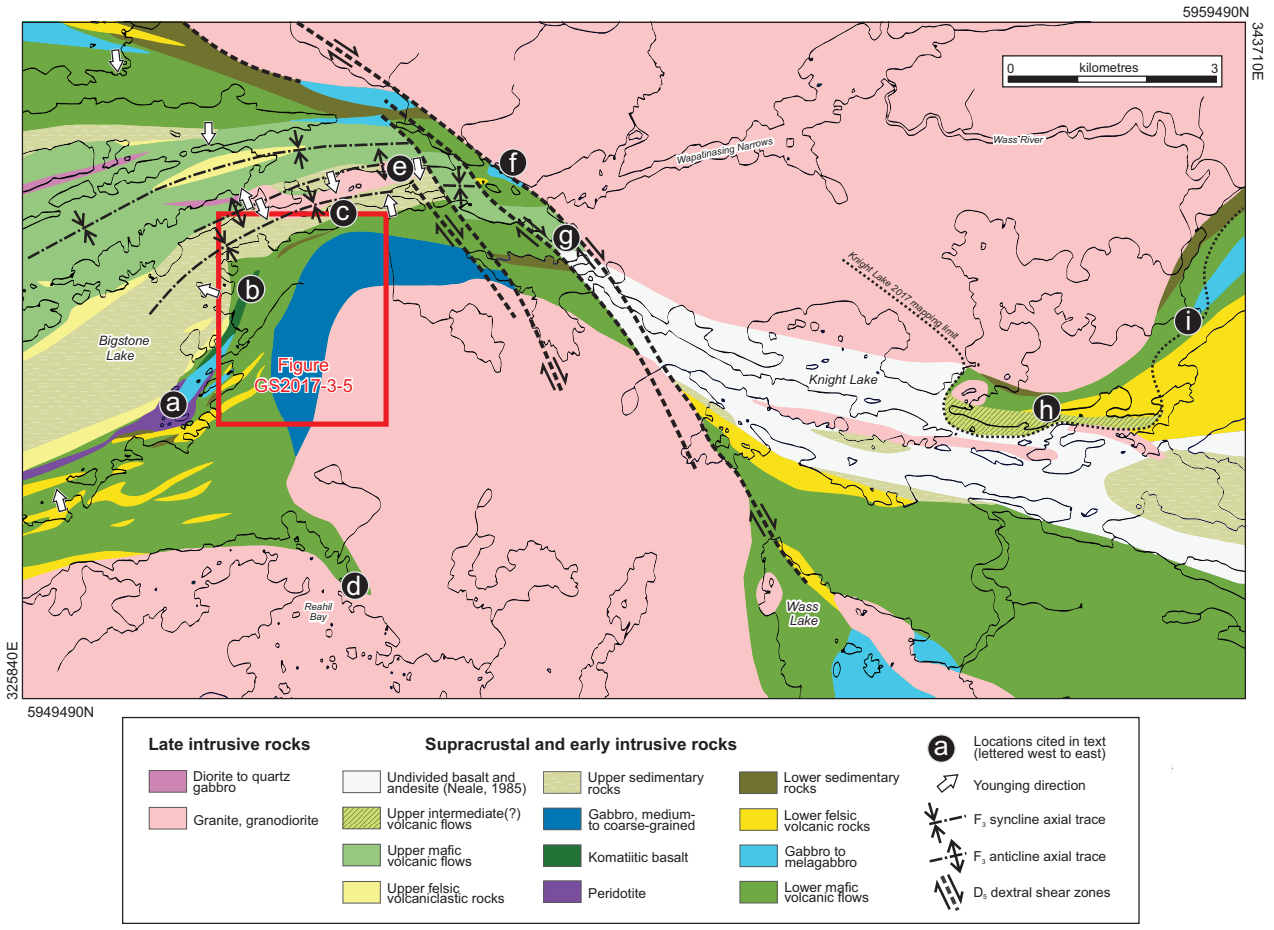

Figure GS2017-3-2: *Simplified geology of the eastern part of Bigstone Lake (modified from Rinne et al., 2016a) and the Knight Lake area (with units south of the 2017 mapping limit mostly after Neale, 1985). Inland geology is based mostly on historical drill data (1938–1988) and traverse stations recorded by McIntosh (1941), Ermanovics et al. (1975), Neale (1984, 1985) and Assessment File 94359 (Manitoba Growth, Enterprise and Trade, Winnipeg). The light grey unit at Knight Lake contains unsubdivided basalt and andesite identified by Neale (1985); it was not visited in 2017. The UTM co-ordinates are in NAD83, zone 15N.*

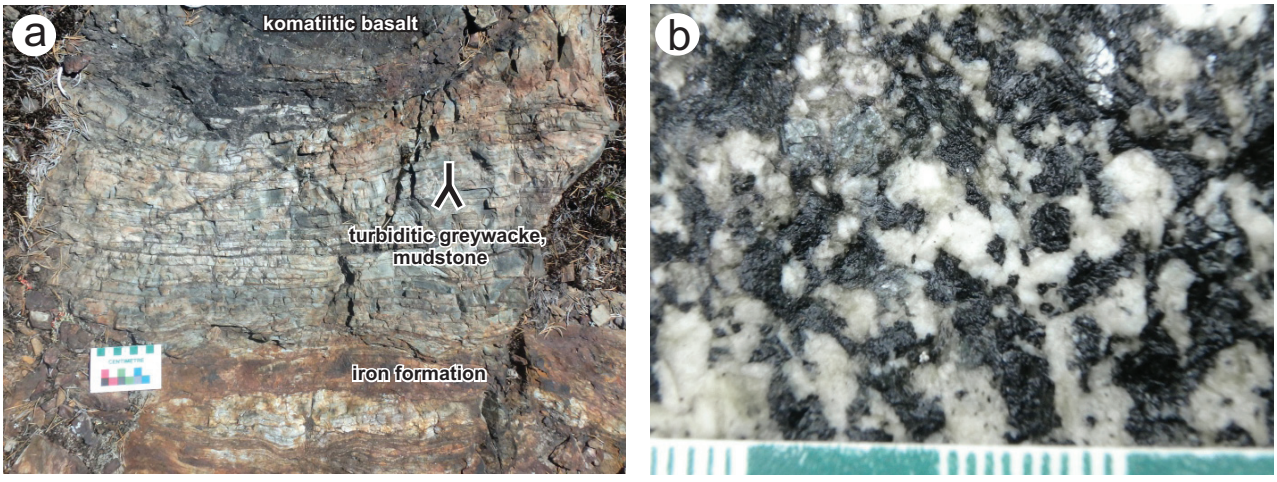

Figure GS2017-3-3: *Outcrop photographs of Bigstone Lake greenstone belt units mapped in 2017, showing* ***a)*** *oxide-facies iron formation conformably overlain by turbiditic greywacke and mudstone (younging to top of image) and komatiitic basalt, which grades over several metres to medium-grained melagabbro;* ***b)*** *medium- to coarse-grained gabbro, which is host to several quartz-carbonate-sulphide±gold veins (see 'Gold mineralization' section).*

across in a felsic-ash matrix. Two stations at Knight Lake contain well-stratified lapilli tuff to tuff breccia, with ungraded layers 2–30 cm thick transposed parallel to the dominant east-northeast-trending foliation.

Four outcrops of plagioclase-phyric dacite were identified along the east-central part of Knight Lake (Figure GS2017-3-2; location h). The rocks contain a fine-grained, quartz-rich groundmass surrounding 20–35% white, subhedral plagioclase phenocrysts 0.1–1 cm long. The dacite is interpreted to be cogenetic with the adjacent and felsic volcaniclastic rocks described above; however, contacts were not observed.

Lower sedimentary rocks

Sedimentary rocks are rare in the lower stratigraphic sequence, with thin (<50 cm) layers forming a minor component of the previously described lower mafic volcanic unit and thicker packages forming mappable units in only a few locations (Figure GS2017-3-2). Turbiditic greywacke and mudstone make up approximately 95% of the lower sedimentary unit; the remainder consists of rare iron formation and pelitic mudstone.

In 2017, turbiditic greywacke–mudstone beds of the lower sequence were described to be in intrusive contact with granodiorite along the northern margin of the greenstone belt at Knight Lake (Figure GS2017-3-2; north of location i). The grey feldspathic greywacke to darker grey mudstone occurs in beds 0.1–8 cm thick that have been transposed along, and isoclinally folded about, an intense north-northeast-trending foliation; structural facing at this location is ambiguous. The rocks transition along strike to the northeast to a felsic tectonite of presumed sedimentary origin.

Large exposures of the lower sedimentary unit were also identified inland from the southwestern corner of Bigstone Lake (west of the area shown in Figure GS2017-3-2). A northeast-trending ridge, visible as a conspicuous rust-coloured feature in high-resolution satellite imagery, was found to contain a sequence of oxide-facies iron formation, turbiditic greywacke–mudstone and komatiitic basalt to melagabbro (Figure GS2017-3-3a). The iron formation occurs in a northeast-trending package at least 5 m in exposed thickness, with approximately equal parts magnetite and quartz (interpreted as recrystallized chert) beds up to 5 cm thick, along with sparse beds of garnetiferous pelitic mudstone. To the southeast, it transitions conformably to a package of turbiditic greywacke–mudstone <1 m thick (Figure GS2017-3-3a) and is in turn overlain by massive komatiitic basalt that transitions over several metres to medium-grained, massive melagabbro. The northwestern contact of the komatiitic basalt is sharp, subtly undulating and crosscuts bedding; this is interpreted as the basal contact of either a thick flow or sill.

Peridotite

Ultramafic rocks occur in the southwestern and eastern parts of Bigstone Lake (Rinne et al., 2016b). Continued mapping of small islands near the eastern shore of Bigstone Lake (Figure GS2017-3-2; location a) revealed relatively unaltered and low-strain examples of peridotite cumulates, mostly pale olive-green on weathered and fresh surfaces. The rocks contain 80% round olivine cumulus crystals ~0.5 mm across and vary from nonmagnetic to weakly magnetic, with no visible sulphides.

Komatiitic basalt

Mafic–ultramafic volcanic rocks were encountered at three shoreline stations in 2017: two on islands adjacent to the peridotite cumulate described above (forming units too small to display in Figure GS2017-3-2); and another inland of the eastern shore of Bigstone Lake (Figure GS2017-3-2; location b). The rocks are aphanitic, highly strained and were identified on the basis of their darker grey-green colour on fresh surfaces. Geochemical results from pillowed outcrops of this unit sampled in 2016 confirm their primitive composition (e.g., 21–24 wt. % MgO; 44–45 wt. % SiO_2; 900–1200 ppm Ni). Contacts with adjacent units were not observed.

Medium- to coarse-grained gabbro

A large intrusion of medium- to coarse-grained and mostly equigranular gabbro occurs inland of the eastern shore of Bigstone Lake (Figure GS2017-3-2). Weathered surfaces are mottled grey-green to beige and fresh surfaces are grey-green, where least altered (Figure GS2017-3-3b). The rock contains an average of 45% pyroxene and 55% plagioclase crystals that vary from 1 to 4 mm across, along with secondary actinolite and chlorite. The gabbro is homogeneous, aside from local strain partitioning and secondary veins and alteration (see 'Gold mineralization' section). A sharp and irregular intrusive contact with basalt was observed at one location, dipping steeply to the east-southeast.

The medium- to coarse-grained gabbro unit is crosscut by granodiorite dikes at several locations and predates the D_3 deformation event, which is manifest in most gabbro outcrops as a weak northeast-trending penetrative S_3 foliation. The unit may be cogenetic with the gabbro and basalt units described above (e.g., a thick synvolcanic sill emplaced during continued development of the overlying volcanic stratigraphy), or it may represent a later, unrelated episode of mafic magmatism. Pending geochemical analyses may help to resolve its relationship with the host stratigraphy.

Upper stratigraphic sequence (Island Lake group)

The upper sequence rocks at Bigstone, Knight and Wass lakes were interpreted by Herd et al. (1987) as stratigraphically equivalent to the Island Lake group, a dominantly sedimentary package that overlies the Hayes River group in the Island Lake greenstone belt. Neale (1984, 1985) tentatively assigned the upper sequence rocks to a separate group, mostly on the basis of the volcanic units they include (which do not form a major component of the Island Lake group; Neale, 1984). The terminology of Herd et al. (1987) is used in this report; investigations into stratigraphic correlations with the Hayes River and Island Lake groups, including U-Pb geochronology, are ongoing.

Upper sedimentary rocks

Rocks of the upper sedimentary unit dominate the older (stratigraphically lower) part of the Island Lake group. The unit consists mostly of turbiditic greywacke–mudstone and locally contains a basal conglomerate. In 2017, the upper sedimentary unit was described at several locations in the eastern part of Bigstone Lake. The unit was not observed in outcrop farther to the east, although Neale (1985) documented several turbidite packages at Knight Lake (south of the mapping limit in Figure GS2017-3-2).

Polymictic conglomerate

Five outcrops of polymictic conglomerate were identified in 2017 along the southern and eastern shorelines of the eastern part of Bigstone Lake, including one highly strained example within 30 m of the inferred unconformity between the upper sedimentary unit and lower mafic volcanic unit (Figure GS2017-3-2; location c). The conglomerate is grey-green to light tan on weathered surfaces, grey to dark grey on fresh surfaces, poorly sorted and crudely bedded to massive. Rounded to subangular clasts 0.5–15 cm long make up 30–60% of the outcrops and are supported in a fine- to medium-grained quartzofeldspathic greywacke matrix. Clast populations resemble those of the conglomerate units documented in 2016 along the southern and northwestern shorelines of Bigstone Lake (Rinne et al., 2016b). The clasts include: grey, fine-grained to pebbly feldspathic greywacke; white, crystalline quartz clasts (possibly vein quartz); light tan to light grey, aphanitic clasts of felsic composition (possibly derived from felsic igneous rocks); and dark grey-green, aphanitic and aphyric mafic clasts (interpreted as basalt derived from the lower mafic volcanic units).

On the basis of clast types and stratigraphic position, the basal conglomerate mapped in 2017 is interpreted as equivalent to polymictic conglomerate or scarp-facies breccia described in the southwestern and northwestern parts of Bigstone Lake (Rinne et al., 2016b) and could thus mark the unconformity between the Hayes River and Island Lake groups; however, this contact has not been observed.

Coarse quartz sandstone

A distinctive coarse sandstone subunit was identified in 2017 along some southeastern shorelines in the eastern part of Bigstone Lake (stations north and west of location b in Figure GS2017-3-2). The sandstone is grey to light tan on weathered surfaces, dark grey to grey-beige on fresh surfaces and occurs in ungraded beds ranging from 2 to 70 cm in exposed thickness. Subangular quartz grains 0.5–3 mm across are distinctive, making up about 60% of the rock, and are supported in a semipelitic mudstone to fine-grained sandstone matrix. Conformable contacts with turbiditic greywacke–mudstone were observed at several locations; contacts with other units were not observed.

Feldspathic greywacke–mudstone turbidite

Most outcrops of the upper sedimentary rocks described in 2017 consist of planar-bedded turbidites, comprising fine-grained feldspathic greywacke and mudstone. The rocks are grey to dark grey on fresh and weathered surfaces and interbedded in a few locations with garnetiferous metapelite beds <40 cm thick, chloritic laminae, and coarse and ungraded quartz sandstone beds. The turbidite beds, commonly transposed parallel to the major S_3 fabric, range from 1 to 30 cm in thickness. Where graded bedding is well preserved, the beds exhibit reversals in younging direction that define a series of belt-parallel F_3 isoclinal folds (Figure GS2017-3-2).

Upper felsic volcaniclastic rocks

The upper felsic unit was identified at only one station in 2017, on the eastern shore of Bigstone Lake (~300 m west of location b in Figure GS2017-3-2). The small outcrop in this location consists of felsic lapilli tuff that contains densely packed plagioclase fragments 0.5–2.5 mm across, in a felsic, fuchsite-altered ash matrix and includes a layer of monomictic felsic volcanic breccia 40 cm thick, with plagioclase-phyric fragments up to 20 cm long. Although contacts were not exposed, conformity with the adjacent upper sedimentary unit was previously documented nearer the centre of Bigstone Lake (Rinne et al., 2016b). Felsic lapilli tuff was also noted to occur conformably throughout the upper mafic volcanic unit (Figure GS2017-3-2).

Upper mafic volcanic flows

The upper mafic flow unit consists of pillow basalt flows that have least altered compositions identical to the lower flow unit. A key distinguishing feature is the presence of abundant (<20%) vesicles in low-strain outcrops of the upper flows. Along the southeast-trending structural corridor at the eastern end of Bigstone Lake (e.g., location g in Figure GS2017-3-2), primary features have been destroyed by deformation. The locations of the upper mafic volcanic packages in this corridor are inferred to preserve stratigraphic continuity with the greenstone belt to the west and east.

Upper intermediate(?) volcanic flows

Highly strained outcrops along the eastern half of Knight Lake (south of location h in Figure GS2017-3-2) were described in the field as either intermediate tectonite or strongly foliated pillowed andesite. In comparison to least altered basalt, these rocks appear slightly lighter grey-green on both weathered and fresh surfaces. Contacts with adjacent units were not identified.

Neale (1985) noted “extensive silicification” in rocks exposed in central Knight Lake, implying the possibility that the ‘intermediate’ rocks are altered basalt as opposed to primary andesite. The upper intermediate volcanic unit could therefore be equivalent to mafic flow units in either the upper or lower sequence. Further work (including the acquisition of geochemical data from least altered equivalents and detailed mapping to establish the nature of the contacts between basalt and silicified basalt) should help to constrain both the primary composition and stratigraphic position of this unit.

Late intrusive rocks

Diorite to quartz gabbro

Porphyritic diorite dikes crosscut all supracrustal units at Bigstone Lake (Rinne et al., 2016b). Examples described in 2017 are light grey dikes up to 60 cm wide, with approximately 10% plagioclase phenocrysts (1–12 mm long) and 10% hornblende phenocrysts (1–6 mm long) in a light grey, fine-grained quartzofeldspathic groundmass. All diorite dikes were overprinted by a steeply dipping S_3 foliation and are in places tightly folded about northeast- to east-trending F_3 axial planes. Quartz gabbro, a rare intrusive phase grouped with the diorite intrusions (Rinne, 2016b), was not encountered during the 2017 field season.

Granite to granodiorite

In addition to thin (<1 m) granitoid dikes occurring throughout the BLGB, granitoid intrusions and contacts were examined along Reahil Bay (Figure GS2017-3-2; location d), the eastern part of Bigstone Lake (near locations e and f), several locations along the northeastern margin of the BLGB at Knight Lake (along the bay north of location h) and 22 widely spaced locations along the Wapatinasing Narrows and Wass River (Figure GS2017-3-2). As described by Rinne et al. (2016b), the intrusions are dominantly medium grained and vary in composition from granodiorite to syenogranite. Consistent with earlier field observations, all contacts between the BLGB and its surrounding granitoid batholith(s) appear to be intrusive and predate D_3 deformation. Granitoid dikes (commonly tightly folded about F_3 axial planes) typically become more abundant within supracrustal units nearest the margins of the greenstone belt; similarly, fine-grained mafic xenoliths up to 2 m across, interpreted to be derived from the BLGB, are more common within granitoid outcrops nearest the greenstone belt.

Late mafic dikes

Minor mafic dikes, which are too small to display as a separate map unit, occur throughout the BLGB, including some that crosscut the previously described diorite dikes (Rinne et al., 2016b). Almost all occurrences are grey-green, aphanitic and aphyric dikes <30 cm thick. A few thicker examples were documented in 2017, notably four fine-grained gabbro dikes up to 1.2 m wide that crosscut the granodiorite batholith in Wapatinasing Narrows. The late mafic dikes, representing the latest intrusive phase recognized in the BLGB, predate D_3 deformation.

Structural geology

Rocks of the BLGB record a complex structural history, as summarized by Rinne et al. (2016b). Results of the 2017 field season are relevant mostly to the D_3, D_5 and D_6 events, as discussed below.

D_3 deformation

The lower stratigraphic units of the BLGB trace the limbs of a broadly northeast- to east-trending and steeply dipping regional F_3 syncline (Figure GS2017-3-2). At Bigstone Lake, the surface trace of the regional F_3 syncline is inferred to extend along the centre of the upper mafic volcanic unit (the northernmost syncline shown in Figure GS2017-3-2). At Knight Lake and Wass Lake, the axial trace of the regional syncline has not yet been defined, but its general location is indicated by the repetition of lower stratigraphic units along the north and south portions of the BLGB (Figure GS2017-3-2; Neale et al., 1986). The syncline is accompanied throughout the BLGB by parasitic F_3 anticlines and synclines; in areas mapped in 2017, these axial planes were not well resolved outside of turbidite-bearing units.

A penetrative and steeply dipping S_3 foliation is the dominant structure in most outcrops, and is broadly parallel to the F_3 axial planes in Figure GS2017-3-2. Moving west to east, the dominant trend of the S_3 foliation in the BLGB varies from

- northeast in the centre of Bigstone Lake (near location a);
- east in the eastern part of Bigstone Lake (location g);
- east-southeast in the western and central parts of Knight Lake (south of location h); to
- northeast in the northeastern part of Knight Lake (location i).

Outside of the BLGB, a pervasive S_3 foliation is commonly observed near batholith margins. However, toward batholith centres most of the granitoid outcrops were noted to contain only steeply dipping spaced cleavages that trend southeast and north-northeast; these are respectively interpreted to correspond to the D_5 and D_6 deformation events.

D_5 deformation

D_5 deformation is expressed throughout the western part of the BLGB as a series of dominantly southeast-trending and steeply dipping shear zones (Rinne et al., 2016b), and is interpreted to be responsible for the regional dextral offset between supracrustal units at Bigstone Lake and Knight and Wass lakes. Rather than a single fault or shear zone (an interpretation offered by Herd et al., 1987), results from 2017 suggest that the regional offset along the centre of the map area was accommodated by a series of dextral shear zones and related planar fabric, resulting in a highly strained corridor containing several offset panels (Figure GS2017-3-2). Rocks in this corridor (e.g., between locations e, f, and g in Figure GS2017-3-2) commonly show a well-developed spaced shear-band cleavage with dextral asymmetry (e.g., Figure GS2017-3-4a). Minor (<20 cm wide) southeast-striking dextral D_5 shears were identified at several stations throughout the structural corridor, and are interpreted to mirror the regional D_5 structure.

D_6 deformation

Northeast- to north-northeast-trending and steeply dipping shear zones from 1 cm to 5 m wide were measured at nine stations in the eastern half of Bigstone Lake. The late shear zones crosscut all previously identified structures (e.g., Figure GS2017-3-4a, b) and show evidence of sinistral

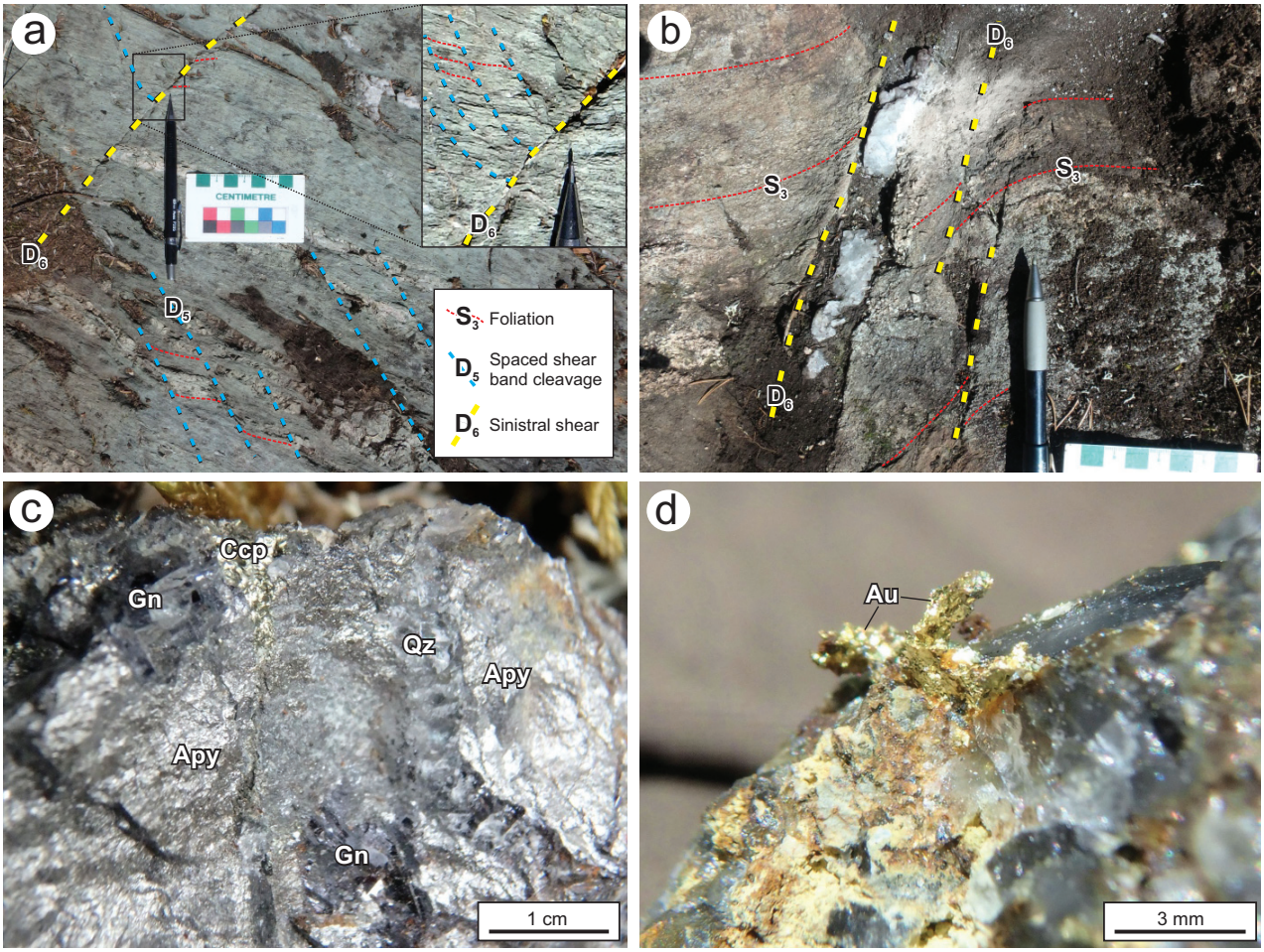

Figure GS2017-3-4: *Photographs illustrating relationships between late-stage shear structures and base-metal–sulphide±gold vein mineralization in the Bigstone Lake greenstone belt:* ***a)*** *S_3 foliation and D_5 shear-band cleavage planes showing deflection along the margins of a minor sinistral D_6 shear;* ***b)*** *north-northeast-trending quartz vein (+trace pyrite) hosted within and parallel to D_6 shear zones showing sinistral deflection of the S_3 foliation;* ***c)*** *arsenopyrite (Apy), galena (Gn) and chalcopyrite (Ccp) in a north-northeast-trending quartz (Qz) vein that ranges up to 60 cm wide;* ***d)*** *wire-gold aggregate exposed on the broken surface of a quartz-calcite-galena-pyrite-chalcopyrite vein.*

movement. Although crosscutting relationships documented so far indicate that D_6 occurred after D_5, further study may indicate mutually crosscutting relationships consistent with a conjugate array of both dextral and sinistral structures. Inland mapping results suggest that the D_6 (and probably D_5) shear structures controlled the locations of vein-hosted gold mineralization.

Gold mineralization

Exploration history

Surface exploration was carried out between 1934 and 1938 in areas east of Bigstone Lake, resulting in the discovery of the Diamond Queen gold occurrence (Figure GS2017-3-5a). In 1938, God's Lake Gold Mines Ltd. bored a series of closely spaced drillholes along the two veins (Figure GS2017-3-5b) to depths of between 19 and 77 m (Assessment File 91148).

Noranda Exploration Company Ltd. collected surface samples from the area from 1983 to 1986. They recognized a 'zone of carbonatization and quartz-carbonate veining' spatially associated with the gabbro contact, along which they discovered a quartz-sulphide vein 50 cm wide that assayed 72.3 ppm Au (Assessment File 94359). The discovery was made approximately 1.5 km north-northeast of the main Diamond Queen vein (Figure GS2017-3-5a) and likely corresponds (based on a hand-drawn sample-location map) with occurrence 7 in Figure GS2017-3-5b. Despite noting promising results, Noranda carried out no drilling on the gold occurrences and abandoned the Bigstone Lake property after 1986.

2017 field mapping results

Several inland traverses were completed in 2017 in order to confirm the gold occurrences, document the vein assemblages and wallrock alteration, investigate the timing and structural

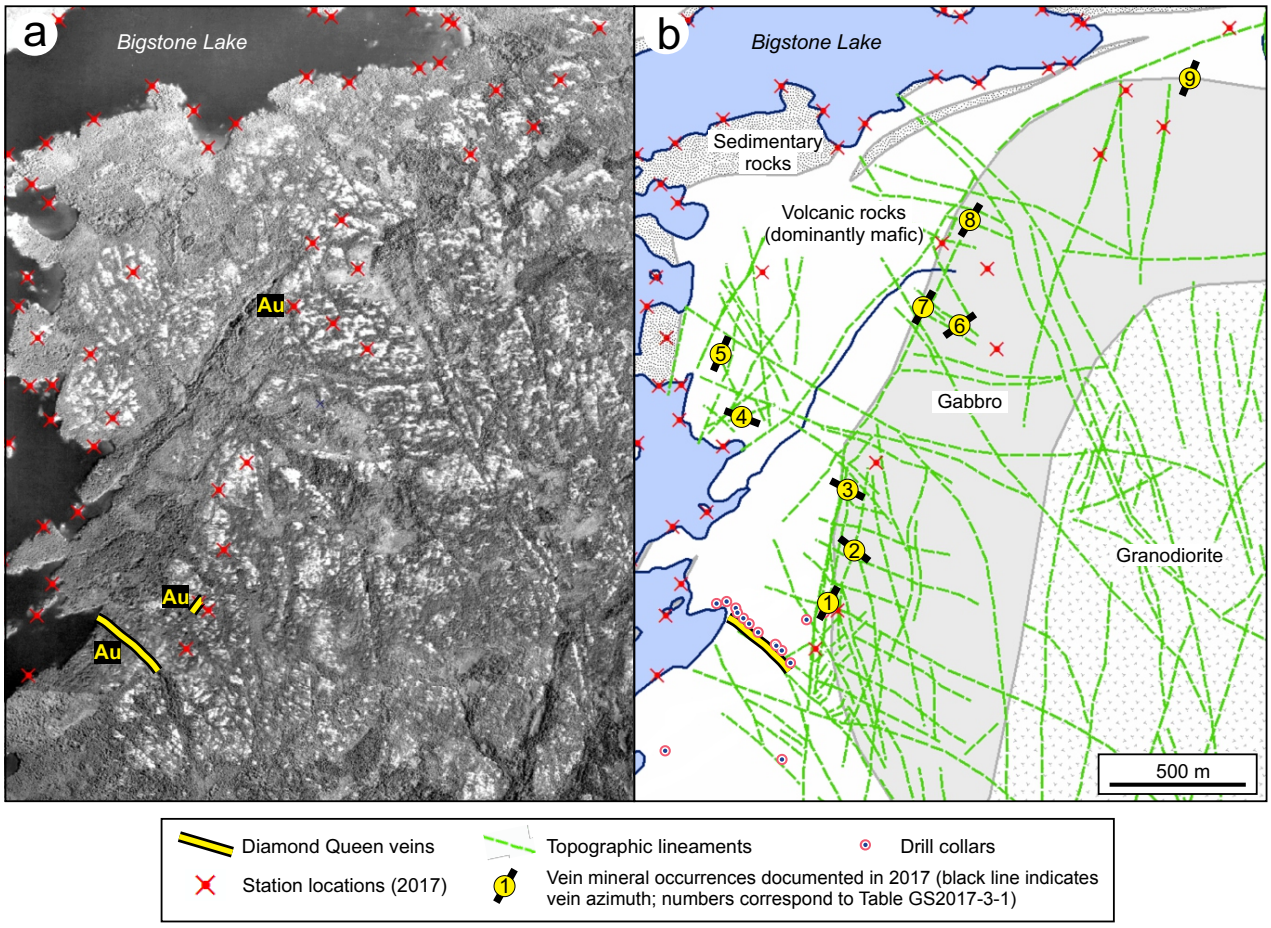

Figure GS2017-3-5: *Locations of quartz-sulphide±gold vein occurrences associated with late shears east of Bigstone Lake:* ***a)*** *airphoto imagery with three known gold occurrences indicated;* ***b)*** *simplified geology, with topographic lineaments, and vein occurrences documented in 2017 numbered south to north. Lineaments are interpreted from airphoto and high-resolution satellite imagery, many likely corresponding to southeast- and north-northeast-trending shear structures that are respectively associated with D_5 and D_6 deformation. The locations of the two Diamond Queen gold veins and adjacent shallow drilling are based on a reassessment of hand-drawn shorelines in Assessment File 91148, Manitoba Growth, Enterprise and Trade, Winnipeg.*

controls on the mineralization, and examine selected north-northeast- and southeast-trending topographic lineaments. Relevant findings are summarized in Table GS2017-3-1 and Figure GS2017-3-5b, and include the recognition of two dominant gold-bearing vein sets, which are described below.

East-southeast- to southeast-trending veins

The main Diamond Queen vein is the first-discovered and largest of the three known gold-mineralized veins in the BLGB, traced in 1938 to a strike length of approximately 350 m (Table GS2017-3-1; Figure GS2017-3-5; McIntosh, 1941; Assessment File 91148). This vein is reported to dip steeply toward the northeast, and contains quartz, pyrite, chalcopyrite and gold (McIntosh, 1941). A planned visit was not possible during the 2017 field season.

Minor quartz-pyrite±chalcopyrite±chlorite veins up to 30 cm wide were described at three locations north of the Diamond Queen vein (occurrences 2–4 in Table GS2017-3-1 and Figure GS2017-3-5b). Striking 114–126° and dipping 69–81° to the southwest, they are hosted within and/or trend parallel to dextral D_5 shear structures. They are potentially related to the southeast-trending Diamond Queen vein on the basis of their similar orientation and contained mineral assemblage; assay results are pending.

North-northeast- to northeast-trending veins

Several quartz-calcite-galena-pyrite-chalcopyrite-arsenopyrite±gold veins were found mostly within 100 m of the contact between gabbro and basalt (Figure GS2017-3-4c, d; occurrences 1 and 5–9 in Table GS2017-3-1 and Figure GS2017-3-5b). The veins range in thickness from 1 cm to 2 m wide, strike 020–034°, and dip 77–88° to the southeast (excepting occurrence 6, which dips steeply to the northwest; Table GS2017-3-1). A few of the north-northeast-trending veins were noted to occur within, but do not appear to have been deformed by, sinistral D_6 shear zones (Figure GS2017-3-4b; Table GS2017-3-1);

Table GS2017-3-1: Summary of vein occurrences east of Bigstone Lake. Numbered occurrences were documented in 2017, with locations shown in Figure GS2017-3-5b. Minor occurrences are included where they illustrate relevant structural relationships.

Vein occurrence	Description (vein mineral assemblage, orientation, associated structures)
Diamond Queen	Quartz-pyrite-chalcopyrite-gold vein, up to 1 m wide; striking average 310/80° to the northeast (McIntosh, 1941; Assessment File 91148). The main Diamond Queen vein was traced by drilling and trenching in 1938 to a strike length of approximately 350 m. Not visited in 2017.
1	Quartz-calcite-galena-pyrite-chalcopyrite-arsenopyrite-gold vein, average 30 cm wide, thinning locally to ~2 cm; striking average 025/79° to the southeast. Trace visible gold occurs in irregular or wiry aggregates <5 mm long (Figure GS2017-3-4d). Assay results are pending. Wallrock is sericite-chlorite-quartz-pyrite schist, interpreted as sericite-altered basalt. Likely corresponds to the northernmost extension of the smaller of two Diamond Queen veins, which was traced in 1938 to a strike length of ~50 m (Assessment File 91148).
2	Quartz-pyrite-chalcopyrite (trace) vein, red, 15 cm wide; striking 126/82° to the southwest.
3	Quartz-chlorite-pyrite vein, 30 cm wide; striking 118/69° to the southwest. Vein contains a D6 cleavage at 202/83° west.
4	Quartz-pyrite veins, 1–6 cm wide; occurring within D_5 dextral shear zones striking 114/81° to the southwest.
5	Quartz-chlorite-pyrite veins, 1–5 cm wide; occurring within D_6 sinistral shear zones striking 024/77° to the southeast.
6	Quartz-galena-chalcopyrite-arsenopyrite vein, 40–60 cm wide; striking 236/78° to the northwest (Figure GS2017-3-4c).
7	Quartz-galena-pyrite-chalcopyrite veins, 10–60 cm wide; striking between 020/84° to the east and 031/80° to the southeast. Wallrock is calcite-altered gabbro. Previously sampled and tagged with flagging tape (label illegible); location roughly matches sample collected by Noranda Exploration Company Ltd. in 1986, with reported 72.3 ppm Au (Assessment File 94359).
8	Quartz-pyrite-chalcopyrite-galena-arsenopyrite ± sphalerite ± secondary covellite veins, 0.2–2 m wide; striking between 025/80° and 034/85° to the southeast. Wallrock is weakly calcite-altered gabbro.
9	Quartz-pyrite (trace) vein 1–3 cm wide; occurring within a D_6 sinistral shear zone striking 023/88° to the southeast (Figure GS2017-3-4b).

the veins are therefore interpreted to have formed during, or possibly following, the D_6 deformation event.

One vein containing visible gold (occurrence 1), identified in 2017 near the centre of a mostly swamp-filled lineament, was traced for approximately 10 m along strike to the south-southwest to a submerged and heavily revegetated blast pit ~1 m wide. Historical drilling plans (God's Lake Gold Mines Ltd.; Assessment File 91148) indicate that this gold occurrence represents the north-northeast portion of the smaller of two Diamond Queen veins defined in 1938 (Figure GS2017-3-5a). The Diamond Queen veins were previously recorded (Manitoba Mineral Resources, 2013) to occur approximately 1 km north of their location indicated in Figure GS2017-3-5.

Alteration

Most of the quartz-sulphide±gold veins mapped in 2017 are hosted in weakly calcite-altered gabbro. Although the distribution of stations is not sufficient to define alteration zones, Noranda geologists noted a zone of carbonate alteration along the dominantly north-northeast-trending gabbro contact (Assessment File 94359). This spatial relationship may indicate that carbonate alteration occurred during development of the north-northeast-trending D_6 structures and veins, although it is also possible that this alteration may be more regional and could entirely predate the D_6 deformation.

The hostrock to the previously described gold-bearing vein (occurrence 1) is tentatively interpreted as altered basalt, based on a small (~10 cm wide) exposure of north-northeast-foliated sericite-chlorite-quartz-pyrite schist and an adjacent outcrop of relatively unaltered massive basalt. Haloes of sericite are commonly documented in the wallrock to Archean shear-hosted gold deposits (e.g., Groves et al., 1998), often representing the most proximal alteration facies. A visit in 2018 is planned to assess the wallrock alteration in better exposed outcrop, and to sample and document the main Diamond Queen vein.

Exploration implications

The available evidence suggests significant potential for lode-gold mineralization east of Bigstone Lake. The most prominent structures in the area are expressed as swamp-filled or densely vegetated valleys (Figure GS2017-3-5a), which presents a challenge for surface exploration. However, modern mapping methods can reveal vectors to buried mineralization and most of the area remains unexplored by drilling (Figure GS2017-3-5b). The exploration targets discussed in this section, relating mostly to the density and refraction of probable controlling structures, are largely untested.

The density of topographic lineaments in Figure GS2017-3-5b could denote increased structural complexity and associated potential for vein development along the western half of the gabbro unit, particularly near occurrence 1. However, interpreted lineament density is only locally relevant as sections of the map area are obscured by overburden. Zones of densely spaced shears could, for example, lie below cover in the creek valley that trends north-northeast of the main Diamond Queen vein (i.e., between occurrences 3 and 4, or west of gold occurrences 1 and 7). Digital elevation models produced from LiDAR (light detection and ranging) data have proven useful for tracing structure in many Archean gold districts and can help to 'see

through' the masking effects of vegetation and thin overburden.

Some of the most prominent east-southeast- to southeast-trending lineaments show clockwise refraction moving southeast across the contact from basalt to gabbro, or in a few cases through the centre of the gabbro unit. Examples include the lineaments north and east of occurrence 3 and east of occurrence 8 (Figure GS2017-3-5b). Clockwise bends along dextral brittle–ductile shears are likely zones of structural dilation and vein infill; a nearly identical scenario has been described at the Rice Lake mine in the Rice Lake greenstone belt of southern Manitoba, wherein the thickest gold-bearing vein segments are associated with the deflection of shears across a gabbro sill contact (Anderson, 2013; D.A. Rhys, unpublished technical report prepared for Harmony Gold (Canada) Inc., 2001).

Several of the north-northeast-trending lineaments occur near or along the gabbro contact (Figure GS2017-3-5b). Any bends or irregularities along the gabbro margin could have generated splays or dilatant zones in contact-parallel shears. Areas of interest in Figure GS2017-3-5b include the curving gabbro contact between occurrences 8 and 9; the gabbro margin north of occurrence 3; and the zone of possible curvilinear splays south of occurrence 1.

At the Rice Lake mine, the shears that host significant gold mineralization have also produced measurable offsets of the host gabbro unit (Anderson, 2013; D.A. Rhys, unpublished technical report prepared for Harmony Gold (Canada) Inc., 2001). Detailed mapping of the gabbro contact at Bigstone Lake, including careful attention paid to evidence of offset, could therefore prove to be an effective strategy to identify new drilling targets. A detailed mapping program may also lead to the recognition of chemically favourable units (e.g., iron formation), alteration zonation (e.g., transitions from chlorite-calcite to vein-proximal ankerite-sericite-pyrite), systematic patterns in pathfinder-element concentrations (e.g., W, As, Bi, B) or other vectors to lode-gold mineralization (Ames et al., 1988; Groves et al., 1998).

Economic considerations

Submarine bimodal volcanic rocks of the BLGB exhibit many characteristics that imply broad potential for VMS mineralization, as discussed in Rinne (2016b). Ultramafic units in the lower stratigraphic package are also possible hosts to magmatic Ni-Cu (±PGE, Cr) mineralization, perhaps similar to the Nickel Island occurrence hosted in potentially equivalent ultramafic units at Island Lake.

Calcite and sericite alteration, in addition to calcite and Cr-bearing mica alteration assemblages documented regionally (Rinne et al., 2016b), may be important guides to lode-gold mineralization in the BLGB (e.g., MacGeehan and Hodgson, 1982; Moritz and Crocket, 1990; Groves et al., 1998). Results from this summer's fieldwork confirm the occurrence of visible gold in quartz-calcite-sulphide veins, and demonstrate that the mineralization is controlled by late shears within a package of dominantly mafic and carbonate (±sericite)-altered stratigraphy. Collectively, these features warrant further attention including, but not limited to, subsurface investigations north-northeast of the Diamond Queen veins.

Acknowledgments

The author thanks G. Fouillard for her exceptional assistance during field mapping and sample cataloguing, and for her keen eye in discovering visible gold at occurrence 1; E. Anderson and N. Brandson (MGS) for their help managing field operations; C. Epp for his assistance with sample preparation; and C. Couëslan and S. Anderson for their reviews. Staff and pilots of Wings Over Kississing provided dependable transportation, with particular thanks to pilot E. Coles for the short-notice evacuation flight through the smoke over Knight Lake.

References

Ames, D.E. 1988: Stratigraphy and alteration of gabbroic rocks near the San Antonio gold mine in the Rice Lake area, southeastern Manitoba; M.Sc. thesis, Carleton University, Ottawa, Ontario, 202 p.

Anderson, S.D. 2013: The Rice Lake mine trend, Manitoba: regional setting, host rock stratigraphy and structural evolution of a classical Archean orogenic gold system; Mineralogical Association of Canada-Geological Association of Canada, Joint Annual Meeting, Winnipeg, MB, May 22–24, 2013, Field Trip Guidebook FT-A1; Manitoba Innovation, Energy and Mines, Manitoba Geological Survey, Open File OF2013-4, 47 p.

Ermanovics, I.F., Park, G., Hill, J. and Goetz, P.A. 1975: Geology of Island Lake map area (53E), Manitoba and Ontario; Geological Survey of Canada, Report of Activities, Part A, Paper 75-1A, p. 311–316.

Groves, D.I., Goldfarb, R.J., Gebre-Mariam, M., Hagemann, S.G. and Robert, F. 1998: Orogenic gold deposits: a proposed classification in the context of their crustal distribution and relationship to other gold deposit types; Ore Geology Reviews, v. 13, p. 7–27.

Herd, R.K., Currie, K.L. and Ermanovics, I.F. 1987: Island Lake area, Manitoba and Ontario; Geological Survey of Canada, Map 1646A, scale 1:250 000, with descriptive notes.

MacGeehan, P.J. and Hodgson C.J. 1982: Environments of gold mineralization in the Campbell Red Lake and Dickenson mines, Red Lake district, Ontario; *in* Geology of Canadian Gold Deposits, R.W. Hodder and W. Petruk (ed.), Canadian Institute of Mining and Metallurgy Special Volume 24, p. 184–207.

Manitoba Mineral Resources 2013: Bedrock geology, Manitoba; *in* Map Gallery–Geoscientific Maps, Manitoba Mineral Resources, URL <http://web33.gov.mb.ca/mapgallery/mgg-gmm.html> [September 2017].

McIntosh, R.T. 1941: Bigstone Lake area; Manitoba Mines and Natural Resources, Mines Branch, Publication 38-1, 12 p., map at 1:63 360 scale.

Moritz, R.P. and Crocket, J.H. 1990: Mechanics of formation of the gold-bearing quartz-fuchsite vein at the Dome mine, Timmins area, Ontario; Canadian Journal of Earth Sciences, v. 27, no. 12, p. 1609–1620.

Neale, K.L. 1984: Bigstone Lake project; *in* Report of Field Activities 1984, Manitoba Energy and Mines; Mineral Resources, p. 126–128.

Neale, K.L. 1985: Geological investigations in the Knight Lake–Bigstone Lake area; *in* Report of Field Activities 1985, Manitoba Energy and Mines; Geological Services/Mines Branch, p. 200–202.

Neale, K.L., Bardsley, J.G. and Lemoine, R.M. 1986: Bigstone Lake; Manitoba Energy and Mines; Minerals Division, Preliminary Map 1986B-1, scale 1:20 000.

Parks, J., Lin, S., Davis, D.W., Yang, X.-M., Creaser, R.A. and Corkery, M.T. 2014: Meso- and Neoarchean evolution of the Island Lake greenstone belt and the northwestern Superior Province: Evidence from lithogeochemistry, Nd isotope data, and U–Pb zircon geochronology; Precambrian Research, v. 246, p 160–179.

Pilkington, M. and Thomas, M.D. 2001: Magnetic and gravity maps with interpreted Precambrian basement, Manitoba: Geological Survey of Canada, Open File 3739, 4 maps, scale 1:1 500 000.

Rinne, M.L., Anderson, S.D. and Reid, K.D. 2016a: Bedrock geology of Bigstone Lake, Manitoba (parts of NTS 53E12, 13), Manitoba Growth, Enterprise and Trade, Manitoba Geological Survey, Preliminary Map PMAP2016-4, scale 1:20 000.

Rinne, M.L., Anderson, S.D. and Reid, K.D. 2016b: Preliminary results of bedrock mapping at Bigstone Lake, northwestern Superior province, Manitoba (parts of NTS 53E12, 13); *in* Report of Activities 2016, Manitoba Growth, Enterprise and Trade, Manitoba Geological Survey, p. 51–62.

Stevenson, R.K. and Turek, A. 1992: An isotopic study of the Island Lake Greenstone Belt, Manitoba: crustal evolution and progressive cratonization in the Late Archean; Canadian Journal of Earth Sciences, v. 29, p. 2200–2210.

Turek, A., Carson, T.M., Smith, P.E., Van Schmus, W.R. and Weber, W. 1986: U-Pb zircon ages for rocks from the Island Lake greenstone belt, Manitoba; Canadian Journal of Earth Sciences, v. 23, p. 92–106.

GS2017-4

Discriminative study of genetically diverse carbonate rocks in the northwestern Pikwitonei granulite domain and Split Lake block, central Manitoba (parts of NTS 63P11, 12, 64A1)

by J.A. Macdonald[1], A.R. Chakhmouradian[1], C.G. Couëslan and E.P. Reguir[1]

[1] Department of Geological Sciences, University of Manitoba, 125 Dysart Road, Winnipeg, MB R3T 2N2

In Brief:

- Genetically diverse types of carbonate rocks identified in the Split Lake block and Pikwitonei granulite domain
- Possible carbonatite discovered at Split Lake; may indicate potential for rare metals
- New petrogenetic interpretations of carbonate rocks help constrain the geodynamic evolution of the Superior Boundary zone

Citation:
Macdonald, J.A., Chakhmouradian, A.R., Couëslan, C.G. and Reguir, E.P. 2017: Discriminative study of genetically diverse carbonate rocks in the northwestern Pikwitonei granulite domain and Split Lake block, central Manitoba (parts of NTS 63P11, 12, 64A1); *in* Report of Activities 2017, Manitoba Growth, Enterprise and Trade, Manitoba Geological Survey, p. 30–41.

Summary

Correct petrogenetic interpretation of carbonate rocks is important for geodynamic reconstruction of structurally complex terranes, and because these rocks can potentially host a variety of mineral resources (e.g., base metals, Mo and W in skarns; rare earths and Nb in carbonatites; diamonds in kimberlites). Carbonate minerals are strongly susceptible to metamorphic decarbonation, and textural and geochemical re-equilibration. Consequently, carbonate rocks of different origins may appear macroscopically similar in metamorphic terranes and require detailed analysis of their trace-element and isotopic compositions to identify their origin. Ten occurrences of carbonate rock in the high-grade Split Lake block and Pikwitonei granulite domain of northern Manitoba are the focus of the present study. Petrographic and quantitative analyses of calcite and dolomite from these rocks were carried out to aid in the determination of their origin. A potential new locality of carbonatite magmatism at Split Lake is identified.

Introduction

Carbonatites are rare mantle-derived igneous rocks that are strongly susceptible to subsolidus processes capable of completely overprinting their primary petrographic features (Chakhmouradian et al., 2016b). Consequently, identification of carbonatites can be difficult, especially in heavily deformed terranes. Altered basalts, hydrothermal veins, supracrustal sediments and carbonatites can all show similar petrographic characteristics after being subjected to even low-grade metamorphism. Furthermore, extrusive and shallow intrusive carbonatites can be easily confused with other carbonate-rich rocks, such as kimberlites and ultramafic lamprophyres, which will have implications for mineral exploration (Chakhmouradian et al., 2009a). Additionally, a correct interpretation of carbonate rocks is essential for geodynamic reconstruction by providing a tectonic context.

Because strongly deformed carbonate rocks are commonly misinterpreted (Le Bas et al., 2002, 2004), nonpetrographic considerations must be taken into account to identify rocks of igneous origin. The presence of pyrochlore suggests a carbonatitic origin (Le Bas et al., 2002), whereas anorthite, scapolite or spinel are more consistent with a sedimentary source (Le Bas et al., 2002). Igneous carbonate is characterized by a high Sr content and typically shows an enrichment in light rare-earth elements (LREE; Chakhmouradian et al., 2016b). However, metamorphic reactions can drastically change the mineralogy (Chakhmouradian et al., 2015), and the distribution of REE in igneous carbonate can be modified by supergene or magmatic processes (Xu et al., 2007; Chakhmouradian et al., 2016a). Element ratios are more robust petrogenetic indicators in that Eu and Ce anomalies are generally lacking in carbonatites, whereas their Y/Ho value approaches that of the primitive mantle (Le Bas et al., 2002, 2004; Chakhmouradian et al., 2016a). Magmatic carbonates generally plot in the ranges $\delta^{13}C_{V\text{-}PDB}$ = –4‰ and –8‰ and $\delta^{18}O_{V\text{-}SMOW}$ = +6‰ and +10‰ on stable-isotope discrimination diagrams (Taylor et al., 1967; Demény et al., 2004). However, various syn- to postemplacement processes can affect the isotopic composition of carbonatites (Demény et al., 2004).

To date, several localities of carbonate rocks of uncertain origin have been reported from the Pikwitonei granulite domain (PGD) and Split Lake block (SLB) of northern Manitoba (Figure GS2017-4-1). With a few exceptions, most these occurrences were first documented in detail by Couëslan (2013, 2014). The present contribution provides a preliminary assessment of 10 significant carbonate-rock occurrences in the PGD and SLB based on the above criteria.

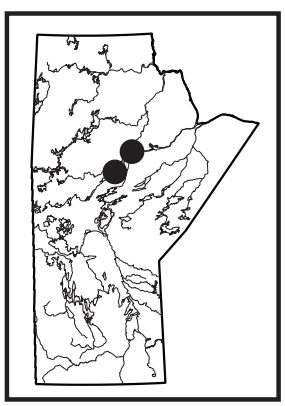

Regional geology

The Superior boundary zone (SBZ) is a transitional structural domain between the Archean continental rocks of the Superior province to the south and east, and the Paleoproterozoic juvenile

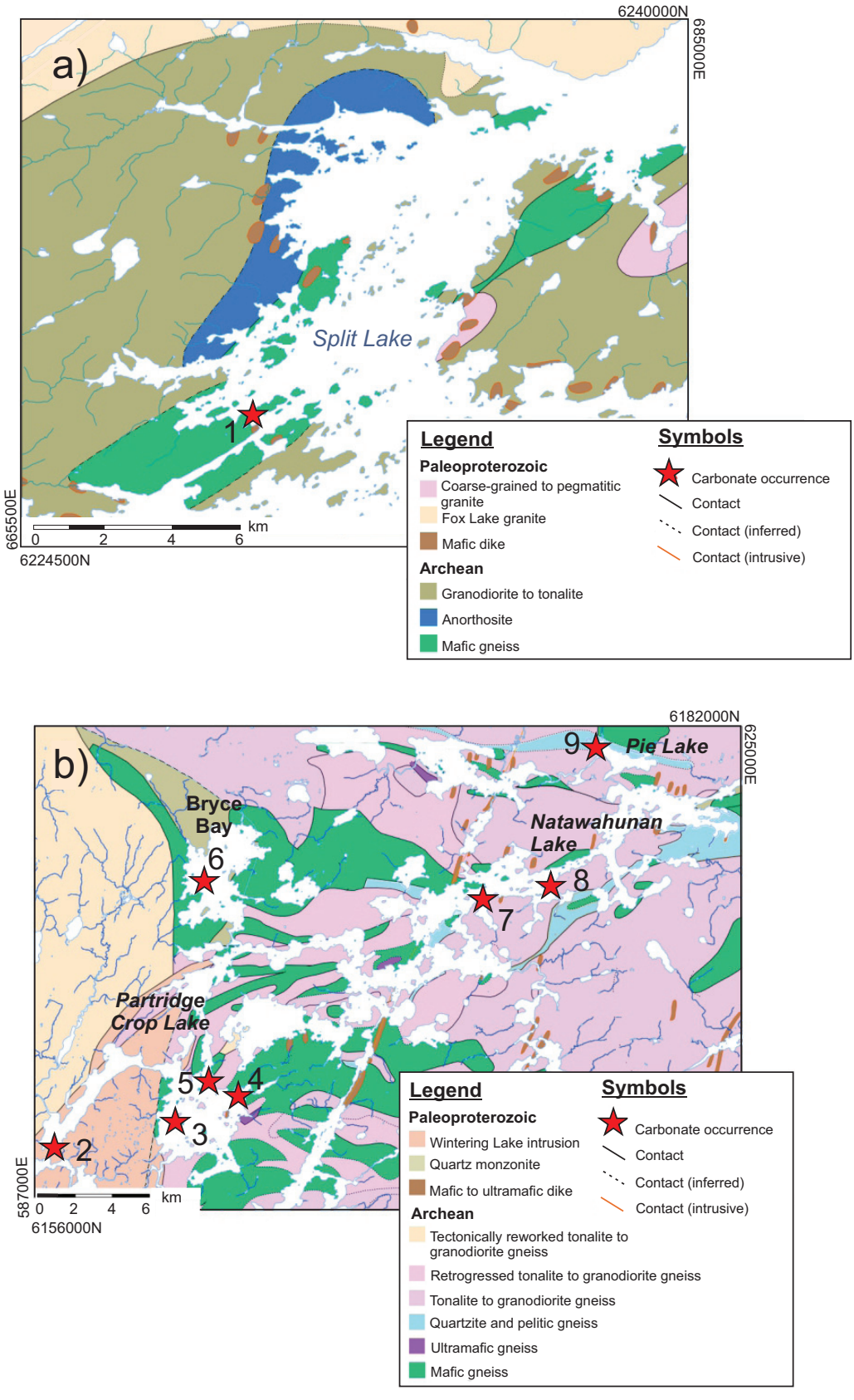

***Figure GS2017-4-1**: Simplified geological maps of the Split Lake **(a)** and Partridge Crop–Natawahunan Lake **(b)** areas (abbreviated PCL and NL, respectively), showing the locations of the studied occurrences of carbonate rocks: 1, Split Lake; 2, PCL-01; 3, PCL-02; 4, PCL-03; 5, PCL-04; 6, Bryce Bay; 7, NL-01 and NL-02 (located ~200 m apart and represented by a single star); 8, NL float; 9, Pie Lake.*

volcanic arc and associated metasedimentary rocks of the Reindeer zone to the north and west. The PGD and SLB represent mid- to deep-crustal rocks of the Superior craton and are separated from each other by shear zones (Hartlaub et al., 2005; Kuiper et al., 2011). The majority of the examined occurrences are located in the PGD, at Partridge Crop and Natawahunan Lakes, with one site in the SLB, at Split Lake (Figure GS2017-4-1).

Split Lake block

The SLB is a geologically distinct terrane bounded by the Assean Lake shear zone to the north and the Aiken River shear zone to the south. It consists largely of metamorphosed igneous rocks with protoliths generated through multiple episodes of magmatism; age relations among these units are unclear (Böhm et al., 1999). Archean rocks in this area consist of supracrustal metapelite, mafic-ultramafic granulite and an igneous complex consisting of anorthosite, gabbro and mafic tonalite. The Archean rocks are often present as disrupted rafts in younger felsic intrusions (Böhm et al., 1999). The same authors also noted that the SLB was isolated from significant Paleoproterozoic deformation. The high-grade terrane is crosscut by weakly metamorphosed Paleoproterozoic mafic dikes and intruded in the north by the Fox Lake granite (ca. 1825 Ma; Heaman et al., 2011). It is hypothesized that the SLB and the PGD share their metamorphic histories at ca. 2.7 Ga (Böhm et al., 1999), but the PGD was unaffected by regional amphibolite-facies retrogression (Hartlaub et al., 2003).

Pikwitonei granulite domain

The Pikwitonei granulite domain (PGD) is an integral part of the Northern Superior superterrane and one of the largest and best-preserved high-grade Neoarchean terranes in the world (Heaman et al., 2011; Couëslan, 2013). The PGD grades into the Thompson Nickel belt (TNB) to the west, and is separated from the SLB to the north by the Aiken River shear zone and from the typical granite-greenstone belts to the south and east by an orthopyroxene isograd (Hartlaub et al., 2005; Heaman et al., 2011; Kuiper et al., 2011). The gradual transition from low-grade rocks to their high-grade equivalents in the PGD represents a continuous oblique crustal cross-section (Heaman et al., 2011). The PGD consists largely of intermediate to felsic, orthopyroxene-bearing gneisses and migmatites, mafic granulites and amphibolites (Heaman et al., 2011). At least four episodes of metamorphism and two major phases of deformation are documented in the PGD. The prominent east-trending S_1 metamorphic layering and isoclinal folding were developed during the first phase (D_1-M_1), which occurred under upper amphibolite– to lower granulite–facies conditions and caused widespread anatexis (Heaman et al., 2011; Couëslan, 2013). This was followed by phase D_2, which generated a strong quartz fabric (S_2) that is axial planar to minor isoclinal folding (Couëslan, 2016). Granulite-facies metamorphism (M_2) resulted in the formation of leucosomes attenuated with S_2, which suggests that they developed synchronously with, or were outlasted by, D_2 (Couëslan, 2016). Paleoproterozoic deformation events caused amphibolite-grade retrogression that increases in intensity toward the TNB.

Partridge Crop Lake is located in the transition zone between the PGD and SBZ, and thus experienced Paleoproterozoic deformation and retrograde metamorphism at amphibolite-facies conditions (Heaman et al., 2011; Couëslan, 2016). The bedrock geology consists of felsic and mafic Archean gneisses interspersed with metamorphosed supracrustal rocks and intruded by granitoids of Paleoproterozoic age (Couëslan, 2013). The Wintering Lake granite dominates the southwestern portion of the area and has been dated at 1846 ±8 Ma and 1822 ±5 Ma (Machado et al., 2011a, b). Mafic and ultramafic dikes crosscut the regional gneissosity in two main orientations, and are tentatively interpreted to represent the Molson dike swarm (ca. 1880 Ma) and possibly an older, east-northeast-trending group of unknown provenance (ca. 2090–2070 Ma; Heaman and Corkery, 1996; Halls and Heaman, 2000; Couëslan, 2013). Peak metamorphic conditions in the Partridge Crop Lake area are approximated at 790–850°C and 8.3–10.7 kbar (Paktunç and Baer, 1986, Mezger et al., 1990).

Natawahunan Lake is located in the western extent of the PGD. The bedrock geology of this area is dominated by granulite- and amphibolite-facies assemblages that were retrogressively metamorphosed to amphibolite- and greenschist-facies assemblages (Weber, 1978; Böhm, 1998; Heaman et al., 2011; Couëslan, 2016). Here, the basement comprises schollen enderbite and orthopyroxene-bearing felsic gneisses (Couëslan, 2016). Other units include mafic and garnet-bearing gneisses and metasedimentary rocks (Couëslan, 2016). A Paleoproterozoic shear zone runs the length of Natawahunan Lake (Couëslan, 2016). Veins consisting of quartz and subordinate carbonate and lined with chlorite are associated with shear zones of Hudsonian age and areas of intense carbonate-chlorite-sericite alteration (Couëslan, 2016). Peak metamorphic conditions at Natawahunan Lake reached 800–830°C and 6.5–8 kbar (Paktunç and Baer, 1986; Mezger et al., 1990).

Carbonate rocks in northeastern Manitoba

The stable C and O isotope data and major- and trace-element compositions of calcite discussed below, as well as the detailed petrographic descriptions of the carbonate rocks, were collected during the present study. Selected occurrences of carbonate rock contain calcite-dolomite pairs that allow the temperature of dolomite equilibration to be calculated (Anovitz and Essene, 1987). An in-depth description of the analytical techniques used is provided with the geochemical data in Data Repository Item DRI2017005 (Macdonald et al., 2017)[2].

[2] MGS Data Repository Item DRI2017005, containing the data or other information sources used to compile this report, is available to download free of charge at http://www2.gov.mb.ca/itm-cat/web/freedownloads.html, or on request from minesinfo@gov.mb.ca or Mineral Resources Library, Manitoba Growth, Enterprise and Trade, 360–1195 Ellice Avenue, Winnipeg, Manitoba, R3G 3P2, Canada.

Split Lake

A sample of apatite-bearing pink carbonate rock (36-77-435-1) was collected at Split Lake and archived by T. Corkery in 1977. This locality was revisited by the authors in 2016 (GS2017-4-1a). Although the original outcrop was not found, a carbonate rock was recognized (Figure GS2017-4-2a). This rock is hosted within a foliated granodiorite, has a dark-green weathered appearance and crosscuts the regional foliation in thin (~4 cm wide) bands in different orientations. The bands are enveloped in a light-green alteration halo several centimetres wide (Figure GS2017-4-2a) and crosscut by felsic veins. Coarse-grained calcite was sampled from one of the bands (Green Bay calcite) and studied along with the material collected by T. Corkery.

Sample 36-77-435-1 consists predominantly of calcite, diopside and apatite. Accessory phases include xenocrystic plagioclase and trace amounts of allanite, pyrite and tremolite. Calcite shows 'patchy' zoning in backscattered-electron scanning electron microscope (BSE) images (Figure GS2017-4-2b), consisting of irregularly shaped core areas that show a relatively high average atomic number (AZ) and areas of lower AZ developed along grain margins and cleavage planes. Some calcite crystals contain small subhedral apatite inclusions (Figure GS2017-4-2b). Apatite occurs as grains measuring 0.5–3.0 mm across, both in the calcite mesostasis and in xenoliths that contain interstitial allanite (Figure GS2017-4-2c). Plagioclase ($An_{31–33}$) is present in highly digested xenoliths, where it is replaced metasomatically by an aggregate of albite (An_9) and muscovite. Plagioclase xenocrysts also exhibit reaction rims zoned from clinozoisite at the xenolith margin to epidote and then allanite in contact with the surrounding calcite.

Major-element compositions of calcite form two populations: one containing no detectable Mg, Mn or Fe and low ΣREE, and the other characterized by higher levels of Mg, Mn, Fe and REE. Both populations are enriched in Sr with respect to the rest of the sample suite (Figure GS2017-4-3a), and the Y/Ho ratios are close to the primitive-mantle value (Figure GS2017-4-3b). The high-AZ variety is enriched in LREE relative to heavy REE (HREE), as reflected in their chondrite-normalized $(La/Yb)_{CN}$ values, whereas the low-AZ variety shows relative depletion in LREE (Figure GS2017-4-4). The normalized profiles of both varieties are flat and lack any Eu anomaly.

The Green Bay calcite contains abundant microscopic inclusions of dolomite, interpreted to have formed by exsolution, and scarce fragments of oscillatory-zoned ankerite and Fe-rich dolomite; both calcite and dolomite show enrichment in Mn. In contrast to sample 36-77-435-1, the Green Bay material contains little Sr or REE (Figure GS2017-4-3a). This calcite has a mantle-like Y/Ho ratio (25 ±2), similar to that in sample 36-77-435-1, but shows extreme enrichment in HREE ($[La/Yb]_{CN}$ << 0.01; Figure GS2017-4-4) where the LREE are at or below detection.

Sample 36-77-435-1 is confidently identified as intrusive calcite carbonatite (sövite), as it shows mineralogical, trace-element and stable-isotope characteristics (Figure GS2017-4-5) consistent with primary igneous carbonate: the presence of allanite and apatite; the absence of a Eu anomaly and a mean Y/Ho value of 26 ±3; enrichment of the calcite in Sr, LREE and light C and O isotopes (as reflected in its $\delta^{13}C_{V\text{-}PDB}$ and $\delta^{18}O_{V\text{-}SMOW}$ values; see Figure GS2017-4-5 for definition of these abbreviations); and 'patchy' zoning in calcite indicative of Sr and REE removal by late-stage fluids (Demény et al., 2004; Le Bas et al., 2004; Chakhmouradian et al., 2016a). Interestingly, this sample is mineralogically and geochemically similar to sövite from Paint Lake, some 120 km southwest of Split Lake in the SBZ (Couëslan, 2008; Chakhmouradian et al., 2009b).

The crosscutting relationships of the carbonate rocks observed on Split Lake in 2016 and their associated green alteration envelope, potentially representing the fenitization process, are consistent with carbonatitic magmatism (Le Bas, 2008). The low Sr and REE abundances in the Green Bay calcite argue against an igneous origin; however, stable C and O isotope data plot in the primary igneous field (Figure GS2017-4-5) and it has been shown that deformation and hydrothermal reworking of igneous carbonates can result in the removal of Sr and REE, generating a variety of REE distribution patterns (Chakhmouradian et al., 2016a).

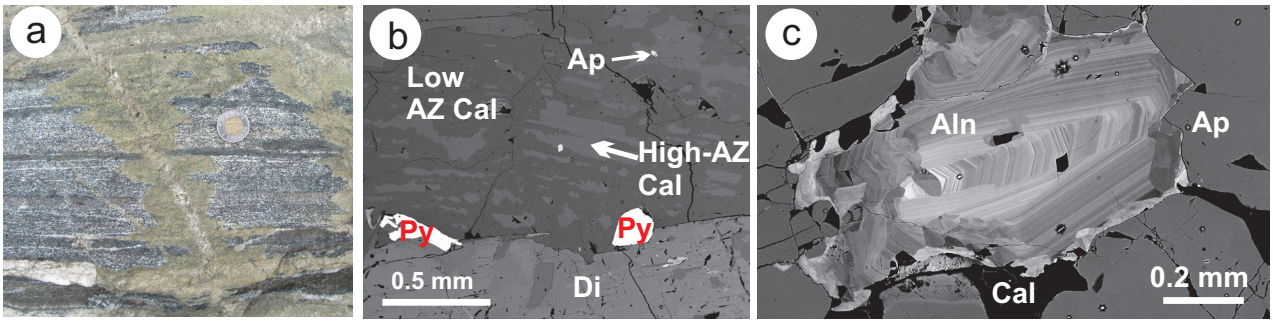

Figure GS2017-4-2: *Structural and textural relations of the carbonate rocks at Split Lake:* ***a)*** *carbonate vein crosscutting gneissic host with associated alteration halo (potentially representing fenitization);* ***b)*** *backscattered-electron scanning electron microscope (BSE) image showing zonation in the calcite from sample 36-77-435-1; note presence of apatite;* ***c)*** *BSE image showing zoned allanite interstitial to apatite in apatite-rich xenolith. Abbreviations: Aln, allanite; Ap, apatite; AZ, average atomic number; Cal, calcite; Di, diopside, Py, pyrite.*

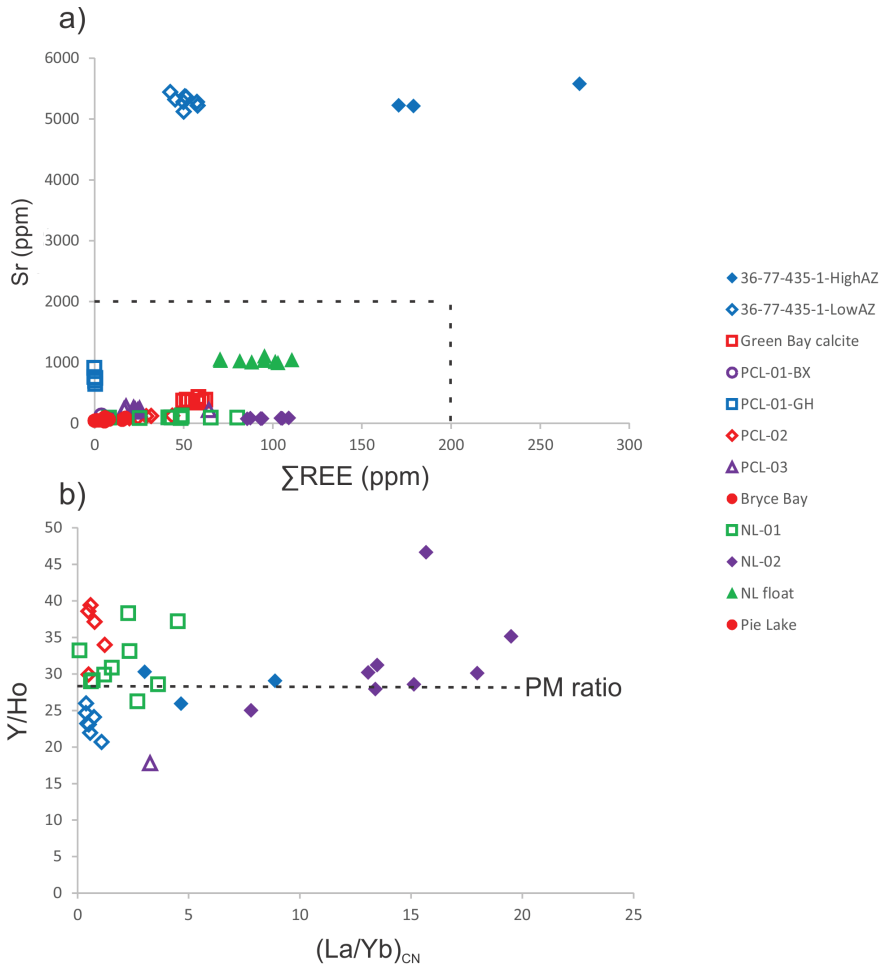

***Figure GS2017-4-3**: Trace-element compositions of calcite from the studied carbonate rocks. Dashed box in lower left corner of **(a)** indicates the inferred Sr and ΣREE contents of sedimentary carbonates (Chakhmouradian et al., 2009b). Dashed line in **(b)** represents the Y/Ho ratio of the primitive mantle; selected occurrences of carbonate rock have been omitted from (b) because one or more of Y, Ho, La or Yb were undetected, so the plotted ratios could not be calculated. Abbreviations: AZ, average atomic number; BX, brecciated variety of carbonate rock at outcrop PCL-01; GH, granite-hosted calcite at outcrop PCL-01; PM, primitive mantle.*

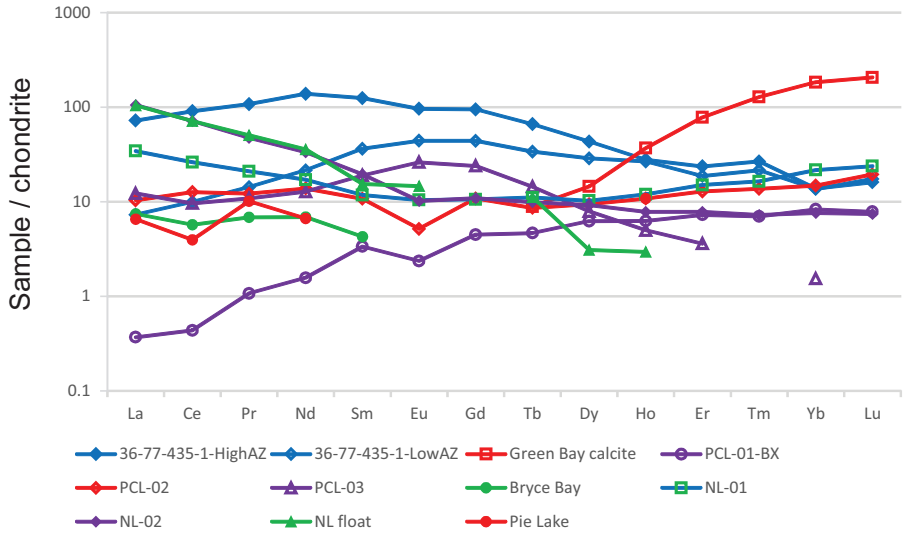

***Figure GS2017-4-4**: Average chondrite-normalized REE profiles of calcite in selected carbonate rocks from this study (normalization values from Anders and Grevesse, 1989). Granite-hosted calcite of outcrop PCL-01 has been omitted because the REE were not confidently detected. Abbreviations: BX, brecciated variety of carbonate rock at outcrop PCL-01.*

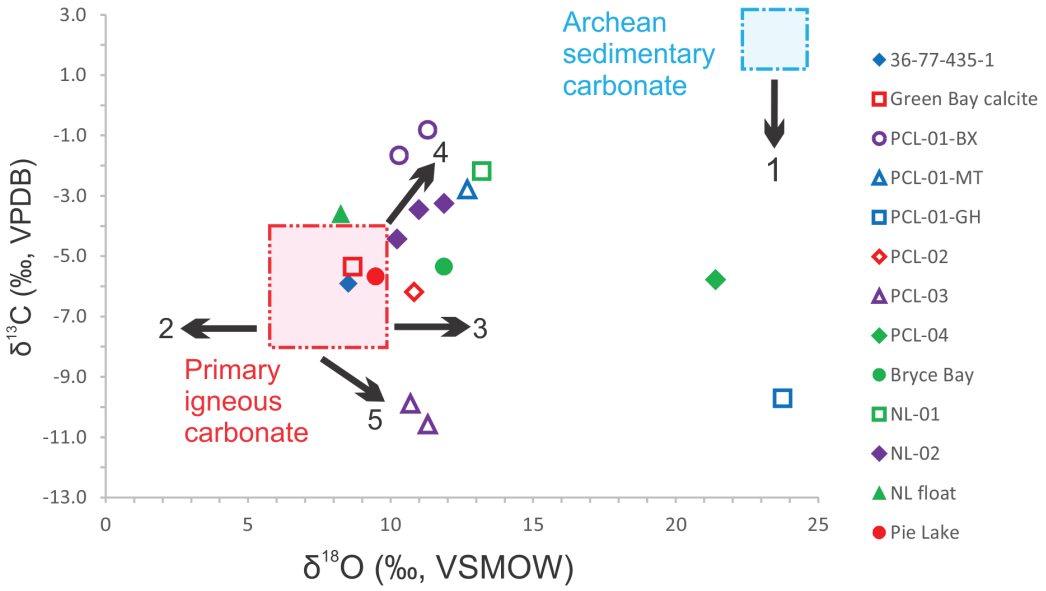

***Figure GS2017-4-5**: Carbon and oxygen stable-isotope compositions of calcite in the carbonate rocks from this study. Solid symbols indicate localities where the samples yielded only calcite; hollow symbols denote localities where the calcite contained dolomite inclusions. Fields of primary igneous carbonate (Taylor et al., 1967) and Archean sedimentary carbonate (Veizer et al., 1989) are shown. Black arrows indicate possible changes in isotopic compositions due to 1) decarbonation during metamorphism (Swain et al., 2015); 2) high-T alteration (Demény et al., 2004); 3) low-T alteration (Demény et al., 2004); 4) sediment assimilation (Demény et al., 2004); and 5) degassing or assimilation of biogenic carbon (Lira and Ripley, 1992; Demény et al., 2004). Abbreviations: BX, brecciated variety of carbonate rock at outcrop PCL-01; MT, magnetite-rich variety of carbonate rock at outcrop PCL-01; GH, granite-hosted calcite at outcrop PCL-01; V-PDB, Vienna Peedee belemnite; V-SMOW, Vienna Standard Mean Ocean Water.*

Outcrop PCL-01

Carbonate rocks in the western part of Partridge Crop Lake (Figure GS2017-4-1b) were first reported by Dawson (1952), and were revisited and resampled in 2013 and 2016. The carbonate rocks are developed in the Wintering Lake granite and Archean mafic gneiss as discontinuous bands extending for up to 75 m along the shoreline. Most volumetrically significant are carbonate breccias that comprise a carbonate matrix showing evidence of ductile deformation (folding and flow; Figure GS2017-4-6a) and abundant clasts aligned with the fold axes.

Less common occurrences of carbonate at this locality are a massive carbonate rock rich in serpentinized olivine and magnetite and confined to the contact with a mafic schist, and pegmatitic veins crosscutting the Wintering Lake granite and hosting medium- to coarse-grained calcite (Figure GS2017-4-6b). The folded clast-rich rock contains felsic clasts and xenocrysts, and is crosscut by granitic veins. Major minerals are calcite, diopside and quartz; minor to accessory phases include microcline, chlorite, amphibole, meionite, titanite, clinozoisite, zeolite, magnetite and plagioclase ($An_{8–39}$). Calcite is inequigranular, shows high-strain deformation features and forms embayments in highly altered diopside grains. The massive rock is composed of calcite, phlogopite, serpentinized forsterite, magnetite, dolomite and spinel, with subordinate chlorite, quartz, pargasite (after diopside), gibbsite (after spinel), ilmenite and zircon. Dolomite forms zoned inclusions in calcite that are interpreted as recrystallized exsolution lamellae and as subhedral grains mantling mafic silicates. Phlogopite is enriched in BaO along the rim (locally up to 6.2 wt. % oxide). The major constituents of the calcite-bearing granitoid veins are albite ($An_{6–7}$; replacing primary plagioclase), quartz, muscovite, chlorite and calcite, with accessory Fe-oxide and relict plagioclase, and trace potassium feldspar and ankerite. Calcite contains abundant inclusions of chlorite and Fe-oxide, and occurs interstitially to the secondary albite-muscovite aggregates.

Calcite from the breccias shows low Sr, Ba and ΣREE abundances in comparison to carbonatites (Figure GS2017-4-3a); its chondrite-normalized REE profiles are characterized by relative enrichment in HREE, a negative Eu anomaly (Figure GS2017-4-4) and Y/Ho ratios that are consistently above the primitive-mantle value (Figure GS2017-4-3b). The granite-hosted calcite has the highest FeO content (2.3–2.7 wt. %) among the studied samples; its Sr abundances are also higher than in the majority of the samples (with the exception of 36-77-435-1), whereas Ba is below detection. Total REE abundances (Figure GS2017-4-3a) are among the lowest measured in this study. Hence, normalized REE profiles and indicator ratios are not available for this sample. The C-O stable-isotope compositions of carbonate from both the brecciated and the olivine-magnetite–rich rocks plot outside the igneous carbonate field toward higher $\delta^{13}C_{V\text{-}PDB}$ and $\delta^{18}O_{V\text{-}SMOW}$ values, whereas the granite-hosted calcite is characterized by a very low $\delta^{13}C_{V\text{-}PDB}$ and high $\delta^{18}O_{V\text{-}SMOW}$ values (Figure GS2017-4-5).

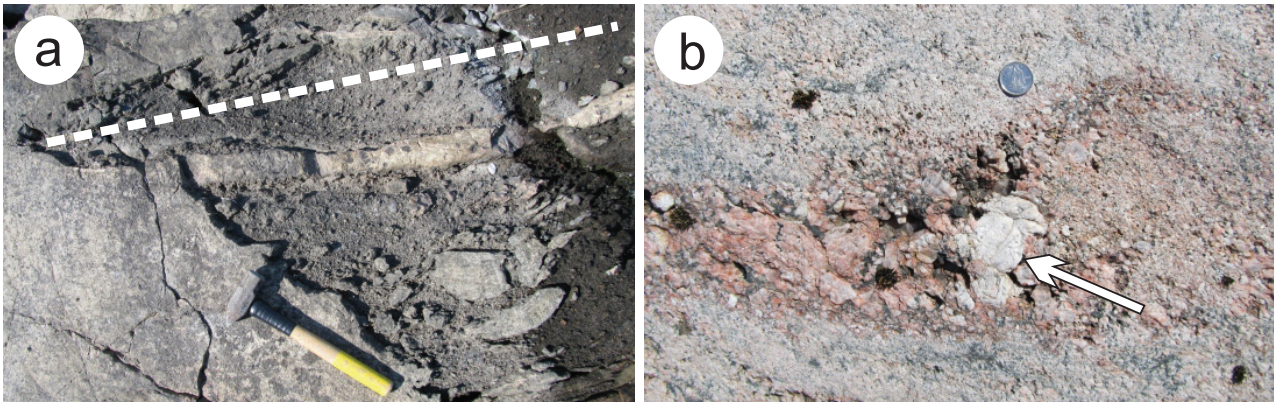

Figure GS2017-4-6*: Structural and textural relations of the carbonate rock at outcrop PCL-01:* ***a)*** *folded and brecciated carbonate rock; note alignment of clasts and vein with fold-axial plane (red dashed line; hammer for scale);* ***b)*** *calcite-bearing granite unit; note coarse calcite grain (~6 cm across; red arrow).*

The structural relations observed among the carbonate rocks of PCL-01 suggest intrusive emplacement of the matrix-supported breccias. Local contamination with silica-undersaturated material from the mafic schist and late-stage remobilization of CO_2 would potentially account for the olivine-magnetite–rich facies and calcite-bearing felsic veins, respectively. However, the observed structures and textures do not necessarily imply magma as a source of carbonate (Le Bas et al., 2002, 2004). In the present case, the presence of spinel and meionite implies a metasedimentary origin (Le Bas et al., 2002), which is consistent with the low Sr and REE levels, negative Eu anomaly, elevated Y/Ho ratios and $\delta^{13}C_{V\text{-}PDB}$ values, and high $\delta^{18}O_{V\text{-}SMOW}$ values in calcite from the clast-rich carbonate rock (Veizer et al., 1989; Le Bas et al., 2002, 2004; Chakhmouradian et al., 2016a). The low $\delta^{13}C_{V\text{-}PDB}$ and high $\delta^{18}O_{V\text{-}SMOW}$ values in the granite-hosted calcite and its intimate association with metasomatized plagioclase are consistent with partial CO_2 remobilization from the carbonate breccias during the emplacement of granitic magma.

Outcrop PCL-02

A large outcrop of layered carbonate-bearing rocks is present on the north side of a large island in the southwestern corner of Partridge Crop Lake (Figure GS2017-4-1b). The outcrop contains several carbonate lenses within a sequence of Archean mafic to ultramafic schists, metapelites, amphibolite and calcsilicate units. The most prominent carbonate unit occurs conformably as vertically stacked boudins with a metapelitic interstitial material, and is bordered by a metapelitic unit to the west and an ultramafic schist to the east. Thin (<4 cm in width) carbonate boudins are present also within the amphibolite and mafic schist. Small-scale isoclinal folds with axial planes parallel to the bedding, as well as repetitive stratigraphy, indicate folding of the sequence. This metamorphic assemblage is crosscut by pegmatite dikes. The carbonate unit comprises predominantly calcite, with dolomite present as exsolution lamellae and rims around mafic-silicate grains. The major silicate phases are serpentinized forsterite, phlogopite, diopside and tremolite. Phlogopite grains are locally enriched in Ba and partially chloritized.

Calcite at PCL-02 contains variable levels of Mg, Fe and Mn. The Sr, Ba and REE abundances in this mineral are much lower than those expected in igneous calcite (Figure GS2017-4-3a), whereas the chondrite-normalized REE profile (Figure GS2017-4-4) is flat and shows a strong negative Eu anomaly. The Y/Ho ratios are consistently above the primitive-mantle value (Figure GS2017-4-3b), but the measured C-O isotope compositions are inconclusive (Figure GS2017-4-5). Dolomite-calcite relationships suggest that the former mineral was overgrown by the latter, or reacted with silicate minerals to yield calcite and Mg-silicates. The low Sr, Ba and REE abundances and indicator REE ratios of the calcite are inconsistent with a magmatic source and imply a metasedimentary origin (Le Bas et al., 2002, 2004; Chakhmouradian et al., 2016a). The low $\delta^{13}C_{V\text{-}PDB}$ value could be produced by partial decarbonation during metamorphism and thus agrees with this interpretation. The calcite-dolomite pairs at PCL-02 give a range of equilibrium temperatures clustering between 674°C and 734°C for the calcite with intermediate Mg contents, and between 822°C and 847°C for the high-Mg grains. However, the analyzed high-Mg areas likely incorporate submicroscopic dolomite lamellae, yielding erroneously high T estimates. Hence, the separation of calcite and dolomite is interpreted to have occurred at ~700°C.

Outcrop PCL-03

This occurrence, located on an island in the southern section of Partridge Crop Lake (Figure GS2017-4-1b), comprises primarily amphibolite crosscut by anastomosing carbonate veins with occasional pockets up to 20 cm across. The fine- to coarse-grained carbonate material filling the veins is locally associated with hornblende. In addition to major calcite, dolomite and amphibole, some of the veins contain accessory diopside, muscovite, clinozoisite, garnet, pyrite and chalcopyrite.

Calcite contains numerous dolomite inclusions. Clinozoisite and muscovite form complete pseudomorphs after an unknown mineral (plagioclase?). Calcite occurs as two distinct varieties that differ in their Fe content yet are similar in their Mg and Mn contents. Dolomite grains overgrown by calcite are

irregularly zoned, with significant variations in Mg, Mn and Fe contents. Barium, Sr and REE levels are low in the calcite, and its chondrite-normalized REE profile displays unusual enrichment in the middle of the lanthanide series, accompanied by a weak positive Eu anomaly (Figure GS2017-4-4). Where both elements could be reliably detected, Y/Ho ratios are close to the primitive-mantle value. The stable-isotope values plot outside the hypothesized field of igneous carbonate (Figure GS2017-4-5). The mineralogical simplicity of carbonate veins at PCL-03, their intimate association with metamorphosed mafic rocks and the composition of their constituent calcite all indicate a noncarbonatitic origin and possible genetic links to metamorphism and removal of Ca and other elements (positive Eu anomaly) from precursor igneous plagioclase by CO_2-rich fluids (Eickmann et al., 2009; Chakhmouradian et al., 2016a).

Outcrop PCL-04

A similar occurrence of carbonate rocks was reported on an island in the northwestern corner of the southern basin of Partridge Crop Lake by Couëslan (2013; Figure GS2017-4-1b). Here, carbonate veins also clearly postdate their Archean mafic hostrock but were subjected to Paleoproterozoic greenschist-facies retrograde metamorphism. The C isotope composition of calcite is consistent with a mantle source, but its enrichment in heavy O is not, possibly indicating remobilization of carbonate material from the amphibolite by low-T fluids (Demény et al., 2004). The mineralogy of the veins, as well as the absence of any evidence of contact metasomatism in their surrounding amphibolite, suggest a low-T hydrothermal origin.

Bryce Bay

On an island in Bryce Bay, amphibolite is crosscut by a carbonate vein (Figure GS2017-4-1b). The vein is ~50 cm wide and contains calcite and orange calcic garnet. The calcite lacks detectable Mg or Fe, and concentrations of Mn, Sr and REE are among the lowest in the sample suite examined during this study (Figure GS2017-4-3a), so none of the indicator REE ratios could be calculated. Although the measured $\delta^{13}C_{V\text{-}PDB}$ and $\delta^{18}O_{V\text{-}SMOW}$ values (Figure GS2017-4-5) plot just outside the range for igneous carbonate, the low trace-element levels of the Bryce Bay calcite and its association with calcic garnet suggest a contact-metamorphic origin. Skarns with similarly low $\delta^{13}C_{V\text{-}PDB}$ and $\delta^{18}O_{V\text{-}SMOW}$ values have been reported in the literature (e.g., Sahlström, 2014).

Outcrop NL-01

This occurrence, initially reported by Dawson (1952), is situated approximately 1 km east of the channel connecting Natawahunan and Partridge Crop Lakes (Figure GS2017-4-1b). The carbonate rock occurs semiconformably within tonalitic basement gneiss and is separated by a calcsilicate unit from pegmatitic granite that crosscuts the gneiss. The carbonate unit hosts granite clasts, which are concentrically mantled by calcsilicate material and a phlogopite-rich rim, as well as folded boudins composed predominantly of diopside with a phlogopite rim (Figure GS2017-4-7a).

The carbonate unit is mineralogically heterogeneous and can be subdivided into two lithological types: forsterite-calcitic and dolomite-calcitic. The former rock type is composed

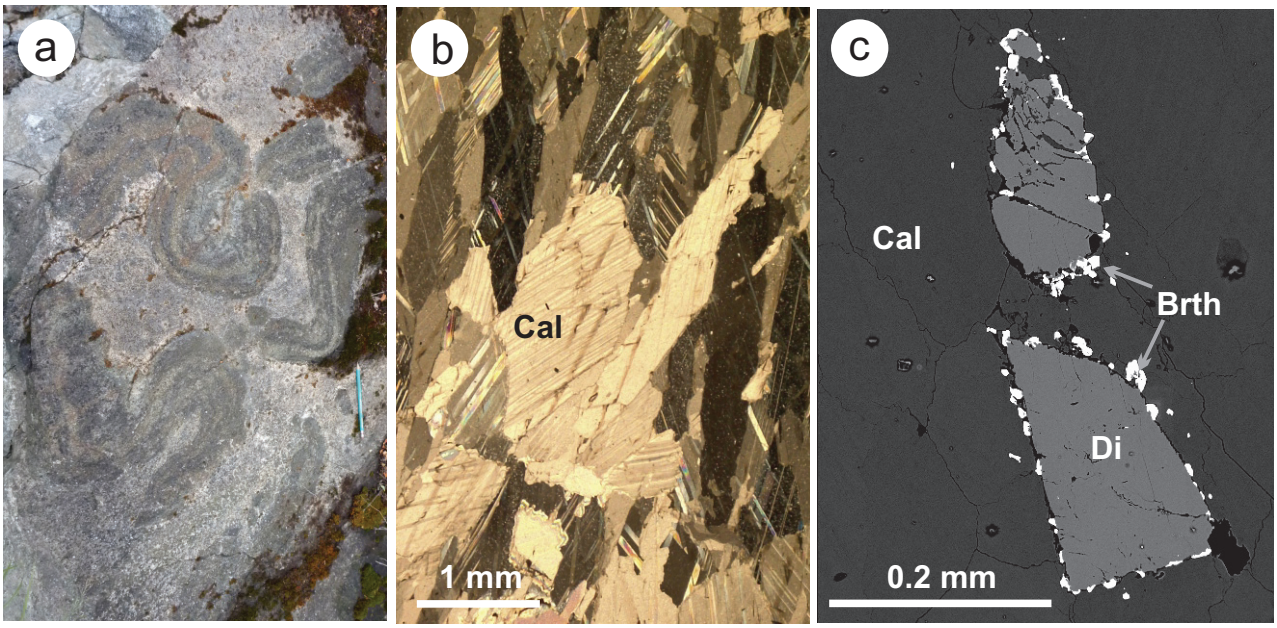

Figure GS2017-4-7*: Textural characteristics of the carbonate rocks from Natawahunan Lake:* ***a)*** *folded diopside-phlogopite boudins hosted in carbonate unit (outcrop NL-01; pencil approximately 20 cm);* ***b)*** *unidirectionally oriented, elongate and polysynthetically twinned calcite grains (outcrop NL-02);* ***c)*** *backscattered-electron scanning electron microscope (BSE) image of diopside with discontinuous britholite rim (NL float). Abbreviations: Cal, calcite; Di, diopside, Brth, britholite.*

predominantly of calcite, serpentinized forsterite and chlorite, whereas accessory phases are magnetite, dolomite, tremolite and barite. Calcite forms the inequigranular groundmass and contains zoned dolomite inclusions interpreted as exsolution lamellae. The second rock type is very heterogeneous in modal composition and consists primarily of calcite, dolomite, diopside, forsterite, phlogopite, tremolite, serpentine and magnetite with accessory chlorite (after phlogopite), plagioclase, pyrrhotite, apatite and barite. In this rock, calcite is similar to that in the forsterite-calcitic type, whereas dolomite also occurs as subhedral rims on silicate phases, where it is associated with magnetite and succeeded by interstitial calcite. In common with the carbonate rocks from outcrop PCL-01, phlogopite at NL-01 is zoned and locally enriched in Ba.

Both examined rock types contain calcite with elevated Mg and Mn levels relative to the majority of other samples in this study. Strontium, Ba and REE abundances, and $(La/Yb)_{CN}$ ratios, are lower than expected for igneous calcite (Figure GS2017-4-3a), and chondrite-normalized REE distributions display an unusual U-shaped profile (Figure GS2017-4-4). There appears to be a small negative Eu anomaly (although Eu/Eu* can be calculated only for a few analyses), whereas the calculated Y/Ho values are mostly above the primitive-mantle value. The calculated temperatures of calcite-dolomite exsolution range from 654 to 742°C. Mixed carbonate samples yield relatively high $\delta^{13}C_{V\text{-}PDB}$ and $\delta^{18}O_{V\text{-}SMOW}$ values that are well outside the igneous carbonate range (Figure GS2017-4-5). Based on these compositional and petrographic characteristics, these rocks are interpreted as a lower-granulite–facies (M_2) silicate-carbonate assemblage (e.g., Bucher and Grapes, 2011) that has been subjected to multistage retrograde metamorphism, as reflected in complex replacement and overgrowth textures.

Outcrop NL-02

Carbonate rocks also occur ~200 m west of the NL-01 outcrop (Figure GS2017-4-1b) as a bifurcating network of veins ~7 m wide that incorporates relict fragments of calcsilicate and pegmatitic material. A phlogopite-rich selvage is present between the carbonate unit and mafic-volcanic country rocks. The carbonate assemblages at this occurrence are highly variable in texture and mineralogy, and contain clasts of several different types. The major constituent minerals are calcite, forsterite, diopside, meionite, phlogopite and serpentine, with accessory magnetite, chlorite, clinozoisite, epidote, grossular, plagioclase, pyrite, spinel, barite and anhydrite. Calcite is the only carbonate mineral observed in the unit and ranges from coarse, elongate grains (Figure GS2017-4-7b) with inclusions of barite and anhydrite to fine, equant grains that infill embayments in silicate phases. Fine- to coarse-grained diopside is ubiquitous across the carbonate unit and is commonly mantled by zoned garnet. Another common reaction product is clinozoisite, which locally grades into epidote intergrown with grossular.

Calcite from outcrop NL-02 contains no detectable Mg, and Mn and Fe values are lower than those in NL-01. Its Sr content is very low, but Ba and REE abundances are higher than in the majority of other samples examined in this study, with the exception of the Split Lake material (Figure GS2017-4-3a). Note that at least some of the measured Ba is probably due to subsurface barite inclusions sampled during laser ablation. The chondrite-normalized REE profile exhibits some enrichment in LREE and a distinct negative Eu anomaly, and level off beyond Gd (Figure GS2017-4-4). In common with the NL-01 samples, this calcite is characterized by elevated Y/Ho ratios (Figure GS2017-4-3b) and relatively heavy C-O isotope compositions (Figure GS2017-4-5). Many geochemical and mineralogical similarities between the carbonate assemblages at the two outcrops suggest that they share a petrogenetic history, but the abundance of Al-rich phases (meionite, grossular, clinozoisite and epidote) and the REE characteristics of calcite at NL-02 imply the presence of a significant pelitic component in its protolith (Bucher and Grapes, 2011; Grizelj et al., 2017).

NL float

In addition to the two outcrops, several angular carbonate cobbles were found on a beach on Natawahunan Lake (Figure GS2017-4-1a) by C. Couëslan. Although their source could not be located, the occurrence of these cobbles in proximity to one another and their angular shape suggest that they were locally derived. Equigranular, evenly distributed calcite constitutes the bulk of this rock; other major minerals are diopside, garnet and meionite. Accessory phases include quartz, chlorite, serpentine, wollastonite, britholite, apatite and microcline. Quartz and wollastonite occur in clasts, whereas garnet is zoned from grossular to andradite and occurs as rims on silicate minerals, pseudomorphs after diopside and euhedral grains with poikilitic rims hosting calcite inclusions. Britholite occurs as minute crystals (<30 μm) intergrown with andradite to form discontinuous rims on diopside and meionite, and as 'necklaces' of such crystals around diopside grains (Figure GS2017-4-7c). A single resorbed grain of apatite mantled by britholite was observed in the calcite matrix.

The calcite in the carbonate cobbles contains low Mg and Mn but elevated Sr and REE relative to the majority of the samples studied (Figure GS2017-4-3a). The chondrite-normalized REE profile shows enrichment in LREE (Figure GS2017-4-4). Of the indicator REE ratios, only Y/Ho could be calculated for some of the laser-ablation measurements and is consistently lower than the primitive-mantle value. The relative enrichment of calcite in LREE and light C and O isotopes (Figure GS2017-4-5) is similar to that found in carbonatitic samples. The Sr content and Y/Ho value are too low for igneous calcite but comparable to those reported for hydrothermal calcite associated with some carbonatites (Chakhmouradian et al., 2016a). The observed mineralogical characteristics are also difficult to reconcile with an igneous source. Although britholite is present and has been described in retrogressively metamorphosed carbonatites (Zaitsev and Chakhmouradian, 2002; Ahijado et al., 2005), this mineral has also been reported as a replacement product after primary REE-bearing phases in some skarns (e.g.,

Smith et al., 2002). The abundance of calcic garnets, meionite and wollastonite in the NL float is characteristic of skarns.

Pie Lake

This occurrence (Figure GS2017-4-1b) is represented by an outcrop of sheared quartz metawacke with minor metapelite, which are locally retrogressed to greenschist facies. Calcite occurs pervasively within an ~1 m wide mylonitic zone developed in the metawacke concordant with the regional metamorphic banding. The examined metawacke sample is texturally heterogeneous owing to mylonitization and associated redistribution of quartz and other minerals into modally distinct domains. The sample is composed of fine-grained, mosaic-textured quartz associated with fine-grained, sub- to anhedral garnet and interstitial calcite. The garnet is zoned from grossular in the core to andradite in the discontinuous rim, whereas calcite occurs interstitially to clinozoisite and increases in abundance and grain size in the quartz-rich domains. Diopside, amphibole and titanite are observed as fractured grains associated with the mosaic quartz.

The calcite contains no detectable Mg or Fe. The measured Sr and REE abundances are among the lowest observed in this study (Figure GS2017-4-3a), so the chondrite-normalized profile is incomplete (Figure GS2017-4-4). Only one analysis gave a meaningful Y/Ho ratio, which is below the primitive-mantle value. The calcite plots within the range of $\delta^{13}C_{V\text{-}PDB}$ and $\delta^{18}O_{V\text{-}SMOW}$ values typical of igneous carbonate (Figure GS2017-4-5). The mylonitic texture of the carbonate unit is not diagnostic of any specific process because strain is typically partitioned into carbonate rocks, which are generally more ductile than their host silicate units (Chakhmouradian et al., 2016b). Although the C-O isotope composition of the Pie Lake calcite is 'carbonatite-like', the extremely low levels of Sr, Ba and REE in this mineral and the absence of any accessory phases characteristic of carbonatites argue against an igneous origin for the host mylonitic rock or its protolith.

Discussion

Of the 10 occurrences examined during this study, only one (sample 36-77-435-1, collected by T. Corkery at Split Lake in 1977) can be classified as carbonatite with a reasonable degree of confidence. The calcite from this occurrence meets all of the trace-element and stable-isotope criteria for igneous carbonate but shows clear evidence of subsolidus re-equilibration with metamorphic (?) fluids (i.e., secondary zoning involving the loss of REE). Notably, however, the trace-element patterns observed in sample 36-77-435-1 differ significantly from those documented in the material collected in 2016. Although hydrothermal processes can potentially account for the observed geochemical variations, a further detailed isotopic investigation of the available material and mapping at Split Lake are needed to establish the provenance of carbonate in this part of the SLB and explore possible geodynamic implications of these findings.

The remaining nine occurrences range from indisputable, high-grade carbonate-silicate assemblages, whose mineralogical complexity reflects the prolonged metamorphic history of the PGD (e.g., outcrop NL-01), to less unequivocal cases where petrogenetic interpretation is impossible in the absence of further data (e.g., NL float). One important outcome of this study is that it demonstrates extensive compositional variations in carbonates of nonigneous origin. From the data presented in this report (Figures GS2017-4-3 to -5), it is clear that no single geochemical criterion can be reliably used to identify the source of carbonate in deformed Precambrian rocks. Specific trace-element and stable-isotope ratios may have limited utility when it comes to metamorphic assemblages that underwent decarbonation and fluid-assisted element remobilization. It is also noteworthy that the inferred metasedimentary carbonate rocks at outcrops PCL-01, PCL-02 and NL-01 contain Ba-rich phlogopite (some with as much as 6.2 wt. % BaO), which implies that Ba was either liberated from an authigenic host (e.g., barite) during metamorphism or introduced with a metamorphic fluid from an external source (Bol et al., 1989). Barium-rich phlogopite is common in alkaline igneous rocks and carbonatites (e.g., Edgar, 1992; Reguir et al., 2009) but relatively rare in metasedimentary rocks. Although it is possible that unusual conditions may be required to stabilize this mineral in high-grade marbles (Bol et al., 1989), an equally likely explanation is the low solubility of barite in fluids and the paucity of potential external sources that could supply fluid-borne Ba (such as carbonatitic magma). The petrogenetic implications of Ba in micas from the PGD rocks remain to be ascertained.

The association of calcite and dolomite in some of the examined rocks allows for the temperature of calcite-dolomite equilibration to be determined (Anovitz and Essene, 1987). The temperatures calculated for the southern basin of Partridge Crop Lake (PCL-02) and Natawahunan Lake (NL-01) are similar, i.e., ~670–730 and 650–740°C, respectively. These estimates are ~100°C lower than the peak metamorphic conditions proposed in the literature (Heaman et al., 2011). Thus, calcite-dolomite exsolution probably occurred during retrograde metamorphism at the amphibolite-facies conditions, as described in Couëslan (2016). Geothermometric calculations can be performed for carbonate inclusions in metamorphic porphyroblasts (e.g., forsterite) and used to study prograde metamorphic processes in granulite-facies terranes (Mizuochi et al., 2010). Calcite or dolomite inclusions do occur in forsterite from the PCL-01, PCL-02, and NL-01 carbonate rocks and, in combination with exsolved calcite-dolomite intergrowths in the groundmass, provide ample opportunity for future work on the metamorphic history of the PGD.

Economic considerations

Rare-earth elements are becoming increasingly relevant as a commodity because their supply is currently limited geographically, whereas the number of technological applications dependent on REE materials, and the volume of industrial production arising from these technologies, have been increasing continuously during the past three decades (Chakhmouradian and Wall, 2012). Carbonatites are of great economic significance as the principal natural source of REE (Chakhmouradian

and Wall, 2012); these rocks host, or are genetically associated with, the world's largest rare-earth deposits (e.g., Maoniuping, Daluxiang, and Bayan Obo deposits, China; Xu et al., 2010; Chakhmouradian and Wall, 2012; Kynicky et al., 2012). In Canada, a number of initiatives have been launched with support from the Federal Government to secure a domestic supply of these increasingly important commodities (Simandl et al., 2012). The results of the present work and recent discoveries of carbonatites and related mantle-derived rocks in the northwestern Superior craton of Manitoba (Anderson et al., 2012; Anderson, 2016) indicate the potential for as-yet untapped rare-earth deposits in this part of the province.

Acknowledgments

The authors thank P. Yang, N. Ball and M. Yun (University of Manitoba) for support with acquisition of analytical data; E. Anderson and N. Brandson for logistical field support; Wings over Kississing for air support; and the Manitoba Hydro Split Lake boat crew for navigational support. A special thanks is extended to T. Martins for organizing the excursion to Split Lake.

References

Ahijado, A., Casillas, R., Nagy, G. And Fernández, C. 2005: Sr-rich minerals in a carbonatite skarn, Fuerteventura, Canary Islands (Spain); Mineralogy and Petrology, v. 84, p. 107–127.

Anders, E. and Grevesse, N. 1989: Abundances of the elements: meteoric and solar; Geochimica et Cosmochimica Acta, v. 53, p. 197–214.

Anderson, S.D. 2016: Alkaline rocks at Oxford Lake and Knee Lake, northwestern Superior province, Manitoba (NTS 53L13, 14, 15): preliminary results of new bedrock mapping and lithogeochemistry; *in* Report of Activities 2016, Manitoba Growth, Enterprise and Trade, Manitoba Geological Survey, p. 16–27.

Anderson, S.D., Kremer, P.D. and Martins, T. 2012: Preliminary results of bedrock mapping at Oxford Lake, northwestern Superior Province, Manitoba (parts of NTS 53L12, 13, 63I9, 16); *in* Report of Activities 2012, Manitoba Innovation, Energy and Mines, Manitoba Geological Survey, p. 6–22.

Anovitz, L.M and Essene, E.J. 1987: Phase equilibria in the system $CaCO_3$-$MgCO_3$-$FeCO_3$; Journal of Petrology, v. 28, p. 389–414.

Böhm, C.O. 1998: Geology of the Natawahunan Lake area; *in* Report of Activities 1998, Manitoba Energy and Mines, Geological Services, p. 56–59.

Böhm, C.O., Heaman, L.M. and Corkery, M.T. 1999: Archean crustal evolution of the northwestern Superior Province margin: U-Pb zircon results from the Split Lake Block; Canadian Journal of Earth Sciences, v. 36, p. 1973–1987.

Bol, L.C.G.M., Bos, A., Sauter, P.C.C. and Jansen, J.B.H., 1989: Barium-titanium-rich phlogopites in marbles from Rogaland, southwest Norway; American Mineralogist, v. 74, p. 439–447.

Bucher, K. and Grapes, R. 2011: Petrogenesis of Metamorphic Rocks; Springer-Verlag, Berlin, 441 p.

Chakhmouradian, A.R. 2006: High-field-strength elements in carbonatitic rocks: geochemistry, crystal chemistry and significance for constraining sources of carbonatites; Chemical Geology, v. 235, p. 18–160.

Chakhmouradian, A.R. and Wall, F. 2012: Rare earth elements: minerals, mines, magnets (and more); Elements, v. 8, p. 333–340.

Chakhmouradian, A.R., Böhm C.O., Demény, A., Reguir, E.P., Hegner, E, Creaser, R.A., Halden, N.M. and Yang, P. 2009a: "Kimberlite" from Wekusko Lake, Manitoba: actually a diamond-indicator-bearing dolomite carbonatite; Lithos, v. 112, p. 347–357.

Chakhmouradian, A.R., Couëslan, C.G. and Reguir, E.P. 2009b: Evidence for carbonatite magmatism at Paint Lake, Manitoba (parts of NTS 6308, 63P5, 12); *in* Report of Activities 2009, Manitoba Innovation, Energy and Mines, Manitoba Geological Survey, p. 118–126.

Chakhmouradian, A.R., Reguir, E.P., Kressall, R.D., Crozier, J., Pisiak, L.K., Sidhu, R. and Yang P. 2015: Carbonatite-hosted niobium deposit at Aley, northern British Columbia (Canada): mineralogy, geochemistry and petrogenesis; Ore Geology Reviews, v. 64, p. 642–666.

Chakhmouradian, A.R., Reguir, E.P., Couëslan, C. and Yang, P. 2016a: Calcite and dolomite in intrusive carbonatites. II. trace-element variations; Mineralogy and Petrology, v. 110, p. 361–377.

Chakhmouradian, A.R., Reguir, E.P. and Zaitsev, A. 2016b: Calcite and dolomite in intrusive carbonatites. I. textural variations; Mineralogy and Petrology, v. 110, p. 333–360.

Couëslan, C.G. 2008: Preliminary results from geological mapping of the west-central Paint Lake area, Manitoba (parts of NTS 63O8, 9, 63P5, 12); *in* Report of Activities 2008, Manitoba Science, Technology, Energy and Mines, Manitoba Geological Survey, p. 99–108.

Couëslan, C.G. 2013: Preliminary results from bedrock mapping in the Partridge Crop Lake area, eastern margin of the Thompson nickel belt, central Manitoba (parts of NTS 63P11, 12); *in* Report of Activities 2013, Manitoba Mineral Resources, Manitoba Geological Survey, p. 34–45.

Couëslan, C.G. 2014: Preliminary results from bedrock mapping in the Partridge Crop Lake area, eastern margin of the Thompson nickel belt, central Manitoba (parts of NTS 63P11, 12); *in* Report of Activities 2014, Manitoba Mineral Resources, Manitoba Geological Survey, p. 18–31.

Couëslan, C.G. 2016: Preliminary results of bedrock mapping in the Natawahunan Lake area, western margin of the Pikwitonei granulite domain, central Manitoba (parts of NTS 63P11, 14); *in* Report of Activities 2016, Manitoba Growth, Enterprise and Trade, Manitoba Geological Survey, p. 28–39.

Dawson, A.S. 1952: Geology of the Partridge Crop Lake area, Cross Lake Mining Division, Manitoba; Manitoba Department of Mines and Natural Resources, Mines Branch, Publication 41-1, 26 p.

Demény, A. Sitnikova, M.A. and Karchevsky, P.I. (2004): Stable C and O isotope compositions of carbonatite complexes of Kola Alkaline Province: phoscorite-carbonatite relationships and source compositions; *in* Phoscorites and Carbonatites from Mantle to Mine: the Key Example of the Kola Alkaline Province, F. Wall and A.N. Zaitsev (ed.), Mineralogical Society of Great Britain and Ireland, London, Mineralogical Society Series, no. 10, p. 407–431.

Edgar, A.P. 1992: Barium-rich phlogopite and biotite from some Quaternary alkali mafic lavas, West Eifel, Germany; European Journal of Mineralogy, v. 4, p. 321–330.

Eickmann, B., Bach, W., Rosner, M. and Peckmann, J. 2009: Geochemical constraints on the modes of carbonate precipitation in peridotites from the Logatchev Hydrothermal Vent Field and Gakkel Ridge; Chemical Geology, v. 268, p. 97–106.

Grizelj, A., Peh, Z., Tibljaš, D., Kovačić, M. and Kurečić, T. 2017: Mineralogical and geochemical characteristics of Miocene pelitic sedimentary rocks from the southwestern part of the Pannonian Basin System (Croatia): implications for provenance studies; Geoscience Frontiers, v. 8, p. 65–80.

Halls, H.C. and Heaman, L.M. 2000: The paleomagnetic significance of new U-Pb age data from the Molson dyke swarm, Cauchon Lake area, Manitoba; Canadian Journal of Earth Sciences, v. 37, p. 957–966.

Hartlaub, R.P., Böhm, C.O., Heaman, L.M. and Simonetti, A. 2005: Northwestern Superior craton margin, Manitoba: an overview of Archean and Proterozoic episodes of crustal growth, erosion and orogenesis (parts of NTS 54D and 64A); *in* Report of Activities 2005, Manitoba Industry, Economic Development and Mines, Manitoba Geological Survey, p. 54–60.

Hartlaub, R.P., Heaman, L.M., Böhm, C.O. and Corkery, M.T. 2003: Split Lake Block revisited: new geological constraints from the Birthday to Gull Rapids corridor of the lower Nelson River (NTS 54D5 and 6); *in* Report of Activities 2003, Manitoba Industry, Trade and Mines, Manitoba Geological Survey, p. 114–117.

Heaman, L.M. and Corkery, T. 1996: U-Pb geochronology of the Split Lake Block, Manitoba: preliminary results; LITHOPROBE Trans-Hudson Orogen Transect, Report of Sixth Transect Meeting, Saskatoon, Saskatchewan, April 1–2, 1996, LITHOPROBE Secretariat, University of British Columbia, Vancouver, British Columbia, Report 55, p. 60–68.

Heaman, L.M., Böhm, Ch.O., Machado, N., Krogh, T.E., Weber, W. and Corkery, M.T. 2011: The Pikwitonei Granulite Domain, Manitoba: a giant Neoarchean high-grade terrane in the northwest Superior Province; Canadian Journal of Earth Sciences, v. 48, p. 205–245.

Kuiper, Y.D., Lin, S. and Böhm C.O., 2011: Himalayan-type escape tectonics along the Superior Boundary Zone in Manitoba, Canada; Precambrian Research, v. 187, p. 248–262.

Kynicky J., Smith M.P. and Xu C. 2012: Diversity of rare earth deposits: the key example of China; Elements v. 8, p. 361–367.

Le Bas, M.J. 2008: Fenites associated with carbonatites; Canadian Mineralogist, v. 46, p. 915–932.

Le Bas, M.J., Ba-bttat, M.A.O., Taylor, R.N., Milton, J.A., Windley, B.F. and Evins, P.M. 2004: The carbonatite-marble dykes of Abyan Province, Yemen Republic: the mixing of mantle and crustal carbonate materials revealed by isotope and trace element analysis; Mineralogy and Petrology, v. 82, p. 105–135.

Le Bas, M.J., Subbaro, K.V. and Walsh, J.N. 2002: Metacarbonatite or marble? – the case of the carbonate, pyroxenite, calcite-apatite rock complex at Borra, Eastern Ghats, India; Journal of Asian Earth Sciences, v. 20, p. 127–140.

Lira. R. and Ripley, E.M. 1992: Hydrothermal alteration and REE-Th mineralization at the Rodeo de Los Molles deposit, Las Chacras batholith, central Argentina; Contributions to Mineralogy and Petrology, v. 110, p. 370–386.

Macdonald, J.A., Chakhmouradian, A.R., Couëslan, C.G. and Reguir, E.P. 2017: Stable C and O isotope and major- and trace-element data, with calcite-dolomite equilibration geothermometry, for genetically diverse carbonate rocks in the Pikwitonei granulite domain and Split Lake block (parts of NTS 63P11, 12, 64A1); Manitoba Growth, Enterprise and Trade, Manitoba Geological Survey, Data Repository Item DRI2017005, Microsoft® Excel® file.

Machado, N., Gapais, D., Potrel, A., Gauthier, G. and Hallot, E. 2011a: Chronology of transpression, magmatism, and sedimentation in the Thompson Nickel Belt (Manitoba, Canada) and timing of Trans-Hudson Orogen–Superior Province collision; Canadian Journal of Earth Sciences, v. 48, p. 295–324.

Machado, N., Heaman, L.M., Krogh, T.E., Weber, W. and Corkery, M.T. 2011b: Timing of Paleoproterozoic granitoid magmatism along the northwestern Superior Province margin: implications for the tectonic evolution of the Thompson Nickel Belt; Canadian Journal of Earth Sciences, v. 48, p. 325–346.

Mezger, K, Bohlen, S.R. and Hanson, G.N. 1990: Metamorphic history of the Archean Pikwitonei Granulite Domain and the Cross Lake Subprovince, Superior Province, Manitoba, Canada; Journal of Petrology, v. 31, p. 483–517.

Mizuochi, H., Satish-Kumar, M., Motoyoshi, Y. and Michibayashi, K. 2010: Exsolution of dolomite and application of calcite-dolomite geothermometry in high-grade marbles: an example from Skallevikshalsen, East Antarctica; Journal of Metamorphic Petrology, v. 28, p. 509–526.

Paktunç, A.D. and Baer, A.J. 1986: Geothermobarometry of the northwestern margin of the Superior Province: implications for its tectonic evolution; Journal of Geology, v. 94, p. 381–394.

Reguir, E.P., Chakhmouradian, A.R., Halden, N.M., Malkovets, V.G. and Yang, P. 2009: Major- and trace-element compositional variation of phlogopite from kimberlites and carbonatites as a petrogenetic indicator; Lithos, v. 112S, p. 372–384.

Sahlström, F. 2014: Stable isotope systematics of skarn-hosted REE-silicate-magnetite mineralisations in central Bregslagen, Sweden; M.Sc. thesis, Uppsala University, Sweden, 82 p.

Simandl, G.J., Prussin, E.A. and Brown, N. 2012: Specialty metals In Canada; British Columbia Geological Survey, Open File 2012-7.

Smith, M.P., Henderson, P. and Jeffries, T. 2002: The formation and alteration of allanite in skarn from the Beinn an Dubhaich granite aureole, Skye; European Journal of Mineralogy, v. 14, p. 471–486.

Swain, S.K., Sarangi, S., Srinivasan, R., Sarkar, A, Bhattacharya, S., Patel, S.C., Pasayat, R.M. and Sawkar, R.H. 2015: Isotope (C and O) composition of auriferous quartz carbonate veins, central lode system, Gadag Gold Field, Dharwar Craton, India: implications to source of fluids; Ore Geology Reviews, v. 70, p. 305–320.

Taylor, H.P., Frechen, J. and Degens, E.T. 1967: Oxygen and carbon isotope studies of carbonatites from the Laacher See District, West Germany and the Alnö District, Sweden; Geochimica et Cosmochimica Acta, v. 31, p. 407–430.

Veizer, J., Hoefs, J., Lowe, D.R. and Thurston, P.C. 1989: Geochemistry of Precambrian carbonates: II. Archean greenstone belts and Archean sea water; Geochimica et Cosmochimica Acta, v. 53, p. 859–871.

Weber, W. 1978: Natawahunan Lake (NTS 63P10, 11, 15 and parts of 64P12, 14, and 64A2); *in* Report of Field Activities 1978, Manitoba Energy and Mines, Mineral Resources Division, p. 47–53.

Xu, C., Campbell, I.H., Allen, C.M., Huang, Z., Qi, L., Zhang, H. and Zhang, G. 2007: Flat rare-earth element patterns as an indicator of cumulate processes in the Lesser Qinling carbonatites, China; Lithos, v. 95, p. 267–278.

Xu, C., Wang, L., Song, W. and Wu, M. (2010) Carbonatites in China: a review for genesis and mineralization; Geoscience Frontiers, v. 1, p. 105–114.

Zaitsev, A.N. and Chakhmouradian, A.R. 2002: Calcite-amphibole-clinopyroxene rock from the Afrikanda complex, Kola Peninsula, Russia: mineralogy and a possible link to carbonatites. II. Oxysalt minerals; Canadian Mineralogist, v. 40, p. 103–120.

GS2017-5

Whole-rock and mineral geochemistry as exploration tools for rare-element pegmatite in Manitoba: examples from the Cat Lake–Winnipeg River and Wekusko Lake pegmatite fields (parts of NTS 52L6, 63J13)

by T. Martins, R.L. Linnen[1], M.A.F. Fedikow[2] and J. Singh[3]

[1] Department of Earth Sciences, Western University, London, ON N6A 5B7
[2] Mount Morgan Resources, 1207 Sunset Drive, Saltspring Island, BC V8K 1E3
[3] Orix Geoscience Inc., 211–428 Portage Ave, Winnipeg, MB R3C 0E2

In Brief:

- Elevated Li, Rb and Cs in mafic metavolcanic country rocks is a useful exploration guide for rare-element pegmatite
- Li-rich amphibole (holmquistite) in country rocks indicates proximity to Li-bearing pegmatite
- Mineral chemistry of feldspar and muscovite provide measures of pegmatite fractionation

Citation:
Martins, T., Linnen, R.L., Fedikow, M.A.F. and Singh, J. 2017: Whole-rock and mineral geochemistry as exploration tools for rare-element pegmatite in Manitoba: examples from the Cat Lake–Winnipeg River and Wekusko Lake pegmatite fields (parts of NTS 52L6, 63J13); *in* Report of Activities 2017, Manitoba Growth, Enterprise and Trade, Manitoba Geological Survey, p. 42–51.

Summary

This report summarizes fieldwork conducted in the Cat Lake–Winnipeg River pegmatite field in southeastern Manitoba and the Wekusko Lake field in west-central Manitoba. Both of these pegmatite fields are endowed with Li mineralization, but their geological settings and ages are different. Country rocks surrounding Li-bearing pegmatite in both fields were analyzed for major and trace elements, revealing anomalous values of highly mobile elements such as Li, Rb and Cs. This study indicates that whole-rock geochemistry can be a very useful tool in exploration programs for rare-element pegmatite. Holmsquistite-bearing assemblages, identified in the country rock to 'Dike 1' in the Wekusko Lake field, can also be used as an exploration tool for Li-bearing pegmatite. In addition, results from mineral-chemistry studies of muscovite and K-feldspar from Dike 1 indicate that it is possible to track pegmatite fractionation using these minerals.

Introduction

Alteration haloes resulting from metasomatism have been documented around many pegmatites, with Cabot Corporation's Tanco mine in the Bird River greenstone belt of southeastern Manitoba being the most studied example in the province (e.g., Trueman, 1978; Morgan and London, 1987; Halden et al., 1989). At Tanco, this type of country-rock metasomatism has been utilized for exploration (Trueman, 1978), and this methodology has since been applied throughout the Bird River greenstone belt (Galeschuk and Vanstone, 2005, 2007; Linnen et al., 2015). Lithium anomalies define the widest haloes adjacent to Li-Cs-Ta (LCT) pegmatites (Linnen et al., 2012) and, in the case of Tanco, Li haloes have been recognized to extend more than 100 m away from the pegmatite body (Černý, 1989). However, dispersion of other elements such as Rb and Cs seems to be more restricted (e.g., Černý, 1989; London, 2008).

This type of country-rock alteration is caused by the influx of pegmatite magma and coexisting fluids rich in incompatible elements. The composition of the fluid phase is related to the magma composition; therefore, the diagnostic elements of the alteration aureoles are related to element enrichments and mineralogy of the associated pegmatite intrusion (Beaus, 1960). In the case of evolved LCT pegmatites, the adjacent country rock is altered by an influx of alkali rare elements (e.g., Li, Rb and Cs) and subsequent interaction between the fluid phase and the country rock, forming a dispersion halo. This interaction results in a change of the composition of pre-existing mineral assemblages in the country rock and stabilization of exotic mineral assemblages. Metasomatism by Li-enriched fluids can produce holmsquistite-bearing assemblages in amphibolitic country rock, as has been documented at several locations, including the Edison pegmatite in the Black Hills of South Dakota (Shearer et al., 1986; Shearer and Papike, 1988) and the Tanco pegmatite in Manitoba (Morgan and London, 1987; Selway et al., 2000). These alteration assemblages can be a good exploration tool and have been used in many pegmatite districts (e.g., Beus, 1960; Truman and Černý, 1982; Norton, 1984; London, 1986).

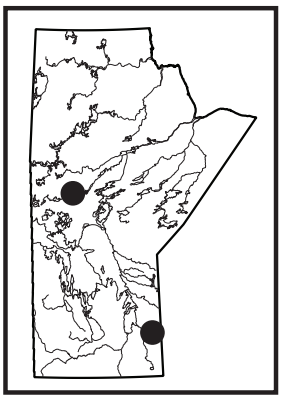

This study focuses on alteration haloes caused by 1) the Dibs LCT pegmatite from the Cat Lake–Winnipeg River pegmatite field in the Archean Bird River greenstone belt, and 2) the Dike 1 LCT pegmatite from the Wekusko Lake pegmatite field in the Paleoproterozoic Flin Flon–Snow Lake greenstone belt. Although the ages differ, both bodies intrude metamorphosed volcanic rocks and the premise for this study is that both would be associated with above-normal background values for elements that are enriched in the pegmatite. There are a number of factors that could influence the metasomatic halo around Li-bearing pegmatites, including 1) the relationship between

dike thickness and the size of the metasomatic halo; 2) the shape of the halo related to the location of the Li mineralization within the pegmatite; 3) fluid pressures at time of emplacement; 4) structural permeability; 5) country-rock composition; 6) emplacement history; and 7) overprinting by later structural, metamorphic or hydrothermal events. All these variables could influence the sampling methodology and the interpretation of the results; one of the goals of this study is to better understand the metasomatic haloes in the context of these various factors.

Regional geology

Cat Lake–Winnipeg River pegmatite field

The Dibs pegmatite is part of the Bernic Lake pegmatite group (Galeschuk and Vanstone, 2005), which includes the Tanco pegmatite, of the Cat Lake–Winnipeg River pegmatite field (Černý et al., 1981) in the Bird River greenstone belt of the Archean Superior province (Figure GS2017-5-1). Most of the supracrustal units of the Bird River greenstone belt range in age from 2.85 to 2.64 Ga (Gilbert et al., 2008) and represent a transitional oceanic–continental margin setting (Gilbert et al., 2008) between the North Caribou terrane to the north and the Winnipeg River terrane to the south (nomenclature of Stott et al., 2010).

The Bird River greenstone belt has been historically described as a large synclinal keel (Trueman, 1980; Černý et al., 1981); however, recent mapping by the Manitoba Geological Survey has led to a reinterpretation of the stratigraphic framework of the belt, summarized by Gilbert et al. (2008). The Bird River belt has been subdivided into two distinct panels (North and South), both of which are composed of ca. 2.75–2.72 Ga, juvenile, arc-type metavolcanic and associated metasedimentary rocks. These two panels are separated by turbidites of the Booster Lake Formation (<2712 ±17 Ma; Gilbert, 2006).

The hostrock for both the Dibs and the Tanco pegmatites is a gabbroic to dioritic body (known as the Tanco gabbro) that is approximately 1.5 km by 3 km in size. It is a relatively homogeneous, equigranular, medium- to coarse-grained intrusion that contains rare pegmatitic phases and intrudes volcanic rocks of the Bernic Lake formation, part of the South panel of the belt (Gilbert et al., 2008; Kremer, 2010). Its margins are characterized by a well-defined, east-trending, steeply dipping foliation and local, narrow, high-strain zones. A sample of pegmatitic gabbro yielded a U-Pb age of 2723.1 ±0.8 Ma, contemporaneous with the age of volcanic rocks in the Bernic Lake Formation (2724.6 ±1.1 Ma) and with the Birse Lake granodiorite (2723.2 ±0.7 Ma), suggesting that these represent components of a single subvolcanic to volcanic system (Gilbert et al., 2008; Kremer, 2010).

Dibs pegmatite

The Dibs pegmatite, which does not outcrop, was discovered during an exploration program carried out by Cabot Corporation (Tanco) during the 1990s and early 2000s (Assessment Files 73144, 74409, Manitoba Growth, Enterprise and Trade, Winnipeg). Galeschuk and Vanstone (2005) described the Dibs pegmatite as a horizontal body at least 500 m in length and up to 100 m in width, with a maximum thickness of approximately 65 m (Figure GS2017-5-2). Five different zones were identified in the Dibs pegmatite (Galeschuk and Vanstone, 2005):

1) the border zone, consisting predominantly of quartz, albite and local black tourmaline;

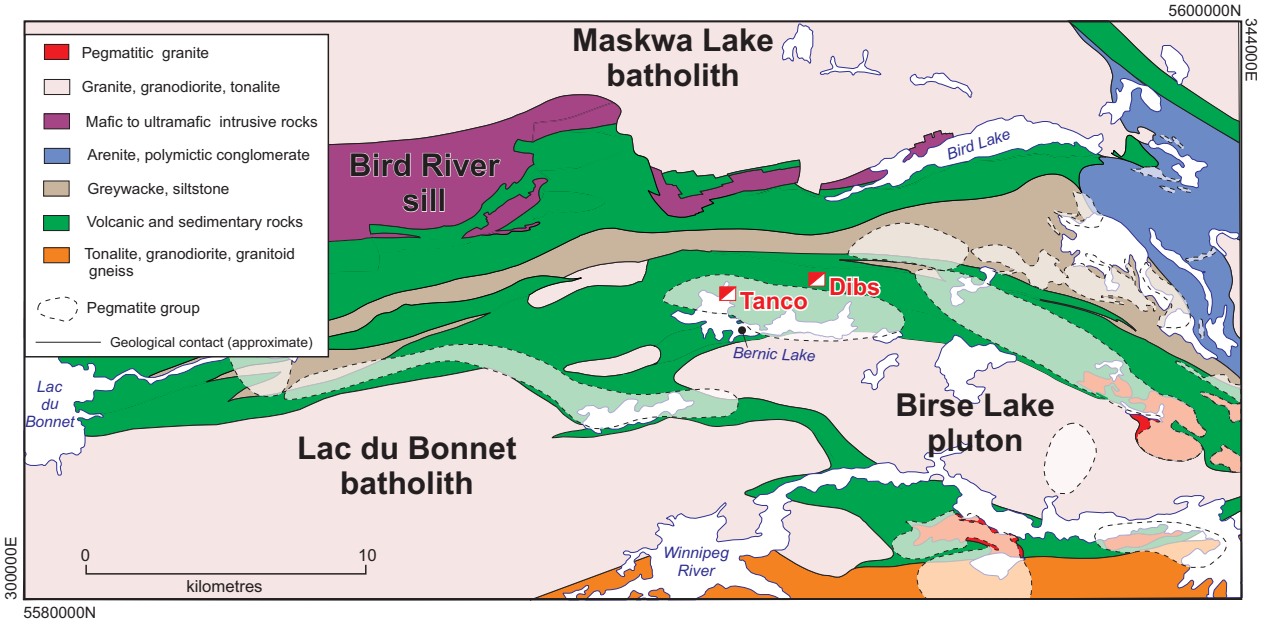

Figure GS2017-5-1: *Simplified regional geology of the Bird River greenstone belt (after Gilbert et al., 2008), showing the locations of the Tanco mine and the Dibs pegmatite.*

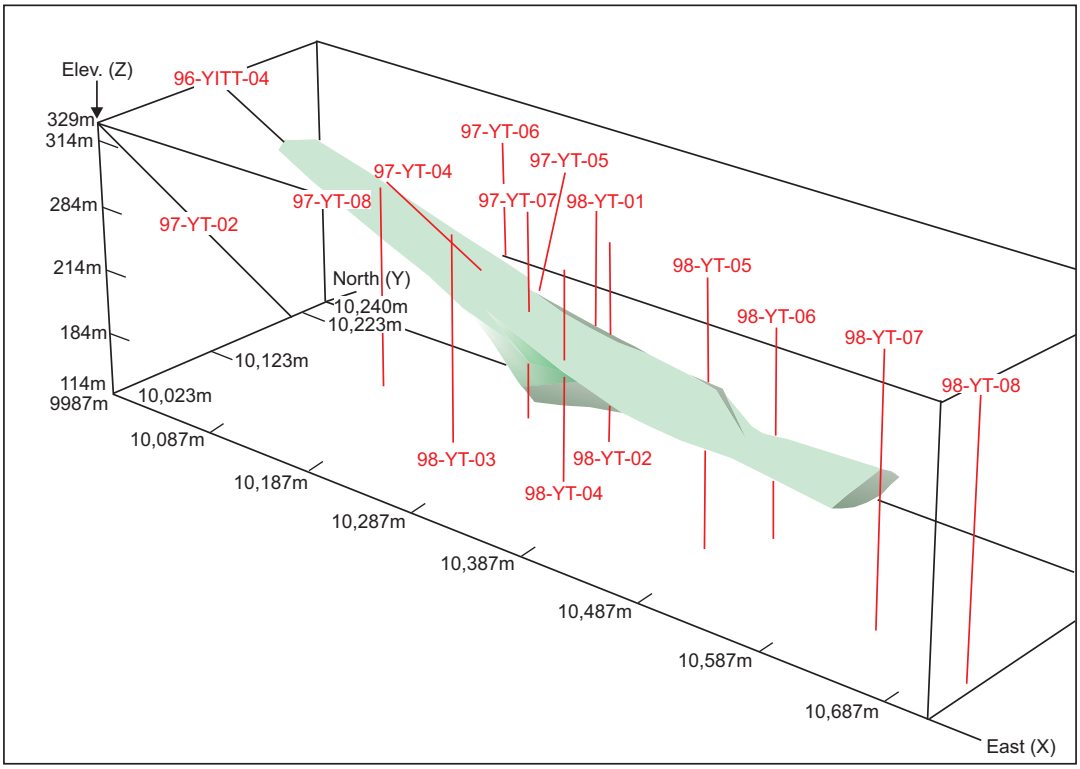

Figure GS2017-5-2: *Three-dimensional block model of the Dibs pegmatite, looking northwest (modified after Galeschuk and Vanstone, 2005).*

2) the wall zone, consisting of K-feldspar, quartz, albite (cleavelandite habit), mica, petalite, tourmaline and minor amblygonite, triphylite, spodumene, lepidolite and smoky quartz;
3) the central intermediate zone, consisting of K-feldspar, quartz-rich sections with masses of muscovite, minerals of the columbite group, and cassiterite;
4) the lower intermediate zone, consisting mainly of K-feldspar, albite (cleavelandite habit), quartz, muscovite, accessory beryl, 'ball peen' mica, petalite, cookeite, amblygonite and smoky cleavable quartz;
5) the quartz±K-feldspar zone or core, composed mainly of massive quartz, K-feldspar and minor petalite, amblygonite and muscovite.

Wekusko Lake pegmatite field

The Dike 1 pegmatite is part of a swarm of at least seven pegmatite dikes that make up the Green Bay group of the Wekusko Lake pegmatite field (Černý et al., 1981). This pegmatite field is located east of Wekusko Lake within the Flin Flon–Glennie complex of the Paleoproterozoic Trans-Hudson orogen (Figure GS2017-5-3; NATMAP Shield Margin Working Group, 1998; Bailes and Galley, 1999). Bedrock exposures east of Wekusko Lake are dominantly Paleoproterozoic metavolcanic and metasedimentary rocks of the Missi group intruded by granitoid rocks (NATMAP Shield Margin Working Group, 1998; Gilbert and Bailes, 2005a). Surface exposures and drillcore indicate that the hostrocks for the Dike 1 pegmatite are ocean-floor mafic volcanic rocks likely deposited between 1.92 and 1.87 Ga (NATMAP Shield Margin Working Group, 1998). Locally in drillcore, the country rock to the Dike 1 pegmatite can also be metasedimentary biotite-garnet-muscovite schist, possibly belonging to the Missi group (NATMAP Shield Margin Working Group, 1998).

Dike 1 pegmatite

The Dike 1 pegmatite is the largest and best known dike of the Green Bay group. It is a north-trending, near-vertical body that extends for at least 280 m along strike, with a maximum thickness of approximately 35 m (Figure GS2017-5-4). The apparent absence of country-rock alteration was commonly noted in historical drill logs (Assessment File 93562). Results from this study however, identified holmquistite in the mafic-volcanic country rock, indicating metasomatic alteration associated with pegmatite intrusion, and lithogeochemical analyses (see below) demonstrate that a broad metasomatic halo is present. The development of holmquistite-bearing assemblages is controlled by the activity of Li introduced into the country rock during pegmatite emplacement. These assemblages reflect greenschist-facies metamorphic conditions and are only found in amphibolitic wallrock, usually replacing hornblende, pyroxene or biotite (Heinrich, 1965; London, 1986). Based on historical (Assessment File 93562) and recent drill-log descriptions, the zonation in the Dike 1 pegmatite can be defined as follows:

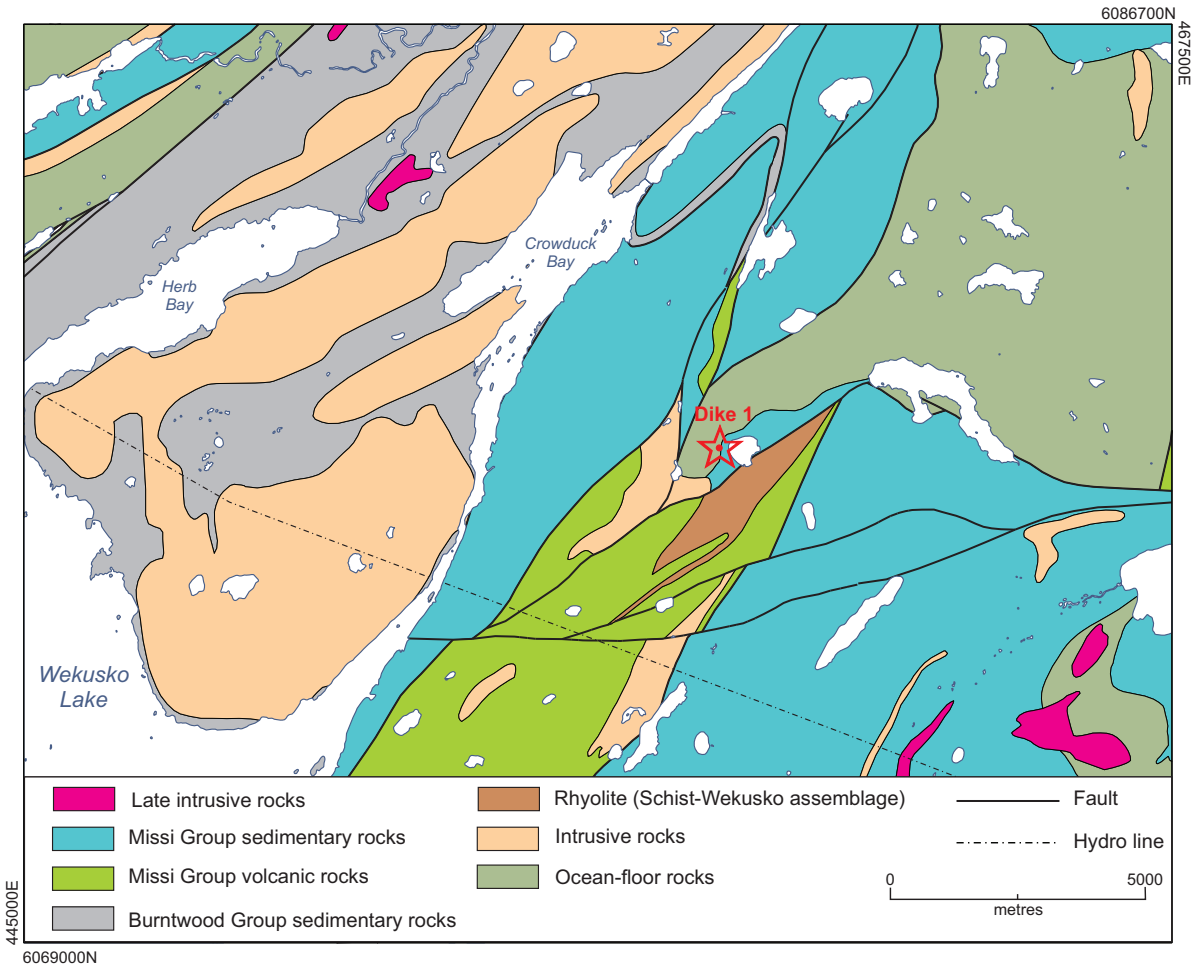

Figure GS2017-5-3: *Regional geology of the east side of Wekusko Lake, with the location of the Dike 1 pegmatite (modified and simplified from NATMAP Shield Margin Working Group, 1998).*

1) the wall zone, composed predominantly of quartz, microcline and muscovite, with accessory tourmaline, hornblende, biotite and rare beryl and spodumene;
2) the intermediate zone, with medium-sized crystals of microcline, albite, quartz, muscovite and spodumene (<5%);
3) the central zone, with abundant spodumene (locally up to 50% but more commonly varying between 10% and 30%), albite, quartz and locally pollucite, and accessory apatite, tourmaline, pyrrhotite, lepidolite, columbite-group minerals and Fe-Mn–phosphate minerals;
4) the core zone, composed mainly of quartz with small- to medium-grained spodumene crystals (although locally 15–20 cm crystals of spodumene are observed) in a quartz matrix, with minor tourmaline and muscovite.

From historical descriptions and recent preliminary petrographic work, it is possible to distinguish at least three different stages of spodumene growth: greenish spodumene with characteristics typical of a primary phase; spodumene-quartz intergrowths, possibly after petalite breakdown (Černý and Ferguson, 1972); and late bands of very fine grained spodumene that crosscut other mineral phases or surround feldspar and muscovite grains. Locally, spodumene crystals are surrounded by fine-grained mica, possibly Li-mica or lepidolite. This could be indicative of a late Li-enriched fluid episode (possibly autometasomatism) that could have produced late Li-enriched mica. Acicular opaque minerals of the columbite group are present, and late bands of fluorite occur locally in fractures (Assessment File 93562). The latest event, identified in thin section, produced late, Fe-rich, quartz-calcite stringers with no preferred orientation crosscutting the pegmatite, which could be similar to the quartz–Fe-carbonate–albite–sericite assemblage described by Galley et al. (1989) in association with Au occurrences east of Wekusko Lake. In thin section, feldspar and muscovite show evidence of deformation (for example, kink bands in muscovite), suggesting that pegmatite emplacement occurred prior to the latest stages of regional deformation.

Methodology

Samples of country rock to the Dibs pegmatite were collected from Tanco's drillcore library to complement and expand on the work carried out by Linnen et al. (2009). Fifty-six

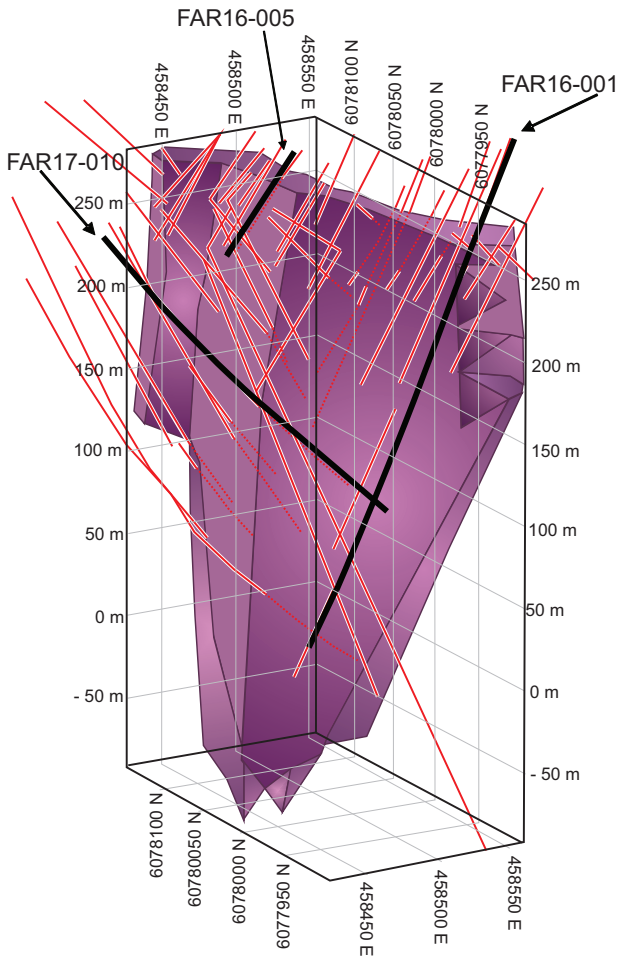

Figure GS2017-5-4: *Three-dimensional block model of the Dike 1 pegmatite, including locations of historical and recent drillholes. Drillholes selected for this study are indicated by arrows.*

samples were selected from drillholes 98-YT-01, 98-YT-03, 98-YT-04, 98-YT-05, 98-YT-08, 06-YT-01, 06-YT-03 and 06-YT-04. Samples were collected from both the hangingwall and footwall at 5–10 m intervals in proximity to the pegmatite contacts, and at 10–20 m intervals distal from the contacts; zones of visible alteration were not sampled. Samples, each consisting of about a 20–30 cm length of drillcore, were crushed at the Midland Sample and Core Library in Winnipeg and the rock powders were sent to Activation Laboratories Ltd. (Ancaster, Ontario) for lithogeochemical analysis. The samples were analyzed using a Li metaborate/tetraborate fusion technique, followed by nitric-acid digestion and analysis by inductively coupled plasma–emission spectrometry (ICP-ES) and inductively coupled plasma–mass spectrometry (ICP-MS). Added element Li was analyzed using total digestion–inductively coupled plasma (TD-ICP). Fluorine was converted to a fuseate and then analyzed by an automated fluoride analyzer.

Three drillholes from the Dike 1 pegmatite were selected for this study: FAR16-001, FAR16-005 and FAR17-010. Sixty-nine samples of mafic-volcanic country rock and one sample of biotite-garnet-muscovite schist were collected from the hangingwall and footwall of the pegmatite dike. Sample spacing was 5 m close to the contact with the pegmatite, and 10 m and 20 m apart farther away from the contact. The samples consisted of about 20 cm of split drillcore. Analyses were performed by Activation Laboratories (Ancaster, Ontario) using a sodium-pyrophosphate fusion technique, followed by ICP-MS. Selected samples of muscovite and K-feldspar from Dike 1 were analyzed using a JEOL JXA-8530F field-emission electron microprobe at Western University. Analytical details are provided in DRI2017004 (Martins and Linnen, 2017)[4].

Results

Whole-rock geochemistry

According to Černý (1989), background values for geochemical anomalies of a certain element can be defined for concentrations that are greater than two standard deviations. Values for Li in the country rock of Dike 1 are generally not available in the literature because this element is not routinely analyzed. Lithium is a moderately incompatible trace element in magmatic systems and its abundance in the mantle is estimated to be about 1.9 ppm (Ryan and Langmuir, 1987). The same authors reported that the world-wide range in Li content for mid-ocean ridge basalt (MORB) is 3–17 ppm (only evolved Fe-Ti basalts have >8 ppm Li), and andesites and dacites from the East Pacific Rise contain up to 30 ppm Li, indicating that Li increases with differentiation. Given that Dike 1 country rock has flat rare-earth element (REE) profiles characteristic of MORB (not plotted; data from Gilbert and Bailes, 2005b), the assumption for this study is that the background concentrations of Li should be low (<8 ppm) in nonmetasomatized country rock to Dike 1. Values for Rb and Cs are more readily available in the literature. Samples from an equivalent unit to the Dike 1 country rock at south Wekusko Lake contain <7 ppm Rb and <0.03 ppm Cs (Gilbert and Bailes, 2005b). Thus, based on available data, values >6 ppm Rb and >0.02 ppm Cs are considered anomalous (twice the values of the standard deviation of data from Gilbert and Bailes, 2005b). For Li background, values are considered to be anomalous at >16 ppm (double the maximum value for non-evolved MORB defined by Ryan and Langmuir, 1987).

At the time of writing, the full dataset of whole-rock geochemistry for the country rocks to the Dibs pegmatite was not available. Therefore, previous work conducted on this dike by Linnen et al. (2009, 2015) will be used for comparison with results obtained during this study for the country rocks to Dike 1. For the country rock to the Dike 1 pegmatite, some of the highest values attained are 1900 ppm Li, 196 ppm Rb and 225 ppm Cs adjacent to the upper contact of the pegmatite,

[4] MGS Data Repository Item DRI2017004, containing the data or other information sources used to compile this report, is available online to download free of charge at http://www2.gov.mb.ca/itm-cat/web/freedownloads.html, or on request from minesinfo@gov.mb.ca or Mineral Resources Library, Manitoba Growth, Enterprise and Trade, 360–1395 Ellice Avenue, Winnipeg, MB R3G 3P2, Canada.

indicating the rare-element character of this dike. The Rb and Cs values are well above what is reported for nonmetasomatized ocean-floor mafic volcanic rocks from the same area (Gilbert and Bailes, 2005b). They are comparable to values obtained by Linnen et al. (2009) in country rock at the upper contact of the Dibs pegmatite: up to 2256 ppm Li, 184.5 ppm and 72.4 ppm Cs.

For the Dibs pegmatite, values of Li, Rb and Cs in the country rock increase substantially toward the contact of the pegmatite (Linnen et al., 2009, 2015). For Dike 1, the maximum concentrations for each element occur mostly in the country rock adjacent to the pegmatite contacts (Figure GS2017-5-5a–f). However, the increase in concentration approaching the contact might not always be a steady one. Within the same drillhole (FAR17-010), values at 11 m for Li, Rb and Cs are 48, 39.1 and 1.1 ppm, respectively (all values above background; Figure GS2017-5-5d–f). These values close to surface are higher than at roughly 70 m downhole (14 ppm Li, 1 ppm Rb, 0.2 ppm Cs). Deeper than 70 m there is a steady increase of Li, Rb and Cs until the pegmatite intrusion at 163 m (922 ppm Li, 51 ppm Rb, 23.9 ppm Cs; Figure GS2017-5-5d–f). This downhole variation in concentration of Li, Rb and Cs could be related to the presence of fractures, the size or shape of the pegmatite (and consequently the metasomatic halo), and the zonation of the pegmatite itself (i.e., location of the Li or Cs mineralization and Rb enrichment within the pegmatite). The data also indicate that above-background concentrations of Li, Rb and Cs in the country rock of Dike 1 can be measured up to 150 m away from the pegmatite contact.

Elements such as Nb and Ta are low and do not show any particular enrichment at the contacts with the pegmatite (Nb <5 ppm; Ta <2 ppm, with only one analysis as high as 8 ppm), indicating low mobility of these elements and a weak enrichment in Dike 1. This is corroborated by mineralogical studies in the Wekusko Lake pegmatite field, in which no minerals of the

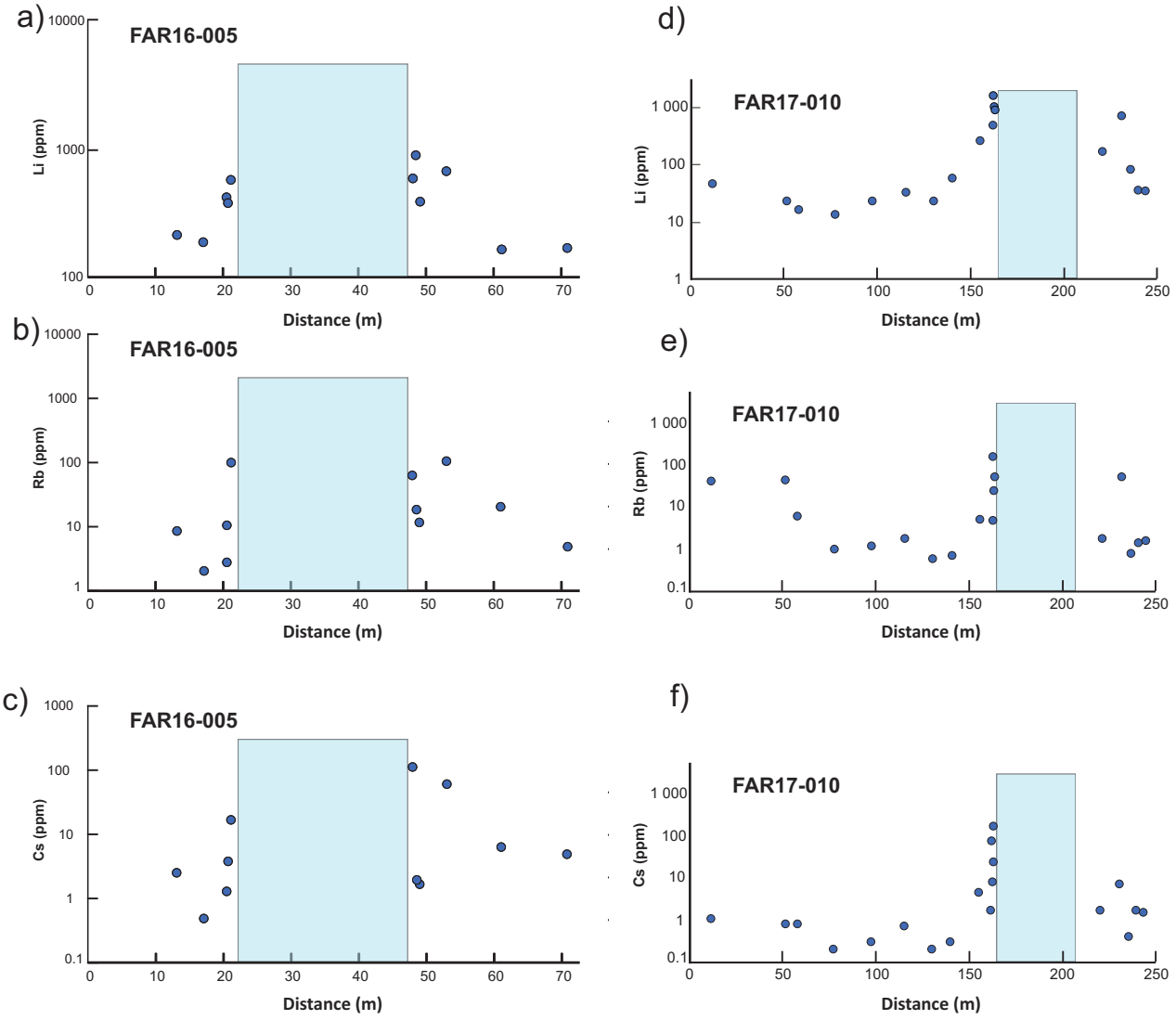

Figure GS2017-5-5: *Element distribution diagrams showing variations along the length of the studied drillholes from Dike 1:* ***a)*** *Li for drillhole FAR16-005;* ***b)*** *Rb for drillhole FAR16-005;* ***c)*** *Cs for drillhole FAR16-005;* ***d)*** *Li for drillhole FAR17-010;* ***e)*** *Rb for drillhole FAR17-010;* ***f)*** *Cs for drillhole FAR17-010. Shaded areas mark the location of the pegmatite.*

columbite group were reported (Černý et al., 1981). However, petrographic work during this study (see above) reveals trace amounts of minerals of the columbite group. Values for Sn are usually <4 ppm, with a few higher values (up to 91 ppm) close to the contact with the pegmatite. Other pegmatite fields show a correlation between Li and Sn mineralization (for example, the Barroso-Alvão pegmatite field in northern Portugal; Martins et al., 2011), but mineralogy studies (Černý et al., 1981) did not identify cassiterite or any other Sn-bearing minerals, suggesting that such a relationship does not occur in the Wekusko Lake pegmatite field. Tellurium and As show dispersion patterns with weak anomalies around the Dibs pegmatite, but this does not seem to be the case for the Dike 1 pegmatite. Values for Tl are usually below detection limit and vary up to 6 ppm. Values for As in the country rock of Dike 1 are elevated (up to 6450 ppm) but could be associated with the Au mineralization known to occur in this area (Galley et al., 1989).

Mineral chemistry of Dike 1 pegmatite

Mineral-chemistry data for both muscovite and K-feldspar obtained during this study are similar to results reported by Černý et al. (1981) for pegmatites from the Green Bay group of the Wekusko Lake pegmatite group. Only ranges will be mentioned in this section. The full dataset of electron microprobe results can be found in DRI2017004 (Martins and Linnen, 2017).

Muscovite

At least two generations of mica were found in Dike 1, but this study focuses on primary muscovite, identified on the basis of the following criteria (Fleet et al., 2003): sharp boundaries, subhedral to euhedral shape, grain size comparable to that of other magmatic minerals, absence of reactions with other minerals, absence of alteration in surrounding minerals, and relative abundance. The mica compositions are all close to the stoichiometric dioctahedral muscovite end-member within the expected values for spodumene-subtype pegmatite (e.g., Selway et al., 2005; Martins et al., 2012). In the diagram for mica classification proposed by Tischendorf et al. (1997) in which (Fe_{tot} + Mn + Ti) – ^{VI}Al is plotted against Mg – Li, the analyzed micas have compositions close to end-member muscovite (Figure GS2017-5-6) and show a trend toward the Li-enriched muscovite end-member. Most of the analyses reveal interlayer occupancies, with Σ(Na + K + Rb + Cs) values varying around the ideal 2.00 atoms per formula unit (apfu; most values ranging from 1.86 to 2.09 apfu, with only a few ranging as high as 2.26 apfu). The octahedral site-occupancy ^{VI}R is higher than the ideal 4.0 apfu, ranging from 4.24 to 4.68 apfu. This is not uncommon for muscovite in pegmatitic environments, as reported by other authors (e.g., Černý et al., 1995; Vieira et al., 2011; Martins et al., 2012). Foord et al. (1995) and du Bray (1994) suggested that the high occupancy of the octahedral site might be indicative of a mixed-layer form, involving both dioctahedral and trioctahedral structures, and could be a sign of disequilibrium crystallization. It is also possible that part of the Li might be an interlayer occupant, or part of the measured FeO is actually Fe^{3+} occupying the tetrahedral site. Note that all Fe is here considered Fe^{2+}. According to Černý and Burt (1984), the existence of FeO is favoured because micas seem to grow under rather reducing conditions, so that Fe^{3+} contents are minor.

With respect to the major-elements, the muscovite samples analyzed show minor variation in their Si and Al content, and Fe contents vary between 0.60 and 4.70 wt. % FeO. Regarding the trace-element concentrations, F varies from below detection limit to 1.53 wt. % F, Rb ranges from 0.18 to 0.81 wt. % Rb_2O, and Cs varies from below detection limit to 0.36 wt. % Cs_2O. The K/Rb ratio values of muscovite in Dike 1

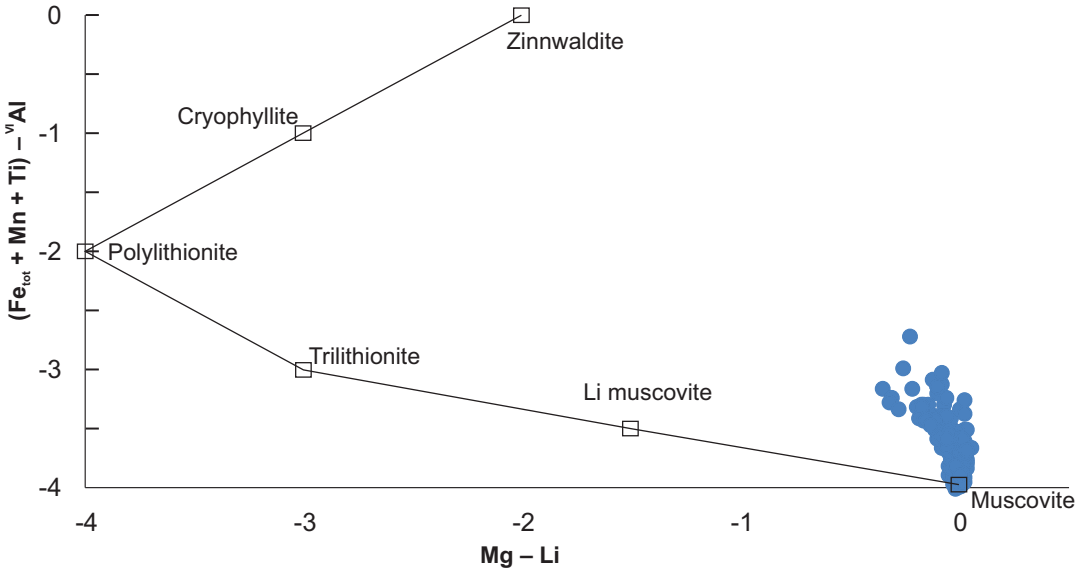

***Figure GS2017-5-6**: Muscovite from Dike 1 (blue dots) plotted on the Mg – Li versus (Fe_{tot} + Mn + Ti) – ^{VI}Al diagram for mica classification (values in apfu; modified after Tischendorf et al., 1997). Squares indicate the ideal locations for mica end-members of this section of the diagram.*

vary between 10.99 and 28.73, comparable to moderately evolved pegmatites from Ontario (Figure GS2017-5-7a; Tindle et al., 2002; Selway et al., 2005) but higher than the highly evolved Tanco pegmatite, in which mica has ratio values varying from 2.9 to 10.6 (Černý, 2005); these results indicate that the Dike 1 pegmatite is less fractionated than the Tanco pegmatite. The K/Cs ratio values of muscovite in Dike 1 vary from 27.89 to 871.48, corroborating the lower level of fractionation of this pegmatite compared to Tanco, in which mica ratio values vary from 14 to 93 (Černý, 2005). (Higher K/Cs ratio values of 1002.59, 1032.18 and 1045.34 are reported in DRI2017004, but they were calculated using Cs results too close to the detection limit of 80 ppm and were not considered for the variation interval.)

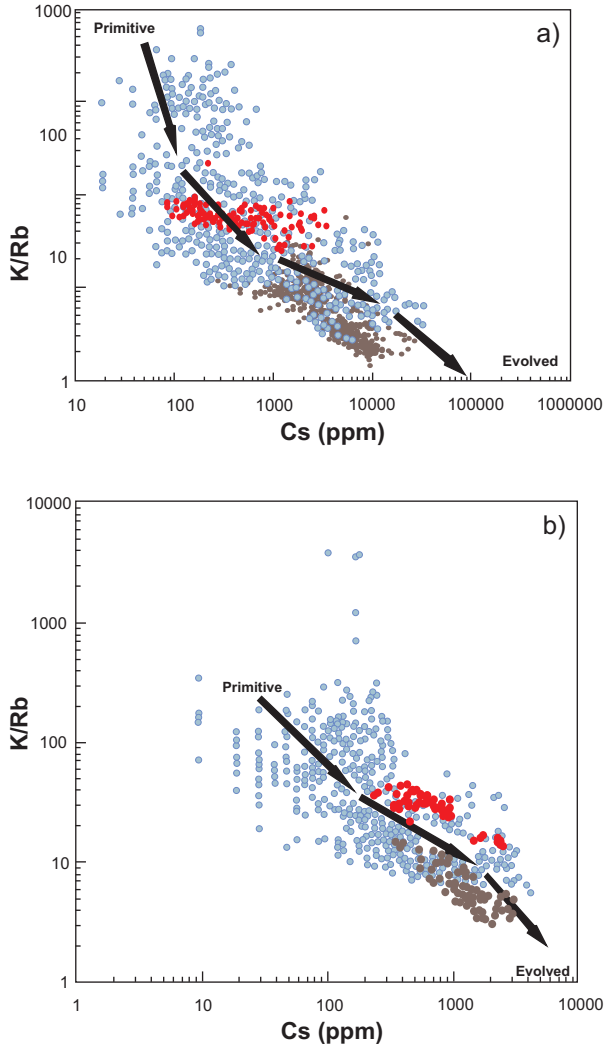

***Figure GS2017-5-7**: Mineral-chemistry results for muscovite and K-feldspar from Dike 1: **a)** general fractionation trend (arrows) for micas from Ontario pegmatites (blue dots; data from Selway et al., 2005) and those from the Tanco pegmatite (brown dots; S. Margison, unpublished data) and Dike 1 (red dots); **b)** general fractionation trend (arrows) for K-feldspar from Ontario pegmatites (blue dots; Selway et al., 2005), Tanco pegmatite (brown dots; data from Brown, 2001) and Dike 1 (red dots).*

K-feldspar

Selected K-feldspar grains were initially considered primary when sampled, but petrography and backscattered imagery indicate albitization. This suggests that the analyzed grains might not be good indicators of high-temperature primary-crystallization processes. The stoichiometry of the analyzed K-feldspar is slightly non-ideal, which is typical for K-feldspar in granitic pegmatites (Černý et al., 2012; Brown et al., 2017). Major elements do not vary significantly throughout the several analyses. Regarding trace elements, Rb varies from below detection limit to 0.70 wt. % Rb_2O and Cs varies from below detection limit to 0.27 wt. % Cs_2O. The values obtained indicate a moderate level of fractionation relative to pegmatites from Ontario (Figure GS2017-5-7b; Tindle et al., 2002; Selway et al., 2005). The K/Rb ratio values vary from 13.45 to 43.92, higher than the values listed for Tanco feldspar (4.0 to 14.2; Černý, 2005) but typical for spodumene-type pegmatites in Ontario (Tindle et al., 2002). The K/Cs ratio values of K-feldspar from Dike 1 vary from 48.26 to 584.62, well above the values reported for the Tanco pegmatite (6 to 26; Černý, 2005), corroborating the lower degree of fractionation of Dike 1.

Economic considerations

The results from this report corroborate the conclusion from other studies (e.g., Halden et al., 1989; Linnen et al., 2009, 2015) that using lithogeochemistry of country rocks is a viable and relatively inexpensive tool to explore for rare-element pegmatites. This is valid for metavolcanic rocks, the country rocks in both of the study areas presented herein, but has not been sufficiently tested for other types of wallrock and should therefore be used with caution. Work by Linnen et al. (2009, 2015) found that a major drawback of using lithogeochemistry of country rocks is the occurrence of Li-Rb-Cs–bearing minerals along fractures, which complicates the interpretation of results. Linnen et al. (2009) suggested that indicator minerals (such as biotite) are potentially more reliable than lithogeochemistry in pegmatite exploration. Despite the potential complication associated with fractures, additional lenses of the Dibs pegmatite were found at depth by following up on Li anomalies occurring below the main body (Linnen et al., 2009).

The presence of holmquistite-bearing assemblages in the amphibolitic country rock to the Dike 1 pegmatite indicates interaction of Li-enriched fluid sourced from the Li-bearing pegmatite. Hence, identification of these assemblages could also be a very useful and inexpensive tool in exploration for Li-bearing pegmatite because they can occur up to 20 m away from pegmatite contacts (Černý et al., 1981). The formation of holmquistite is not restricted to early episodes of interaction between pegmatite fluid and the amphibolite country rock, but can occur at any time from pegmatite injection to final consolidation (London, 1986).

Mineral-chemistry results for muscovite and K-feldspar indicate that Dike 1 is a moderately fractionated pegmatite (Figure GS2017-5-7a, b; Martins and Linnen, 2017). This kind of information could be a useful tool for understanding fractionation

trends within a pegmatite field. According to Selway et al. (2005), compositions of K-feldspar and muscovite are excellent exploration tools because these minerals are common in barren and fertile granites as well as rare-element pegmatites, allowing for an understanding of fractionation trends. Research shows that Rb and Cs contents increase in K-feldspar and muscovite with increasing fractionation of a granitic melt (e.g., Selway et al., 2005; Černý et al., 2012; Martins et al, 2012; Brown et al., 2017). Similarly, pegmatites with the highest degree of fractionation (and thus the most economic potential for Li-Cs-Ta) usually contain K-feldspar with >3 000 ppm Rb, K/Rb <30, and >100 ppm Cs (Tindle et al., 2002; Selway et al., 2005). Pegmatites with the most economic potential contain muscovite with >2 000 ppm Li, >10 000 ppm Rb, >500 ppm Cs and >65 ppm Ta (Tindle et al., 2002; Selway et al., 2005).

Expanding the mineral-chemistry study to other pegmatite dikes in the area might help in understanding fractionation paths in the Wekusko Lake pegmatite field and establishing areas of higher probability of finding pegmatite dikes with higher degrees of fractionation. Further petrographic studies of mineralogy and zonation would also give a better idea of the degree of fractionation of the Dike 1 pegmatite and a better understanding of the Li mineralization and its associations. Future work in the area around the Dike 1 pegmatite could also include rock, vegetation or soil geochemical surveys and selective-extraction analytical techniques, which have been widely used in other areas with LCT potential (Galeschuk and Vanstone, 2005). Collectively, the techniques presented in this report can provide effective exploration tools for identifying and characterizing Li-bearing pegmatite dikes.

Acknowledgments

The authors thank G. Fouillard for providing enthusiastic field assistance, as well as N. Brandson and E. Anderson for logistical support. Support by C. Epp from the Midland Sample and Core Library is gratefully appreciated. Access to drillcore at the Tanco mine was facilitated by C. Deveau. Logistical support and all analytical work for the Dike 1 pegmatite was supported by Far Resources Ltd. (Zoro project). B. Lenton is acknowledged for her help preparing figures. E. Yang, C. Böhm and S. Anderson are acknowledged for improving this report with their reviews.

References

Bailes, A.H. and Galley, A.G. 1999: Evolution of the Paleoproterozoic Snow Lake arc assemblage and geodynamic setting for associated volcanic-hosted massive sulphide deposits, Flin Flon Belt, Manitoba, Canada; Canadian Journal of Earth Sciences, v. 36, p. 1789–1805.

Beus, A.A. 1960: Geochemistry of beryllium and genetic types of beryllium deposits; Academy of Science, USSR, Moscow (in Russian; translation, Freeman & Co, San Francisco, 1966), 329 p.

Brown, J.A. 2001: Mineralogy and geochemistry of alkali feldspars from the Tanco pegmatite, southeastern Manitoba; M.Sc. thesis, University of Manitoba, Winnipeg, Manitoba, 238 p.

Brown, J.A., Martins, T. and Černý, P. 2017: The Tanco pegmatite at Bernic Lake, Manitoba, XVII: mineralogy and geochemistry of alkali feldspars; Canadian Mineralogist, v. 55, p. 483–500.

Černý, P. 1989: Exploration strategy and methods for pegmatite deposits of tantalum; *in* Lanthanides, Tantalum and Niobium, P. Möller, P. Černý and F. Saupé (ed.), Springer-Verlag, Heidelberg, p. 274–310.

Černý, 2005: The Tanco rare element pegmatite deposit, Manitoba: regional context, internal anatomy and global comparisons; *in* Rare Element Geochemistry and Ore Deposits, R.L. Linnen and I.M. Samson (ed.), Geological Association of Canada, Short Course Notes, v. 17, p. 127–158.

Černý, P. and Burt, D.M. 1984: Paragenesis, crystallochemical characteristics, and geochemical evolution of micas in granite pegmatites; *in* Micas, S.W. Bailey (ed.), Reviews in Mineralogy, v. 13, p. 257–297.

Černý, P. and Ferguson, R.B. 1972: The Tanco pegmatite at Bernic Lake, Manitoba. IV. Petalite and spodumene relations; The Canadian Mineralogist, v. 11, pt. 3, p. 660–678.

Černý, P., Trueman, D.L., Ziehlke, D.V., Goad, B.E. and Paul, B.J. 1981: The Cat Lake–Winnipeg River and the Wekusko Lake pegmatite fields, Manitoba; Manitoba Department of Energy and Mines, Mineral Resources Division, Economic Geology Report ER80-1, 215 p.

Černý, P., Staněk, J., Novák, M., Baadsgaard, H., Rieder, M., Ottolini, L., Kavalová, M. and Chapman, R. 1995: Geochemical and structural evolution of micas in the Rožná and Dobrá Voda pegmatites, Czech Republic; Mineralogy and Petrology, v. 55, p. 177–201.

Černý, P., Teertstra, D.K., Chapman, R., Selway, J.B., Hawthorne, F.C., Ferreira, K., Chackowsky, L.E., Wang, X.-J. and Meintzer, R.E. 2012: Extreme fractionation and deformation of the leucogranite-pegmatite suite at Red Cross Lake, Manitoba, Canada. IV. mineralogy; Canadian Mineralogist, v. 50, p. 1839–1875.

du Bray, E.A. 1994: Compositions of micas in peraluminous granitoids of the eastern Arabian Shield: implications for petrogenesis and tectonic setting of highly evolved, rare-metal enriched granites; Contributions to Mineralogy and Petrology, v. 116, p. 381–397.

Fleet, M.E., Deer, W.A., Howie, R.A. and Zussman, J. 2003: Rock-Forming Minerals. 3A. Sheet Silicates: Micas (Second Edition); The Geological Society, London, United Kingdom, 758 p.

Foord, E.E., Černy, P., Jackson, L.L., Sherman, D.M. and Eby, R.K. 1995: Mineralogical and geochemical evolution of micas from miarolitic pegmatites of the anorogenic Pikes Peak batholith, Colorado; Mineralogy and Petrology, v. 55, p. 1–26.

Galeschuk, C.R. and Vanstone, P.J. 2005: Exploration for buried rare-element pegmatites in the Bernic Lake area of southeastern Manitoba; *in* Rare-Element Geochemistry and Mineral Deposits, R.L. Linnen and I.M. Samson (ed.), Geological Association of Canada, Short Course Notes, v. 17, p. 153–167.

Galeschuk, C.R. and Vanstone, P.J. 2007: Exploration techniques for rare-element pegmatite in the Bird River greenstone belt, southeastern Manitoba; *in* Proceedings of Exploration 07: Fifth Decennial International Conference on Mineral Exploration, B. Milkereit (ed.), 2007, p. 823–839.

Galley, A.G., Ames, D.E. and Franklin, J.M. 1989: Results of studies on the gold metallogeny of the Flin Flon Belt; Geological Survey of Canada, Open File 2133, p. 25–32.

Gilbert, H.P. 2006: Geological investigations in the Bird River area, southeastern Manitoba (parts of NTS 52L5N and 6); *in* Report of Activities 2006, Manitoba Science, Technology, Energy and Mines, Manitoba Geological Survey, p. 184–205.

Gilbert, H.P. and Bailes, A.H. 2005a: Geology of the southern Wekusko Lake area, Manitoba (NTS 63J12NW); Manitoba Industry, Economic Development and Mines, Manitoba Geological Survey, Geoscientific Map MAP2005-2, scale 1:20 000.

Gilbert, H.P. and Bailes, A.H. 2005b: Lithological and lithogeochemical data and field photographs for the southern Wekusko Lake area, Manitoba (NTS 63J12NW); Manitoba Industry, Economic Development and Mines, Manitoba Geological Survey, Data Repository Item DRI2005003, Microsoft® Excel® file.

Gilbert, H.P., Davis, W.D., Duguet, M., Kremer, P.D., Mealin, C.A. and MacDonald J. 2008: Geology of the Bird River Belt, southeastern Manitoba (parts of NTS 52L5, 6); Manitoba Science, Technology, Energy and Mines, Manitoba Geological Survey, Geoscientific Map MAP2008-1, scale 1:50 000.

Halden, N.M., Meintzer, R.E. and Černý, P. 1989: Trace element characteristic and controls of element mobility in the metasomatic aureole to the Tanco pegmatite; *in* Report of Field Activities 1989, Manitoba Energy and Mines, Minerals Division, p. 152–155.

Heinrich, E.W. 1965: Holmquistite and pegmatitic lithium exomorphism; Indian Mineralogist, v. 6, p. l–13.

Kremer, P.D. 2010: Structural geology and geochronology of the Bernic Lake area in the Bird River greenstone belt, Manitoba: evidence for syn-deformational emplacement of the Bernic Lake pegmatite group; M.Sc. thesis, University of Waterloo, Waterloo, Ontario, 91 p.

Linnen, R.L., Galeschuk, C. and Halden, N.M., 2015: The use of fracture minerals to define metasomatic aureoles around rare-metal pegmatites; 27th International Applied Geochemistry Symposium, Tucson, Arizona, 5 p., URL <https://www.appliedgeochemists.org/images/stories/IAGS_2015/Abstracts/27th%20IAGS_Linnen%20et%20al_Fracture%20Chlorites%20in%20Exploration.pdf> [October 2017].

Linnen, R.L., Galeschuk, C, Halden, N.M. and Lau, L. 2009: Dispersion haloes around rare-metal pegmatites: a case study of the Dibs LCT pegmatite, Manitoba, Canada; Estudos Geológicos, v. 19, no. 2, p. 25–29.

Linnen, R.L., van Lichtervelde, M. and Černý, P. 2012: Granitic pegmatites as sources of strategic metals; Elements, v. 8, p. 275–280.

London, D. 1986: Holmquistite as a guide to pegmatitic rare-metal deposits; Economic Geology, v. 81, p. 704–712.

London, D. 2008: Pegmatites; Canadian Mineralogist, Special Publication 10, 347 p.

Martins, T., Lima, A., Simmons, W.B., Falster, A.U. and Noronha, F. 2011: Geochemical fractionation of Nb-Ta oxides in Li-bearing pegmatites from the Barroso-Alvão pegmatite field, northern Portugal; Canadian Mineralogist, v. 49, p. 777–791.

Martins, T. and Linnen, R.L. 2017: Whole-rock and mineral geochemistry as an exploration tool for rare-element pegmatites in Manitoba: examples from the Cat Lake–Winnipeg River and the Wekusko Lake pegmatite fields (parts of NTS 52L6, 63J13); Manitoba Growth, Enterprise and Trade, Manitoba Geological Survey, Data Repository Item DRI2017004, Microsoft® Excel® file.

Martins, T., Roda-Robles, E., Lima, A. and Parseval, P. 2012: Geochemistry and evolution of micas in the Barroso-Alvão pegmatite field, northern Portugal; Canadian Mineralogist, v. 50, p. 1117–1129.

Morgan, G.B. and London, D. 1987: Alteration of amphibolitic wallrocks around the Tanco rare-element pegmatite, Bernic Lake, Manitoba; American Mineralogist, v. 72, p. 1097–1121.

NATMAP Shield Margin Project Working Group 1998: Geology, NATMAP Shield Margin Project Area (Flin Flon Belt), Manitoba/Saskatchewan; Geological Survey of Canada, Map 1968A, scale 1:100 000.

Norton, J.J. 1984: Lithium anomaly near Pringle, southern Black Hills, South Dakota, possibly caused by unexposed rare-mineral pegmatite; United States Geological Survey, Circular 889, p. 1–7.

Ryan, J.G. and Langmuir, C.H. 1987: The systematics of lithium abundances in young volcanic rocks; Geochimica et Cosmochimica Acta, v. 51, p. 1727–1741.

Selway, J.B., Breaks, F.W. and Tindle, A.G. 2005: A review of rare-element (Li-Cs-Ta) pegmatite exploration techniques for the Superior Province, Canada, and large worldwide tantalum deposits; Exploration and Mining Geology, v. 14, no. 1–4, p. 1–30.

Selway, J.B., Novák, M., Černý, P. and Hawthorne, F.C. 2000: The Tanco pegmatite at Bernic Lake, Manitoba. XIII. Exocontact tourmaline; Canadian Mineralogist, v. 38, p. 869–876.

Shearer, C.K. and Papike, J.J. 1988: Pegmatite-wallrock interaction: holmquistite-bearing amphibolite, Edison pegmatite, Black Hills, South Dakota; American Mineralogist, v. 73, p. 324–337.

Shearer, C.K., Papike, J.J., Simon, S.B. and Laul, J.C. 1986: Pegmatite-wallrock interactions, Black Hills, South Dakota: interaction between pegmatite-derived fluids and quartz-mica schist wallrock; American Mineralogist, v. 71, p. 518–539.

Stott, G.M., Corkery, M.T., Percival, J.A., Simard, M. and Goutier, J. 2010: Project units 98-006 and 98-007: a revised terrane subdivision of the Superior Province; *in* Summary of Field Work and Other Activities 2010, Ontario Geological Survey, Open File Report 6260, p. 20-1–20-10.

Tindle, A.G., Selway, J.B. and Breaks, F.W. 2002: Electron microprobe and bulk analyses of fertile peraluminous granites and related rare-element pegmatites, Superior province, northwest and northeast Ontario: Operation Treasure Hunt; Ontario Geological Survey, Miscellaneous Release–Data 111.

Tischendorf, G., Gottesmann, B., Förster, H.-J. and Trumbull, R.B. 1997: On Li-bearing micas: estimating Li from electron microprobe analyses and an improved diagram for graphical representation; Mineralogical Magazine, v. 61, p. 809–834.

Trueman, D.L. 1978: Exploration methods in the Tanco Mine area of southeastern Manitoba, Canada; Energy, v. 3, p. 293–297.

Trueman, D.L. 1980: Stratigraphy, structure and metamorphic petrology of the Archean greenstone belt at Bird River, Manitoba; Ph.D. thesis, University of Manitoba, Winnipeg, Manitoba, 150 p.

Trueman, D.L. and Černý, P., 1982: Exploration and processing; *in* Granitic Pegmatites in Science and Industry, Mineralogical Association of Canada, Short Course Notes, v. 8, p. 463–493.

Vieira, R., Roda-Robles, E., Pesquera, A. and Lima, A. 2011: Chemical variation and significance of micas from the Fregeneda-Almendra pegmatitic field (Central Iberian Zone, Spain and Portugal); American Mineralogist, v. 96, p. 637–645.

GS2017-6

Evaluation of diamond-drill core from the Tower Cu-Zn-Ag-Au deposit, sub-Phanerozoic Thompson nickel belt, central Manitoba (part of NTS 63G14)

by C.G. Couëslan

In Brief:

- Drillcore re-evaluation places the Tower Cu-Zn-Ag-Au deposit within the Ospwagan group of the Thompson nickel belt
- Stratiform mineralization (T2 zone) may have formed by sub-seafloor hydrothermal replacement
- Potential exists for additional deposits along strike in the Ospwagan group

Citation:
Couëslan, C.G. 2017: Evaluation of diamond-drill core from the Tower Cu-Zn-Ag-Au deposit, sub-Phanerozoic Thompson nickel belt, central Manitoba (part of NTS 63G14); *in* Report of Activities 2017, Manitoba Growth, Enterprise and Trade, Manitoba Geological Survey, p. 52–64.

Summary

The Tower Cu-Zn-Ag-Au deposit is a pelitic-mafic or Besshi-type volcanogenic massive-sulphide (VMS) system located in the sub-Phanerozoic Thompson nickel belt (TNB). Preliminary findings suggest that the deposit is hosted in Pipe formation rocks of the Ospwagan group. A simplified stratigraphy for the deposit consists of impure chert and siliceous rock of the Pipe formation P1 member, overlain by pelite and local sulphide-facies iron formation of the P2 member. This is overlain by laminated calcareous rock and a thick sequence of impure chert with intercalations of calcsilicate, iron formation, siliceous rock and minor carbonate, constituting the P3 member. The upper portion of the P3 member hosts a heterogeneous chlorite schist unit that has not been identified in the Pipe formation from other parts of the TNB and appears to result from hydrothermal alteration, likely during sulphide deposition.

The T1 zone mineralization is discordant to stratigraphy and is hosted within the P2 member in the north and P3 member in the south. The T1 zone varies from a sulphidic schist to a sulphide breccia, the latter consisting of fragments of wall-rock, interpreted to result from mobilization along a late (D_3-D_4) structure. The T2 zone mineralization and associated chlorite schist may represent a stratiform zone of sub-seafloor hydrothermal replacement that is mostly in situ.

It is suggested that mafic to ultramafic magmatism, associated with either the Bah Lake assemblage or ca. 1883 Ma Molson-age intrusions, could have provided the heat source to drive the hydrothermal circulation system required to generate the Tower VMS deposit. Both of these magmatic events are of regional extent, suggesting there could be potential for VMS mineralization throughout the TNB. Volcanogenic massive-sulphide systems typically occur in clusters, suggesting that additional deposits could be found along strike from the Tower deposit.

Introduction

The Tower Cu-Zn-Ag-Au deposit is located along the eastern margin of the sub-Phanerozoic Thompson nickel belt (TNB; Figure GS2017-6-1). It was discovered by Falconbridge Ltd. (now Glencore plc) in September of 2000 during exploration for Ni-sulphide deposits in the William Lake area (Assessment Files 73953 and 73950, Manitoba Growth, Enterprise and Trade, Winnipeg). Follow-up drilling in the autumn of 2000 and winter of 2001 intersected significant Cu-Zn-Au mineralization in what has become known as the T1 zone of the Tower deposit (Assessment File 63G13256). The property was then acquired by Pure Nickel Inc. in August of 2007 (Beaudry, 2007). Rockcliff Resources Inc. (now Rockcliff Copper Corporation) entered an option and joint-venture agreement with Pure Nickel to explore the Tower deposit in February of 2008. Rockcliff Resources completed drill programs from 2010 to 2014 to further delineate the deposit, and additional mineralization was discovered in the T2 zone during the 2012 drill program (Assessment Files 63G13256, 63G14375). An indicated-resource estimate released in 2013 included 1 Mt at 3.7% Cu, 1.0% Zn, 17 g/t Ag and 0.5 g/t Au (Caracle Creek International Consulting Inc., 2013). In April of 2015, Rockcliff Resources agreed to sell its interest in the Tower property to Akuna Minerals Inc., and Pure Nickel sold its remaining interest to Akuna Minerals in June of the same year. Akuna Minerals is working toward developing the Tower deposit, and hopes to bring the deposit into production in the near future.

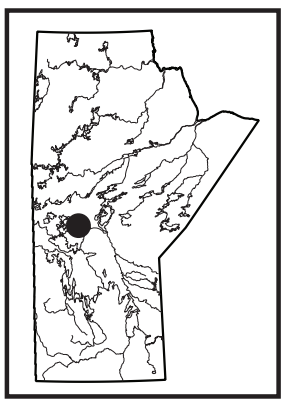

The significance of volcanogenic massive-sulphide (VMS) mineralization within a metallotect known for its magmatic Ni deposits is uncertain and brings into question the affinity of the hostrocks. Initial work by Falconbridge suggested that the mineralization is hosted by metasedimentary rocks of the Ospwagan group intruded by altered ultramafic rocks (Beaudry, 2007; Assessment Files 73953, 73950), implying that the Precambrian rocks in the area are part of the TNB; however, later work by Rockcliff Resources suggested that the metasedimentary rocks are subordinate to metavolcanic rocks and metamorphosed ultramafic intrusions (Assessment File 63G13256), possibly more in keeping with greenstone belts in the adjacent Superior province or Trans-Hudson

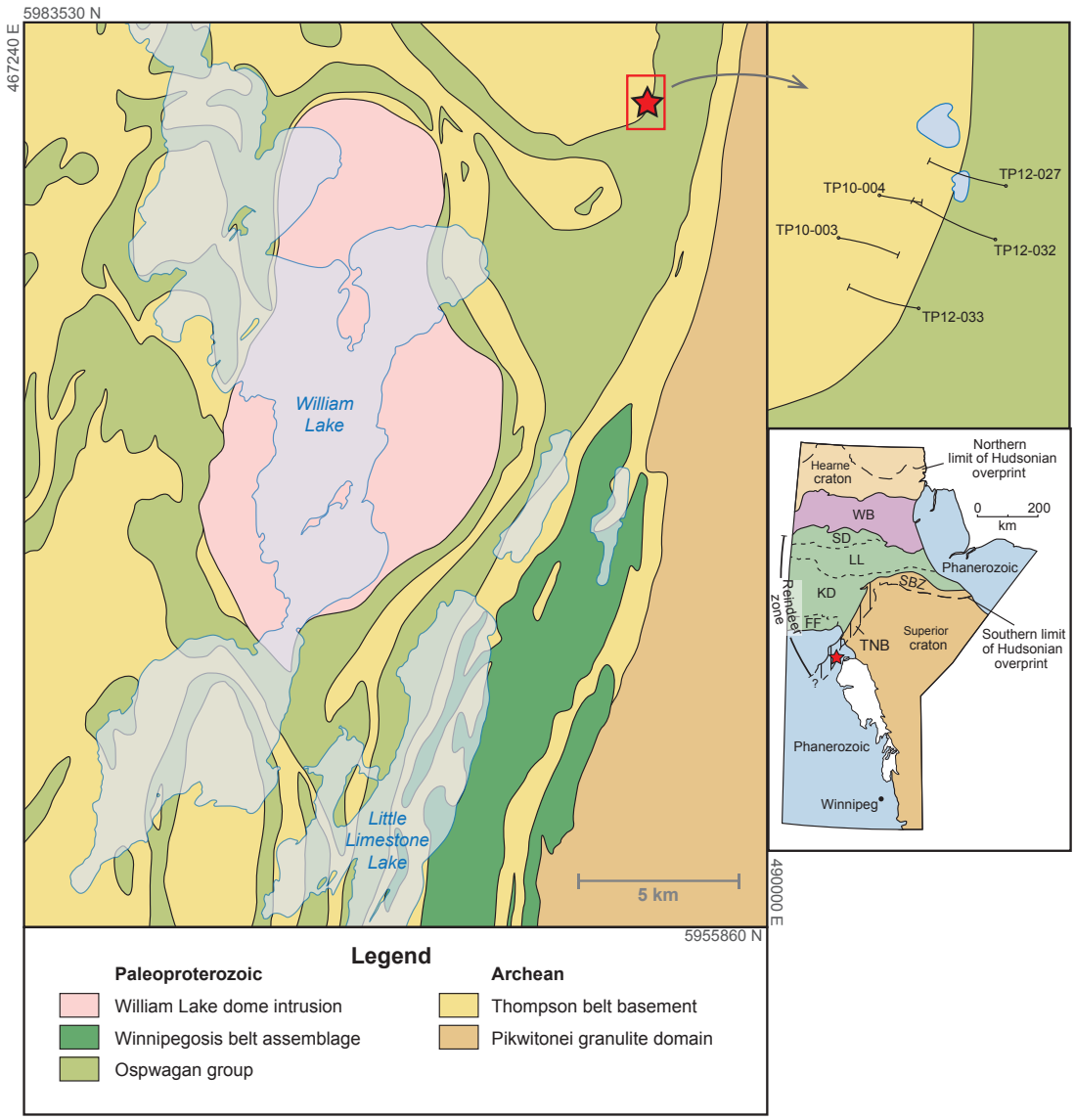

Figure GS2017-6-1: *Simplified lithology of the William Lake area (modified from Macek et al., 2006). The red star indicates the location of the Tower deposit. Abbreviations: FF, Flin Flon domain; KD, Kisseynew domain; LL, Lynn Lake domain; SBZ, Superior boundary zone; SD, Southern Indian domain; TNB, Thompson nickel belt; WB, Wathaman batholith.*

orogen (THO). Garnet, amphibole and biotite are described as common constituents in the ultramafic rocks: this association (garnet-bearing ultramafic rocks) is unknown in the Paleoproterozoic of the TNB but is described in the adjacent Pikwitonei granulite domain (PGD) of the Superior province (Böhm, 2005a, b; Couëslan, 2014). In contrast, VMS deposits have not been documented in the TNB or PGD but are widespread in the Flin Flon domain (FFD) of the THO: several deposits have been discovered to date in the eastern sub-Phanerozoic FFD, including the Talbot deposit, located roughly 32 km northwest of the Tower deposit (Simard et al., 2010). In this regard, it is possible that the rocks hosting the Tower deposit could represent a klippe of juvenile FFD rocks lying unconformably on TNB rocks.

The aim of this project is to evaluate the rocks hosting the Cu-Zn-Ag-Au mineralization at Akuna Minerals' Tower property, establish any genetic affiliation to the FFD, TNB or PGD, and identify possible VMS-related hydrothermal alteration. Identifying the provenance of the hostrocks could expand the mineral potential of the TNB or PGD, or expand the known area of the sub-Paleozoic FFD. Identifying VMS-related hydrothermal alteration could also provide exploration vectors to additional mineralization.

Regional geology

The TNB forms a segment of the Superior boundary zone, flanked to the northwest by the Kisseynew domain of the Trans-Hudson orogen and to the southeast by the PGD of the Superior craton. The TNB is underlain largely by reworked Archean gneiss of the Superior craton, which is typically quartzofeldspathic with enclaves of mafic to ultramafic rock. It is commonly

migmatitic and characterized by complex internal structures that are the result of multiple generations of Archean and Paleoproterozoic deformation and metamorphism; clearly recognizable paragneiss is rare. The gneiss is interpreted to be derived from the adjacent PGD, which was subjected to amphibolite- to granulite-facies metamorphic conditions from ca. 2720 to 2640 Ma (Hubregtse, 1980; Mezger et al., 1990; Heaman et al., 2011; Guevara et al., 2016a, b). The granulites of the PGD were exhumed and unconformably overlain by the Paleoproterozoic supracrustal rocks of the Ospwagan group (TNB) prior to intrusion of the Molson dike swarm and associated ultramafic intrusions at ca. 1883 Ma (Bleeker, 1990; Zwanzig et al., 2007; Heaman et al., 2009; Scoates et al., 2017). The Archean basement gneiss and Ospwagan group were subjected to multiple generations of deformation and metamorphic conditions ranging from middle-amphibolite facies to lower-granulite facies during the Trans-Hudson orogeny (Bleeker, 1990; Burnham et al., 2009; Couëslan and Pattison, 2012).

The dominant phase of penetrative deformation is D_2, which affected the Ospwagan group and ca. 1883 Ma magmatic rocks. This deformation phase resulted in the formation of F_2 nappe structures, which incorporated the underlying Archean gneiss. The nappe structures have been interpreted as either east verging (Bleeker, 1990; White et al., 2002) or southwest verging (Zwanzig et al., 2007; Burnham et al., 2009). The recumbent folds are associated with regionally penetrative S_2 fabrics. The D_2 phase of deformation is interpreted to be the result of convergence between the Superior craton margin and the Reindeer zone of the Trans-Hudson orogen from ca. 1830 to 1800 Ma. The D_3 phase of deformation resulted in isoclinal folds with vertical to steeply southeast-dipping axial planes (Bleeker, 1990; Burnham et al., 2009). Mylonite zones with subvertical stretching lineations parallel many of the regional F_3 folds. Tightening of D_3 structures continued during D_4, marked by localized retrograde greenschist metamorphism along northeast-striking, mylonitic and cataclastic shear zones that commonly record southeast-side-up sinistral movement (Bleeker, 1990; Burnham et al., 2009). Although all rocks described in this report have been subjected to at least amphibolite-facies metamorphic conditions, the 'meta-' prefix has been omitted from rock names for brevity.

Review of the Ospwagan group stratigraphy

The following summary of the Ospwagan group is sourced largely from Bleeker (1990) and Zwanzig et al. (2007). The Paleoproterozoic Ospwagan group unconformably overlies Archean basement gneiss in the TNB. The lowermost unit of the Ospwagan group is the Manasan formation, which consists of two members: the lower M1 member, consisting of layered to laminated sandstone with local conglomerate layers near the base; and the overlying M2 member, consisting of semipelitic rock (Figure GS2017-6-2). The Manasan formation is interpreted as a transgressive, fining-upward sequence deposited along a passive margin. This siliciclastic system grades into the overlying calcareous sedimentary rocks of the Thompson formation.

The Thompson formation consists of three members: the T1 member comprises a variety of calcareous–siliceous rocks including chert, calcsilicate and impure marble; the T2 member is a semipelitic calcareous gneiss that is rarely present; and the T3 member consists of impure dolomitic marble with local horizons of calcsilicate (Figure GS2017-6-2). The Thompson formation represents a transition from a siliciclastic-dominated to a carbonate-dominated system.

The Pipe formation is subdivided into three members (Figure GS2017-6-2). The P1 member consists of a graphite-rich, sulphide-facies iron formation at the base (the locus of the Pipe II and Birchtree orebodies), overlain by a silicate-facies iron formation. The top of the P1 member consists of a reddish, laminated, siliceous rock. The P1 member grades into the overlying pelitic rocks of the P2 member, the top of which is marked by a sulphide-facies iron formation (the locus of the Thompson orebody). The overlying P3 member consists of a wide variety of rock types, including laminated, siliceous sedimentary rocks; silicate-, carbonate- and local oxide-facies iron formations; and semipelitic rocks, calcsilicate and a local horizon of relatively pure dolomitic marble. The Pipe formation represents a mix of chemical sediments and fine to very fine siliciclastics that were deposited in either an open-marine environment (Zwanzig et al., 2007) or during the development of a foredeep basin (Bleeker, 1990).

The Setting formation is divided into two members and is defined to include all siliciclastic rocks above the iron formation of the uppermost P3 member (Figure GS2017-6-2). The S1 member consists of rhythmically interbedded quartzite and pelitic schist with local calcareous concretions, which are very characteristic of the S1 member. The S2 member consists of thickly layered greywacke, with local horizons grading from conglomeratic at the base to pelitic at the top. No contact has been observed between the S1 and S2 members. It is possible that they represent a lateral facies change as opposed to a vertical succession. The S2 member appears to be missing altogether in the area of the Pipe mine, where contacts between the S1 member and the overlying Bah Lake assemblage are exposed. The Setting formation is interpreted to have been deposited by turbidity currents in a relatively deep-marine environment, possibly a foredeep basin (Bleeker, 1990). The coarse clastic material and thick turbidite bedding of the S2 member may record the onset of active tectonism, or a lateral sedimentary facies change, possibly to a submarine-channel or upper-fan environment.

At the top of the Ospwagan group is the Bah Lake assemblage, which consists of mafic to ultramafic volcanic rocks dominated by massive to pillowed basalt flows with local picrite and minor synvolcanic intrusions (Figure GS2017-6-2). The Bah Lake assemblage is dominated by a high-Mg suite (similar to normal mid-ocean ridge basalt; N-MORB) that occurs throughout much of the main TNB, and an incompatible-element–enriched suite (similar to enriched mid-ocean ridge basalt; E-MORB) that occurs in the northwestern Setting Lake area and along the margin of the Kisseynew domain (Zwanzig, 2005). The enriched suite is interpreted to overlie the high-Mg suite;

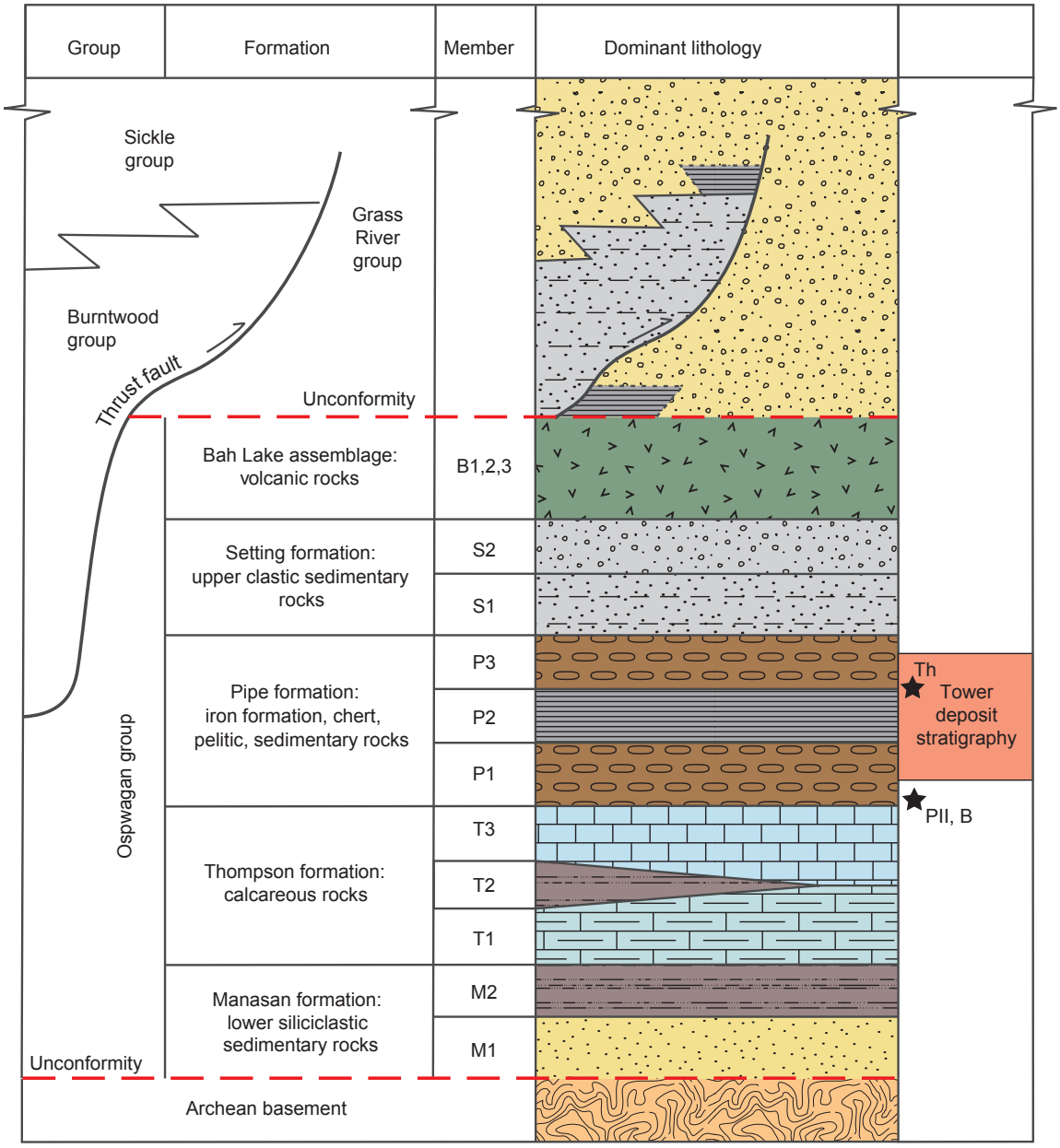

Figure GS2017-6-2: *Schematic tectonostratigraphic and lithostratigraphic section of the Ospwagan group of the Thompson nickel belt, and the Grass River and Burntwood groups of the adjoining Kisseynew domain (modified from Bleeker, 1990; Zwanzig et al., 2007). Black stars indicate the stratigraphic positions of the Birchtree (B), Pipe II (PII) and Thompson (Th) orebodies. A more detailed description of the Ospwagan group is found in the text.*

however, it is uncertain if this represents a stratigraphic or tectonic relationship. The Bah Lake assemblage may suggest the onset of active rifting in the TNB (Zwanzig, 2005; Zwanzig et al., 2007), or that the foredeep was magmatically active (Bleeker, 1990).

A minimum age for the Ospwagan group is provided by crosscutting amphibolitized dikes interpreted to be part of the Molson dike swarm, and the possibly comagmatic Ni-ore–bearing ultramafic sills, which intruded the Ospwagan group at all stratigraphic levels at ca. 1883 Ma (Bleeker, 1990; Zwanzig et al., 2007; Heaman et al., 2009; Scoates et al., 2017).

Geology of the Tower deposit

The Tower deposit occurs along the eastern margin of the sub-Phanerozoic TNB (Figure GS2017-6-1). The Precambrian rocks are overlain by 70–170 m of Paleozoic limestone and sandstone (Beaudry, 2007). Falconbridge geologists described the mineralization as being hosted in a thick package of Pipe formation pelitic and siliceous sedimentary rocks intruded by altered ultramafic rocks (Assessment Files 73953, 73950), consistent with the compilation map of Macek et al. (2006), which suggests that much of the Tower property is underlain by Pipe formation. Approaching the mineralization from the hangingwall, the

sequence consists of magnetite-bearing silicate-facies iron formation, turbidite, and then a thick sequence of pelitic sedimentary rocks intruded by an altered ultramafic sill (Beaudry, 2007). The mineralization is hosted in the pelitic sedimentary rocks in proximity to the ultramafic body.

Conversely, work conducted by Rockcliff Resources determined the Tower property to be underlain by dominantly volcanic and ultramafic rocks with subordinate sedimentary rocks (Assessment File 63G13256). The volcanic rocks are dark green and fine to medium grained, contain possible pillow selvages, and have sharp contacts with adjacent units. The ultramafic rocks are described as peridotite, as well as dark green to black, fine- to coarse-grained rocks variably enriched in amphibole, garnet and biotite. In contrast to the Falconbridge work, the mineralization of the T1 zone was interpreted to occur within the ultramafic rocks, in proximity to the sedimentary rocks that consist of grey pelitic rocks containing fine-grained garnet and muscovite, interpreted to be part of the Pipe formation.

The mineralization of the T1 zone has a strike of approximately 013° with a dip of 75–85° to the east (Assessment File 73953). The mineralization transects the regional foliation and is characterized by rounded to subangular, millimetre- to centimetre-scale fragments of wallrock within a matrix of semi-solid to solid sulphide (Assessment Files 73953, 63G13256 and 63G14375), interpreted to be mobilized from the source and forming the matrix of a fault breccia. Mineralization of the T2 zone is interpreted to be in situ, within pervasively altered volcanic rocks approximately 200 m northeast of the T1 zone (Rockcliff Resources Inc., 2013; Assessment File 63G13256).

The Cu- and Zn-rich nature of the mineralization is unusual for the TNB, as are the low concentrations of Ni and platinum-group elements (Beaudry, 2007). The mineralization is more akin to VMS deposits west of the TNB in the sub-Phanerozoic Flin Flon belt (Simard et al., 2010), and has been interpreted as a Besshi-type VMS system (Beaudry, 2007).

Methodology

Five drillholes were selected for re-examination. Drillholes TP10-003 and TP10-004 were both collared in the footwall and drilled toward the east, across strike through the T1 zone, and into the hangingwall (Figure GS2017-6-1). Drillholes TP12-027, TP12-032 and TP12-033 were collared in the hangingwall and drilled toward the west, across strike through the T1 zone, and into the footwall. Drillholes TP10-004 and TP12-032 were collared roughly across strike from each other, allowing for the construction of a continuous section from the footwall into the hangingwall of the deposit.

The core from each drillhole was laid out in its entirety, allowing for the entire sequence to be viewed and separated into petrographically distinct intervals. Each interval was then described petrographically and an interpretation of the protolith was made based on the mineral assemblages. Protolith interpretations were made within the context of the Ospwagan group stratigraphy; however, it is possible that the units represent varying types and intensities of hydrothermal alteration affecting volcanic rocks, which can be easily mistaken for sedimentary rocks (cf. Tinkham and Karlapalem, 2008). With this in mind, 27 samples were collected from key stratigraphic units for whole-rock lithogeochemical and Sm-Nd isotopic analyses. These analyses will be compared with the well-documented lithogeochemical and Sm-Nd isotopic compositions of the Ospwagan group (Zwanzig et al., 2007; Böhm et al., 2007) and published analyses from the sub-Phanerozoic Flin Flon belt (Simard et al., 2010). Thin sections were also made from each of the 27 samples to augment petrographic descriptions. The findings of this report should be considered preliminary and of an interpretive nature, pending the results of these analyses.

Stratigraphy of the Tower deposit

Iron formations are present throughout the footwall and hangingwall stratigraphy of the deposit (Figure GS2017-6-3). Because iron formations are only described from the Pipe formation of the Ospwagan group (Bleeker, 1990; Zwanzig et al., 2007), all sedimentary rocks intersected by the five drillholes are interpreted to be from the Pipe formation. The following stratigraphic description is from the footwall in the west to the hangingwall on the east side of the Tower deposit. The widths of stratigraphic units are reported as approximate true width, while thicknesses of potentially discordant intrusive units are reported as the length of the core intercept. Because of intense deformation, stratigraphic units commonly pinch and swell, and significant variations should be expected along strike. The stratigraphy presented below is idealized and based only on the five examined drillholes. All units were metamorphosed to amphibolite-facies conditions, and typically have moderate to strong foliations.

P1 member

The lowermost unit intersected in the footwall consists of grey, medium-grained and laminated to layered, impure chert (Figure GS2017-6-4a). The impure chert is garnet, biotite and amphibole bearing, and forms a package at least 22 m thick with intercalations, <20 cm thick, of garnet-bearing and biotite- and amphibole-rich silicate-facies iron formation. Upsection from the impure chert is a grey, fine- to coarse-grained, diffusely layered siliceous rock, 4.5–11 m thick (Figure GS2017-6-4b). The siliceous rock is garnet and biotite bearing, and could represent either quartz-rich siltstone or impure chert. The siliceous rock contains bands of, and is locally gradational into, biotite-bearing and amphibole-rich impure chert. Sparse sulphidic horizons, <25 cm thick, are present.

The siliceous rock has a mineral assemblage similar to the red laminated chert of the Pipe formation P1 member, exposed at the Pipe II mine near Thompson (Macek and Bleeker, 1989; Bleeker, 1990). The presence of this unit adjacent to pelitic schist (see P2 member) is in general agreement with this interpretation. Therefore, this package of rocks is tentatively interpreted as part of the Pipe formation P1 member.

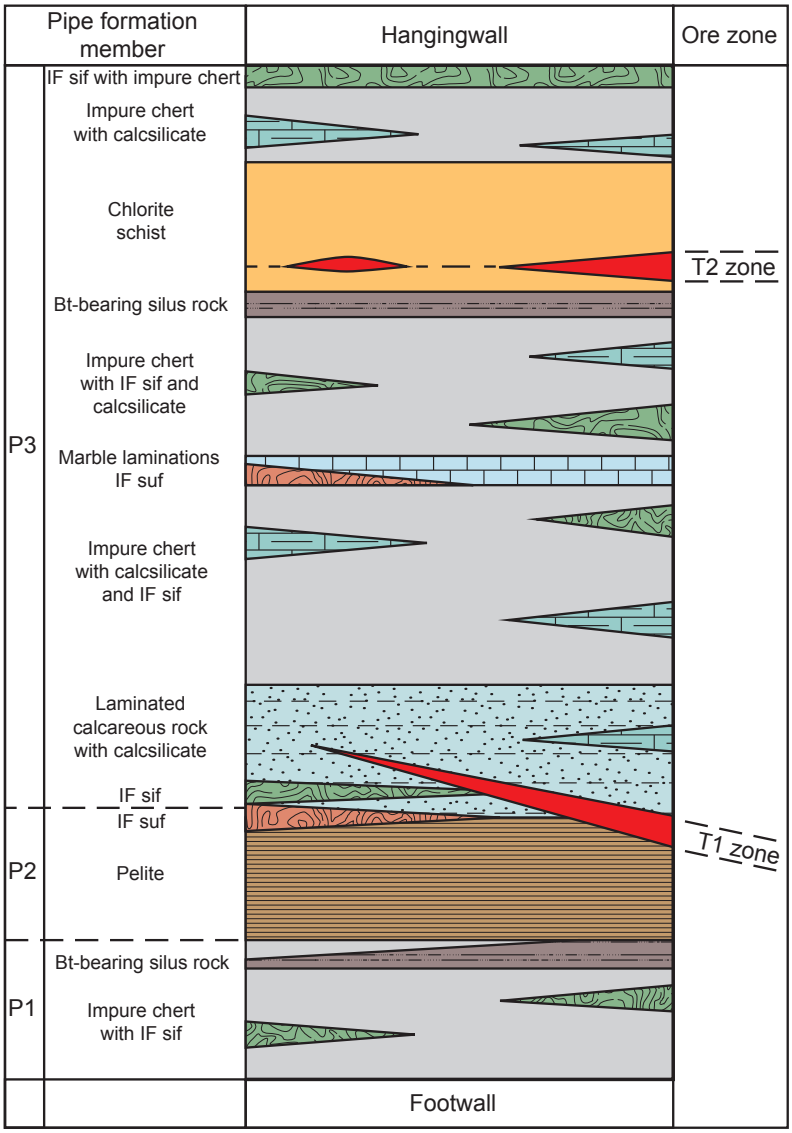

Figure GS2017-6-3: *Schematic lithostratigraphic section of the Pipe formation rocks hosting the Tower deposit. Abbreviations: Bt, biotite; IF sif, silicate-facies iron formation; IF suf, sulphide-facies iron formation; silus, siliceous.*

P2 member

Upsection from the siliceous rocks is a grey-brown, medium- to coarse-grained and diffusely layered pelitic schist (Figure GS2017-6-5a). The pelite can be 4–120 m thick, and is garnet bearing and enriched in muscovite and biotite. Staurolite occurs locally and the pelite locally becomes increasingly sulphidic in the uppermost part of the section. Spinel was identified in a thin section from the sulphidic portion of the pelite. Above the pelite is a 1.0–2.3 m thick sulphidic schist (Figure GS2017-6-5b) that is brown-grey, medium to coarse grained, gradationally banded and strongly magnetic in places. It is sulphide bearing and biotite and quartz rich, and is locally gradational into sulphidic chert.

The presence of iron formation on either side of the pelite (see P3 member) is a strong indicator that it is the Pipe formation P2 member. The sulphidic schist is likely correlative with a sulphide-facies iron formation of regional extent that marks the top of the P2 member (Bleeker, 1990; Zwanzig et al., 2007). This provides a good indicator that the sedimentary sequence is younging toward the east, from the footwall into the hangingwall of the deposit, and that the deposit remains structurally and stratigraphically upright.

P3 member

The sulphidic schist is locally overlain by silicate-facies iron formation (Figure GS2017-6-5b). The iron formation is grey to dark green, medium grained and strongly magnetic. It can be up to 3 m thick and is sulphide, grunerite, magnetite and biotite bearing, hornblende rich and siliceous. Magnetite forms discrete, equant porphyroblasts. The iron formation varies from relatively homogeneous to banded at a scale of <2 cm.

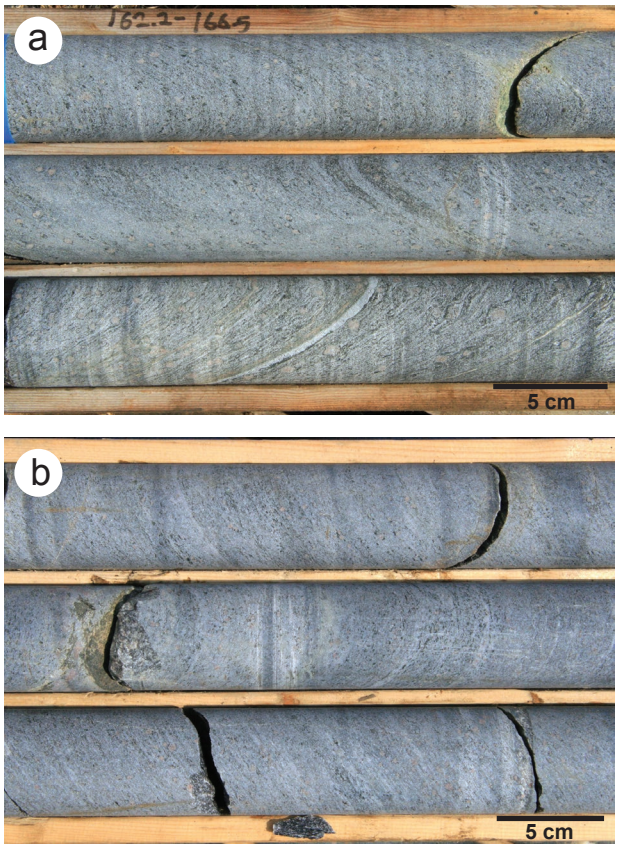

Figure GS2017-6-4: *P1 member rocks at the Tower deposit:* ***a)*** *garnet- and amphibole-bearing impure chert with incipient silicate-facies iron formation (bottom row; TP10-004, 162.2 m);* ***b)*** *garnet- and biotite-bearing siliceous rock (TP12-032, 578.6 m).*

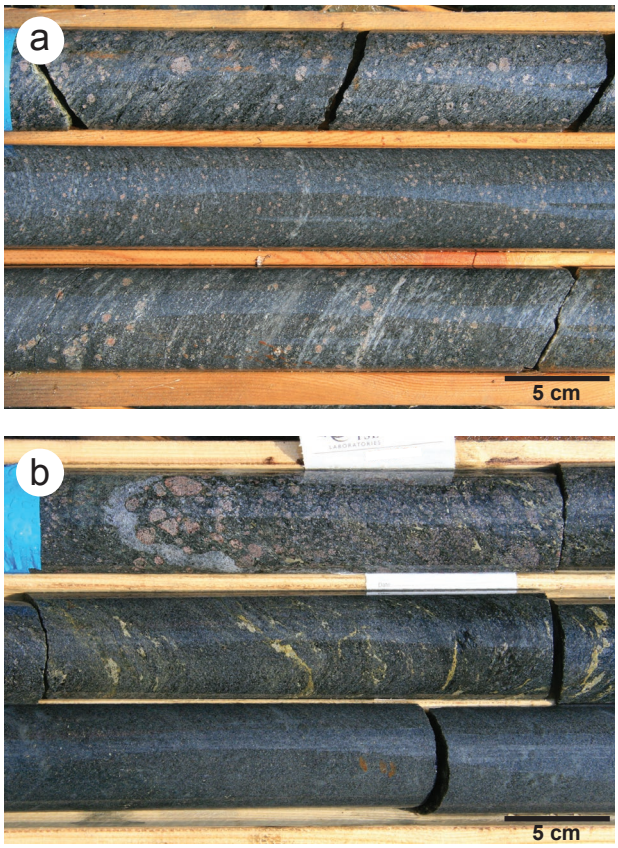

Figure GS2017-6-5: *P2 member rocks at the Tower deposit:* ***a)*** *garnet-bearing, muscovite- and biotite-rich pelitic schist (TP12-032, 573.6 m);* ***b)*** *sulphide- and garnet-bearing pelite (top row), sulphidic schist (middle row), and P3 member magnetite-bearing, silicate-facies iron formation (bottom row; TP10-004, 206.15 m).*

More typically, the sulphidic schist and pelite are overlain by an 8.9–38 m thick sequence of laminated calcareous rock (Figure GS2017-6-6a). The rock is grey-green, medium grained and weakly magnetic in places. It is typically laminated, but local zones can have diffuse bands <20 cm thick. The rock is siliceous, biotite bearing and hornblende rich. Local layers can be garnet bearing or clinozoisite bearing, and minor sulphide can be present. Intercalations of calcsilicate occur as clinozoisite-rich bands <10 cm thick. The calcsilicate varies from layered to mottled.

The calcareous rock is overlain by a thick (54–100 m) sequence of impure chert with intercalations of calcsilicate, silicate-facies iron formation and biotite-bearing siliceous rock (Figure GS2017-6-6b). The impure chert is typically grey to green-grey, medium to coarse grained, nonmagnetic and laminated to crudely layered on a scale <3 m. The chert is typically garnet bearing and siliceous with varying proportions of hornblende and biotite. The hornblende and biotite combined generally make up <30% of the rock. Local layers may be clinozoisite bearing. The chert locally grades into bands of silicate-facies iron formation <2.5 m thick. The iron formation is dark green-grey and contains a greater amount of garnet and hornblende (up to 40%) than the impure chert. Laminations of stringy chert are locally present within the iron formation (Figure GS2017-6-6b). The calcsilicate occurs as light green-grey, mottled to layered bands <20 cm thick. The calcsilicate is typically rich in clinozoisite±tremolite, with minor carbonate. The siliceous rock occurs as bands <40 cm thick that are garnet bearing and biotite rich with little to no hornblende. Sparse laminations of carbonate can be present within this sequence and become more abundant toward the upper contact.

The impure chert is locally overlain by a thin (25–85 cm) sulphide-facies iron formation (Figure GS2017-6-6c). The iron formation is brown-grey, fine to medium grained and weakly to moderately magnetic. The composition varies from a sulphide- and biotite-rich siliceous rock to a biotite- and hornblende-bearing, grunerite- and sulphide-rich rock.

Laminations and thin layers (<1 cm) of carbonate appear to form a local marker horizon at the Tower property (Figure GS2017-6-6d). These layers commonly occur in clusters within impure chert, just above the sulphide-facies iron formation when present. The carbonate layers are commonly interlayered

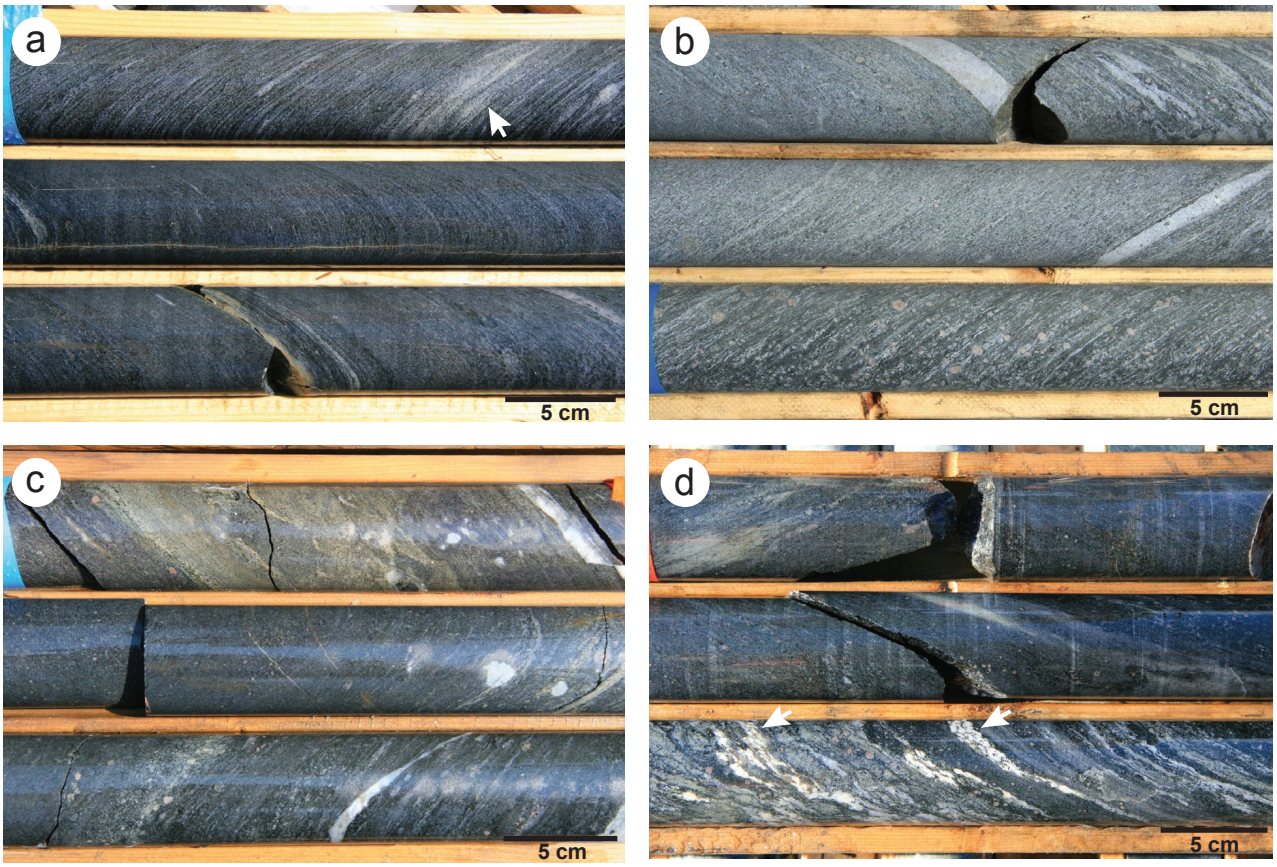

Figure GS2017-6-6: *P3 member rocks at the Tower deposit:* ***a)*** *amphibole-rich, laminated calcareous rock with diffuse clinozoisite-rich calcsilicate band (arrow; TP10-004, 227.1 m),* ***b)*** *garnet-bearing and amphibole-rich impure chert (top two rows) and iron formation with stringy chert laminations (bottom row; TP10-004, 274.5 m);* ***c)*** *sulphide-facies iron formation (top row) and impure chert (bottom two rows; TP12-032, 425.5 m),* ***d)*** *impure chert with diffuse bands of calcsilicate and thin carbonate layers (arrows; TP12-033, 350.5 m).*

with clinozoisite-rich and locally garnet-bearing calcsilicate. The impure chert sequence continues above the carbonate layers for an additional 64–150 m, and is similar to the sequence described below the sulphide-facies iron formation.

The impure chert is overlain by a 7–34 m thick sequence of garnet- and hornblende-bearing, biotite-rich siliceous rock (Figure GS2017-6-7a). The siliceous rock is brown-grey, medium grained and moderately magnetic in places. Chlorite and magnetite are present in minor amounts. The siliceous rock is interbedded with layers of impure chert, <2 m thick, which are generally enriched in clinozoisite. Local layers of silicate-facies iron formation, <1 m thick, can be present. The iron formation is strongly magnetic, garnet and magnetite bearing, and rich in grunerite. The magnetite occurs as discrete equant grains (Figure GS2017-6-7a). The siliceous rock grades over 3–5 m into the overlying chlorite schist.

The chlorite schist is the uppermost unit in two of the three drillholes collared in the hangingwall. Drillhole TP12-032 intersected the entire interval of schist, which is approximately 42 m thick. It is dark green to purplish green to brown, coarse grained, crudely banded on a scale of <50 cm, variably magnetic and compositionally heterogeneous (Figure GS2017-6-7b). The schist is typically quartz and chlorite rich with variable amounts of garnet, staurolite, magnetite and biotite, and minor sulphide±carbonate, hornblende and muscovite. Garnet porphyroblasts up to 10 cm across locally form up to 70% of the rock. Quartz occurs as discrete laminations, layers and pods <10 cm thick. A sulphidic horizon up to 4 m thick occurs near the base of the unit (Figure GS2017-6-7c). The contact between the chlorite schist and overlying impure chert is gradational over approximately 1 m (Figure GS2017-6-7d).

The units above the chlorite schist are described from drillhole TP12-032, and their continuity along strike is not known. The chlorite schist is overlain by a 14 m thick sequence of impure chert with intercalations of calcsilicate, <40 cm thick, that are most abundant toward the base of the unit. The impure chert is green-grey, fine to medium grained and magnetic in places. It varies from laminated to diffusely banded at a scale of <5 cm. The rock is siliceous, typically garnet bearing and hornblende rich with varying amounts of biotite and clinozoisite. The calcsilicate is light greenish yellow, fine grained and locally magnetic.

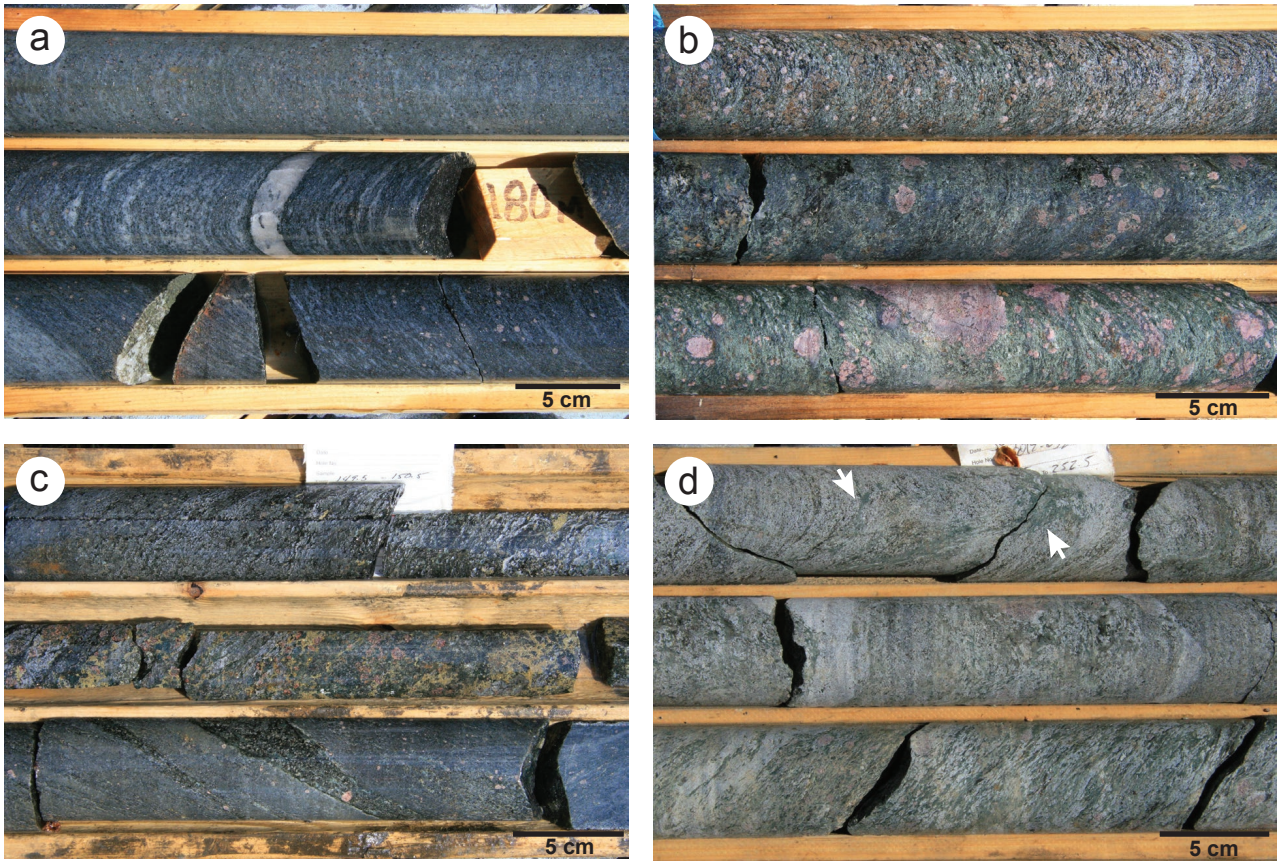

*Figure **GS2017-6-7:** P3 member rocks at the Tower deposit: **a)** magnetite-bearing, silicate-facies iron formation (top row) and garnet- and biotite-bearing siliceous rock (bottom two rows; TP12-027, 178.4 m); **b)** garnet-bearing and staurolite-rich chlorite schist (top row) grading into garnet-rich chlorite schist (bottom row; TP12-032, 285.85 m); **c)** chlorite schist with pods of semimassive sulphide from the T2 zone (middle row; TP12-033, 149.3 m); **d)** diffuse chlorite-rich bands in impure chert (arrows, top row) overlying chlorite schist (bottom two rows; TP12-032, 251.4 m).*

It is diffusely layered to massive, biotite bearing and clinozoisite rich with minor carbonate.

The impure chert is overlain by a sequence of silicate-facies iron formation and impure chert at least 11 m thick. The iron formation is dark brown-grey, medium grained and locally magnetic. It is laminated to layered with local stringy chert laminations; sulphide, biotite and garnet bearing; and hornblende rich. The iron formation is compositionally gradational into impure chert, which forms bands <2 m thick intercalated throughout the sequence. The chert is grey, fine to medium grained and nonmagnetic. It consists of a garnet- and hornblende-bearing siliceous rock with minor biotite.

The progression from pelite to sulphide-facies iron formation (see P2 member) to a sequence of predominantly chert, silicate-facies iron formation and calcsilicate suggests that the latter sequence represents the Pipe formation P3 member (Bleeker, 1990; Zwanzig et al., 2007). The silicate-facies iron formation with stringy chert laminations is similar to iron formation with stringy or 'ornamental' chert occurring in the lower part of the P3 member at the Pipe II mine (Macek and Bleeker, 1989). The carbonate laminations and layers that form a local marker horizon at the Tower deposit may represent incipient carbonate deposition correlative with the P3 member dolomite present along the Pipe mine–Birchtree mine trend in the exposed TNB. Although the carbonate layers and laminations appear to be conformable, they could represent carbonate veins that formed during diagenesis or during early prograde metamorphism and became transposed during the D_2 and D_3 deformation events.

The chlorite schist does not to correlate with any known part of the Ospwagan group sequence. No feldspar is present in thin sections of the schist, suggesting very low concentrations of Na. Calcium is likely present in only small amounts, contained in the minor amounts of carbonate. The K content is likely variable, contained within biotite and the minor amounts of muscovite. High concentrations of Mg-Fe and Al are suggested by the abundance of chlorite, garnet and staurolite. Overall, the mineral assemblage of the schist is that of a rock low in alkalis (especially Na and Ca) and rich in Al, Mg and Fe. Rocks of this bulk composition are characteristic of the proximal hydrothermal alteration zones associated with VMS deposits (Lydon, 1988; Franklin et al., 2005; Bailes et al., 2016; Buschette and Piercy, 2016). It should be noted that the sulphidic horizon toward the base of this unit is coincident with the T2

zone mineralization in drillhole TP12-027 (Assessment File 63G13256). The chlorite schist appears to be conformable with the Pipe formation stratigraphy; however, it is possible that it could be a discordant conduit that was transposed during the D_2 and D_3 phases of deformation. The gradational nature of the upper and lower contacts of this unit could indicate the waning influence of the hydrothermal fluids away from the alteration horizon or conduit (Figure GS2017-6-7d).

Intrusions

The Ospwagan group stratigraphy was intruded by various igneous bodies ranging in composition from ultramafic to felsic. Ultramafic schist, likely representing altered bodies of peridotite, occurs at various stratigraphic levels within the P3 member (Figure GS2017-6-8a) in intersections ranging from 10–100 m long. The ultramafic schist is pale grey-green, medium to coarse grained and weakly to strongly magnetic. It typically consists of varying amounts of talc, anthophyllite, chlorite, carbonate and serpentine, with minor magnetite and carbonate. The ultramafic schist commonly grades into ultramafic amphibolite at the margins, possibly representing a pyroxenitic envelope. It is possible that the ultramafic bodies intersected in holes TP10-003 and TP12-033 are correlative; however, it is not possible to correlate the host stratigraphy.

Bands of plagioclase amphibolite were intersected in all drillholes and occur at all stratigraphic levels (Figure GS2017-6-8b). The amphibolite is dark green-grey, medium to coarse grained, relatively homogeneous and nonmagnetic. Minor biotite, and rarely garnet, can be present. Although generally <6 m long, an intersection of amphibolite in hole TP10-003 was approximately 113 m long. The plagioclase amphibolite is interpreted as metamorphosed diabase and gabbro dikes, likely related to the Molson dike swarm (Heaman et al., 2009), or possibly one of the older Paleoproterozoic dike swarms of the northwestern Superior province (Heaman and Corkery, 1996; Halls and Heaman, 2000).

Small granitoid dikes <2 m thick occur sporadically in the core. An intersection of granodiorite >73 m long occurs directly below the Phanerozoic unconformity in hole TP12-032 (Figure GS2017-6-8c). The granodiorite is biotite and muscovite bearing and strongly foliated to protomylonitic. The intrusion could be related to the nearby William Lake dome (Layton-Matthews et al., 2007).

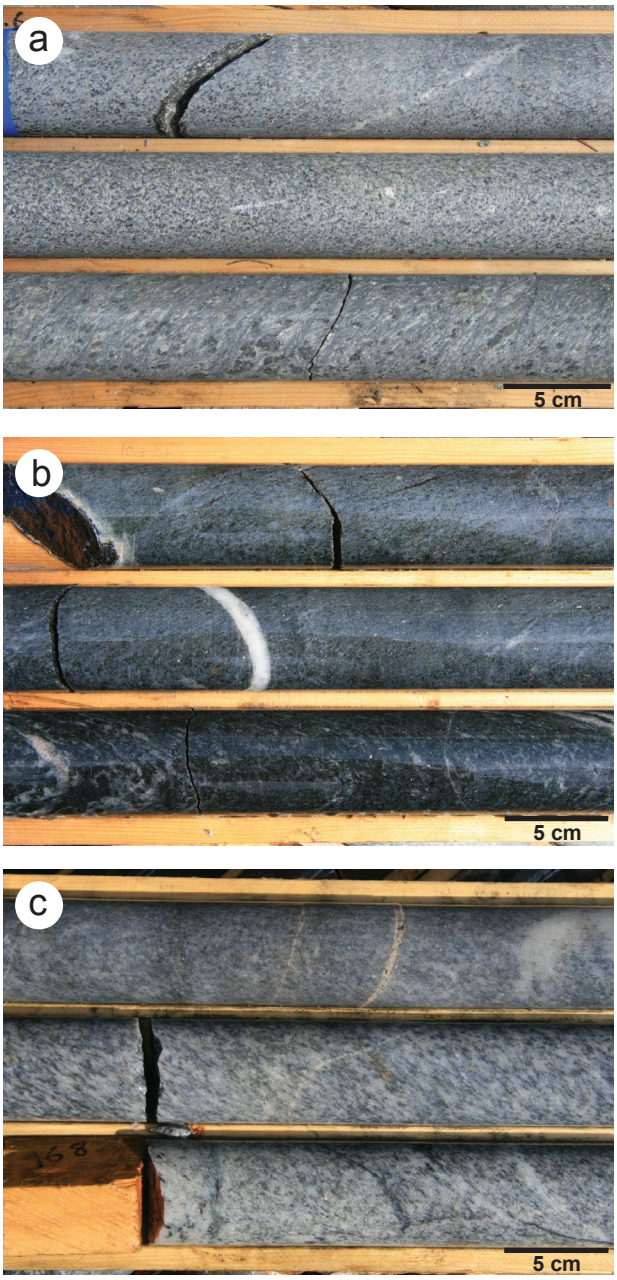

Figure GS2017-6-8: *Intrusive rocks at the Tower deposit:* ***a)*** *altered peridotite now represented by talc- and anthophyllite-rich ultramafic schist (TP10-003, 566.45 m);* ***b)*** *gabbro dike now represented by plagioclase amphibolite (TP10-003, 183.85 m;* ***c)*** *high-strain granodiorite (TP12-032, 167.6 m).*

Mineralization

The main focus of this study is the rocks that host the Tower deposit; however, the mineralization of the T1 and T2 zones is discussed here briefly in relation to the stratigraphy. For more information regarding mineralization and resource estimates, the reader is referred to Assessment Files 63G1148 and 63G13256, and Caracle Creek International Consulting Inc. (2013).

T1 zone

The nature of the T1 zone mineralization varies along strike from that of a sulphidic schist with foliation-parallel sulphide stringers to solid sulphide. The sulphidic schist is typically biotite rich and contains up to 12% net-textured sulphide (Figure GS2017-6-9a). The solid sulphide occurs as the matrix to a breccia that contains rounded fragments of ultramafic amphibolite and rounded to angular fragments of white quartz and impure chert <7 cm across (Figure GS2017-6-9b).

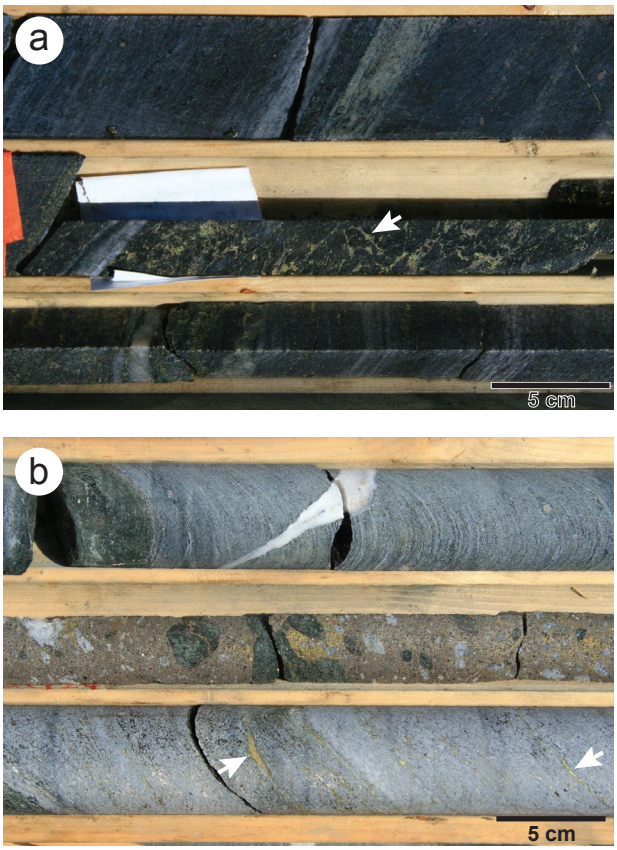

Figure GS2017-6-9: *Mineralization in the T1 zone of the Tower deposit:* ***a)*** *sulphidic schist with stringers of chalcopyrite and pyrrhotite (middle row, arrow indicates crosscutting veinlets of sulphide; TP12-027, 438.4 m);* ***b)*** *sulphide breccia with fragments of ultramafic amphibolite and white quartz (middle row); foliation-parallel stringers of chalcopyrite are visible in the laminated calcareous rock (arrows, bottom row; TP12-032, 565.7 m).*

The fragments are unsorted and matrix supported with rotated fabrics. The contacts of the breccia are locally marked by a seam of siliceous mylonite <5 mm thick. Local foliation-parallel stringers of chalcopyrite are present in the core up to 2 m away from the sulphide breccia. The T1 zone appears to be slightly discordant to the stratigraphy. In the northernmost intersection (TP12-027), the T1 zone occurs in place of the sulphide-facies iron formation, immediately above the P2 member pelite, whereas the mineralization in the southernmost intersection (TP10-003) occurs within the P3 member stratigraphy approximately 96 m above the upper contact of the P2 member pelite. The discordant nature of the mineralization and its occurrence as a sulphide breccia has led to the interpretation that the sulphide was mobilized from its source, forming a fault breccia (Assessment File 63G13256). The brittle-ductile nature of the structure suggests it likely belongs to the later D_3-D_4 phase of deformation.

T2 zone

Mineralization of the T2 zone occurs as disseminated sulphide blebs <1 cm across, and as stringers and pods of semisolid sulphide <5 cm across within the chlorite schist (Figure GS2017-6-7c). The stringers and pods typically have diffuse margins, parallel the foliation and appear to be concentrated toward the bottom of the chlorite schist unit. Of the selected drillcore, the T2 zone was only described from TP12-027 (Assessment File 63G13256); however, mineralization was also described from the same stratigraphic level in TP12-033, and weak Cu mineralization is present in TP12-032. This suggests that, although the T2 zone may pinch and swell, it appears to form a continuous horizon toward the bottom of the chlorite schist across the Tower property, suggesting that it may be stratiform and in situ.

Economic considerations

Volcanogenic massive-sulphide deposits of the pelitic-mafic lithofacies association, or Besshi type, are typically hosted in argillite and siltstone; and, to a lesser extent, in marl, chert and iron formation, intercalated with mafic flows, dikes or sills (Franklin et al., 2005; Piercey, 2011). The mafic magmas commonly have a mid-ocean ridge basalt (MORB) affinity, although magmas of alkali/ocean-island basalt affinity are also reported (Piercey, 2011). Deposits of this type are typically related to arc-rifting in oceanic environments (Franklin et al., 2005; Piercey, 2011). Regional semiconformable hydrothermal-alteration zones are poorly documented within the pelitic-mafic lithofacies association; however, footwall alteration zones with chlorite and quartz-sericite alteration are typically well developed and mineralized (Franklin et al., 2005). The association of potentially stratiform, in situ Cu-Zn mineralization with hydrothermally altered, low-alkali and high–Fe-Mg-Al rocks (T2 zone) strongly suggests that the Tower deposit is of VMS affinity. The pelite and chert-rich chemical sedimentary rocks that host the Tower deposit appear to be part of the Ospwagan group Pipe formation, intruded by mafic and ultramafic sills and dikes. Hostrocks of this type are suggestive of a pelitic-mafic lithofacies association, or Besshi-type, VMS deposit.

Volcanogenic massive-sulphide deposits form in areas of high heat flow, typically related to upwelling mafic magmas in extensional basins (Franklin et al., 2005; Galley et al., 2007; Piercey, 2011). The thinned crust and pooled mafic magmas provide the necessary heat to drive the hydrothermal circulation required to scavenge, transport and deposit base metals (Piercey, 2011). Mafic and ultramafic intrusive rocks are common in the stratigraphy that hosts the Tower deposit and are likely related to the ca. 1883 Ma Molson dike swarm and coeval ultramafic intrusions associated with magmatic Ni deposits in the TNB. Although not intersected in the drillcore at Tower, mafic to ultramafic volcanic rocks occur in the Bah Lake assemblage at the top of the Ospwagan group. Both of these suites are characterized by MORB-like trace-element signatures, which suggests relatively shallow partial melting of the mantle, likely in an extensional environment and accompanied by high heat flow. Hydrothermal activity sufficient to form VMS deposits could be associated with either suite of mafic-ultramafic rocks.

Cummingtonite-cordierite schist is reported from northern Setting Lake (Macek et al., 2006). Rocks of this composition

are commonly interpreted to result from metamorphism of intense chlorite alteration (Baldwin, 1976; Pan and Fleet, 1995; Peck and Smith, 2005; Zheng et al., 2011). Although the schist is hosted in the Setting formation, it is in spatial proximity to the Bah Lake assemblage, which could suggest a paragenetic relationship. The Bah Lake assemblage is most abundant in the Setting, Ospwagan, Liz, and Mystery lakes areas but has been largely avoided by exploration programs because of its stratigraphic position upsection from the more prospective Pipe formation. These areas may warrant more detailed study if the VMS mineralization at the Tower property is found to be paragenetic with the Bah Lake assemblage. Examples of Molson-age mafic and ultramafic dikes are ubiquitous in the TNB; if the Tower deposit is found to be contemporaneous with Molson-age intrusions, the entire strike length of the TNB could have notional potential for VMS deposits.

The relationship between the Bah Lake assemblage and the Molson and ultramafic magmatism is disputed. Bleeker (1990) and Zwanzig (2005) called for discrete periods of magmatism, with the Bah Lake volcanism occurring prior to ca. 1890 Ma (Zwanzig, 2005). Conversely, Heaman et al. (2009) considered the Molson-age intrusions to be feeders to the Bah Lake assemblage. In either scenario, the mafic magmatism largely postdates the sedimentation of the Ospwagan group. This has implications for the hydrothermal alteration and mineralization of the T2 zone. If the VMS system was contemporaneous with magmatism, the T2 zone must have formed after deposition of the Pipe formation. This implies that the T2 zone formed either through sub-seafloor replacement, as hydrothermal fluids percolated laterally through the Pipe formation, or the T2 zone represents a transposed footwall stringer zone. Regardless, the alteration and variably mineralized T2 zone can be traced along strike at the deposit scale.

The T1 zone consists of mobilized sulphide, likely within a later D_3-D_4 (brittle-ductile) structure. What remains unclear is the source of this mineralized sulphide. One possibility is that it was sourced from the T2 zone. In this scenario, the T1 zone should continue to climb, up-stratigraphy, to the southwest until it intersects the T2 zone. Another possibility is that the T1 zone is sourced from elsewhere in the stratigraphy. Of note is the relative proximity of the T1 zone to the regionally extensive sulphide-facies iron formation at the top of the P2 member. If this sulphide-rich horizon is the source of the mineralization, it would imply that this horizon could be prospective for VMS mineralization as well as magmatic Ni. Another possibility is that the T1 zone sulphide was sourced from farther up the stratigraphy, where sulphide mounds formed on the paleoseafloor.

Volcanogenic massive-sulphide deposits typically occur in clusters, around calderas or along linear rifts (Galley et al., 2007). The MORB-like character of the mafic magmas in the TNB is suggestive of an extensional environment. This, combined with the apparent lack of a volcanic edifice in the Tower property area, suggests that the VMS system likely developed along an extensional fault. Hence, there may be potential for additional deposits along strike. Although not on trend, intersections of anomalous Cu and Zn have been encountered in drillholes on the adjacent William Lake property (Beaudry, 2007), suggesting that VMS mineralization may well be more widespread than is currently recognized in the sub-Phanerozoic portion of the TNB.

Acknowledgments

The author thanks N. Clark, M. Stocking and S. Walker for providing enthusiastic field assistance; N. Brandson and E. Anderson for logistical support; and S. Anderson, S. Gagné and K. Reid for reviewing earlier versions of this manuscript. This project was made possible by Akuna Minerals Inc. and Rockcliff Copper Corporation, who provided access to the Tower property core. Thanks go to M. Lapierre for looking after our needs at the Rockcliff core-storage facility and for cutting samples. Special thanks are due to an anonymous mentor for discussions regarding the geology of the Ospwagan group and the sub-Phanerozoic TNB.

References

Bailes, A.H., Galley, A.G., Paradis, S. and Taylor, B.E. 2016: Variations in large synvolcanic alteration zones at Snow Lake, Manitoba, Canada, with proximity to associated volcanogenic massive sulphide deposits; Economic Geology, v. 111, p. 933–962.

Baldwin, D.A. 1976: Cordierite-anthophyllite rocks at Rat Lake, Manitoba: a metamorphosed alteration zone; Manitoba Mines, Resources and Environmental Management, Mineral Resources Division, Open File Report 76/1, 30 p.

Beaudry, C. 2007: Technical report on the William Lake property, Grand Rapids, Manitoba, Canada; NI 43-101 report prepared for Pure Nickel Inc., 133 p., URL <http://www.purenickel.com/i/pdf/wl_43101_techreport.pdf> [August 2017].

Bleeker, W. 1990: Evolution of the Thompson Nickel Belt and its nickel deposits, Manitoba, Canada; Ph.D. thesis, University of New Brunswick, Fredericton, New Brunswick, 400 p.

Böhm, C.O. 2005a: Bedrock geology of northern and central Wintering Lake, Manitoba (parts of NTS 63P5 and 12); *in* Report of Activities 2005, Manitoba Industry, Economic Development and Mines, Manitoba Geological Survey, p. 32–39.

Böhm, C. 2005b: Bedrock geology of northern and central Wintering Lake, Manitoba; Manitoba Industry, Economic Development and Mines, Manitoba Geological Survey, Manitoba Mining and Minerals Convention 2012, Winnipeg, Manitoba, November 17–19, 2005, poster presentation.

Böhm, C.O., Zwanzig, H.V. and Creaser, R.A. 2007: Sm-Nd isotopic technique as an exploration tool: delineating the northern extension of the Thompson Nickel Belt, Manitoba, Canada; Economic Geology, v. 102, p. 1217–1231.

Burnham, O.M., Halden, N., Layton-Matthews, D., Lesher, C.M., Liwanag, J., Heaman, L., Hulbert, L., Machado, N., Michalak, D., Pacey, M., Peck, D.C., Potrel, A., Theyer, P., Toope, K. and Zwanzig, H. 2009: CAMIRO project 97E-02, Thompson Nickel Belt: final report, March 2002, revised and updated 2003; Manitoba Science, Technology, Energy and Mines, Manitoba Geological Survey, Open File OF2008-11, 434 p. plus appendices and GIS shape files for use with ArcInfo®.

Buschette, M.J. and Piercey, S.J. 2016: Hydrothermal alteration and lithogeochemistry of the Boundary volcanogenic massive sulphide deposit, central Newfoundland, Canada; Canadian Journal of Earth Sciences, v. 53, p. 506–527.

Caracle Creek International Consulting Inc. 2013: Independent technical report, Tower property, Grand Rapids, Manitoba; Rockcliff Resources Inc., NI 43-101 technical report, 161 p.

Couëslan, C.G. 2014: Preliminary results from bedrock mapping in the Partridge Crop Lake area, eastern margin of the Thompson nickel belt, central Manitoba (parts of NTS 63P11, 12); *in* Report of Activities 2014, Manitoba Mineral Resources, Manitoba Geological Survey, p. 18–31.

Couëslan, C.G. and Pattison, D.R.M. 2012: Low-pressure regional amphibolite-facies to granulite-facies metamorphism of the Paleoproterozoic Thompson Nickel Belt, Manitoba; Canadian Journal of Earth Sciences, v. 49, p. 1117–1153.

Franklin, J.M., Gibson, H.L., Jonasson, I.R. and Galley, A.G. 2005: Volcanogenic massive sulphide deposits; *in* Economic Geology One Hundredth Anniversary Volume 1905–2005, J.W. Hedenquist, J.F.H. Thompson, R.J. Goldfarb and J.P. Richards (ed.), Society of Economic Geologists, p. 523–560.

Galley, A.G., Hannington, M.D. and Jonasson, I.R. 2007: Volcanogenic massive sulphide deposits; *in* Mineral Deposits of Canada: A Synthesis of Major Deposit-Types, District Metallogeny, the Evolution of Geological Provinces, and Exploration Methods, W.D. Goodfellow (ed.), Geological Association of Canada, Mineral Deposits Division, Special Publication 5, p. 141–161.

Guevara, V.E., Dragovic, B., Caddick, M.J., Kylander-Clark, A.R.C. and Couëslan, C.G. 2016a: Ultrahigh temperature metamorphism of the Archean Pikwitonei granulite domain; Geological Society of America, Annual Meeting, Denver, Colorado, September 25–28, 2016, Abstracts with Programs, v. 48, paper 270-4, URL <https://gsa.confex.com/gsa/2016AM/webprogram/Paper284904.html> [August 2017].

Guevara, V., MacLennan, S.A., Schoene, B., Dragovic, B., Caddick, M.J., Kylander-Clark, A.R. and Couëslan, C.G. 2016b: Quantifying the timescales of Archean UHT metamorphism through U-Pb monazite and zircon petrochronology; American Geophysical Union, Fall Meeting, San Francisco, California, December 12–16, 2016, abstract V51B-07, URL <https://agu.confex.com/agu/fm16/meetingapp.cgi/Paper/175259> [August 2017].

Halls, H.C. and Heaman, L.M. 2000: The paleomagnetic significance of new U-Pb age data from the Molson dyke swarm, Cauchon Lake area, Manitoba; Canadian Journal of Earth Sciences, v. 37, p. 957–966.

Heaman, L.M. and Corkery, T. 1996: U-Pb geochronology of the Split Lake Block, Manitoba: preliminary results; LITHOPROBE Trans-Hudson Orogen Transect, Report of Sixth Transect Meeting, Saskatoon, Saskatchewan, April 1–2, 1996, LITHOPROBE Secretariat, University of British Columbia, Vancouver, British Columbia, Report 55, p. 60–68.

Heaman, L.M., Böhm, C.O., Machado, N., Krogh, T.E., Weber, W. and Corkery, M.T. 2011: The Pikwitonei Granulite Domain, Manitoba: a giant Neoarchean high-grade terrane in the northwest Superior Province; Canadian Journal of Earth Sciences, v. 48, p. 205–245.

Heaman, L.M., Peck, D. and Toope, K. 2009: Timing and geochemistry of 1.88 Ga Molson Igneous Events, Manitoba: insights into the formation of a craton-scale magmatic and metallogenic province; Precambrian Research, v. 172, p. 143–162. doi:10.1016/j.precamres.2009.03.015

Hubregtse, J.J.M.W. 1980: The Archean Pikwitonei granulite domain and its position at the margin of the northwestern Superior Province (central Manitoba); Manitoba Energy and Mines, Manitoba Geological Survey, Geological Paper GP80-3, 16 p.

Layton-Matthews, D., Lesher, C.M., Burnham, O.M., Liwanag, J., Halden, N.M., Hulbert, L., and Peck, D.C. 2007: Magmatic Ni-Cu-platinum-group element deposits of the Thompson nickel belt; *in* Mineral Deposits of Canada: A Synthesis of Major Deposit-Types, District Metallogeny, the Evolution of Geological Provinces, and Exploration Methods, W.D. Goodfellow (ed.), Geological Association of Canada, Mineral Deposits Division, Special Publication 5, p. 409–432.

Lydon, J.W. 1988: Volcanogenic massive sulphide deposits, part 1: a descriptive model; *in* Ore Deposit Models, R.G. Roberts and P.A. Sheahan (ed.), Geological Association of Canada, Geoscience Canada, Reprint Series 3, p. 145–153.

Macek, J.J. and Bleeker, W. 1989: Thompson Nickel Belt project – Pipe pit mine, Setting and Ospwagan lakes; *in* Report of Field Activities 1989, Manitoba Energy and Mines, Minerals Division, p. 73–87.

Macek, J.J., Zwanzig, H.V. and Pacey, J.M. 2006: Thompson nickel belt geological compilation map, Manitoba (parts of NTS 63G, J, O, P and 64A and B); Manitoba Science, Technology, Energy and Mines, Manitoba Geological Survey, Open File Report OF2006-33.

Mezger, K., Bohlen, S.R. and Hanson, G.N. 1990: Metamorphic history of the Archean Pikwitonei granulite domain and the Cross Lake subprovince, Superior Province, Manitoba, Canada; Journal of Petrology, v. 31, p. 483–517.

Pan, Y. and Fleet, M.E. 1995: Geochemistry and origin of cordierite-orthoamphibole gneiss and associated rocks at an Archean volcanogenic massive sulphide camp, Manitouwadge, Ontario, Canada; Precambrian Research, v. 74, p. 73–89.

Peck, W.H. and Smith, M.S. 2005: Cordierite-gedrite rocks from the Central Metasedimentary Belt boundary thrust zone (Grenville Province, Ontario): Mesoproterozoic metavolcanic rocks with affinities to the Composite Arc Belt; Canadian Journal of Earth Sciences, v. 42, p. 1815–1828.

Piercey, S.J. 2011: The setting, style, and role of magmatism in the formation of volcanogenic massive sulphide deposits; Mineralium Deposita, v. 46, p. 449–471.

Rockcliff Resources Inc. 2012: Rockcliff reports discovery of new copper zone at Tower: additional DPEM anomalies identified with copper potential; Rockcliff Resources Inc., news release, May 23, 2012, URL <http://www.sedar.com/search/search_en.htm> [August 2017].

Scoates, J.S., Scoates, J.R.F., Wall, C.J., Friedman, R.M. and Couëslan, C.G. 2017: Direct dating of ultramafic sills and mafic intrusions associated with Ni-sulfide mineralization in the Thompson nickel belt, Manitoba, Canada; Economic Geology, v. 112, p. 675–692.

Simard, R-L., McGregor, C.R., Rayner, N., and Creaser, R.A. (2010): New geological mapping, geochemical, Sm-Nd isotopic and U-Pb age data for the eastern sub-Phanerozoic Flin Flon belt, west-central Manitoba (parts of NTS 63J3-6, 11, 12, 14, 63K1-2, 7–10); *in* Report of Activities 2010, Manitoba Innovation, Energy and Mines, Manitoba Geological Survey, p. 69–87.

Tinkham, D.K. and Karlapalem, N. 2008: Hydrothermal alteration and metamorphism of the Sherridon structure, Sherridon area, Manitoba (part of NTS 63N3); *in* Report of Activities 2008, Manitoba Science, Technology, Energy and Mines, Manitoba Geological Survey, p. 79–86.

White, D.J., Lucas, S.B., Bleeker, W., Hajnal, Z., Lewry, J.F. and Zwanzig, H.V. 2002: Suture-zone geometry along an irregular Paleoproterozoic margin: the Superior boundary zone, Manitoba, Canada; Geology, v. 30, p. 735–738.

Zheng, Y.C., Gu, L., Tang, X., Wu, C., Li, C. and Liu, S. 2011: Geology and geochemistry of highly metamorphosed footwall alteration zones in the Hongtoushan volcanogenic massive sulphide deposit, Liaoning Province, China; Resource Geology, v. 61, p. 113–139.

Zwanzig, H.V. 2005: Geochemistry, Sm-Nd isotope data and age constraints of the Bah Lake assemblage, Thompson Nickel Belt and Kisseynew Domain margin: relation to Thompson-type ultramafic bodies and a tectonic model (NTS 63J, O and P); *in* Report of Activities 2005, Manitoba Industry, Economic Development and Mines, Manitoba Geological Survey, p. 40–53.

Zwanzig, H.V., Macek, J.J. and McGregor, C.R. 2007: Lithostratigraphy and geochemistry of the high-grade metasedimentary rocks in the Thompson Nickel Belt and adjacent Kisseynew Domain, Manitoba: implications for nickel exploration; Economic Geology, v. 102, p. 1197–1216.

GS2017-7

Sub-Phanerozoic basement geology south of Wekusko Lake, eastern Flin Flon belt, north-central Manitoba (parts of NTS 63J5, 12, 63K8, 9): insights from drillcore observations and whole-rock geochemistry of mafic rocks

by K.D. Reid

In Brief:

- Basaltic rocks south of Wekusko Lake are chemically analogous to modern juvenile arc and mid-ocean ridge basalts
- Prospective stratigraphy, including felsic volcanic rocks, extends along strike from the Kofman deposit
- Mafic volcanic associations locally contain orogenic-style gold mineralization

Citation:
Reid, K.D. 2017: Sub-Phanerozoic basement geology south of Wekusko Lake, eastern Flin Flon belt, north-central Manitoba (parts of NTS 63J5, 12, 63K8, 9): insights from drillcore observations and whole-rock geochemistry of mafic rocks; *in* Report of Activities 2017, Manitoba Growth, Enterprise and Trade, Manitoba Geological Survey, p. 65–77.

Summary

Twenty-five historical exploration drillcores from the area south and east of Wekusko Lake were re-examined over a three-week period in the summer of 2017. Data from 20 of these drillcores were combined with data from 18 drillcores examined during the 2016 field season to provide wide-spaced coverage over a large area south of Wekusko Lake, roughly equivalent to a 1:50 000 map area. This work is part of a broader project to create a series of 1:50 000 scale maps for the eastern portion of the sub-Phanerozoic Flin Flon belt. These maps will provide new data to constrain poorly understood geology and better inform exploration models. Four drillcores from east of the current study area facilitated a preliminary investigation of the geology in the adjacent map sheet, whereas the review of one drillcore from the Watts River volcanogenic massive-sulphide (VMS) deposit allowed examination of hostrocks and the collection of one sample for U-Pb dating. The objectives of this season's fieldwork were to 1) document the rock types in the eastern and southern portions of the map area; 2) obtain additional whole-rock geochemical data for volcanic and plutonic rocks not covered by previous regional compilations in order to facilitate correlations; and 3) identify samples suitable for U-Pb dating within both volcanic and sedimentary sequences.

Introduction

The Flin Flon belt (FFB) consists of a series of oceanic assemblages that were formed and tectonically juxtaposed during closure of the Proterozoic Manikewan Ocean (e.g., Stauffer, 1984; Syme and Bailes, 1993), and is one of a series of belts that make up the internal Reindeer zone of the Paleoproterozoic Trans-Hudson orogen (Lewry and Collerson, 1990). Volcanic assemblages (ca. 1.9–1.8 Ga) include juvenile island-arc, juvenile ocean-floor/back-arc, and ocean-island basalt (Syme et al., 1999). Following the accretion of oceanic volcanic assemblages was the emplacement of 'successor'-arc plutons (1.87–1.83 Ga; e.g., Whalen et al., 1999). Fluvial-alluvial sandstone and conglomerate of the Missi group (1.85–1.83 Ga) unconformably overlie older volcanic rocks (e.g., Ansdell et al., 1992; Syme et al., 1999). Burntwood group (1.85–1.84 Ga) greywacke and argillite is considered the lateral facies equivalents to the Missi group (e.g., Ansdell et al., 1995).

The FFB is one of the most prolific volcanogenic massive-sulphide (VMS)–hosting greenstone belts in the world, with the majority of deposits hosted by arc and arc-rift volcanic sequences (Syme et al., 1999). Exploration in the FFB has matured from prospecting in the exposed portions to deep-penetrating airborne geophysical surveys coupled with diamond drilling in areas with little or no exposure. Airborne geophysical surveys (magnetic and electromagnetic) flown within the past 25 years can resolve differences in magnetic susceptibility and conductivity beneath as much as 300 m of cover, allowing exploration to proceed in areas overlain by Phanerozoic strata. As a result, several VMS deposits have been discovered beneath Phanerozoic cover since the mid 1990s. However, when plotted on existing geological maps, several of these VMS deposits coincide with areas identified as being predominantly sedimentary, such as the East Kisseynew domain (e.g., Watts River, Harmin, Fenton and Talbot deposits; Figure GS2017-7-1), rather than being associated with volcanic domains similar to those that host major VMS deposits in the exposed portion of the FFB. This has brought into focus the need for updated geological maps for the sub-Phanerozoic portion of the eastern FFB. A new mapping program involving re-examination of exploration drillcore and compilation of geochemical and geophysical data is currently underway to facilitate a better understanding of the basement geology in the covered portion of the FFB and its economic potential.

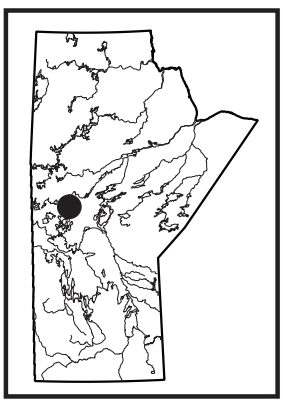

Previous work in the south Wekusko Lake area

The eastern FFB includes both exposed and sub-Phanerozoic portions (Figure GS2017-7-1). The exposed portion is subdivided into tectonostratigraphic assemblages on the basis of bedrock

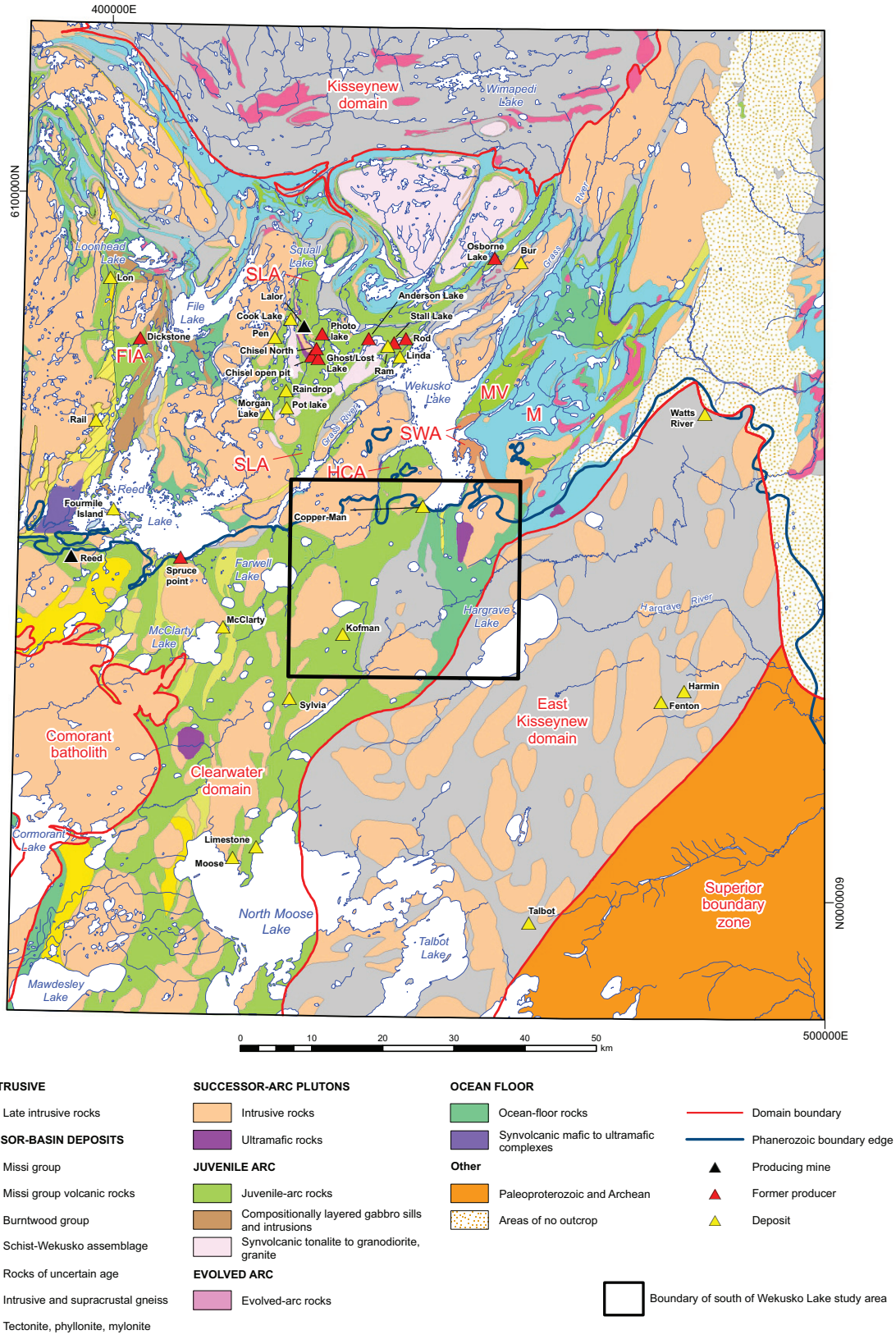

LATE INTRUSIVE
- Late intrusive rocks

SUCCESSOR-BASIN DEPOSITS
- Missi group
- Missi group volcanic rocks
- Burntwood group
- Schist-Wekusko assemblage
- Rocks of uncertain age
- Intrusive and supracrustal gneiss
- Tectonite, phyllonite, mylonite

SUCCESSOR-ARC PLUTONS
- Intrusive rocks
- Ultramafic rocks

JUVENILE ARC
- Juvenile-arc rocks
- Compositionally layered gabbro sills and intrusions
- Synvolcanic tonalite to granodiorite, granite

EVOLVED ARC
- Evolved-arc rocks

OCEAN FLOOR
- Ocean-floor rocks
- Synvolcanic mafic to ultramafic complexes

Other
- Paleoproterozoic and Archean
- Areas of no outcrop

- Domain boundary
- Phanerozoic boundary edge
- Producing mine
- Former producer
- Deposit
- Boundary of south of Wekusko Lake study area

Figure GS2017-7-1: *Generalized geology of the exposed and sub-Phanerozoic eastern Flin Flon belt, showing major tectonostratigraphic assemblages/domains and volcanogenic massive-sulphide deposits (modified from Leclair and Viljoen, 1997; NATMAP Shield Margin Project Working Group, 1998). Box outlines the south Wekusko Lake study area in GS2017-7-2. Exposed tectonostratigraphic assemblages: FIA, Fourmile Island assemblage; HCA, Hayward Creek assemblage, M, Missi group; MV, Missi group volcanic rocks; SLA, Snow Lake assemblage; SWA, Schist-Wekusko assemblage. Thick red lines define sub-Phanerozoic domains.*

mapping (e.g., Syme et al., 1995; Bailes and Galley, 2007) whereas Leclair et al. (1997) subdivided the sub-Phanerozoic portion into three domains on the basis of geophysical mapping: the Cormorant batholith, the Clearwater domain and the East Kisseynew domain (GS2017-7-1). The Clearwater domain consists of relatively lower grade (greenschist to lower-amphibolite facies) volcanic rocks that vary in composition from mafic to felsic and include different depositional facies. Farther east in the East Kisseynew domain, the metamorphic grade increases dramatically to upper-amphibolite facies, such that primary textures are obscured and protolith identification is difficult. Nevertheless, this domain is thought to consist of highly recrystallized Burntwood group turbidites and plutons (Figure GS2017-7-1).

Figure GS2017-7-2 shows the simplified geology of the exposed portion of the eastern FFB based on mapping (e.g., Gilbert and Bailes, 2005; Bailes and Galley, 2007). Gilbert and Bailes (2005) described the geology of the southern half of Wekusko Lake and outlined five tectonostratigraphic blocks from west to east: 1) Hayward Creek assemblage of juvenile-arc affinity; 2) Burntwood group turbidites; 3) South Wekusko assemblage of ocean-floor affinity; 4) Schist-Wekusko assemblage of successor-arc affinity; and 5) Missi group sandstone and conglomerate (Figure GS2017-7-2). Multiple large intrusions of successor-arc age (1.87–1.83 Ga) intrude and some cases stitch the stratigraphic assemblages.

The Hayward Creek assemblage, consisting of arc-volcanic, intrusive and sedimentary rocks, forms a lozenge south of Goose Bay and is bounded to the west by Hayward Creek before extending south beneath Phanerozoic cover (Figure GS2017-7-2). The age of the Hayward Creek assemblage is uncertain but it has many similarities to the Snow Lake assemblage (Gilbert and Bailes, 2005). At the core of the Hayward Creek assemblage is the Southwest Wekusko Lake pluton, which varies from granodiorite to diorite (Figure GS2017-7-2).

Burntwood group greywacke and mudstone, interpreted to be in thrust contact with the Hayward Creek assemblage, is observed along the western shoreline (and on some islands) of Wekusko Lake near Goose Bay. At the southern end of Wekusko Lake, a package, <1 km wide at the lakeshore, widens and extends approximately 25 km to the south (Figure GS2017-7-2).

East of the Burntwood group at the south end of Wekusko Lake is a sequence of pillowed basalt flows and related gabbro sills, which are geochemically akin to the 1.90 Ga Elbow-Athapapuskow and Northeast Reed ocean-floor basalt assemblages (Stern et al., 1995b; Syme et al., 1995). These rocks are termed the South Wekusko assemblage by Gilbert and Bailes (2005).

The Crowduck Bay fault is a crustal-scale fault that can be traced to the north of Broad Bay before trending northeast in Crowduck Bay (Figure GS2017-7-2). Toward the north, it separates Burntwood group turbidites from Schist-Wekusko assemblage successor-arc volcanic rocks, and younger Missi group volcanic and sedimentary rocks (Connors and Ansdell, 1994; Ansdell et al., 1999; Gilbert and Bailes, 2005). At the south end of Wekusko Lake, the Crowduck Bay fault is a phyllonitic package of chlorite-carbonate schist within the South Wekusko assemblage, and extends beneath the Phanerozoic cover (Figure GS2017-7-2).

Drillcore examination

Twenty-five historical exploration drillcores from the area south and east of Wekusko Lake were re-examined over a three-week period in the summer of 2017. Data from these historical exploration drillcores were combined with data from 18 drillcores examined during the 2016 field season (Reid and Gagné, 2016). Drillcore observations from 25 of these drillholes are discussed with reference to the Clearwater and East Kisseynew domains (Leclair et al., 1997; Figures GS2017-7-1, -2). Clearwater domain rocks are subdivided into four lithological associations: bimodal volcanic; mafic-dominated; plutonic; and sedimentary. Only bimodal volcanic, mafic-dominated and plutonic associations are described in this report. Due to heterogeneity between drillcores, rocks of the East Kisseynew domain are not presently subdivided.

Drillholes near the western edge of the study area in the Clearwater domain, which were examined by Gagné (2015, GS2017-9, this volume), are briefly mentioned and shown in Figure GS2017-7-2.

Clearwater domain

Bimodal volcanic association

Drillcores CP-11-017, 94-15 and SL91-7 (Assessment files 63J1159, 72778, 72326, Manitoba Growth, Enterprise and Trade, Winnipeg) all contain significant intervals (25–100 m) of weakly to moderately strained, intermediate to felsic volcaniclastic rocks (crystal tuff to heterolithic tuff breccia) that show moderate pervasive epidote-silica and local discordant chlorite-carbonate alteration (Figure GS2017-7-3a, b).

The upper half (94.7–247.3 m) of drillcore CP-11-017 is a thick sequence of moderately to strongly foliated quartz-phyric dacite, which is separated from heterolithic lapilli tuff in the lower part of the drillcore (320.0–422.8 m) by a package of graphitic greywacke and argillite (247.3–320.0 m). Between 372.7 and 403.0 m a fine- to medium-grained, leucocratic granodiorite is present. The last two metres of the drillcore (422.8–425.0 m) is a moderately foliated, equigranular, medium-grained mesocratic gabbro.

The upper portion of drillcore 94-15 is a massive, dark green, aphanitic basalt flow that contains scattered 0.2–1 cm quartz amygdules before gradationally becoming a heterolithic breccia (the mafic matrix of the breccia also contains amygdules—flow-top breccia, intrusion breccia or peperite?) at 102.0 m. The heterolithic breccia contains angular, light grey, aphanitic, felsic fragments (20%; 1–15 cm) and subangular epidote-altered mafic fragments (30%; 2–10 cm) in a silicified feldspar-pyroxene crystal tuff matrix. This breccia grades into a thick sequence (128–195.5 m) of intermediate to felsic ash tuff/greywacke, which contains local centimetre-scale seams of pyrite and graphite, the lower contact to this unit is marked

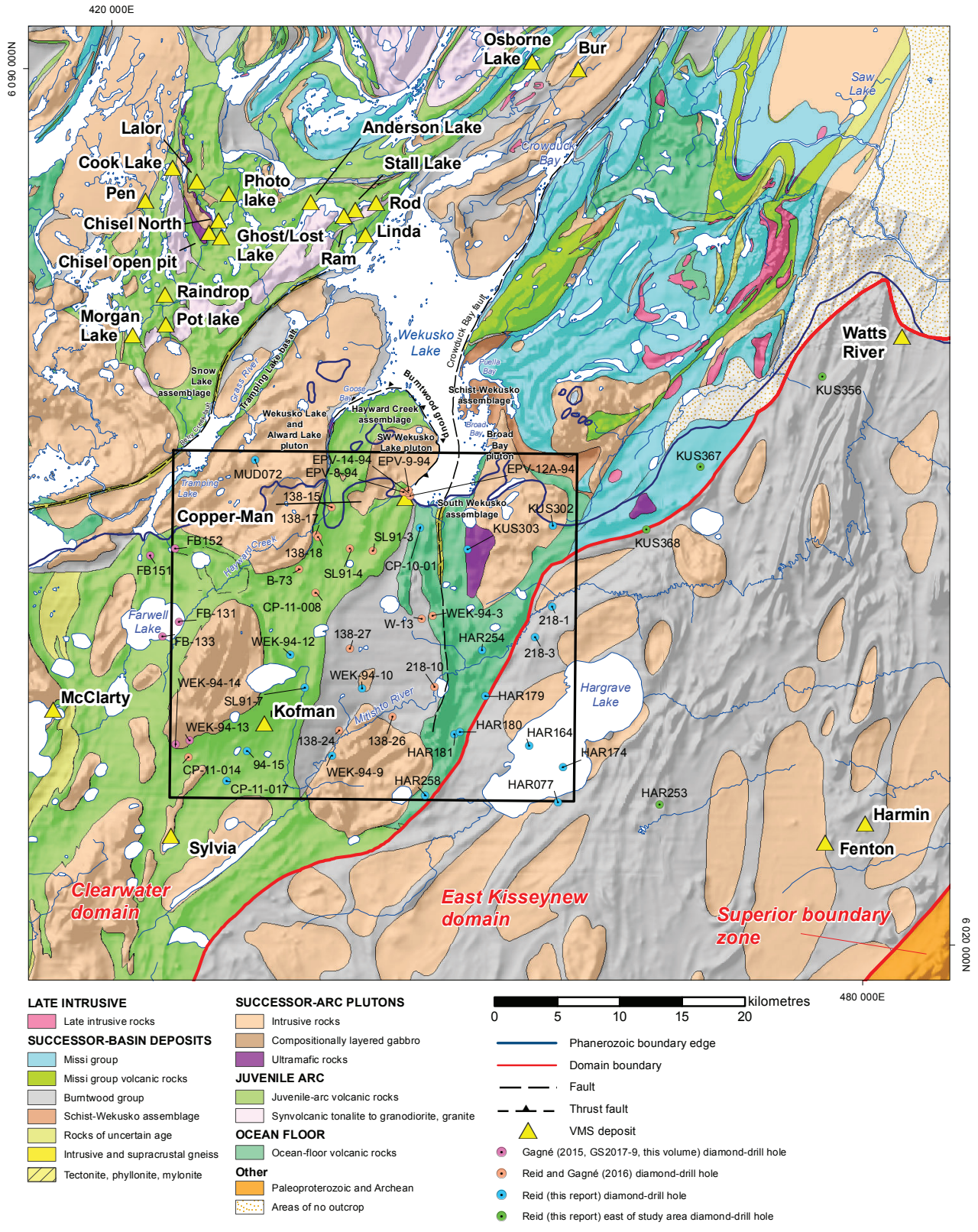

Figure GS2017-7-2: *Geology of the south Wekusko Lake area (modified from NATMAP Shield Margin Project Working Group, 1998), showing the collar locations discussed in this report. Abbreviation: SW, Southwest.*

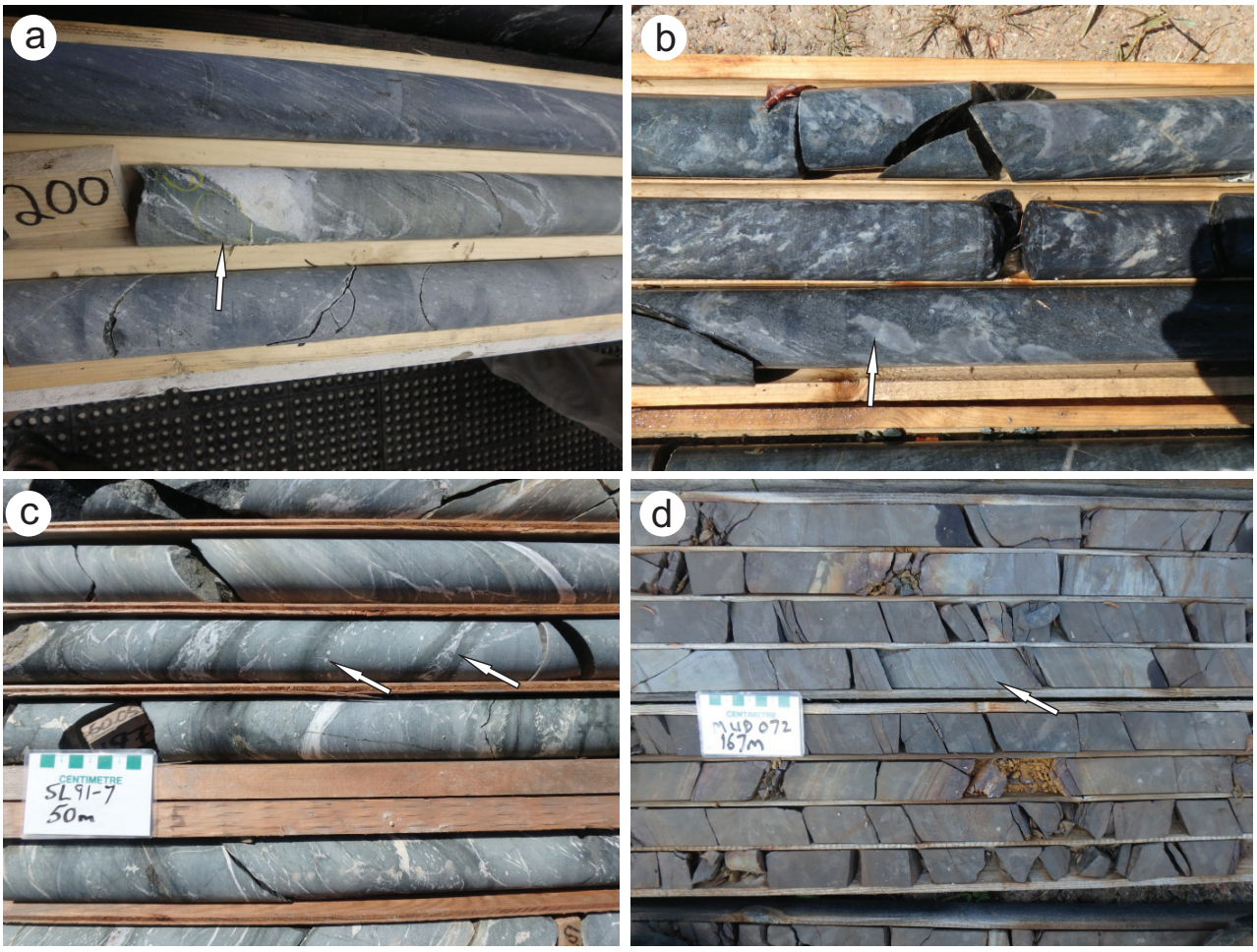

Figure GS2017-7-3: *Volcanic rocks of various composition in the Clearwater domain:* ***a)*** *wispy domains of chlorite-carbonate with trace specks of chalcopyrite (arrow) cutting mafic rocks that are adjacent to quartz-eye dacite, drillcore CP-11-017, 200.0 m, NQ;* ***b)*** *angular felsic fragments (arrow) in a epidote-silica–altered matrix, drillcore 94-15, 124.5 m, NQ;* ***c)*** *pillow basalt with carbonate amygdules and dark green selvages (right arrow), drillcore SL91-7, 50.0 m, NQ;* ***d)*** *laminated tuff/graphitic argillite with weak zinc-copper mineralization (arrow), drillcore MUD072, 167.0 m, BQ. Core diameter: NQ, 4.76 cm; BQ, 3.65 cm.*

by the appearance of angular blocks of rhyolite (5–20 cm) that have very distinctive 1–8 mm blue quartz phenocrysts. The blue quartz–porphyritic fragmental rhyolite and massive rhyolite extend to the end of the hole (227.0 m). Well-preserved pillowed mafic flows, which have calcite amygdules around the pillow margins, dark green selvages and interpillow hyaloclastite, occur between 43.0 and 75.2 m in drillcore SL91-7 (Figure GS2017-7-3c). Thinly laminated graphitic argillite (75.2–82.6 m) grades into intermediate lapilli tuff (82.6–109.0 m) that is intruded by equigranular, medium-grained gabbro in drillcore SL91-7.

The WEK-94-12 (Assessment File 94654) is a short drillcore (125 m) that intersects dark grey–black, aphanitic to fine-grained rock of mafic composition (59.9–125 m); aside from grain-size decreasing downhole, it contains no textural clues to indicate whether it is an extrusive volcanic or a hypabyssal intrusion.

Drillhole MUD072 (Assessment File 74711) is collared in what is mapped as successor-arc intrusive rocks related to the Alward Lake pluton (Figure GS2017-7-2; NATMAP Shield Margin Project Working Group, 1998). However, the drillcore consists of several successions of intermediate feldspar-crystal lapilli tuff to crystal tuff several metres thick. Graded beds indicate that the package is overturned. At a depth of 112.3 m, a thick package (77.7 m) of thinly laminated (millimetre-scale) sulphide-graphite–bearing argillite/ash tuff is present (Figure GS2017-7-3d). The remainder of the drillcore, from 190.0 to 224.0 m, is feldspar-crystal tuff similar to that observed above the argillite.

Drillcore FB152, examined in the summer of 2015, is described as a package of amygdaloidal mafic flows (50 m thick) followed by a thick interval of heterolithic felsic tuff breccia whereas drillhole FB151 encountered mainly mafic volcaniclastic rocks (see Gagné, 2015 for more details). Descriptions of volcanic rocks observed in drillcores FB-131 and FB-133 during the 2017 field season are in this volume (Gagné, GS2017-9, this volume).

Mafic-dominated association

Drillcores CP-10-01 and KUS303 (Assessment files 74903, 74423) consist mainly of aphanitic to fine-grained, dark green basalt, which in places contains faint pillow selvages (Figure GS2017-7-4a); heterogeneous ductile deformation represented by discrete shear zones, varying from a few centimetres to several metres wide, is observed in both drillcores. Given its proximity to the inferred contact between Burntwood group sediments and South Wekusko assemblage ocean-floor basalt, and descriptions of graphitic argillite in company drill logs, drillcore CP-10-01 was examined in detail. Narrow intervals of dark grey, thinly laminated greywacke between 107.5–125.0 m and a poorly consolidated graphitic fault zone from 155.0 to 170.0 m, typical of the Burntwood group, possibly represent structural imbricates within the monotonous dark green mafic rocks that characterize this drillcore. The upper portion of drillcore KUS303 (29.86–53.0 m) contains an intermediate rock that has a distinct spotted texture imparted by medium- to coarse-grained pyroxene phenocrysts in a fine- to medium-grained light grey groundmass. Several narrow intervals (<2 m to several metres) of felsic rocks are intercalated within the mafic rocks in drillcore KUS303, but the contact relationships are obscured by ductile deformation; these could represent dikes or structurally emplaced blocks. From 131.0 to 161.7 m laminated mafic wacke grades into felsic (chert?) fragmental rock, which has a matrix of grunerite and magnetite (Figure GS2017-7-4b), and then grades into laminated chert.

Drillcores HAR179, HAR180, HAR181, HAR254 and HAR258 (Assessment files 74565, 74942) all have relatively similar rock types, the most common being millimetre- to centimetre-scale layered mafic wacke (Figure GS2017-7-4c), which is massive in places. Each drillcore intersects a quartz-rich sulphide-mineralized interval ranging from 5 to 10 m in width (up to 40 m in drillcore HAR181); the mineralization varies from 1–5% disseminated pyrite along laminations in mafic wacke to net-textured pyrrhotite and pyrite (up to 50%) in narrow (<50 cm) stockworks associated with brecciated quartz fragments. The absence of laminations in felsic fragments suggests they are part of a quartz vein system that cuts the mineralized mafic wacke; later ductile deformation dismembered the vein and remobilized pyrrhotite into the stockworks. Intermediate to felsic feldspar-phyric dikes (<1.5 m) with chilled margins

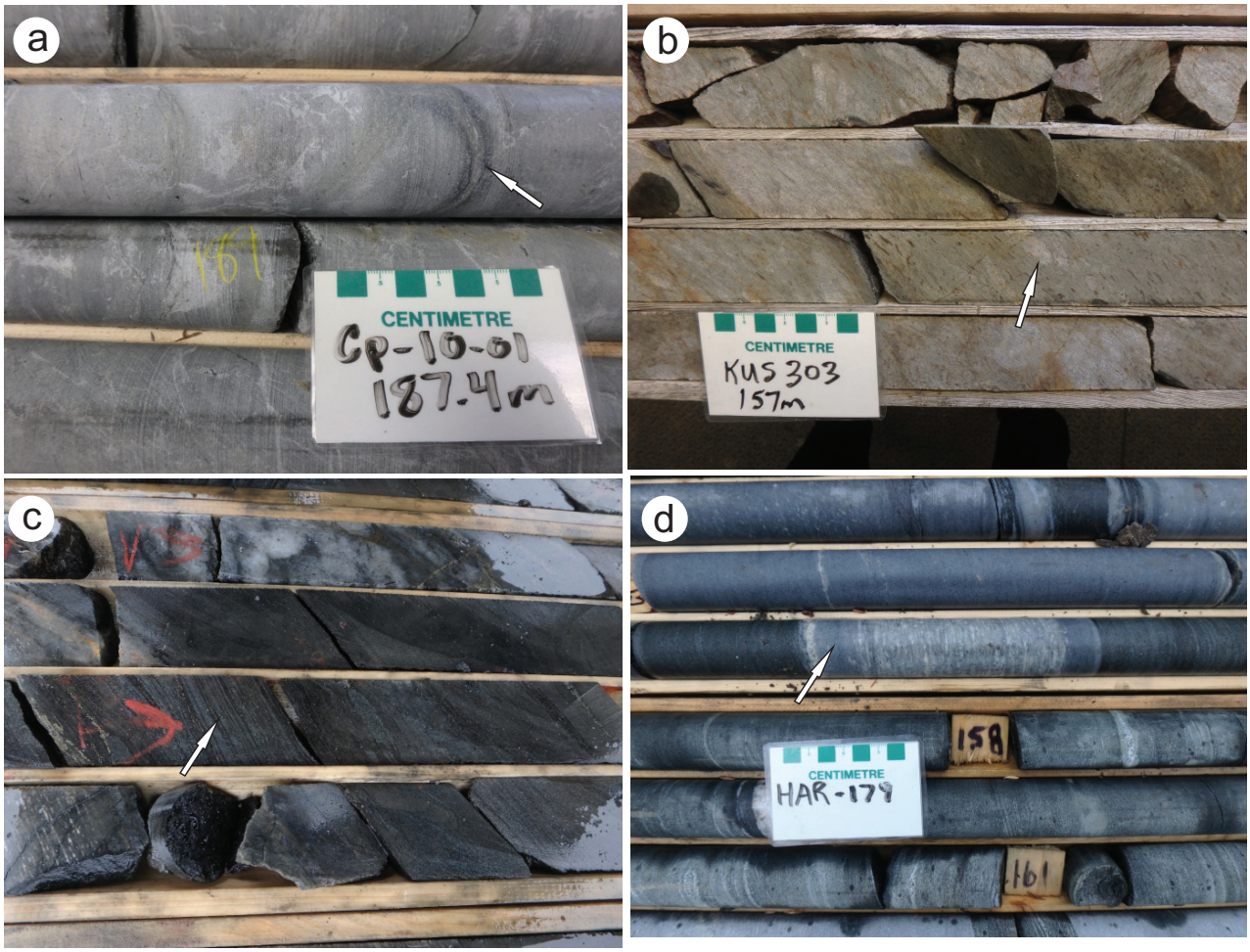

Figure GS2017-7-4: *Mafic-dominated rocks of the Clearwater domain:* ***a****) green basalt with dark green pillow selvage (arrow), drillcore CP-10-01, 187.4 m, NQ;* ***b****) grunerite-magnetite—bearing rock with felsic fragments (arrow), drillcore KUS303, 157.0 m, NQ;* ***c****) laminated mafic wacke (arrow), drillcore HAR181, 164.0 m, NQ;* ***d****) feldspar-phyric felsic dike with a chilled margin (arrow) cutting mafic wacke, drillcore HAR179, 156.4 m, NQ. Core diameter: NQ, 4.76 cm; BQ, 3.65 cm.*

commonly cut the mafic wacke (Figure GS2017-7-4d). Their absence in the mineralized mafic wacke might indicate that they predate them.

Plutonic association

Drillcores WEK-94-9 and WEK-94-10 (Assessment File 94654) both intersect homogeneous, massive, equigranular, moderately magnetic, medium-grained mesocratic gabbro (Figure GS2017-7-5a); these are similar to the gabbro in drillcores 138-27 and 138-24 (Reid and Gagné, 2016). Primary pyroxene is replaced by secondary amphibole in drillcore WEK-94-9, however, the timing and significance of this alteration is unknown. Drillcores WEK-94-13 and WEK-94-14 contain gabbro similar to that described here (see Gagné, GS2017-9, this volume for more details).

Drillcore KUS302 (Assessment File 73949) contains a complex package of rocks that varies from a greenish-black, medium- to coarse-grained amphibolite to a lighter grey, pyroxene-porphyritic intermediate rock of uncertain protolith. The intermediate rock appears to contain 1–2 cm, subangular fragments; these may be lithic fragments in a volcaniclastic precursor. However, diffuse contacts around the fragments do not allow positive identification. Intruding the above-mentioned units is a light grey, medium-grained, equigranular granodiorite (Figure GS2017-7-5b).

East Kisseynew domain

Mafic and felsic gneiss

Rocks in the East Kisseynew domain are distinctly different from rocks in the Clearwater domain in that they are heterogeneous, medium-grained, foliated to granoblastic with gneissic layering at the centimetre- to metre-scale, which is interpreted to result from pooling/segregation of leucosome derived from partial melting. These rocks vary from dark green amphibolite (mafic; Figure GS2017-7-6a) to a distinct blue-grey, quartz-feldspar-hornblende gneiss (intermediate; Figure GS2017-7-6b). Light grey to pink, medium- to coarse-grained, strongly foliated granite is intercalated with the mafic and intermediate gneiss and has a width in drillcore from a few centimetres to 35 m (Figure GS2017-7-6c). The youngest intrusive rocks are narrow granitic aplite dikes that postdate the gneissic fabric (Figure GS2017-7-6c) and may be related to pegmatite injections that formed late in the deformation history. Drillcore HAR077 (Assessment File 73949), though injected with pegmatite, does not show extensive recrystallization and contains bedded quartz-feldspar arenite that is cut by a mafic dike (Figure GS2017-7-6d). Amphibolite and quartz-feldspar arenite alternate at >10 m intervals throughout the remainder of the drillcore. The amphibolite has a layered appearance due to ubiquitous carbonate and light green amphiboles concentrated along foliation-parallel centimetre-scale seams.

East of the south Wekusko Lake study area

Drillcores HAR253, KUS356 and KUS367 (Assessment files 74844, 74705), from near the Watts River and Harmin VMS deposits to the east of the study area, are similar in that they intersect two distinct packages of rocks separated by graphite- and sulphide-bearing zones no more than a few metres wide. These zones most likely represent late faults with significant displacements, as rocks above and below show differing amounts of recrystallization and migmatization, which likely record different metamorphic histories.

Drillcore HAR253 contains grey-green, weakly layered, medium-grained, intermediate gneiss (84.7–245.4 m) that locally appears to contain flattened 2–4 cm clasts (Figure GS2017-7-7a). Minor centimetre-scale pegmatitic melt segregations occur throughout the upper portion of the drillcore; a thick interval of massive plagioclase-rich pegmatite (tonalite in composition) resides between 220.0 and 232.5 m. Fine- to medium-grained amphibolite, which has layered green to dark green domains with abundant disseminated calcite, is present

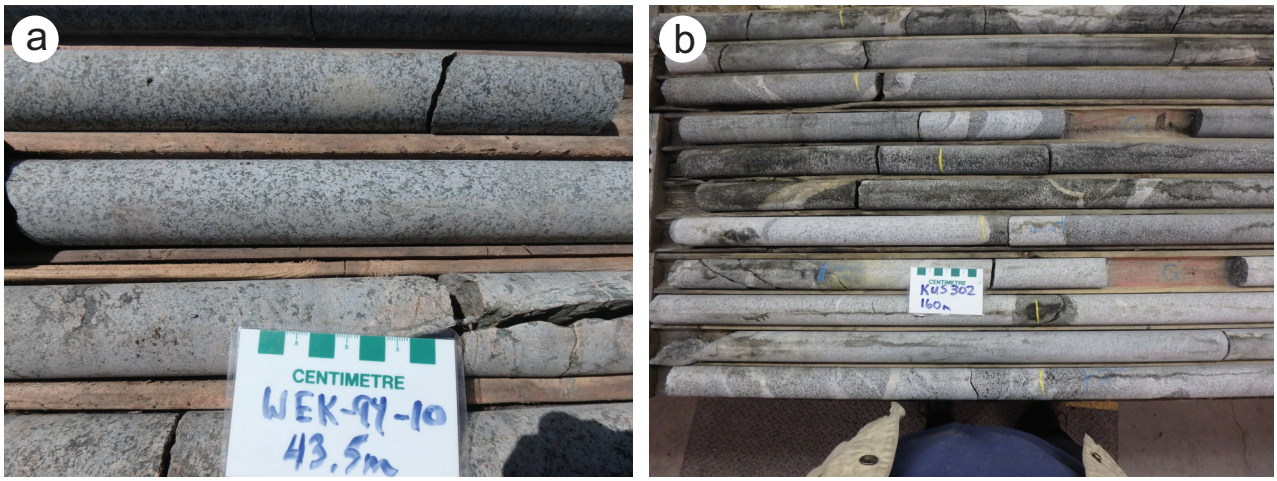

Figure GS2017-7-5: *Plutonic rocks of the Clearwater domain:* ***a)*** *medium-grained mesocratic gabbro, drillcore WEK-94-10, 43.5 m, NQ;* ***b)*** *medium-grained amphibolite intruded by granodiorite, drillcore KUS302, 160.0 m, BQ. Core diameter: NQ, 4.76 cm; BQ, 3.65 cm.*

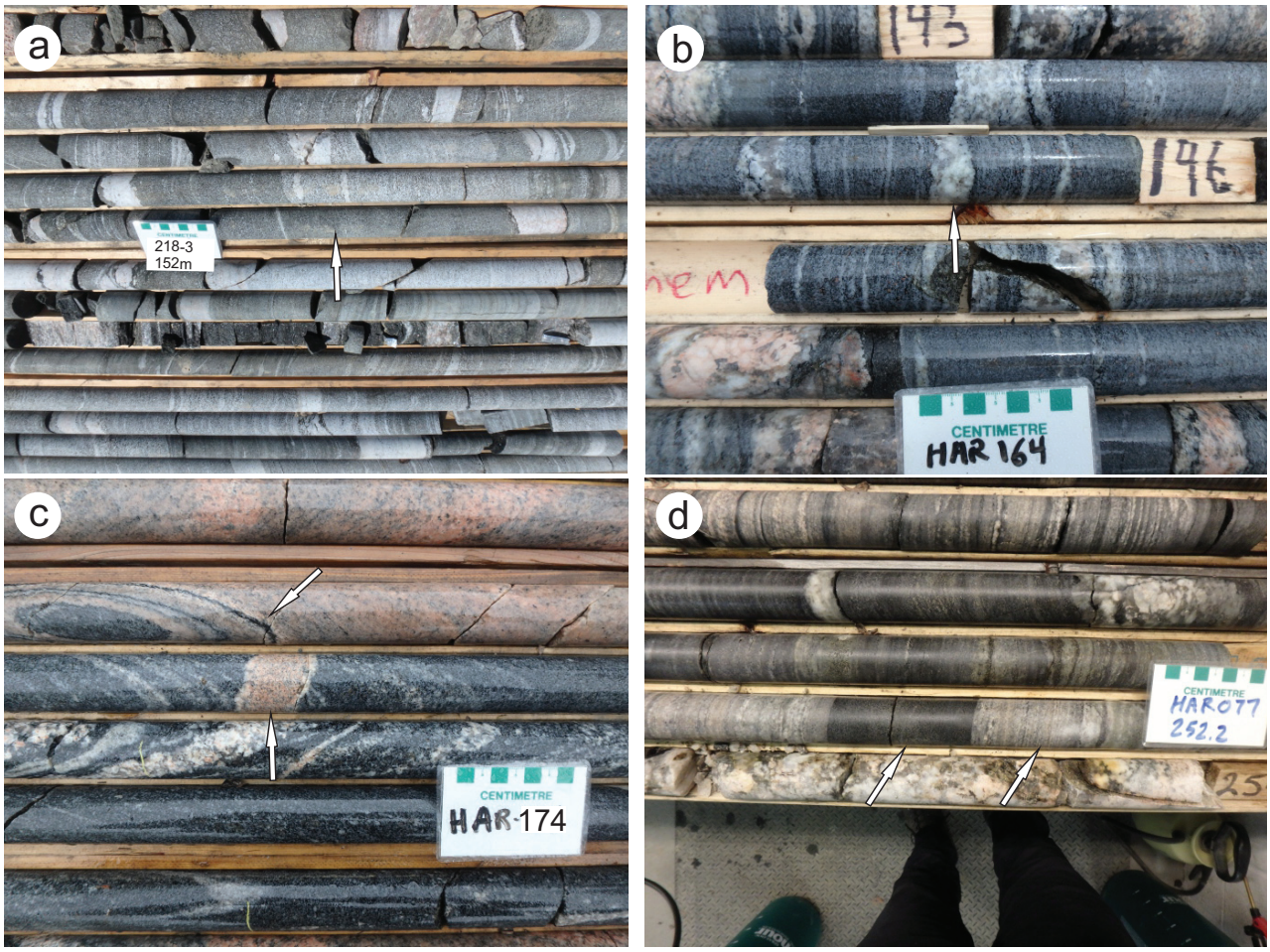

Figure GS2017-7-6: *Mafic and felsic gneiss of the East Kisseynew domain:* ***a)*** *weakly gneissic amphibolite (arrow) and granodiorite cut by pegmatitic segregations, drillcore 218-3, 152.0 m, BQ (Assessment File 71118, Manitoba Growth, Enterprise and Trade, Winnipeg);* ***b)*** *grey quartzofeldspathic gneiss with abundant migmatite sweats and biotite-rich melanosome (arrow), drillcore HAR164, 146.0 m, NQ (Assessment File 74565);* ***c)*** *gneissic amphibolite with pegmatitic injections and foliated pink granite (upper arrow); note the granitic aplite that cuts the gneissic fabric (lower arrow), drillcore HAR174, 272.0 m, NQ (Assessment File 74565);* ***d)*** *thin amphibolite dike (left arrow) in bedded quartz-feldspar arenite (right arrow), drillcore HAR077, 252.2 m, BQ. Core diameter: NQ, 4.76 cm; BQ, 3.65 cm.*

in both the lower half of HAR253 (245.4–377.0 m) and the upper section of KUS356 (49.5–189.6 m). The amphibolite in drillcore KUS356 differs in that ~5% of the unit is cut by <1 m feldspar-phyric intermediate dikes that are similar to the previously described dikes that cut mafic-dominated rocks (see 'Mafic-dominated association' section). The lower section of drillcore KUS356 (200–272 m) contains a blue-grey gneiss that is medium- to coarse-grained, layered (because of mineral segregation) and contains abundant centimetre-scale migmatite with biotite-bearing melanosome along the margins. Absence of melt-related textures in combination with the relatively fine-grained character of amphibolite in both HAR253 and KUS356 when compared to their recrystallized intermediate gneiss counterparts suggests that they evolved under differing metamorphic conditions and were tectonically juxtaposed.

Similar to the rocks described above, drillcore KUS367 contains two distinctly different packages of rocks. In the upper portion (36.1–117.7 m), intervals (1–3 m) of garnet-bearing greywacke grade into biotite-garnet±staurolite gneiss, with the contact with the next greywacke interval being sharp. The gradational nature of the two rock types followed by the abrupt truncations and is interpreted to define a series of thick beds that graded from greywacke at the base to mudstone at the top and now display reverse metamorphic grading due to enhanced recrystallization of the mudstone (Figure GS2017-7-7b). Separating the upper from the lower section is a graphite-sulphide–bearing horizon between 117.7 and 120.0 m. The lower half of the drillcore (120.0–197.0 m) includes feldspar-biotite-hornblende gneiss and hornblende amphibolite (mafic wacke protolith?), which in places contains up to 5% medium- to coarse-grained garnet porphyroblasts; contacts are gradational. The feldspar-biotite-hornblende gneiss locally contains fine wisps of a light grey, fibrous mineral, possibly sillimanite.

Drillcore KUS368 (Assessment File 74705) intersects a heterogeneous package of medium-grained feldspar-biotite-hornblende gneiss and hornblende amphibolite with two

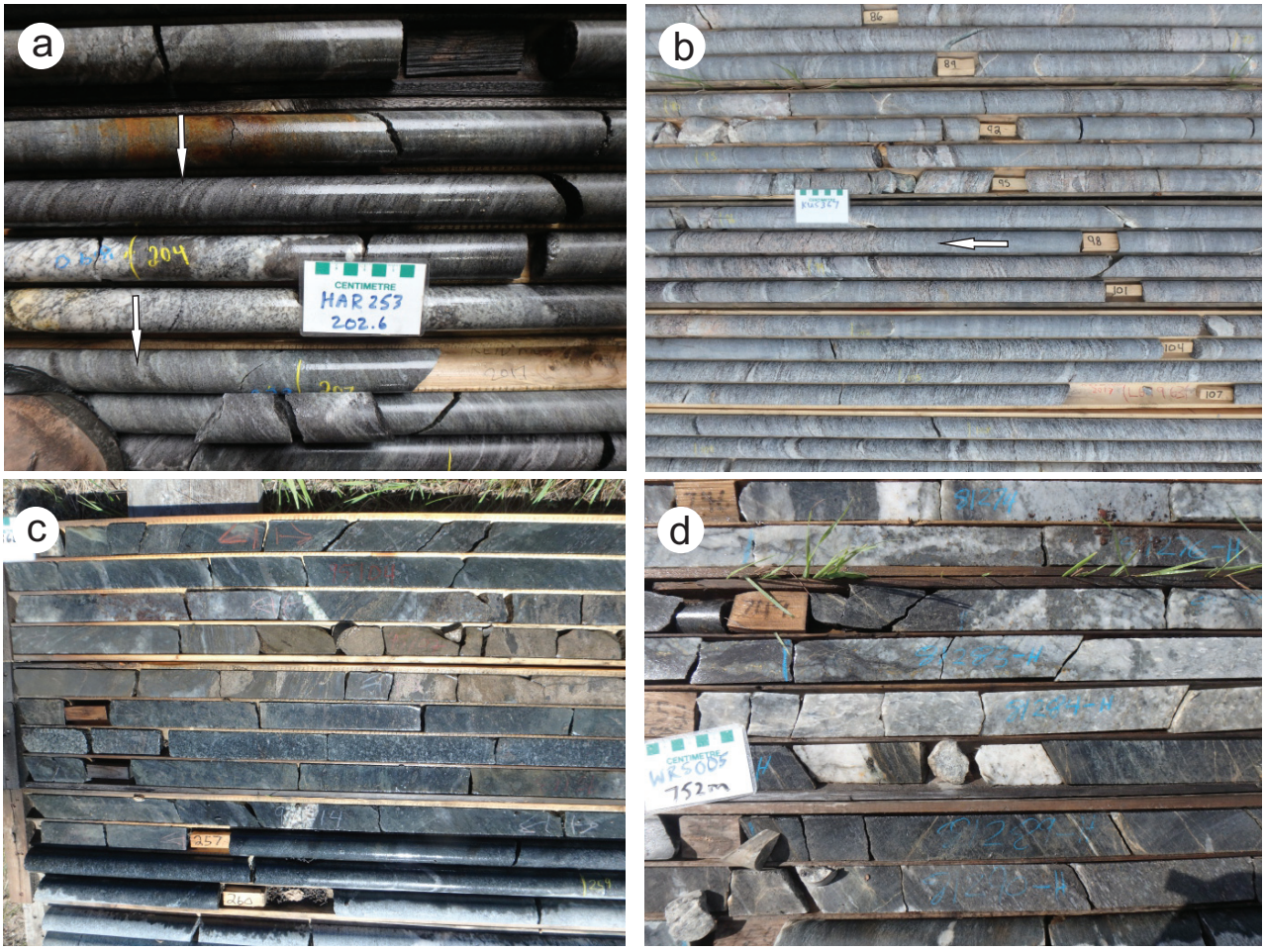

Figure GS2017-7-7: *Drillholes east of the south Wekusko Lake study area:* ***a)*** *intermediate volcanic (?) fragments (arrows) and white tonalitic pegmatite, drillcore HAR253, 202.6 m, NQ;* ***b)*** *garnet-bearing greywacke and biotite-garnet-staurolite gneiss (arrow shows direction of reverse metamorphic grading in normally graded beds), drillcore KUS367, 77–113 m, NQ;* ***c)*** *gold-bearing semi-massive pyrrhotite in intermediate gneiss, drillcore KUS368, 251.0 m, BQ;* ***d)*** *sillimanite-bearing siliceous rock beneath mineralized zone and biotite-bearing intermediate quartzofeldspathic gneiss, drillcore WRS-005, 752.0 m, BQ. Core diameter: NQ, 4.76 cm; BQ, 3.65 cm.*

sulphide-bearing zones. The first sulphide zone consists of highly tectonized pyrrhotite and pyrite, between 120 and 122 m, and is associated with light grey–green siliceous rocks that range from centimetre-scale layered rock to feldspar porphyritic rock that resembles rhyolite. The lower sulphide zone (247–251 m) is a package of semi-massive to stringer pyrrhotite that contains trace specks of chalcopyrite (GS2017-7-7c).

Drillcore WRS-005 (located at the Watts River deposit, Figure GS2017-7-2 [drillhole not shown]; Assessment File 74251) intersects copper-zinc mineralization associated with the Watts River VMS deposit (Bailes, 2015). Drillcore from 680 to 786 m was re-examined to identify the rock types that host mineralization and to select a sample for U-Pb zircon dating. Rocks from this drillcore are moderately recrystallized, medium grained and have few recognizable primary textures. However, in the structural hangingwall, from 680 to 701 m, a clast-supported felsic breccia grades downward into less recognizable intermediate quartzofeldspathic gneiss from 701.0 to 723.5 m. The contact between the relatively unaltered intermediate gneiss in the hanging wall and the mineralized zone below is sharp. The mineralized zone (723.5–734.0 m) consists of disseminated, stringer and semi-massive chalcopyrite, sphalerite, pyrrhotite and pyrite hosted by biotite±cordierite gangue. Beneath the main mineralized zone, from 734.0 to 753.0 m, is a distinctive light grey, aphanitic to fine-grained, weakly mineralized siliceous rock that contains 5–10% wisps of sillimanite (2–5 mm long; Figure GS2017-7-7d). From 753.0 to 760.0 m, the biotite content increases to ~10% and the rock contains 5–10% subrounded (1–2 cm diameter) fine aggregates of quartz and sillimanite. Downcore from 760.0 m the rock becomes an intermediate quartzofeldspathic gneiss that continues to the end of the hole (786.0 m), a sample of the relatively homogeneous intermediate quartzofeldspathic gneiss from 760.0 to 783.7 m was selected for future geochronology work.

Whole-rock geochemistry of mafic rocks

Whole-rock samples were collected by the Manitoba Geological Survey (MGS) in 2016 and analyzed at Activation

Laboratories Ltd. (Ancaster, Ontario) using lithium metaborate/tetraborate fusion for both major oxides and trace elements. HudBay Minerals Inc. collected samples from 2002 to 2012 and they were analyzed by Acme Analytical Laboratories Ltd. (now Bureau Veritas Minerals; Vancouver, British Columbia) by using a combination of lithium metaborate fusion for major oxides and digestion in a mixture of $HF:HClO_4:HNO_3$ acids for trace elements. In both cases, concentrations of analytes were measured by quadrapole inductively coupled plasma–mass spectrometry (ICP-MS). The data was imported and handled in REFLEX's ioGAS™ and subalkaline basaltic rocks were identified using the Zr/Ti versus Nb/Y diagram of Winchester and Floyd (1977; modified by Pearce, 1996); these rocks are the focus of the following descriptions. Plutonic and epiclastic sedimentary rocks were removed from the dataset. Magmatic affinity was determined using the parameters of Ross and Bédard (2009), and trace-element concentrations were plotted on spider diagrams, normalized to normal (N-type) mid-ocean–ridge basalt (N-MORB) using the values of Sun and McDonough (1989).

Rocks of basaltic composition from the bimodal volcaniclastic association in the Clearwater domain are of tholeiitic to transitional magmatic affinity (Figure-GS2017-7-8a), N-MORB–normalized trace-element diagrams have slightly concave, negatively sloped profiles with depleted Sm-Lu and well-developed negative Nb and Zr, and to a lesser extent Ti anomalies (Figure GS2017-7-8b). Heavy rare-earth elements (HREE) are relatively unfractionated, whereas the light rare-earth elements (LREE) are strongly fractionated. These features are characteristic of juvenile-arc volcanic rocks (Stern et al., 1995a; Syme et al., 1999).

Pillow basalt, massive basalt and mafic wacke from the mafic-dominated association of the Clearwater domain are mostly tholeiitic with a few samples of transitional affinity (Figure GS2017-7-8c). The N-MORB–normalized profiles are flat to slightly negatively sloped with incompatible abundances that are similar to N-MORB, with very subtle Nb, Zr and Ti anomalies (Figure GS2017-7-8d).

Based on a limited dataset, amphibolite from the East Kisseynew domain in the eastern corner of the map area and farther east (drillcores HAR077, HAR164 [Assessment File 74565], HAR253, KUS356, KUS367, KUS368) have tholeiitic to transitional magmatic affinities (Figure GS2017-7-8e, g), flat to gently negative-sloped N-MORB–normalized profiles and incompatible element abundances near that of N-MORB (Figure GS2017-7-8f, h). It is noted that these amphibolites have been affected by varying amounts of calcsilicate alteration, which may account for some variation in incompatible element contents.

Discussion

The bimodal volcanic association in the Clearwater domain shows highly variable lithology and alteration from one drillcore to the next, but some common features are apparent. Quartz-phyric dacite/rhyolite and associated volcaniclastic rocks are texturally similar in drillcores CP-11-008 (Assessment File 63J1159), 94-15 and CP-11-017, and are similar to rocks associated with VMS mineralization at the Kofman deposit (Simard et al., 2010, drillcores K08-01, K08-06, K08-07). The drillcores in this study lie along a magnetic lineament that extends southwest and northeast of the Kofman VMS deposit and possibly indicates a stratigraphic trend favourable for VMS deposits (Figure GS2017-7-2); these felsic rocks will be a focus of future geochemical investigations.

In contrast, volcanic rocks of the mafic-dominated association show less lithological variation, consisting mostly of mafic volcanic rocks, with felsic dikes and volcaniclastic rocks, chert- and silicate-facies (grunerite-magnetite) iron formation forming a volumetrically minor component. Noteworthy is a change from pillowed basalt in the west half of the mafic-dominated association (CP-10-01, KUS303) to mafic wacke/tuff in the east (HAR179, HAR180, HAR181, HAR254). Regardless of this change in facies, all basaltic samples have incompatible trace-element abundances typical of N-MORB (Figure GS2017-7-8d), though elevated Th/Nb is characteristic of basalt produced in a back-arc basin (Stern et al., 1995b).

Feldspar-biotite-hornblende gneiss, amphibolite and granite are the main rock types in the East Kisseynew domain, and have previously been interpreted as higher grade equivalents to the Burntwood group (Leclair et al., 1997). However, no aluminosilicate-bearing assemblages, typical of argillite and greywacke that has been metamorphosed to amphibolite facies, are present in the drillcores examined. Only drillcore KUS367 is interpreted to contain Burntwood group sedimentary rocks. Quartz-feldspar arenite with intercalated amphibolite (HAR077) is not common in the juvenile oceanic–arc, ocean-floor and back-arc assemblages of the Flin Flon belt. However, quartz-feldspar sandstone and conglomerate, with interleaved basalt, in the Saw Lake area are interpreted to be part of the Missi group (Bailes, 1985) and could be a lithological analogue. Of particular interest is the fact that amphibolite (of subalkaline basaltic composition) in the East Kisseynew domain that was examined has incompatible trace-element abundances typical of N-MORB and lack well-developed negative Nb, Zr and Ti anomalies characteristic of subduction-related processes. Similar to basaltic rocks in the mafic-dominated association of the Clearwater domain, elevated Th/Nb ratios may indicate that these rocks were produced in a setting that is transitional between oceanic arc and ocean floor, such as a back-arc basin (Figure GS2017-7-8f, g; e.g., Stern et al., 1995b; Syme et al., 1999).

Economic considerations

Volcanogenic massive-sulphide deposits form in active rifts in a number of geodynamic settings, including mid-ocean ridges, back-arc basins, intraoceanic arcs and continental arcs (Franklin et al., 2005; Galley et al., 2007). Geochemical studies and fieldwork have shown that most VMS deposits in the Flin Flon belt are associated with oceanic-arc volcanism, particularly during the initial stages of arc development and intra-arc rifting (Syme and Bailes, 1993; Syme et al., 1999). The geochemistry of

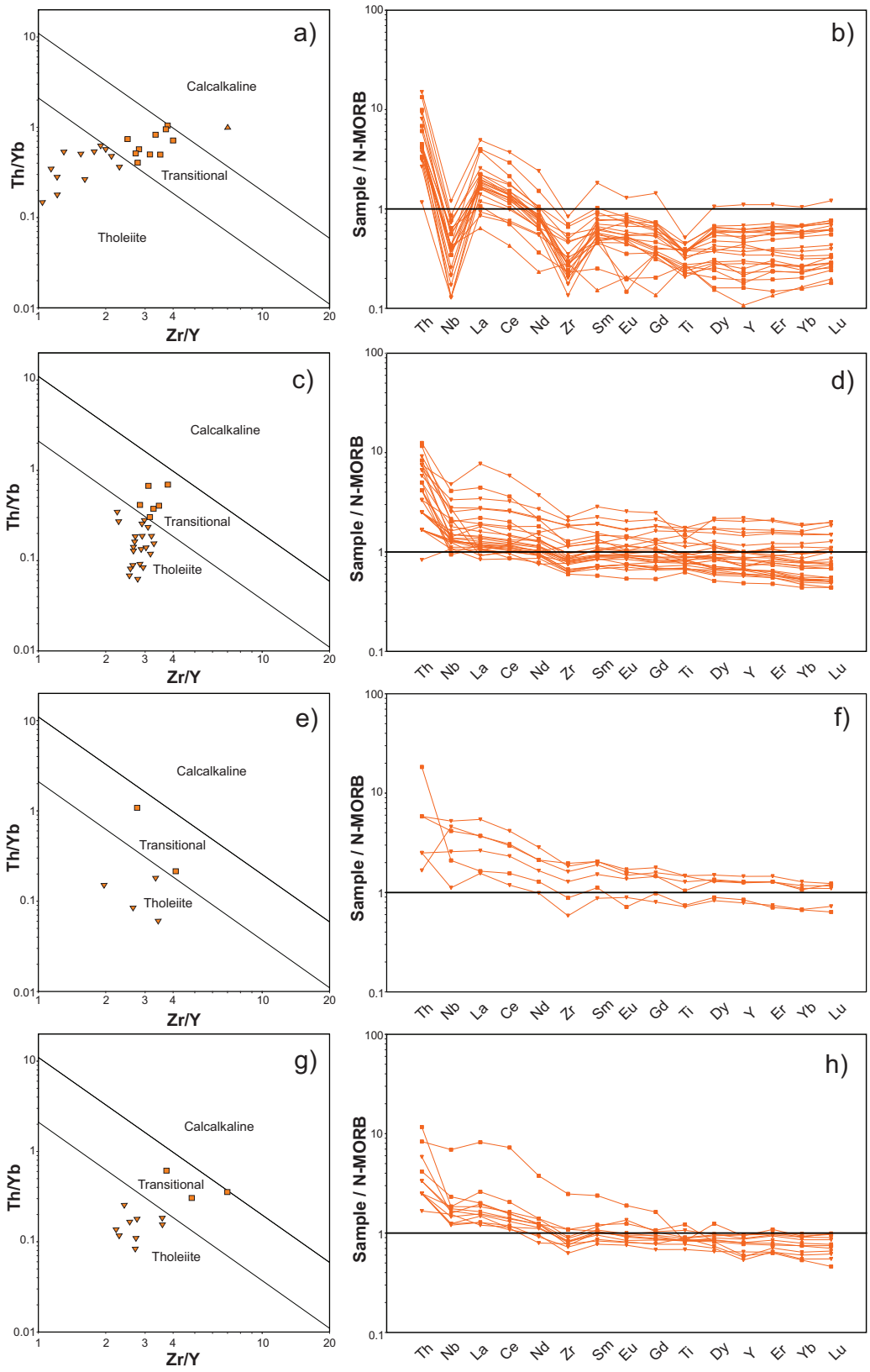

Figure GS2017-7-8: *Log Zr/Y versus log Th/Yb plots (Ross and Bédard, 2009) of magmatic affinity (down triangles, tholeiite; squares, transitional; up triangles, calcalkaline) and spider diagrams showing incompatible trace elements normalized to normal (N-type) mid-ocean–ridge basalt (N-MORB; Sun and McDonough, 1989):* ***a)*** *and* ***b)*** *bimodal volcaniclastic association in the Clearwater domain,* ***c)*** *and* ***d)*** *mafic-dominated association in the Clearwater domain,* ***e)*** *and* ***f)*** *amphibolite gneiss in the East Kisseynew domain,* ***g)*** *and* ***h)*** *amphibolite east of the study area into the East Kisseynew domain.*

rocks to the southwest of Wekusko Lake is indicative of juvenile-arc settings, suggesting above-average potential to host VMS mineralization. This is corroborated by the presence of the Copper-Man and Kofman VMS deposits (Figures GS2017-7-1, -2). Anomalous zinc and copper (2100 ppm Zn, 740 ppm Cu; Assessment File 72778) associated with quartz-phyric dacite/rhyolite, similar to that associated with the Kofman deposit, was intersected in drillhole 94-15, which is approximately 2.5 km farther to the south along strike indicating that the host stratigraphy may extend at least this far.

Of particular economic significance is the presence of feldspar-crystal tuff and associated weakly mineralized argillite/siliceous ash tuff in drillcore MUD072, with assays indicating that the latter rock type contains up to 0.08 g/t Au, 3.35 g/t Ag, 0.19% Zn, 0.05% Cu over 77.8 m (Assessment File 74711). Existing maps of the geology indicate that this drillhole is collared in plutonic rocks (Figure GS2017-7-2; NATMAP Shield Margin Project Working Group, 1998), but it is apparent that volcanic rocks are also present.

Basaltic rocks of the mafic-dominated association in the eastern Clearwater domain have trace-element signatures indicative of basalt produced in an ocean-floor or back-arc setting, and would thus be considered less prospective for VMS. However, laminated to brecciated siliceous fragments, possibly representing dismembered quartz veins, locally contain elevated gold and trace copper values (e.g., drillcore HAR181, 0.41 g/t Au from 194.0 to 195.08 m, Assessment File 74565; drillcore HAR258, 0.45 g/t Au from 167.79 to 168.49 m, Assessment File 74942; drillcore WEK-94-2, 1.56 g/t Au from 113.2 to 113.8 m [not shown on GS2017-7-2, ~1 km southeast of drillhole WEK-94-3], Assessment File 94654). Proximity to a major metamorphic gradient and crustal-scale fault (Crowduck Bay fault) suggests that this area has potential for orogenic gold mineralization. To the east, drillcore KUS368 intersects semi-massive to stringer pyrrhotite that contains significant gold values (3.58 g/t Au over 3 m, Assessment File 74705) indicating that gold-bearing fluids inundated these rocks, although the timing and style of this mineralization is not understood.

Acknowledgments

The fieldwork was made possible through the co-operation of HudBay Minerals Inc. and Royal Nickel Corporation who allowed access to their facilities to examine drillcore. The author also thanks M. Stocking, C. Stocki and S. Walker for their excellent assistance, both in the field and at the Midland Sample and Core Library. Thanks also go to C. Epp for preparing samples and thin sections, and to S. Gagné and S.D. Anderson for reviewing this manuscript.

References

Ansdell, K.M., Connors, K.A., Stern, R.A. and Lucas, S.B. 1999: Coeval sedimentation, magmatism, and fold-thrust belt development in the Trans-Hudson Orogen: geochronological evidence from the Wekusko Lake area, Manitoba, Canada; Canadian Journal of Earth Sciences, v. 36, p. 293–312.

Ansdell, K.M., Kyser, K., Stauffer, M. and Edwards, G. 1992: Age and source of detrital zircons from the Missi group: a Proterozoic molasses deposit, Trans-Hudson orogen, Canada; Canadian Journal of Earth Sciences, v. 29, p. 2583–2594.

Ansdell, K.M., Lucas, S.B., Connors, K. and Stern, R.A. 1995: Kisseynew metasedimentary gneiss belt, Trans-Hudson orogen (Canada): back-arc origin and collisional inversion; Geology, v. 23, p. 1039–1043.

Bailes, A.H. 1985: Geology of the Saw Lake area; Manitoba Energy and Mines, Manitoba Geological Survey, Geological Report GR83-2, 47 p.

Bailes, A.H. 2015: Geological setting of the Watts River base metal massive sulphide deposit; HudBay Minerals Inc., unpublished internal geological report, 70 p.

Bailes, A.H. and Galley, A.G. 2007: Geology of the Chisel–Anderson lakes area, Snow Lake, Manitoba (NTS areas 63K16SW and west half of 63SE); Manitoba Science, Technology, Energy and Mines, Manitoba Geological Survey, Geoscientific Map MAP2007-1, scale 1:20 000.

Connors, K.A. and Ansdell, K.M. 1994: Revision of stratigraphy of and structural history in the Wekusko Lake area, eastern Tran-Hudson orogen; *in* Report of Activities 1994, Manitoba Energy and Mines, Minerals Division, p. 104–107.

Gagné, S. 2015: Examination of exploration drillcore from the Reed Lake area, Flin Flon belt, west-central Manitoba (parts of NTS 63K9, 10): implications for the stratigraphy of the Fourmile Island assemblage and setting of VMS deposits; *in* Report of Activities 2015, Manitoba Mineral Resources, Manitoba Geological Survey, p. 38–51.

Galley, A.G., Syme, E.C. and Bailes, A.H. 2007: Metallogeny of the Paleoproterozoic Flin Flon Belt, Manitoba and Saskatchewan; *in* Mineral Deposits of Canada: A Synthesis of Major Deposit Types, District Metallogeny, the Evolution of Geological Provinces, and Exploration Methods, W.D. Goodfellow (ed.), Geological Association of Canada, Mineral Deposits Division, Special Publication 5, p. 509–531.

Gilbert, H.P. and Bailes, A.H. 2005: Geology of the southern Wekusko Lake area, Manitoba (NTS 63J12NW); Manitoba Industry, Economic Development and Mines, Manitoba Geological Survey, Geoscientific Map MAP2005-2, scale 1:20 000.

Franklin, J.M., Gibson, H.L., Galley, A.G. and Jonasson, I.R. 2005: Volcanogenic massive sulfide deposits; Economic Geology, 100th year Anniversary Volume, p. 523–560.

Leclair, A.D. and Viljoen, H.J. 1997: Geology of Precambrian basement beneath Phanerozoic cover, Flin Flon Belt, Manitoba and Saskatchewan; Geological Survey of Canada, Open File 3427, scale 1:250 000.

Leclair, A.D., Lucas, S.B., Broome, H.J., Viljoen, D.W. and Weber, W. 1997: Regional mapping of Precambrian basement beneath Phanerozoic cover in southeastern Trans-Hudson Orogen, Manitoba and Saskatchewan; Canadian Journal of Earth Sciences, v. 34, p. 618–634.

Lewry, J.F. and Collerson, K.D. 1990: Trans-Hudson Orogen: extent, subdivisions, and problems; *in* The Proterozoic Trans-Hudson Orogen of North America, J.F. Lewry and M.R. Stauffer (ed.), Geological Association of Canada, Special Publication 37, p. 1–14.

NATMAP Shield Margin Project Working Group 1998: Geology, NATMAP Shield Margin Project area, Flin Flon belt, Manitoba/Saskatchewan; Geological Survey of Canada, Map 1968A, scale 1:100 000.

Pearce, J.A. 1996: A user's guide to basalt discrimination diagrams; *in* Trace Element Geochemistry of Volcanic Rocks: Applications for Massive Sulphide Exploration, D.A. Wyman (ed.), Geological Association of Canada, Short Course Notes, v. 12, p. 79–113.

Reid, K.D. and Gagné, S. 2016: Examination of exploration drillcore from the south Wekusko Lake area, eastern Flin Flon belt, north-central Manitoba (parts of NTS 63J5, 12, 63K8, 9); *in* Report of Activities 2016, Manitoba Growth, Enterprise and Trade, Manitoba Geological Survey, p. 74–86.

Ross, P.-S. and Bédard, J.H. 2009: Magmatic affinity of modern and ancient sub-alkaline volcanic rocks determined from trace-element discriminant diagrams; Canadian Journal of Earth Sciences, v. 46, p. 823–839.

Simard, R.L., McGregor, C.R., Rayner, N. and Creaser, R.A. 2010: New geological mapping, geochemical, Sm-Nd isotopic and U-Pb data for the eastern sub-Phanerozoic Flin Flon belt, west-central Manitoba (parts of NTS 63J3-6, 11, 12, 14, 63K1-2, 7–10); *in* Report of Activities 2010, Manitoba Innovation, Energy and Mines, Manitoba Geological Survey, p. 69–87.

Stauffer, R.A. 1984: Manikewan: an early Proterozoic ocean in central Canada: its igneous history and orogenic closure; Precambrian Research, v. 25, p. 257–281.

Stern, R.A., Syme, E.C., Bailes, A.H. and Lucas, S.B. 1995a: Paleoproterozoic (1.90–1.86 Ga) arc volcanism in the Flin Flon belt, Trans-Hudson Orogen, Canada; Contributions to Mineralogy and Petrology, v. 119, no. 2–3, p. 117–141.

Stern, R.A., Syme, E.C. and Lucas, S.B. 1995b: Geochemistry of 1.9 Ga MORB- and OIB-like basalts from the Amisk collage, Flin Flon belt, Canada: evidence for an intra-oceanic origin; Geochimica et Cosmochimica Acta, v. 59, no. 15, p. 3131–3154.

Sun, S.-s. and McDonough, W.F. 1989: Chemical and isotopic systematics of ocean basalts: implications for mantle composition and processes; *in* Magmatism in the Ocean Basins, A.D. Sauders and M.J. Norry (ed.), Geological Society, London, Special Publications, v. 42, p. 313–345.

Syme, E.C. and Bailes, A.H. 1993: Stratigraphic and tectonic setting of early Proterozoic volcanogenic massive sulfide deposits, Flin Flon, Manitoba; Economic Geology, v. 88, no. 3, p. 566–589.

Syme, E.C., Bailes, A.H. and Lucas, S.B. 1995: Geology of the Reed Lake area (parts of 63K/9 and 63K/10); *in* Report of Activities 1995, Manitoba Energy and Mines, Geological Services, p. 42–60.

Syme, E.C., Lucas, S.B., Bailes, A.H. and Stern, R.A. 1999: Contrasting arc and MORB-like assemblages in the Paleoproterozoic Flin Flon belt, Manitoba, and the role of intra-arc extension in localizing volcanic-hosted massive sulphide deposits; Canadian Journal of Earth Sciences, v. 36, p. 1767–1788.

Whalen, J.B., Syme, E.C. and Stern, R.A. 1999: Geochemical and Nd isotopic evolution of Paleoproterozoic arc-type magmatism in the Flin Flon belt, Trans-Hudson orogeny, Canada; Canadian Journal of Earth Sciences, v. 36, p. 227–250.

Winchester, J.A. and Floyd, P.A. 1977: Geochemical discrimination of different magma series and their differentiation products using immobile elements; Chemical Geology, v. 20, p. 325–343.

GS2017-8

New occurrences of kimberlite-like intrusive rocks in drillcore from south of Wekusko Lake, eastern Flin Flon belt, north-central Manitoba (NTS 63J12)

by A.R. Chakhmouradian[1] and K.D. Reid

[1] Department of Geological Sciences, University of Manitoba, 125 Dysart Road, Winnipeg, MB

In Brief:

- Narrow, porphyritic, carbonate-rich dikes cut Paleoproterozoic rocks south of Wekusko Lake
- Mineralogy includes macrocryst and groundmass dolomite, phlogopite, spinel and ilmenite
- Preliminary data indicate hypabyssal kimberlite, rather than magnesiocarbonatite

Citation:
Chakhmouradian, A.R. and Reid, K.D. 2017: New occurrences of kimberlite-like intrusive rocks in drillcore from south of Wekusko Lake, eastern Flin Flon belt, north-central Manitoba (NTS 63J12); *in* Report of Activities 2017, Manitoba Growth, Enterprise and Trade, Manitoba Geological Survey, p. 78–90.

Summary

Two exploration drillholes that penetrate Precambrian basement rocks beneath the Phanerozoic limestone cover south of Wekusko Lake contain narrow but macroscopically distinguishable intercepts of dolomite-phlogopite–bearing intrusive dikes that crosscut the Paleoproterozoic rocks. These intrusive rocks were recognized during re-examination of the drillcore by the Manitoba Geological Survey during the 2016 and 2017 field seasons as part of a broader project to develop a series of 1:50 000 scale maps for the eastern portion of the sub-Phanerozoic Flin Flon belt. Both dike occurrences contain brownish-grey, predominantly inequigranular rocks that are macroscopically similar to kimberlite. Textures in the dikes vary from macrocrystic and composed of subrounded phlogopite (±serpentinized olivine) crystals set in a fine- to medium-grained dolomitic groundmass, to relatively equigranular, to quasi-globular owing to the presence of abundant ovoid, polygonal and irregularly shaped dolomitic aggregates. The modal composition of both dikes is broadly similar to magnesiocarbonatite previously described in the southwest corner of Wekusko Lake, but the trace-element data show greater similarity to hypabyssal kimberlite.

Presented in this report are the geological setting, drillcore observations and preliminary compositional data for dolomite, phlogopite, spinel and ilmenite from the dike sampled in 2016. Detailed petrographic and mineralogical work on the samples collected in 2017 is currently underway. If these occurrences of 'kimberlite-like' intrusive rocks are genetically related to the magnesiocarbonatite found in the southwest corner of Wekusko Lake, the area of mantle magmatism in the Flin Flon belt may be extended to at least 50 km^2. Implications of these new findings for diamond exploration are discussed.

Introduction

From a statistical perspective, Manitoba is relatively well endowed with respect to the number of known carbonatite occurrences, although examples of kimberlite remain elusive. Archean examples of carbonatite include those in the Oxford Lake and Knee Lake areas (Anderson et al., 2012; Anderson, 2016) and Paleoproterozoic examples were found at Eden Lake in the Trans-Hudson orogen and Paint Lake in the Superior boundary zone (Mumin, 2002; Chakhmouradian et al., 2008, 2009a; Couëslan, 2008). Carbonatite magmas are rare but known to produce significant economic concentrations of rare-earth elements, niobium and zirconium (e.g., Chakhmouradian and Wall, 2012; Chakhmouradian et al., 2015; Smith et al., 2015). In some cases, they contain more common metals, including copper, iron and molybdenum, such as at Palabora in South Africa (Aldous, 1986), Kovdor in Russia (Krasnova et al., 2004) and Huanglongpu in China (Xu et al., 2010).

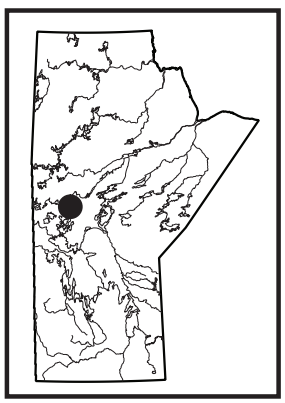

The rich mining history of copper-zinc (±gold±silver) volcanogenic massive sulphide (VMS) deposits in the Flin Flon belt (FFB) has resulted in exploration efforts in the region being focused heavily on its base-metal potential. Thus, it is not surprising that mantle-derived rocks of alkaline affinity were first intersected in the FFB by Falconbridge Nickel Mines Ltd. in 1983 during drill testing of the Copper-Man VMS deposit in the southwest corner of Wekusko Lake (Figure GS2017-8-1). Further drilling by European Ventures Inc. in the same location intersected what was described as a "kimberlitic rock" and reported to contain G10, G9 and possible eclogitic garnets, indicative of diamond potential. It is noteworthy that kimberlite and other carbonate-rich mantle-derived rocks (e.g., carbonatites and ultramafic lamprophyres) cannot be distinguished reliably based on their textural characteristics, but require a detailed geochemical and mineralogical analysis for their identification. A detailed petrographic study of the samples from the Falconbridge and European Ventures drillholes was undertaken by Chakhmouradian et al. (2009b) in order to identify these rocks and examine their affinity to various types of mantle-derived CO_2-rich magma. Their findings were that the mineralogy and geochemistry of the studied samples were inconsistent

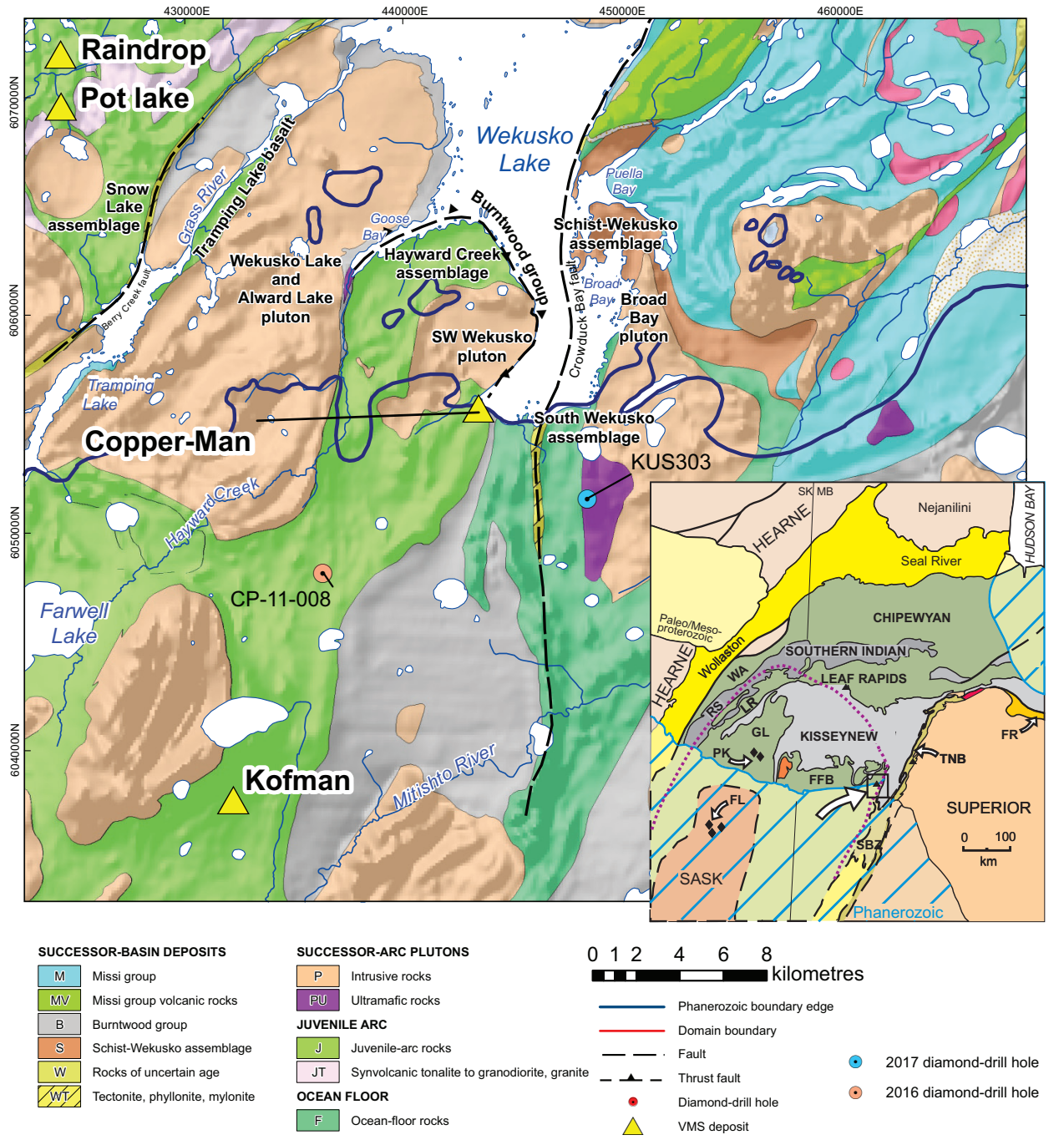

Figure GS2017-8-1: *Geology of the south Wekusko Lake area (modified from NATMAP Shield Margin Project Working Group, 1998), showing the Copper-Man VMS deposit, where magnesiocarbonatite has been identified in drillholes GBO-16 (Assessment file 73676) and EPV-12a (Chakhmouradian et al., 2009a, b; Assessment file 70569), and two new occurrences of texturally similar intrusive rocks in drillholes CP-11-008 (Assessment File 63J1159) and KUS303 (Assessment File 74423).* ***Inset*** *(modified after Zwanzig and Bailes, 2010): large white arrow shows location of south Wekusko Lake area in the Flin Flon belt (FFB) and its relation to the Kisseynew domain (KD), Superior boundary zone (SBZ), Thompson nickel belt (TNB), Fox River belt (FR), Glennie complex (GL), La Ronge belt (LR), Rottenstone domain (RS), Wathaman batholith (WA) and sub-Phanerozoic Sask craton (SASK). Fort à la Corne (FL) and Pikoo (PK) kimberlite fields indicated by diamond symbols, and triangles show Paleoproterozoic and younger carbonatite occurrences. Purple dashed line shows possible extent of Sask Craton in the lower crust.*

with kimberlite. Given the modal, isotopic and trace-element composition, Chakhmouradian et al. (2009b) interpreted these rocks as primary dolomite carbonatite contaminated by mantle material (including diamond-indicator minerals) and isotopically re-equilibrated with low-temperature crustal fluids. Recent re-examination of drillcore from the area south of Wekusko Lake has identified two new occurrences of inequigranular rock that is superficially similar to kimberlite and comprises largely the same minerals as those found in the dikes near the Copper-Man VMS deposit.

Geological setting

Wekusko Lake is at the eastern end of the FFB in the Reindeer zone of the Paleoproterozoic Trans-Hudson orogen (Lewry and Collerson, 1990). The FFB is a series of oceanic tectonostratigraphic assemblages structurally juxtaposed during intraoceanic accretion, intruded by successive arc-magma series and ultimately entrained during terminal collision of the Hearne, Superior and Sask cratons (e.g., Lucas et al., 1996; Syme et al., 1999; Hajnal et al., 2005). The belt is flanked to the north by metasedimentary gneisses of the Kisseynew domain and to the east by the Superior boundary zone, and to the south is covered by Phanerozoic sedimentary rocks (Figure GS2017-8-1).

The exposed geology of the southern section of Wekusko Lake was mapped by Gilbert and Bailes (2005) at 1:20 000 scale. Their work outlined five tectonostratigraphic blocks, from west to east the: 1) Hayward Creek assemblage of juvenile-arc affinity; 2) Burntwood Group turbidites; 3) South Wekusko assemblage of ocean-floor affinity; 4) Schist-Wekusko assemblage of successor-arc affinity; and 5) Missi group sandstone and conglomerate (see Figure GS2017-8-1). These are crosscut by multiple large intrusions of 'successor-arc' age.

The Crowduck Bay fault is a crustal-scale fault that can be traced to the north of Broad Bay before trending northeast in Crowduck Bay (not shown on Figure GS2017-8-1); it separates the Burntwood Group turbidites (2) from the South Wekusko ocean-floor basalt (3) to the east (Figure GS2017-8-1). At the south end of Wekusko Lake, the Crowduck Bay fault is traced as chlorite-carbonate schist before disappearing beneath the Phanerozoic cover (Figure GS2017-8-1).

Kimberlite-like intrusive rocks in drillcore

Drillhole CP-11-008

Drillhole CP-11-008 (Assessment File 63J1159) intersects predominantly heterolithic lapilli tuff with an overall dacitic composition. This unit is distinctive in that it contains ~5% quartz phenocrysts and 5–10% dark green, flattened mafic fragments. It then grades into a 50 m thick package comprising feldspathic wacke before grading back into dacitic feldspar-crystal tuff (Reid and Gagné, 2016). Overall the volcaniclastic rocks are moderately strained with a well-developed penetrative fabric.

Between depths of 307.75 and 308.10 m, the feldspar-crystal tuff is cut by a heterogeneous intrusive rock that varies in colour from buff brown to brownish grey (Figure GS2017-8-2a); the lateral extent of this intrusive rock is unknown and, for discussion purposes, it is referred to as a dike. Although material along the contacts with the wallrock is not well preserved, it is evident that both contacts are sharp and associated with brittle fracturing and cryptic alteration that extends approximately 1 cm into the adjacent wallrock (Figure GS2017-8-2b). The intrusive rock is texturally heterogeneous due to the presence of layering (flow banding?) and exotic xenoliths. Figure GS2017-8-2c shows a dolomite-rich layer that contains ovoid segregations of fine-grained dolomite 1–2 mm across and is in sharp contact with a darker grey layer that contains medium- to coarse-grained phlogopite macrocrysts in an aphanitic oxide-dolomite groundmass. Figure GS2017-8-2d shows a sharp but irregular lower contact between the darker grey macrocryst-rich domain and the lower dolomite-rich domain that contains several abraded xenoliths of biotite schist. A distinct, large (~4 cm) angular xenolith of mica schist occurs in a phlogopite-dolomite–rich material close to the lower contact (Figure GS2017-8-2e). Portions of the intrusive rock are texturally similar to some material from Wekusko Lake (drillhole EPV-12a) and many hypabyssal kimberlites (e.g., Wemindji in Quebec; Zurevinski and Mitchell, 2011).

Drillhole KUS303

The predominant rock type in drillhole KUS303 (Assessment File 74423) is dark green, fine-grained basalt with subordinate (<1.5 m in apparent thickness) intrusive rocks of intermediate to felsic composition, mafic wacke, finely laminated siliceous chert, and grunerite-bearing iron formation. Near the end of the drillhole, between depths of 215 and 230 m, a number of centimetre- to decimetre-scale ductile shear structures are present, and the rock type changes from basalt to gabbro (Reid, GS2017-7, this volume). Intruding a portion of the ductile shear zone is an approximately 2 m thick (227–229 m) interval of fine- to medium-grained, brownish-grey, dolomite-rich rocks that contain 5–10 vol. % orange-brown (altered?) phlogopite macrocrysts measuring up to 1.5 cm in diameter (Figure GS2017-8-3a). This interval is bounded by intensely fractured rock hosting abundant calcite- and dolomite-filled fractures. A 20 cm interval above the main intercept shows very poorly preserved intrusive material separated from the wallrock by a sharp but diffuse contact over a distance of several millimetres (Figure GS2017-8-3b). The upper contact of the main intercept is brecciated (at 226.95 m), with angular chlorite schist wallrock fragments surrounded by minor fine-grained intrusive matrix (Figure GS2017-8-3c).

Farther downhole (at 227.0 m), the brecciated rock varies from clast to matrix supported, with dark grey subangular schist fragments and late carbonate-filled fractures, the latter of which cut both wallrock and fine-grained intrusive rock (Figure GS2017-8-3d). The distribution of phlogopite macrocrysts is heterogeneous throughout the intercept, with 0.5–1.5 cm subangular to amoeboid grains of orange-brown colour concentrated at 227.1 m and, to a lesser extent, elsewhere (Figure GS2017-8-3e). At 227.7 m, the intrusive rock is characterized by a relatively equigranular groundmass hosting 0.5–2.0 mm

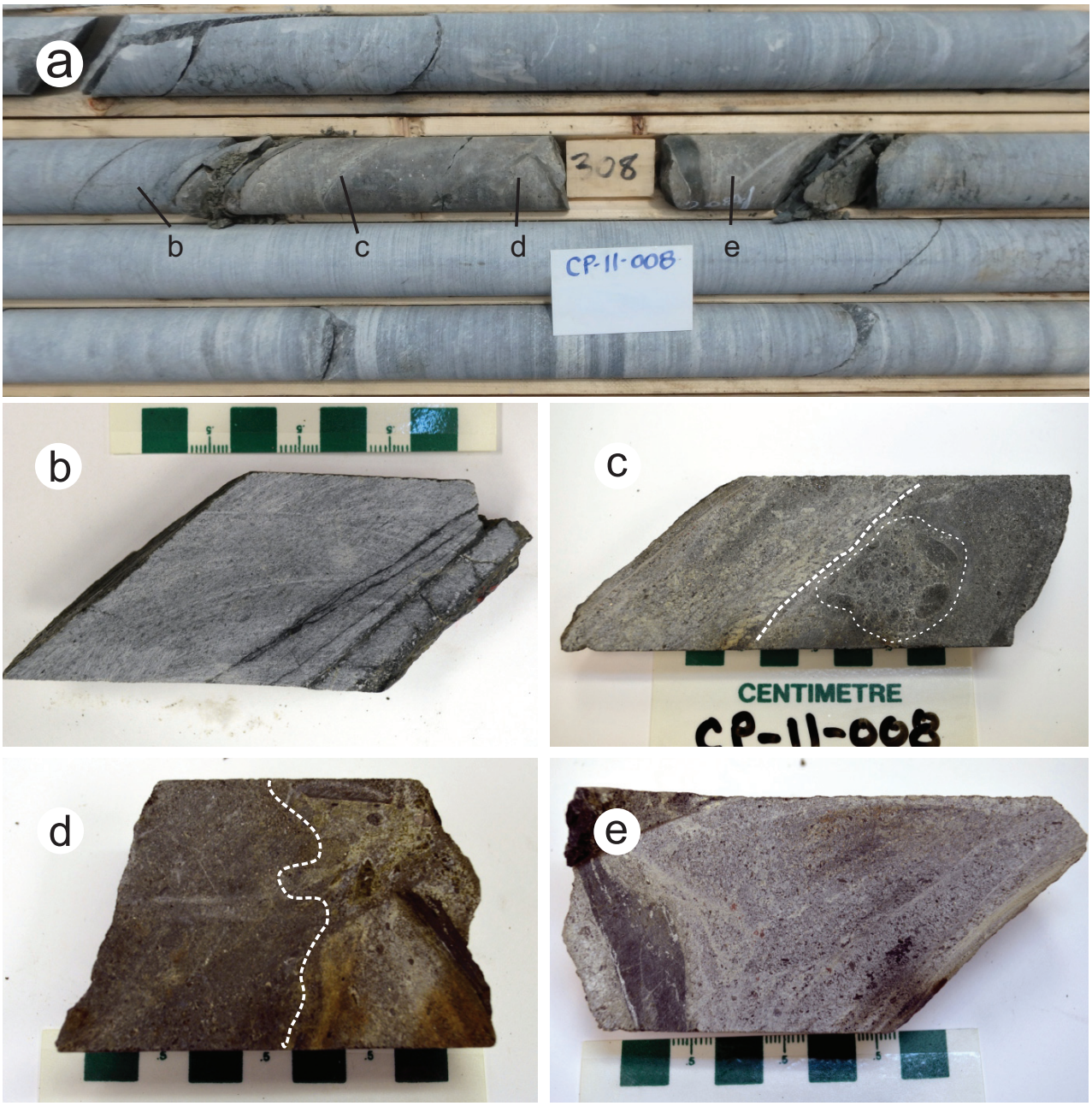

Figure GS2017-8-2: *Drillcore photos from drillhole CP-11-008 (Assessment File 63J1159):* ***a)*** *brownish-grey intrusive rock with sharp contacts, 307.75–308.10 m; letters show the location of close-up photos;* ***b)*** *sharp upper contact between felsic lapilli tuff and the intrusive rock, 307.70–307.75 m;* ***c)*** *internal structural heterogeneity of the intrusive rock, defined by layers rich in dolomite segregations (white dashed line), phlogopite macrocrysts (circular white dashed lines) and xenoliths, 307.75–307.90 m;* ***d)*** *sharp but irregular contact (dashed white line) between darker grey phlogopite-rich and dolomite-rich layers near the lower contact, 307.90–308.00 m;* ***e)*** *large mica schist xenolith in equigranular dolomite-phlogopite layer, 308.00–308.10 m. Core is NQ diameter (4.76 cm).*

rounded aggregates of fine-grained dolomite and minor phlogopite phenocrysts but few to no phlogopite macrocrysts (Figure GS2017-8-3f). The groundmass texture becomes more variable closer to the lower contact owing to intercalations of fine-grained phaneritic and aphanitic material (Figure GS2017-8-3g). The brown macrocryst-rich intrusive rock from drillhole KUS303 is superficially similar to altered hypabyssal kimberlite, alnoite and other carbonate-rich mantle-derived rocks, and thus cannot be identified with any degree of confidence in the absence of detailed petrographic, geochemical and mineralogical data.

Petrography

To date, four samples representing the upper ~25 cm of the dike intersected by drillhole CP-11-008 have undergone detailed

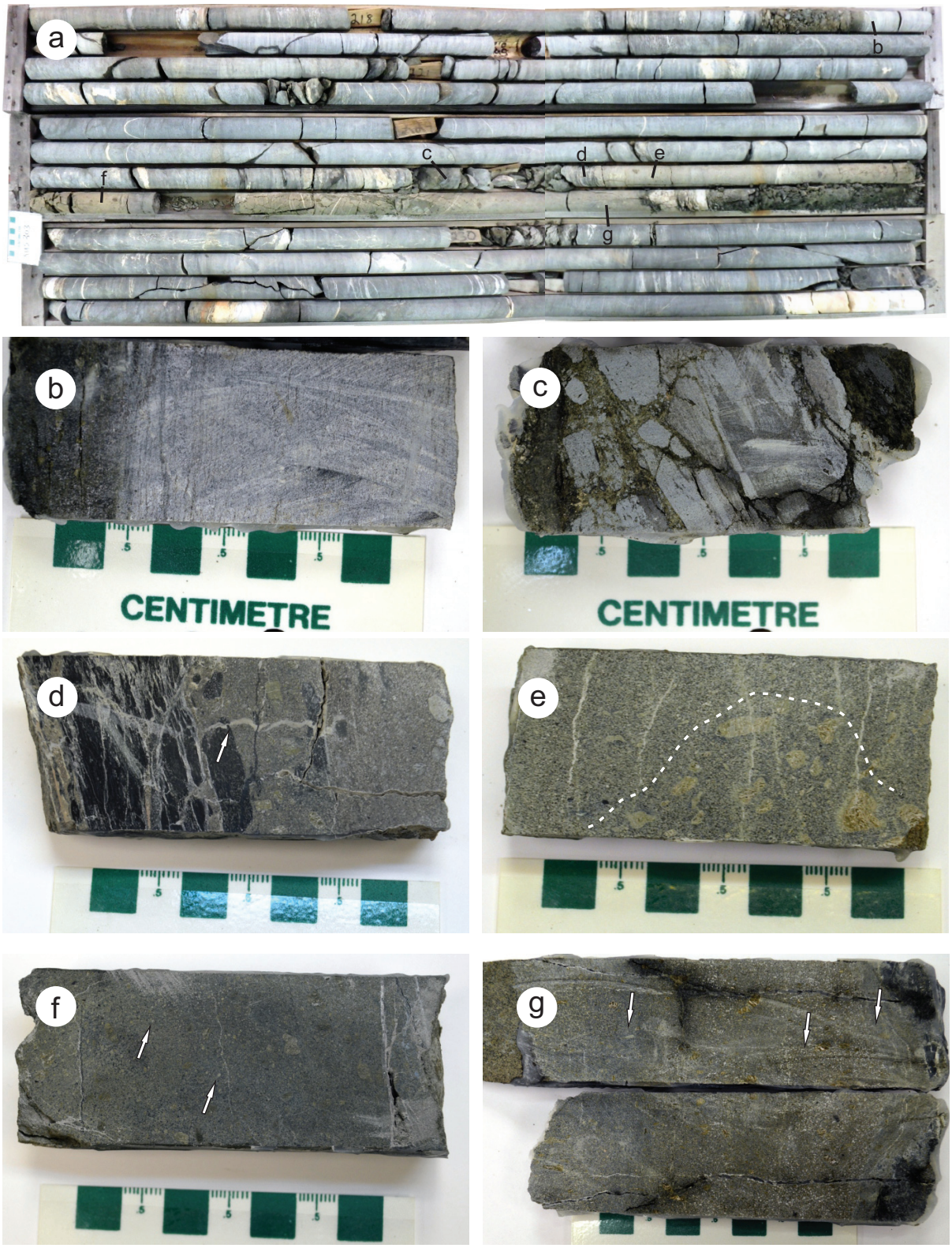

Figure GS2017-8-3: *Drillcore photos from drillhole KUS303 (Assessment File 74423):* ***a)*** *main intrusive intercept (227–229 m); letters show the location of close-up photos;* ***b)*** *sharp but diffuse contact between the intrusive material and wallrock metadacite, 218.8 m;* ***c)*** *clast-supported, chlorite schist breccia with a carbonate matrix, 226.95 m;* ***d)*** *gradation from clast-supported to matrix-supported breccia at the intrusive rock contact, 227.0 m; arrow points to a late-stage carbonate-filled vein;* ***e)*** *locally concentrated phlogopite macrocrysts (dashed line), 227.10 m;* ***f)*** *relatively equigranular igneous material with ovoid dolomite aggregates (arrows), 227.70 m;* ***g)*** *texturally heterogeneous (possibly layered) intrusive material with grain-size variations in the groundmass, 228.55 m. Core is BQ diameter (3.65 cm).*

petrographic and mineralogical study. The rock examined is remarkably heterogeneous in texture. A thin (~5 mm) selvage adjacent to the contact with the host metadacitic rock contains numerous phlogopite crystals and slender laths of dolomite up to 1 mm in length arranged at 50–90° to the contact (Figure GS2017-8-4a). The laths are 'sheathed' in microcrystalline granular dolomite and resemble quench textures observed in the selvages of some carbonatite dikes (e.g., Chakhmouradian et al., 2016, Figures 3c, 5c), as well as mantled microphenocrysts in some hypabyssal kimberlites (Chakhmouradian, unpublished data). In the contact zone, dolomite also occurs as ovoid aggregates of minute (20–60 μm across) polygonal grains and in the groundmass (Figure GS2017-8-4a). The groundmass also contains euhedral grains of spinel-group minerals, phlogopite and apatite surrounded by serpentine. The proportion of ovoid aggregates and phlogopite increases in abundance away from the contact, whereas dolomite laths and spinel-group minerals decrease, and the former disappear completely within 1 cm from it. Both phlogopite plates and dolomite laths are oriented obliquely to the intrusive contact outside the selvage zone (Figure GS2017-8-4b). In addition to these morphological changes, phlogopite crystals and groundmass grains are appreciably larger in the interior of the dike relative to the selvage zone.

Dolomite aggregates, phlogopite crystals and polymineralic groundmass remain the major structural elements up to a distance of ~5 cm from the upper contact. Within this interval, the rock is crudely layered and light coloured. Three types of dolomite aggregates were identified (listed in order of decreasing abundance): ovoid, irregularly shaped and polygonal (Figure GS2017-8-4c). Both ovoid and polygonal aggregates do not exceed 1.2 mm across and are composed of fine-grained (20–60 μm across) dolomite coarsening inward (Figure GS2017-8-4d), whereas the irregularly shaped aggregates are larger (up to 3 mm across) and contain generally coarser grains (locally up to 0.6 mm across). Phlogopite occurs in the groundmass and

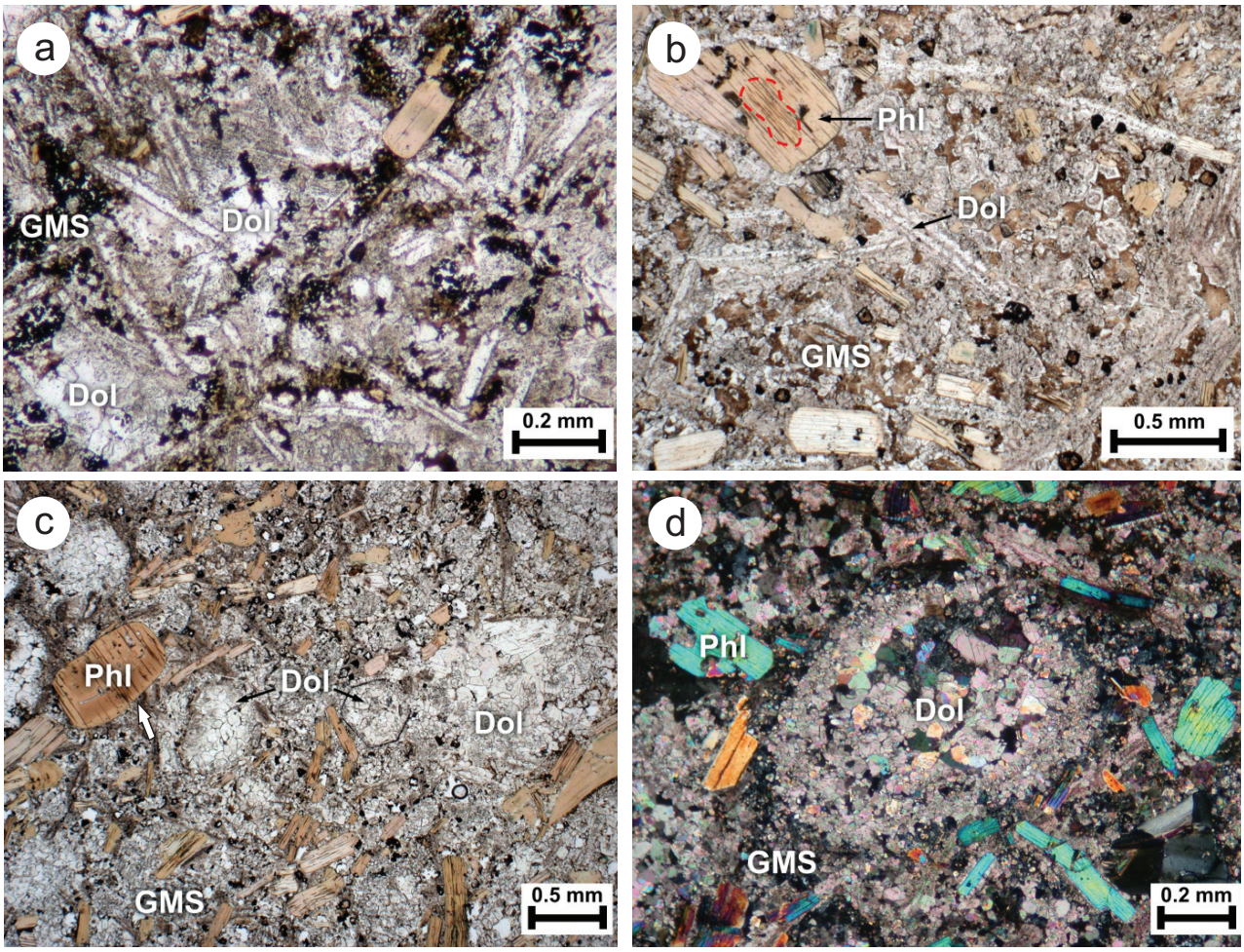

Figure GS2017-8-4: *Thin-section photomicrographs of carbonate intrusive rock near its upper contact with metadacite (~307.8 m), drillhole CP-11-008:* ***a)*** *dolomite laths (Dol) in a groundmass (GMS) composed of granular dolomite, spinel-group minerals, phlogopite, apatite and serpentine;* ***b)*** *phlogopite crystals (Phl) and dolomite laths (Dol) oriented subparallel to the upper contact and set in a finer grained groundmass, similar to that shown in (a) but containing a lower proportion of spinel (opaque);* ***c)*** *ovoid (left), polygonal (centre) and irregularly shaped (right) dolomite (Dol) aggregates, ~1.5 cm from the upper contact; note the abundance of macrocrystic and groundmass phlogopite and a relatively small proportion of spinel in this part of the dike;* ***d)*** *characteristic concentric, granular structure of ovoid dolomite aggregate (Dol), showing an inward pattern of grain coarsening.*

as thick tabular crystals up to 2 mm in length that show simple zoning and evidence of resorption, both at the core-rim boundary and along their margin (Figure GS2017-8-4c, white arrow). Because the larger tabular crystals were clearly not in equilibrium with their host melt, they will be referred to hereafter as macrocrysts rather than phenocrysts.

At a distance of ~5 cm from the contact, the rock colour changes to dark greenish grey, and its texture to massive and conspicuously inequigranular (Figure GS2017-8-2c). In this part of the dike, which extends for ~10 cm inward, the rock is composed of abundant phlogopite macrocrysts similar to those in the layered zone. However, it also contains minor chlorite, serpentine pseudomorphs after olivine (or, less likely, monticellite), phlogopite macrocrysts up to 2 mm in length (Figure GS2017-8-5a) and rounded biotite-quartz xenoliths up to 4 mm in diameter (Figure GS2017-8-5b) set in a fine-grained polymineralic groundmass. The groundmass comprises euhedral atoll-textured spinel-group minerals, cube-shaped rutile (±parisite) pseudomorphs after perovskite[2], hopper apatite crystals, platy phlogopite and anhedral dolomite grains set in a serpentine mesostasis (Figure GS2017-8-5c). The spinels and pseudomorphs after perovskite do not exceed 150 μm across, whereas apatite prisms are generally much smaller (<20 μm in diameter). Identification of the petrogenetically important accessory mineral perovskite (e.g., Reguir et al., 2010; Chakhmouradian et al., 2013), the precursor mineral to the parisite-rutile pseudomorphs, was determined from quantitative analysis of scarce unaltered cubic crystals and its Raman spectrum.

The proportions of serpentinized olivine and biotite-quartz xenoliths vary appreciably across the massive zone, whereas macrocrystic phlogopite is distributed relatively uniformly but exhibits an increasing degree of chloritization toward the centre of the intrusive interval. The central zone is texturally heterogeneous owing to the presence of randomly oriented crustal

[2] Parisite is a fluorocarbonate of light rare-earth elements with the general formula $CaREE_2(CO_3)_3F_2$; perovskite is a complex oxide mineral with the formula $(Ca,Na,REE)(Ti,Nb,Fe)O_3$.

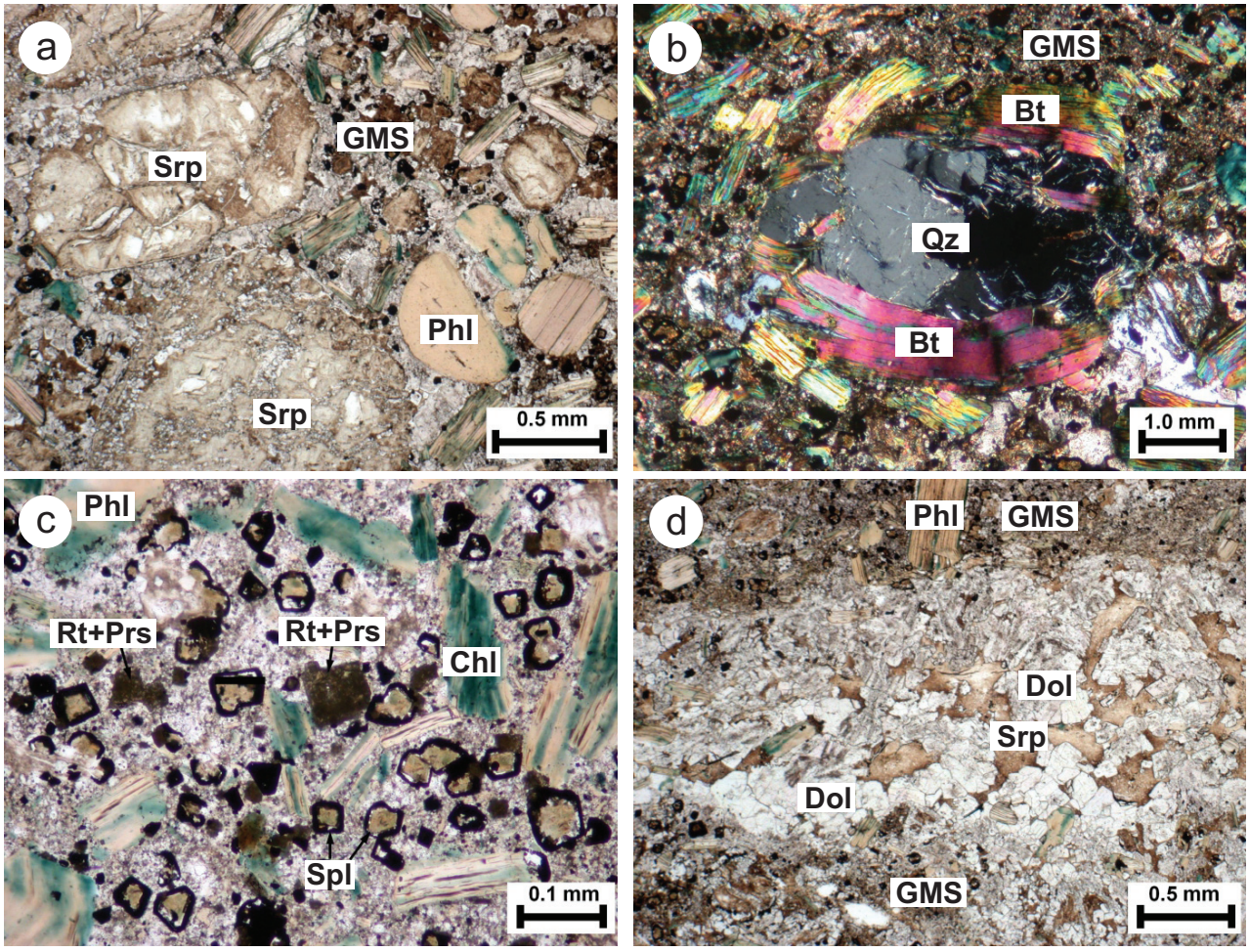

Figure GS2017-8-5: *Thin-section photomicrographs of carbonate intrusive rock near its axial zone (~308 m), drillhole CP-11-008:* ***a)*** *serpentinized macrocrysts of olivine or monticellite (Srp) and phlogopite (Phl) macrocrysts set in a groundmass (GMS) of dolomite, phlogopite, serpentine and opaque phases;* ***b)*** *rounded xenolith composed of quartz (Qz) and biotite (Bt);* ***c)*** *rutile-parisite (Rt+Prs) pseudomorphs after perovskite, atoll-textured spinel crystals (Sp) and partially chloritized (Chl) phlogopite (Phl) in the groundmass;* ***d)*** *lenticular aggregate of euhedral dolomite (Dol) crystals with interstitial serpentine (Srp); note grain-size contrast relative to the adjacent groundmass (GMS).*

xenoliths (some as large as 4 cm), domains enriched in dolomite aggregates and those enriched in serpentinized olivine. Texturally, this zone is characterized by the presence of 1) elongate light-coloured patches composed of coarser grained (relative to the surrounding groundmass) euhedral dolomite and occasional chloritized phlogopite set in a serpentine mesostasis (Figure GS2017-8-5d); 2) dolomite mantles around serpentinized olivine; and 3) relatively coarse (up to 1 mm across), zoned dolomite grains in the groundmass. The remainder of the groundmass is similar to that in the massive zone (i.e., comprises atoll-textured spinel-group minerals, rutile pseudomorphs after perovskite, apatite, chloritized phlogopite and serpentine).

Perhaps the most notable mineralogical feature of the dike in drillhole CP-11-008 is the abundance of opaque macrocrysts throughout the four texturally distinct zones described above. Most common are abraded ilmenite grains up to 2 mm across. Most of these macrocrysts are extremely irregular in shape and often fractured, and exhibit an embayed margin decorated with euhedral rutile-parisite pseudomorphs after perovskite; these pseudomorphs, in turn, are partially overgrown by spinel-group minerals (Figure GS2017-8-6a). The reaction-induced rim is variable in thickness and spongy, indicating the loss of some chemical components during the replacement. Notably, ilmenite was not observed in the groundmass. Spinel-group minerals occur both in the groundmass and as atoll-textured macrocrysts up to 0.6 mm across (Figure GS2017-8-6a). Some of the macrocrysts are abraded and lack an atoll-type rim. The chemical composition of these minerals is described in the next section.

Mineral chemistry

Selected minerals from the CP-11-008 dike were analyzed for major and minor elements using a Cameca SX100 automated electron microprobe operated at an accelerating voltage of 15 kV and a beam current of 20 nA. A carefully selected set of standards and peak-measurement parameters was used in each case to minimize matrix effects and potential peak overlaps. The empirically determined lower detection limits were <800 ppm for all elements reported here.

Dolomite is the principal constituent throughout the dike and shows great morphological diversity (see above). However, the compositions of all dolomite varieties fall within a fairly limited range (i.e., $Dol_{75–85}Ank_{11–24}Rds_{0–4}$, where Dol = $CaMg[CO_3]_2$, Ank = $CaFe[CO_3]_2$ and Rds = $CaMn[CO_3]_2$]. The SrO content ranges from 0.1 to 0.6 wt. %, whereas Ba is below its detection limit. Of all the morphological types, zoned crystals from the centre of the dike are characterized by the greatest compositional variation, involving a decrease in their Fe content coupled with an increase in Mg, Mn and Sr from the core outward.

The C and O stable-isotope ratios were measured in dolomite from all parts of the dike that have been petrographically studied. Eight powdered samples were digested in H_3PO_4 to produce CO_2 gas, which was analyzed using a Finnigan GasBench II on-line gas preparation and introduction system connected to a Thermo Finnigan Delta V Plus isotope-ratio mass spectrometer. Calibration was performed by analyzing two international calcite standards at the beginning, middle and end of each sample run. For quality check, calibrated internal calcite and dolomite standards were analyzed simultaneously with the samples. Multiple analyses of these standards yielded results within the standard deviation from the reference values (±0.10‰ for $\delta^{13}C_{V\text{-}PDB}$ and ±0.15‰ for $\delta^{18}O_{V\text{-}SMOW}$). The measured isotope ratios show very limited variation that cannot be correlated with any specific morphological type of dolomite ($\delta^{13}C_{V\text{-}PDB}$ = –3.8 to –4.0‰; $\delta^{18}O_{V\text{-}SMOW}$ = 19.5 to 22.2‰) and are therefore consistent with the electron-microprobe results.

Mica crystals show an extensive compositional variation and form two discrete populations on element-correlation diagrams. The darker coloured cores of some strongly zoned macrocrysts are biotite characterized by low mg# (molar Mg/[Mg+Fe]), ranging between 0.32 and 0.49, low Ti (1.4–2.5 wt. %

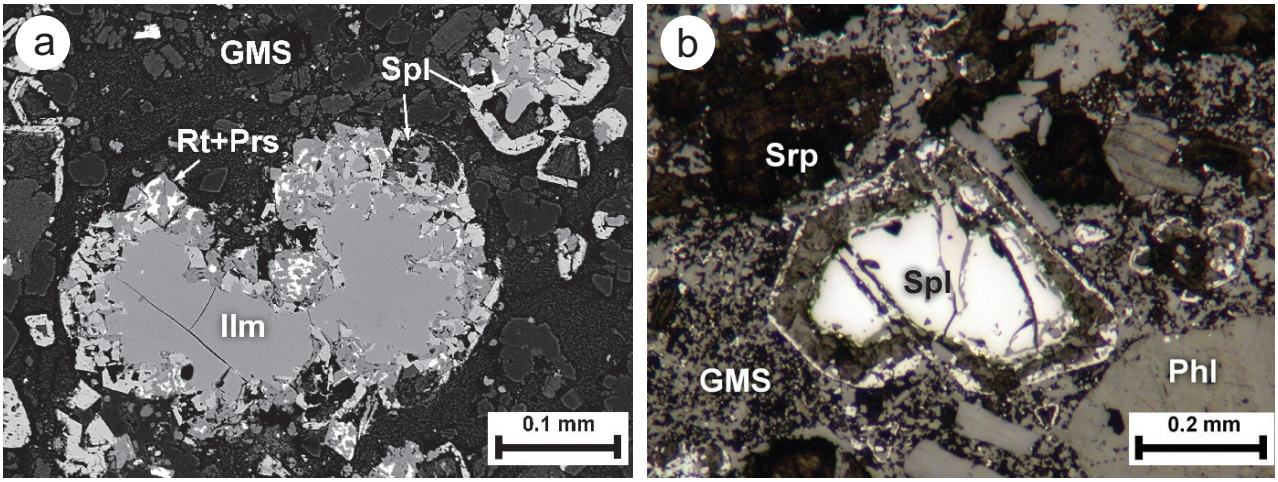

Figure GS2017-8-6: *Morphology of mantle-indicator minerals from the carbonate intrusive rock intersected by drillhole CP-11-008:* ***a)*** *backscattered-electron scanning electron microscope image of heavily resorbed ilmenite (Ilm) macrocrysts that are discontinuously overgrown by perovskite, now completely replaced by 'spongy' rutile-parisite (Rt+Prs) pseudomorphs and spinel (Spl);* ***b)*** *atoll-textured spinel (Spl) macrocryst set in apatite-serpentine-phlogopite-dolomite groundmass (GMS).*

TiO_2) and absence of detectable Cr. Macrocryst rims and groundmass grains define a single phlogopite population enriched in Mg (mg# = 0.70–0.78), Ti and Cr (up to 3.5 and 0.7 wt. % of the respective oxides). Individual zoned macrocrysts show a rimward increase in Fe coupled with a decrease in Cr and Ti.

Ilmenite macrocrysts are devoid of zoning and high in Mg and Cr (10.4–12.5 and up to 6.5 wt. % of the respective oxides; Figure GS2017-8-7a) but poor in Mn (0.2–0.5 wt. % MnO). Notably, all analyzed grains also contain detectable Al (0.3–0.5 wt. % Al_2O_3), which is rarely reported in published electron-microprobe data for ilmenite. The measured compositions show a somewhat lower-than-expected TiO_2 content (Figure GS2017-8-7b), owing to the presence of Fe^{3+} substituting for Ti in ilmenite. The formulae calculated on a stoichiometric basis (two cations and three oxygen atoms) give between 4 and 7 mol. % Fe_2O_3 (i.e., are lower than the Fe_2O_3 levels suggested

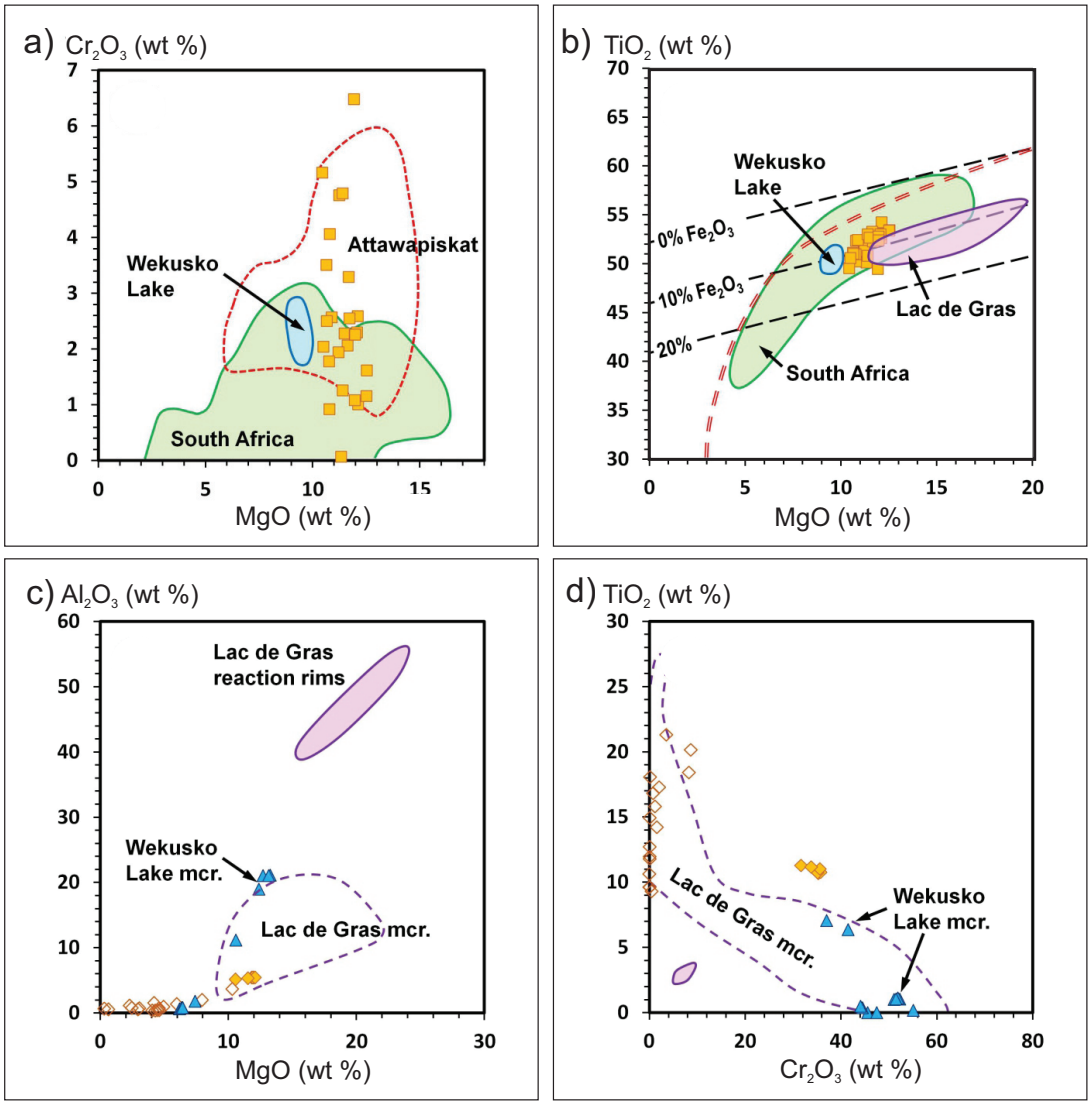

Figure GS2017-8-7: *Compositional variation (wt. % oxides) of ilmenite and spinel-group minerals from the carbonate intrusive rock intersected by drillhole CP-11-008:* ***a)*** *MgO vs. Cr_2O_3 in ilmenite macrocrysts from CP-11-008 (brown squares) compared to those from Wekusko Lake dolomite carbonatites (Chakhmouradian et al., 2009b), South African kimberlites (Wyatt et al., 2004) and Attawapiskat, Ontario kimberlites (Kong et al., 1999);* ***b)*** *MgO vs. TiO_2 in ilmenite macrocrysts from CP-11-008 (brown squares) compared to those from Wekusko Lake dolomite carbonatites (Chakhmouradian et al., 2009), South African kimberlites (Wyatt et al., 2004) and Lac de Gras, Northwest Territories kimberlites (Chakhmouradian, unpublished data); dashed lines indicate estimated Fe_2O_3 content and double-dashed line separates fields of kimberlitic (right) and nonkimberlitic (left) ilmenite (according to Wyatt et al., 2004);* ***c)*** *MgO vs. Al_2O_3 in macrocrysts and groundmass grains of spinel-group minerals (filled and empty diamonds, respectively) compared to macrocrysts from Wekusko Lake dolomite carbonatites (Chakhmouradian et al., 2009b) and Lac de Gras kimberlites (Chakhmouradian, unpublished data); purple field shows compositional range of reaction rims on macrocrysts from Lac de Gras kimberlites;* ***d)*** *TiO_2 vs. Cr_2O_3 in macrocrysts and groundmass grains of spinel-group minerals (filled and empty diamonds, respectively) compared to macrocrysts from Wekusko Lake dolomite carbonatites (Chakhmouradian et al., 2009b) and Lac de Gras kimberlites (Chakhmouradian, unpublished data). Abbreviation: mcr., macrocrysts.*

by the discrimination diagram of Wyatt et al. [2004]). The most likely reason for this discrepancy is the enrichment of the current samples in Cr and Al, which substitute for Ti in the structure and thus would account for some of the apparent Ti deficit.

Spinel macrocrysts (Figure GS2017-8-7c, d) are rich in Mg, Al, Ti and Cr (10.3–12.1, 5.2–5.5, 10.7–11.3 and 31.7–35.8 wt. % respective oxides) at low Mn levels. They can be classified as magnesiochromite (~45 mol. % $MgCr_2O_4$) with significant proportions of ulvöspinel (Fe_2TiO_4), magnetite ($FeFe_2O_4$) and spinel ($MgAl_2O_4$). Groundmass grains and rims on ilmenite and spinel macrocrysts correspond to Al-Cr–poor (<2.0 and 3.5 wt. % respective oxides) but relatively Mg-Ti–rich magnetite (2.3–7.9 and 9.6–21.3 wt. % respective oxides). In addition to Ti, the Mn content is also elevated in the magnetite relative to the macrocrysts (0.6–1.7 vs. 0.2–0.4 wt. % MnO, respectively).

Geochemistry

Bulk-rock major- and trace-element data are available only for one sample (total-digestion ICP-MS; # K08914, HudBay Minerals Inc., unpublished data) from the KUS303 core (depth 228.0 m). The rock is ultrabasic and carbonate rich (all values in wt. %): 29.03% SiO_2, 2.97% TiO_2, 2.33% Al_2O_3, 23.76% MgO, 9.86% CaO, 0.21% MnO, 9.41% FeO_{total}, 0.44% Na_2O, 0.51% K_2O, 14.80% CO_2, 0.19% P_2O_5, 19.80% LOI. Of particular note are the high levels of both compatible and incompatible trace elements (e.g., 155 ppm V, 958 ppm Cr, 844 ppm Ni, 195 ppm Zr, 143 ppm Nb, 325 ppm Ba, 470 ppm REE, 23 ppm Th). The abundances of trace elements normalized to the primitive-mantle values (McDonough and Sun, 1995) are shown in Figure GS2017-8-8. Key petrogenetic ratios are as follows: K/Sr = 7.4, Co/Ni = 0.11, Ga/Al = 0.00049, $(La/Yb)_{CN}$ = 37, Zr/Hf = 20, Th/U = 2.8, Nb/Ta = 16.

Discussion

Based on the currently available mineralogical and geochemical evidence, the intrusive rocks intersected in drillholes CP-11-008 and KUS303 bear a strong resemblance to the Wekusko Lake carbonatite dikes described by Chakhmouradian et al. (2009a, b). The principal similarities are 1) the extremely inequigranular nature of these rocks; 2) the presence of basement xenoliths and abundance of dolomite, phlogopite and oxide macrocrysts in their modal composition; and 3) their enrichment in Cr and REE (among other incompatible elements). Although bulk-rock data are not yet available for the CP-11-008 sample, its enrichment in Cr is clearly manifested in the compositions of phlogopite, ilmenite and spinel macrocrysts, whereas the abundance of parisite also implies high levels of REE. Dolomite from drillhole CP-11-008 is very similar to that from drillhole GBO-16 (Wekusko Lake) in its major-element and C-O stable-isotope compositions (i.e., both are low-Fe, relatively Sr-rich varieties showing low $\delta^{13}C_{V\text{-}PDB}$ but high $\delta^{18}O_{V\text{-}SMOW}$ values). Significant mineralogical differences, however, are observed between the Wekusko Lake dikes and the CP-11-008 samples. The latter contain serpentinized olivine, magnetite and (pseudomorphed) perovskite in the groundmass but lack zircon and apatite phenocrysts. Mineralogically, the CP-11-008 dike is more similar to hypabyssal kimberlites, and this resemblance is underscored by some of its microtextural characteristics, such as the perovskite-magnetite reaction rims on ilmenite macrocrysts, TiO_2 pseudomorphs after perovskite (Chakhmouradian and Mitchell, 2000) and mantled dolomite microphenocrysts (Chakhmouradian, unpublished data).

The compositions of ilmenite and spinel macrocrysts from CP-11-008 are compared to those in the Wekusko Lake dikes and bona fide kimberlites in Figure GS2017-8-7. In terms of

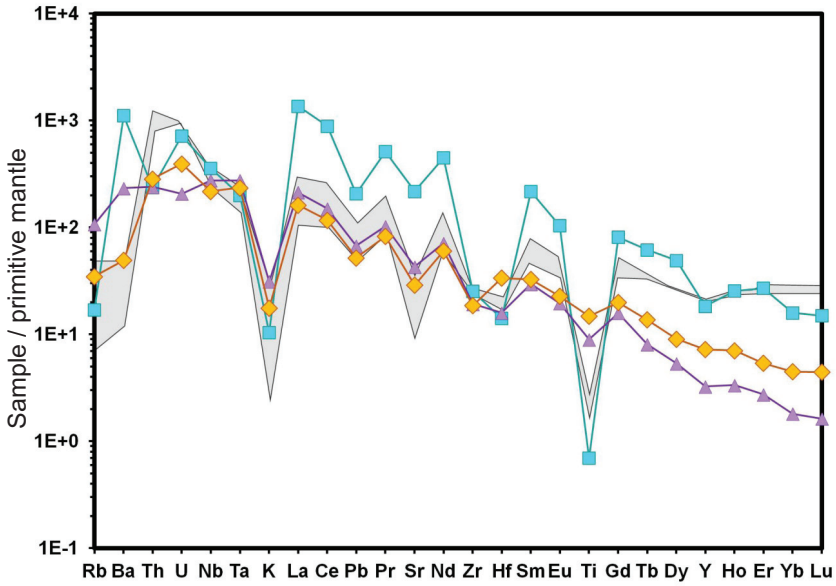

Figure GS2017-8-8: *Chondrite-normalized trace-element profile of carbonate intrusive rock from drillhole KUS303 (yellow diamonds; normalized to the primitive-mantle values of McDonough and Sun, 1995), compared to the average profiles of hypabyssal kimberlites (purple triangles; Chakhmouradian et al., 2013) and anorogenic dolomite carbonatites (blue squares; Chakhmouradian et al., 2009b), and to the profile of the Wekusko Lake dolomite carbonatite dikes (grey field).*

its Mg, Cr and Mn contents, ilmenite examined in this study is similar to macrocrysts from on-craton kimberlites worldwide. Note, however, that compositionally similar macrocrysts were also reported previously from carbonatites and carbonate-rich ultramafic lamprophyres (Chakhmouradian et al., 2009b; Tappe et al., 2009), so their presence in a mantle-derived rock cannot be used for its reliable identification. Macrocrystic spinel in kimberlites (e.g., Mitchell, 1986, 1995) and other mantle-derived carbonate-rich rocks (Tappe et al., 2006, 2009; Chakhmouradian et al., 2009b; Brady and Moore, 2012) is similar to the macrocrysts examined in this study in terms of its Mg, Al and Cr contents (comparison to Lac de Gras kimberlite spinel is shown in Figure GS2017-8-7c, d) but usually shows lower levels of Ti (<9 wt. % TiO_2). Groundmass grains correspond to low–Cr-Al and high–Mg-Ti compositions, akin to the magnesioferrite-ulvöspinel-magnetite series characteristic of kimberlites (Mitchell, 1986, 1995).

The sample from drillhole KUS303 analyzed by HudBay Minerals is geochemically akin to kimberlites; in fact, with the exception of somewhat lower Rb and Ba abundances and higher levels of heavy REE (Gd-Lu), this rock is almost identical to the average hypabyssal kimberlite (Figure GS2017-8-8). Dolomite carbonatites are characterized by generally higher levels of divalent large-ion lithophile elements and REE (Figure GS2017-8-8). More importantly, however, carbonatites and kimberlites can be reliably distinguished on the basis of certain element ratios, which are sensitive to both the nature of mantle sources of these rocks and petrogenetic processes involved in their evolution (Chakhmouradian, 2006; Chakhmouradian et al., 2009b, 2013). In kimberlites, these indicator ratios approach primitive-mantle (and chondritic) values (e.g., K/Sr = 9 vs. 12, Co/Ni = 0.07 vs. 0.05, Nb/Ta = 18 vs. 18, respectively). In contrast, anorogenic carbonatites exhibit a very different trace-element signature (e.g., K/Sr = 0.6, Co/Ni = 2.7, Nb/Ta = 39 for dolomitic rocks), implying their derivation from an unusual mantle source or their geochemically evolved nature. The KUS303 dike shows primitive-mantle–like indicator ratios similar to those in kimberlites and no evidence of element loss through fractionation or wall-rock metasomatism.

To summarize, the currently available evidence strongly indicates that the intrusive rocks identified in drillholes CP-11-008 and KUS303 may be related to those intersected farther north beneath Wekusko Lake or, at least, are derived from a similar mantle source enriched in carbon and incompatible elements. At all three localities, the emplacement of parental magma must have been rapid enough to preserve mantle-derived indicator minerals and to facilitate the entrainment of wallrock material. The structures and textures observed in the drillcore and thin sections imply emplacement by injection into fractured basement rocks below the surface of magma fluidization. True segregation textures, such as those typifying the transitional facies of some kimberlite intrusions (Hetman et al., 2004; Skinner and Marsh, 2004), are not observed in the dikes at any of the three localities. That the level of fluidization was not reached is also consistent with the stable-isotope data, which do not indicate any significant CO_2 loss, as would have occurred during magma fluidization. The stable-isotope data for both the Wekusko Lake and the CP-11-008 dikes, however, do record re-equilibration of primary igneous dolomite with a low-temperature, ^{18}O-enriched reservoir, potentially representing Lower Paleozoic seawater (for further discussion, see Chakhmouradian et al., 2009b). A detailed mineralogical and geochemical study of the newly discovered intrusive dikes is presently underway as a collaborative project between the University of Manitoba and the Manitoba Geological Survey.

Economic considerations

Although indicator minerals such as Mg-Cr–rich ilmenite and spinel cannot be used to identify the type of magma that transported them (Mitchell et al., 1999; Chakhmouradian et al., 2009b; Tappe et al., 2009; Brady and Moore, 2012), their occurrence in the rock is an important hallmark of mantle-derived silica-undersaturated and carbonate-rich intracontinental magmatism that is known to produce diamond deposits. In this context, kimberlite is not the only type of magma that is of potential interest in diamond exploration, other notable examples being ultramafic lamprophyres and carbonatites (Mitchell et al., 1999; Digonnet et al., 2000). As has been emphasized numerous times in the literature (e.g., Raeside and Helmstaedt, 1982; Mitchell, 1983, 1995; Reguir et al., 2009), reliable identification of (potentially) diamondiferous rocks requires a painstaking analysis of their petrography, of compositional variations exhibited by major and accessory phases, and of the whole-rock trace-element budget. With the two new localities of kimberlite-like rocks described in this report, the extent of ultrabasic, carbonate-rich magmatism in the southern Wekusko Lake area may be greater than 50 km^2 (Figure GS2017-8-1).

It is also noteworthy that young cryptovolcanic structures have been documented farther south, at Shoulderblade Island in South Moose Lake (Bezys and Bamburak, 1994) and at Easterville (Bezys et al., 1996). Although the data available for these localities are presently insufficient to claim any petrogenetic connection to the Wekusko area dikes, they do indicate that this part of the Trans-Hudson orogen (and underlying Sask craton: Hajnal et al., 2005) has experienced (possibly, more than once) extensional tectonic reactivation and associated magmatism since the Paleoproterozoic. Further indicator-mineral sampling and geophysical exploration are warranted along the southern margin of the FFB and into the Interlake Region to ascertain the extent of kimberlite-like magmatism in this part of Manitoba.

Acknowledgments

The authors thank M. Stocking, C. Stocki, and S. Walker for providing enthusiastic field assistance, as well as N. Brandson and E. Anderson for thorough logistical support. Additional thanks go to C. Epp and C. Stocki for help handle of samples in the laboratory. They are grateful to HudBay Minerals Inc. and Royal Nickel Inc. for providing access and facilities to examine drillcore. The Natural Sciences and Engineering Research Council of Canada provided funding for micro-analytical analyses

through a grant to A. Chakhmouradian (University of Manitoba).

References

Aldous, R.T.H. 1986: Copper-rich fluid inclusions in pyroxenes from the Guide copper mine, a satellite intrusion of the Palabora igneous complex, South Africa; Economic Geology, v. 81, p. 143–155.

Anderson, S.D. 2016: Preliminary results of bedrock mapping at central Knee Lake, northwestern Superior province, Manitoba (parts of NTS 53L15, 53M2); *in* Report of Activities 2016, Manitoba Growth, Enterprise and Trade, Manitoba Geological Survey, p. 1–15.

Anderson, S.D., Kremer, P.D. and Martins, T. 2012: Preliminary results of bedrock mapping at Oxford Lake, northwestern Superior province, Manitoba (parts of NTS 53L12, 13, 63I9, 16); *in* Report of Activities 2012, Manitoba Innovation, Energy, and Mines, Manitoba Geological Survey, p. 6–22.

Bezys, R.K. and Bamburak, J.D. 1994: Geological investigation of Shoulderblade Island structure, South Moose Lake, NTS 63F16; *in* Report of Activities 1994, Manitoba Energy and Mines, Minerals Division, p. 142–143.

Bezys, R.K., Fedikow, M.A.F. and Kjarsgaard, B.A. 1996: Evidence of Cretaceous(?) volcanism along the Churchill–Superior Boundary Zone, Manitoba (NTS 63G/4); *in* Report of Activities 1996, Manitoba Energy and Mines, Minerals Division, p. 122–126.

Brady, A.E. and Moore, K.R. 2012: A mantle-derived dolomite silicocarbonatite from the southwest coast of Ireland; Mineralogical Magazine, v. 76, p. 357–376.

Chakhmouradian, A.R., 2006: High-field-strength elements in carbonatitic rocks: geochemistry, crystal chemistry and significance for constraining the sources of carbonatites; Chemical Geology, v. 235, p. 138–160.

Chakhmouradian, A.R. and Mitchell, R.H. 2000: Occurrence, compositional variation and alteration of perovskite in kimberlites; Canadian Mineralogist, v. 38, p. 975–994.

Chakhmouradian, A.R. and Wall, F. 2012: Rare earth elements: minerals, mines, magnets (and more); Elements, v. 8, p. 333–340.

Chakhmouradian, A.R., Böhm, C.O., Demény, A., Reguir, E.P., Hegner, E., Creaser, R.A., Halden, N.M. and Yang, P. 2009b: "Kimberlite" from Wekusko Lake, Manitoba: actually a diamond-indicator bearing dolomite carbonatite; Lithos, v. 112, p. 347–357.

Chakhmouradian, A.R., Couëslan, C.G. and Reguir, E.P. 2009a: Evidence for carbonatite magmatism at Paint Lake, Manitoba (parts of NTS 63O8, 63P5, 12); *in* Report of Activities 2009, Manitoba Science, Technology, Energy and Mines, Manitoba Geological Survey, p. 118–126.

Chakhmouradian, A.R., Mumin, A.H., Demény, A. and Elliott, B. 2008: Postorogenic carbonatites at Eden Lake, Trans-Hudson Orogen (northern Manitoba, Canada): geological setting, mineralogy and geochemistry; Lithos, v. 103, p. 503–526.

Chakhmouradian, A.R., Reguir, E.P., Kamenetsky, V.S., Sharygin, V.V. and Golovin, A.V. 2013: Trace-element partitioning in perovskite: implications for the geochemistry of kimberlites and other mantle-derived undersaturated rocks; Chemical Geology, v. 353, p. 112–131.

Chakhmouradian, A.R., Reguir, E.P., Kressall, R.D., Crozier, J., Pisiak, L.K., Sidhu, R. and Yang, P. 2015: Carbonatite-hosted niobium deposit at Aley, northern British Columbia (Canada): mineralogy, geochemistry and petrogenesis; Ore Geology Reviews, v. 64, p. 642–666.

Chakhmouradian, A.R., Reguir, E.P. and Zaitsev, A.N. 2016: Calcite and dolomite in intrusive carbonatites. I. Textural variations; Mineralogy and Petrology, v. 110, p. 333–360.

Couëslan, C.G. 2008: Preliminary results from geological mapping of the west-central Paint Lake area, Manitoba (parts of NTS 63O8, 9, 63P5, 12); *in* Report of Activities 2008, Manitoba Science, Technology, Energy and Mines, Manitoba Geological Survey, p. 99–108.

Digonnet, S., Goulet, N., Bourne, J., Stevenson, R. and Archibald, D. 2000: Petrology of the Abloviak aillikite dykes, New Québec: evidence for a Cambrian diamondiferous alkaline province in northeastern North America; Canadian Journal of Earth Sciences, v. 37, p. 517–533.

Gilbert, H.P. and Bailes, A.H. 2005: Geology of the southern Wekusko Lake area, Manitoba (NTS 63J12NW); Manitoba Industry, Economic Development and Mines, Manitoba Geological Survey, Geoscientific Map MAP2005-2, scale 1:20 000.

Hajnal, Z., Lewry, J., White, D., Ashton, K., Clowes, R., Stauffer, M., Gyorfi, I. and Takacs, E. 2005: The Sask Craton and Hearne Province margin: seismic reflection studies in the western Trans-Hudson Orogen; Canadian Journal of Earth Sciences, v. 42, p. 403–419.

Hetman, C.M., Scott-Smith, B.H., Paul, J.L. and Winter, F. 2004: Geology of the Gahcho Kué kimberlite pipes, NWT, Canada: root to diatreme magmatic transition zones; Lithos, v. 76, p. 51–74.

Kong, J.M., Boucher, D.R. and Scott-Smith, B.H. 1999: Exploration and geology of the Attawapiskat kimberlites, James Bay Lowlands, northern Ontario, Canada; *in* Proceedings of the VIIth International Kimberlite Conference (Volume 1); Red Roof Design, Cape Town, South Africa, p. 452–467.

Krasnova, N.I., Petrov, T.G., Balaganskaya, E.G., Garcia, D., Moutte, J., Zaitsev, A.N. and Wall, F. 2004: Introduction to phoscorites: occurrence, composition, nomenclature and petrogenesis; *in* Phoscorites and Carbonatites from Mantle to Mine: The Key Example of the Kola Alkaline Province, F. Wall and N. Zaitsev (ed.), Mineralogical Society of Great Britain and Ireland, London, p. 45–74.

Lewry, J.F., and Collerson, K.D. 1990: Trans-Hudson Orogen: extent, subdivision, and problems, *in* The Early Proterozoic Trans-Hudson Orogen of North America, J.F. Lewry and M.R. Stauffer (ed.), Geological Association of Canada, Special Publication 37, p. 1–14.

Lucas, S.B., Stern, R.A., Syme, E.C., Reilly, B.A. and Thomas, D.J. 1996: Intraoceanic tectonics and the development of continental crust: 1.92–1.84 Ga evolution of the Flin Flon Belt, Canada; Geological Society of America Bulletin, v. 108, p. 602–629.

McDonough, W.F. and Sun, S.-s. 1995: The composition of the Earth; Chemical Geology, v. 120, p. 223–253.

Mitchell, R.H. 1983: The Ile Bizard intrusion, Montreal, Quebec – kimberlite or lamprophyre? Discussion; Canadian Journal of Earth Sciences, v. 20, p. 1493–1496.

Mitchell, R.H. 1986: Kimberlites: Mineralogy, Geochemistry and Petrology; Plenum, New York, New York, 442 p.

Mitchell, R.H. 1995: Kimberlites, Orangeites, and Related Rocks; Plenum, New York, New York, 410 p.

Mitchell, R.H., Scott-Smith, B.H. and Larsen, L.M. 1999: Mineralogy of ultramafic dikes from the Sarfartoq, Sisimiut and Maniitsoq areas, West Greenland; *in* Proceedings of the VIIth International Kimberlite Conference; Red Roof Design, Cape Town, South Africa, p. 574–583.

Mumin, A.H. 2002: Discovery of a carbonatite complex at Eden Lake (NTS 64C9), Manitoba, *in* Report of Activities 2002, Manitoba Industry, Trade and Mines, Manitoba Geological Survey, p. 187–197.

NATMAP Shield Margin Project Working Group 1998: Geology, NATMAP Shield Margin Project area, Flin Flon belt, Manitoba/Saskatchewan; Geological Survey of Canada, Map 1968A, scale 1:100 000.

Raeside, R.P. and Helmstaedt, H. 1982: The Ile Bizard intrusion, Montreal, Quebec – kimberlite or lamprophyre? Canadian Journal of Earth Sciences, v. 19, p. 1996–2011.

Reguir, E.P., Camacho, A., Yang, P., Chakhmouradian, A.R., Kamenetsky, V.S. and Halden, N.M. 2010: Trace-element study and uranium-lead dating of perovskite from the Afrikanda plutonic complex, Kola Peninsula (Russia) using LA-ICP-MS; Mineralogy and Petrology, v. 100, p. 95–103.

Reguir, E.P., Chakhmouradian, A.R., Halden, N.M., Malkovets, V.G. and Yang, P. 2009: Major- and trace-element compositional variation of phlogopite from kimberlites and carbonatites as a petrogenetic indicator; Lithos, v. 112S, p. 372–384.

Reid, K.D. and Gagné, S. 2016: Examination of exploration drillcore from the south Wekusko Lake area, eastern Flin Flon belt, north-central Manitoba (parts of NTS 63J5, 12, 63K8, 9); *in* Report of Activities 2016, Manitoba Growth Enterprise and Trade, Manitoba Geological Survey, p. 74–86.

Skinner, E.M.W. and Marsh, J.S. 2004: Distinct kimberlite pipe classes with contrasting eruption processes; Lithos, v. 76, p. 183–200.

Smith, M.P., Campbell, L.S. and Kynicky, J. 2015: A review of the genesis of the world class Bayan Obo Fe-REE-Nb deposits, Inner Mongolia, China: multistage processes and outstanding questions; Ore Geology Reviews, v. 64, p. 459-476.

Syme, E.C., Lucas, S.B., Bailes, A.H. and Stern, R.A. 1999: Contrasting arc and MORB-like assemblages in the Paleoproterozoic Flin Flon Belt, Manitoba, and the role of intra-arc extension in localizing volcanic-hosted massive sulphide deposits; Canadian Journal of Earth Sciences, v. 36, p. 1767–1788.

Tappe, S., Foley, S.F., Jenner, J.A., Heaman, L.M., Kjarsgaard, B.A., Romers, R.L., Stracke, A., Joyces, N. and Hoefs, J. 2006: Genesis of ultramafic lamprophyres and carbonatites at Aillik Bay, Labrador: a consequence of incipient lithospheric thinning beneath the North Atlantic craton; Journal of Petrology, v. 47, p. 1261–1315.

Tappe, S., Steenfelt, A., Heaman, L.M. and Simonetti, A. 2009: The newly discovered Jurassic Tikiusaaq carbonatite-aillikite occurrence, West Greenland, and some remarks on carbonatite-kimberlite relationships; Lithos, v. 112S, p. 385–399.

Wyatt, B.A., Baumgartner, M., Anckar, E and Grutter, H., 2004: Compositional classification of “kimberlitic” and “non-kimberlitic” ilmenite; Lithos, v. 77, p. 819–840.

Xu, C., Kynicky, J., Chakhmouradian, A.R., Qi, L. and Song, W. 2010: A unique Mo deposit associated with carbonatites in the Qinling orogenic belt, central China; Lithos, v. 118, p. 50–60.

Zurevinski, S.E. and Mitchell, R.H. 2011: Highly evolved hypabyssal kimberlite sills from Wemindji, Quebec, Canada: insights into the process of flow differentiation in kimberlite magmas; Contributions to Mineralogy and Petrology, v. 161, p. 765–776.

Zwanzig, H.V. and Bailes, A.H. 2010: Geology and geochemical evolution of the northern Flin Flon and southern Kisseynew domains, Kississing –File Lake areas, Manitoba (parts of NTS 63K, N); Manitoba Growth, Enterprise and Trade, Manitoba Geological Survey, Geoscientific Report GR2010-1, 134 p.

GS2017-9

Examination of exploration drillcore from the Reed Lake area and the sub-Phanerozoic extension of the Paleoproterozoic Flin Flon belt, west-central Manitoba (parts of NTS 63K7, 8, 9, 10)

by S. Gagné

In Brief:

- Drillcore re-examination indicates areas with potential for volcanogenic Cu-Zn-Au-Ag deposits
- Favorable targets for magmatic Ni-Cu deposits identified
- Detailed lithological and geochemical data provide additional context for base metal mineralization at Reed Lake

Citation:
Gagné S. 2017: Examination of exploration drillcore from the Reed Lake area and the sub-Phanerozoic extension of the Paleoproterozoic Flin Flon belt, west-central Manitoba (parts of NTS 63K7, 8, 9, 10); *in* Report of Activities 2017, Manitoba Growth, Enterprise and Trade, Manitoba Geological Survey, p. 91–103.

Summary

Three weeks of drillcore examination were conducted in June 2017 as part of a comprehensive multiyear compilation and geological mapping project of the Paleoproterozoic Flin Flon belt exposed in the Reed Lake area and its sub-Phanerozoic extension directly to the south. Thirty-five recent and historical exploration drillcores were examined, documented and sampled. These complement a set of 74 drillcores examined previously (2010–2016). The objectives of the program are to: 1) document the volcanic and sedimentary rocks from areas of the sub-Phanerozoic Flin Flon belt not yet examined; 2) provide a better understanding of the stratigraphic sequences hosting the Fourmile Island and Reed Lake volcanogenic massive sulphide (VMS) deposits by examining additional drillcore from the vicinity of the deposits; and 3) acquire additional samples for whole-rock geochemical analysis in order to expand the regional database and facilitate correlation of volcanic stratigraphy.

Key observations from this summer include the identification of several sulphide- and graphite-bearing mudstone successions, which contain local interbedded greywacke and form both thick sequences and thin intercalations within volcanic successions throughout the Reed Lake area. Intervals of sulphide-rich mudstone along the margins of late gabbroic intrusions indicate that these plutons may have the potential to host magmatic Ni-Cu mineralization, analogous to the Rice Island deposit at Wekusko Lake. The volcanic succession peripheral to the Reed VMS deposit contains a much larger proportion of felsic volcaniclastic rock than the sequence that hosts the deposit, which is dominated by coherent mafic flows and subordinate quartz-porphyry dikes. This change in lithological facies and composition is interpreted to reflect a key part of the internal stratigraphy of the Fourmile Island assemblage and will be investigated further using whole-rock geochemical data. Areas with variably altered bimodal volcanic and volcaniclastic rocks of possible arc to arc-rift origin have been extended to the Dolomite Lake–Cooper Lake area, as well as to Farwell Lake. Drillcore from the Cooper Lake to McClarty Lake area has mineral assemblages indicative of lower- to middle-amphibolite facies metamorphic conditions, in contrast to the rest of the Reed Lake region where the metamorphic grade is lower and the rocks contain lower- to upper-greenschist facies assemblages. Despite higher metamorphic grades, several intervals of potential volcaniclastic rocks were identified, expanding the known area of variably altered bimodal volcanic and volcaniclastic rocks with potential for VMS mineralization.

All geological data from drillcore and surface mapping have been integrated and compiled with a regional geochemical database and geophysical airborne surveys to produce two new preliminary maps, one for the exposed Flin Flon belt in the Reed Lake area and the other for its sub-Phanerozoic extension to the south.

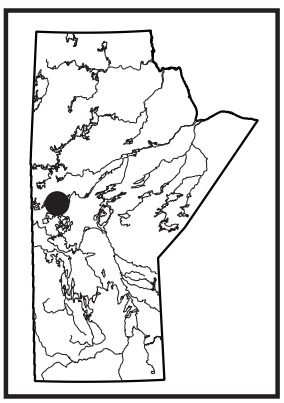

Introduction

Paleoproterozoic rocks in the Reed Lake area (Figure GS2017-9-1) are a component of a larger tectonic collage of volcano-plutonic and sedimentary rocks assembled during the closure of an ancient ocean (ca. 1.9–1.8 Ga) and collectively termed the 'Flin Flon belt' (FFB). The Flin Flon belt contains numerous base-metal VMS deposits and is among the world`s most prolific VMS districts (Syme et al., 1999). The Flin Flon belt in the Reed Lake area, and its extension to the south beneath Phanerozoic sedimentary rocks, has significant potential to host additional VMS deposits. Despite the presence of several economic deposits, including the currently producing Reed Cu-Zn mine (Figure GS2017-9-1), the geological setting of VMS deposits in the Reed Lake area is not well understood. Previous workers (Stern et al., 1995a) recognized that significant stratigraphic, geochemical and isotopic differences exist between arc-volcanic rocks in the Flin Flon (Amisk collage) and Snow Lake areas, suggesting that these two segments of the FFB formed in distinct tectonic settings

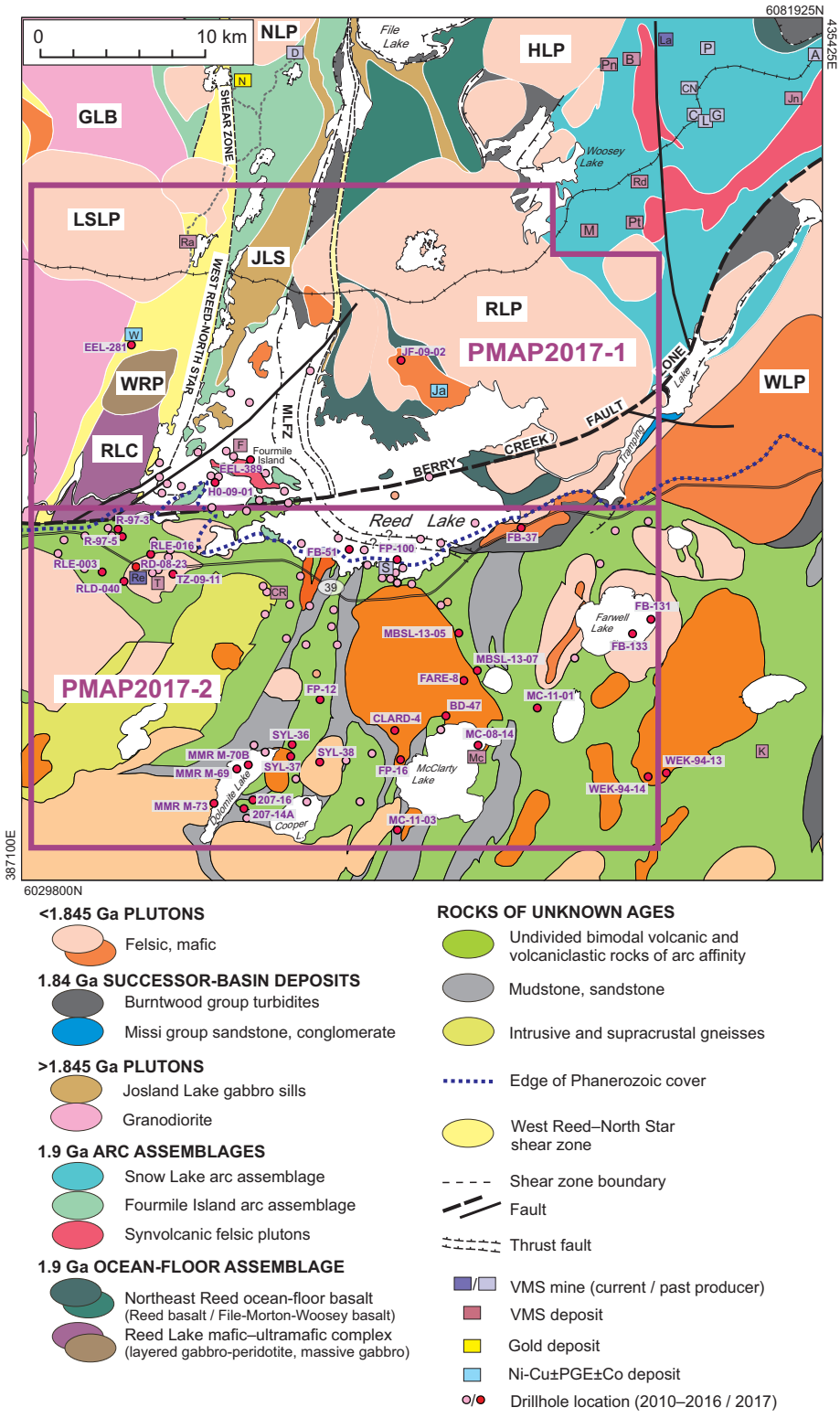

***Figure GS2017-9-1**: Generalized geology of the Reed Lake area (after Syme et al., 1995a), including the sub-Phanerozoic Flin Flon belt (Leclair and Viljoen, 1997; NATMAP Shield Margin Project Working Group, 1998) and showing the locations of drillholes included in this study. Intrusive rocks: GLB, Gants Lake batholith; HLP, Ham Lake pluton; JLS, Josland Lake sills; LSLP, Little Swan Lake pluton; NLP, Norris Lake pluton; RLC, Reed Lake mafic–ultramafic complex; RLP, Reed Lake pluton; WLP, Wekusko Lake pluton; WRP, West Reed pluton. Structural feature: MLFZ, Morton Lake fault zone. Mines (active or closed) and deposits: A, Anderson; B, Bomber; C, Chisel; CN, Chisel North; CR, Cowan River zone; D, Dickstone; F, Fourmile Island; G, Ghost; Ja, Jackfish; Jn, Joannie; K, Kofman; L, Lost; La, Lalor; M, Morgan; Mc, McClarty; N, North Star; P, Photo; Pn, Pen; Pt, Pot; Ra, Rail; Rd, Raindrop; Re, Reed; S, Spruce Point; T, Tower; W, Wine. Other abbreviations: PGE, platinum-group elements; VMS, volcanogenic massive sulphide.*

(Lucas et al., 1996). The Reed Lake area represents a critical bridge between these two segments, as it lies at the boundary between the Amisk collage *sensu stricto* and the Snow Lake segment. One of the key geological units of the Reed Lake area, the Fourmile Island assemblage (FIA), is a bimodal succession of volcanic and volcaniclastic rocks of arc or arc-rift affinity that are known to host several VMS deposits.

To gain a better understanding of the geological framework and mineral potential of the Reed Lake area, a multiyear field-mapping and compilation project was initiated in 2013. A drillcore examination and sampling component was added to the project in 2015 to complement data acquired through surficial geological mapping. Drillcore provides essential information in areas that lack surface exposure. Previous geological work (Leclair et al., 1997) and geophysical data show that arc-affinity rocks extend south of Reed Lake beneath Phanerozoic cover for a distance of more than 50 km. Therefore, a better understanding of the exposed and sub-Phanerozoic geology of the Reed Lake area has important implications for base-metal exploration in this complex and challenging area.

Previous work

Reconnaissance mapping of Reed Lake was completed at 1:50 000 scale during a joint Manitoba Geological Survey–Geological Survey of Canada project in the summer of 1995 (Syme et al., 1995b). The results of follow-up geochemical and structural studies were presented by Syme and Bailes (1996). Prior to 1995, supracrustal rocks at Reed Lake were subdivided into mafic volcanic, volcaniclastic and sedimentary types (e.g., Stanton, 1945; Rousell, 1970). Preliminary Map PMAP1995F-1 (Syme et al., 1995a) was compiled from older maps, including those of Rousell (1970) and Stanton (1945), and new data from the 1995 field season, resulting in a significantly improved understanding of the local geology. Morrison and Whalen (1995) mapped granitoid rocks in the area west of Reed Lake (NTS 63K10); a simplified version of their map was included in Preliminary Map PMAP1995F-1 (Syme et al., 1995a) and their complete work was presented in Morrison et al. (1996). In 2013, the northwestern Reed Lake area, including Rail, Sewell and Prieston lakes, was mapped at 1:10 000 scale (Gagné, 2013a, b), and the inland area west of Reed Lake was subsequently mapped in 2014 at 1:20 000 scale (Gagné and Anderson, 2014a, b).

The southern shore of Reed Lake coincides with the northern extent of Phanerozoic sedimentary rocks, which unconformably overlie the Precambrian basement and increase in thickness southward from a few metres to 30 m in the area immediately south of Reed Lake. Despite geophysical discoveries of significant base-metal mineralization in the sub-Phanerozoic basement in the 1960s and 1970s, the geology of this area remained poorly understood. The NATMAP Shield Margin Project produced the first regional 1:100 000 scale map of the sub-Phanerozoic portion of the FFB by integrating high-resolution aeromagnetic and gravity data with drillcore information (Leclair et al., 1997; Leclair and Viljoen, 1997). Only a small number of drillcores from the area south of Reed Lake were examined.

The recent discovery of the Reed VMS deposit has resulted in renewed interest in the sub-Phanerozoic geology south of Reed Lake. To address this interest, 74 drillcores were examined and sampled from the Reed Lake area (Simard et al., 2010; Gagné, 2015; Gagné, 2016). This report presents the preliminary results from the examination and sampling of an additional 35 drillcores from this area. A companion project focused on the sub-Phanerozoic basement immediately east of the Reed Lake area, south of Wekusko Lake, is ongoing (Reid and Gagné, 2016; Reid, GS-7, this volume). A compilation of geological data from surface mapping and drillcore was integrated with regional geochemistry and airborne geophysical surveys to produce two new preliminary maps, one for the exposed Flin Flon belt in the Reed Lake area (PMAP2017-1; Gagné et al., 2017) and the other for its sub-Phanerozoic extension to the south (PMAP2017-2; Gagné, 2017).

Geological framework of the Reed Lake area

The exposed portion of the FFB at Reed Lake contains several distinct fault-bounded panels of juvenile-arc volcanic rocks, some of which also contain interleaved slices of ocean-floor volcanic rocks, younger sedimentary rocks of the Burntwood group and successor-arc plutonic rocks (Figure GS2017-9-1). The juvenile-arc volcanic rocks are internally complex due to faulting and folding (e.g., Bailes and Syme, 1989) and include a wide range of typical bimodal, arc-related volcanic, volcaniclastic and synvolcanic intrusive rocks (e.g., Bailes and Syme, 1989; Syme and Bailes, 1993; Stern et al., 1995a; Lucas et al., 1996; Bailes and Galley, 2007). Ocean-floor volcanic rocks consist primarily of mid-ocean ridge basalt (MORB) and related kilometre-scale, layered, mafic–ultramafic intrusions (Syme and Bailes, 1993; Stern et al., 1995b). Voluminous successor-arc plutons and coeval volcanic and sedimentary rocks (1.88—1.83 Ga) occur throughout the Reed Lake area and include the Missi and Burntwood groups (Syme et al., 1995b). The Missi group is characterized by fluvial-alluvial conglomerate and sandstone, whereas the Burntwood group comprises basinal-marine turbiditic greywacke, mudstone and rare conglomerate.

The western Reed Lake area includes a regionally extensive (kilometres wide) north-trending zone of tectonite referred to as the West Reed–North Star (WRNS) shear zone, which was previously thought to juxtapose rocks of ocean-floor affinity on the west with rocks of juvenile-arc affinity (FIA) to the east (Syme et al., 1995a, b). Rocks east of the WRNS shear zone are further divided into two domains, separated by the Morton Lake fault zone: the FIA in the footwall and the Northeast Reed assemblage, Reed Lake pluton and Snow Lake arc assemblage in the hangingwall (Figure GS2017-9-1; Syme et al., 1995a, b; Syme and Bailes, 1996). The fault zone includes a narrow panel of Burntwood group rocks. The Berry Creek fault zone (BCFZ), a major east-trending fault, transects the southern part of Reed Lake near the northern limit of the Phanerozoic cover (Figure GS2017-9-1, -2).

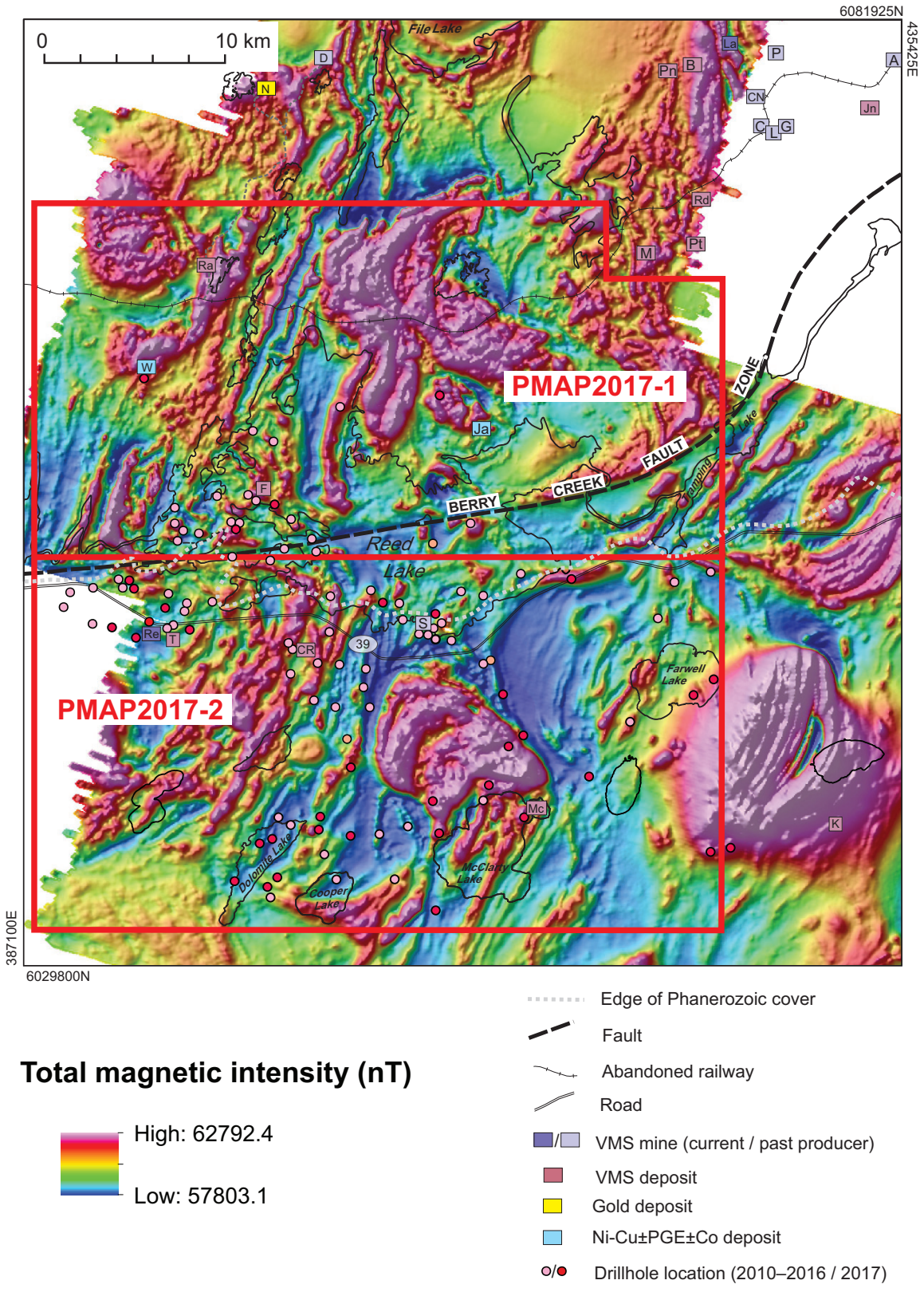

***Figure GS2017-9-2**: Total magnetic intensity of the Reed Lake area from a 1995 regional Spectrem airborne survey (Assessment File 73859, Manitoba Growth, Enterprise and Trade, Winnipeg), showing the locations of drillholes included in this study. Mines (active or closed) and deposits: A, Anderson; B, Bomber; C, Chisel; CN, Chisel North; CR, Cowan River zone; D, Dickstone; F, Fourmile Island; G, Ghost; Ja, Jackfish; Jn, Joannie; K, Kofman; L, Lost; La, Lalor; M, Morgan; Mc, McClarty; N, North Star; P, Photo; Pn, Pen; Pt, Pot; Ra, Rail; Rd, Raindrop; Re, Reed; S, Spruce Point; T, Tower; W, Wine. Other abbreviations: PGE, platinum-group elements; VMS, volcanogenic massive sulphide.*

Syme et al. (1995a) proposed that the exposed volcanic stratigraphy north and south of the BCFZ are related in a general sense. However, correlation of units across the BCFZ is hampered by poor exposures at Reed Lake, the presence of Phanerozoic cover farther south, and uncertainty surrounding the sense and magnitude of displacement on the fault zone.

The Phanerozoic cover in the Reed Lake area typically consists of 1–2 m of Ordovician quartz-rich sandstone (Winnipeg Formation) overlain by 12–25 m of Ordovician dolomitic limestone (Red River Formation), atop which generally sits several metres of unconsolidated glacial sediments and organic material. Precambrian rocks beneath the Ordovician cover are weathered to depths ranging from 5 to 30 m.

Drillcore logging

This report provides a summary of observations made from drillcore in 2017. In addition to the examination of 35 drillcores, 317 samples have been collected for reference purposes, whole-rock geochemistry, thin-section petrography, Sm-Nd isotopic analysis and U-Pb radiometric dating.

Mineral assemblages in the study area indicate lower greenschist– to middle amphibolite–facies metamorphism. However, in the interest of brevity, the prefix 'meta-' is not used in this report and the rocks are described in terms of their protoliths.

Fourmile Island deposit area

Two drillcores, EEL-389 and HO-09-01 (Assessment Files 72909, 74753), were examined to further refine the stratigraphy of volcanic rocks in the vicinity of the Fourmile Island deposit (Figure GS2017-9-1). Both drillholes encountered a diverse sequence of volcanic and volcaniclastic rocks, and displayed intervals of weak to moderate pervasive chlorite or silica±epidote alteration. On the north side of Fourmile Island, drillhole EEL-389 intersected a succession of andesite flows and mafic lapilli and crystal tuff showing weak to moderate, pervasive chlorite alteration and sporadic patches of weak silica alteration. The midsection of the drillcore consists of 50 m of thinly bedded, fine-grained sandstone and mudstone with minor graphite and local laminations (1–3 mm) of pyrite (2–5%). The drillhole terminates in mafic ash tuff and mafic wacke. Drillhole HO-09-01, collared on the south side of Fourmile Island and drilled to a depth of 1052 m, provides a long section through the deposit stratigraphy. Only the interval from 520 m to 890 m was re-examined, as it seemed to provide a representative section and offered the best interval of felsic volcanic rocks for geochronological sampling. A diverse succession of intercalated mafic and felsic flows and volcaniclastic rocks is present in the observed section. Andesite flows, 5–30 m thick, vary from aphyric to plagioclase phyric and are affected by weak to moderate, pervasive chlorite alteration. Quartz-phyric to quartz- and plagioclase-phyric felsic volcanic rocks form massive flows, 10–30 m thick, that vary in composition from dacitic to rhyolitic (Figure GS2017-9-3a). Felsic crystal tuff and lapilli tuff form 5–20 m thick intervals and display varying intensity of silicification and sericitization.

Reed deposit area

Seven drillcores from the Reed Lake area were re-examined and sampled (Figure GS2017-9-1). Drillcores from adjacent to the Reed VMS deposit show much larger proportions of felsic volcaniclastic rocks than the sequence hosting the deposit (dominated by coherent mafic flows). Rocks in the Fourmile Island area on Reed Lake show a similar lithofacies transition (Gagné, 2015). Further geochemical fingerprinting of units and development of cross-sections will help investigate the detailed stratigraphy of the two areas and compare the two packages separated by the BCFZ (Figure GS2017-9-1, -2). Two drillholes northwest of the Reed deposit (R-97-3, R-97-5) show intense deformation and indicate the presence of a ductile high-strain zone; it could be a splay fault from the BCFZ zone to the north.

The company log for drillhole RD-08-23 (Assessment File 63K1127; collared 200 m west of the Reed deposit) indicates that it intersected a thick sequence of felsic flows and felsic volcaniclastic rocks; however, re-examination of the drillcore revealed a sequence of andesite flows and minor fragmental horizons that are light grey due to moderate to strong silicification (Figure GS2017-9-3b). One narrow dike of quartz-phyric rhyolite occurs near the middle of the silicified andesite succession. The andesite locally has late chlorite alteration developed along fractures, as well as in the matrix of some fragmental horizons. Drillhole RLD-040 (Assessment File 63K12199) was collared approximately 500 m southwest of the Reed deposit and intersected alternating successions of mafic crystal tuff and andesitic flows that are low strain and have weak to moderate chlorite alteration (Figure GS2017-9-3c). Drillhole RLE-003 (Assessment File 63K1143) was drilled about 1.2 km west of the Reed deposit and intersected a package consisting of several different intrusive phases. The upper portion of the drillhole includes a quartz-phyric phase with abundant (20–30%) angular, aphyric, mafic volcanic fragments (Figure GS2017-9-3d), followed by an altered gabbroic phase; the lower portion comprises massive quartz-plagioclase–phyric dacite.

Drillhole TZ-09-11 (Assessment File 74860), located 1.8 km east of the Reed deposit, intersected a sequence of aphyric and quartz-phyric rhyolite flows (Figure GS2017-9-3e) that are intruded by a multicomponent gabbro-diorite-feldspar porphyry intrusive unit. Drillhole RLE-016 (Assessment File 63K1151) intersected a thick sequence of plagioclase-rich crystal tuff with broken quartz amygdules, and includes a thin interval (30 m) of mafic tuff breccia followed by an approximately 20 m thick mineralized zone; the zone contains mainly disseminated sulphides but also a few narrow sections (<2 m thick) of near-solid to solid sulphides (mostly pyrrhotite-pyrite and minor chalcopyrite). Structurally above the mineralized zone is a halo of pervasive and patchy silica alteration that increases in intensity toward the mineralization (Figure GS2017-9-3f).

Two drillholes (R-97-3, R-97-5; Assessment File 73220), located ~2.7 km northwest of the Reed deposit, intersected

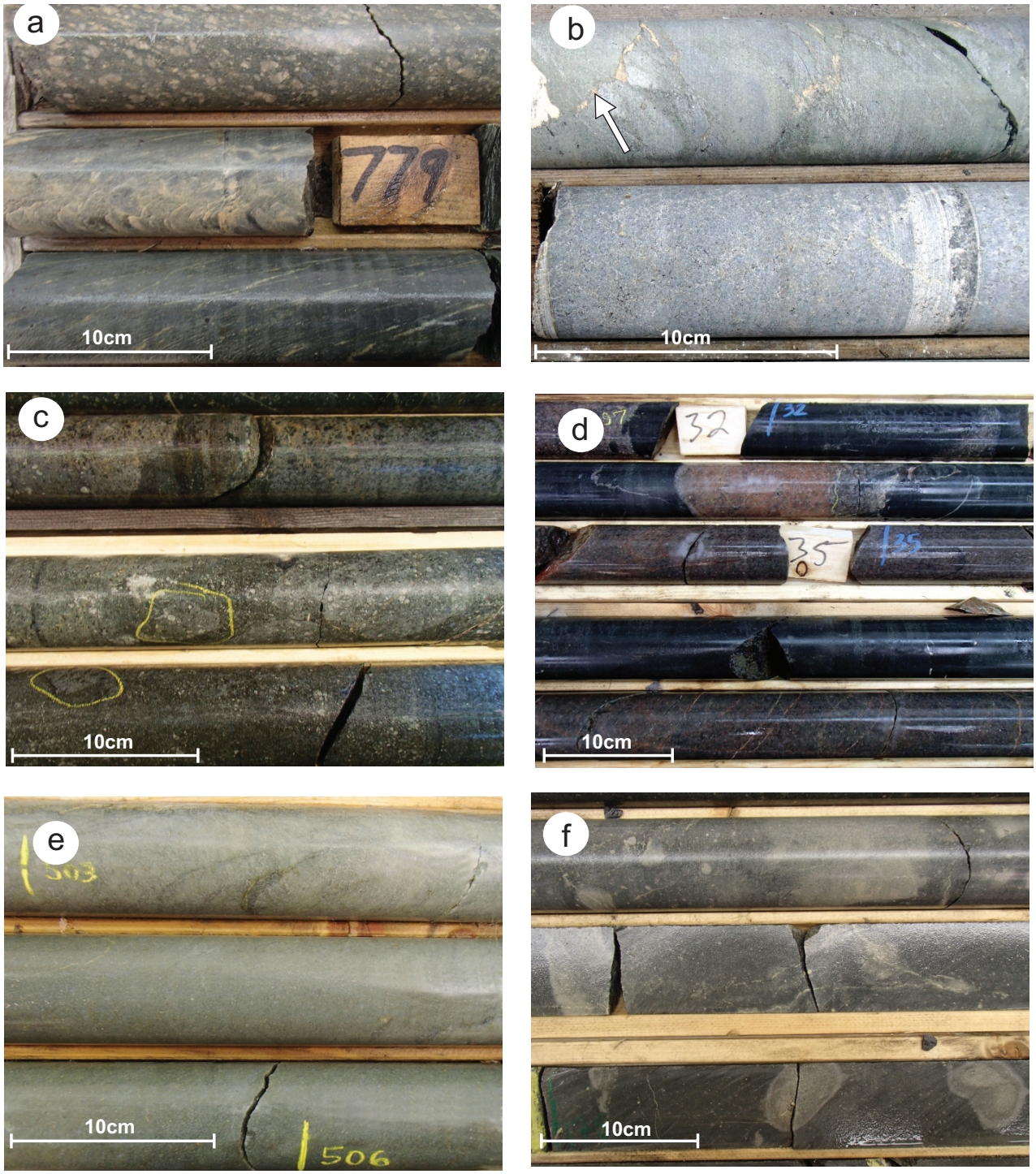

Figure GS2017-9-3*: Drillcore photos:* ***a)*** *quartz-phyric felsic lapilli tuff (first row) underlain by sparsely quartz-phyric and weakly sericitized massive rhyolite flow, drillhole HO-09-01 (NQ core; start of interval [upper left] at 778.4 m);* ***b)*** *relict domains of intense silica alteration (light grey, upper row), replaced by late pervasive chlorite alteration (greenish colour) and cut by late carbonate veinlets (light brown colour; white arrow), drillhole RD-08-23; andesite in lower row is strongly silicified and shows very little late pervasive chlorite overprint (NQ core; 197 m);* ***c)*** *mafic lapilli tuff with ~30–50% plagioclase-pyroxene–phyric fragments (circled in yellow) in a plagioclase-pyroxene crystal-rich matrix, drillhole RLD-040 (NQ core; 137.1 m);* ***d)*** *quartz-phyric intrusion (pink to pinkish grey) with enclaves (dark green; 5–60 cm) of aphyric andesite, drillhole RLE-003 (NQ core; 31.9 m);* ***e)*** *massive, aphyric rhyolite with weak pervasive sericite alteration, drillhole TZ-09-11 (NQ core; 503 m);* ***f)*** *mafic crystal tuff with patchy silicification and circular silicification haloes developed around quartz amygdules, ~6 m above a narrow (1.5 m) solid-sulphide interval, drillhole RLE-016 (NQ core, 177 m). Drillcore diameter: NQ, 47.6 mm.*

thick sequences of dominantly volcaniclastic rocks. Drillhole R-97-3 intersected mafic crystal tuff and lapilli tuff that contain fragments of amygdaloidal andesite (Figure GS2017-9-4a). These rocks vary from moderately to strongly foliated, with local transposition and isoclinal folding (Figure GS2017-9-4b). Moderate pervasive chlorite alteration is often overprinted by moderate to intense pervasive silica alteration. Drillhole R-97-5, collared only a few hundred metres south of R-97-3, also intersected a sequence of dominantly mafic lapilli and crystal tuff but also contains two sections (~30 m each) of felsic flows and lapilli tuff. The succession intersected in R-97-5 is strongly foliated and shows widespread chlorite alteration. Pervasive silica alteration is stronger and more widespread in R-97-5 than in R-97-3.

Spruce Point mine

Two drillcores from the vicinity of the past-producing Spruce Point mine (Figure GS2017-9-1, drillholes FP-100, FB-51; Assessment Files 98470, 94450) were re-examined. Drillhole FP-100 was collared in the footwall of the Spruce Point VMS deposit and intersected the near-vertical deposit sequence in reverse order. First encountered in the drillcore is a thick succession (~120 m) of footwall felsic lapilli tuff that is intruded by massive andesite (43 m thick) with sharp intrusive contacts. Sericite- and silica-altered massive rhyolite to rhyolite tuff breccia form the stratigraphic base of the solid-sulphide lens. The top of the lens is in sharp contact with massive andesite, suggesting that the andesite may be intrusive (Figure GS2017-9-4c).

Drillhole FB-51 intersected a sequence dominated by interbedded (2–20 mm) mudstone-sandstone (Figure GS2017-9-4d) with an interval (~56 m) of graphite- and sulphide-bearing mudstone. The low strain and metamorphic grade of these rocks allowed for the preservation of several good graded beds, all indicating an uphole younging direction. The bottom of the drillhole cuts through a sequence of thick-bedded sandstone (10–40 cm).

Dolomite Lake–Cooper Lake area

Nine drillholes (207-14A, 207-16, FP-12, MMR M-69, MMR M-70B, MMR M-73, SYL-36, SYL-37, SYL-38; Figure GS2017-9-1) from the Dolomite Lake–Cooper Lake region were selected for re-examination. Three drillholes east and northeast of Dolomite Lake (SYL-36, SYL-37, FP-12; Assessment Files 93486, 99449) confirmed that the north-trending package of supracrustal rocks just east of Dolomite Lake is dominated by mafic to intermediate volcanic and volcaniclastic rocks with minor intervals of sedimentary and felsic volcanic rocks. A package of sedimentary rocks (mudstone and greywacke) between Dolomite and Cooper lakes was confirmed by drillholes 207-14A and 207-16 (Assessment File 94808). Drillcore from MMR M-70B and MMR M-69 (Assessment File 99377) confirmed the presence of a sedimentary interval structurally juxtaposed to a sequence dominated by volcanic rocks. Representative core from two intrusions was examined in drillholes MMR M-73 and SYL-38 (Assessment Files 99377, 93486).

The upper section of drillcore FP-12 consists of massive to pillowed andesite with minor intervals of amoeboid flow-top breccia. Near the bottom of the drillhole, a short interval of graphitic mudstone (~5 m) and sulphide-facies iron formation (7 m) lies above a massive dacite flow (~3 m). The drillhole terminated in massive andesite that is similar in appearance to the andesite in the upper section. Drillholes SYL-36 and SYL-37 both contain a thick sequence of massive and pillowed basaltic flows intercalated with minor intervals of mafic crystal/lapilli tuffs. Local quartz amygdules (1–2%, 2–8 mm) are present in the mafic flows. Near the end of drillhole SYL-37, a short interval (~18 m) of thinly bedded, graphite-bearing (locally sulphidic) mudstone and sandstone is interlayered with narrow, intermediate ash tuff horizons.

Drillholes 207-14A, 207-16, MMR M-69 and MMR M-70B were examined to further document the sedimentary sequence from the Dolomite Lake area (Figure GS2017-9-1). The upper portion of drillhole MMR M-69 consists of aphyric, massive andesite flows overlying a thick sequence of greywacke interbedded with minor mudstone. The contact between these units is marked by a narrow high-strain zone (Figure GS2017-9-4e).

A thick sequence of massive, amygdaloidal, aphyric andesite flows overlies thinly bedded (1–3 cm) to massive, mafic crystal and ash tuff with broken quartz amygdules in drillhole MMR M-70B. Thin beds of tuff consistently become finer grained downhole, indicating that the sequence is overturned. The upper half of the core from drillhole 207-14A consists of a thick package of mudstone and sandstone interbedded with narrow intervals of sulphidic mudstone. The lower section of the core comprises mostly thick-bedded sandstone and feldspathic wacke with rare argillaceous bands containing traces of graphite. Small euhedral garnet porphyroblasts (1–3%, 1–3 mm) occur locally throughout drillhole 207-14A. Drillhole 207-16 intersected a thick sequence of quartzofeldspathic biotite gneiss, interpreted as metagreywacke, interbedded with narrower bands of quartzofeldspathic biotite-hornblende gneiss that may represent metamorphosed mafic wacke. An interval (~20 m) of sulphidic mudstone containing thin (1–3 mm) pyrite-rich laminations was intersected near the base of the hole.

Drillhole MMR M-73 intersected the northeastern margin of the Cormorant Lake batholith, encountering fine- to medium-grained, homogeneous and weakly foliated, leucocratic biotite granodiorite that includes minor phases of pink leucocratic granite pegmatite and aplite. The granodiorite intrudes medium-grained, homogeneous, massive to weakly foliated, mesocratic hornblende-biotite quartz diorite. Drillcore SYL-38 comprises granodiorite and gabbro (Figure GS2017-9-4f) with a narrow interval (~12 m) of thinly bedded sulphidic mudstone and sandstone that likely represents a large raft.

McClarty Lake area

Five drillholes from the McClarty Lake area were examined. All drillcore reviewed contains mineral assemblages indicative of amphibolite-facies peak metamorphic conditions. Two drillholes (MC-08-14, MC-11-01; Assessment Files 74613,

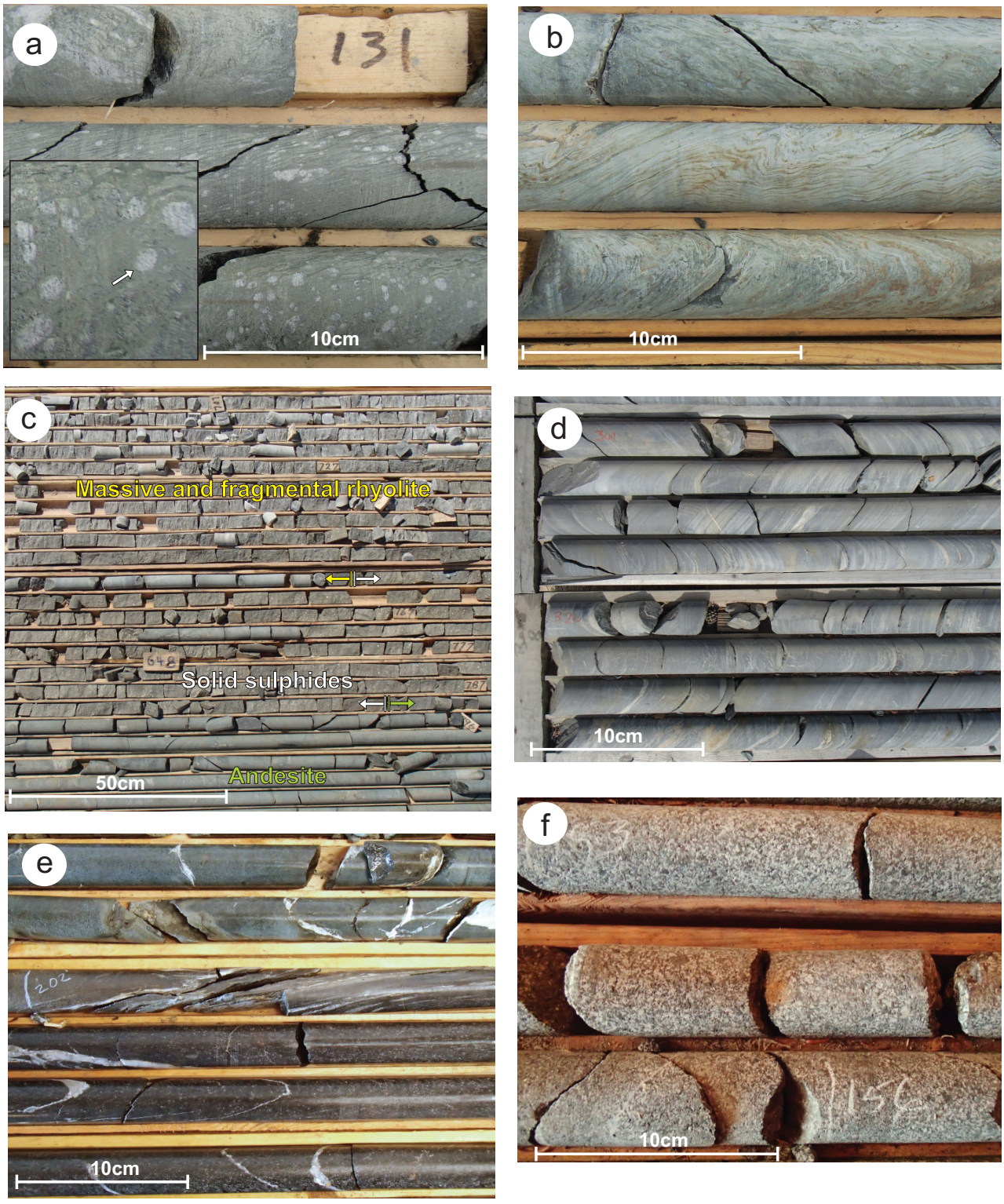

Figure GS2017-9-4*: Drillcore photos:* ***a)*** *foliated mafic crystal tuff with 3–5% broken quartz amygdules (3–15 mm), 5–15% plagioclase crystals and sparsely distributed pyroxene, drillhole R-97-3 (BQ core; 130.9 m);* ***b)*** *strongly flattened, chloritized and carbonate-altered mafic lapilli tuff, drillhole R-97-3 (BQ core, 218.1 m);* ***c)*** *drillcore interval displaying the Spruce Point solid-sulphide horizon with overlying rhyolite (stratigraphic footwall) and underlying pillowed andesite, drillhole FP-100, (AQ core, 214.9–248.7 m [705–816 ft.]);* ***d)*** *thinly bedded wacke and mudstone, drillhole FB-51 (BQ core, 91.7 m [301 ft.]);* ***e)*** *massive, aphyric andesite (upper two rows) in sheared contact with underlying greywacke, drillhole MMR M-69 (AQ core, shear zone at 61.9 m [203 ft.]);* ***f)*** *massive, homogeneous, equigranular gabbro, drillhole SYL-038 (BQ core; 153 m). Drillcore diameter: AQ, 27 mm; BQ, 36.5 mm.*

63K1171) were collared through sequences of variably altered rocks interpreted to be of volcanic origin. The other three drillholes (CLARD-4, FP-16, MC-11-03; Assessment Files 70825, 99449, 63K1171) intersected sequences of metamorphosed metasedimentary rocks.

The company log for drillhole MC-11-01, collared 3 km northeast of McClarty Lake (Figure GS2017-9-1), indicates that a sequence of mafic and intermediate volcanic rocks is interbanded with tonalite in the upper portion of the hole. However, re-examination of the drillcore showed that the entire interval is a thick sequence of mafic crystal and lapilli tuff with mafic tuff breccia horizons. Homogeneous to crudely stratified intervals of plagioclase-rich crystal tuff of intermediate composition represents horizons initially identified as tonalite. The tuff breccia horizons are matrix supported and heterolithic; the fragments are diverse but mostly of volcanic derivation. Several larger mafic fragments show concentric zonation, suggesting pre-metamorphic alteration (Figure GS2017-9-5a). The Edwards formation of the Snow Lake assemblage has many similarities to these heterolithic mafic breccias in that they both display complex and varied alteration, including fragments with haloes of silica and epidote replacement that developed during regional semi-conformable alteration associated with VMS deposit formation (Bailes et al., 2016). The rocks of MC-11-01 are also of higher metamorphic grade, as indicated by such mineral assemblages as biotite-hornblende-plagioclase-quartz-garnet-sillimanite.

Drillhole MC-11-03, 8 km southeast of McClarty Lake, intersected moderate to strongly foliated mafic to intermediate gneisses with centimetre-scale compositional layering, suggesting a possible sedimentary precursor. The gneisses are cut by several granitic injections (0.3–8 m). Mineral assemblages in the gneiss include biotite, hornblende, plagioclase, quartz, garnet and sillimanite. Horizons of quartzofeldspathic gneiss, initially logged as tonalite, are herein interpreted as metasedimentary.

Drillhole MC-08-14 was collared just north of the McClarty deposit to test the presence of mineralization along strike. It encountered granite and granodiorite in the upper third of the hole, whereas the remainder of the core is a sequence of mafic to intermediate volcaniclastic rocks with minor felsic bands. The rocks are generally well foliated and recrystallized, and have amphibolite-facies mineral assemblages that include various combinations of biotite, hornblende, plagioclase, quartz, garnet, sillimanite, anthophyllite, cordierite and staurolite (Figure GS2017-9-5b). Variations in composition and in the intensity and nature of alteration makes it difficult to recognize protoliths. Kutluoglu and Bailes (2008) indicated that textures and alteration assemblages in this drillcore are similar to those observed in the footwall of the Chisel and Lalor deposits in the Snow Lake area.

Drillhole CLARD-4 contains thinly bedded sandstone and graphitic mudstone with pyrite-bearing laminations. The drillcore terminates in a foliated mafic crystal tuff with centimetre-scale compositional layering. Drillhole FP-16 was located on the southwest edge of the McClarty Lake gabbro and intersected a thick sequence of graphitic mudstone that is thinly interbedded with sandstone. The graphitic mudstone typically has trace to a few percent pyrite; however, one interval (~10 m) has pyrite content varying from 30 to 50%. The sequence of sedimentary rocks is underlain by fine- to medium-grained quartzofeldspathic biotite gneisses, which may represent recrystallized greywacke.

Southeast Reed Lake

Five drillcores from the Farwell Lake area were examined. Drillholes FB-131 and FB-133, collared in the middle of an interpreted pluton (Figure GS2017-9-1), intersected bimodal sequences of volcanic and volcaniclastic rocks. Drillholes MBSL-13-05, MBSL-13-07 and FB-37 (Figure GS2017-9-1; Assessment Files 63K13307, 94334) were collared along the same linear trend of moderate to high magnetic intensity (Figure GS2017-9-2); the first two drillholes intersected successions of mafic volcaniclastic rocks with minor sulphidic mudstone horizons, whereas as the latter drillhole encountered a thick succession of sandstone and graphitic mudstone with minor pyrite content.

Drillholes FB-131 and FB-133 (Assessment File 73218) were collared on the eastern shore of Farwell Lake about 1.8 km apart. The top of drillcore FB-131 contains an ~15 m section of medium-grained, homogeneous equigranular gabbro, followed by an ~50 m sequence of massive andesitic flows with 1–2% quartz-carbonate veins. Two narrow intervals (2–3 m) of silicified mafic fragmental rocks occur near the middle of the sequence, and a few narrow bands of variolitic andesite occur near the lower part of the interval. A second, sill-like body (~18 m) of medium-grained, homogeneous equigranular gabbro was encountered in the middle of the hole. The last ~100 m of the drillcore consists of massive, aphyric andesitic flows with 1–2% quartz-carbonate veins and contains an ~30 m interval of aphyric, felsic lapilli tuff (Figure GS2017-9-5c) that includes narrow (0.2–0.8 m; ~40% of the interval) dikes of andesite. Drillhole FB-133 intersected an ~30 m sequence of regolith and thinly laminated, chloritized mafic crystal tuff followed by a narrow interval (~13 m) of hematized, medium-grained, equigranular massive gabbro. Downhole of the gabbro is a thick sequence of matrix-supported, mafic lapilli tuff that contains 10–30% prominently flattened, intermediate to felsic clasts (0.5–3 cm) in a chlorite-rich matrix. Below that is ~40 m of graphitic argillite and greywacke. The graphitic sedimentary rocks transition downhole into mafic lapilli tuff that becomes progressively more felsic and grades into a 10 m interval of clast-supported (>90% fragments) rhyolitic lapilli tuff. The felsic fragmental interval is in sharp contact with the underlying matrix-supported mafic lapilli tuff (<10% felsic fragments). The core has a strong penetrative foliation made evident by flattened fragments. Graphite is common on foliation surfaces of more schistose volcaniclastic rocks and may be related to narrow zones of ductile shearing.

Drillholes MBSL-13-05 and MBSL-13-07 were drilled along the eastern margin of the McClarty Lake gabbro (located 5.6 km

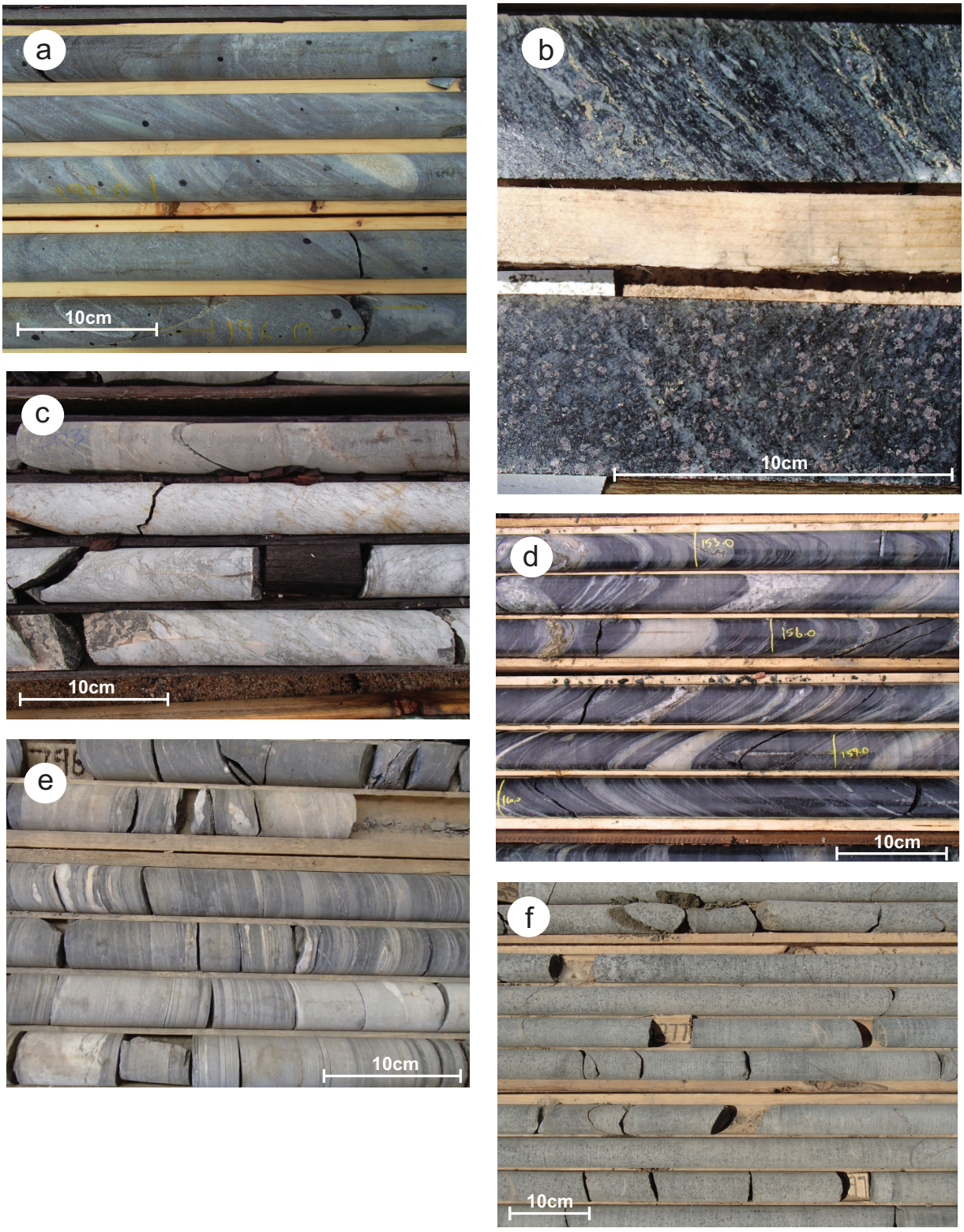

***Figure GS2017-9-5**: Drillcore photos: **a)** mafic heterolithic tuff breccia, drillhole MC-11-01; most fragments have a bleached rim, indicating silica replacement after deposition (NQ core; 189.9 m); **b)** strongly foliated biotite-sillimanite quartzofeldspathic gneiss (upper row) and more massive biotite-garnet quartzofeldspathic gneiss (lower row), drillhole MC-08-14; the rocks in the upper and lower rows may represent, respectively, intermediate tuffaceous and flow facies (NQ core, 236.5 m); **c)** massive, aphyric andesite (upper row) and rhyolitic lapilli tuff with a chloritized matrix, drillhole FB-131 (BQ core, 61.9 m [203 ft.]); **d)** foliated, mafic heterolithic tuff breccia, with flattened light-coloured felsic fragments and darker mafic fragments, drillhole MBSL-13-07 (NQ core, 152.7 m); **e)** thinly bedded wacke and mudstone (BQ core, 242.6 m [796 ft.]), drillhole FB-37; **f)** medium-grained, massive, homogeneous melanocratic gabbro, drillhole FARE-8 (BQ core; 78.3 m [257 ft.]). Drillcore diameter: BQ, 36.5 mm; NQ, 47.6 mm.*

and 7.8 km, respectively, southeast of the Spruce Point mine) and intersected similar stratigraphy, consisting of intermediate to mafic, thinly bedded volcaniclastic rocks. The fine-grained bedded rocks include bands with lapilli-size fragments of rhyolite and andesite, as well as sparse broken quartz amygdules and epidosite fragments, demonstrating a volcanogenic origin (Figure GS2017-9-5d). Sequences of mudstone with thin pyrite laminations vary from a few metres to tens of metres in thickness, and may indicate that these sediments were derived from both volcanic/hydrothermal activity and pelagic sources.

Drillhole FB-37, collared 8.3 km east-northeast of the Spruce Point mine along Highway 39, intersected a sequence of thickly laminated sandstone and mudstone (Figure GS2017-9-5e) that is locally graphitic and contains trace to a few percent pyrite. The rocks are strongly deformed, with attenuated quartz veinlets, isoclinal folds and transposed bedding.

Mafic–ultramafic intrusions

A series of six drillholes (BD-47, EEL-281, JF-09-02, FARE-8, WEK-94-14, WEK-94-13), collared in various mafic–ultramafic intrusions within the Reed Lake project area, were examined. Samples were collected from each drillcore for whole-rock geochemical analyses. All of the sampled mafic–ultramafic intrusions appear to truncate the dominant geophysical fabrics (Assessment File 73859), indicating they likely were emplaced late or after the main deformation event. The intrusions typically display minor lithological variations, from leucogabbro to mesogabbro, and rare diorite and pyroxenite. The gabbroic intrusions generally lack a penetrative foliation but are cut by ductile shear zones (a weak to moderate foliation extends on the metre scale away from these structures).

Drillholes BD-47 and FARE-8 (Assessment Files 72094, 93754) were collared in a large (8 by 8 km) ovoid gabbroic intrusion that extends from north of McClarty Lake to just south of the Spruce Point mine (Figure GS2017-9-2). Drillhole FARE-8 intersected a massive, medium-grained to locally fine-grained, homogeneous melanocratic gabbro (Figure GS2017-9-5f). The upper portion of hole BD-47 intersected pyroxenite followed by a zone of gabbro with minor quartz diorite. Mineralization within the pyroxenite consists of interstitial pyrrhotite and pyrite, with trace to a few percent pentlandite. The highest base-metal values from BD-47 were 0.39% Cu and 0.61% Ni over a length of 2.45 m (Assessment File 72094).

Drillholes WEK-94-13 and WEK-94-14 (Assessment File 94654) were collared in homogeneous, meso- to melanocratic, medium-grained massive gabbro at the southern extent of a large (12 by 9 km) ovoid mafic intrusion located immediately southeast of Farwell Lake.

Drillhole JF-09-02 (Assessment File 74754) was collared in the northwestern portion of the Jackfish gabbro. The hole intersected a layered gabbroic intrusion, as well as several granite to granitic pegmatite dikes. Sporadic blebs of pyrrhotite and pyrite were encountered in this drillhole, but no substantive mineralization was encountered.

Drillhole EEL-281 (Assessment File 94657), collared ~350 m west of the Wine Ni-Cu-Co-PGE occurrence (Figure GS2017-9-1), encountered an interval of heterogeneous, fine- to medium-grained, leucocratic to mesocratic gabbro that contains bands of disseminated to near-solid sulphide (at 20.7–24.3 m [68–80 ft.] and 26.2–27.7 m [86–91 ft.] in the hole), although no significant base-metal values were reported (Assessment File 94657). The mineralized zone at the Wine deposit is described as disseminated sulphides and stringers associated with a mafic magmatic breccia hosted by leucogabbro (Augsten, unpublished company report, 2006; Assessment Files 94660, 94667, 94669). It is interpreted that EEL-281 was drilled through the same gabbro that hosts the Wine occurrence.

Economic considerations

Bimodal volcanic and volcaniclastic rocks were recognized in drillcore throughout the Reed Lake area and the sub-Phanerozoic extension of the Flin Flon belt to the south, indicating that these volcanic successions were deposited in arc or arc-rift settings. The presence of moderate to intense pervasive alteration and local sulphide mineralization suggests that most volcanic-arc assemblages in these areas have potential to host significant VMS mineralization. Recent drillcore examination has extended the area of known, variably altered, bimodal volcanic and volcaniclastic rocks of possible arc to arc-rift origin to the Dolomite Lake–Cooper Lake area, as well as to Farwell Lake, which further expands the area with VMS potential. However, establishing the key criteria to target specific favourable horizons within these packages is the focus of ongoing work. One component of this work is deciphering the internal stratigraphy of the Fourmile Island assemblage using data collected from both the Reed deposit area and the Fourmile Island area.

Widespread occurrence of graphitic and locally sulphidic mudstone sequences throughout the sub-Phanerozoic basement south of Reed Lake has several implications. Regular narrow intercalations of sedimentary rocks within volcanic sequences suggest that at least some of the sediment was deposited during volcanism (ca. 1880–1890 Ma) and is thus significantly older than the ca. 1840 Ma Burntwood group metaturbidites. The deposition of sulphidic and graphitic mudstone may represent periods of volcanic quiescence with contemporaneous hydrothermal venting, and could represent significant stratigraphic markers. Thicker sequences of argillite and greywacke found in the sub-Phanerozoic may belong to the Burntwood group; they are often located at major boundaries between tectonostratigraphic blocks with different geological histories, suggesting they may indicate the locations of major structures, such as early thrust faults. Consequently, these sequences could be analogous to those in the Snow Lake and Reed Lake areas, where the Burntwood group rocks are tectonically juxtaposed with older volcanic rocks. Identifying the location of major structural breaks can help generate targets for orogenic gold mineralization. Finally, sulphide-rich mudstones provide an excellent source of sulphur when assimilated by gabbroic intrusions; the coincidence of these two rock types provides exploration targets for magmatic Ni-Cu (±PGE) deposits.

Mafic to ultramafic intrusions of various sizes occur in the Reed Lake area. Although no mineable deposits have been identified to date, several occurrences and zones of Ni-Cu sulphide mineralization have been identified. The Jackfish gabbro, just west of the Reed Lake pluton (Figure GS2017-9-2), is host to a Cu-Ni occurrence with minor to solid pyrrhotite and lesser pentlandite, pyrite and chalcopyrite in a gabbro/norite hostrock (Ferreira and Fedikow, 1990). Another occurrence of Ni-Cu mineralization is found along the southern margin of the gabbro intrusion between the Spruce Point mine and McClarty Lake (drillhole BD-47). These two gabbroic intrusions, as well as a few others (drillholes WEK-94-13, WEK-94-14), locally intrude S-rich sedimentary rocks in areas that have seen little exploration drilling and may thus represent strong exploration targets. The Rice Island Ni-Cu-Co deposit, located 30 km northeast of Reed Lake, is hosted by a late- to post-tectonic gabbro that intruded Burntwood group sedimentary rocks and represents an important example of this style of mineralization.

On the west shore of Reed Lake, the Reed Lake mafic–ultramafic complex (RLC) and the West Reed pluton (WRP; Figure GS2017-9-2) both represent prospective targets for PGE exploration. Grab samples collected on a transect along the Grass River indicate minor enrichment of PGE in the basal portion of the RLC (Williamson, 1993). Farther north, the Wine Ni-Cu-Co-PGE occurrence is associated with a mafic magmatic breccia hosted by leucogabbro (Figure GS2017-9-2; Augsten, unpublished company report, 2006) and was discovered through drilling of a ground geophysical anomaly by Hudson Bay Exploration and Development Co. Ltd. in the early 1980s. The northern margin of the WRP includes examples of leucogabbro-hosted magmatic breccia, locally associated with trace to a few percent sulphides (pyrrhotite±chalcopyrite), indicating that the WRP may have potential to host mineralization similar to that of the Wine showing.

Acknowledgments

This project has been facilitated by the co-operation of Hudbay Minerals Inc., Royal Nickel Corp. (formerly VMS Ventures Inc.) and Rockcliff Copper Corp., who provided access to, and allowed sampling of, drillcore. This co-operation has significantly expanded the scope of the drillcore examination program. The author also thanks C. Stocki and M. Stockings for their excellent assistance, both in the field and at the Midland Rock Preparation Laboratory, as well as N. Brandson and E. Anderson for efficient and reliable logistical support. Thanks also go to C. Epp for preparing samples and thin sections, and to K. Reid, C. Couëslan, and S.D. Anderson for reviewing this manuscript.

References

Bailes, A.H. and Galley, A.G. 2007: Geology of the Chisel–Anderson lakes area, Snow Lake, Manitoba (NTS areas 63K16/SW and west half of 63J13/SE); Manitoba Science, Technology, Energy and Mines, Manitoba Geological Survey, Geoscientific Map MAP2007-1, scale 1:20 000.

Bailes, A.H., Galley, A.G., Paradis, S. and Taylor, B.E. 2016: Variations in large synvolcanic alteration zones at Snow Lake, Manitoba, Canada, with proximity to associated volcanogenic massive sulphide deposits; Economic Geology, v. 111, p. 933–962.

Bailes, A.H. and Syme, E.C. 1989: Geology of the Flin Flon–White Lake area; Manitoba Energy and Mines, Geological Services, Geological Report GR87-1, 313 p.

Ferreira, K.J. and Fedikow, M.A.F. 1990: Mineral deposits and occurrences in the Tramping Lake area, NTS 63K/9; Manitoba Energy and Mines, Geological Services, Mineral Deposit Series Report 7, 96 p. plus 1 map at 1:50 000 scale.

Gagné, S. 2013a: Geological investigations in the Rail Lake–Sewell Lake area, Flin Flon–Snow Lake greenstone belt, west-central Manitoba (parts of NTS 63K10, 15); *in* Report of Activities 2013, Manitoba Mineral Resources, Manitoba Geological Survey, p. 95–105.

Gagné, S. 2013b: Geology of the Rail Lake–Sewell Lake area, Flin Flon–Snow Lake greenstone belt, west-central Manitoba (parts of NTS 63K10, 15); Manitoba Mineral Resources, Manitoba Geological Survey, Preliminary Map PMAP2013-8, scale 1:10 000.

Gagné, S. 2015: Examination of exploration drillcore from the Reed Lake area, Flin Flon belt, west-central Manitoba (parts of NTS 63K9, 10); *in* Report of Activities 2015, Manitoba Mineral Resources, Manitoba Geological Survey, p. 38–51.

Gagné, S. 2016: Examination of exploration drillcore from the Reed Lake area, Flin Flon belt, west-central Manitoba (parts of NTS 63K7, 8, 9, 0); *in* Report of Activities 2016, Manitoba Growth, Enterprise and Trade, Manitoba Geological Survey, p. 63–73.

Gagné, S. 2017: Sub-Phanerozoic geology of the Reed Lake area, Flin Flon belt, west-central Manitoba (parts of NTS 63K7, 8, 9, 10); Manitoba Growth, Enterprise and Trade, Manitoba Geological Survey, Preliminary Map PMAP2017-2, scale 1:30 000.

Gagné, S. and Anderson, S.D. 2014a: Bedrock geology west of Reed Lake, Flin Flon greenstone belt, Manitoba (parts of NTS 63K10); Manitoba Mineral Resources, Manitoba Geological Survey, Preliminary Map PMAP2014-5, scale 1:20 000.

Gagné, S. and Anderson, S.D. 2014b: Update on the geology and geochemistry of the west Reed Lake area, Flin Flon greenstone belt, west-central Manitoba (part of NTS 63K10); *in* Report of Activities 2014, Manitoba Mineral Resources, Manitoba Geological Survey, p. 77–93.

Gagné, S., Syme, E.C., Anderson, S.D. and Bailes, A.H. 2017: Geology of the exposed basement in the Reed Lake area, Flin Flon belt, west-central Manitoba (parts of NTS 63K9, 10, 15, 16); Manitoba Growth, Enterprise and Trade, Manitoba Geological Survey, Preliminary Map PMAP2017-1, scale 1:30 000.

Kutluoglu, R. and Bailes, A.H. 2008: 2008 technical (NI 43-101) report on the McClarty Lake property, located in the Snow Lake area, The Pas Mining District, NTS 63/K8; NI 43-101 report prepared for Troymet Exploration Corp., 277 p., URL <https://www.troymet.com/assets/docs/projects/McClarty%2043-101%20Rpt_Jun08.pdf> [June 2008].

Leclair, A.D. and Viljoen, D. 1997: Geology of Precambrian basement beneath Phanerozoic cover, Flin Flon Belt, Manitoba and Saskatchewan; Geological Survey of Canada, Open File 3427, scale 1:250 000.

Leclair, A.D., Lucas, S.B., Broome, H.J., Viljoen, D.W. and Weber, W. 1997: Regional mapping of Precambrian basement beneath Phanerozoic cover in southeastern Trans-Hudson Orogen, Manitoba and Saskatchewan; Canadian Journal of Earth Sciences, v. 34, p. 618–634.

Lucas, S.B., Stern, R.A., Syme, E.C., Reilly, B.A. and Thomas, D.J. 1996: Intraoceanic tectonics and the development of continental crust: 1.92–1.84 Ga evolution of the Flin Flon Belt, Canada; Geological Society of America Bulletin, v. 108, no. 5, p. 602–629.

Morrison, D.W. and Whalen, J.B. 1995: Granitoid plutons and major structures in the Iskwasum Lake sheet, Manitoba: a portion of the Flin Flon Domain of the Trans-Hudson Orogen; *in* Current Research, Part C, Geological Survey of Canada, Paper 1995-C, p. 225–234.

Morrison, D.W., Syme, E.C. and Whalen, D. 1996: Geology, Iskwasum Lake, Manitoba (part of NTS 63K10); Geological Survey of Canada, Open File 2971, scale 1:50 000.

NATMAP Shield Margin Project Working Group 1998: Geology, NATMAP Shield Margin Project area, Flin Flon belt, Manitoba/Saskatchewan; Geological Survey of Canada, Map 1968A, scale 1:100 000.

Reid, K.D. and Gagné, S. 2016: Examination of exploration drillcore from the south Wekusko Lake area, eastern Flin Flon belt, north-central Manitoba (parts of NTS 63J5, 12, 63K8, 9); *in* Report of Activities 2016, Manitoba Growth, Enterprise and Trade, Manitoba Geological Survey, p. 74–86.

Rousell, D.H. 1970: Geology of the Iskwasum Lake area (east half); Manitoba Mines Branch, Publication 66-3, 26 p.

Simard, R.-L., McGregor, C.R., Rayner, N. and Creaser, R.A. 2010: New geological mapping, geochemical, Sm-Nd isotopic and U-Pb age data for the eastern sub-Phanerozoic Flin Flon Belt, west-central Manitoba (parts of NTS 63J3-6, 11, 12, 14, 63K1–2, 7–10); *in* Report of Activities 2010, Manitoba Innovation, Energy and Mines, Manitoba Geological Survey, p. 69–87.

Stanton, M.S. 1945: Tramping Lake; Geological Survey of Canada, Map 906A, scale 1:63 630.

Stern, R.A., Syme, E.C., Bailes, A.H. and Lucas, S.B. 1995a: Paleoproterozoic (1.90–1.86 Ga) arc volcanism in the Flin Flon Belt, Trans-Hudson Orogen, Canada; Contributions to Mineralogy and Petrology, v. 119, no. 2–3, p. 117–141.

Stern, R.A., Syme, E.C. and Lucas, S.B. 1995b: Geochemistry of 1.9 Ga MORB- and OIB-like basalts from the Amisk collage, Flin Flon Belt, Canada; evidence for an intra-oceanic origin; Geochimica et Cosmochimica Acta, v. 59, no. 15, p. 3131–3154.

Syme, E.C. and Bailes, A.H. 1993: Stratigraphic and tectonic setting of early Proterozoic volcanogenic massive sulfide deposits, Flin Flon, Manitoba; Economic Geology, v. 88, no. 3, p. 566–589.

Syme, E.C. and Bailes, A.H. 1996: Geochemistry of arc and ocean-floor metavolcanic rocks in the Reed Lake area, Flin Flon belt; *in* Report of Activities 1996, Manitoba Energy and Mines, Geological Services, p. 52–65.

Syme, E.C., Bailes, A.H. and Lucas, S.B. 1995a: Reed Lake, parts of NTS 63K/9, 63K/10; Manitoba Energy and Mines, Geological Services, Preliminary Map 1995F-1, scale 1:50 000.

Syme, E.C., Bailes, A.H. and Lucas, S.B. 1995b: Geology of the Reed Lake area (parts of NTS 63K/9 and 10); *in* Report of Activities 1995, Manitoba Energy and Mines, Geological Services, p. 42–60.

Syme, E.C., Lucas, S.B., Bailes, A.H., and Stern, R.A. 1999: Contrasting arc and MORB-like assemblages in the Paleoproterozoic Flin Flon Belt, Manitoba, and the role of intra-arc extension in localizing volcanic-hosted massive sulphide deposits; Canadian Journal of Earth Sciences, v. 36, p. 1767–1788.

Williamson, B.L. 1993: Petrologic studies of the Reed Lake and Claw Lake gabbroic complex; *in* Report of Activities 1993, Manitoba Energy and Mines, Geological Services, p. 119.

GS2017-10

Prehnite-pumpellyite– to amphibolite-facies metamorphism in the Athapapuskow Lake area, west-central Manitoba (parts of NTS 63K12, 13)

by M. Lazzarotto[1], D.R.M. Pattison[1] and S. Gagné

[1] Department of Geosciences, University of Calgary, 2500 University Drive NW, Calgary, AB T2N 1N4

In Brief:

- Regional metamorphic grade increases from prehnite-pumpellyite-facies in the south to amphibolite-facies in the north
- Key isograds associated with major fluid release (hornblende-in and chlorite-out) have been mapped and quantified
- Isograd mapping has implications for understanding the genesis and localization of orogenic gold deposits

Citation:

Lazzarotto, M., Pattison, D.R.M. and Gagné, S. 2017: Prehnite-pumpellyite– to amphibolite-facies metamorphism in the Athapapuskow Lake area, west-central Manitoba (parts of NTS 63K12, 13); *in* Report of Activities 2017, Manitoba Growth, Enterprise and Trade, Manitoba Geological Survey, p. 104–116.

Summary

The Athapapuskow Lake area is part of a tectonic collage situated in the Flin Flon greenstone belt, Manitoba. It consists of accreted terranes comprising metamorphosed ocean-floor and island-arc assemblages that are unconformably overlain by sedimentary rocks and intruded by successor-arc plutons. The area consists of blocks bound by faults and major shear zones, within which both regional and contact metamorphism are observed. The regional metamorphic grade generally increases northward across the Flin Flon greenstone belt from prehnite-pumpellyite–facies rocks in the south, through to amphibolite-facies rocks in the north. Rocks in contact metamorphic aureoles around plutons record amphibolite-facies conditions. Late shear zones disrupt the regional metamorphic grade and overprint contact aureoles. A preliminary map of metamorphic-mineral assemblages and isograds of the area is presented. Isograds that were identified include actinolite-in, prehnite- and pumpellyite-out, hornblende-in, oligoclase-in, actinolite-out, chlorite-out and garnet-in. Two spatially important isograds are the hornblende-in and chlorite-out isograds. These have been demonstrated to be associated with major fluid release that can have implication for the generation of orogenic gold deposits. Isochemical phase diagram modelling of equilibration conditions of the rocks indicates that, in the Athapapuskow Lake area, for both contact and regional metamorphic sequences, the hornblende-in isograd occurs at pressures of 3.7–4.2 kbar and temperatures around 450°C, whereas the chlorite-out isograd yields similar pressures but higher temperatures (500–550°C).

Introduction

In 2015, a new project involving the tectonic and metamorphic study of parts of the Flin Flon greenstone belt, was initiated by the University of Calgary, in collaboration with the Manitoba Geological Survey. Greenstone belts are zones of variably metamorphosed mafic to ultramafic volcanic sequences, associated sedimentary rocks and granitoid intrusive bodies that occur within Precambrian cratons. The rocks in such belts commonly record events of regional metamorphism, contact metamorphism and hydrothermal alteration. In addition to providing insight into the tectonic evolution of the area, study of such rocks allows better understanding of metamorphic processes, such as the behavior of rocks at the transition from low-grade (prehnite-pumpellyite facies) to medium–high-grade (greenschist- to amphibolite-facies) metamorphism, that result in the release of hydrothermal fluids. An improved understanding of the metamorphic and alteration events that affected these areas provides information to constrain exploration models for volcanogenic massive sulphide (VMS) and orogenic gold deposits in the region.

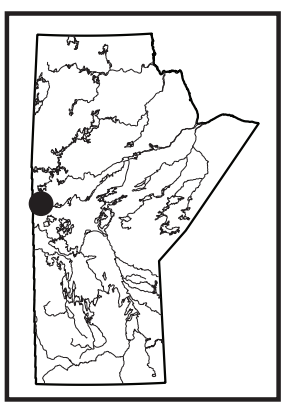

The objective of the project is to refine the metamorphic and tectonic history of the Athapapuskow Lake area established by previous workers (e.g., Bailes and Syme, 1989; Gilbert 2012; Syme, 2015) based on new field mapping and petrography. Previous workers in the area have identified rocks of prehnite-pumpellyite to amphibolite facies in the region (e.g., Digel and Gordon, 1995; Starr, 2016).

The Athapapuskow Lake area was selected for several reasons: 1) the area straddles the transition from prehnite-pumpellyite, through greenschist, to amphibolite facies; 2) several different shear zones and faults of regional tectonic relevance cut the area, juxtaposing blocks of sometimes considerably different origin and metamorphic grade; and 3) relationships between metamorphism in contact aureoles and the later regional metamorphic overprint can be studied around several plutons. Investigation of these different aspects will allow to test the traditional model for the tectonic evolution of the western Flin Flon belt (i.e., early intra-oceanic accretion, followed by successor-arc plutonism, followed by regional thermotectonism; Lucas et al., 1996).

During three field seasons (summers of 2015, 2016 and 2017), targeted mapping and sampling was completed in the Athapapuskow Lake area and in the nearby North Star and File lakes areas. This report focuses on results from the Athapapuskow Lake area. A new map of metamorphic-mineral assemblages and isograds of the Athapapuskow Lake area is presented, together with preliminary results from thermodynamic phase-equilibria modelling. All mineral abbreviations are after Whitney and Evans (2010).

Future research will focus on the investigation of relationships between metamorphosed mafic volcanic rocks and metamorphosed sedimentary rocks along a north–south transect in the File and North Star lakes areas, and building an integrated metamorphic map of the whole Flin Flon–Snow Lake greenstone belt.

Regional geology

The Athapapuskow Lake area is situated in the western Flin Flon belt, Manitoba (part of NTS 63K12, 13). It is part of the juvenile Reindeer zone of the Trans-Hudson orogen (Figure GS2017-10-1; Hoffmann, 1988), a domain formed from the convergence between the Hearne, Superior and Sask cratons. The result is a geological setting characterized mainly by the juxtaposition of juvenile-arc and juvenile–ocean-floor rocks, accompanied by contaminated-arc, ocean-island and ocean-plateau rocks (Stern et al., 1995a, b; Syme et al., 1999; Whalen et al., 2016).

Circa 1920–1880 Ma juvenile-arc and ocean-floor rocks, including tholeiitic, calcalkalic and lesser shoshonitic and boninitic rocks, were juxtaposed in an accretionary collage, probably as a consequence of arc-arc collision at about 1880–1870 Ma (Lucas et al., 1996). This became the starting point for postaccretion and successor-arc magmatism, which resulted in the emplacement of calcalkalic plutons ca. 1870–1830 Ma (Lucas et al., 1996). Between 1850 and 1840 Ma, continental sediments of the Missi and Burntwood groups were deposited (Ansdell et al., 1995; Lucas et al., 1996). The complex imbrication of sedimentary and volcanic assemblages along pre-peak metamorphic structures (Lucas et al., 1996; Stern et al., 1999) is the consequence of two additional collisional events: the first involving the Sask craton at 1840–1830 Ma and, immediately afterwards, a second event involving the Superior craton at 1830–1800 Ma (Bleeker, 1990; Ellis et al., 1999; Ashton et al., 2005), resulting in what is known as the 'Amisk collage' (Lucas et al., 1996).

Today the Athapapuskow Lake area of the Flin Flon–Snow Lake greenstone belt consists of imbricated juvenile-arc, ocean-floor and sedimentary rocks, intruded by granitoid plutons, and is characterized by internally complex patterns of faults and folds (Figure GS2017-10-2a; Bailes and Syme, 1989; Stern et al, 1995a; Lucas et al, 1996). The arc-related assemblages comprise a wide range of volcanic, volcaniclastic and related synvolcanic intrusive rocks, whereas the ocean-floor assemblages are mainly composed of mid-ocean-ridge–like basalt and related mafic–ultramafic complexes (Syme and Bailes, 1993; Stern et al., 1995b; Lucas et al., 1996). Sedimentary rocks principally consist of thick sequences of continentally derived conglomerate and sandstone, and marine turbidites.

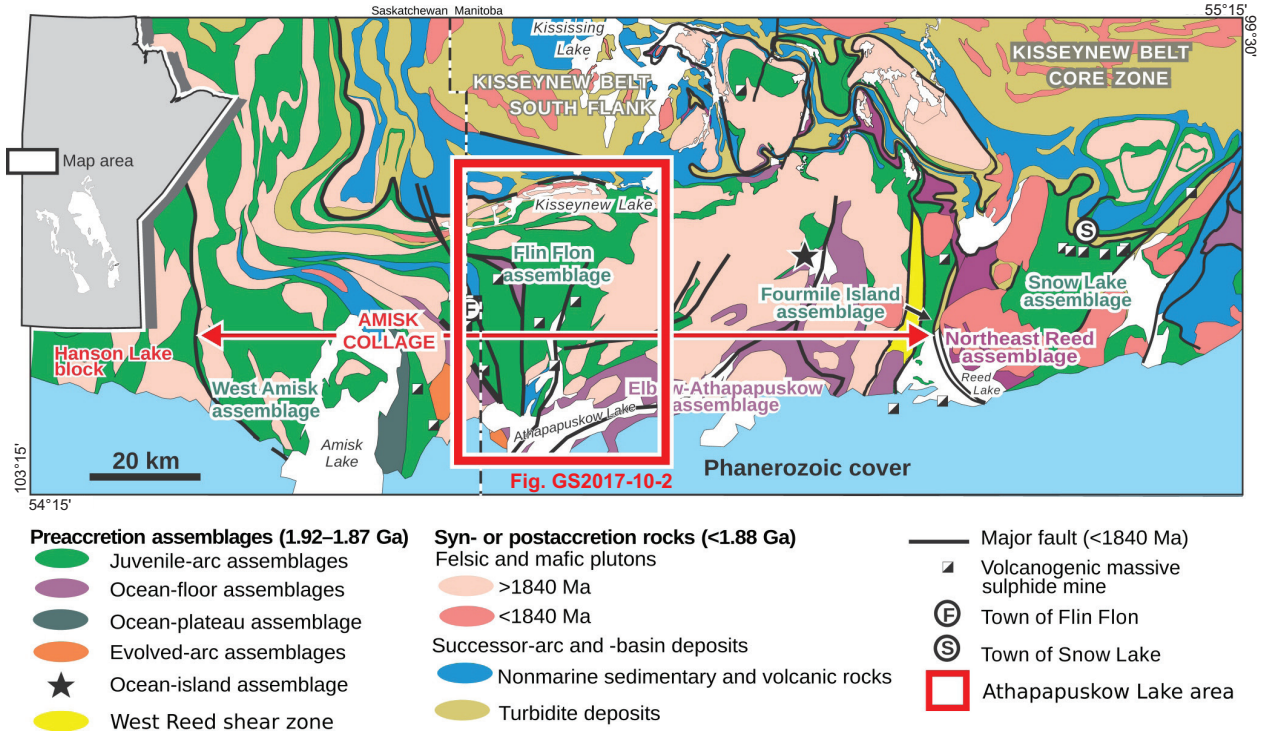

Figure GS2017-10-1: *Simplified geology of the Flin Flon–Snow Lake greenstone belt (modified from NATMAP Shield Margin Project Working Group, 1998). The box outlined in red indicates the Athapapuskow Lake area (Figure GS2017-10-2a, b).*

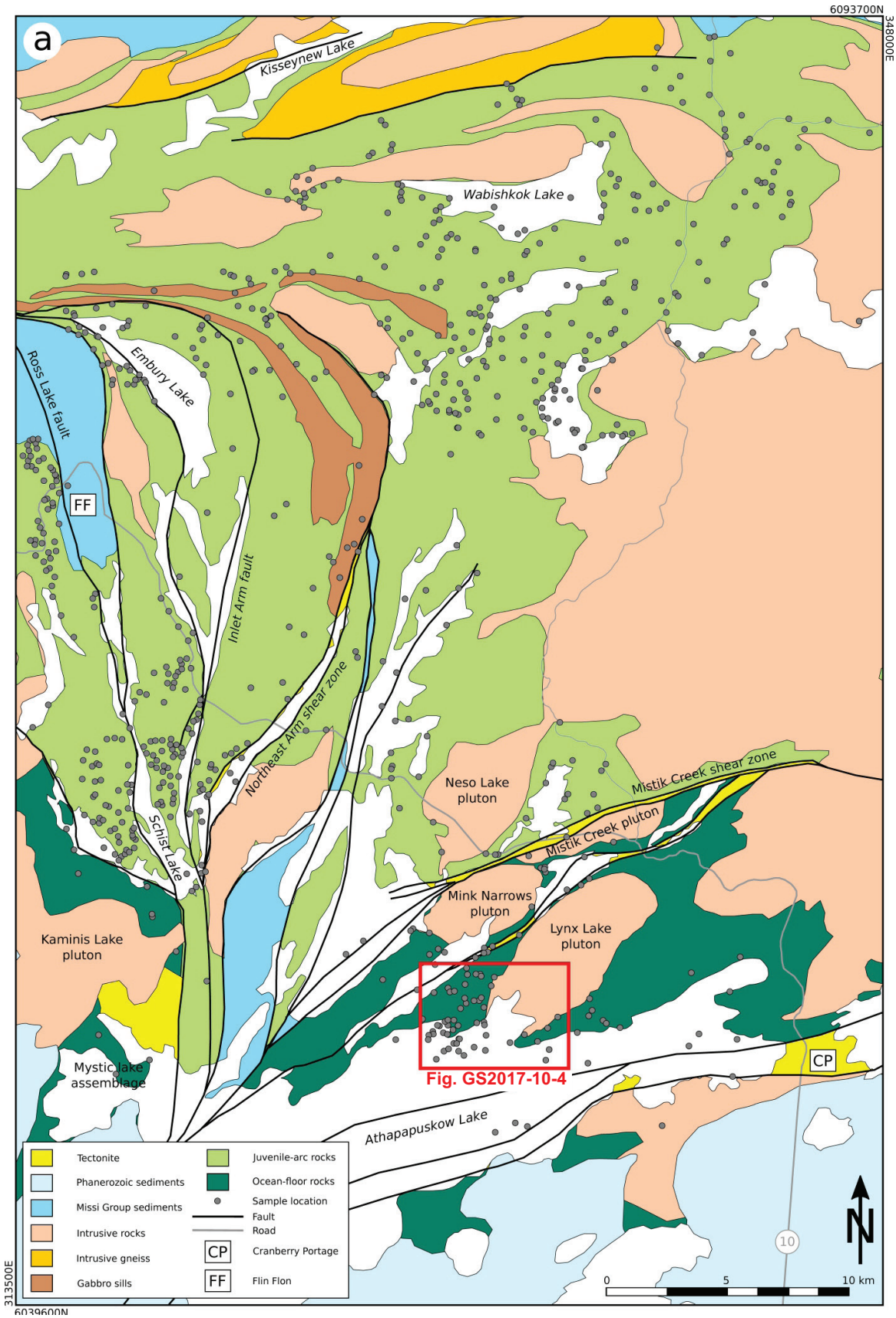

Figure GS2017-10-2a: *Simplified geology of the Athapapuskow Lake study area. Box outlined in red indicates location of Figure GS2017-10-4.*

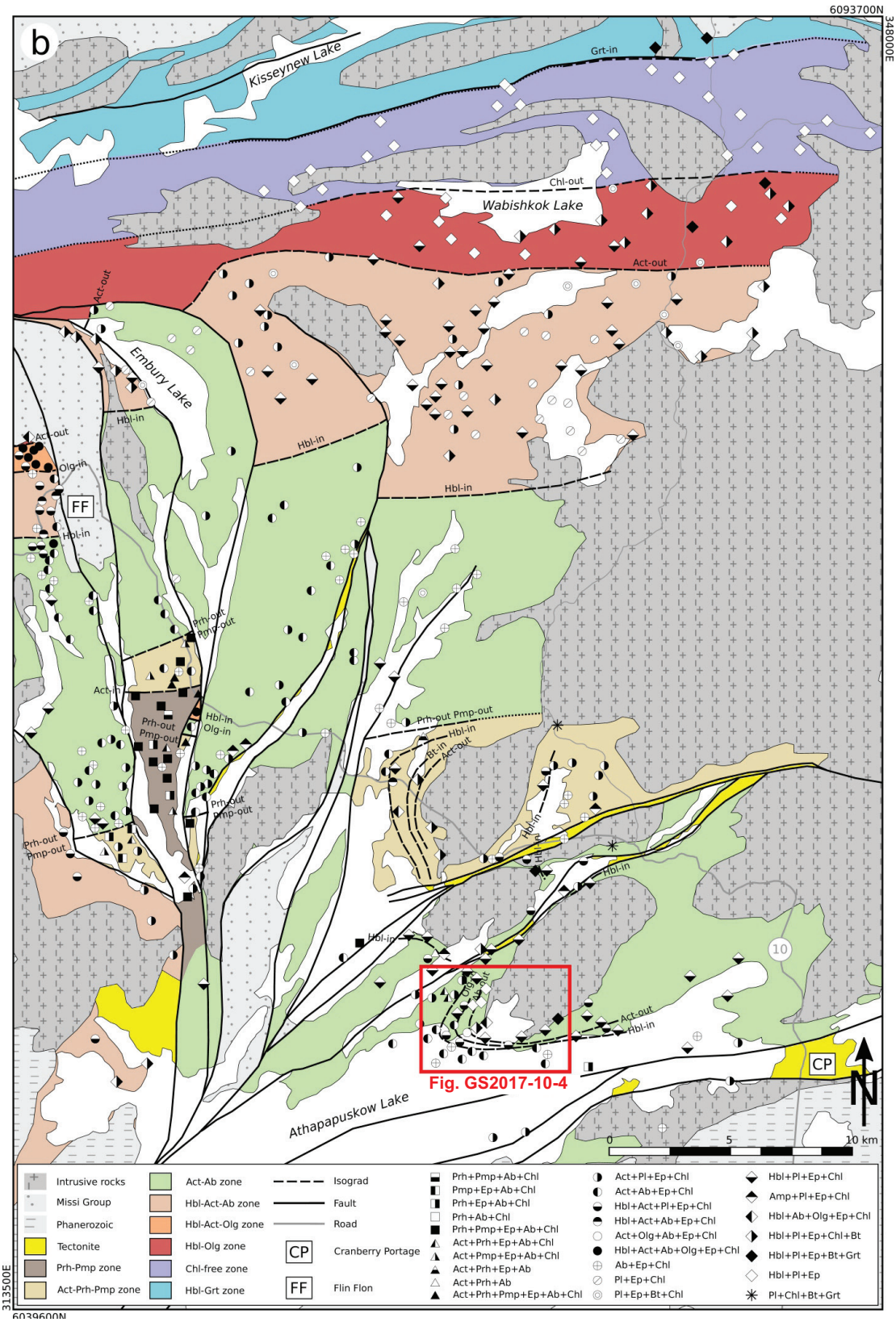

Figure GS2017-10-2b: *Preliminary map of metamorphic-mineral assemblages and isograds of the Athapapuskow Lake study area; zones are coloured according to regional metamorphic grade and thus exclude contact metamorphic areas. Data compiled from Bailes and Syme (1989), Gilbert (2012), Syme (2015) and Starr (2016), and samples collected by the authors. Abbreviations: Ab, albite; Act, actinolite; Amp, amphibole; Bt, biotite; Chl, chlorite; Ep, epidote; Grt, garnet; Hbl, hornblende; Olg, oligoclase; Pl, plagioclase; Prh, prehnite; Pmp, pumpellyite.*

Fedorowich et al. (1995) and Schneider et al. (2007) suggested three main episodes of metamorphism in the Flin Flon–Snow Lake greenstone belt: 1) early amphibolite-facies contact metamorphism due to the emplacement of successor-arc plutons ca. 1860–1840 Ma; 2) regional subgreenschist to amphibolite metamorphism (Digel and Gordon, 1995; Syme, 2015) ca. 1820–1790 Ma; and 3) retrograde overprint at 1790–1690 Ma. A northward increase in metamorphic grade within single fault-bounded blocks is observed (Bailes and Syme, 1989; Digel and Gordon, 1995; Syme, 2015; Starr, 2016). In general, the grade changes northward from prehnite-pumpellyite, through greenschist, to amphibolite facies.

Metamorphism

With the exception of the Phanerozoic sedimentary cover south of Athapapuskow Lake, all rocks in the Athapapuskow Lake area are metamorphosed. Two distinct types of metamorphism are recognized in the area: regional metamorphism and contact metamorphism. In this study, the Missi group sediments and the successor-arc intrusive rocks were not investigated due to limited access to samples and data.

Metamorphic textures and igneous remnants

In most analyzed samples from the subgreenschist and greenschist facies, metamorphic-minerals are randomly oriented and igneous fabrics are well preserved, whether in contact or regional metamorphic setting. Preservation of igneous texture is less common in samples from the regional-metamorphic amphibolite facies.

Distribution of metamorphic-mineral assemblages in individual samples is controlled by relict igneous textures such as phenocrysts and amygdules, which are common in metamorphosed flow and pillow basalt, and are found throughout the study area. Metamorphic pseudomorphs after pyroxene and calcic plagioclase phenocrysts, are mainly composed of actinolite, hornblende or sodic plagioclase, respectively. They vary in size from < 0.1 to 10 mm. Amygdules are generally filled with quartz, epidote and carbonate (with the addition of prehnite and pumpellyite in the subgreenschist facies). They are rounded to subrounded and range in size from <0.1 to 20 mm. The matrix is usually composed of crystals with considerably finer grain size than phenocrysts or amygdules.

At outcrop scale, igneous structures are preserved in the form of pillows and flows (Figure GS2017-10-3a). Typically, pillow cores are rich in epidote and contain few, small amygdules, whereas the rims contain more chlorite and actinolite/hornblende, with lots of large amygdules. Pseudomorphed plagioclase and/or pyroxene porphyroblasts are often aligned, preserving the trachytic texture typical for magmatic flows. Only in areas of high strain do metamorphic minerals such as chlorite or amphibole define a foliation.

Preservation of igneous mineralogy is rare. Only a few samples within the subgreenschist-facies contain relict igneous pyroxene. Generally, pyroxene is replaced by actinolite or hornblende (or both) and chlorite, depending on metamophic grade. Igneous calcic plagioclase was not identified in any sample. In the subgreenschist facies, plagioclase is usually replaced by albite (with minor prehnite, pumpellyite and epidote), whereas at higher grade it is replaced by oligoclase (with minor albite, epidote and carbonate).

Regional metamorphism

Map of metamorphic-mineral assemblages and isograds

Figure GS2017-10-2b shows a preliminary map of metamorphic-mineral assemblages and isograds for the entire study area. The map was compiled using data from Bailes and Syme (1989), Gilbert (2012), Syme (2015) and Starr (2016), and samples collected by the authors during fieldwork between 2015 and 2017. The plotted mineral assemblages only comprise diagnostic minerals used to define the different metamorphic zones (full mineral assemblages are recorded, but are not shown in this report). The grouping of mineral assemblages allows for the definition of a pattern of regional metamorphic zones, ranging from prehnite-pumpellyite to amphibolite facies. These metamorphic zones are defined through combinations of key minerals, including prehnite, pumpellyite, actinolite, hornblende, albite, oligoclase, chlorite, epidote and garnet. A series of seven isograds were identified separating the different metamorphic zones. From south to north, these isograds are actinolite-in, prehnite- and pumpellyite-out, hornblende-in, oligoclase-in, actinolite-out, chlorite-out and garnet-in. A northerly increase in metamorphic grade is visible, from prehnite-pumpellyite facies in the southern part of Schist Lake to garnet-amphibolite facies at the contact with the Kisseynew domain at Kisseynew Lake. An exception is the cryptic amphibolite-facies domain, referred to as the 'Mystic lake assemblage' after its type area in Saskatchewan (Thomas, 1991), outcropping in the southwestern part of the study area. Major shear zones (e.g., Northeast Arm shear zone) and late brittle faults (e.g., Ross Lake fault, Inlet Arm fault) disrupt the otherwise continuous metamorphic succession of zones and isograds.

Subgreenschist facies: prehnite-pumpellyite zone

The prehnite-pumpellyite zone is defined as the area down-grade of the actinolite-in isograd and is characterized by the mineral assemblage Prh+Pmp+Ab+Chl+Ep+Qtz±Ttn±Cb±Ap (Figure GS2017-10-3b). Prehnite and pumpellyite typically, but not always, coexist within samples of this zone, with prehnite being present in considerably higher modal amount compared to pumpellyite. These two minerals are easily identified in amygdules, but are also found as very fine-grained crystals in the matrix intergrown with albite, chlorite and epidote, which are the most abundant minerals found in rocks from the prehnite-pumpellyite zone. These minerals replace phenocrysts or are found as part of the matrix assemblage. Radial or granular epidote and chlorite, together with quartz, can also fill amygdules. Rare igneous pyroxene is preserved in a few samples of this zone, mostly within partially replaced phenocrysts.

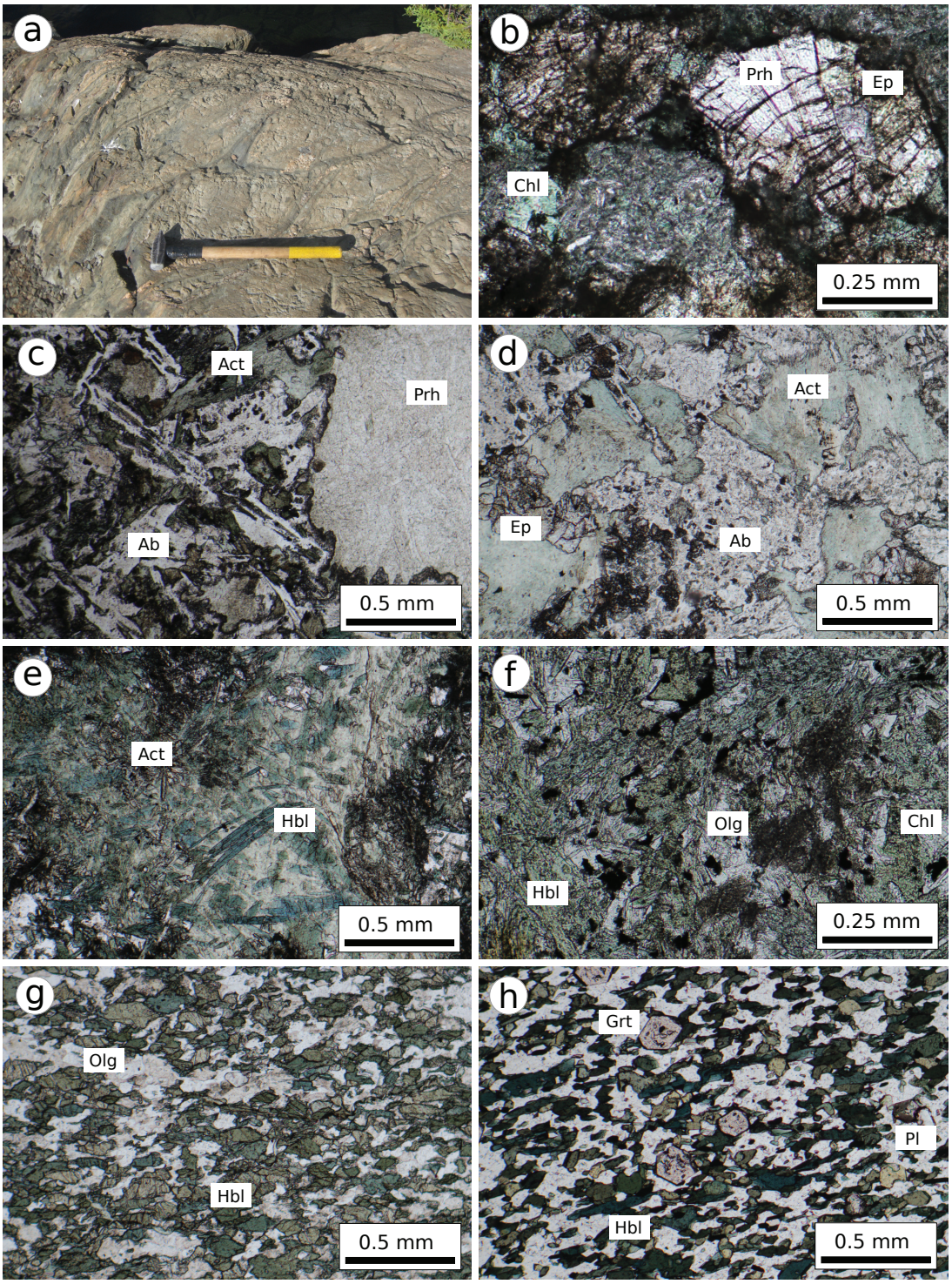

Figure GS2017-10-3: *Outcrop picture and photomicrographs of different metamorphic zones in the study area:* ***a)*** *metamorphosed basalt with well-preserved pillow structure from Act-Ab zone (sample 47-4, UTM Zone 14U, 315657E, 6067795N, NAD 83);* ***b)*** *prehnite, epidote and chlorite in amygdule of sample from the prehnite-pumpellyite zone, in plane polarized light (ppl; sample 52-85-342-1, UTM 320372E, 6059778N);* ***c)*** *prehnite-filled amygdule in contact with actinolite in sample from the actinolite-prehnite zone (ppl; sample 71-1, UTM 330568E, 6061945N);* ***d)*** *actinolite, epidote and albite in sample from the actinolite-albite zone (ppl; sample 52-88-3010-1, UTM 316899E, 6062467N);* ***e)*** *distinct crystals of hornblende and actinolite in sample from the hornblende-actinolite-albite zone (ppl; sample 52-86-1010-1, UTM 316412E, 6057885N);* ***f)*** *hornblende and oligoclase in matrix of sample from the hornblende-oligoclase zone (ppl; sample 32-01-0362-1, UTM 343722E, 6085680N);* ***g)*** *hornblende and oligoclase in matrix of sample from the chlorite-free zone (ppl; sample 32-01-0198-1, UTM 338638E, 6088670N);* ***h)*** *hornblende and garnet in sample from the hornblende-garnet zone (ppl; sample 32-03-0062-1, UTM 342677E, 6092696N). Abbreviations: Ab, albite; Act, actinolite; Chl, chlorite; Ep, epidote; Grt, garnet; Hbl, hornblende; Olg, oligoclase; Pl, plagioclase; Prh, prehnite.*

Subgreenschist facies: actinolite-prehnite-pumpellyite zone

The actinolite-prehnite-pumpellyite zone is defined as the area between the actinolite-in and prehnite- and pumpellyite-out isograds. The characteristic metamorphic-mineral assemblage of rocks within this zone is Act+Prh+Pmp+Ab+Chl+Ep+Qtz±Ttn±Cb±Ap (Figure GS2017-10-3c). Even though the characteristic assemblage implies the coexistence of actinolite with either or both of prehnite and pumpellyite within the same sample, the more common assemblages in the zone are Prh+Pmp+Ab+Chl+Ep+Qtz±Ttn±Cb±Ap and Act+Ab+Chl+Ep+Qtz±Ttn±Cb±Ap. Usually, actinolite occurs as fine acicular grains (only visible using scanning electron microscopy) intergrown with prehnite and pumpellyite (where present) within the matrix. Prehnite and pumpellyite are typically present in amygdules, and as very fine grained crystals in the matrix. Epidote is usually found as subidiomorphic grains overgrowing the matrix. Chlorite fills vesicles or grows interstitially within the matrix. Carbonate is usually associated with prehnite, pumpellyite, chlorite, epidote and quartz within amygdules. In the actinolite-prehnite-pumpellyite zone, the nondiagnostic assemblage Ab-Chl-Ep is common.

Greenschist facies: actinolite-albite zone

The actinolite-albite zone defines the greenschist facies and occupies the area between the prehnite- and pumpellyite-out and the hornblende-in isograds. This zone is the largest metamorphic zone in the study area. Rocks in this area contain the typical greenschist-facies assemblage Act+Ab+Ep+Chl+Qtz±Ttn±Bt±Ap±Opq (Figure GS2017-10-3d). Primary igneous textures are usually well preserved within samples of this zone. Pyroxene and plagioclase phenocrysts are pseudomorphed by actinolite and albite, respectively. Amygdules are typically filled with fine-grained quartz, granular or radial epidote, chlorite and carbonate. Tiny, green needles of actinolite, together with fine-grained albite, granular epidote, interstitial chlorite and quartz make up the bulk of the matrix. Minor titanite, carbonate, apatite and opaque minerals are also found as part of the matrix. Very fine grained biotite is present in some samples. In most cases the biotite-bearing rocks are missing the diagnostic mineral actinolite.

Lower-amphibolite facies: hornblende-actinolite-albite zone

The hornblende-actinolite-albite zone is defined as the area found between the hornblende-in and the oligoclase-in isograds. The zone is characterized by the mineral assemblage Hbl+Act+Ab+Ep+Chl+Qtz±Ttn±Bt±Ap±Opq (Figure GS2017-10-3e). Several different textural relationships between actinolite and hornblende have been identified, including distinct grains, patchy intergrowths and core–rim microstructures. Even though the typical assemblage contains both hornblende and actinolite, some assemblages contain only one of the two minerals. Hornblende occurs as rare, small blebs in samples from the southern part of the zone. The modal amount of hornblende, together with its grain size, increases toward the north. Close to the oligoclase-in isograd, hornblende is characterized by dark green needles, needle aggregates or blades, up to several millimetres long, in the eastern part of the study area. Actinolite persists throughout the zone and typically consists of pale green to green needle aggregates that vary in size depending on whether it is part of the matrix or replacing phenocrysts. Plagioclase phenocrysts are replaced by albite, which is also present as a fine-grained component of the matrix. Granular epidote, chlorite and fine-grained quartz are common in the matrix and within amygdules. Minor titanite, apatite and opaque minerals are found as part of the matrix assemblage.

Lower-amphibolite facies: hornblende-actinolite-oligoclase zone

The hornblende-actinolite-oligoclase zone is defined as the area between the oligoclase-in and actinolite-out isograds. This zone was only identified in the Flin Flon block. The typical metamorphic-mineral assemblage is Hbl+Act+Olg+Ab+Ep+Chl+Qtz±Ilm±Ttn±Bt±Ap±Opq. In this zone only large amygdules and phenocrysts are preserved. Hornblende is identifiable in the field as fine black needles, just north of the oligoclase-in isograd, and coarsens toward the north. Relatively coarse-grained intergrown hornblende and actinolite build a network of elongate crystals. Fine-grained interstitial oligoclase (accompanied in some cases by albite), acicular chlorite and skeletal epidote fill the space between, and in some cases overgrow, the amphibole network. Ilmenite is the main Ti-bearing phase, replacing titanite. Late retrograde(?) titanite rims the ilmenite.

Amphibolite facies: hornblende-oligoclase zone

The zone between the actinolite-out and chlorite-out isograd is defined as the hornblende-oligoclase zone. The characteristic metamorphic-mineral assemblage for this zone is Hbl+Ab+Olg+Ep+Chl+Qtz±Bt±Ilm±Ttn±Ap±Opq (Figure GS2017-10-3f). The most common plagioclase is oligoclase, with minor to no albite. Oligoclase is found as interstitial grains between fairly coarse-grained, dark green, hornblende blades or needle aggregates up to 1 mm long. Brown to green biotite is present in most of the samples as plates or blades of variable size in association with the hornblende crystals. Skeletal epidote, usually <1 mm across, and acicular or fibrous chlorite are also present between the hornblende grains. Ilmenite is commonly rimmed by retrograde(?) titanite.

Amphibolite facies: chlorite-free zone

The zone north of the chlorite-out and south of the garnet-in isograd is defined as the chlorite-free zone. This zone is characterized by the absence of chlorite, with the key mineral assemblage being Hbl+Pl+Ep+Qtz±Bt±Ilm±Ttn±Ap±Opq (Figure GS2017-10-3g). Hornblende is found as green blades, less than a millimetre to several millimetres long, or as tiny, pale green needles, typically creating a tight network of crystals. The main plagioclase is oligoclase, which is usually present as an interstitial phase filling the spaces in the amphibole network. Rare

pseudomorphed igneous plagioclase phenocryst relicts are found in the eastern part of the chlorite-free zone. Epidote crystals are skeletal to granular and range in size from <0.1 to 0.5 mm. Several samples contain brown to green biotite as plates or blades varying in size from <0.1 mm to 0.5 mm. Ilmenite is enveloped by titanite.

Amphibolite facies: hornblende-garnet zone

The northernmost zone begins just north of the garnet-in isograd and is defined as the hornblende-garnet zone. It occurs south of the transition into the Kisseynew gneiss belt. The characteristic mineral assemblage for this zone is Hbl+Pl+Ep+Bt+Grt +Qtz±Ilm±Ttn±Ap±Opq (Figure GS2017-10-3h). Green to blue hornblende grains less than a millimetre to several millimetres long create a decussate texture. Garnet porphyroblasts overgrowing the amphibole reach up to 3 mm in diameter. Plagioclase is present as interstitial fill between hornblende grains. Small epidote grains are found dispersed within the matrix. In some cases skeletal epidote is present, as are subidiomorphic brown to green biotite plates or blades.

Contact metamorphism

Contact metamorphic aureoles around plutons are usually recognized in the field through a general darkening of the fresh and weathered surfaces. The rocks are very fine grained and the mineral assemblages difficult to identify in hand sample or optically. With the aid of electron-microprobe analysis of thin sections, contact metamorphic assemblages within the aureole could be identified. For the purpose of this study, a contact aureole is defined as the area around an intrusive pluton where mafic rocks consist of a metamorphic-mineral assemblage containing hornblende, rather than only actinolite, typical for unaffected rocks outside the contact aureole in areas of low-grade metamorphic overprint.

In the eastern part of the Athapapuskow Lake area, contact aureoles extend for approximately 1 km outward from the margins of the Lynx Lake (1847 ±4 Ma; Gordon et al, 1990) and Neso Lake (1858 ±3 Ma; Syme et al., 1991) plutons. Narrower aureoles surround the Mink Narrows and the Mistik Creek plutons (Figure GS2017-10-2a). Rocks in the contact aureole of the intrusions generally consist of metamorphosed massive or pillowed basalt showing little to no deformation and characterized by dark grey to black weathering. Fresh surfaces are dark green, with some lighter patches due to epidotization. Igneous textures, such as phenocrysts and pillow or flow structures, are typically preserved, whereas primary igneous minerals are pseudomorphed. Primary pyroxene is usually replaced by actinolite and/or hornblende, whereas calcic plagioclase is replaced by sodic plagioclase. The typical mineral assemblage observed in thin section is Hbl±Act+Pl(Ab or Olg)+Qtz+Bt±Ep±Chl±Opq. Discrete actinolite grains are intergrown with hornblende where the two amphiboles are present together. Granular epidote, acicular or fibrous chlorite and fine-grained quartz occur in veins, amygdules or as part of the matrix. Biotite is present as small, brown to green, platy grains. Red to purple garnet porphyroblasts <1 mm in diameter are locally found. The garnet occurs in mafic domains, within rhyolitic units. The mafic domains are interpreted as zones of premetamorphic alteration.

A well-developed aureole surrounds the Lynx Lake pluton (Figure GS2017-10-4) within the regional actinolite-albite zone. Several observations indicate the presence of this contact aureole around the Lynx Lake pluton: 1) a slight increase in grain size of amphibole is observed with proximity to the pluton; 2) the metamorphic-mineral assemblage changes from Act+Ab+Ep+Chl+Qtz±Ttn±Opq outside the aureole, to Hbl+Olg+Ep+Chl+Qtz±Ilm±Ttn±Opq close to the pluton; and 3) the modal amount of epidote decreases toward the intrusion. Garnet porphyroblasts are locally found in the internal part of the contact aureole at one locality on the southern side of the Lynx Lake pluton in an assemblage comprising Hbl+Olg+Ep+Grt+Qtz+Opq. The limited occurrence of this assemblage suggests local variations in bulk composition. The aureole is narrower south of the Lynx Lake pluton, where greenschist-facies assemblages occur about 800 m from the pluton. These greenschist-facies assemblages are interpreted as the result of regional metamorphism and are therefore outside of the contact aureole as defined in this study.

A contact aureole was interpreted by Syme (2015) to extend for about 1 km around the Kaminis Lake pluton (1856 ±2 Ma; Stern and Lucas, 1994) in the western part of the Athapapuskow Lake area (Figure GS2017-10-2a). The aureole is less well defined compared to the Lynx Lake, Mink Narrows, Neso Lake and Mistik Creek plutons. Rocks immediately adjacent to the Kaminis Lake pluton in the northern and northwestern parts of the aureole are characterized by pale green to grey weathered surfaces and are dark grey to black on fresh surfaces. Local porphyritic basalt contains pseudomorphs of pyroxene and/or plagioclase phenocrysts. A metamorphic-mineral assemblage consisting of Hbl+Act+Pl+Bt+Chl+Qtz±Opq±Ap is commonly observed in this part of the aureole. Domains in the eastern and southeastern parts of the aureole show a strong foliation oriented approximately 150°/80°. Up-grade of the hornblende-in isograd, it becomes difficult to differentiate between a regional and a contact metamorphic origin for the mineral assemblages.

A region of amphibolite-facies rocks approximately 5 km wide is present southeast of the Kaminis Lake pluton (Mystic lake assemblage; Figure GS2017-10-2b). Rocks in this area consist of strongly foliated amphibolite interlayered with fine-grained granitic layers, consistently oriented 130°/90°. These relatively fine-grained amphibolite bands, usually 5–20 cm wide, are grey to green on weathered surfaces and dark green on fresh surfaces. The characteristic mineral assemblage for metabasic rocks of this area is Hbl+Pl+Bt+Chl+Qtz±Opq±Ap. The granitic layers vary between a few millimetres and several centimetres in thickness, and consist of fine-grained quartz and feldspar. No contact aureole on the southeastern side of the Kaminis Lake pluton could be distinguished.

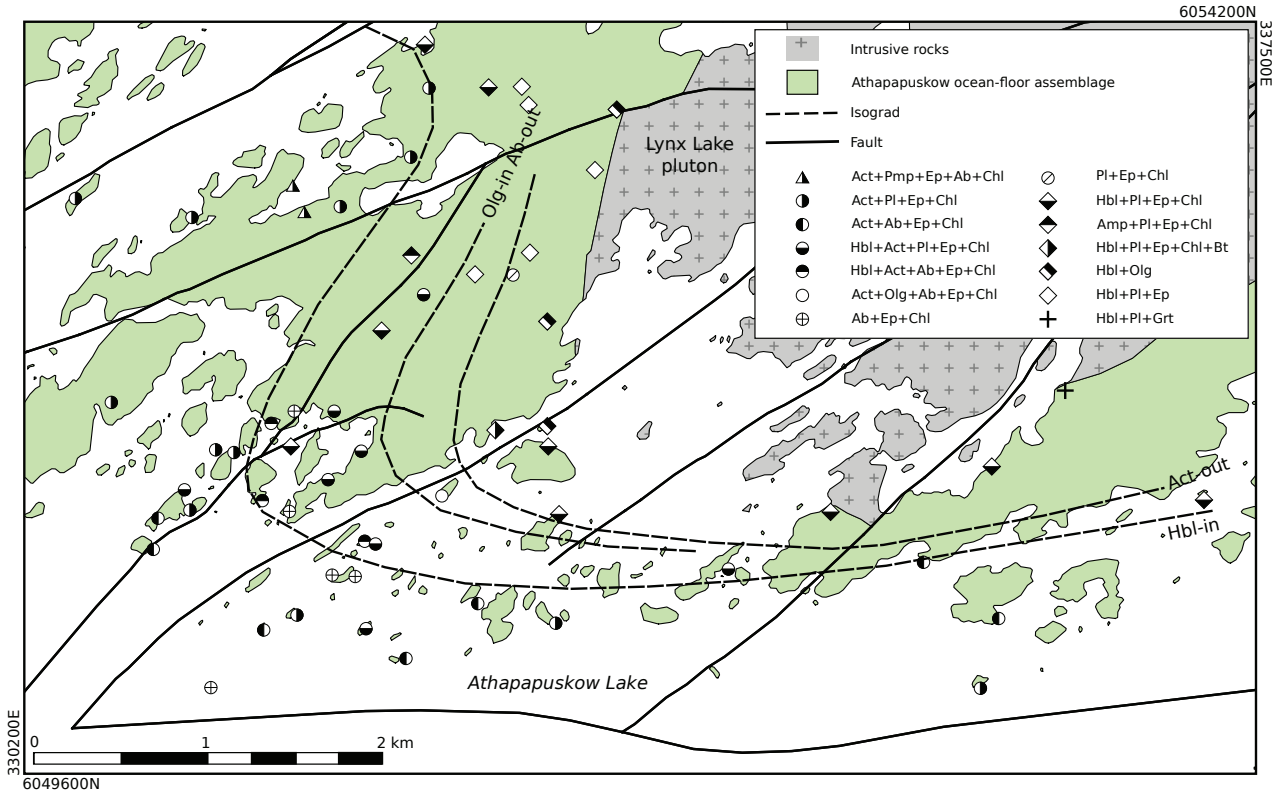

Figure GS2017-10-4: *Map of the metamorphic-mineral assemblages and isograds for the Lynx Lake contact aureole. Abbreviations: Ab, albite; Act, actinolite; Amp, amphibole (undefined); Bt, biotite; Chl, chlorite; Ep, epidote; Grt, garnet; Hbl, hornblende; Olg, oligoclase; Pl, plagioclase; Pmp, pumpellyite.*

Thermodynamic modelling

Phase-equilibria diagram sections were calculated for representative average bulk compositions of the juvenile-arc rocks and the ocean-floor–assemblage rocks (Table GS2017-10-1), in order to estimate pressure and temperature conditions at the peak of metamorphism. The Gibbs energy minimization software Theriak-Domino (de Capitani and Brown, 1987; de Capitani and Petrakakis, 2010) was used, together with the thermodynamic dataset of Holland and Powell (1998; updated to version ds5.5). Activity-composition models (a-X models) for clinoamphibole (Diener et al., 2007, revised by Diener and Powell, 2012), clinopyroxene (Green et al., 2007; Diener and Powell, 2012), garnet (White et al., 2007), chloritoid (White et al., 2000), chlorite (Holland et al., 1998), white mica (Coggon and Holland, 2002), biotite (White et al., 2007), epidote (Holland and Powell, 1998), spinel (White et al., 2002), ilmenite-hematite (White et al., 2000) and feldspar (Cbar1 field; Holland and Powell, 2003) were integrated. The phase-equilibria modelling was performed in the Na_2O-CaO-K_2O-FeO-MgO-Al_2O_3-SiO_2-H_2O-TiO_2-Fe_2O_3 (NCKFMASHTO) chemical system. This system was selected because it is a good approximation of the analyzed composition of the rocks. Iron oxide (Fe_2O_3) was estimated as 15% of the total FeO^T, based on the presence of accessory Fe-bearing phases, wet titration of selected samples, and iterative T-XFe^{3+} and pressure-temperature(P-T) equilibrium modelling for different iron contents and pressures. Manganese was not considered as a component due to its low abundance (usually MnO <0.1 wt. %) and to avoid overstabilization of garnet, which is the main mineral thermodynamically incorporating Mn. Phosphorous is assumed to be completely incorporated in apatite. Hydrogen was set at a large value to obtain H_2O in excess over the whole calculated P-T range.

Figure GS2017-10-5 shows the isochemical phase diagrams for the average juvenile-arc bulk composition (Figure GS2017-10-5a) and the average ocean-floor bulk composition (Figure GS2017-10-5b) in the NCKFMASHTO chemical system. The same colour scheme used in the map of metamorphic-mineral assemblages and isograds (see legend of Figure GS2017-10-2b) is applied to facilitate comparison.

The calculated diagrams for the two different bulk compositions show a number of similar features. In both sections, a large field containing the assemblage Act+Ab+Chl+Ep+Bt+Qtz+Ttn is present below 450°C. Just up-grade of this field are two successive, relatively narrow fields (<20°C) containing coexisting albite and plagioclase, followed by coexisting hornblende and actinolite. The overlap in pressure between the two fields varies between bulk compositions. In the case of the average juvenile-arc assemblage, the overlap spans over a pressure range of 3.7–4.2 kbar, whereas for the average ocean-floor assemblage, the overlap range is 2.7–4.4 kbar. The stability fields, where hornblende coexists with epidote, become narrower and eventually disappear with decreasing pressure. For the juvenile-arc rocks,

Table GS2017-10-1: Whole-rock geochemical data used to calculate phase-equilibria diagrams of figure GS2017-10-5. Average calculated based on selected data from Bailes and Syme (1989), Gilbert (2012), Syme (2015) and Starr (2016), and samples collected by the authors.

wt. % oxides	SiO_2	TiO_2	Al_2O_3	Fe_2O_3	FeO	MgO	CaO	Na_2O	K_2O	P_2O_5	LOI	Total
Average juvenile-arc assemblage	53.84	0.617	14.94	1.911	9.745	4.98	7.8	2.692	0.699	0.126	2.619	99.97
Average ocean-floor assemblage	48.92	1.193	14.09	2.266	11.56	7.147	8.722	2.513	0.214	0.137	3.524	100.3
mol% cations	**Si**	**Ti**	**Al**	**Fe3+**	**Fe2+**	**Mg**	**Ca**	**Na**	**K**	**P**	**H**	**Total**
Average juvenile-arc assemblage	52.16	0.449	17.06	1.393	7.896	7.193	7.926	5.057	0.864	0	100	200
Average ocean-floor assemblage	47.61	0.873	16.17	1.66	9.405	10.37	8.906	4.742	0.266	0	100	200

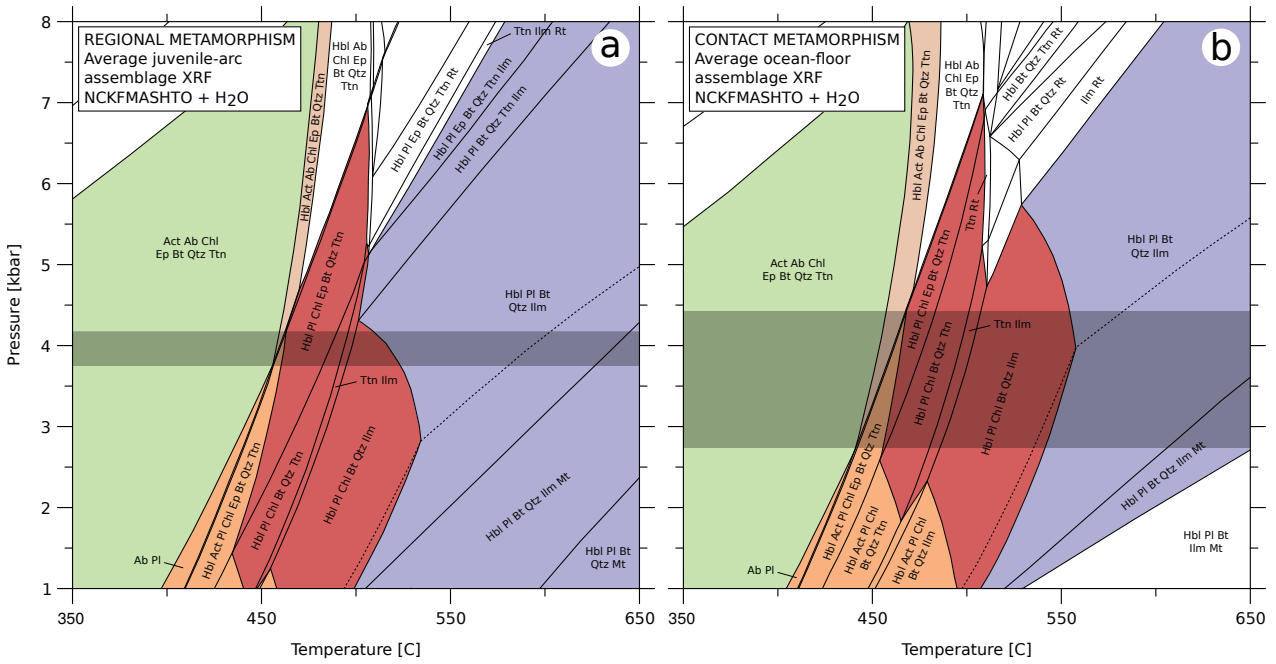

Figure GS2017-10-5: *Pressure-temperature–equilibrium phase diagram constructed for* ***a)*** *the average juvenile-arc assemblage, and* ***b)*** *the ocean-floor assemblages in the NCKFMASHTO chemical system. Fields use the same colour scheme as in Figure GS2017-10-2b to facilitate comparison. The grey overlay indicates the estimated equilibration-pressure range, based on the sequence of isograds observed (regional metamorphic gradient for the juvenile-arc assemblage and Lynx Lake pluton contact aureole for the ocean-floor assemblage). Abbreviations: Ab, albite; Act, actinolite; Bt, biotite; Chl, chlorite; Ep, epidote; Hbl, hornblende; Ilm, ilmenite; Mt, magnetite; Pl, plagioclase; Qtz, quartz; Rt, rutile; Ttn, titanite; XRF, X-ray fluorescence.*

this occurs at about 0.5 kbar, whereas for the ocean-floor rocks, it happens at 1.5 kbar. Up-grade of the hornblende-oligoclase zone, the chlorite-out reaction occurs at slightly lower temperatures in the juvenile-arc assemblage, compared to the ocean-floor assemblage (525°C in the juvenile-arc assemblage, 550°C in the ocean-floor assemblage). Up-grade of the chlorite-out reaction, an amphibole phase is predicted to be stable (upgrade of dashed line). This phase is a calculated amphibole, created to handle order-disorder of Fe, Mg and Al within the crystal structure for minerals, where the partitioning between these elements is unknown (camo1 and camo2; see Diener et al., 2007, Holland and Powell, 2006). In the natural sequences analyzed in this study, no additional amphibole other than actinolite and hornblende was observed, neither through optical microscopy nor through microprobe analysis. The calculated amphibole stability field up-grade of the dashed line is therefore interpreted as hornblende. At relatively low pressures (<3.5 kbar) and temperatures >500°C magnetite is stable. Biotite is stable over the entire P-T range.

Comparison of the calculated phase diagrams, with the sequence of isograds observed in the field (Hbl-in, Olg-in, Ab-out, Act-out and Chl-out), allows an approximation of the

pressure during metamorphism, assuming the models provide a reasonable representation of the natural reactions. The grey band on each diagram represents the range of possible pressures. According to the calculated models, rocks from the regional metamorphic juvenile-arc assemblage equilibrated at pressures between 3.7–4.2 kbar, whereas rocks from the contact metamorphic ocean-floor assemblages experienced pressures of 2.7–4.4 kbar. Within the estimated pressure range, for both the regional metamorphic juvenile-arc assemblage and the contact metamorphic ocean-floor assemblage, the hornblende-in isograd occurs around 440–450°C, followed by the oligoclase-in at 450°C and actinolite-out at 450–460°C. The chlorite-out isograd is situated at approximately 525°C for the juvenile-arc assemblage and at 550°C for the ocean-floor assemblage.

Discussion and conclusion

The new map of metamorphic-mineral assemblages, together with the phase-equilibria modelling, confirms the general increase in metamorphic grade from south to north within the studied part of the Flin Flon greenstone belt. The offset of metamorphic zones by faults and shear zones suggests at least one episode of late tectonic activity (i.e., post-peak regional metamorphism?).

Within the study area, two major metamorphic-facies transitions in metamorphosed basic rocks are observed: the prehnite-pumpellyite– to greenschist-facies transition-and the greenschist- to amphibolite-facies transition. The first is characterized by the first appearance of actinolite, and the last appearence of prehnite and pumpellyite, resulting in a zone where the three minerals coexist. The second is a domain where hornblende coexists with actinolite, located between the hornblende-in isograd and the actinolite-out isograd.

Based on the sequence of isograds observed in the field within the regional metamorphic sequence of the juvenile-arc rocks and the contact metamorphic sequence of the ocean-floor rocks, thermodynamic phase-diagram modelling suggests that the greenschist- to amphibolite-facies transition within the Athapapuskow Lake area is situated at pressures of 3.7–4.2 kbar and temperatures close to 450°C.

Isochemical phase diagrams were calculated using an estimated amount of Fe_2O_3 of 15% of the total FeO^T. Investigation of the influence of ferric iron on the topology of the calculated phase-diagram sections shows that by increasing the amount of Fe_2O_3 to 20%, the equilibration-pressure range of the observed sequence is lowered by more than 1 kbar. In contrast, decreasing the amount of Fe_2O_3 to 10% yields pressures in excess of 1 kbar. This indicates that care should be taken when interpreting results obtained from phase-equilibria modelling of rocks containing ferric iron.

Previous work has demonstrated that important dehydration reactions, which release significant volumes of fluid, are associated with the greenschist- to amphibolite-facies transition. Identifying this transition and the controlling reactions related to the hornblende-in and chlorite-out isograds carries implications for orogenic gold exploration and targeting (e.g., Phillips and Powell, 1993; Starr, 2016). Further work will be directed toward estimating the volume of the fluids released.

Economic considerations

The Flin Flon greenstone belt is host to a variety of mineral deposits and occurrences, including VMS and orogenic gold deposits. Volcanogenic massive sulphide deposits form by seafloor venting of metalliferous hydrothermal fluids in active volcanic settings (e.g., Galley et al., 2007). The Athapapuskow Lake area contains bimodal volcanic successions of mafic and felsic rocks that are characteristic of extensional tectonic regimes and are similar to the volcanic sequence that hosted the Flin Flon and Callinan VMS deposits (e.g., Bailes and Syme, 1989; Syme and Bailes, 1993), indicating excellent exploration potential. Because they formed early in the tectonic evolution of the region, these deposits are overprinted, and in some cases strongly remobilized, via metamorphic and deformational processes. Recognizing the effects of metamorphism on these deposits and their alteration haloes (e.g., Starr, 2016) is important for exploration.

Orogenic-Au deposits form later with respect to regional deformation, magmatism and metamorphism, and the associated release of fluids. The controls on orogenic gold deposits are thus strongly related to metamorphic and tectonic processes. Dehydration reactions, for example at the transition from greenschist to amphibolite facies in metabasites, has been interpreted to provide fluids for the transport of gold (e.g., Phillips and Powell, 1993). Identifying these transitions therefore has implications for gold exploration. In addition, crustal-scale shear zones can create pathways and/or traps for the transport and deposition of base metals and gold in solution (e.g, Dubé and Gosselin, 2007). Constraining the magmatic, tectonic and metamorphic framework of the region, combined with a better understanding of the mechanisms and processes involved in mineral alteration and transport, may therefore help focus base- and precious-metals exploration in the Flin Flon belt.

Acknowledgments

The authors thank J. MacDonald, R. Ponto, S. Walker and R. Ashton for providing enthusiastic field assistance, as well as all the staff at Midland Rock Preparation Laboratory for thorough logistical support and sample preparation. The authors also thank C. Coueslan for reviewing an earlier version of this manuscript.

References

Ansdell, K.M., Lucas, S.B., Connors, K. and Stern, R.A. 1995: Kisseynew metasedimentary gneiss belt, Trans-Hudson Orogen (Canada): back-arc origin and collisional inversion; Geology, v. 23, p. 1039–1043.

Ashton, K.E., Lewry, J.F., Heaman, L.M., Hartlaub, R.P., Stauffer, M.R. and Tran, H.T. 2005: The Pelican Thrust Zone: basal detachment between the Archean Sask Craton and Paleoproterozoic Flin Flon–Glennie Complex, western Trans-Hudson Orogen; Canadian Journal of Earth Sciences, v. 42, p. 685–706.

Bailes, A.H. and Syme, E.C. 1989: Geology of the Flin Flon–White Lake area; Manitoba Energy and Mines, Minerals Division, Geological Report GR87-1, 313 p.

Bleeker, W. 1990: New structural-metamorphic constraints on Early Proterozoic oblique collision along the Thompson Nickel Belt, Manitoba, Canada; *in* The Early Proterozoic Trans-Hudson Orogen of North America, J.F. Lewry and M.R. Stauffer (ed.), Geological Association of Canada, Special Paper 37, p. 57–73.

Coggon, R. and Holland, T.J.B. 2002: Mixing properties of phengitic micas and revised garnet-phengite thermobarometers; Journal of Metamorphic Geology, v. 20, no. 7, p. 683–696.

de Capitani, C. and Brown, T.H. 1987: The computation of chemical equilibrium in complex systems containing non-ideal solutions; Geochimica et Cosmochimica Acta, v. 51, no. 10, p. 2639–2652.

de Capitani, C. D. and Petrakakis, K. 2010: The computation of equilibrium assemblage diagrams with Theriak/Domino software; American Mineralogist, v. 95, no. 7, p. 1006–1016.

Digel, S. and Gordon, T.M. 1995: Phase relations in metabasites and pressure-temperature conditions at the prehnite-pumpellyite to greenschist facies transition, Flin Flon, Manitoba, Canada; *in* Low-Grade Metamorphism of Mafic Rocks, P. Schiffman and H.W. Day (ed.), Geological Society of America, Special Paper 296, p. 67–80.

Diener, J.F.A., Powell, R., White, R.W. and Holland, T.J.B. 2007: A new thermodynamic model for clino-and orthoamphiboles in the system Na_2O-CaO-FeO-MgO-Al_2O_3-SiO_2-H_2O-O; Journal of Metamorphic Geology, v. 25, no. 6, p. 631–656.

Diener, J.F.A. and Powell, R. 2012: Revised activity–composition models for clinopyroxene and amphibole; Journal of Metamorphic Geology, v. 30, no. 2, p. 131–142.

Dubé, B. and Gosselin, P. 2007: Greenstone-hosted quartz-carbonate vein deposits; *in* Mineral Deposits of Canada: a Synthesis of Major Deposit-Types, District Metallogeny, the Evolution of Geological Provinces, and Exploration Methods, W.D. Goodfellow (ed.), Geological Association of Canada, Mineral Deposits Division, Special Publication no. 5, p. 49–73.

Ellis, S., Beaumont, C. and Pfiffner, O.A. 1999: Geodynamic models of crustal-scale episodic tectonic accretion and underplating in subduction zones; Journal of Geophysical Research, v. 15, p. 169–184.

Fedorowich, J.S., Kerrich, R. and Stauffer, M.R. 1995: Geodynamic evolution and thermal history of the central Flin Flon Domain, Trans-Hudson Orogen: constraints from structural development, $^{40}Ar/^{39}Ar$, and stable isotope geothermometry; Tectonics, v. 14, no. 2, p. 472–503.

Galley, A.G., Hannington, M.D. and Jonasson, I.R., 2007: Volcanogenic massive sulphide deposits; *in* Mineral Deposits of Canada: a Synthesis of Major Deposit-Types, District Metallogeny, the Evolution of Geological Provinces, and Exploration Methods, W.D. Goodfellow (ed.), Geological Association of Canada, Mineral Deposits Division, Special Publication no. 5, p. 141–161.

Gilbert, H.P. 2012: Geology and geochemistry of arc and ocean-floor volcanic rocks in the northern Flin Flon Belt, Embury–Wabishkok–Naosap lakes area, Manitoba (parts of NTS 63K13, 14); Manitoba Innovation, Energy and Mines, Manitoba Geological Survey, Geoscientific Report GR2011-1, 46 p., 1 DVD.

Gordon, T.M., Hunt, P.A., Bailes, A.H. and Syme, E.C. 1990: U-Pb zircon ages from the Flin Flon and Kisseynew belts, Manitoba: chronology of crust formation at an Early Proterozoic accretionary margin; *in* The Early Proterozoic Trans-Hudson Orogen of North America, J.F. Lewry and M.R. Stauffer (ed.), Geological Association of Canada, Special Paper 37, p. 177–199.

Green, E., Holland, T. and Powell, R. 2007: An order-disorder model for omphacitic pyroxenes in the system jadeite-diopside-hedenbergite-acmite, with applications to eclogitic rocks; American Mineralogist, v. 92, no. 7, p. 1181–1189.

Hoffman, P.F. 1988: United Plates of America, the birth of a craton: Paleoproterozoic assembly and growth of proto-Laurentia; Annual Review of Earth and Planetary Sciences, v. 16, p. 543–603.

Holland, T., Baker, J. and Powell, R. 1998: Mixing properties and activity-composition and relationships of chlorites in the system MgO-FeO-Al_2O_3-SiO_2-H_2O; European Journal of Mineralogy, v. 10, no. 3, p. 395–406.

Holland, T.J.B. and Powell, R. 1998: An internally consistent thermodynamic data set for phases of petrological interest; Journal of Metamorphic Geology, v. 16, no. 3, p. 309–343.

Holland, T. and Powell, R. 2003: Activity-composition relations for phases in petrological calculations: an asymmetric multicomponent formulation; Contributions to Mineralogy and Petrology, v. 145, no. 4, p. 492–501.

Holland, T.J.B. and Powell, R., 2006. Mineral activity–composition relations and petrological calculations involving cation equipartition in multisite minerals: a logical inconsistency; Journal of Metamorphic Geology, v. 24, no. 9, p. 851–861.

Lucas, S.B., Stern, R.A., Syme, E.C., Reilly, B.A. and Thomas, D.J. 1996: Intraoceanic tectonics and the development of continental crust: 1.92–1.84 Ga evolution of the Flin Flon belt, Canada; Geological Society of America Bulletin, v. 108, p. 602–629.

NATMAP Shield Margin Project Working Group 1998: Geology, NATMAP Shield Margin Project area, Flin Flon belt, Manitoba/Saskatchewan; Geological Survey of Canada, Map 1968A, scale 1:100 000.

Phillips, G.N. and Powell, R., 1993: Link between gold provinces; Economic Geology, v. 88, no. 5, p. 1084–1098.

Schneider, D.A., Heizler, M.T., Bickford, M.E., Wortman, G.L., Condie, K.C. and Perilli, S. 2007: Timing constraints of orogeny to cratonization: thermochronology of the Paleoproterozoic Trans-Hudson orogen, Manitoba and Saskatchewan, Canada; Precambrian Research, v. 153, no. 1, p. 65–95.

Starr, P.G. 2016: Sub-greenschist to lower amphibolite facies metamorphism of basalts: examples from Flin Flon, Manitoba and Rossland, British Columbia; Ph.D. thesis, University of Calgary, Calgary, AB, 511 p.

Stern, R.A. and Lucas, S.B. 1994: U-Pb zircon age constraints on the early tectonic history of the Flin Flon accretionary collage, Saskatchewan; *in* Radiogenic Age and Isotopic Studies: Report 8, Geological Survey of Canada, Current Research 1994-F, p. 75–86.

Stern, R.A., Machado, N., Syme, E.C., Lucas, S.B. and David, J. 1999: Chronology of crustal growth and recycling in the Paleoproterozoic Amisk Collage (Flin Flon belt), Trans-Hudson Orogen, Canada; Canadian Journal of Earth Sciences, v. 36, p. 1807–1827.

Stern, R.A., Syme, E.C., Bailes, A.H. and Lucas, S.B. 1995a: Paleoproterozoic (1.90–1.86 Ga) arc volcanism in the Flin Flon belt, Trans-Hudson Orogen, Canada; Contributions to Mineralogy and Petrology, v. 119, p. 117–141.

Stern, R.A. Syme, E.C. and Lucas, S.B. 1995b: Geochemistry of 1.9 Ga MORB- and OIB-like basalts from the Amisk Collage, Flin Flon belt, Canada: evidence for an intra-oceanic origin; Geochimica et Cosmochimica Acta, v. 59, p. 3131–3154.

Syme, E.C. 2015: Geology of the Athapapuskow Lake area, western Flin Flon belt, Manitoba (part of NTS 63K12); Manitoba Mineral Resources, Manitoba Geological Survey, Geoscientific Report GR2014-1, 209 p.

Syme, E.C. and Bailes, A.H. 1993: Stratigraphic and tectonic setting of volcanogenic massive sulfide deposits, Flin Flon, Manitoba; Economic Geology, v. 88, p. 566–589.

Syme, E.C., Hunt, P.A. and Gordon, T.M. 1991: Two U-Pb zircon crystallization ages from the western Flin Flon belt, Trans-Hudson orogen, Manitoba; *in* Radiogenic Age and Isotopic Studies: Report 4, Geological Survey of Canada, Paper 90-2, p. 25–34.

Syme, E.C., Lucas, S.B., Bailes, A.H. and Stern, R.A. 1999: Contrasting arc and MORB-like assemblages in the Paleoproterozoic Flin Flon belt, Manitoba, and the role of intra-arc extension in localizing volcanic-hosted massive sulphide deposits; Canadian Journal of Earth Sciences, v. 36, p. 1767–1788.

Thomas, D.J. 1991: Revision bedrock geological mapping: Bootleg Lake–Birch Lake area (parts of NTS 63K-12 and 63L-9); in Summary of Investigations 1991, Saskatchewan Geological Survey, Saskatchewan Energy Mines, Miscellaneous Report 91-4, p. 2–8

Whalen, J.B., Perhsson, S. and Rayner, N.M. 2016: Significance of pre–1860 Ma granitoid magmatism for crustal evolution and exploration targeting in the Flin Flon assemblage, Trans-Hudson Orogen, Canada; Economic Geology, v. 111, no. 4, p. 1021–1039, doi: 10.2113/econgeo.111.4.1021

White, R.W., Powell, R., Holland, T.J.B. and Worley, B.A. 2000: The effect of TiO_2 and Fe_2O_3 on metapelitic assemblages at greenschist and amphibolite facies conditions: mineral equilibria calculations in the system K_2O-FeO-MgO-Al_2O_3-SiO_2-H_2O-TiO_2-Fe_2O_3; Journal of Metamorphic Geology, v. 18, no. 5, p. 497–512.

White, R.W., Powell, R. and Clarke, G.L. 2002: The interpretation of reaction textures in Fe-rich metapelitic granulites of the Musgrave Block, central Australia: constraints from mineral equilibria calculations in the system K_2O-FeO-MgO-Al_2O_3-SiO_2-H_2O-TiO_2-Fe_2O_3; Journal of Metamorphic Geology, v. 20, no. 1, p. 41–55.

White, R.W., Powell, R. and Holland, T.J.B. 2007: Progress relating to calculation of partial melting equilibria for metapelites; Journal of Metamorphic Geology, v. 25, no. 5, p. 511–527.

Whitney, D.L. and Evans, B.W. 2010: Abbreviations for names of rock-forming minerals; American Mineralogist, v. 95, no. 1, p. 185–187.

GS2017-11

Geological investigations of the Wasekwan Lake area, Lynn Lake greenstone belt, northwestern Manitoba (parts of NTS 64C10, 15)

by X.M. Yang and C.J. Beaumont-Smith

In Brief:

- New detailed mapping provides an updated geological context for gold mineralization in the Johnson shear zone
- Important controls on Au mineralization include structural and chemical traps along contacts between map units of contrasting rheology
- Granitoid intrusions locally provide an empirical guide to mineralization

Citation:
Yang, X.M. and Beaumont-Smith, C.J. 2017: Geological investigations of the Wasekwan Lake area, Lynn Lake greenstone belt, northwestern Manitoba (parts of NTS 64C10, 15); *in* Report of Activities 2017, Manitoba Growth, Enterprise and Trade, Manitoba Geological Survey, p. 117–132.

Summary

In 2017, the Manitoba Geological Survey continued a multiyear bedrock mapping project in the Paleoproterozoic Lynn Lake greenstone belt. Detailed mapping at 1:20 000 scale focused on the southern supracrustal belt in the Wasekwan Lake area to resolve questions regarding the geological context of Au mineralization and support ongoing exploration activity in the vicinity of the Burnt Timber Au deposit. This detailed mapping also aligns with the broader objectives of the project, which are to constrain the complex geology and geodynamic evolution of the Lynn Lake greenstone belt, and to identify key factors controlling the formation of its diverse mineral deposits (e.g., orogenic Au, magmatic Ni-Cu-PGE, volcanogenic massive-sulphide Cu-Zn).

Preliminary mapping indicates that the area is dominantly underlain by massive to pillowed basalt, with minor basaltic andesite, dacite, rhyolite and related volcaniclastic rocks, along with subordinate sedimentary rocks. The volcanic sequence is spatially and temporally associated with reworked volcaniclastic and epiclastic rocks, as well as banded iron formation (BIF), features suggestive of deposition in a setting comparable to modern volcanic arcs or back-arc basins. These supracrustal rocks are intruded by various granitoid intrusions, in addition to being overprinted by multiple phases of deformation and metamorphism.

Additional findings from the 2017 field season include: 1) Au mineralization appears to be spatially associated with structural contacts between volcaniclastic rocks (unit 1), Fe-rich mafic volcanic rocks (unit 2) and sedimentary rocks (unit 3) that occur along, or adjacent to, the Johnson shear zone and associated structures, which may have created traps (structural and chemical) for Au-bearing fluids; 2) the presence of garnet-hornblende porphyroblasts well preserved in feldspathic greywacke (unit 3), that suggests it, together with the other supracrustal rocks, may have experienced middle-amphibolite facies metamorphism, although the presence of actinolite–tremolite and sodic plagioclase in mafic volcaniclastic rocks (unit 1) indicates that they have been subject to greenschist-facies retrograde overprint; 3) gabbroic intrusions of unit 4 may have potential to host magmatic Ni-Cu-Co-(Pt) mineralization but require further evaluation; and 4) late granitic porphyry dikes (unit 7) and granitoid plutons (unit 6) need to be investigated for their potential connection to Au mineralization.

Introduction

The Manitoba Geological Survey initiated a detailed bedrock mapping project in the Paleoproterozoic Lynn Lake greenstone belt (LLGB) of northwestern Manitoba (Figure GS2017-11-1) in 2015. The broader objectives of this project are to compile all available information and produce an up-to-date synthesis for the belt to accompany a seamless series of 1:50 000 scale maps covering nine NTS sheets. Thus far, fieldwork has been focused around the past-producing MacLellan and Farley Lake Au deposits, with emphasis on investigating their geology and geodynamic evolution as they relate to the Au metallogeny of the belt. In addition, key factors controlling the formation of various types of mineral deposits are being reviewed (e.g., orogenic Au, magmatic Ni-Cu-PGE, volcanogenic massive-sulphide Cu-Zn). These new bedrock geological maps incorporate lithogeochemistry, radiogenic-isotope analysis and a GIS compilation of historical data.

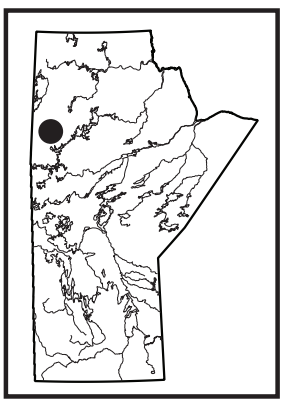

Detailed mapping at a scale of 1:20 000 in the summer of 2017 focused on the Wasekwan Lake area, particularly around the Burnt Timber (BT) Au deposit. The BT deposit occurs within the Johnson shear zone (JSZ; Figure GS2017-11-1; Peck et al., 1998; Jones, 2005; Jones et al., 2006) and displays significant differences to the MacLellan and Farley Lake deposits, which are hosted in the regionally extensive Agassiz metallotect (Figure GS2017-11-1; Fedikow and Gale, 1982; Fedikow, 1992; Ma et al., 2000; Ma and Beaumont-Smith, 2001; Park et al., 2002; Yang and Beaumont-Smith, 2015a, 2016a, b). Understanding these differences will provide important constraints for understanding the Au metallogeny of the Lynn Lake belt. In addition, gabbroic intrusions (e.g., Cockeram

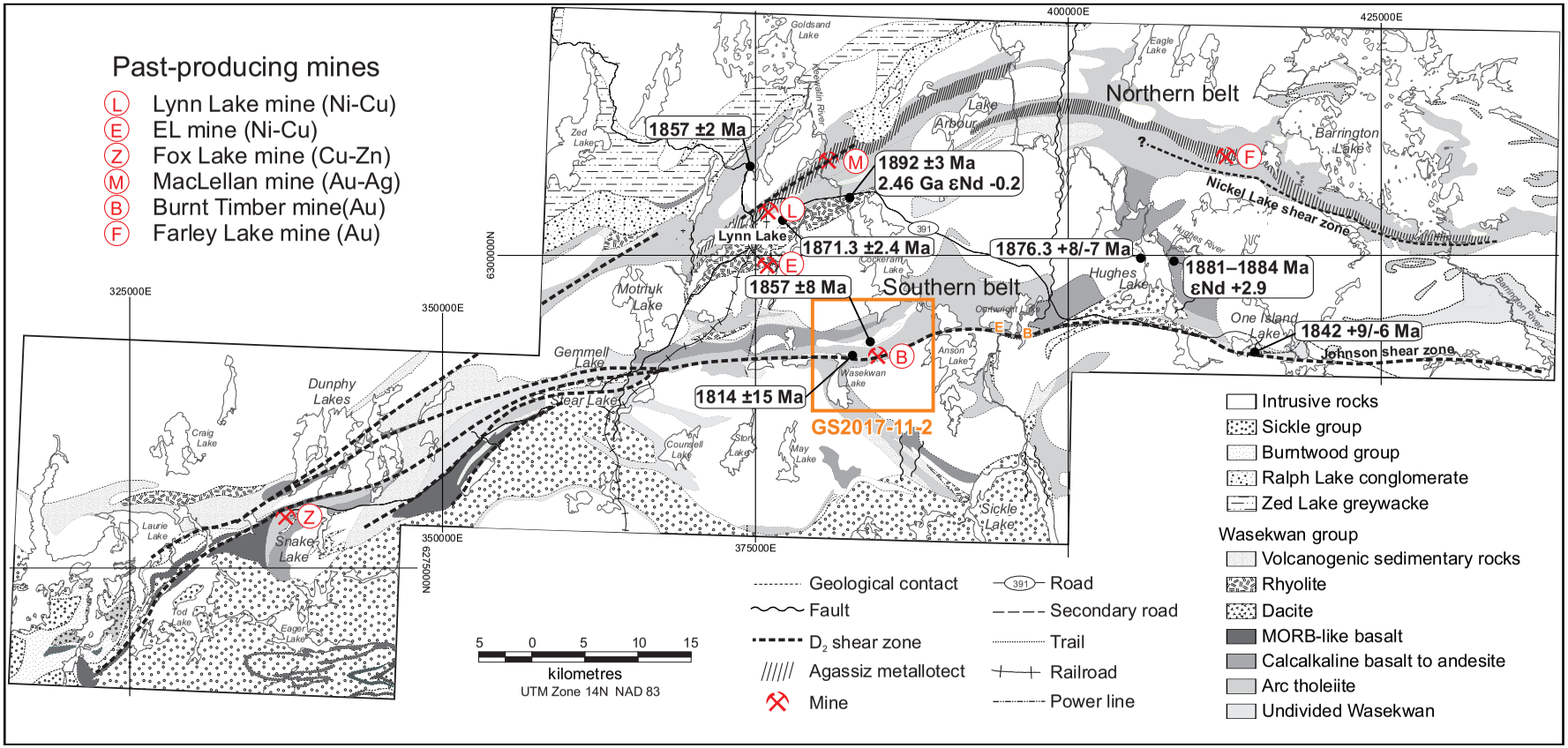

***Figure GS2017-11-1**: Regional geology with zircon U-Pb ages and Nd-isotopic compositions of the Lynn Lake greenstone belt (modified and compiled from Gilbert et al., 1980; Manitoba Energy and Mines, 1986; Gilbert, 1993; Zwanzig et al., 1999; Beaumont-Smith et al., 2000, 2006; Turek et al., 2000; Beaumont-Smith and Böhm, 2002, 2003, 2004; Beaumont-Smith, 2008; Jones, 2005; Jones et al., 2006; C.J. Beaumont-Smith, unpublished data, 2006). The detailed mapping area is indicated by the box and includes the Burnt Timber Au deposit (labelled). Abbreviations: B, Bonanza Au deposit; E, Esker Au showing; MORB, mid-ocean–ridge basalt.*

Lake intrusion) in the map area are petrologically similar to the Lynn Lake gabbroic intrusion that hosts the Lynn Lake magmatic Ni-Cu-Co mine (Pinsent, 1980; Jurkowski, 1999; Yang and Beaumont-Smith, 2015a, b), suggesting that the Wasekwan Lake area also has potential for this type of deposit.

The preliminary map (Yang and Beaumont-Smith, 2017) associated with this report is generated from 279 field stations (this study), compiled historical data (138 stations from Gilbert et al., 1980; 84 stations from C.J. Beaumont-Smith, unpublished data, 2006) and detailed airborne electromagnetic-survey data provided by Carlisle Goldfields Ltd. (now Alamos Gold Inc.).

Regional geology

The LLGB (Bateman, 1945) is an important tectonic element of the Reindeer zone of the Trans-Hudson orogen (Stauffer, 1984; Lewry and Collerson, 1990), which is the largest Paleoproterozoic orogenic belt of Laurentia (Hoffman, 1988; Corrigan et al., 2007, 2009). The LLGB is bounded to the north by the Southern Indian domain, a mixed metasedimentary and metaplutonic domain; to the south, it is bounded by the Kisseynew metasedimentary domain (Gilbert et al., 1980; Syme, 1985; Zwanzig et al., 1999; Beaumont-Smith and Böhm, 2004). Similar Paleoproterozoic greenstone belts also occur to the east (Rusty Lake belt), to the west (La Ronge belt) and to the far south (Flin Flon belt; e.g., Ansdell et al., 1999; Ansdell, 2005; Corrigan et al., 2007, 2009).

The LLGB consists of two east-trending, steeply dipping belts that contain various supracrustal rocks of the Wasekwan group (Bateman, 1945; Gilbert et al., 1980), along with younger molasse-type sedimentary rocks of the Sickle group (Figure GS2017-11-1; Norman, 1933). The southern and northern belts are separated by granitoid plutons of the Pool Lake intrusive suite (Figure GS2017-11-1; Gilbert et al., 1980; Baldwin et al., 1987) which are divided into pre- and post-Sickle intrusions based on their temporal relationships to the Sickle group. In the central and southern parts of the LLGB, the Sickle group overlies the Wasekwan group and felsic–mafic plutonic rocks of the Pool Lake intrusive suite along an angular unconformity. The Sickle group correlates well with the 1850–1840 Ma MacLennan group in the La Ronge greenstone belt in Saskatchewan in terms of composition, stratigraphic position and contact relationships (Ansdell et al., 1999; Ansdell, 2005), although it could be as old as 1865 Ma, based on regional correlations in the Trans-Hudson orogen (Corrigan et al., 2007, 2009). Cutting the entire belt are the much younger Mackenzie dikes (ca. 1267 Ma; Baragar et al., 1996), indicated by regional aeromagnetic data.

The northern Lynn Lake belt consists mostly of subaqueous, tholeiitic, mafic metavolcanic and metavolcaniclastic rocks interpreted as an overall north-facing, steeply dipping succession that occupies the upright limb of a major antiformal structure (Gilbert et al., 1980). Included in the northern belt is the Agassiz metallotect (Fedikow and Gale, 1982; Fedikow, 1986, 1992), a relatively narrow, stratigraphically and structurally distinct entity consisting of ultramafic flows (picrite), banded oxide-facies iron formation and associated exhalative and epiclastic rocks (Ma et al., 2000; Ma and Beaumont-Smith, 2001; Park et al., 2002). The Agassiz metallotect contains Au mineralization (Figure GS2017-11-1) and intense deformation fabrics (Beaumont-Smith and Böhm, 2004).The northern belt is unconformably overlain to the north by marine conglomerate and turbiditic sedimentary rocks, known as the Ralph Lake conglomerate and Zed Lake greywacke, respectively (Gilbert et al., 1980; Manitoba Energy and Mines, 1986; Zwanzig et al., 1999). This clastic succession is derived largely from the Wasekwan group and plutonic rocks, with the majority of detrital zircons returning ca. 1890 Ma ages (Beaumont-Smith and Böhm, 2004).

The southern belt consists largely of subaqueous tholeiitic to calcalkalic metavolcanic and metavolcaniclastic rocks, including minor amounts of metabasalt with geochemical signatures comparable to modern mid-ocean–ridge basalt. The tholeiitic to calcalkalic rocks include older (ca. 1890 Ma) contaminated-arc rocks, as well as younger (ca. 1855 Ma) juvenile-arc volcanic rocks (Peck and Smith, 1989; Zwanzig et al., 1999; Zwanzig, 2000; Beaumont-Smith and Böhm, 2003, 2004). Structural analysis of the LLGB suggests that it is highly transposed (Beaumont-Smith and Rogge, 1999; Beaumont-Smith and Böhm, 2002), calling into question previous stratigraphic and structural interpretations.

Significant differences in the geology and geochemistry of the northern and southern belts reflect this complex structural scenario and/or regional differences in tectonic setting (Syme, 1985; Zwanzig et al., 1999). This complexity leads to the suggestion that the term 'Wasekwan group' should be abandoned because it contains the diverse volcanic assemblages structurally juxtaposed in the evolution of LLGB (see Zwanzig et al., 1999) and thus may represent a tectonic collage similar to that described in the Flin Flon greenstone belt (e.g., Stern et al., 1995). However, this report and accompanying preliminary map (Yang and Beaumont-Smith, 2017) retain the term 'Wasekwan group' to maintain consistency with previous LLGB-related literature.

Geology of the Wasekwan Lake area

The Wasekwan Lake area is located in the southern belt of the LLGB (Figure GS2017-11-1) and consists dominantly of the Wasekwan group supracrustal rocks intruded by plutons of the Pool Lake intrusive suite (Figure GS2017-11-2). Following the convention of previous workers (e.g., Beaumont-Smith and Böhm, 2004), intrusions cutting the Wasekwan group (i.e., the Pool Lake intrusive suite of Gilbert et al., 1980) and those cutting the Sickle group are called, respectively, the pre-Sickle and post-Sickle (e.g., Milligan, 1960) suites; both are cut by a late intrusive suite (Yang and Beaumont-Smith, 2015a, b), identified in the area of the MacLellan Au mine.

Eight map units, including 15 subunits, were defined during the course of bedrock mapping (Table GS2017-11-1). These map units are described in the following sections and shown in Figure GS2017-11-2 (see Yang and Beaumont-Smith, 2017). The supracrustal rocks in the LLGB were metamorphosed in the greenschist to amphibolite facies (Gilbert et al., 1980;

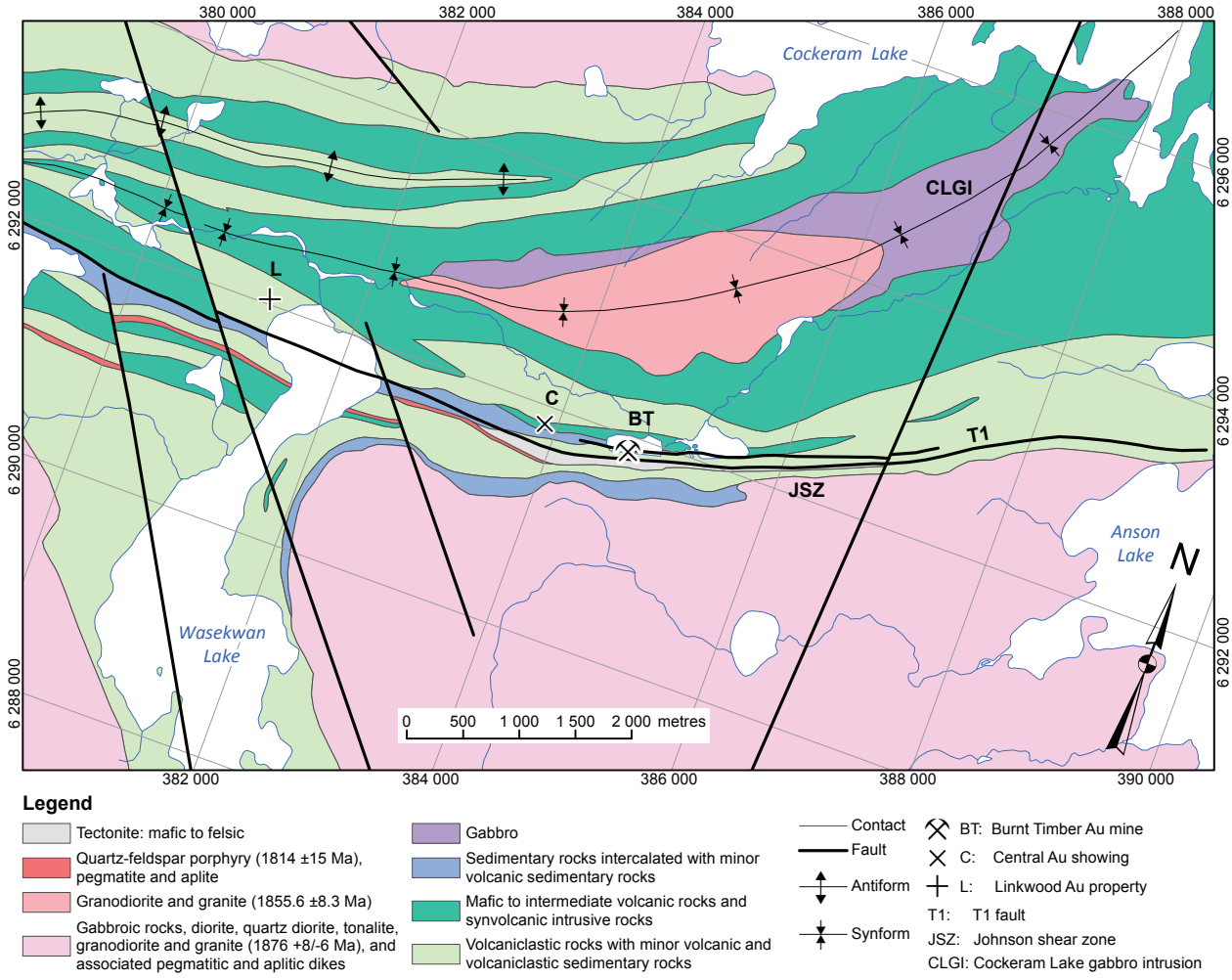

***Figure GS2017-11-2**: Simplified geology of the Wasekwan Lake area, Lynn Lake greenstone belt, northwestern Manitoba (modified from Yang and Beaumont-Smith, 2017).*

Beaumont-Smith and Böhm, 2004; Yang and Beaumont-Smith, 2015a, 2016a); however, for brevity, the prefix 'meta' is omitted in this report.

Volcaniclastic rocks with minor volcanic rocks and volcanic sedimentary rocks (unit 1)

Rocks of unit 1 are widespread in central, southwestern and western parts of the map area (Figure GS2017-11-2). Unit 1 consists mainly of mafic volcaniclastic rocks and lesser amounts of intermediate to felsic volcanic and volcaniclastic rocks that in places appear to have been reworked by sedimentary processes. The volcaniclastic rocks of unit 1 include mafic breccia, tuff breccia, lapillistone, lapilli tuff and tuff, and minor intermediate to felsic lapilli tuff and tuff (Table GS2017-11-1).

Despite being less abundant, outcrops of strongly foliated dacite and rhyolite (subunit 1a) are significant in terms of correlation to similar rocks in the northern belt. Subunit 1a is mainly exposed in the central and west-central portions of the map area (Figure GS2017-11-2). These felsic to intermediate rocks are very fine grained, pale grey to white on weathered surfaces and light to medium grey on fresh surfaces, and preserve primary features (i.e., flow banding, porphyritic texture) despite being strongly foliated and recrystallized (Figure GS2017-11-3a). Porphyritic dacite and rhyolite contain equant or subrounded quartz (0.5–1.3 mm) and locally subhedral to euhedral K-feldspar (0.5–1.5 mm) phenocrysts embedded in a very fine grained to aphanitic groundmass. Locally associated with these rocks is disseminated pyrite and mesoscopic hydrothermal alteration represented by an assemblage of amphibole (actinolite?), chlorite, sericite and carbonate, manifested by dark bluish patches and/or zones up to 20 cm in width that gradually transition to less-altered felsic to intermediate volcanic rocks. It is not uncommon that boudinaged vein quartz occurs along the main S_2 foliation planes (note that the structural terms used in this report follow those in Beaumont-Smith and Böhm, 2003, 2004), some of which contains fine-grained pyrite grains.

Felsic volcaniclastic rocks are less abundant than dacite and rhyolite rocks (subunit 1a). They consist primarily of felsic lapilli tuff that contains very fine to fine-grained rhyolite to

Table GS2017-11-1: Lithostratigraphic units of the Wasekwan Lake area, Lynn Lake greenstone belt, northwestern Manitoba.

Unit[1]	Rock type	Affiliation
8	Tectonite: mafic to felsic in composition	Tectonite
	Structural contact	
7	Quartz-feldspar porphyry (1814 ±15 Ma[2,4]), pegmatite and aplite	Late intrusive suite
	Intrusive contact	
6	Granodiorite and granite (1855.6 ±8.3 Ma[4])	
6a	Granodiorite	Post-Sickle intrusive suite
6b	Granite	
	Intrusive contact	
5	Gabbroic rocks, diorite, quartz diorite, tonalite, granodiorite, and granite (1876 +8/-6 Ma[3]) and associated pegmatitic and aplitic dikes	
5a	Tonalite, granodiorite and granite and associated pegmatitic and aplitic dikes	Pre-Sickle intrusive suite
5b	Diorite, quartz diorite and minor gabbroic rocks	
4	Gabbro	
	Structural contact	
3	Sedimentary rocks intercalated with minor volcanic sedimentary rocks	
3a	Argillite and greywacke	
3b	Banded iron formation	
3c	Volcanic mudstone and arenite	
	Structural contact	
2	Mafic to intermediate volcanic rocks and synvolcanic intrusive rocks	
2a	Diabase and gabbro	
2b	Porphyritic basaltic andesite	Wasekwan group
2c	Plagioclase-phyric basalt and aphyric basalt	
2d	Pillow basalt	
	Structural contact	
1	Volcaniclastic rocks with minor volcanic rocks and volcanic sedimentary rocks	
1a	felsic to intermediate volcanic and volcaniclastic rocks	
1b	Intermediate lapilli tuff and tuff	
1c	Mafic lapillistone, mafic lapilli tuff, tuff and minor mafic mudstone	
1d	Mafic tuff breccia and breccia	
	?	

[1] on Preliminary Map PMAP2017-3 (Yang and Beaumont-Smith, 2017)
[2] Jones (2005)
[3] Baldwin et al. (1987)
[4] C.J. Beaumont-Smith, unpublished data, 2006

dacite (elongated, subangular to irregular shape; 4–10 mm), feldspar and quartz crystal fragments (2–3 mm) in a tuff matrix that contains lithic (1–2 mm) and mineral fragments (<2 mm; plagioclase, K-feldspar, quartz and biotite).

Intermediate lapilli tuff and tuff (subunit b) typically display millimetre- to centimetre- scale layers, interpreted to represent beds even though they are foliated and, in places, folded. Lapilli tuff contains elongated lithic fragments up to 6 cm in diameter of variable composition (e.g., diorite, rhyolite, porphyritic andesite, aphanitic basalt) that are embedded in a fine-grained matrix consisting of amphibole, biotite, chlorite, epidote, plagioclase and aphanitic material. In places, alternating ~0.5–1 cm thick, dark grey and pale yellow-grey layers represent mafic and intermediate–felsic intercalations. Lapilli tuff appears to grade laterally to fine-grained tuff that contains interbedded mafic and felsic laminae (~0.5–2 mm), and in which larger lapilli-sized lithic fragments are rare or absent. Some tuff and lapilli tuff are moderately to strongly magnetic due to the presence of scattered, euhedral to subhedral magnetite porphyroblasts (up to 1%; 0.5–2 mm). Noteworthy are plagioclase crystal tuff and lapilli tuff, with thin felsic layers up to 1 cm thick (Figure GS2017-11-3b) that contain a large amount of plagioclase fragments of varied shape (e.g., angular, irregular) ranging in size from 0.1 to 10 mm across, and which are unevenly distributed at the outcrop scale. This feature distinguishes the plagioclase crystal tuff and lapilli tuff from plagioclase-phyric

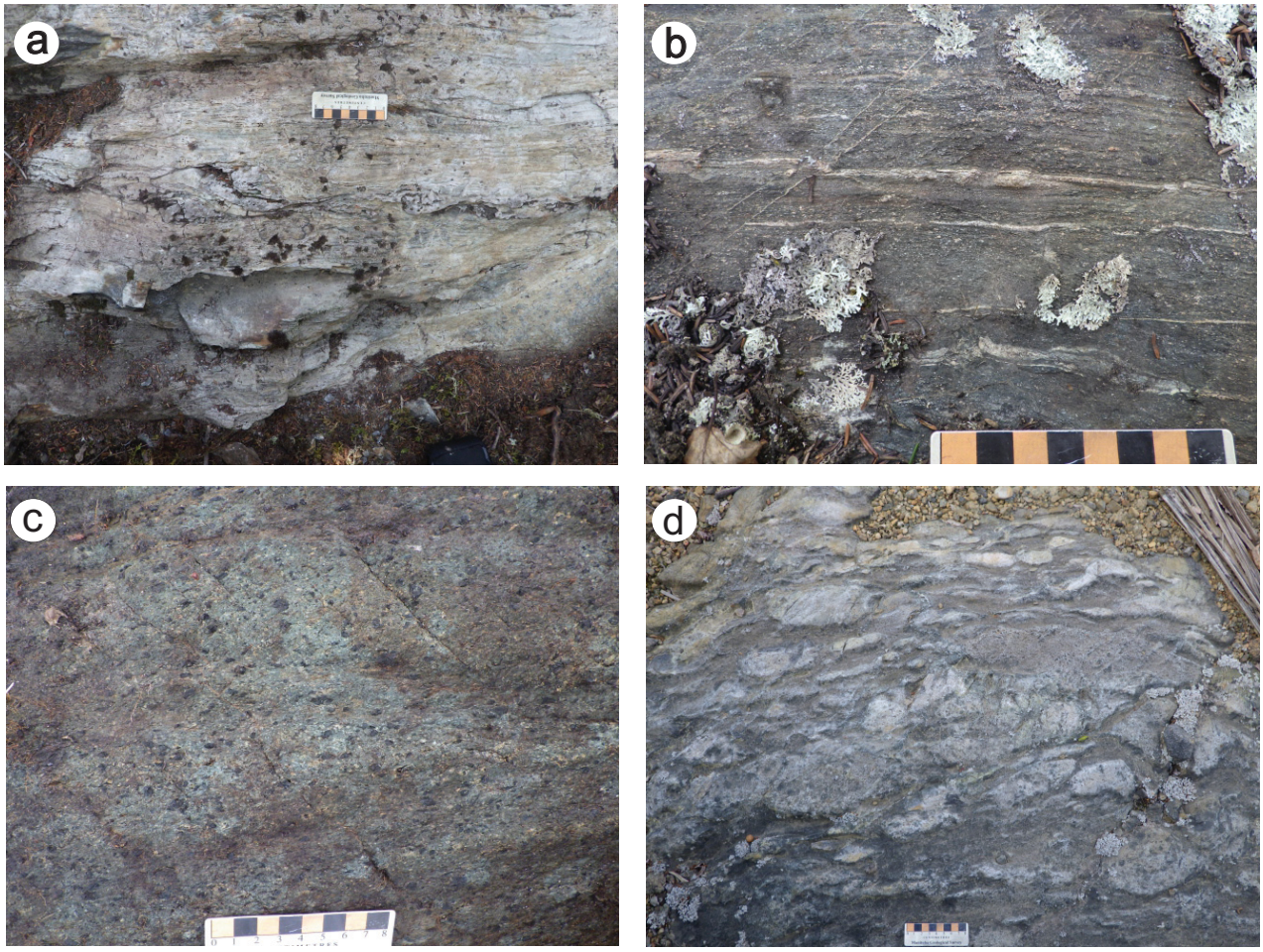

Figure GS2017-11-3: *Field photographs of unit 1 volcaniclastic rocks with minor volcanic and volcanic sedimentary rocks of the Wasekwan group:* ***a)*** *strongly foliated felsic to intermediate volcanic rock (subunit 1a; UTM Zone 14N, 380148E, 6292197N, NAD 83) with a boudinaged quartz vein along S_2 foliation plane; asymmetrical fabric indicates sinistral shear sense;* ***b)*** *mafic to intermediate plagioclase crystal tuff and lapilli tuff with thin felsic layers (subunit 1b; UTM 381903E, 6290514N);* ***c)*** *foliated lapilli tuff to tuff with amphibole (pseudomorph of clinopyroxene) and plagioclase crystal fragments in fine-grained mafic matrix (subunit 1c; UTM 380522E, 6293155N);* ***d)*** *mafic tuff breccia and breccia with plagioclase- and amphibole-phyric basalt fragments and blocks in lapilli tuff to tuff matrix (subunit 1d; UTM 380288E, 6292917N).*

basalt (see unit 2c of unit 2 described below). Again, pyrite-bearing quartz veins and veinlets are common along or cross-cutting S_2 foliation in these rocks.

Mafic volcaniclastic rocks have been broken into two subunits; subunit 1c consists of minor mafic mudstone, tuff and lapilli-tuff, whereas subunit 1d consists of mafic tuff breccia and breccia (Table GS2017-11-1). Mafic lapillistone, lapilli tuff and tuff (subunit 1c) are characterized by the presence of mafic lithic fragments in a chloritic matrix. Minor greenish grey, very fine grained, thinly-bedded mafic mudstone is also included in subunit 1c (Table GS2017-11-1), which usually weathers light greenish brown to light grey and contains disseminated pyrrhotite and pyrite. Mafic volcaniclastic rocks are commonly epidote altered. Dark green, acicular amphibole (actinolite?) porphyroblasts (up to 5–10 mm) concentrated in foliation or fracture planes in mafic tuff and lapilli tuff are interpreted to have formed by retrograde metamorphism to greenschist facies. Some outcrops of mafic tuff and lapilli tuff contain 1–2% euhedral magnetite porphyroblasts (1–3 mm) and coincide with very strong magnetic features on aeromagnetic maps.

The mafic lapilli tuff and tuff (subunit 1c) are generally moderate to strongly foliated and range from texturally variable to relatively homogeneous. These rocks consist of varied amounts of aphyric lithic fragments, plagioclase (up to 40%; 0.1–5 mm) and chloritic amphibole pseudomorphs after pyroxene (up to 15%; 0.2–12 mm) in a fine-grained mafic tuff matrix (Figure GS2017-11-3c). Magnetite and amphibole porphyroblasts are evident in places. Mafic lapilli-sized fragments make up <25% of subunit 1c, but can locally account for up to 80% of the rocks, which are thus termed mafic lapillistone.

Subunit 1d consists of moderate to strongly deformed and foliated heterolithic mafic tuff breccia and breccia. Lithic fragments, ranging from 8 to 25 cm in length, include plagioclase-phyric basalt, plagioclase-amphibole–phyric basalt, aphyric

basalt, lapilli tuff, very fine grained andesite and minor rhyolite clasts embedded in a lapilli tuff and tuff matrix (Figure GS2017-11-3d). The basaltic fragments are subrounded to subangular, varying in shape from irregular to rarely ellipsoidal, and have been stretched along the generally east- to southeast-trending foliation (S_2). Some of the aphanitic basalt fragments display epidote alteration and others show reaction rims with very fine grained assemblages of chlorite, epidote, sericite and albite. Some porphyritic basalt blocks contain well-preserved plagioclase and amphibole (after pyroxene) phenocrysts, and are moderately to strongly magnetic. Rare pyrrhotite and pyrite disseminations are evident in both the basaltic fragments and the matrix, suggesting that the basaltic magmas may have been sulphide saturated.

Chert and thin layers of BIF or fragments of these rocks are not observed within mafic tuff breccia and breccia of subunit 1d in the Wasekwan Lake area. This is similar to the mafic volcaniclastic rocks in the area of the Farley Lake Au mine (Yang and Beaumont-Smith, 2016a), but contrasts with the mafic volcaniclastic rocks in the area of the MacLellan Au mine, which contain fragments of thinly bedded chert and BIF (see Ma et al., 2000; Yang and Beaumont-Smith, 2015a).

Mafic to intermediate volcanic rocks and synvolcanic intrusive rocks (unit 2)

Unit 2 volcanic rocks mainly occur in the northeastern and southwestern parts of the map area (Figure GS2017-11-2). The volcanic succession of unit 2 in the Wasekwan Lake area is dominated by plagioclase-phyric and aphyric basalts as well as pillow basalts, with subordinate porphyritic basaltic andesite, and synvolcanic diabase and gabbro dikes (Table GS2017-11-1).

Pillowed basalts (subunit 2d) are well preserved in a low-strain window exposed along the southeastern shore of Cockeram Lake (Figure GS2017-11-2). Pillow size ranges from 30 to 100 cm, with well-preserved selvages up to 5 cm thick, epidote alteration and subrounded to round quartz±carbonate amygdules up to 1.5 cm in diameter that are concentrated along the inner margin (Figure GS2017-11-4a). In some cases, the concentration of amygdules is asymmetrical, which may be an indicator of younging direction. However, fragments of brecciated pillows with abundant quartz±carbonate±feldspar amygdules of varied shape (e.g., subrounded to irregular) and size (1–10 mm) make it difficult to unambiguously determine younging directions. In high-strain areas, such as the northwestern part of Wasekwan Lake, pillows are strongly deformed and contain a penetrative foliation with width to length ratios up to 1:10. Some pillow selvages are still recognizable, and contain stretched vesicles and quartz amygdules that align parallel to S_2 foliation planes (Figure GS2017-11-4b). Notably, layers of very fine grained interpillow chert up to 5 cm thick are present between some of the strongly deformed pillows, reflecting subaqueous hydrothermal activity associated with basalt eruption.

The plagioclase-phyric basalt of subunit 2c is similar to rocks in the northern belt as described in Gilbert et al. (1980) and by Yang and Beaumont-Smith (2015a, 2016a). This porphyritic basalt weathers greenish grey to dark grey-black and is green to dark grey on fresh surfaces. It comprises varied amounts of plagioclase phenocrysts and glomerocrysts (in the range of 5 to 50% but most commonly 20 to 30%), and rare amphibole phenocrysts (pseudomorphs after pyroxene) in a fine-grained groundmass of plagioclase, amphibole, epidote, chlorite, carbonate and iron-oxide minerals. Amphibole and magnetite porphyroblasts occur rarely in the basalt. The plagioclase phenocrysts are subhedral and commonly equant (0.5–5 mm), although some glomerocrysts or single plagioclase grains are up to 10 mm. The plagioclase-phyric basalt is texturally homogeneous and moderately to strongly foliated; in high-strain zones, relict plagioclase phenocrysts occur as finer recrystallized aggregates aligned along the S_2 foliation. Distinct light greenish grey epidote-altered domains are common. Trace disseminated pyrrhotite and/or chalcopyrite are evident in many outcrops, and pyrite is common in fractures and faults cutting basalt flows.

Porphyritic basaltic andesite (subunit 2b) contains amphibole (±biotite) and lesser amounts of plagioclase phenocrysts in a fine-grained groundmass, although in some cases it lacks plagioclase phenocrysts. Biotite and sericite alteration is a common feature of these rocks. When plagioclase and amphibole phenocrysts coexist in basaltic andesite (subunit 2b), it is difficult to distinguish it from plagioclase-phyric basalt (subunit 2c), although the latter commonly lacks amphibole (±biotite) phenocrysts. In such circumstances, whole-rock geochemistry and mineral chemistry of plagioclase may help distinguish between the rocks.

Massive aphyric basalt (subunit 2c) is also commonly seen in the map area (Figure GS2017-11-4c). Vesicles and quartz±calcite amygdules are present in some outcrops. Variation in vesicle abundance, size and shape in some exposures indicates that the volcanic sequence at the northwestern part of Wasekwan Lake youngs to the south. This basalt is greyish green on weathered surfaces and dark greyish green on fresh surfaces. In most cases, it is aphanitic. Chlorite and epidote alteration is common in the aphyric basalt, as shown by epidote domains, a few centimetres to a metre across. These epidote domains are generally irregular to ovoid, displaying sharp to gradational contacts with the host aphyric basalt though some epidote is fracture controlled as veins or veinlets, similar to those described in Gilbert et al. (1980), Gilbert (1993) and Yang and Beaumont-Smith (2016a).

Synvolcanic diabase and gabbroic rocks usually occur as dikes and small plugs intruded into unit 2 volcanic rocks, and in some cases into unit 1 volcaniclastic rocks. These mafic intrusive rocks are assigned to subunit 2a. The diabase dikes weather greenish grey to medium grey and are medium to dark green on fresh surfaces; they are very fine to medium grained, porphyritic, and moderately to strongly deformed and foliated (Figure GS2017-11-4d). Equant to subhedral plagioclase phenocrysts (up to 10 mm) occur in a fine-grained groundmass of plagioclase, amphibole, chlorite and iron oxides. Generally, the diabase and gabbroic rocks consists of 50–60% amphibole and 40–50% plagioclase. Grain boundaries between phenocrysts

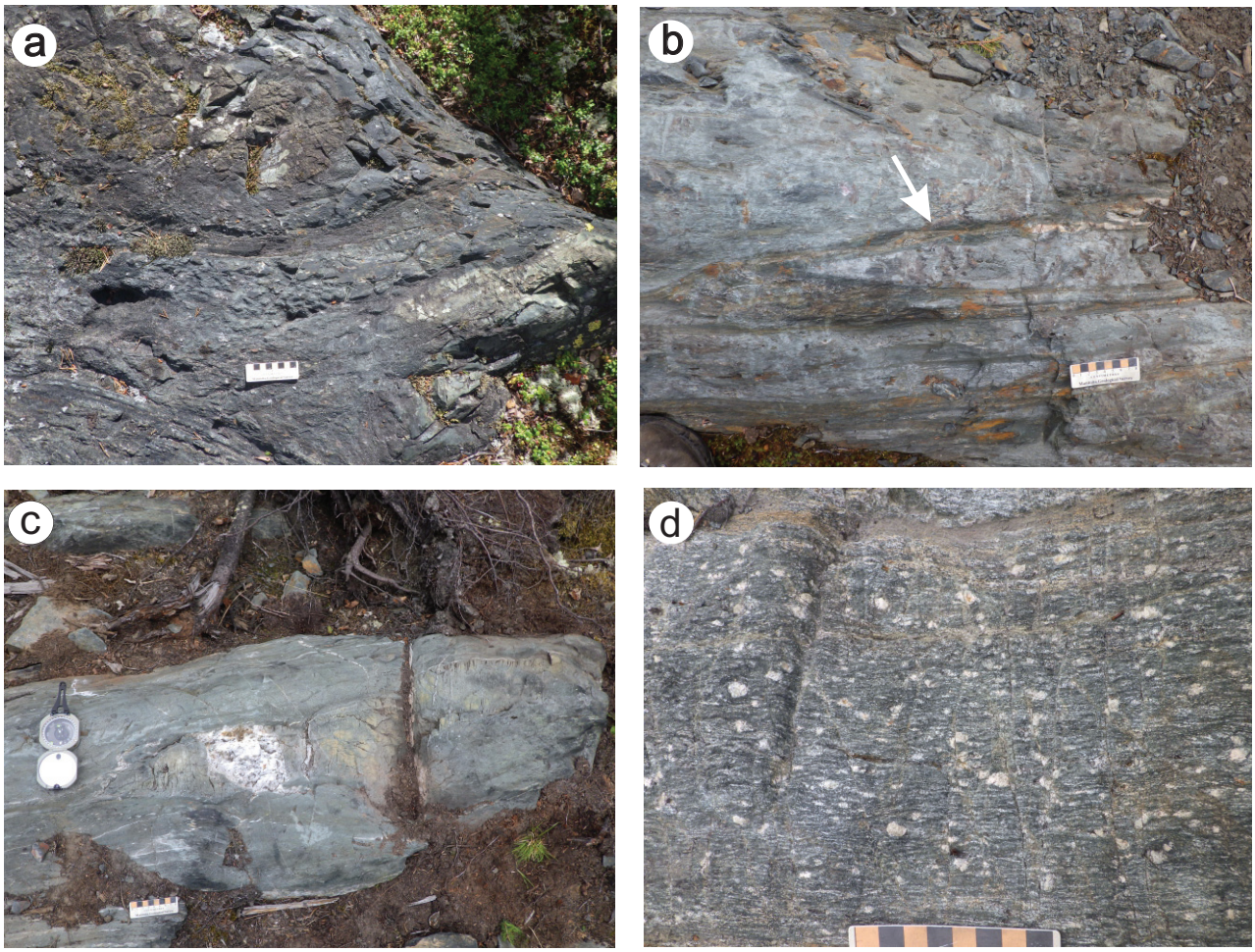

Figure GS2017-11-4*: Field photographs of mafic to intermediate volcanic rocks and synvolcanic intrusive rocks (unit 2) of the Wasekwan group:* ***a)*** *pillow basalt with well-preserved selvage up to 5 cm thick and subrounded quartz±carbonate amygdules (centre right; subunit 2d; UTM Zone 14N, 387265E, 6296232N, NAD83);* ***b)*** *strongly deformed and foliated pillow basalt with recognizable selvages (as indicated by arrow) parallel S_2 foliation (subunit 2d; UTM 381153E, 6292415N);* ***c)*** *foliated amphibole-phyric basaltic andesite (subunit 2b; UTM 380379E, 6293137N);* ***d)*** *very fine grained, foliated, aphyric basalt with epidote-altered domain cut by late quartz veins (subunit 2c; UTM 381146E, 6292386N).*

and the groundmass are diffuse due to sericite and chlorite alteration, regardless of the extent of deformation. Disseminated sulphides (e.g., pyrrhotite and/or pyrite; ~0.5–1 mm) are locally evident.

Sedimentary rocks intercalated with minor volcanic sedimentary rocks (unit 3)

Unit 3 sedimentary rocks are subordinate to volcanic and volcaniclastic rocks in the Wasekwan Lake area. The sedimentary rocks are mainly exposed in the central and southwestern portions of the map area (Figure GS2017-11-2). This unit consists of argillite and greywacke (subunit 3a), and BIF (subunit 3b), intercalated with minor volcanic mudstone and arenite (subunit 3c; Table GS2017-11-1).

Quartz feldspathic greywacke and sandstone (subunit 3a) are dominant in the sedimentary succession. The greywacke contains more than 15% clay materials in its matrix, whereas sandstone has much less clays in the matrix. Primary bedding (S_0) in the sediments is completely transposed by the regional S_2 foliation. These medium- to coarse-grained greywacke and sandstone are medium tan to yellowish grey on weathered surfaces, and light grey on fresh surfaces. Quartz, feldspar, amphibole and lithic clasts (1.3–2 mm) are angular to subrounded, and well aligned on foliation planes, whereas euhedral to subhedral dark pink garnet (1–3.5 mm) and dark green hornblende (2–3 mm) porphyroblasts are more randomly oriented (Figure GS2017-11-5a, b), albeit that biotite flakes define foliation planes. The mineral assemblage of garnet, hornblende ±biotite in these sedimentary rocks reveals that they have experienced middle-amphibolite facies metamorphism, similar to their counterparts in the northern belt (Yang and Beaumont-Smith, 2015a, 2016a). Scattered sulphide minerals dominated by pyrite are evident in the greywacke and sandstone; in many cases they are associated with quartz veins and veinlets.

In the northeastern part of the Wasekwan Lake area, primary bedding in thin- to medium-bedded argillite and mudstone (subunit 3a) is locally well preserved at the outcrop scale

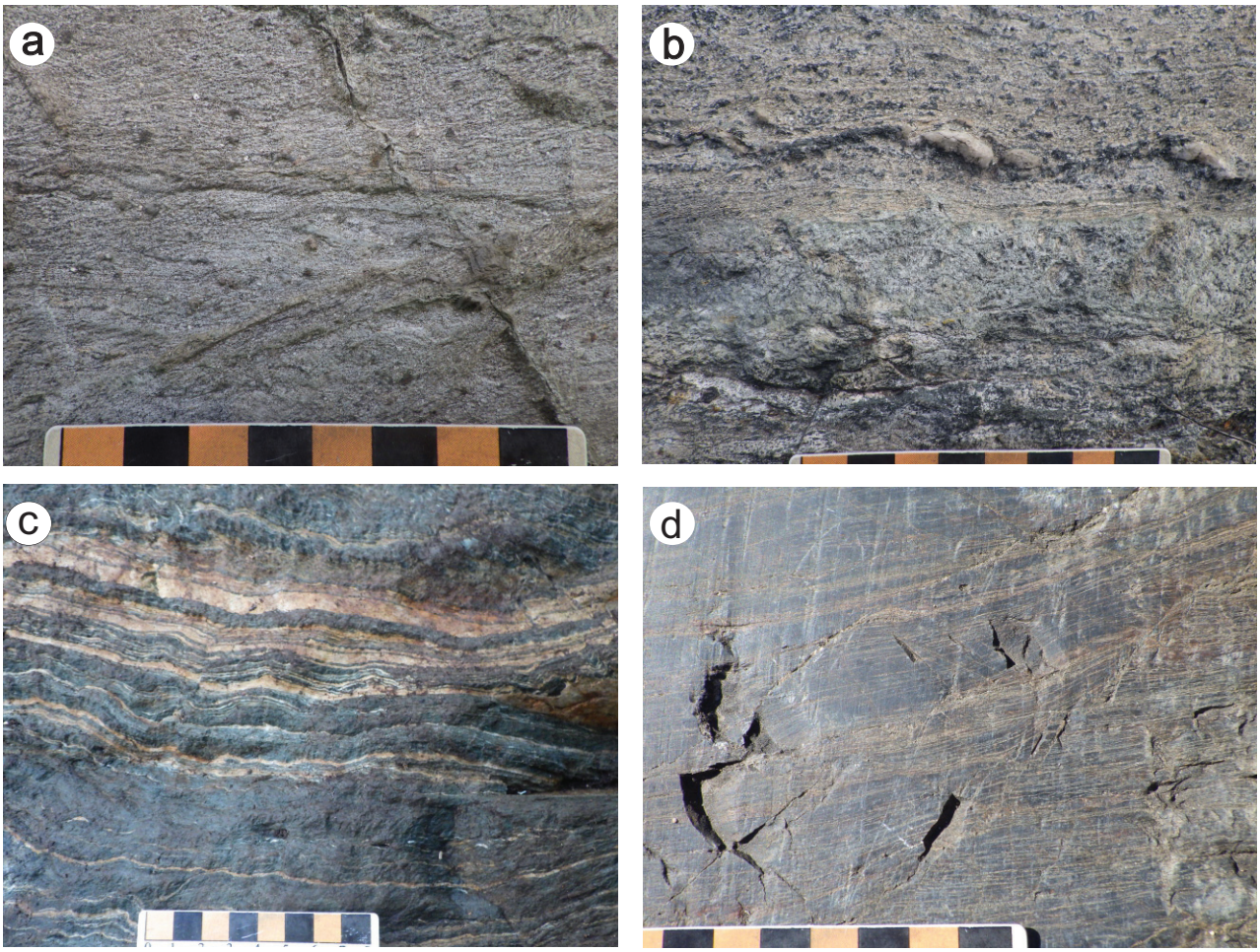

Figure GS2017-11-5*: Field photographs of sedimentary rocks intercalated with minor volcanic sedimentary rocks (unit 3) of the Wasekwan group:* ***a)*** *quartz feldspathic greywacke containing dark pink garnet and hornblende porphyroblasts (subunit 3a; UTM 383443E, 6291886N, NAD 83);* ***b)*** *sandstone with hornblende and garnet porphyroblasts, late quartz veinlets occurring along S_2 foliation that has transposed S_0 primary bedding (subunit 3a; UTM 383527E, 6291914N);* ***c)*** *thinly bedded argillite and mudstone dominated by mafic materials (subunit 3a; UTM 382530E, 6291206N);* ***d)*** *banded iron formation consisting of alternating laminae of very fine grained magnetite, biotite-rich mudstone and chert, with bedding transposed by S_2 foliation (subunit 3b; UTM Zone 14N, 384995E, 6291845N).*

(Figure GS2017-11-5c), although they are foliated and folded. Millimetre- to centimetre-thick, dark green mafic to light tan felsic layers alternate to form laminae; the mafic laminae are rich in amphibole and chlorite, whereas the felsic laminae contain abundant feldspar and lesser quartz, in addition to minor fine-grained biotite (<0.2 mm) and disseminated pyrite. In a few locations, graded beds indicate that the stratigraphic sequence is younging to the south, consistent with the observed southward younging of mafic volcanic rocks (subunit 2c).

The BIFs (subunit 3b) are rarely exposed southeast of the BT Au deposit (Figure GS2017-11-2), but correlate with highly east-trending magnetic domains in detailed airborne magnetic surveys. At the outcrop scale, BIFs typically display very thin alternating laminae ranging from 1 to 6 mm (locally up to 15 mm). These laminae consist of chert, jasper, mudstone, greywacke and very fine grained magnetite±hematite (Figure GS2017-11-5d). Very fine grained biotite is concentrated in the mudstone layers and imparts a unique brownish colour; the jasper layers are up to 1 cm thick. Layering in the BIFs locally displays mesoscopic Z-asymmetric folds and a penetrative foliation.

Thin beds of minor volcanic sedimentary rocks (subunit 3c) are present in the upper section of unit 3 and consist of volcanic mudstone and sandstone (Table GS2017-11-1). A section >1 m thick of this subunit is exposed west of Wasekwan Lake. A similar exposure of rocks, about 10 m in thickness, is observed in the Keewatin River area in the northern belt (Yang and Beaumont-Smith, 2015a).

Pre-Sickle intrusive suite (units 4 and 5)

Plutonic rocks in the pre-Sickle intrusive suite occur as intrusions or plutons that are emplaced into the Wasekwan group but overlain unconformably by the Sickle group (Gilbert

et al., 1980; Baldwin et al., 1987; Beaumont-Smith and Bohm, 2004). Unit 4 gabbro and unit 5 granitoid rocks, diorite, quartz diorite and minor gabbroic rocks are included in this suite (Table GS2017-11-1).

Gabbro (unit 4)

Gabbro of unit 4 is represented by the Cockeram Lake intrusion, which intrudes unit 2 and unit 1 in the northeastern to central part of the map area (Figure GS2017-11-2). The gabbro occurs as an elongated intrusion or a sill-like body occupying the core of a macroscopic F_2 fold that trends in an east-northeast direction through the central portion of the map area; the gabbro is then cut by granitic intrusions. This gabbro weathers greenish grey and is dark greenish grey to dark grey on fresh surfaces. It is medium grained, equigranular, massive and moderately to locally strongly foliated. The gabbro consists of 40–45% plagioclase laths (1–3 mm), 55–60% amphibole (pseudomorphs after pyroxene), minor iron-oxide minerals, and trace pyrrhotite and chalcopyrite (Figure GS2017-11-6a). The edges of both plagioclase and amphibole crystals are diffuse due to chlorite and sericite alteration. This gabbro contains a greenschist-facies metamorphic assemblage (chlorite, actinolite, epidote and albite). Quartz veinlets and veins (~2–5 cm wide) are locally common along extensional fractures, and some of these veins contain pyrite and/or chalcopyrite.

The gabbro (unit 4) is petrologically similar to the Lynn Lake gabbro, which is dated at 1871.3 ±2.4 Ma by Turek et al. (2000) and hosts the past producing Ni-Cu mine (22.2 Mt of ore grading 1.0% Ni and 0.5% Cu).

Granitoid rocks (subunit 5a)

Granitoid plutons of the pre-Sickle intrusive suite (unit 5) are exposed in northern and southern parts of the map area (Figure GS2017-11-2), and include a variety of rock types, such as diorite, quartz diorite, tonalite, granodiorite, granite and associated pegmatitic and aplitic dikes, with minor gabbro. A tonalite sample of this suite at Norrie Lake was dated at 1876 +8/–6 Ma by Baldwin et al. (1987) using zircon U-Pb geochronology. These intrusive rocks (Table GS2017-11-1) are divided into two subunits based on the field relations and rock types: tonalite, granodiorite and granite and associated pegmatitic and aplitic rocks (subunit 5a); and diorite, quartz diorite and minor gabbroic rocks (subunit 5b).

Subunit 5a granitoid rocks comprise tonalite, granodiorite and granite, and minor related pegmatitic and aplitic dikes. Granodiorite is the dominant phase of the Cockeram Lake pluton and intrudes subunits 2c and 2d (Figure GS2017-11-6b). The granodiorite is medium to coarse grained, massive, equigranular to locally porphyritic, and is weakly to moderately foliated. It weathers greyish pink to light beige and consists of 20–30% anhedral quartz, 25–35% subhedral plagioclase laths, 20–25% K-feldspar, 5–10% biotite (±hornblende) and accessory iron-oxide minerals. This mineral assemblage is consistent with I-type granite of Chappell and White (1974) or the magnetite-series granite of Ishihara (1981). Minor granite of subunit 5a is differentiated from granodiorite by slightly higher K-feldspar and quartz content than the granodiorite. In places, medium- to coarse-grained granite dikes intrude unit 1 and are folded and foliated (Figure GS2017-11-6c). This granite is likely formed by differentiation of the same parent magma(s) and thus is considered part of the I-type and magnetite-series granites.

In the southern part of the map area, the supracrustal rocks of units 1 to 3 are cut by granitoid rocks ranging from tonalite to granodiorite to granite. The tonalite is fine to medium grained, grey to light grey, equigranular, moderately foliated and locally porphyritic. Its mineralogy consists of 15–25% quartz, 50–60% plagioclase, 15–20% amphibole and minor biotite, and is also characterized by chlorite and sericite alteration. At the contact zone, scattered disseminated pyrite is evident in the tonalite.

Pegmatite and/or aplite of unit 5a are more commonly associated with granite and granodiorite than with tonalite. They occur as dikes that are a few centimetres to a few metres wide and consist of quartz, feldspar and minor biotite (±muscovite).

Diorite, quartz diorite and minor gabbroic rocks (subunit 5b)

Diorite and quartz diorite (subunit 6b) mostly occur as marginal phases of the Cockeram Lake pluton in the northern part, and as a small stock exposed in the central part of the map area. Quartz diorite is medium to dark grey on weathered and fresh surfaces, fine to medium grained, massive, equigranular and moderately to strongly foliated. Locally, the quartz diorite is porphyritic, containing plagioclase phenocrysts up to 1 cm in a fine- to medium-grained groundmass (Figure GS2017-11-6d). It consists of 5–10% anhedral quartz, 50-60% plagioclase laths with diffuse grain boundaries, 20–30% hornblende and minor biotite. Contacts between quartz diorite, diorite, granodiorite and granite are not observed in the Wasekwan Lake area, but many outcrops in the northern belt show that similar quartz diorite (and diorite) is cut by granodiorite (Yang and Beaumont-Smith, 2015c).

Minor gabbroic dikes cutting the quartz diorite are assigned to subunit 6b, similar to those observed in the Farley Lake area in the northern belt of the LLGB (Yang and Beaumont-Smith, 2016a).

Post-Sickle intrusive suite (unit 6)

Post-Sickle intrusive rocks of unit 6 occur as an elongated stock exposed mainly in the central portion of the map area (Figure GS2017-11-2). This unit comprises two subunits (Table GS2017-11-1): granodiorite (subunit 6a) and granite (subunit 6b), defined by a domain of muted magnetic response in detailed airborne magnetic data. Granitic rocks at the contact zone consist of dikes and veins to veinlets cutting unit 2 basalt (Figure GS2017-11-6e), although the dikes do not display notable deformation. The unit 6 granitoid intrusion cuts the Cockeram Lake gabbro (unit 4) in the northern part of map area (Figure GS2017-11-2). Subunit 6a returned an age determined at 1855.6 ±8.3 Ma (Beaumont-Smith, unpublished data, 2006)

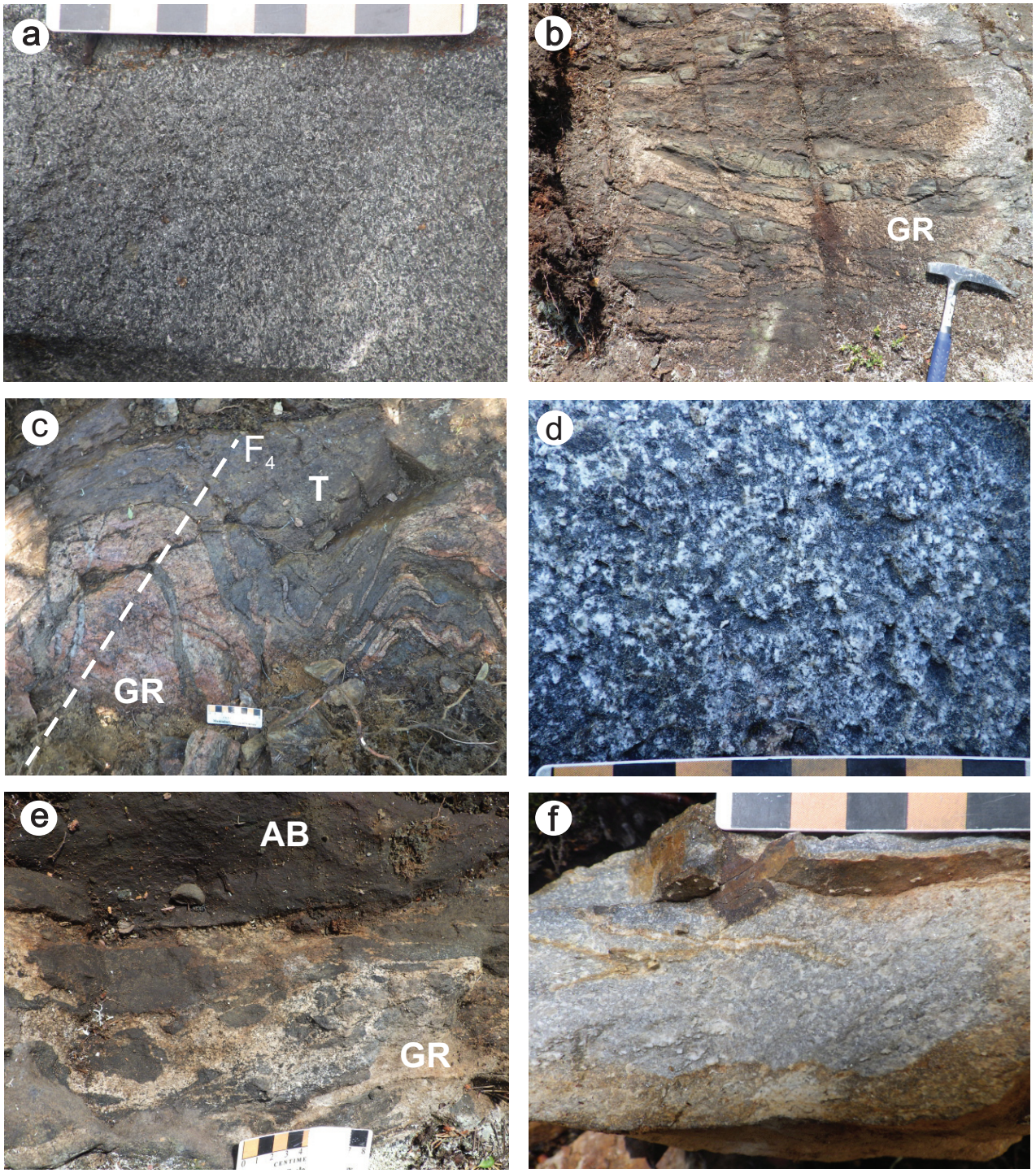

Figure GS2017-11-6: *Outcrop photographs of map units 4, 5, 6 and 7 on PMAP2017-3 (Yang and Beaumont-Smith, 2017) in the Wasekwan Lake area:* ***a)*** *weakly foliated, massive, medium-grained, equigranular gabbro (unit 4; UTM Zone 14N, 387901E, 6296217N, NAD 83);* ***b)*** *dikes of medium grained, porphyritic to equigranular granodiorite (subunit 5a) intruding basalt of unit 2c at the contact zone (UTM 380752E, 6294014N);* ***c)*** *medium- to coarse-grained granite dikes cutting unit 1 intermediate tuff and folded by* F_4 *fold that plunges 045º/57º (subunit 5a; UTM 380238E, 6291506N);* ***d)*** *porphyritic quartz diorite with plagioclase phenocrysts up to 1 cm in a fine- to medium-grained groundmass (subunit 5b; UTM 379465E, 6294010N);* ***e)*** *medium-grained granodiorite (unit 6a) as veins and veinlets cutting strongly foliated basalt (subunit 2c; UTM 384451E, 6292943N);* ***f)*** *quartz-feldspar porphyry dike ~2 m wide, containing fine-grained pyrite disseminations, cutting unit 3 quartz feldspathic greywacke and unit 2 mafic volcanic rocks (subunit 7; UTM 383547E, 6291899N). Abbreviations: AB, aphanitic basalt; GR, granodiorite; T, mafic tuff.*

by zircon U-Pb geochronology, which is within analytical uncertainties of the Burge Lake pluton (1857±2 Ma; see Beaumont-Smith et al., 2006) in the northern belt. It is noted that the granodiorite and granite in the current map area correspond with magnetic lows, which is characteristic of reduced I-type and ilmenite-series granites (see Chappell and White, 1974; Ishihara, 1981) that may be associated with intrusion-related Au mineralization as reported elsewhere (e.g., Thorne et al., 2008; Yang et al., 2008).

The granodiorite of subunit 6b is pinkish on fresh surfaces and weathers beige to tan, is medium to coarse grained, foliated and equigranular to locally porphyritic. This granodiorite consists of 5–8% hornblende (partly altered to biotite), 3-5% discrete biotite flakes, 25–30% quartz, 30–40% plagioclase and 25–30% K-feldspar.

Late intrusive suite (unit 7)

Unit 7 quartz-feldspar porphyry, pegmatite and/or aplite occur mostly as dikes in the southwestern and central portions of the map area (Figure GS2017-11-2). These dikes tend to be isolated, relatively lesser deformed and are not able to trace back to any plutons nearby on the surface. Their association with the pre- and post-Sickle intrusive suites (unit 5 and unit 6, respectively) is unknown. At the Central Manitoba Au occurrence, a quartz-feldspar porphyry dike, 2–3 m in thickness, cutting unit 3 greywacke and unit 2 mafic volcanic rocks contains pyrite (±arsenopyrite?; Figure GS2017-11-6f). The age of the dike was determined at 1814 ±15 Ma by zircon U-Pb geochronology (Jones, 2005; C.J. Beaumont-Smith, unpublished data, 2006), revealing that it is much younger than the granitic rocks from unit 5 pre-Sickle and unit 6 post-Sickle intrusive suites.

Unit 7 pegmatite and aplite commonly have muscovite (±tourmaline) in addition to biotite; this indicates that they are less likely to be related to I-type or magnetite-series granitoid rocks of both the pre-Sickle and post-Sickle intrusive suites, both of which typically lack muscovite.

Tectonite (unit 8)

Tectonite of unit 8 comprises mylonitic mafic to felsic rocks within the JSZ (Figure GS2017-11-2) characterized by intense transposition and the development of S_2 tectonic fabric. The protoliths of such high-strain rocks are difficult to determine in the field, although feldspar and quartz relicts may be partly preserved in felsic tectonite. Mafic tectonite derived from lava flows and/or volcaniclastic rocks are indistinguishable, in particular, those that are altered to very fine grained chlorite and sericite. In some cases, the tectonite shows evidence of multiple deformation events (Figure GS2017-11-7a). Quartz-carbonate (±pyrite) veins or veinlets occur in tectonite, and are primarily concentrated along the S_2 foliation.

Structural geology

Structural geology has been extensively investigated at both regional and deposit scales in the LLGB (Gilbert et al., 1980; Gilbert, 1993; Peck et al., 1998; Beaumont-Smith and Rogge, 1999; Beaumont-Smith and Edwards, 2000; Beaumont-Smith et al., 2000; Ma et al., 2000; Anderson and Beaumont-Smith, 2001; Ma and Beaumont-Smith, 2001; Beaumont-Smith et al., 2001; Park et al., 2002; Beaumont-Smith and Böhm, 2002, 2003, 2004; Jones, 2005; Jones et al., 2006; Yang and Beaumont-Smith, 2015a, 2016a). Beaumont-Smith and Böhm (2002, 2004) defined as many as six deformation events (D_1 to D_6) in the LLGB. Although not all deformation fabrics are observed in the Wasekwan Lake area, this report follows the terms used by Beaumont-Smith and Böhm (2002, 2004) to describe the characteristics of the D_1 to D_6 structures. The D_1 deformation is interpreted to be related to the assembly of volcanic terranes comprising the LLGB, but these fabrics and structures are mostly obscured by later deformation.

In the Wasekwan Lake area, D_2 structures are the most penetrative and manifest as a steeply north-dipping S_2 foliation and tight to isoclinal folds (F_2) that have shallowly plunging hinges and associated minor chevron folds. Ductile shear zones that generally define unit contacts are thought to be related to D_2 deformation, as the intensity of S_2 fabrics and tightness of F_2 folds increase toward contacts. The D_2 shear zones are characterized by dextral shear-sense indicators on horizontal surfaces and steeply plunging, generally down-dip to slightly oblique (easterly pitch) stretching lineations. The structural geometry of the Wasekwan Lake area is characterized by shallowly plunging F_2 fold axes, which steepen to subvertical within D_2 shear zones.

The JSZ, a regional east–west trending shear zone, transects the southern part of the map area (Figure GS2017-11-2) and can be traced over 100 km along strike. The JSZ is a protracted and dominantly dextral transpressional fault zone (Beaumont-Smith and Rogge, 1999; Jones, 2005; Jones et al., 2006). Numerous dextral shear sense indicators are observed on the horizontal surface within the JSZ. The development of narrow zones of shallowly plunging stretching lineations in the core of the shear zone reflects kinematics consistent with shear-zone development in response to dextral transpression.

The fabrics of D_3 deformation are represented by close to tight, S-asymmetric F_3 folds and northwest-trending, axial-planar S_3 crenulation cleavages in the map area (Figure GS2017-11-7b). Also, F_4 folds are pervasive throughout the map area. These folds plunge steeply to the northeast and are associated with steeply dipping, northeast-striking, axial-planar S_4 crenulation cleavages. Mesoscopic structures associated with D_5 deformation include open F_5 conjugate folds, kink bands and crenulations, and a brittle D_5 fault (Figure GS2017-11-7c). The post-mineralization 'T1 fault' at the BT mine open pit (Peck et al., 1998; Figure GS2017-11-2) is most likely a D_5 structure.

The D_6 deformation was brittle to ductile, represented by sinistral reactivation of D_2 shear zones (Beaumont-Smith and Böhm, 2004). In places, retrograde actinolite crystals up to 1.5 cm (Figure GS2017-11-7d) are randomly oriented on the planes of associated planar structures (cleavages, fractures).

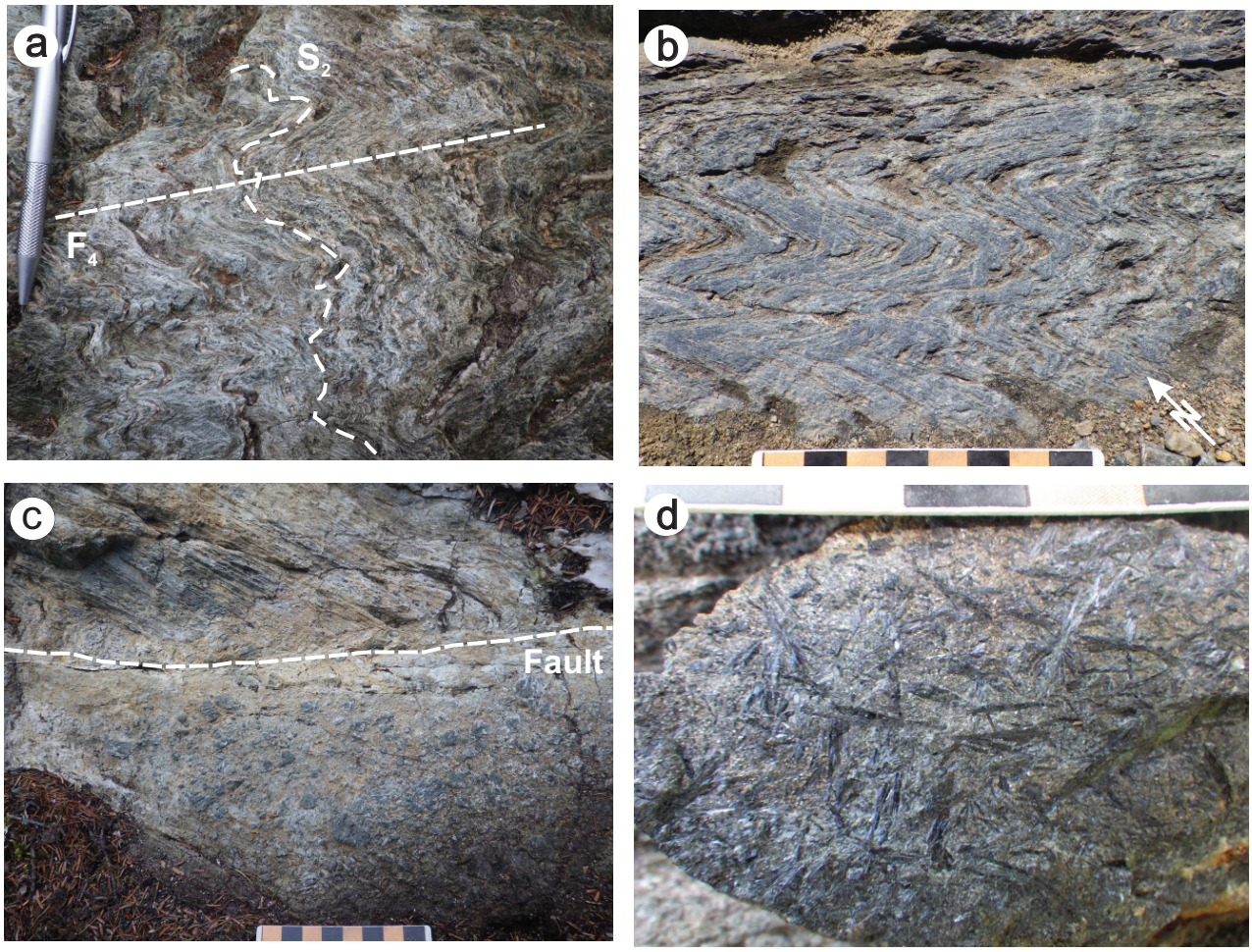

Figure GS2017-11-7*: Outcrop photographs of map unit 7 tectonite, structural features and retrograde metamorphic rocks on PMAP2017-3 (Yang and Beaumont-Smith, 2017) in the Wasekwan Lake area:* ***a)*** *mafic tectonite showing S_2 foliation and associated quartz veins folded by F_4 folds (UTM Zone 14N, 383945E, 6291623N, NAD 83);* ***b)*** *F_3 fold vertically plunging to the northwest within the Johnson shear zone (UTM 385018E; 6291878N);* ***c)*** *drag-folding along hangingwall contact of a brittle fault (215º/35º), which is related to D_5 deformation and cuts unit 1a felsic volcanic rock and actinolite alteration, suggests reverse movement (UTM 380159N, 6291960N);* ***d)*** *randomly oriented acicular actinolite crystals related to retrograde metamorphism (UTM 381326E, 6292353N).*

Economic considerations

The presence of significant Au mineralization at the BT deposit and Linkwood property along or adjacent to the JSZ demonstrates the economic potential of this long-lived structure in the Wasekwan Lake area. The BT open-pit operation produced 2457 kg (79 000 oz.) of Au from 1993 to 1996 (Richardson et al., 1996; Jones et al., 2006). Puritch et al. (2012) estimated that remaining mineral resources at the BT deposit are 1.021 Mt grading 1.4 g/t Au (45 000 oz. in the indicated category) and 2.344 Mt grading 1.04 g/t Au (78 500 oz. in the inferred category). Noteworthy is the Linkwood Au property, located approximately 3.5 km west-northwest of the BT mine, which also contains a significant mineral resource, with 30.84 Mt grading 1.16 g/t Au in both indicated and inferred categories (~820 000 oz. Au; see Puritch et al., 2013). Old trenches expose part of the Central Au occurrence, 1 km west of the BT mine, where Au is hosted in a quartz-feldspar porphyry. A surface grab sample returned 4.5 g/t Au (Bateman, 1945; Ferreira and Baldwin, 1997), whereas two feldspar porphyry samples yielded 1.45 and 3.15 g/t Au, respectively (Jones et al., 2006).

New mapping suggests that rheological differences between volcaniclastic rocks (unit 1), Fe-rich mafic volcanic rocks (unit 2) and sedimentary rocks (unit 3) acted as foci for ductile strain during multiple phases of deformation along the JSZ (and associated subsidiary D_2 structures), focusing Au-bearing fluids into structural and chemical traps. Potential structural traps include areas where D_2 shear zones and D_3 and D_4 fabrics intersect as these may locally form dilatant zones. The sources of auriferous fluids are the subject of ongoing collaborative research between the Manitoba Geological Survey and the Geological Survey of Canada.

Jones et al. (2006) noted that Au-bearing quartz-sulphide veins are hosted in granitoid intrusions and dikes that are rheologically more competent than the surrounding mafic volcanic and volcaniclastic rocks. Gold-bearing (pyrite+galena) quartz veins also cut deformed quartz-feldspar porphyry at the

Bonanza deposit approximately 12 km east of the BT deposit (Peck, 1985; Jones et al., 2006; Figure GS2017-11-1). Ten kilometres east of the BT deposit, the Esker Au showing consists of pyrite- and chalcopyrite-bearing quartz veins cutting variably foliated granodiorite (Jones et al., 2006; Figure GS2017-11-1). Interestingly, Jones et al. (2006) point out that high-grade mineralized zones (up to 120 g/t Au) in the BT deposit are locally associated with folded and boudinaged quartz-pyrite veins hosted in carbonate- and sericite-altered feldspar porphyry dikes that cut the shear zone. Such observations suggest that quartz-pyrite vein systems hosted in granitic intrusions of the post-Sickle intrusive suite (unit 6) and late intrusive suite (unit 7) are potentially an important Au-exploration target in the region.

The unit 4 gabbro intrusions are saturated with sulphides (e.g., Cockeram Lake intrusion), and are petrologically similar to the Lynn Lake gabbro intrusion that hosts the Lynn Lake Ni-Cu-Co deposit, which suggests that these intrusions may also have potential for magmatic Ni-Cu-Co (±PGE). In addition, relatively oxidized I-type granitoid intrusions of unit 5 may have potential for porphyry Cu-Au (Mo) mineralization, but more work is required to look into the emplacement depth of these granitoid intrusions (e.g., Yang, 2017) and their petrogenetic types (e.g., Chappell and White, 1974; Ishihara, 1981) to fully assess their mineral potential.

Acknowledgments

The authors thank J. Watts for providing enthusiastic and capable field assistance, E. Anderson and N. Brandson for thorough logistical support. Thanks go to Carlisle Goldfields Ltd. and Alamos Gold Inc. for providing detailed airborne geophysical data and LiDAR (light detection and ranging) data. This study benefited from discussions with M. Rein (Alamos Gold Inc.), C. Lawley (Geological Survey of Canada) and S.D. Anderson in the field. Thanks go to P. Lenton and G. Keller for technical support; L. Chackowsky and B. Lenton for providing GIS data, digitizing map data and drafting figures; M. Pacey for assembling the digital database for a hand-held data acquisition system; and C. Epp for cataloguing, processing and preparing the samples. The manuscript benefited greatly from constructive reviews by K.D. Reid and S.D. Anderson, and from technical editing by M.-F. Dufour.

References

Anderson, S.D. and Beaumont-Smith, C.J. 2001: Structural analysis of the Pool Lake–Boiley Lake area, Lynn Lake greenstone belt (NTS 64C/11); *in* Report of Activities 2001, Manitoba Industry, Trade and Mines, Manitoba Geological Survey, p. 76–85.

Ansdell, K.M. 2005: Tectonic evolution of the Manitoba-Saskatchewan segment of the Paleoproterozoic Trans-Hudson Orogen, Canada; Canadian Journal of Earth Sciences, v. 42, p. 741–759.

Ansdell, K.M., Corrigan, D., Stern, R. and Maxeiner, R. 1999: SHRIMP U-Pb geochronology of complex zircons from Reindeer Lake, Saskatchewan: implications for timing of sedimentation and metamorphism in the northwestern Trans-Hudson Orogen; Geological Association of Canada–Mineralogical Association of Canada, Joint Annual Meeting, Program with Abstracts, v. 24, p. 3.

Baldwin, D.A., Syme, E.C., Zwanzig, H.V., Gordon, T.M., Hunt, P.A. and Stevens, R.P. 1987: U-Pb zircon ages from the Lynn Lake and Rusty Lake metavolcanic belts, Manitoba: two ages of Proterozoic magmatism; Canadian Journal of Earth Sciences, v. 24, p. 1053–1063.

Baragar, W.R.A., Ernst, R.E., Hulbert, L. and Peterson, T. 1996: Longitudinal petrochemical variation in the Mackenzie dyke swarm, northwestern Canadian Shield; Journal of Petrology, v. 37, p. 317–359.

Bateman, J.D. 1945: McVeigh Lake area, Manitoba; Geological Survey of Canada, Paper 45-14, 34 p.

Beaumont-Smith, C.J. 2008: Geochemistry data for the Lynn Lake greenstone belt, Manitoba (NTS 64C11-16); Manitoba Science, Technology, Energy and Mines, Manitoba Geological Survey, Open File OF2007-1, 5 p.

Beaumont-Smith, C.J. and Böhm, C.O. 2002: Structural analysis and geochronological studies in the Lynn Lake greenstone belt and its gold-bearing shear zones (NTS 64C10, 11, 12, 14, 15 and 16), Manitoba; *in* Report of Activities 2002, Manitoba Industry, Trade and Mines, Manitoba Geological Survey, p. 159–170.

Beaumont-Smith, C.J. and Böhm, C.O. 2003: Tectonic evolution and gold metallogeny of the Lynn Lake greenstone belt, Manitoba (NTS 64C10, 11, 12, 14, 15 and 16), Manitoba; *in* Report of Activities 2003, Manitoba Industry, Economic Development and Mines, Manitoba Geological Survey, p. 39–49.

Beaumont-Smith, C.J. and Böhm, C.O. 2004: Structural analysis of the Lynn Lake greenstone belt, Manitoba (NTS 64C10, 11, 12, 14, 15 and 16); *in* Report of Activities 2004, Manitoba Industry, Economic Development and Mines, Manitoba Geological Survey, p. 55–68.

Beaumont-Smith, C.J. and Edwards, C.D. 2000: Detailed structural analysis of the Johnson shear zone in the west Gemmell Lake area (NTS 64C/11); *in* Report of Activities 2000, Manitoba Industry, Trade and Mines, Manitoba Geological Survey, p. 64–67.

Beaumont-Smith, C.J. and Rogge, D.M. 1999: Preliminary structural analysis and gold metallogeny of the Johnson shear zone, Lynn Lake greenstone belt (parts of NTS 64C/10, 11, 15); *in* Report of Activities 1999, Manitoba Energy and Mines, Geological Services, p. 61–66.

Beaumont-Smith, C.J., Anderson, S.D. and Böhm, C.O. 2001: Structural analysis and investigations of shear-hosted gold mineralization in the southern Lynn Lake greenstone belt (parts of NTS 64C/11, /12, /15, /16); *in* Report of Activities 2001, Manitoba Industry, Trade and Mines, Manitoba Geological Survey, p. 67–75.

Beaumont-Smith, C.J., Lentz, D.R. and Tweed, E.A. 2000: Structural analysis and gold metallogeny of the Farley Lake gold deposit, Lynn Lake greenstone belt (NTS 64C/16); *in* Report of Activities 2000, Manitoba Industry, Trade and Mines, Manitoba Geological Survey, p. 73–81.

Beaumont-Smith, C.J., Machado, N. and Peck, D.C. 2006: New uranium-lead geochronology results from the Lynn Lake greenstone belt, Manitoba (NTS 64C11-16); Manitoba Science, Technology, Energy and Mines, Manitoba Geological Survey, Geoscientific Paper GP2006-1, 11 p.

Chappell, B.W. and White, A.J.R. 1974: Two contrasting granite types; Pacific Geology, v. 8, p. 173–174.

Corrigan, D., Galley, A.G. and Pehrsson, S. 2007: Tectonic evolution and metallogeny of the southwestern Trans-Hudson Orogen; *in* Mineral Deposits of Canada: A Synthesis of Major Deposit-Types, District Metallogeny, the Evolution of Geological Provinces, and Exploration Methods, W.D. Goodfellow (ed.), Geological Association of Canada, Mineral Deposits Division, Special Publication 5, p. 881–902.

Corrigan, D., Pehrsson, S., Wodicka, N. and de Kemp, E. 2009: The Palaeoproterozoic Trans-Hudson Orogen: a prototype of modern accretionary processes; *in* Ancient Orogens and Modern Analogues, J.B. Murphy, J.D. Keppie, and A.J. Hynes (ed.), Geological Society of London, Special Publications, v. 327, p. 457–479.

Fedikow, M.A.F. 1986: Geology of the Agassiz stratabound Au-Ag deposit, Lynn Lake, Manitoba; Manitoba Energy and Mines, Geological Services, Open File Report OF85-5, 80 p.

Fedikow, M.A.F. 1992: Rock geochemical alteration studies at the MacLellan Au-Ag deposit, Lynn Lake, Manitoba; Manitoba Energy and Mines, Geological Services, Economic Geology Report ER92-1, 237 p.

Fedikow, M.A.F. and Gale, G.H. 1982: Mineral deposit studies in the Lynn Lake area; *in* Report of Field Activities 1982, Manitoba Department of Energy and Mines, Mineral Resources Division, p. 44–54.

Ferreira, K.J. and Baldwin, D.A. 1997: Mineral deposits and occurrences in the Cockeram Lake area, NTS 64C/15; Manitoba Energy and Mines, Geological Services, Mineral Deposit Series Report No. 8, 154 p.

Gilbert, H.P. 1993: Geology of the Barrington Lake–Melvin Lake–Fraser Lake area; Manitoba Energy and Mines, Geological Services, Geological Report GR87-3, 97 p.

Gilbert, H.P., Syme, E.C. and Zwanzig, H.V. 1980: Geology of the metavolcanic and volcaniclastic metasedimentary rocks in the Lynn Lake area; Manitoba Energy and Mines, Mineral Resources Division, Geological Paper GP80-1, 118 p.

Hoffman, P.H. 1988: United plates of America, the birth of a craton: Early Proterozoic assembly and growth of Laurentia; Annual Reviews of Earth and Planetary Sciences, v. 16, p. 543–603.

Ishihara, S. 1981: The granitoid series and mineralization; Economic Geology, 75th Anniversary Volume, p. 458–484.

Jones, L.R. 2005: Geology of the shear-hosted Burnt Timber deposit, Lynn, northern Manitoba; M.Sc. thesis, Laurentian University, Sudbury, Ontario, 63 p.

Jones, L.R., Lafrance, B. and Beaumont-Smith, C.J. 2006: Structural controls on gold mineralization at the Burnt Timber Mine, Lynn Lake Greenstone Belt, Trans-Hudson Orogen, Manitoba; Exploration and Mining Geology, v. 15, p. 89–100.

Jurkowski, J.S. 1999: Uranium-lead geochronology study of Lynn Lake greenstone belt, Manitoba; M.Sc. thesis, University of Windsor, Windsor, Ontario, 95 p.

Lewry, J.F. and Collerson, K.D. 1990: The Trans-Hudson Orogen: extent, subdivisions and problems; *in* The Early Proterozoic Trans-Hudson Orogen of North America, J.F. Lewry and M.R. Stauffer (ed.), Geological Association of Canada, Special Paper 37, p. 1–14.

Ma, G. and Beaumont-Smith, C.J. 2001: Stratigraphic and structural mapping of the Agassiz Metallotect near Lynn Lake, Lynn Lake greenstone belt (parts of NTS 64C/14, /15); *in* Report of Activities 2001, Manitoba Industry, Trade and Mines, Manitoba Geological Survey, p. 86–93.

Ma, G., Beaumont-Smith, C.J. and Lentz, D.R. 2000: Preliminary structural analysis of the Agassiz Metallotect near the MacLellan and Dot lake gold deposits, Lynn Lake greenstone belt (parts of NTS 64C/14, /15); *in* Report of Activities 2000, Manitoba Industry, Trade and Mines, Manitoba Geological Survey, p. 51–56.

Manitoba Energy and Mines 1986: Granville Lake, NTS 64C; Manitoba Energy and Mines, Minerals Division, Bedrock Geology Compilation Map Series, Map 64C, scale 1:250 000.

Milligan, G.C. 1960: Geology of the Lynn Lake district; Manitoba Department of Mines and Natural Resources, Mines Branch, Publication 57-1, 317 p.

Norman, G.W.H. 1933: Granville Lake district, northern Manitoba; Geological Survey of Canada, Summary Report, Part C, p. 23–41.

Park, A.F., Beaumont-Smith, C.J. and Lentz, D.R. 2002: Structure and stratigraphy in the Agassiz Metallotect, Lynn Lake greenstone belt (NTS 64C/14 and /15), Manitoba; *in* Report of Activities 2002, Manitoba Industry, Trade and Mines, Manitoba Geological Survey, p. 171–186.

Peck, D.C., 1985, Geological investigations at Cartwright Lake, Manitoba: Manitoba Energy and Mines, Geological Services, *in* Report of Field Activities 1985, p. 37–40.

Peck, D.C. and Smith, T.E, 1989: The geology and geochemistry of an Early Proterozoic volcanic-arc association at Cartwright Lake: Lynn Lake greenstone belt, northwestern Manitoba; Canadian Journal of Earth Sciences, v. 26, p. 716–736.

Peck, D.C., Lin, S., Atkin, K. and Eastwood, A.M. 1998: Reconnaissance structural studies of Au metallotects in the Lynn Lake greenstone belt (parts of NTS 63C/10, C/11, C/15); *in* Report of Activities 1998, Manitoba Energy and Mines, Geological Services, p. 69–74.

Pinsent, R.H. 1980: Nickel-copper mineralization in the Lynn Lake gabbro; Manitoba Energy and Mines, Geological Services, Economic Geology Report ER79-3, 138 p.

Puritch, E., Burga, D. and Wu, Y. 2012: Technical report and resource estimate on the Burnt Timber property, Lynn Lake, Northern Manitoba, Canada; NI-43-101 & 43-101F1, P & E Mining Consultants Inc., Technical Report No. 248, 96 p.

Puritch, E., Burga, D. and Wu, Y. 2013: Technical report and resource estimate on the Linkwood property, Lynn Lake, Northern Manitoba, Canada; NI-43-101 & 43-101F1, P & E Mining Consultants Inc., Technical Report No. 252, 80 p.

Richardson, D.J., Ostry, G., Weber, W. and Fogwill, W.D. 1996: Gold deposits of Manitoba; Manitoba Energy and Mines, Economic Geology Report ER86-1 (2nd Edition), 114 p.

Stauffer, M.R. 1984: Manikewan: an Early Proterozoic ocean in central Canada, its igneous history and orogenic closure; Precambrian Research, v. 25, p. 257–281.

Stern, R.A., Syme, E.C. and Lucas, S.B. 1995: Geochemistry of 1.9 Ga MORB- and OIB-like basalts from the Amisk collage, Flin Flon Belt, Canada: evidence for an intra-oceanic origin; Geochimica et Cosmochimica Acta, v. 59, p. 3131–3154.

Syme, E.C. 1985: Geochemistry of metavolcanic rocks in the Lynn Lake Belt; Manitoba Energy and Mines, Geological Services/Mines Branch, Geological Report GR84-1, 84 p.

Thorne, K.G., Lentz, D.R., Hoy, D., Fyffe, L.R. and Cabri, L.J. 2008: Characteristics of mineralization at the Main Zone of the Clarence Stream Gold Deposit, southwestern New Brunswick, Canada: evidence for an intrusion-related gold system in the northern Appalachian Orogen; Exploration and Mining Geology, v. 17, p. 13–49.

Turek, A., Woodhead, J. and Zwanzig H.V. 2000: U-Pb age of the gabbro and other plutons at Lynn Lake (part of NTS 64C); *in* Report of Activities 2000, Manitoba Industry, Trade and Mines, Manitoba Geological Survey, p. 97–104.

Yang, X.M. 2017: Estimation of crystallization pressure of granite intrusions; Lithos, v. 286–287, p. 324–329.

Yang, X.M. and Beaumont-Smith, C.J. 2015a: Geological investigations of the Keewatin River area, Lynn Lake greenstone belt, northwestern Manitoba (parts of NTS 64C14, 15); *in* Report of Activities 2015, Manitoba Mineral Resources, Manitoba Geological Survey, p. 52–67.

Yang, X.M. and Beaumont-Smith, C.J. 2015b: Bedrock geology of the Keewatin River area, Lynn Lake greenstone belt, northwestern Manitoba (parts of NTS 64C14, 15); Manitoba Mineral Resources, Manitoba Geological Survey, Preliminary Map PMAP2015-3, scale 1:20 000.

Yang, X.M. and Beaumont-Smith, C.J. 2015c: Granitoid rocks in the Lynn Lake region, northwestern Manitoba: preliminary results of reconnaissance mapping and sampling; *in* Report of Activities 2015, Manitoba Mineral Resources, Manitoba Geological Survey, p. 68–78.

Yang, X.M. and Beaumont-Smith, C.J. 2016a: Geological investigations in the Farley Lake area, Lynn Lake greenstone belt, northwestern Manitoba (part of NTS 64C16); *in* Report of Activities 2016, Manitoba Growth, Enterprise and Trade, Manitoba Geological Survey, p. 99-114.

Yang, X.M. and Beaumont-Smith, C.J. 2016b: Bedrock geology of the Farley Lake area, Lynn Lake greenstone belt, northwestern Manitoba (part of NTS 64C16); Manitoba Growth, Enterprise and Trade, Manitoba Geological Survey, Preliminary Map PMAP2016-5, scale 1:20 000.

Yang, X.M. and Beaumont-Smith, C.J. 2017: Bedrock geology of the Wasekwan Lake area, Lynn Lake greenstone belt, northwestern Manitoba (parts of NTS 64C10, 15); Manitoba Growth, Enterprise and Trade, Manitoba Geological Survey, Preliminary Map PMAP2017-3, scale 1:20 000.

Yang, X.M., Lentz, D.R., Chi, G. and Thorne, K.G. 2008: Geochemical characteristics of gold-related granitoids in southwestern New Brunswick, Canada; Lithos, v. 104, p. 355–377.

Zwanzig, H.V. 2000: Geochemistry and tectonic framework of the Kisseynew Domain–Lynn Lake belt boundary (part of NTS 63P/13); *in* Report of Activities 2000, Manitoba Industry, Trade and Mines, Manitoba Geological Survey, p. 91–96.

Zwanzig, H.V., Syme, E.C. and Gilbert, H.P. 1999: Updated trace element geochemistry of ca. 1.9 Ga metavolcanic rocks in the Paleoproterozoic Lynn Lake belt; Manitoba Industry, Trade and Mines, Geological Services, Open File Report OF99-13, 46 p.

GS2017-12

Update on Paleozoic stratigraphic correlations in the Hudson Bay Lowland, northeastern Manitoba and northern Ontario

by M.P.B. Nicolas and D.K. Armstrong[1]

[1] Earth Resources and Geoscience Mapping Section, Ontario Geological Survey, Sudbury, ON P3E 6B5

In Brief:

- Long distance onshore correlations in the Hudson Bay Basin inform petroleum and mineral exploration and land-use planning
- Stratigraphic correlations of Devonian and Silurian strata are challenging, but resolvable using stable isotopes

Citation:
Nicolas, M.P.B. and Armstrong, D.K. 2017: Update on Paleozoic stratigraphic correlations in the Hudson Bay Lowland, northeastern Manitoba and northern Ontario; *in* Report of Activities 2017, Manitoba Growth, Enterprise and Trade, Manitoba Geological Survey, p. 133–147.

Summary

This work summarizes the continued collaborations between the Manitoba Geological Survey and the Ontario Geological Survey as part of the Hudson-Ungava Project of the Geo-mapping for Energy and Minerals program, Phase 2 (GEM-2; 2013–2020). The objective of this project is to advance the understanding of the sedimentological and stratigraphic framework of the onshore component of the Hudson Bay Basin to support mineral exploration and land-use planning in this underexplored frontier region.

The stratigraphic correlations for the Paleozoic sequence in northeastern Manitoba and northern Ontario have been resolved using a combination of lithostratigraphy, biostratigraphy and chemostratigraphy. This report presents the correlations based on the lithostratigraphic and chemostratigraphic findings in the Silurian and Devonian formations of the onshore extent of the Hudson Bay Basin.

Introduction

The Manitoba Geological Survey (MGS) is a partner in the Geological Survey of Canada's (GSC) Geo-mapping for Energy and Minerals 2 (GEM-2) program, which runs from 2013 to 2020. The MGS is participating in the Hudson-Ungava project (Nicolas et al., 2014), which includes multijurisdictional partners, including Ontario Geological Survey (OGS), Canada–Nunavut Geoscience Office, Laurentian University and University of Manitoba. In Manitoba, the purpose of the project is to enhance the understanding of the stratigraphic and sedimentological framework and structural complexities of the onshore component of the Hudson Bay Basin (HBB) in the Hudson Bay Lowland (HBL) in northeastern Manitoba, and correlate them to the onshore sections in Ontario in order to build a seamless stratigraphic framework for the southern part of the Hudson Platform. The Hudson Platform includes the HBB in northeastern Manitoba and northern Ontario and the Moose River Basin (MRB) in northeastern Ontario. This information will then be integrated with offshore and northern models for the basin to create a basin-wide sedimentological framework, which will form the basis for petroleum potential assessments, exploration in the basin and land-use planning in the region.

A number of cores have been drilled through the onshore Paleozoic sequence of the HBB in northeastern Manitoba and northern Ontario (Figure GS2017-12-1; Nicolas and Lavoie, 2012; Armstrong et al., 2013a). The thickest sections, up to approximately 1000 m, were intersected in two onshore wells, Sogepet Aquitaine Kaskattama Prov. No. 1 (Kaskattama; Oil and gas licence number 2168, Manitoba Growth, Enterprise and Trade, Winnipeg) and Aquitaine Sogepet et al. Pen No. 1 (Pen No. 1; Oil and gas licence number T002784, Ontario Ministry of Natural Resources and Forestry, Peterborough), located in the HBL of northeastern Manitoba and northern Ontario, respectively (Figure GS2017-12-1). These sections have been logged and sampled for biostratigraphy (Nicolas and Lavoie, 2012; Armstrong et al., 2013b) and stable-isotope chemostratigraphy as part of this project. Lithological logs and stable-isotope profiles for other cores in Manitoba, including Kaskattama, Houston Oils et al. Comeault Prov. No. 1 (Comeault; Oil and gas licence number 2337) and Merland et al. Whitebear Creek Prov. (Whitebear; Oil and gas licence number 2454) have been reported on by Nicolas (2016a, b). This report presents the stratigraphy, lithology and stable-isotope profile for the Foran Mining Kaskattama Kimberlite No. 1 (KK1; Assessment File 74223, Manitoba Growth, Enterprise and Trade, Winnipeg) core, and revised Devonian and Silurian stratigraphy for the Kaskattama, Comeault, Whitebear and Pen No. 1 wells. The analysis of the Selco Pennycutaway No. 1 (Pennycutaway; Assessment File 91728) core results were still under evaluation at the time of this writing. Regional correlations of Ordovician strata in the southern HBB are part of an ongoing related study (Hahn et al., 2016).

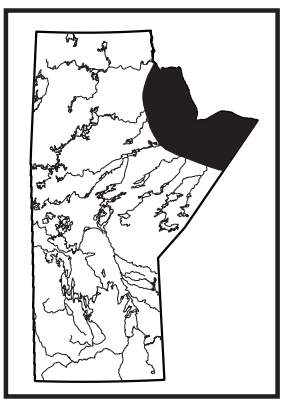

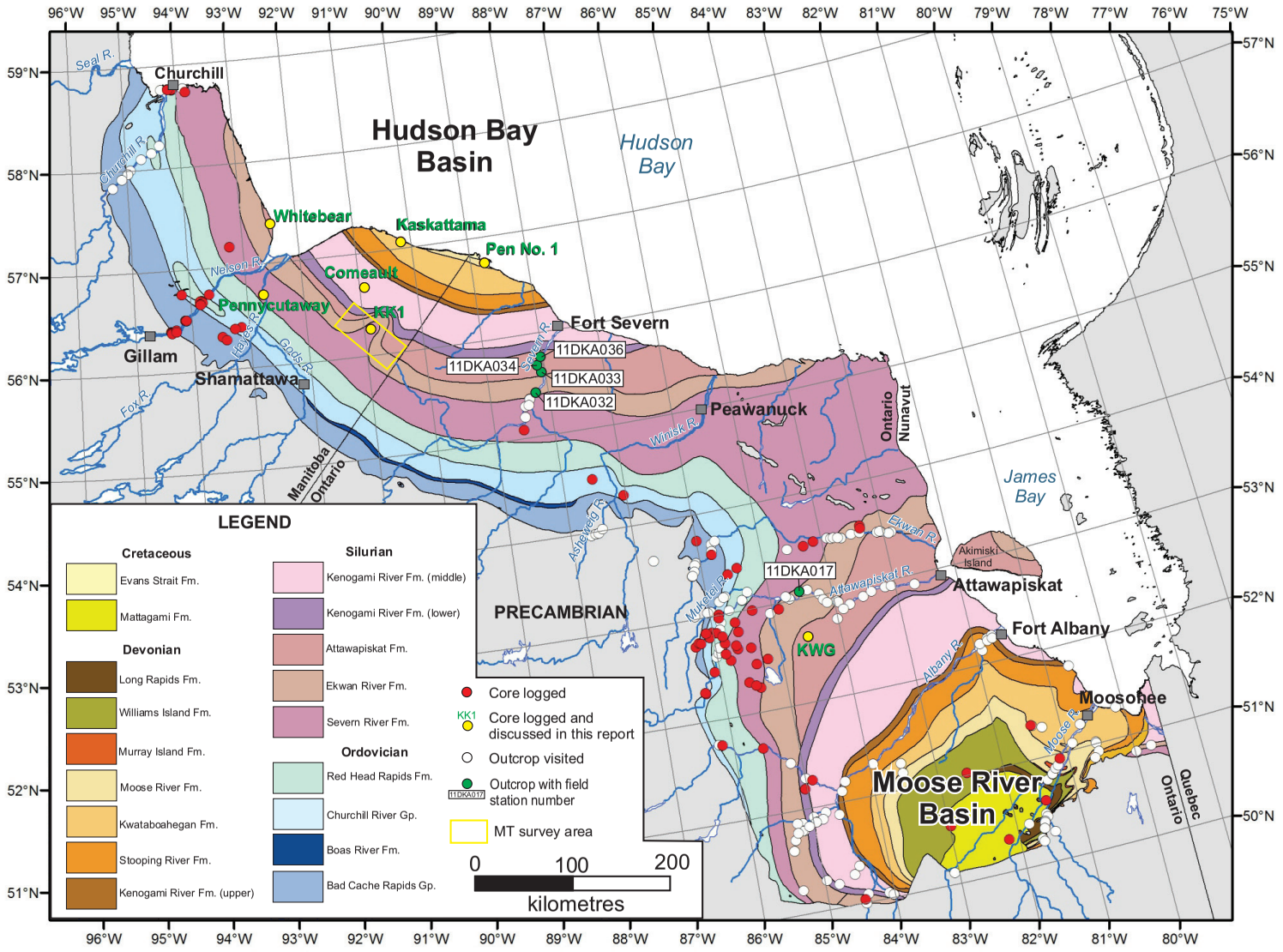

Figure GS2017-12-1: *Regional Phanerozoic geological map of the southern Hudson Platform showing locations of drillholes and outcrops studied for this project. Manitoba geology is modified from Nicolas et al. (2014); Ontario and Nunavut (Akimiski Island) geology is modified from Sanford and Grant (1998) and Ontario Geological Survey (2011). Abbreviations: Comeault, Houston Oils et al. Comeault Prov. No. 1; Kaskattama, Sogepet Aquitaine Kaskattama Prov. No. 1; KK1, Foran Mining Kaskattama Kimberlite No. 1; KWG, KWG-Spider Resources DR-94-19; MT, magnetotelluric; Pen No. 1, Aquitaine Sogepet et al. Pen No. 1; Pennycutaway, Selco Pennycutaway No. 1; Whitebear, Merland et al. Whitebear Creek Prov.*

Overview of Hudson Bay Basin onshore cores

The HBB Silurian and Devonian sections (Figure GS2017-12-2) in the HBL region have been a challenge to correlate confidently. The Pen No. 1 core in Ontario is continuous through the entire HBB section (217.32–1021.33 m vertical depth), beginning in the Devonian upper member of the Kenogami River Formation through to the Ordovician Bad Cache Rapids Group and Precambrian basement (Armstrong et al., 2013a) and is considered a good reference core for this region. The Kaskattama core intervals begin higher in the section, in the Devonian Kwataboahegan Formation, but have shorter telescoped core intervals rather than continuous core. Both the Pen No. 1 and Kaskattama wells have a small suite of downhole geophysical logs to assist in correlations and help fill in core gaps. In the Kaskattama well, gaps in core recovery or preservation have meant that many formational contacts have not been recovered, resulting in significant gaps in the interpretations. The Comeault core provides a complete view of the section starting in the Silurian lower member of the Kenogami River Formation; however, the upper ~60 m of this core has intermittent poor recovery. The Whitebear core has excellent continuous core recovery but provides only a part of the Silurian section.

Stable-isotope results

This past year, the last of the isotope results for the Manitoba cores were received from the multiwell sampling program conducted in 2014 (for sampling details see Nicolas et al., 2014). Nicolas (2016a, b) presented the data and a preliminary analysis of the first batch of $\delta^{13}C$ and $\delta^{18}O$ stable-isotope results. The latest batch of results covers the middle member of the Kenogami River Formation in the Kaskattama core; short interval samples from the entire KK1 and Pennycutaway cores; and outcrop samples collected in 2014 (Nicolas and Young, 2014) from along the Churchill River and along the coast near the town of Churchill. The new $\delta^{13}C$ and $\delta^{18}O$ stable-isotope results are presented in Nicolas (2017)[2].

[2] MGS Data Repository Item DRI2017002, containing the data or other information sources used to compile this report, is available online to download free of charge at http://www2.gov.mb.ca/itm-cat/web/freedownloads.html, or on request from minesinfo@gov.mb.ca or Mineral Resources Library, Manitoba Growth, Enterprise and Trade, 360–1395 Ellice Avenue, Winnipeg, Manitoba R3G 3P2, Canada.

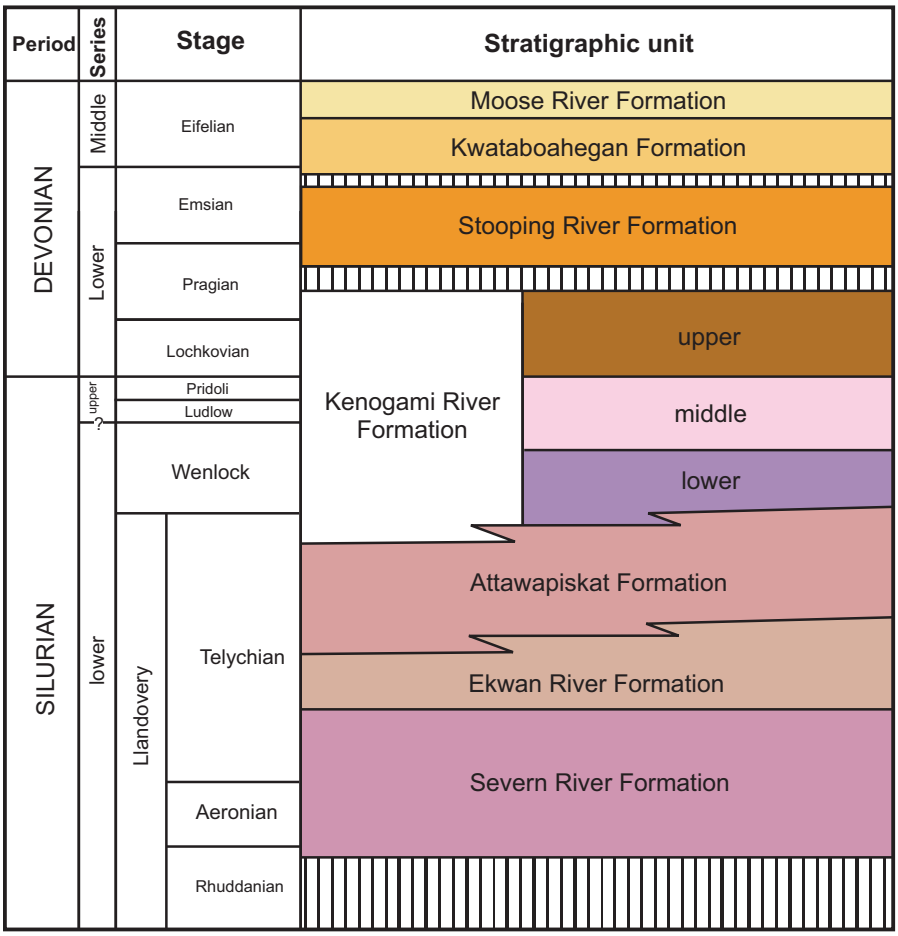

Figure GS2017-12-2: *Time-stratigraphic framework for the Silurian and Devonian succession in the Hudson Bay Basin in northeastern Manitoba and northern Ontario (excludes northeastern Ontario). Series and stages are from the International Commission on Stratigraphy (2017), but their relationships to the formations are based on Norford (1997) and Zhang and Barnes (2007) for the Silurian, and Sanford and Norris (1975) for the Devonian.*

The carbon and oxygen stable-isotope profiles for the Kaskattama core, including the new results for the middle member of the Kenogami River Formation are shown in Figure GS2017-12-3, along with the revised Silurian and Devonian stratigraphic tops (discussed later in this report). The Kaskattama core has intermittent core recovery through the middle member of the Kenogami River Formation, however, the overall trend of the $\delta^{13}C$ profile resembles that of Pen No. 1 (Figure GS2017-12-4), which has a more completely sampled section.

Kaskattama highland and KK1 core

The KK1 drillhole was drilled in 2006 by the Foran Mining Corporation near Bouchard Lake on the Kaskattama highland, northeast of the First Nation community of Shamattawa, northeastern Manitoba (Figure GS2017-12-1). Core was intermittently cut from 16.8 to 332.2 m (Figure GS2017-12-5) and the stratigraphic, lithological/sedimentological and stable-isotope profiles for the Paleozoic core of the KK1 are shown in Figure GS2017-12-5.

This drillhole encountered an unusually thick section of Quaternary sediments (mostly till), overlying a black shale followed by Paleozoic carbonate rocks. The age of the black shale is uncertain, with micropaleontological analyses indicating ages ranging from Cretaceous to Tertiary[3] and Quaternary (McCracken, 2014). The stratigraphic position, lithology and texture of the Kaskattama highland black shale closely resembles Cretaceous black shales in southwestern Manitoba, supporting a more probable age of Cretaceous. In addition to the unusual thickness of sediments overlying the Paleozoic, KK1 is missing a thick section of expected strata as compared to the Comeault core. Preliminary logging of KK1 (Nicolas et al., 2014) reported the Severn River Formation at the top of the Paleozoic bedrock section, rather than the expected (from previous geological maps) Attawapiskat and Ekwan River formations. Biostratigraphy results for KK1 confirmed a Silurian age and Severn River Formation assignment (McCracken, 2014), which is supported by comparing its chemostratigraphic profile to those of nearby cores. This may help in understanding the character and origin of the Kaskattama trough, which is interpreted to run through this area, based on work done by Hobson (1964) and Nelson and Johnson (1966).

A magnetotelluric (MT) ground geophysical survey was undertaken in July 2017 over the Kaskattama highland (Figure GS2017-12-1) as part of the GEM-2 program by J. Craven and B. Roberts from the GSC and I. Ferguson and N. Clark from the University of Manitoba to investigate this anomalous area (for more details see Craven et al., 2017). The MT survey will provide valuable information on the general bedrock composition and structure in the area of the Kaskattama trough. The results from the survey are pending.

Stratigraphic resolutions

Nicolas (2016a) presented the preliminary stratigraphic sections for the Kaskattama, Comeault and Whitebear drillcores along with their $\delta^{13}C$ and $\delta^{18}O$ stable-isotope profiles, and Nicolas and Lavoie (2012) presented the section for the KK1 drillcore. Armstrong et al. (2013b) presented the preliminary section for the Pen No. 1 well. The stable-isotope profiles for these wells were reviewed and compared. Where necessary, cores were re-examined to help resolve stratigraphic inconsistencies. The updated stratigraphic tops for select wells are shown in Table GS2017-12-1, and are displayed graphically in Figures GS2017-12-3 to -7, along with their lithological logs, $\delta^{13}C$ and $\delta^{18}O$ stable-isotope profiles, and spontaneous potential or gamma ray downhole geophysical log traces. These stratigraphic revisions replace those published in Nicolas (2011, 2016a) and Armstrong et al. (2013b). The stratigraphic assignments in the Whitebear and Comeault cores were changed significantly from Nicolas (2011, 2016a), and some adjustments were also made to formation top picks in the Kaskattama core. Revision of formational assignments and top picks was based on comparison of $\delta^{13}C$ and $\delta^{18}O$ stable-isotope profiles among all the cores and review of core descriptions and photographs.

Below is a detailed rationale for formational picks and correlations of the Silurian section in the onshore section of the HBB.

Attawapiskat Formation

The top of the Attawapiskat Formation was intersected in the Pen No. 1, Kaskattama and Comeault cores. The Pen No. 1 core has the best recovery of the Attawapiskat Formation, including the preservation of the upper and lower contacts, and a natural gamma-ray (GR) downhole log and therefore is considered the best reference log for this formation. Kaskattama has intermittent core recovery, but has a GR log, whereas Comeault has variable core recovery and only spontaneous potential (SP) and resistivity logs. All three cores have $\delta^{13}C$ isotope profiles (Figures GS2017-12-3, -4, -6), however, variable recovery through this interval in the Comeault and Kaskattama cores resulted in coarser isotopic profiles for these wells. Accurate formation top picks based on $\delta^{13}C$ may not be reliable, depending on sample frequency (which can in turn be affected by core recovery). Isotopic profiles can, however, corroborate other lines of evidence, such as lithological changes and geophysical responses.

The top of the Attawapiskat Formation in Pen No. 1 (Figure GS2017-12-4) is marked lithologically by a relatively rapid upward transition from porous, granular-looking, dolomitic limestone (including the “Nuia” grainstone reported by Suchy [1992] and Suchy and Stearn [1993]) to massive or laminated, variably argillaceous dolomudstones of the lower Kenogami River Formation. Lithologically, the contact can be picked at a

[3] ‘Tertiary’ is an historical term. The International Commission on Stratigraphy recommends using ‘Paleogene’ (comprising the Paleocene to Oligocene epochs) and ‘Neogene’ (comprising the Miocene and Pliocene epochs). The author used the term ‘Tertiary’ because it was used in the source material for this report.

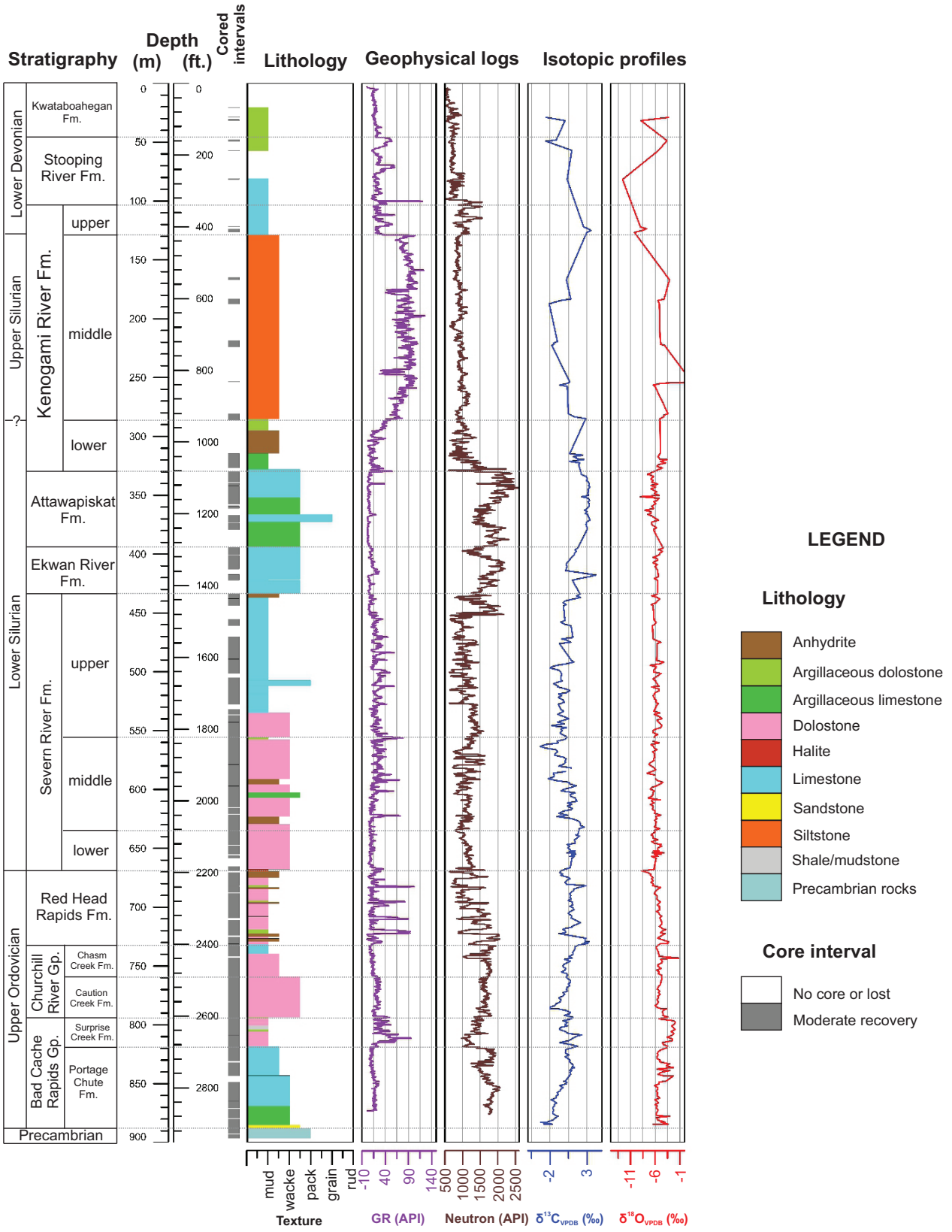

Figure GS2017-12-3: *Profile of the Sogepet Aquitaine Kaskattama Prov. No. 1 core (Oil and gas licence number 2168, Manitoba Growth, Enterprise and Trade, Winnipeg), showing tracks for lithology, geophysical logs, and $\delta^{13}C$ and $\delta^{18}O$ stable-isotope profiles (modified from Nicolas, 2016a). Abbreviations: grain, grainstone; GR, gamma ray; mud, mudstone; pack, packstone; rud, rudstone; VPDB, Vienna Peedee Belemnite; wacke, wackestone.*

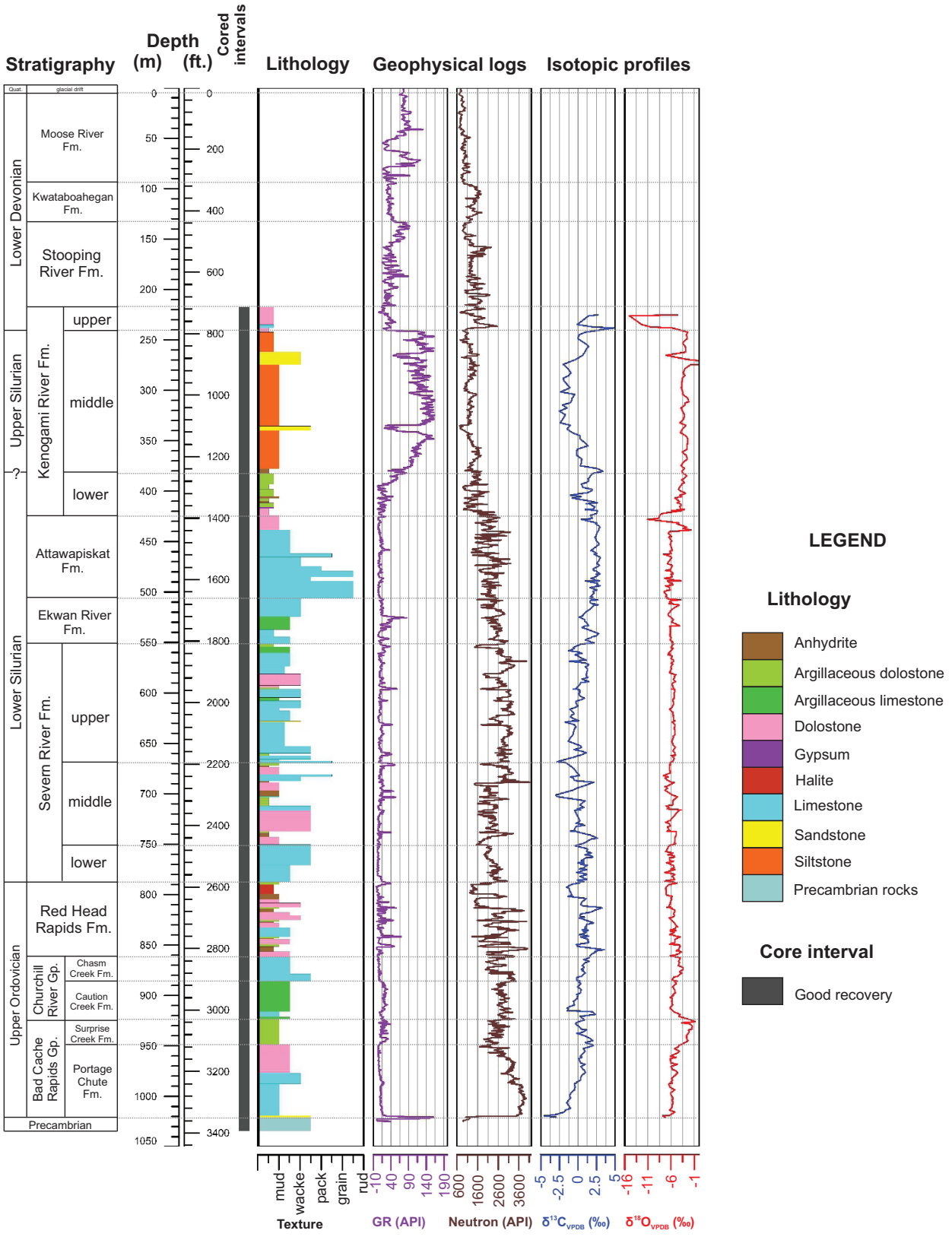

Figure GS2017-12-4: *Profile of the Aquitaine Sogepet et al. Pen No. 1 core (Oil and gas licence number T002784, Ontario Ministry of Natural Resources and Forestry, Peterborough), showing tracks for lithology, geophysical logs, and $\delta^{13}C$ and $\delta^{18}O$ stable-isotope profiles (modified from Armstrong et al., 2013b). Abbreviations: grain, grainstone; GR, gamma ray; mud, mudstone; pack, packstone; rud, rudstone; VPDB, Vienna Peedee Belemnite; wacke, wackestone.*

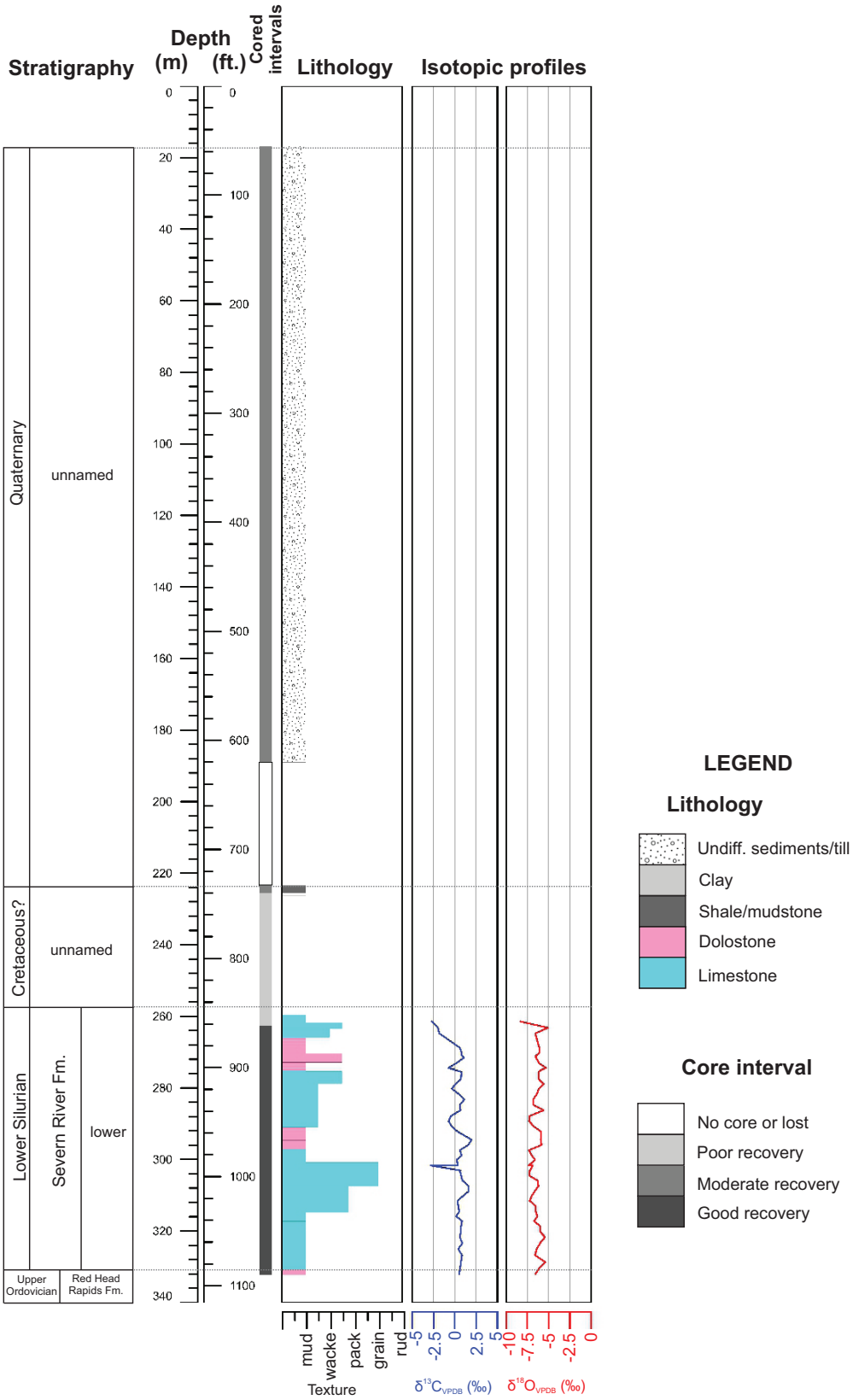

Figure GS2017-12-5: *Profile of the Foran Mining Kaskattama Kimberlite No. 1 (KK1) core (Assessment File 74223, Manitoba Growth, Enterprise and Trade, Winnipeg), showing tracks for the stratigraphy, lithology, and $\delta^{13}C$ and $\delta^{18}O$ stable-isotope profiles. Abbreviations: grain, grainstone; GR, gamma ray; mud, mudstone; pack, packstone; rud, rudstone; Undiff., undifferentiated; VPDB, Vienna Peedee Belemnite; wacke, wackestone.*

Table GS2017-12-1: Stratigraphic tops for select wells in the Hudson Bay Lowland in northeastern Manitoba and northern Ontario. Dashes indicate that stratigraphic unit is not present in the core or could not be picked up from geophysical logs. Abbreviation: Comeault, Houston Oils et al. Comeault Prov. No. 1; Kaskattama, Sogepet Aquitaine Kaskattama Prov. No. 1; KK1, Foran Mining Kaskattama Kimberlite No. 1; n/a, information not available; Pen No. 1, Aquitaine Sogepet et al. Pen No. 1; Whitebear, Merland et al. Whitebear Creek Prov.

	Core	KK1		Whitebear		Comeault		Kaskattama		Pen No.1	
Era/epoch	**Formation/member**	**Depth (m)**	**Depth (ft.)**	**Depth (m)**	**Depth (ft.)**	**Depth (m)**	**Depth (ft.)**	**Depth (m)**	**Depth (ft.)**	**Depth (m)**	**Depth (ft.)**
Quaternary	Glacial drift (till and gravel)	16.80	55.12	n/a	n/a	n/a	n/a	0	0	3.00	10.00
	Base of glacial drift	223.40	732.94	n/a	n/a	n/a	n/a	7.01	23.00	41.76	137.00
Paleogene/Neogene or Cretaceous	Unnamed	223.40	732.94	-	-	-	-	-	-	-	-
Devonian	Moose River Formation	-	-	-	-	-	-	-	-	41.76	137.00
	Kwataboahegan Formation	-	-	-	-	-	-	7.01	23.00	95.10	312.00
	Stooping River Formation	-	-	-	-	-	-	46.02	151.00	133.50	438.00
	Kenogami River Formation	-	-	-	-	<60.96	<200	103.33	339.00	216.41	710.00
	upper member	-	-	-	-	-	-	103.33	339.00	216.41	710.00
Silurian	middle member	-	-	-	-	-	-	128.93	423.00	240.79	790.00
	lower member	-	-	-	-	<60.96	<200	283.52	930.20	382.40	1254.60
	Attawapiskat Formation	-	-	-	-	122.22	401.00	329.79	1082.00	425.50	1396.00
	Ekwan River Formation	-	-	-	-	158.59	520.30	393.50	1291.00	506.36	1661.30
	Severn River Formation	257.10	843.50	<30.48	<100.00	200.04	656.30	433.43	1422.00	551.66	1809.90
	upper member	-	-	<30.48	<100.00	200.10	656.50	433.43	1422.00	551.66	1809.90
	middle member	-	-	130.15	427.00	323.09	1060.00	555.35	1822.00	669.65	2197.00
	lower member	257.10	843.50	194.77	639.00	382.52	1255.00	634.90	2083.00	750.42	2462.00
Ordovician	Red Head Rapids Formation	330.70	1084.97	220.68	724.00	411.60	1350.40	667.97	2191.50	787.45	2583.50
	Churchill River Group			269.44	884.00	466.88	1531.75	731.89	2401.20	861.91	2827.80
	Chasm Creek Formation			269.44	884.00	466.88	1531.75	731.89	2401.20	861.91	2827.80
	Caution Creek Formation			299.92	984.00	492.80	1616.80	758.95	2490.00	886.05	2907.00
	Bad Cache Rapids Group			328.57	1078.00	529.47	1737.10	793.70	2604.00	924.15	3032.00
	Surprise Creek Formation			328.57	1078.00	529.47	1737.10	793.70	2604.00	924.15	3032.00
	Portage Chute Formation			359.66	1180.00	564.22	1851.12	818.39	2685.00	948.38	3111.50
	member 2			359.66	1180.00	564.22	1851.12	818.39	2685.00	948.38	3111.50
	member 1			391.97	1286.00	614.32	2015.50	884.83	2903.00	1018.95	3343.00
Precambrian	Precambrian (weathered)			396.54	1301.00	616.00	2021.00	887.67	2912.30	1021.38	3351.00
	Precambrian (fresh)					617.22	2025.00	889.41	2918.00		
Total depth of borehole		332.20	1089.90	427.02	1401.00	647.70	2125.00	896.42	2941.00	1034.19	3393.00

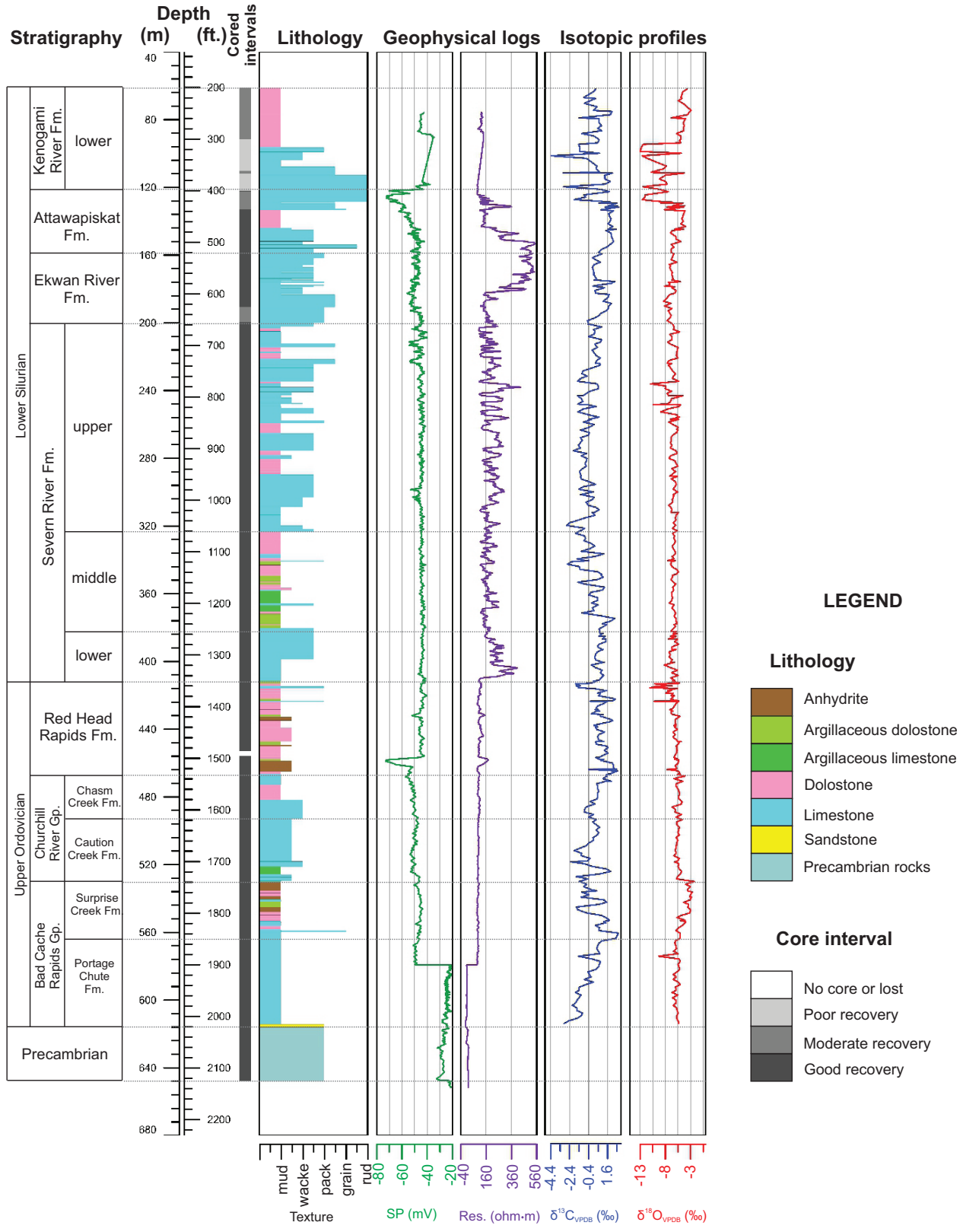

Figure GS2017-12-6: *Profile of the Houston Oils et al. Comeault Prov. No. 1 core (Oil and gas licence number 2337, Manitoba Growth, Enterprise and Trade, Winnipeg), showing tracks for lithology, geophysical logs, and $\delta^{13}C$ and $\delta^{18}O$ stable-isotope profiles. Abbreviations: grain, grainstone; mud, mudstone; pack, packstone; Res., resistivity; rud, rudstone; SP, spontaneous potential; V, volt; VPDB, Vienna Peedee Belemnite; wacke, wackestone.*

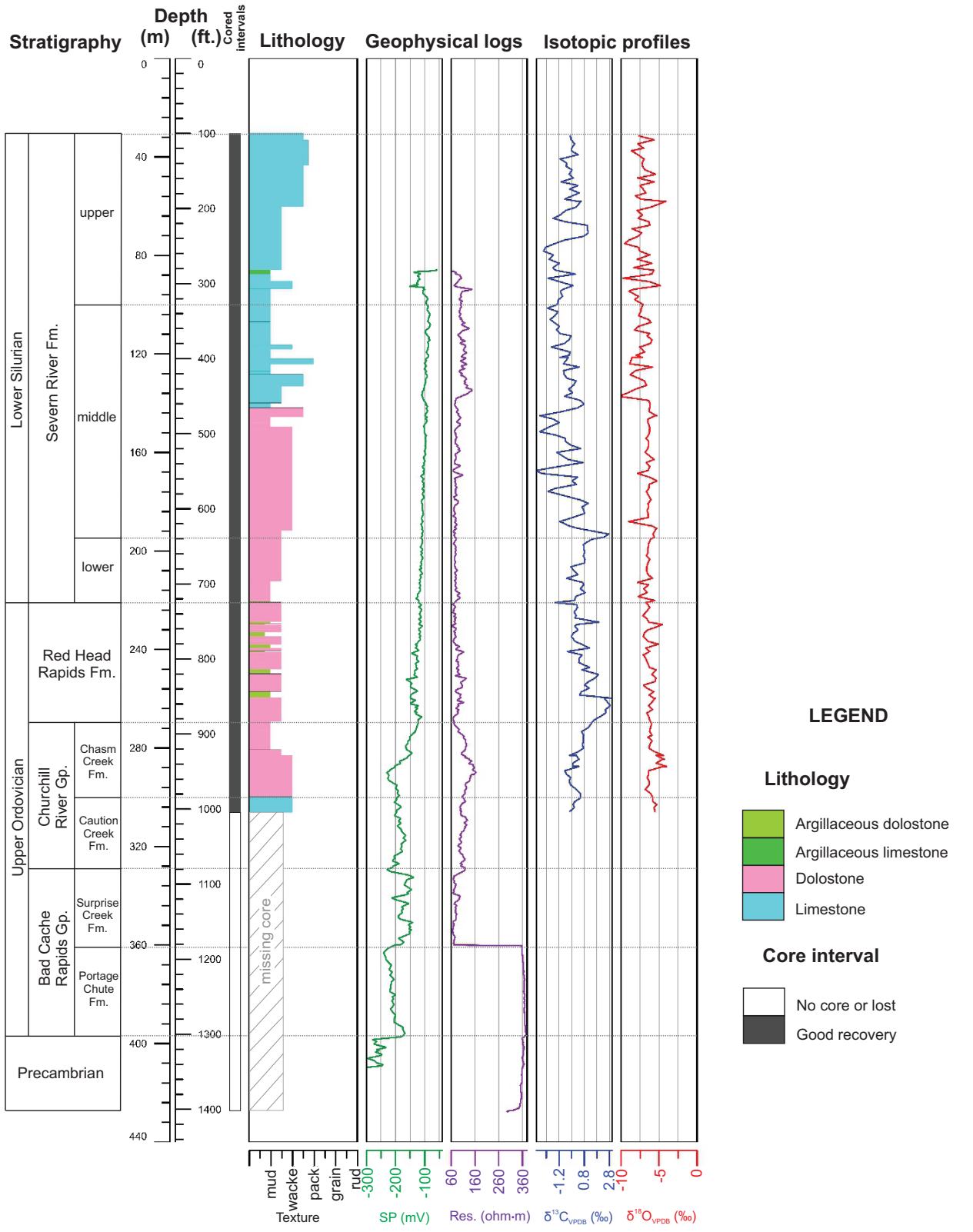

Figure GS2017-12-7: *Profile of the Merland et al. Whitebear Creek Prov. core (Oil and gas licence number 2454, Manitoba Growth, Enterprise and Trade, Winnipeg), showing tracks for lithology, geophysical logs, and $\delta^{13}C$ and $\delta^{18}O$ stable-isotope profiles. Abbreviations: grain, grainstone; mud, mudstone; pack, packstone; Res., resistivity; rud, rudstone; SP, spontaneous potential; V, volt; VPDB, Vienna Peedee Belemnite; wacke, wackestone.*

depth of 424.07 m (1391.3 ft.) in the Pen. No. 1 core, although glauconite (sometimes indicative of slow sedimentation rate and possible disconformity) occurs a few metres deeper at 427.33 m (1402 ft.). The GR log for Pen No. 1 shows a small positive spike at 425.20 m (1395 ft.) followed (downwards) by a drop in the GR baseline. This appears to reflect the transition from the more argillaceous Kenogami River Formation to the cleaner carbonate of the Attawapiskat Formation. Based on this rationale and specifically the GR log signature, the Attawapiskat Formation top contact is picked at 425.50 m (1396 ft.) in Pen No.1.

Using this GR-based pick, the top of the Attawapiskat Formation in the Kaskattama well is picked at 329.79 m (1082 ft.; Figure GS2017-12-3). This fits lithologically as well, although core recovery for this interval of Kaskattama well is poor.

Correlation to the Comeault well is complicated by variable core recovery and lack of a GR log. Correlation is based on the $\delta^{13}C$ profiles among the three wells. In Pen No. 1 (Figure GS2017-12-4), the $\delta^{13}C$ profile for the Kenogami River Formation is erratic, possibly characteristic of an evaporitic intertidal to supratidal environment. The profile for the Attawapiskat Formation in Pen No. 1 is generally smoother and with $\delta^{13}C$ values typically between +2 and +3 ‰. A negative spike (approaching 0 ‰) occurs at 427.88 m (1403.8 ft.), approximately 8 m below the top contact of 425.50 m (1396 ft.). This may indicate diagenesis related to an overlying disconformity, however, until confirmed with more closely spaced sampling, this single-point spike should be considered a possible outlier.

A transect across exposed bedrock in the Severn River in northern Ontario (south of the Pen No. 1 location), showed a similar chemostratigraphic relationship (Figure GS2017-12-8). Samples from the Attawapiskat Formation (biohermal) outcrops (location 11DKA034 in Armstrong, 2011) yielded $\delta^{13}C$ values ranging from +2.27 to +3.28 ‰, and stratigraphically higher, laminated dolostones (location 11DKA036 in Armstrong, 2011) yielded values ranging from +0.93 to +2.17 ‰ (Armstrong et al., 2013a). The latter unit was mapped as uppermost Attawapiskat Formation, but should likely be considered lowermost Kenogami River Formation. In the Kaskattama well, this contact is marked by a similar shift in $\delta^{13}C$ from about +2 ‰ in the lowest portions of the Kenogami River Formation to consistent values of around +3 ‰ in the Attawapiskat Formation.

Lithologically, the Kenogami River–Attawapiskat–Ekwan River formations interval in the Comeault core has significant differences with that observed in the Kaskattama and Pen No. 1 cores. In the Comeault core (Figure GS2017-12-6), a biohermal lithofacies of the Attawapiskat Formation occurs between 122.22 and 133.50 m (401–438 ft.), and represents Norford's (1971) "upper tongue of Attawapiskat Formation". Above 122.22 m (401 ft.) rock types are dominated by dolosiltite, which is characteristic of the lower member of the Kenogami River Formation. From 133.50–145.05 m (438.0–475.9 ft.) the rock types appear more similar to the lower Kenogami River Formation than either the Attawapiskat or Ekwan River formations. The interval from 145.05–153.92 m (475.9–505.0 ft.) consisting of tan to light brown, interbedded wackestones and packstones could, based on lithology alone, be assigned

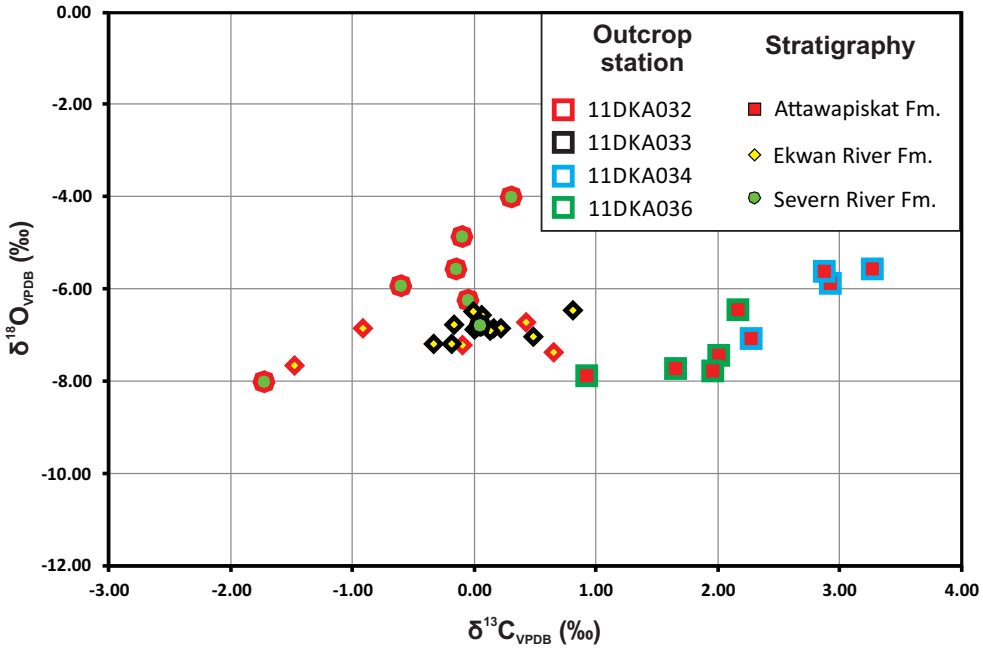

Figure GS2017-12-8: *Plot of $\delta^{18}O$ versus $\delta^{13}C$ for outcrop samples of the Ekwan and Attawapiskat formations along the Severn River in northern Ontario. Outcrop stations (from Armstrong, 2011), plotted on Figure GS2017-12-1, are 11DKA032 (Ekwan and Severn River formations), 11DKA033 (Ekwan River Formation), 11DKA034 (Attawapiskat Formation), 11DKA036 (upper Attawapiskat Formation or lower Kenogami River Formation). Symbol outline colour is coded according to station number, and symbol shape and fill is coded according to stratigraphic assignment. Abbreviations: VPDB, Vienna Peedee Belemnite.*

to either Ekwan River or Severn River formations. The interval from 153.92–158.59 m (505.0–520.3 ft.) consists of a biohermal lithofacies and corresponds closely to Norford's (1971) "lower tongue of Attawapiskat Formation". The top of the higher biohermal interval (122.22 m) is selected as the official top pick of Attawapiskat Formation in this core.

Nomenclature challenges

The interbedded nature of the formations (or lithofacies characteristics of specific formations) identified in the Comeault core by Norford (1971) comes with its challenges. Traditional lithostratigraphic top selections seldom allow for the recording of the interbedded nature of a section, that is, the occurrence of a formation top more than once in a well that is not structurally disturbed, and so it is seldom recorded that a particular formation occurs more than once in a given location. This is mostly due to the constraints of computer database architecture, and the challenge of handling multiple entries for the same unit. Previous authors (e.g., Lavoie et al., 2015) have acknowledged the complex inter-relationship of these units, and refer to "Attawapiskat reefs" within the Ekwan River Formation, rather than a stand-alone Attawapiskat Formation. The inter-relationship of these formations and their constituent facies remains a subject for further investigation.

Ekwan River Formation

The key lithological difference between the Ekwan River Formation and the overlying Attawapiskat Formation is the former's bedded biostromal nature and the latter's biohermal nature (Savage and Van Tuyl, 1919; Norris, 1993). In the Pen No. 1 core, the Attawapiskat Formation consists of two biohermal zones separated by bedded limestones, which on their own might be interpreted as Ekwan River Formation. As discussed above, the intercalated lithofacies suggest these formations may at least in part be equivalent or, as some have suggested (e.g., Lavoie et al., 2015), the Attawapiskat reef facies should be part of the Ekwan River Formation. For this report, however, the present formational status of these units is retained.

Lithostratigraphically, the top of the Ekwan River Formation is placed at the base of the lowest biohermal limestone (i.e., basal Attawapiskat Formation). In the Pen No. 1 core (Figure GS2017-12-4), this is a sharp contact at 506.36 m (1661.3 ft.). It is also marked by a sharp but small increase (downward) in the average GR response, reflecting the difference between clean carbonate of the Attawapiskat Formation and the slightly higher argillaceous content in the Ekwan River Formation.

Despite the lack of core through this interval in the Kaskattama well (Figure GS2017-12-3), the lithological difference between the Attawapiskat and Ekwan River formations is consistent within Pen No. 1, and is supported by a similar GR log response. The upper contact of the Ekwan River Formation is picked on the GR log at 393.50 m (1291 ft.) in the Kaskattama well.

Isotopically, in these two wells (Figures GS2017-12-3, -4), the top of Ekwan River Formation (identified lithologically) is located near the base of the broad $\delta^{13}C$ high that characterizes the overlying Attawapiskat Formation and immediately above the top of two small positive spikes (albeit more subtle in the Kaskattama core).

The $\delta^{13}C$ isotopic profile for the Ekwan River Formation is best exhibited in the Pen No. 1 core (Figure GS2017-12-4), and generally consists of positive values (+2 to +3 ‰) in the upper part, similar to or slightly lower than values for the overlying Attawapiskat Formation. The middle part of the Ekwan Formation exhibits lower $\delta^{13}C$ values, down to about 0 ‰, but can contain some positive spikes, whereas the lower part of the formation exhibits high values, similar to the top. Below this, passing into the underlying Severn River Formation, average $\delta^{13}C$ values decrease to about 0 ‰.

In the Comeault core (Figure GS2017-12-6), the top of the Ekwan River Formation, based on the $\delta^{13}C$ isotope profile, is at 158.59 m (520.30 ft.), but the lithological change exhibited at this depth is not typical of the Attawapiskat Formation–Ekwan River Formation contact. Lithologically, below 158.59 m (520.30 ft.) and with increasing depth, the rock becomes dominantly a wackestone to wackestone-packstone, greyer in colour, slightly more argillaceous and allochems decrease in abundance. In the isotope profile, the two small positive spikes below 158.59 m (520.30 ft.) in the Comeault core may correlate with similar double spikes that are coincident with the top of the Ekwan River Formation in the Kaskattama and Pen No. 1 wells. The upper unit of the Ekwan River Formation in the Comeault core extends down to 173.77 m (570.0 ft.), and includes some packstone interbeds. Below this, from 173.77 to 182.88 m (570.0–600 ft.), there are variable carbonate rock types, ranging from laminated mudstones to packstones to calcarenites. The allochems (crinoids, brachiopods, horn corals, stromatoporoids, gastropods) between 158.59 and 182.88 m (520.30–600 ft.) are characteristic of the Ekwan River Formation, however, the lithological character of this interval in the Comeault core differs significantly from the Ekwan River Formation in the Kaskattama and Pen No. 1 cores.

Severn River Formation

The Severn River Formation is the thickest Silurian carbonate unit in the southern (onshore) part of the HBB. It has been informally subdivided into three members: lower, middle and upper (LeFèvre et al., 1976; Norris, 1993; Armstrong et al., 2013b).

Although it contains a variety of rock types, the most common lithology of the Severn River Formation is a light tan, burrow-mottled carbonate. Wackestones and packstones dominate the upper and lower members, but can also occur in the middle member. Thin, bioclastic, and locally intraclastic, grainstone beds occur throughout, and appear to be best developed in the lower member, where they occur in association with *Virgiana decussata*-rich limestones. Mudstones, either laminated or massive, also occur throughout but are generally subordinate to the wackestones and packstones, except in the middle member. Dolomudstone and anhydrite beds and

nodules characterize the middle member, although mudstones, wackestones and packstones are also present. Nodular and bedded anhydrite is limited to the upper member in the Kaskattama well. These various lithofacies appear to be arranged in sequences that represent shallowing upward cycles. This is especially evident in the middle member where cycles include anhydrite beds capped by greenish, argillaceous, dolomudstone to dolosiltstone beds. These green beds stand out in GR logs as sharp positive spikes. Green argillaceous beds also occur in the upper member but are not as numerous (cycles may not be as well developed). The lower member is defined by its position beneath the evaporative middle member and the occurrence of locally abundant *Virgiana decussata* brachiopods. The lower part of the lower member is marked by a decrease in allochem abundance, grading downwards from *Virgiana*- and coral-bearing grainstones and packstones to wackestones and ultimately lime mudstone (or locally dolomudstone) at its base. The lime mudstone (or dolomudstone) grades rapidly into grey siliciclastic mudstones of the Red Head Rapids Formation.

The top of the upper member of the Severn River Formation is exposed in two outcrops, map station 11DKA032 on the Severn River (Armstrong, 2011) and map station 11DKA017 (Armstrong, 2011; same as map station 15DKA063 in Armstrong, 2015) on the Attawapiskat River (Figure GS2017-12-9), and in numerous cores (e.g., Comeault, Kaskattama, Pen No. 1, KWG-Spider Resources DR-94-19 [KWG; Ratcliffe and Armstrong, 2013]). Despite these numerous occurrences, the top of the upper member of the Severn River Formation is difficult to pick in the subsurface.

Outcrop exposures on the Severn and Attawapiskat rivers reveal a sharp disconformable contact; although the uppermost lithofacies of the Severn River Formation differs in each case (Figure GS2017-12-9). In the Severn River outcrop (11DKA032; Armstrong, 2011), the uppermost Severn River Formation lithofacies is a thin-platy bedded, greenish (weathering to yellowish), argillaceous dolosiltstone, similar to the uppermost Severn River Formation in the Pen No. 1 core. Farther to the east in Ontario, in the MRB, on the Attawapiskat River (at outcrop 11DKA017; Armstrong, 2011) the uppermost Severn River Formation is a very fine-grained, burrow-mottled wackestone with thin packstone beds. It looks similar to the basal beds of the overlying Ekwan River Formation, except that the latter have a coarser grained matrix. The disconformable nature of the contact is obvious at this locality and was described by Suchy (1992).

In core from the MRB, such as core KWG (also map station 13LMR004 in Ratcliffe and Armstrong, 2013), the contact is subtle and hard to pick. Many of the thin grainstone beds in the upper Severn River Formation have sharp bases, which can easily be mistaken for the contact. Key lithological indicators to recognizing this contact include an increase in matrix grainsize in the Ekwan River Formation, as well as the occurrence and abundance of stromatoporoids, tabulate corals and crinoidal fragments. Chert also tends to be more prevalent in the Ekwan River Formation, where it is locally very abundant (especially in the lower half of the formation). In the KWG core, there is an interval (67.5–70.22 m) of creamy tan to light grey lime mudstone-siltite in the middle of the formation, which could be interpreted as the uppermost Severn River Formation. Below this, however, there is an interval (72.8–79.33 m) of grey, wackestone-packstone-grainstone beds with abundant stromatoporoids, tabulate corals and chert—classic Ekwan River Formation lithofacies. The lowest bed is intraclastic overlying a disconformity. Underlying it is a grey-tan, burrow-mottled, lime

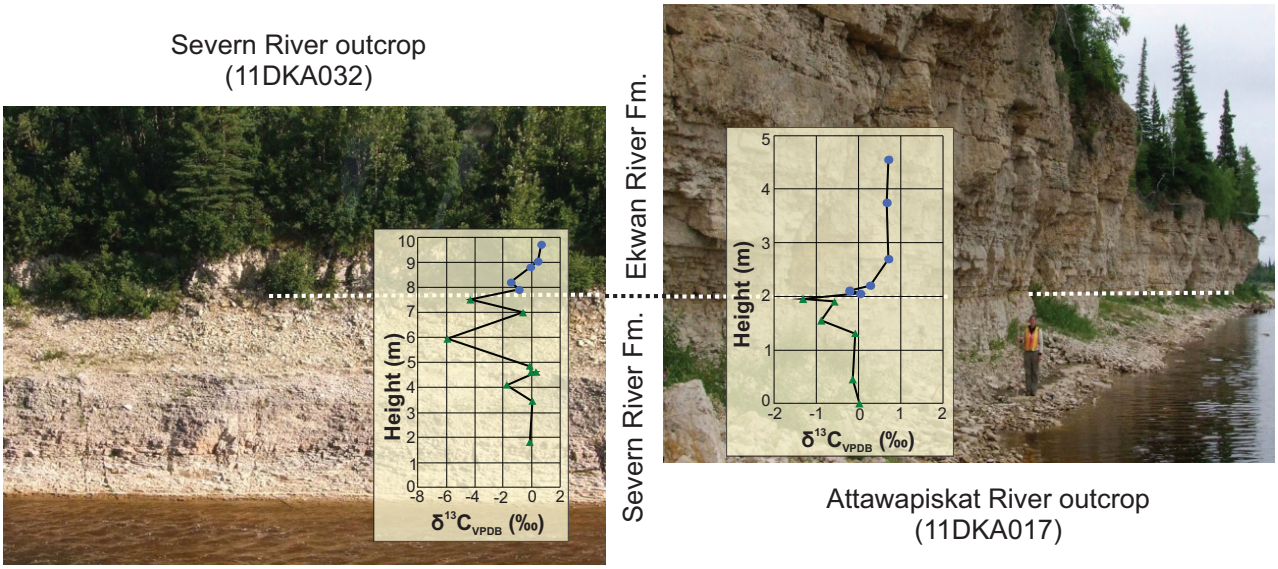

Figure GS2017-12-9: *Outcrops showing the disconformable contact between the Ekwan River and Severn River formations, on the Severn River (left; station 11DKA032 from Armstrong, 2011) and 365 km to the southeast on the Attawapiskat River (right; station 11DKA017 from Armstrong, 2011). Outcrop photographs are overlain with their respective $\delta^{13}C$ isotopic profiles. Data points are colour coded to formations: blue dots are Ekwan River Formation and green triangles are Severn River Formation.*

mudstone to sparsely fossiliferous wackestone, similar to the uppermost Severn River Formation in the Attawapiskat River outcrop. These key lithological indicators are also present in the Comeault core.

Isotopically, the top of the Severn River Formation is marked by a downward decrease in $\delta^{13}C$ from values around +2 ‰ in the lower Ekwan River Formation to values typically ranging from –1 to +1 ‰ in the upper Severn River Formation. In Ontario, the isotopic profile across the contact is consistent among cores and outcrops in both the HBB (Severn River outcrops and Pen No.1 core) and MRB (Attawapiskat River outcrops and KWG core; Figure GS2017-12-9; Armstrong et al., 2013b; Ratcliffe and Armstrong, 2013). In most cases, the contact is marked by a negative $\delta^{13}C$ spike in the uppermost Severn River Formation, possibly related to the overlying disconformity. In Pen No. 1, the spike occurs at 558.79 m (1833.3 ft.; Figure GS2017-12-4), and at 441.96 m (1450 ft.) in Kaskattama (Figure GS2017-12-3) and 200.04 m (656.3 ft.) in Comeault (Figure GS2017-12-6).

The top of the Severn River Formation in Pen No. 1 (Figure GS2017-12-4), as defined lithologically and isotopically, occurs in a GR low between two moderate GR positive spikes and at the top of a negative shift in the neutron log. This corresponds to a depth of about 438.91 m (1440 ft.) in the Kaskattama well (Figure GS2017-12-3), with both the GR log and isotopic profiles in agreement. This is, however, in conflict with the top of the Severn River Formation in the Kaskattama well being picked lithologically at the top of the anhydrite at 433.43 m (1422 ft.). The discrepancy between the lithological pick, isotopic signature and GR logs for this well is likely due to intermittent core recovery.

In the Whitebear core (Figure GS2017-12-7), the isotopic signature between 30.48 and 220.68 m (100.0–724.0 ft.) follows the pattern typical of the Severn River Formation in Comeault, thus confirming the absence of the Attawapiskat and Ekwan River formations in this core.

Economic considerations

The Hudson Bay Lowland in Manitoba is a large frontier area with good potential for local hydrocarbon accumulations. The stratigraphic information described here guides the long-distance correlations of rock units, as well as predictability of the depositional environment that formed the rocks. This provides a basic geological framework for the sedimentary basin including its structure and lithologies, which is required to attract exploration investment. Geographic predictability, particularly in a large basin like the HBB, helps a company identify focus areas for exploration. The information gathered from this project supports exploration of natural resources and informs decisions on land-use planning that balance conservation and responsible resource development.

Economic benefits from collaborative programs such as GEM-2 can be measured in terms of industry attraction and investments over the long term. The program also provides access for the MGS to expertise and services from world-class GSC laboratories, as well as training opportunities for students to develop themselves as new geoscience experts in Manitoba, benefits that can be applied to other projects in the future.

Acknowledgments

The authors would like to acknowledge D. Lavoie from the Geological Survey of Canada, the leader of the Hudson-Ungava Project of the Geo-mapping for Energy and Minerals program, Phase 2 (GEM-2; 2013–2020), for his continued support.

The authors thank C. Epp (Manitoba Geological Survey) and the summer students at the Midland Sample and Core Library for help in preparing the core for viewing, and for general assistance with rock cutting and sample preparation. Finally, thanks go to J. Harrison (University of Manitoba) for her diligent isotope sampling and note taking. The authors would like to thank the numerous student assistants who have over the course of this project worked in the field, logged core, sampled for isotopic analyses and assisted in data analysis. Special thanks go to K. Yeung (Ontario Geological Survey) for help with all GIS-related issues.

References

Armstrong, D.K. 2011: Re-evaluating the hydrocarbon resource potential of the Hudson Platform: interim results from northern Ontario; *in* Summary of Field Work and Other Activities 2011, Ontario Geological Survey, Open File Report 6270, p. 27-1–27-11.

Armstrong, D.K. 2015: Hudson Platform Project: Paleozoic geology of the McFaulds Lake, South Moosonee, Ekwan River and Attawapiskat River areas, James Bay Lowland; *in* Summary of Field Work and Other Activities 2015, Ontario Geological Survey, Open File Report 6313, p. 31-1–31-20.

Armstrong, D.K., Lavoie, D., McCracken, A.D., Asselin, E. and Galloway, J.M. 2013a: Stratigraphy and source rocks of the Hudson Platform in northern Ontario (abstract); Geological Association of Canada–Mineralogical Association of Canada, Joint Annual Meeting, Winnipeg, Manitoba, May 21–24, 2013, Program with Abstracts, p. 63–64.

Armstrong, D., McCracken, A D., Asselin, E. and Brunton, F.R. 2013b: The Hudson Platform Project: stratigraphy of the Aquitaine Sogepet et al. Pen No. 1 core; *in* Summary of Field Work and Other Activities 2013, Ontario Geological Survey, Open File Report 6290, p. 34-1–34-21.

Craven, J.A., Ferguson, I.J., Nicolas, M.P.B., Zaprozan, T., Hodder, T., Roberts, B.R. and Clarke, N. 2017: Report of activities for the ground geophysical survey across the Kaskattama highland, Manitoba: GEM-2 Hudson-Ungava Project; Geological Survey of Canada, Open File OF8321, 30 p.

Hahn, K.E., Armstrong, D.K., Turner, E.C. and Nicolas, M.P.B. 2016: Toward a sequence stratigrapic framework for the Ordovician Hudson Bay and Moose River basins, northern Ontario; *in* Summary of Field Work and Other Activies 2016, Ontario Geological Survey, Open File Report 6323, p. 28-1–28-10.

Hobson, G.D. 1964: Nine reversed refraction seismic profiles, Hudson Bay Lowland, Manitoba; *in* Summary of Activities: Office and Laboratory, 1963, Geological Survey of Canada, Paper 64-2, p. 33–40.

International Commission on Stratigraphy 2017: International chronostratigraphic chart v.2017/02; International Commission on Stratigraphy, URL <http://www.stratigraphy.org/ICSchart/ChronostratChart2017-02.jpg> [October 2017].

Lavoie, D.N.P., Dietrich, J. and Chen, Z. 2015: The Paleozoic Hudson Bay Basin in northern Canada: new insights into hydrocarbon potential of a frontier intracratonic basin; America Association of Petroleum Geologists, Bulletin, v. 99, no. 2, p. 859–888.

LeFèvre, J.A., Barnes, C.R. and Tixier, M. 1976: Paleoecology of Late Ordovician and Early Silurian conodontophorids, Hudson Bay Basin; *in* Conodont Paleoecology, C.R. Barnes (ed.), Geological Association of Canada, Special Paper no. 15, p. 69–89.

McCracken, A.D. 2014: Report on 10 conodont samples (9 from the Early Silurian, early Llandovery Severn River Formation, 1 barren conodont sample from the Ordovician Red Head Rapids Formation) in the Foran Mining Kaskattama Kimberlite 1 (KK1) core (near Bouchard Lake and Kaskattama River), Hudson Bay Lowland, northeastern Manitoba, submitted in 2014 by Michelle Nicolas (Manitoba Geological Survey), NTS 054B/07, Con. No. 1973; Geological Survey of Canada, Paleontological Report 3-ADM-2014, 9 p.

Nelson, S.J. and Johnson, R.D. 1966: Geology of Hudson Bay Basin; Bulletin of Canadian Petroleum Geology, v. 14, no. 4, p. 520–578.

Nicolas, M.P.B. 2011: Stratigraphy of three exploratory oil-well cores in the Hudson Bay Lowland, northeastern Manitoba (parts of NTS 54B10, F8, G1); *in* Report of Activities 2011, Manitoba Innovation, Energy and Mines, Manitoba Geological Survey, p. 165–170.

Nicolas, M.P.B. 2016a: Carbon and oxygen stable-isotope profiles of Paleozoic core from the Hudson Bay Basin, northeastern Manitoba (parts of NTS 54B7, 8, 54F8, 54G1); *in* Report of Activities 2016, Manitoba Growth, Enterprise and Trade, Manitoba Geological Survey, p. 142–149.

Nicolas, M.P.B. 2016b: Carbon and oxygen stable-isotope results from three petroleum-exploration Paleozoic cores from the Hudson Bay Basin, northeastern Manitoba (parts of NTS 54B7, 8, 54F8, 54G1); Manitoba Growth, Enterprise and Trade, Manitoba Geological Survey, Data Repository Item DRI2016002, Microsoft® Excel® file.

Nicolas, M.P.B. 2017: Carbon and oxygen stable-isotope results from Paleozoic cores and outcrops from the Hudson Bay Basin, northeastern Manitoba (NTS 54B7, 54C10, 54G1, parts of 54E, K, L); Manitoba Growth, Enterprise and Trade, Manitoba Geological Survey, Data Repository Item DRI2017002, Microsoft® Excel® file.

Nicolas, M.P.B. and Lavoie, D. 2012: Oil shale and reservoir rocks of the Hudson Bay Lowland, northeastern Manitoba (part of NTS 54); *in* Report of Activities 2012, Manitoba Innovation, Energy and Mines, Manitoba Geological Survey, p. 124–133.

Nicolas, M.P.B. and Young, G.A. 2014: Reconnaissance field mapping of Paleozoic rocks along the Churchill River and Churchill coastal area, northeastern Manitoba (parts of NTS 54E, L, K); *in* Report of Activities 2014, Manitoba Mineral Resources, Manitoba Geological Survey, p. 148–160.

Nicolas, M.P.B., Lavoie, D. and Harrison, J. 2014: Introduction to the GEM-2 Hudson-Ungava Project, Hudson Bay Lowland, northeastern Manitoba; *in* Report of Activities 2014, Manitoba Mineral Resources, Manitoba Geological Survey, p. 140–147.

Norford, B.S. 1971: Silurian stratigraphy of northern Manitoba; *in* Geoscience Studies in Manitoba, A.C. Turnock (ed.), Geological Association of Canada, Special Paper 9, p. 199–207.

Norford, B.S. 1997: Correlation chart and biostratigraphy of the Silurian rocks of Canada; Geological Survey of Norway, International Union of Geological Sciences, Publication No. 33, 77 p.

Norris, A.W. 1993: Hudson Platform - Geology; *in* Chapter 8 of Sedimentary Cover of the Craton in Canada, D.F. Stott and J.D. Aitken (ed.), Geological Survey of Canada, Geology of Canada, no. 5 and Geological Society of America, The Geology of North America, v. D-1, p. 653–700.

Ontario Geological Survey 2011: 1:250 000 scale bedrock geology of Ontario; Ontario Geological Survey, Miscellaneous Release—Data 126–Revision 1.

Ratcliffe, L.M. and Armstrong, D.K. 2013: The Hudson Platform Project: 2013 field work and drill-core correlations, western Moose River Basin; *in* Summary of Field Work and Other Activities 2013, Ontario Geological Survey, Open File Report 6290, p. 36-1–39-19.

Sanford, B.V. and Grant, A.C. 1998: Paleozoic and Mesozoic geology of the Hudson and southeast Arctic Platforms; Geological Survey of Canada, Open File 3595, 1 colour map, scale 1:2 500 000.

Sanford, B.V. and Norris, A.W. 1975: Devonian stratigraphy of the Hudson platform: part I: stratigraphy and economic geology; Geological Survey of Canada, Memoir 379, 124 p.

Savage, T.E. and Van Tuyl, F.M. 1919: Geology and stratigraphy of the area of Paleozoic rocks in the vicinity of Hudson and James bays; Geological Society of America, Bulletin, v. 30, p. 339–377.

Suchy, D.R. 1992: Hudson Bay Platform: Silurian sequence stratigraphy and paleoenvironments; Ph.D. thesis, McGill University, Montreal, Quebec, 207 p.

Suchy, D.R. and Stearn, C.W. 1993: Lower Silurian reefs and post-reef beds of the Attawapiskat Formation, Hudson Bay Platform, northern Ontario; Canadian Journal of Earth Sciences, v. 30, p. 575–590.

Zhang, S. and Barnes, C.R. 2007: Late Ordovician-Early Silurian conodont biostratigraphy and thermal maturity, Hudson Bay Basin; Bulletin of Canadian Petroleum Geology, v. 55, p. 179–216.

GS2017-13

Sedimentary facies variability of the Upper Ordovician Williams Member in the Williston Basin, southern Manitoba: lithostratigraphic implications

by C.Y.C. Zheng[1], M.G. Mángano[1] and L.A. Buatois[1]

[1] Department of Geological Science, University of Saskatchewan, 114 Science Place, Saskatoon, SK S7N 5E2

In Brief:

- The Williams Member is refined and placed into the Stony Mountain Formation
- Long-range correlations are challenging, with two depositional environments and correlation options proposed

Citation:
Zheng, C.Y.C., Mángano, M.G. and Buatois, L.A. 2017: Sedimentary facies variability of the Upper Ordovician Williams Member in the Williston Basin, southern Manitoba: lithostratigraphic implications; *in* Report of Activities 2017, Manitoba Growth, Enterprise and Trade, Manitoba Geological Survey, p. 148–157.

Summary

The Upper Ordovician Williams Member is analyzed based on the study of seven stratigraphic cores in the subsurface of Manitoba. Two remarkably different sedimentary facies, representing tidal flat and nearshore complex environments, have been traditionally included in this member. Confusion regarding the use of this member also generates debate on its placement at the top of the Stony Mountain Formation or the base of the lower Stonewall Formation. In this report, the Williams Member is redefined to include only the deposits of the last stage Stony Mountain Formation with two suggested correlations: 1) the member is limited to the nearshore deposits in southwestern Manitoba, or 2) the member includes tidal flat deposits toward the north and nearshore deposits toward the south. In addition, the tidal flat deposits situated above the Stony Mountain Formation should not be assigned to the Williams Member and should be included in the lower interval of the Stonewall Formation.

Introduction

The Upper Ordovician succession in the Williston Basin is characterized by the basal sandstone unit of the Winnipeg Formation, with overlying epeiric carbonate-anhydrite cycles that compose the Red River, Stony Mountain and Stonewall formations. A disconformity situated at the top of the Stonewall Formation marks a prolonged hiatus separating the Ordovician from the Silurian (Demski et al., 2015). Different subdivisions of these epeiric sea deposits have been adopted not only between Saskatchewan and Manitoba, but also in outcrop and subsurface due to a complex facies pattern. For instance, the Stony Mountain Formation was divided, from base to top, into the Hartaven, Gunn and Gunton members in Saskatchewan (Kendall, 1976). In Manitoba, the formation was divided into the Gunn, Penitentiary, Gunton and Williams members based on type sections in the outcrop belt (Elias et al., 2013b), whereas the formation was divided into the Hartaven, Gunn/Penitentiary and Gunton members in the subsurface of southwestern Manitoba (Nicolas and Barchyn, 2008). There is disagreement between these subdivisions. Specifically, the Williams Member, in places capped by the basal Stonewall anhydrite, was placed at the base of the lower Stonewall Formation in the subsurface of southwestern Manitoba (Bezys and Bamburak, 2004; Nicolas and Barchyn, 2008). However, the member was first proposed for the uppermost part of the Stony Mountain Formation based on outcrops in the Stonewall quarry (Smith, 1963; Cowan, 1971). The decision to move the Williams Member into the Stonewall Formation was based on detailed stratigraphic investigations conducted jointly by the Manitoba Geological Survey (MGS), Saskatchewan Geological Survey and the Geological Survey of Canada (R. Bezys, pers. comm., 2017), and even though a formal publication of that decision is not available, the stratigraphic reassessment is mentioned in Martiniuk (1992) and Norford et al. (1998). A recent study placed the upper contact of the member at a disconformity in the Stonewall quarry, suggesting its inclusion in the uppermost interval of the Stony Mountain Formation as well (Elias et al., 2013b).

The purpose of this study is to provide a preliminary assessment of the sedimentary facies variability of the Williams Member in the subsurface, aiming to clarify its definition and distribution, based on seven stratigraphic cores in southern Manitoba (Figure GS2017-13-1, Table GS2017-13-1).

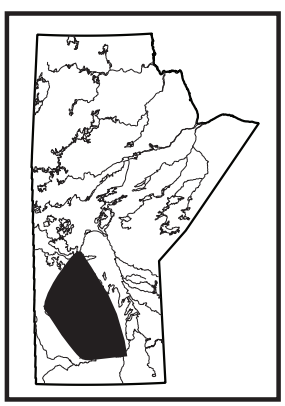

Stratigraphic setting

In the Williston Basin, Late Ordovician sedimentation began with a large-scale marine transgression from the southeast. This punctuated transgression led to the deposition of shoreface sandstone to offshore mudstone of the Winnipeg Formation (Kreis, 2004; Dorador et al., 2014). Detailed lateral facies correlation at this stratigraphic level is complicated due to complex stratal architectures resulting from a series of topographic depressions on the underlying Cambrian

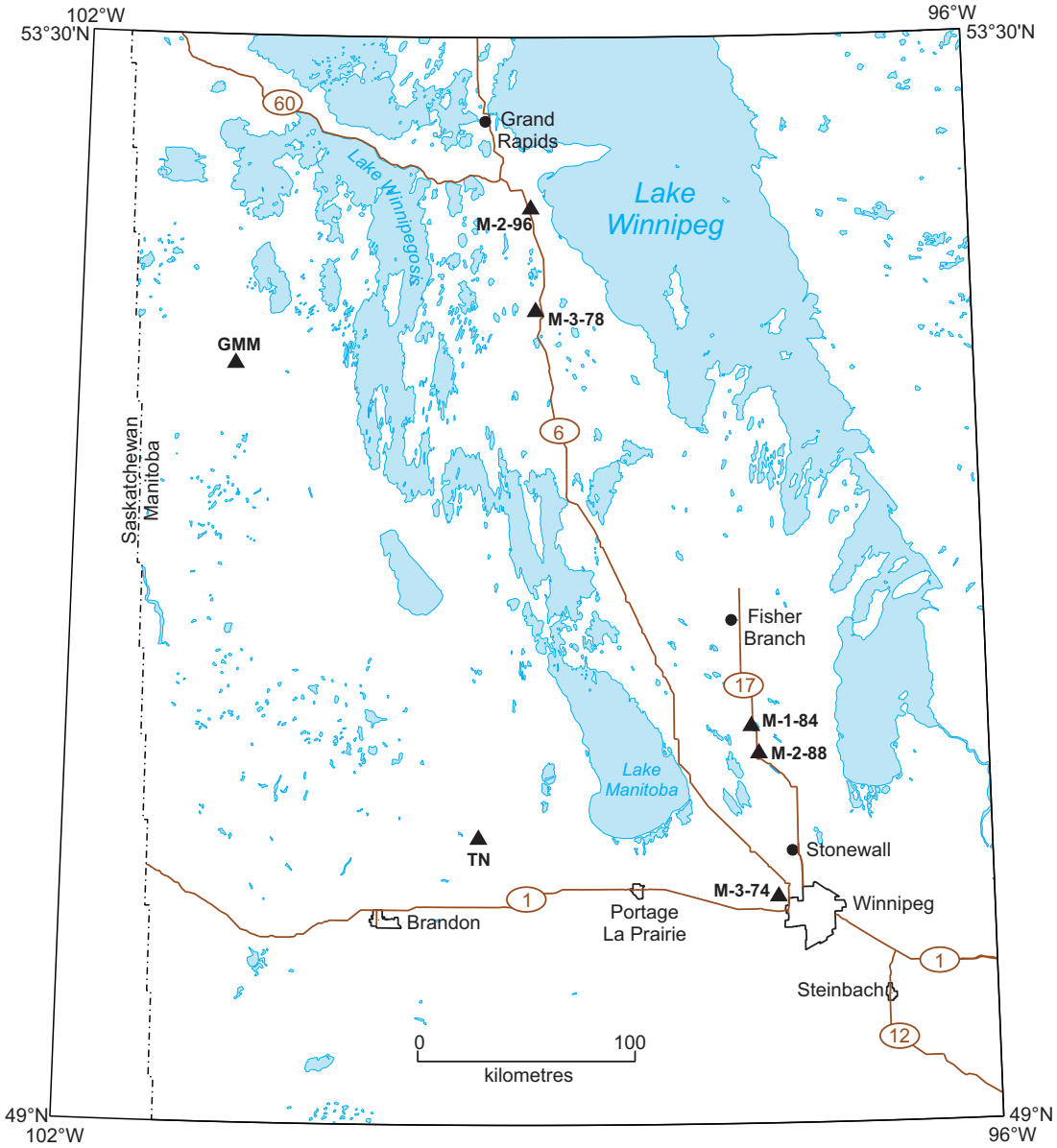

Figure GS2017-13-1: *Location map of the seven stratigraphic cores (black triangles) studied in southern Manitoba. Abbreviations: GMM, Gulf Minerals Minitonas; TN, Tudale Neepawa.*

Table GS2017-13-1: Details of well locations and cored intervals for the seven stratigraphic cores studied in southern Manitoba.

Drillhole	Location	Core interval
M-3-78	12-07-40-10W1*	73.6–98 m
M-3-74	01-21-11-01E1	2.0–27.7 m (6.6–90.9 ft.)
M-2-96	03-28-44-11W1	11.0–37.0 m
M-2-88	04-11-18-01W1	40.0–56.8 m
M-1-84	04-15-19-01W1	17.00–42.65 m
Tudale Neepawa	15-29-14-14W1	534.0–562.7 m (1752–1846 ft.)
Gulf Minerals Minitonas	03-29-36-25W1	381.0–402.3 m (1250–1320 ft.)

*L.S. 12, Sec. 7, Twp. 40, Rge. 10, W 1st Mer.

Deadwood Formation (Vigrass, 1971; Potter, 2006). Subsequent Late Ordovician sedimentation in the Williston Basin is characterized by carbonate-evaporite tripartite cycles. These cycles typically contain fossiliferous wackestones at the base, grading into parallel-laminated mudstone, and capped by anhydrite beds (Kent and Christopher, 1994; Norford et al., 1994). The Red River Formation records the first two cycles, whereas the Stony Mountain Formation and the lower interval of the Stonewall Formation together record the third cycle (Figure GS2017-13-2; Kendall, 1976). These cycles are variably preserved across the basin. The complete succession is preserved in a basin-centre position in southeastern Saskatchewan, whereas in Manitoba the capping anhydrites are commonly absent (Nicolas and Barchyn, 2008). Depositional trends in the Red River and Stony Mountain formations show a similar overall pattern in the Williston Basin, exhibiting the thickest strata in southern Manitoba and thinning toward the north (Bezys and Bamburak, 2004; Nicolas and Barchyn, 2008). Furthermore, subsurface correlations in the basin demonstrate continuous southwest-trending strata with minor lithological changes, and indicate depositional and erosional thinning of stratigraphic units from the southeast toward the northwest (Norford et al., 1994). In contrast, although the thickness and lithology of the Stonewall Formation are uniform throughout the outcrop belt (Bezys and McCabe, 1996), subsurface correlations of the formation exhibit a thinning trend toward the outcrop belt in the north and east (Nicolas and Barchyn, 2008). Subsequent erosion highly constrained the present distribution of these Ordovician carbonate successions. In the Williston Basin, erosion on the Transcontinental, Severn, Peace River and Sweetgrass–North Battlefield arches removed parts of the underlying deposits in the east, northeast, northwest and west of the basin, respectively (Norford et al., 1994). The widespread Ordovician epeiric carbonate deposits were correlated from northern Mexico to northern Greenland and from eastern Quebec to eastern Alaska, with the maximum distribution marked by the Red River–Stony Mountain coral province (Ross et al., 1982; Elias, 1991; Elias et al., 2013a).

In the subsurface of southwestern Manitoba, the Stony Mountain Formation was subdivided, from base to top, into the Hartaven, Gunn/Penitentiary and Gunton members. The Stonewall Formation was subdivided into the lower Stonewall Formation, which contained the basal Williams Member, and the upper Stonewall Formation. In places, the Gunton anhydrite and the basal Stonewall anhydrite capped the Gunton Member and the Williams Member, respectively (Figure GS2017-13-3; Nicolas and Barchyn, 2008). Although the precise lithostratigraphic position of the Williams Member is still ambiguous, this member serves as a transition between the underlying Gunton Member and the overlying lower Stonewall Formation.

The Williams Member was first characterized within the standard section at the Winnipeg Supply and Fuel Company quarry (Stonewall quarry) near the town of Stonewall and at that time it was included in the Stony Mountain Formation (Smith, 1963; Cowan, 1978). The member consists of argillaceous, mottled, dense arenaceous dolomite with coarse, well-rounded, frosted and pitted, quartz sand grains abundant

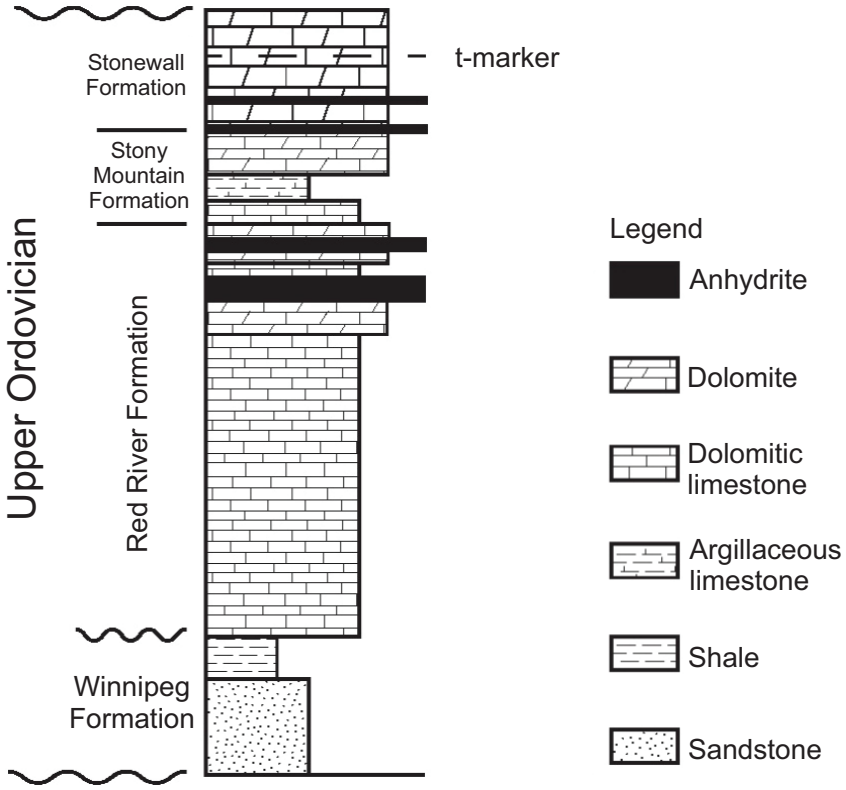

Figure GS2017-13-2: *The Upper Ordovician succession in the Williston Basin (modified from Kendall, 1976).*

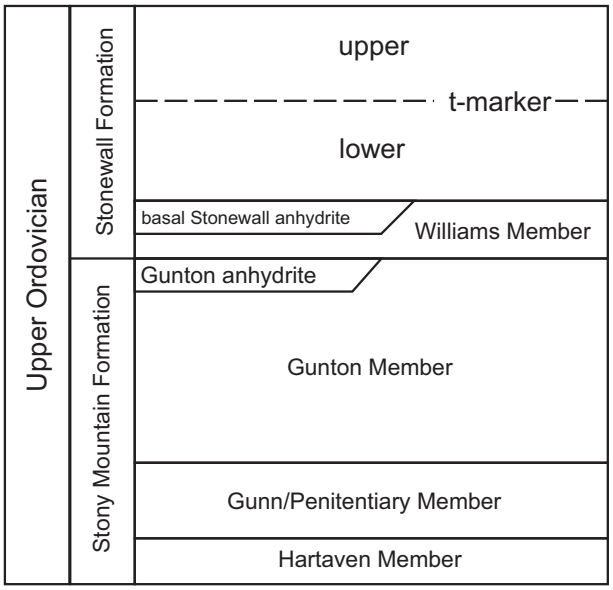

Figure GS2017-13-3: *Stratigraphy of the Upper Ordovician Williston Basin in the subsurface of Manitoba (modified from Nicolas and Barchyn, 2008).*

toward the base. In places, there is laminated to crossbedded and conglomeratic dolostone. This unit is recessive, pinching out toward the north, with the only other exposure around Fisher Branch (Smith, 1963; Cowan, 1978; Glass, 1990). Recent carbon-isotope profiling of the type section supported placing the formational boundary between the Williams Member of the Stony Mountain Formation and the overlying Stonewall Formation at a sharp, irregular contact (Elias et al., 2013b) located at a stratigraphically higher position than the original contact assigned by Smith (1963). This contact is indicative of a period of subaerial exposure and significant erosion, occurring after deposition of the bed that contains rounded, sand-size carbonate clasts and frosted quartz grains and before deposition of the overlying dolostone. Furthermore, the Williams Member was suggested to have been deposited during the final regressive stage of the Stony Mountain Formation (Elias et al., 2013b). On the other hand, at outcrops in the Grand Rapids uplands the Williams Member consists of planar-laminated to crossbedded dolostone, in places containing fine, subrounded quartz sand grains, with a subaerially exposed upper contact at the top of a thrombolitic interval. Therefore, the member was suggested to be part of the Stony Mountain Formation, having been formed under a tidal flat to restricted lagoon environment during a regression (Stewart, 2012; Elias et al., 2013b).

Discrepancies also occurred during subsurface investigations. In the subsurface, the Williams Member has an argillaceous marker bed defining the upper contact of the Stony Mountain Formation across southwestern Manitoba and southern Saskatchewan (Cowan, 1971; Kendall, 1976). Kendall (1976) suggested that the equivalent beds of the upper Williams Member in Saskatchewan have a conformable contact with the overlying lower Stonewall Formation, but unconformably rests on the underlying beds of the lower Williams Member. Therefore, Kendall (1976) discarded the Williams Member and put the lower equivalent beds into the Gunton Member and the upper equivalent beds into the overlying lower Stonewall Formation. In the subsurface of southwestern Manitoba, early subsurface investigations placed the member at the top of the Stony Mountain Formation (McCabe, 1978, 1979, 1984, 1988; Bannatyne, 1988). However, later core descriptions and subsurface studies in southwestern Manitoba relocated these strata within the lower Stonewall Formation (Norford et al., 1998; Bezys and Bamburak, 2004; Nicolas and Barchyn, 2008). In addition, the member was assigned to inconsistent positions in the successions.

Sedimentary facies variability

The sedimentary facies were examined in seven cores (Figure GS2017-13-1) with detailed study of trace fossils to help decipher the depositional environment. Assessing sedimentary facies variability in these strata is crucial to achieving a better correlation. Whereas previous studies focused on body fossils (Young et al., 2007; Stewart, 2012; Elias et al., 2013b), trace fossil analysis has proven useful for facies delineation in overall muddy environmental settings, where body fossils are scarce and severe dolomitization hampers detailed microfacies analysis. Various degrees of bioturbation are assessed following the bioturbation index (BI) scheme established by Taylor and Goldring (1993). Although dolomitization is pervasive in all sections, the lithological description below follows Dunham's (1962) classification of carbonate rocks.

In this study, two remarkably different deposits were included in the Williams Member in the subsurface at various locations in southern Manitoba: 1) the parallel-laminated mudstone predominated toward the northwest (cores M-3-78 [L.S. 12, Sec. 7, Twp. 40, Rge. 10, W 1st Mer., abbreviated 12-07-40-10W1], M-2-96 [03-28-44-11W1], GMM [Gulf Minerals Minitonas; 03-29-36-25W1]), and 2) arenaceous dolostone, parallel-laminated mudstone and mottled wackestone sharply underlain by parallel-laminated mudstone dominated toward the southeast (cores M-3-74 [01-21-11-01E1], M-1-84 [04-15-19-01W1], TN [Tudale Neepawa; 15-29-14-14W1]). The dense dolostone in the M-2-88 [04-11-18-01W1] core has an unusually low sand content and the reason for its unusual preservation will be the subject of future study.

Parallel-laminated mudstone

These deposits consist of parallel-laminated carbonate mudstone intercalated with crosslaminated to crossbedded grainstone (Figure GS2017-13-4a). An alternation of very fine sand-size and mud-size carbonate produces the centimetre-scale laminations. Body fossils and trace fossils are absent within the laminated intervals (BI 0). Locally, moulds of dissolved fossils occur, forming thin sheets (3–5 cm; Figure GS2017-13-4b). Sparsely bioturbated (BI 2), 5–10 cm thick intervals are intercalated within parallel-laminated intervals and contain monospecific suites of *Phycosiphon* (Figure GS2017-13-4c) and *Chondrites*. The grainstone is composed of medium- to

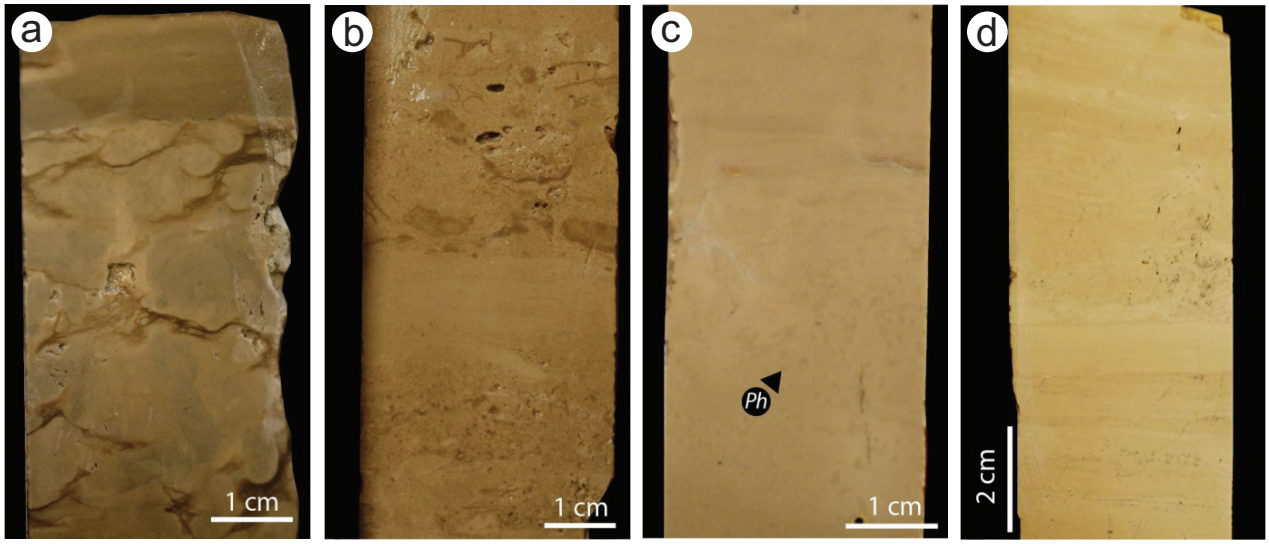

Figure GS2017-13-4: *Sedimentary facies of the parallel-laminated mudstone:* ***a)*** *sharp, basal contact of the parallel-laminated mudstone resting on top of nodular, mottled wackestone; depth 33.3 m in core M-2-96;* ***b)*** *bioclasts forming thin sheets (<5 cm) intercalated within the parallel-laminated mudstone; depth 12.2 m (40 ft.) in core M-3-74;* ***c)*** *a thin interval (BI 2–3) containing* Phycosiphon *(Ph) represents the establishment of short-term subtidal conditions between tidal flat progradations; depth 46 m in core M-2-88; and* ***d)*** *the upper part of this core interval contains crosslamination, whereas the bottom of the core interval contains planar-lamination; vugs are possibly remnants of dissolved bioclasts; depth 21.3 m (70 ft.) in core M-3-74. Top direction of the core is at the top of photo.*

fine-grained sand-size peloids and is characterized by scoured bases commonly with a basal lag underlying the low-angle crosslamination. Bioturbation is absent (BI 0) in this interval (Figure GS2017-13-4d).

Similar to the upper Red River Formation, some authors ascribed the parallel-laminated mudstone to intertidal and supratidal settings (Roehl, 1967; Kendall, 1976; Clement, 1985; Derby and Kilpatrick, 1985; Ruzyla and Friedman, 1985). However, the lack of evaporites and structures indicative of subaerial exposure may argue against a supratidal setting (Ginsburg et al., 1977). The scarcity of fossils, together with the presence of monospecific trace fossil suites, suggests restricted conditions. Whereas the producers of *Phycosiphon* and *Chondrites* would have colonized the sediment under subtidal conditions during refreshing events, the laminated intervals represent intertidal deposits formed during restricted conditions that prevented bioturbation. In contrast, the interbedded, crosslaminated grainstone records high energy sand shoals (Gonzalez and Eberli, 1997). In this case, nonbioturbation may have resulted from rapid deposition. Stewart (2012) suggested that the Williams Member in the Grand Rapids uplands was deposited under the shallowest and most restricted conditions in the Stony Mountain Formation, possibly in tidal flat and restricted lagoon environments.

Arenaceous dolostone, parallel-laminated mudstone and mottled wackestone

These deposits consist of a complex array of facies, ranging from arenaceous dolostone, parallel-laminated mudstone to mottled wackestone. In places, where bedding is well developed, the succession consists of basal medium- to fine-grained sandstone (up to tens of centimetres thick) intercalated with argillaceous dolostone, sharply overlain by parallel-laminated mudstone to mottled wackestone with a capping, thin, red-stained, argillaceous dolostone layer. The sandstone interval is rarely bioturbated (Figure GS2017-13-5a). Body fossils are absent. Sedimentary structures are remarkably rare and restricted to a few medium-grained sandstone beds, showing crossbedding and parallel lamination. The mottled wackestone is moderately to intensely bioturbated (BI 3–4), and characterized by *Thalassinoides*-like structures. Some sparse fenestrae in the mottled wackestone may be voids left by dissolved centimetre-scale skeletal remains (Figure GS2017-13-5b). Alternatively, in places where bedding was not well developed, deposits are characterized by arenaceous dolostone locally blackened by pyrite crystals (Figure GS2017-13-5c). Sand content varies at different locations, with visible quartz grains occurring locally. Crosslaminated to planar-laminated, medium-grained sandstone layers intercalate within this interval. Body fossils and trace fossils are usually absent. Certain intervals of arenaceous dolostone were stained by the red argillaceous layers intercalated within the successions.

As noted above, the parallel-laminated mudstone represents tidal flat deposits. The mottled wackestone with *Thalassinoides*-like structures has been interpreted as recording deposition in shallow subtidal settings (Kendall, 1977; Myrow, 1995; Zenger, 1996; Jin et al., 2012). Generally, shallow-marine, restricted conditions are characterized by the lack of macrofossils (Elias et al., 2013b) together with sparsely preserved bioturbation. Therefore, the *Phycosiphon* producer may have colonized during short-term refreshings likely related to flooding events, whereas the occurrence of *Thalassinoides*-like

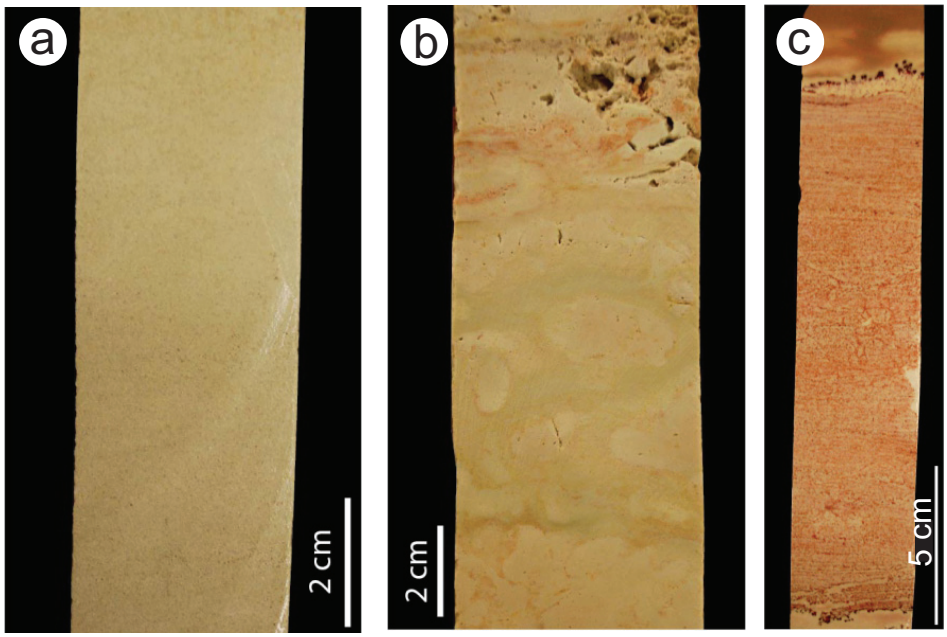

Figure GS2017-13-5: *Sedimentary facies of the arenaceous dolostone and mottled wackestone:* ***a)*** *a medium- to fine-grained sandstone layer (10 cm thick) intercalated within the arenaceous dolostone interval; depth 15.7 m (51.4 ft.) in core M-3-74;* ***b)*** *mottled wackestone; the nodular appearance results from the presence of burrows attributed to* Thalassinoides*; the upper part of the core interval contains vugs of body fossils; depth 10.4 m (34 ft.) in core M-3-74;* ***c)*** *planar-laminated to crosslaminated arenaceous dolostone, containing high sand content; black dots are pyrite crystals; depth 16.5 m (54 ft.) in core M-3-74. Top direction of the core is at the top of photo.*

burrows represents more open marine conditions. The whole succession, recording all the subenvironments interpreted above, is <10 m thick. This significant vertical change in sedimentary facies suggests a highly complex facies mosaic, probably representing a nearshore environment that encompassed a wide variety of subenvironments. Further evidence of a relative sea-level fall is provided by the capping arenaceous dolostone in the type section, which was interpreted to be the result of a period of subaerial exposure (Elias et al., 2013b).

Discussion

It can be surmised that confusion regarding the precise placement of the Williams Member originates from the application of different definitions. Specifically, in core M-2-96, the parallel-laminated mudstone, representing tidal flat deposits (depth 28.0–33.3 m), was included in the Williams Member and placed within the lowermost Stonewall Formation (R.K. Bezys and K. Horsman, unpublished core description, 1996; Figure GS2017-13-6). On the other hand, very different facies in core M-3-74, comprising vuggy, mottled, argillaceous dolostone intercalated with arenaceous dolostone representing nearshore deposits (depth 6.5–18 m [21.3–59.1 ft.]), were also placed within the lowermost Stonewall Formation (H.R. McCabe, unpublished core description, 1974; Figure GS2017-13-6). H.R. McCabe (unpublished core description, 1974) initially assigned the Stonewall Formation–Stony Mountain Formation contact to depth 12.6 m (41.3 ft.) but later moved it to depth 18.0 m (59.1 ft.; Figure GS2017-13-6).

Correlation problems lie not only in the different nature of these deposits, but also in the fact that significant diachronism is involved. A single thin dolomitic mudstone bed containing angular clasts of the same lithology as the underlying facies underlies the Williams Member in core M-3-74. These types of contacts commonly cap the tidal flat deposits toward the northwest, specifically at depths 388.6 m (1275 ft.) and 79.7 m in cores GMM and M-3-78, respectively. The underlying successions of the Stony Mountain Formation become dominated by the mottled, nodular wackestone at these places. Also, this contact is believed to mark the fragmental, sharp top of the Williams Member at depth 28.0 m in core M-2-96. Thin, shaly layers invariably mantled these contacts toward the northwest, and are comparable to the marker bed at the top of the Stony Mountain Formation in the subsurface of Saskatchewan (Kendall, 1976). These strata are analogous to equivalent strata in the Big Horn Dolomite in Wyoming, where similar contacts represent subaerial exposure at the termination of the parasequences of the Horseshoe Mountain Member (Holland and Patzkowsky, 2012). It is possible that intervals between three thin shaly marker beds situated higher in the sequence, in places mixed with patterned dolomite, record parasequences overlying the Stony Mountain Formation in southern Manitoba (Figure GS2017-13-7b, c). These possible parasequences could have been formed during a transition from a greenhouse climate to an icehouse climate preceding the Hirnantian glaciation (Holland and Patzkowsky, 2012). Coincidently, three to four informally assigned, reddish-stained marker beds characterize the lower Stonewall Formation in the subsurface of southern

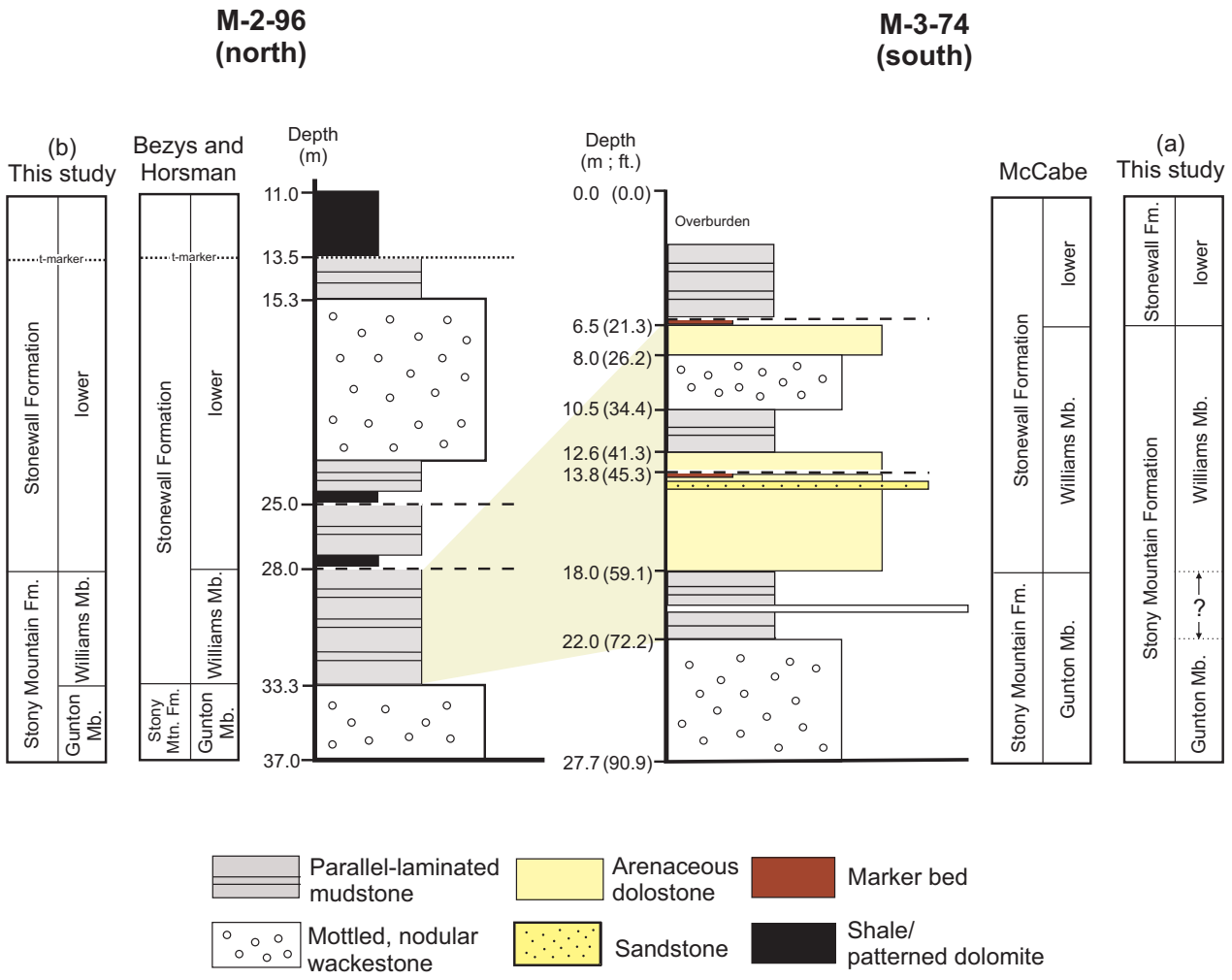

Figure GS2017-13-6: *Correlation between cores M-2-96 and M-3-74, showing previous subdivisions assigned to the two cores and alongside are the two possible revised subdivisions (labelled a and b) recommended from this study. The beige shaded area marks one revised correlation (b) of the Williams Member of the Stony Mountain Formation. The long dash lines mark shaly marker beds in core M-2-96 and reddish-stained marker beds in core M-3-74. Bezys and Horsman from unpublished core descriptions (1996) and McCabe from unpublished core descriptions (1974). Abbreviation: Mtn., Mountain.*

Manitoba (Figure GS2017-13-7a). In early investigations, the Williams Member was assigned to the intervals overlying the contacts at places where the Williams Member was considered to be the dolomite with shale interbeds, and overlying the contact, at 73.6–79.7 m in M-3-78, was placed in the Stony Mountain Formation (McCabe, 1978). Later identification of the upper Stony Mountain Formation contact and the capping marker bed is believed to be the reason for moving the Williams Member to within the lower Stonewall Formation (Norford et al., 1998).

The type section of the Williams Member in the Stonewall quarry is representative of the member in southern Manitoba, and Smith (1963) suggested deposition was continuous from the Gunton Member to the Williams Member. However, problems arose correlating the members toward the northwest, where the transitional intervals between the Gunton Member and the lower Stonewall Formation become dominated by parallel-laminated mudstone, representing tidal flat deposits with no sand influx. The authors agree with Elias et al. (2013b) that the Williams Member should be included in the upper part of the Stony Mountain Formation. Therefore, identifying the upper contact or marker bed of the Stony Mountain Formation is crucial. In addition, the parallel-laminated mudstone with shaly interbeds situated above the upper contact of the Stony Mountain Formation should not be assigned to the Williams Member.

The strata in the 6.5–18.0 m (21.3–59.1 ft.) depth interval in M-3-74 is comparable to the Williams Member section in the Stonewall quarry, and the Stonewall Formation–Stony Mountain Formation contact identified in the quarry is suggested to be placed at the top of the interval in M-3-74. In M-2-96, the upper contact of the Stony Mountain Formation is placed at a depth of 28.0 m. The Williams Member should not be assigned to the parallel-laminated mudstone with shaly interbeds situated

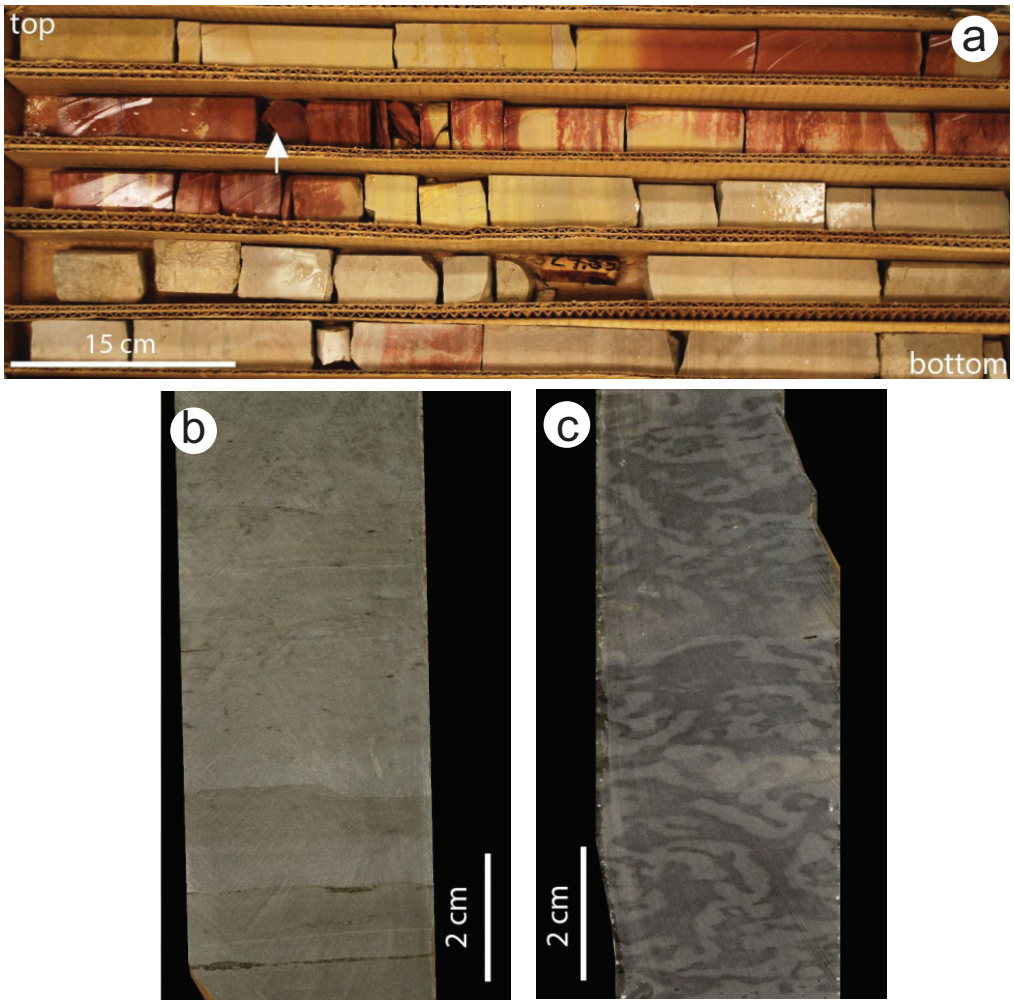

Figure GS2017-13-7: *Marker beds in the subsurface of southern Manitoba:* ***a)*** *an argillaceous, red-stained marker bed (indicated by arrow) intercalated within parallel-laminated mudstone and arenaceous dolostone in the Williams Member; depth 27.75–29.15 m in core M-1-84;* ***b)*** *a shaly layer punctuated within argillaceous dolostone caps the Stony Mountain Formation; depth 386.5 m (1268 ft.) in core Gulf Minerals Minitonas (GMM);* ***c)*** *a thin patterned dolomite layer marks the lower Stonewall Formation; depth 75.3 m in core M-3-78.*

above depth 28.0 m in M-2-96 (Figure GS2017-13-6). To address these issues, two possible stratigraphic revisions are proposed herein.

The first revision suggests that based on the characteristic sand content in the type section, the Williams Member in southern Manitoba should be limited to the intervals rich in clastic material and indicative of nearshore deposits. In this scenario, the member occurs in the south and pinches out toward the north, and is comparable to the trend in the outcrop belt. However, the distinct tidal flat deposits of the uppermost part of the Stony Mountain Formation cannot be differentiated from the underlying thick, mottled, nodular wackestone of the Gunton Member. These distinct tidal flat deposits are absent within the Gunton Member. For instance, the Williams Member of the Stony Mountain Formation is assigned to the interval at depth 6.5–18.0 m (21.3–59.1 ft.) in M-3-74 and pinches out toward the northwest. Although the 28.0–33.3 m depth interval in M-2-96 correlates to the 18.0–22 m depth interval in M-3-74, the intervals are absent within the Gunton Member (Figure GS2017-13-6, stratigraphic column a).

The second revision suggests that in the Williams Member in the subsurface of southern Manitoba the nearshore deposits in the south correlate to the tidal flat deposits in the north with a northward decrease in arenaceous content. In this case, both the tidal flat deposits and nearshore deposits would be included in the uppermost interval of the Stony Mountain Formation. In this scenario, the Williams Member is assigned to intervals of 28.0–33.3 m (Figure GS2017-13-6, stratigraphic column b) and 6.5–22.0 m (21.3–72.2 ft.; correlation shown in beige in Figure GS2017-13-6) in M-2-96 and M-3-74, respectively, and is included in the uppermost Stony Mountain Formation.

Depositional trend implications of the Williston Basin

Longman and Haidl (1996) proposed that the boundaries between members in the Willston Basin were isochronous

based on a layer-cake stratigraphy and the assumption of basin-wide environmental changes. However, the apparent layer-cake stratigraphy partially originated from the loose definition of members. If the revised definitions of the Williams Member are adopted then progradational sedimentation with diachronous boundaries between facies is expected since this unit represents the maximum regressive phase of the uppermost part of the Stony Mountain Formation. Allogenic controls, especially eustatic fluctuations, undoubtedly impacted on stratal architecture, highlighting the need for high-resolution sequence stratigraphic studies, which may assist with intrabasinal correlation of key surfaces. Future studies applying sequence stratigraphic concepts to the study of these epeiric deposits may help to provide a more accurate picture of Ordovician facies distribution and depositional history for the Williston Basin.

Economic considerations

Although only two oil shows have been reported in the Stony Mountain Formation (Nicolas and Barchyn, 2008), the revised schemes proposed in this study may help to refine subsurface stratigraphy and long-range correlations. This is critical in understanding the oil pathways, which in turn help petroleum companies create exploration models they can use to build their wildcat exploration programs.

Acknowledgments

This research was funded by the American Association Petroleum Geologists Foundation Grants-in-Aid program and a SEPM student research grant to the first author, together with Natural Sciences and Engineering Research Council of Canada (NSERC) Discovery Grants 311727-05/08/13 and 311726-05/08/15 to the second author and third author, respectively. Special thanks are given to M. Nicolas (Manitoba Geological Survey), who provided core information, guided the visit to the quarries and helped with this report; C. Epp (Manitoba Geological Survey), who provided enthusiastic and invaluable assistance in the Midland Sample and Core Library; and all the staff of the Midland Sample and Core Library, who assisted in preparing the core for viewing. The authors especially appreciate R. Elias' (University of Manitoba) extensive reviewing and insightful suggestions.

References

Bannatyne, B.B. 1988: Dolomite reservoirs of southern Manitoba; Manitoba Industry, Economic Development and Mines, Manitoba Geological Survey, Economic Geology Report ER85-1, 39 p.

Bezys, R.K. and Bamburak, J.D. 2004: Lower to middle Paleozoic stratigraphy of southwestern Manitoba; Manitoba Industry, Trade and Mines, Manitoba Geological Survey, WCSB/TGI II Field Trip guidebook, Winnipeg, Manitoba, May 25–28, 2004, 72 p.

Bezys, R.K. and McCabe, H.R. 1996: Lower to middle Palaeozoic stratigraphy of southwestern Manitoba; Geological Association of Canada–Mineralogical Association of Canada, Joint Annual Meeting, Winnipeg, Manitoba, May 27–29, 1996, Field Trip Guidebook B4, 92 p.

Clement, J.H. 1985: Depositional sequences and characteristics of Ordovician Red River reservoirs, Pennel Field, Williston Basin, Montana; *in* Carbonate Petroleum Reservoirs, P.O. Roehl and P.W. Choquette (ed.), Springer-Verlag, New York, New York, p. 71–84.

Cowan, J.R. 1971: Ordovician and Silurian stratigraphy of the Interlake area, Manitoba; *in* Geoscience Studies in Manitoba, A.C. Turnock (ed.), Geological Association of Canada, Special Paper 9, p. 235–241.

Cowan, J.R. 1978: Ordovician and Silurian stratigraphy in the Interlake area, Manitoba; M.Sc. thesis, University of Manitoba, Winnipeg, Manitoba, 73 p.

Demski, M.W., Wheadon, B.J., Stewart, L.A., Elias, R.J., Young, G.A., Nowlan, G.S. and Dobrzanski, E.P. 2015: Hirnantian strata identified in major intracratonic basins of central North America: implications for uppermost Ordovician stratigraphy; Canadian Journal of Earth Sciences, v. 52, no. 1, p. 68–76.

Derby, J.R. and Kilpatrick, J.T. 1985: Ordovician Red River dolomite reservoirs, Killdeer Field, North Dakota; *in* Carbonate Petroleum Reservoirs, P.O. Roehl and P.W. Choquette (ed.), Springer-Verlag, New York, New York, p. 59–69.

Dorador, J., Buatois, L.A., Mángano, M.G. and Rodríguez-Tovar, F.J. 2014: Ichnologic and sedimentologic analysis of the Upper Ordovician Winnipeg Formation in southeastern Saskatchewan; *in* Summary of Investigations 2014, Volume 1, Saskatchewan Geological Survey, Saskatchewan Ministry of the Economy, Miscellaneous Report 2014-4.1, Paper A-4, 15 p.

Dunham, R.J. 1962: Classification of carbonate rocks according to depositional texture; *in* Classification of Carbonate Rocks, W.E. Ham (ed.), American Association of Petroleum Geologists, Memoir 1, p. 108–121.

Elias, R.J. 1991: Environmental cycles and bioevents in the Upper Ordovician Red River-Stony Mountain solitary rugose coral province of North America; *in* Advances in Ordovician Geology, C.R. Barnes and S.H. Williams (ed.), Geological Survey of Canada, Paper 90-9, p. 205–211.

Elias, R.J., Young, G.A., Lee, D.-J. and Bae, B.-Y. 2013a: Coral biogeography in the Late Ordovician (Cincinnatian) of Laurentia; *in* Early Palaeozoic Biogeography and Palaeogeography, D.A.T. Harper and T. Servais (ed.), Geological Society of London, Memoir no. 38, p. 97–115.

Elias, R.J., Young, G.A., Stewart, L.A., Demski, M.W., Porter, M.J., Lukie, T.D., Nowlan, G.S. and Dobrzanski, E.P. 2013b: Ordovician-Silurian boundary interval in the Williston Basin outcrop belt of Manitoba: a record of global and regional environmental and biotic change; Geological Association of Canada–Mineralogical Association of Canada, Joint Annual Meeting, Field Trip Guidebook FT-C5, Winnipeg, Manitoba, May 22–24, 2013, 49 p.

Ginsburg, R.N., Hardie, L.A., Bricker, O.P., Garrett, P. and Wanless, H.R. 1977: Exposure index: a quantitative approach to defining position within the tidal zone; *in* Sedimentation on the Modern Carbonate Tidal Flats of Northwest Andros Island, Bahamas, L.A. Hardie (ed.), The Johns Hopkins University Studies in Geology, v. 22, p. 7–11.

Glass, D.J. (ed.) 1990: Lexicon of Canadian Stratigraphy, Volume 4, Western Canada, including eastern British Columbia, Alberta, Saskatchewan and southern Manitoba; Canadian Society of Petroleum Geologists, Calgary, Alberta, 772 p.

Gonzalez, R. and Eberli, G.P. 1997: Sediment transport and bedforms in a carbonate tidal inlet, Lee Stocking Island, Exumas, Bahamas; Sedimentology, v. 44, issue 6, p. 1015–1030.

Holland, S.M. and Patzkowsky, M.E. 2012: Sequence architecture of the Bighorn Dolomite, Wyoming, USA: transition to the Late Ordovician icehouse; Journal of Sedimentary Research, v. 82, no. 8, p. 599–615.

Jin, J., Harper, D.A., Rasmussen, J.A. and Sheehan, P.M. 2012: Late Ordovician massive-bedded *Thalassinoides* ichnofacies along the palaeoequator of Laurentia; Palaeogeography, Palaeoclimatology, Palaeoecology, v. 367, p. 73–88.

Kendall, A.C. 1976: The Ordovician carbonate succession (Bighorn Group) of southeastern Saskatchewan; Saskatchewan Department of Mineral Resources, Saskatchewan Geological Survey, Sedimentary Geology Division, Report no. 180, 186 p.

Kendall, A.C. 1977: Origin of dolomite mottling in Ordovician limestones from Saskatchewan and Manitoba; Bulletin of Canadian Petroleum Geology, v. 25, p. 480–504.

Kent, D.M. and Christopher, J.E. 1994: Geological history of the Williston Basin and Sweetgrass arch; *in* Geological Atlas of the Western Canada Sedimentary Basin, G.D. Mossop and I. Shetsen (comp.), Canadian Society of Petroleum Geologists, Calgary, Alberta and Alberta Research Council, Edmonton, Alberta, p. 421–429.

Kreis, L.K. 2004: Geology of the Middle Ordovician Winnipeg Formation in Saskatchewan; *in* Lower Paleozoic Map Series – Saskatchewan, Saskatchewan Industry and Resources, Miscellaneous Report 2004-8, Sheet 3.

Longman, M.W. and Haidl, F.M. 1996: Cyclic deposition and development of porous dolomites in the Upper Ordovician Red River Formation, Williston Basin; *in* Paleozoic Systems of the Rocky Mountain Region, M.W. Longman and M.D. Sonnenfeld (ed.), SEPM, Rocky Mountain Section, p. 29–46.

Martiniuk, C.D. 1992: Lower Paleozoic sequence, southwestern Manitoba - an overview; Manitoba Energy and Mines, Petroleum Branch, Petroleum Open File, POF13-92, 40 p.

McCabe, H.R. 1974: Stratigraphic core hole program; *in* Summary of Geological Field Work 1974, Manitoba Department of Mines, Resources and Environmental Management, Mineral Resources Division, Exploration and Geological Survey Branch, Geological Paper GP2/74, p. 53–54.

McCabe, H.R. 1978: Stratigraphic core hole and mapping programme; *in* Report of Field Activities 1978, Manitoba Department of Mines, Resources and Environmental Management, Mineral Resources Division, p. 64–67.

McCabe, H.R. 1979: Stratigraphic mapping program; *in* Report of Field Activities 1979, Manitoba Department of Mines, Natural Resources and Environment, Mineral Resources Division, p. 72–75.

McCabe, H.R. 1984: Stratigraphic mapping and stratigraphic and industrial minerals core hole program; *in* Report of Field Activities 1984, Manitoba Energy and Mines, Mineral Resources, p. 136–143.

McCabe, H.R. 1988: Stratigraphic mapping and core hole program; *in* Report of Field Activities 1988, Manitoba Energy and Mines, Minerals Division, p. 130–138.

Myrow, P.M. 1995: *Thalassinoides* and the enigma of Early Paleozoic open-framework burrow systems; Palaios, v. 10, p. 58–74.

Nicolas, M.P.B. and Barchyn, D. 2008: Williston Basin Project (Targeted Geoscience Initiative II): summary report on Paleozoic stratigraphy, mapping and hydrocarbon assessment, southwestern Manitoba; Manitoba Science, Technology, Energy and Mines, Manitoba Geological Survey, Geoscientific Paper GP2008-2, 21 p.

Norford, B.S., Haidl, F.M., Bezys, R.K., Cecile, M.P., McCabe, H.R. and Paterson, D.F. 1994: Middle Ordovician to lower Devonian strata of the Western Canada Sedimentary Basin; *in* Geological Atlas of the Western Canada Sedimentary Basin, G.D. Mossop and I. Shetsen (comp.), Canadian Society of Petroleum Geologists, Calgary, Alberta and Alberta Research Council, Edmonton, Alberta, p. 109–127.

Norford, B.S., Nowlan, G.S., Haidl, F.M. and Bezys, R.K. 1998: The Ordovician-Silurian boundary interval in Saskatchewan and Manitoba; *in* Eighth International Williston Basin Symposium, J.E. Christopher and C.F. Gilboy (ed.), Saskatchewan Ministry of Energy and Resources, Saskatchewan Geological Society, Special Publication no. 13, p. 27–45.

Potter, D. 2006: Relationships of Cambro-Ordovician stratigraphy to paleotopography on the Precambrian basement, Williston Basin; *in* Saskatchewan and Northern Plains Oil & Gas Symposium (2006), C.F. Gilboy and S.G. Whittaker (ed.), Saskatchewan Geological Society, Special Publication 19, p. 63–73.

Roehl, P.O. 1967: Stony Mountain (Ordovician) and Interlake (Silurian) facies analogs of Recent low-energy marine and subaerial carbonates, Bahamas; American Association of Petroleum Geologists, Bulletin 51, p. 1979–2032.

Ross, R.J., Jr., Adler, F.J., Amsden, T.W., Bergstrom, D., Bergstrom, S.M., Carter, C., Churkin, M., Cressman, E.A., Derby, J.R., Dutro, J.T.J., Ethington, R.L., Finney, S.C., Fisher, D.W., Fisher, J.H., Harris, A.G., Hintze, L.F., Kentner, K.B., Kolata, D.L., Landing, E., Neuman, R.B., Sweet, W.C., Pojeta, J.J., Potter, A.W., Rader, E.K., Repetski, J.E., Shaver, R.H., Thompson, T.L. and Webers, G.F. 1982: The Ordovician System in the United States; International Union of Geological Sciences, Publication 12, 73 p.

Ruzyla, K. and Friedman, G.M. 1985: Factors controlling porosity in dolomite reservoirs of the Ordovician Red River Formation, Cabin Creek Field, Montana; *in* Carbonate Petroleum Reservoirs, P.O. Roehl and P.W. Choquette (ed.), Springer-Verlag, New York, New York, p. 39–58.

Smith, D.L. 1963: A lithologic study of the Stony Mountain and Stonewall formations in southern Manitoba; M.Sc. thesis, University of Manitoba, Winnipeg, Manitoba, 219 p.

Stewart, L.A. 2012: Paleoenvironment, paleoecology, and stratigraphy of the uppermost Ordovician section, north of Grand Rapids, Manitoba; M.Sc. thesis, University of Manitoba, Winnipeg, Manitoba, 254 p.

Taylor, A.M. and Goldring, R. 1993: Description and analysis of bioturbation and ichnofabric; Journal of the Geological Society, v. 150, p. 141–148.

Vigrass, L.W. 1971: Depositional framework of the Winnipeg Formation in Manitoba and eastern Saskatchewan; *in* Geoscience Studies in Manitoba, A.C. Turnock (ed.), Geological Association of Canada, Special Paper no. 9, p. 225–234.

Young, G.A., Rudkin, D.M., Dobrzanski, E.P., Robson, S.P. and Nowlan, G.S. 2007: Exceptionally preserved Late Ordovician biotas from Manitoba, Canada; Geology, v. 35, p. 883–886.

Zenger, D.H. 1996: Dolomitization patterns in widespread “Bighorn Facies” (Upper Ordovician), western craton, USA; Carbonates and Evaporites, v. 11, p. 219–225.

GS2017-14

Detailed examination of drillcore RP95-17, west-central Manitoba (NTS 63C7): evidence of potential for Mississippi Valley–type lead-zinc deposits

by K. Lapenskie and M.P.B. Nicolas

In Brief:

- In situ Pb-Zn mineralization have been identified in Paleozoic carbonates
- Two new occurrences of galena and sphalerite in the Winnipegosis area have been identified in core
- Structural and geological controls indicate that the Mississippi Valley-type deposits may occur in Manitoba

Citation:
Lapenskie, K. and Nicolas, M.P.B. 2017: Detailed examination of drillcore RP95-17, west-central Manitoba (NTS 63C7): evidence of potential for Mississippi Valley–type lead-zinc deposits; *in* Report of Activities 2017, Manitoba Growth, Enterprise and Trade, Manitoba Geological Survey, p. 158–172.

Summary

Several examples of in situ lead-zinc mineralization have been found in Paleozoic carbonate rocks in the Williston Basin, which extends into southwestern Manitoba. The Manitoba Geological Survey (MGS) and several companies have undertaken exploratory investigations into occurrences of carbonate-hosted sphalerite-galena mineralization in the province but have yet to find any deposits. In the 1990s, Cominco Ltd. conducted several exploration programs in the Lake Winnipegosis area, looking for base-metal potential in the Superior boundary zone, which lies beneath a Phanerozoic cover. A re-examination of Paleozoic strata in drillcore from one of these programs has identified two new occurrences of in situ mineralization with a style comparable to that in Mississippi Valley–type deposits. Galena was identified in dolostone of the Ordovician Red River Formation and sphalerite was observed in a subvertical, calcite-lined fracture in dolostone of the lower member of the Devonian Winnipegosis Formation. Numerous structural and geological conditions in the province indicate that the Mississippi Valley–type model may be applicable within Manitoba. Platformal carbonates, shales, evaporites, karsting and reefal structures, often associated with Mississippi Valley–type deposits, are all present in southwestern Manitoba. Also, the Superior boundary zone may have acted as a source of base-metal–bearing fluids and provided conduits for fluid flow.

Introduction

There is evidence to suggest potential for Mississippi Valley–type (MVT) deposits in Manitoba, specifically in the Williston Basin (Gale and Conley, 2000; Bamburak and Klyne, 2004), which is part of the larger Western Canada Sedimentary Basin (WCSB). There are 16 known MVT deposits in Canada, with the significant Pine Point deposit in the Northwest Territories located within the WCSB. Southwestern Manitoba is blanketed by a thick package of southwesterly dipping Phanerozoic sedimentary rocks, which was deposited within this basin. Underlying these strata are the Precambrian igneous and metamorphic rocks belonging to the Superior craton and Trans-Hudson orogen (THO), which are sutured together along the Superior boundary zone (SBZ).

Mississippi Valley–type deposits consist of stratabound, carbonate-hosted assemblages of sphalerite, galena and iron sulphides, typically occurring within marine platform dolostone and limestone near basinal edges (Paradis et al., 2007; Leach et al., 2010). It is generally understood that metalliferous, saline basinal waters driven by large-scale tectonic events are the source of ore fluids. Mississippi Valley–type deposits often occur in clusters of tens to hundreds of individual ore bodies that make up a broad district. The ore bodies are typically controlled by local lithological and structural features, such as solution collapse breccias, faults/fractures and shale-carbonate facies changes.

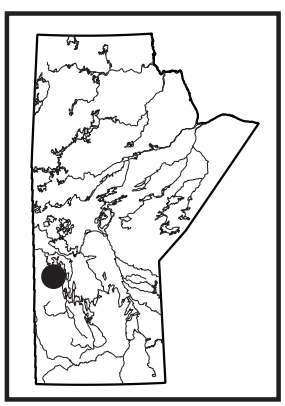

Cominco Ltd. conducted an exploration program in the Lake Winnipegosis area in 1995, targeting Precambrian base-metal mineralization. Drillcore RP95-17 (Assessment File 94638, Manitoba Growth, Enterprise and Trade, Winnipeg) was recently examined by the authors, and resulted in the discovery of galena in the Ordovician Red River Formation and sphalerite in the Devonian Winnipegosis Formation. The former represents the first known occurrence of in situ carbonate-hosted galena in the Williston Basin.

Previous work

Exploration for MVT deposits in Manitoba was prompted by the discovery of a galena pebble in surficial, glacially derived sediments near Balmoral (Figure GS2017-14-1, Table GS2017-14-1; McCabe, 1969). Cubic grains of galena may have been identified from the Winnipeg Formation near Grindstone Point, however, it was noted that the grains could have been tarnished pyrite (Genik, 1952). No samples were collected and no analyses were done of these cubic minerals, therefore, it

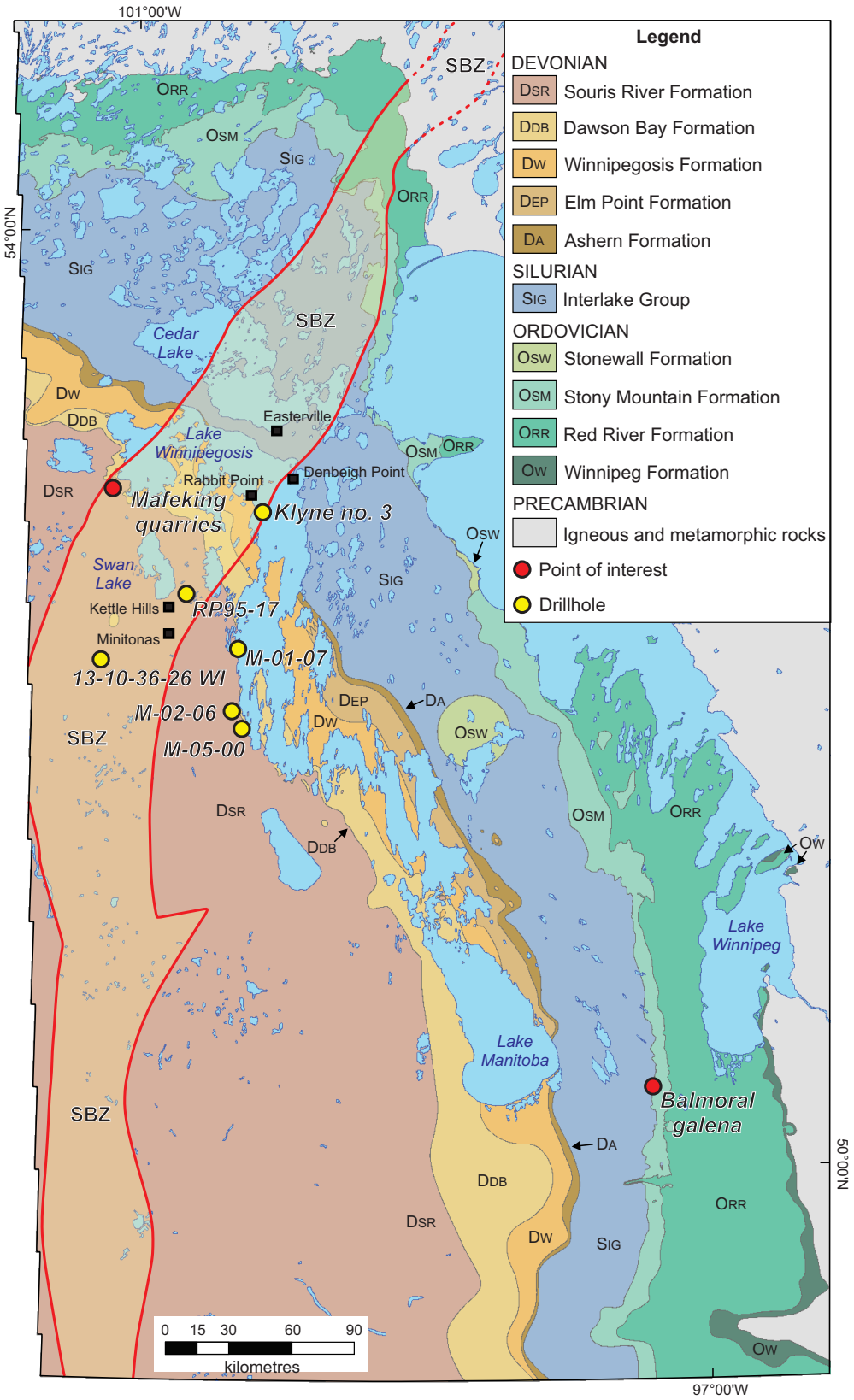

Figure GS2017-14-1: *Regional bedrock geology of southwestern Manitoba (after Nicolas et al., 2010); formations younger than the Souris River Formation are not shown. The region consists of sedimentary rocks of the Williston Basin draped over Precambrian igneous and metamorphic rocks (exposed in the northern and eastern parts of the map area). The limits of the Superior boundary zone (SBZ) are projected to surface. Also indicated are occurrences of Pb-Zn mineralization and the locations of other features of relevance to the search for Mississippi Valley–type (MVT) deposits in Manitoba.*

Table GS2017-14-1: Reported occurrences of in situ carbonate-hosted sphalerite-galena and lithological features in Manitoba that are comparable to Mississippi Valley–type districts elsewhere. The UTM co-ordinates are in NAD83, Zone 14.

	Easting	Northing	Mineralization	Depth (m)	Stratigraphic unit	Reference
Balmoral pebble	NE¼-26-14-1-E1[1]		Galena	n/a	Surficial sediments	Gale and Conley (2000)
Mafeking quarries	361740	5855814	Prairie-type	n/a	Point Wilkins Member, Souris River Formation	Fedikow et al. (2004)
13-10-36-26W1 drillhole	356371	5772556	Sphalerite	429.2	Stony Mountain Formation	Assessment File 92116 (Manitoba Growth, Enterprise and Trade, Winnipeg)
Klyne no. 3 drillhole	433525	5842645	Sphalerite (black-jack and ruby-jack)	8.5; 15.2; 16.8; 17.7; 18.6	Upper Interlake Group	Bamburak and Klyne (2004); Assessment File 74128
M-05-00 drillhole	423445	5739324	Sphalerite, minrecordite, stilleite	114.2	Upper member, Winnipegosis Formation	Bamburak (2007)
M-02-06 drillhole	415171	5739363	Sphalerite	72.8	Second Red Bed Member, Dawson Bay Formation	Bamburak (2006, 2007)
M-01-07 drillhole	421088	5774977	Saddle dolomite; hydrothermal dolomite	80.81–122.52	Cedar Lake Formation, Interlake Group	Bamburak (2007), Rawluk (2010)
RP95-17 drillhole	396816	5803656	Sphalerite; galena	109.95–110.28; 344.87 (TVD)	Lower member, Winnipegosis Formation; lower Red River Formation	Assessment File 94638

[1] No UTM coordinates available; galena pebble was collected in NE ¼, Sec. 26, Twp. 14, Rge. 1, E 1st Mer.
Abbreviations: n/a, not applicable; TVD, total vertical depth

should not be considered as a confirmed occurrence of in situ Pb-Zn mineralization.

Geological, geochemical and geophysical exploration programs to investigate MVT potential in Manitoba began in 1970 and lasted until the present day. Cominco Ltd. worked in the Easterville and Denbeigh Point area from 1970 to 1971, attempting to locate Pb-Zn mineralization (Assessment File 91785). During that same time period, Husky Oil Ltd. conducted an electromagnetic survey and drill program in the vicinity of Dawson Bay (Assessment files 91776, 92239).

Gulf Minerals Canada Ltd. drilled four holes in the Minitonas area in 1976 to examine the base-metal content of Paleozoic carbonates (Assessment File 92116). The Pb, Zn and Cu values from core were insufficient to warrant further work in this area. However, a single occurrence of sphalerite was noted from one of the cores (13-10-36-26W1) and is described below (see 'Carbonate-hosted Pb-Zn mineralization in Manitoba' section).

From 1979 to 1983, Canadian Nickel Company Limited (Canico) applied several techniques to explore for MVT deposits in the Dawson Bay area. A soil, rock and water sampling program was initially conducted, with numerous geochemical anomalies detected; geophysical surveys were also conducted (Assessment files 93877, 93878). Exploration activities culminated in a drill program, however, none of the holes intersected Pb-Zn mineralization (Assessment File 92830). Canico terminated exploration for MVT deposits in Manitoba in 1983.

To date, the best known example of carbonate-hosted Pb-Zn mineralization in Manitoba is located near Pemmican Island, in the north basin of Lake Winnipegosis. In 2004, Klyne Exploration drilled three holes near the island, with Klyne no. 3 encountering a 15 cm interval of pyrite and sphalerite within uppermost Interlake Group dolostone (Figure GS2017-14-1, Table GS2017-14-1; Bamburak and Klyne, 2004; Assessment File 74128). Analyses demonstrated the sulphide interval was 4.59% Zn, 0.41% Pb and 0.014% Cu. Previous work in the area also demonstrated that sulphide-bearing dolostone clasts along the shorelines of the north basin of Lake Winnipegosis contained elevated values of Ni, Zn and Pb, among other base metals (Bamburak et al., 2002). The mineralogy of the sulphides was not determined.

The MGS previously conducted investigations into the potential for MVT deposits in Manitoba. A large-scale sampling program by Gale and Conley (2000) involved analyzing approximately 6300 samples from various stratigraphic drillcores. This program demonstrated widespread anomalous values of Cu, Zn, Pb and Ni in Paleozoic strata across the Williston Basin. Gale and Conley (2000) concluded that the anomalous values obtained through this study, along with other geological features, indicated potential for MVT deposits west of Lake

Winnipegosis. Fedikow et al. (2004) investigated 'Prairie-type microdisseminated mineralization' in the Late Devonian Point Wilkins Member of the Souris River Formation in the Mafeking area. Altered and silicified cone structures in the high-calcium limestone were found to contain precious and base metals (Au, Zn, Ni, Co, Fe), and indicated that processes favourable for MVT deposits had occurred in this area. During a MGS stratigraphic drillcore program, several drillcores were chosen for further exploration for sphalerite-galena mineralization based on previous findings (Bezys, 2000; Bamburak, 2006, 2007). However, only a few of these cores intersected Pb-Zn mineralization (see 'Carbonate-hosted Pb-Zn mineralization in Manitoba' section).

Regional geology

Southwestern Manitoba is blanketed by a thick succession of sedimentary rocks that were deposited in the Williston Basin during the Phanerozoic (Figure GS2017-14-1). Deposition during the Paleozoic spanned the Cambrian to the Mississippian periods, with significant episodes of nondeposition and/or erosion occurring between the Cambrian and Ordovician, and the Silurian and Devonian periods. These Paleozoic rocks are composed predominantly of marine platform carbonate rocks, with lesser amounts of siliciclastic and evaporitic rocks (Figure GS2017-14-2).

Underlying these sedimentary strata are Precambrian igneous and metamorphic rocks. The SBZ is a 40–50 km wide suture zone between the Archean Superior craton to the southeast and the Paleoproterozoic THO to the northwest (Bleeker, 1990). The SBZ extends from the southwestern corner of Manitoba beneath the Williston Basin, and continues northeastward through the Hudson Bay Lowland, beneath the Hudson Bay Basin (Figure GS2017-14-1). The Manitoba portion of the Hudson Bay Basin comprises a series of Paleozoic carbonates and could also theoretically host MVT deposits.

The SBZ hosts magmatic Ni-Cu deposits of the Thompson nickel belt, with some of these deposits occurring below the Phanerozoic cover of the Williston Basin. The Minago (Ni-Cu-platinum group elements [PGE]) and Tower (Cu-Zn) deposits both occur along the SBZ beneath the northeastern portion of the Williston Basin, north of William Lake. There are also known Cu-Zn and Ni-Cu-PGE deposits that occur beneath the northern margin of the Williston Basin, hosted within the Flin Flon and Snow Lake greenstone belts of the THO (Gagné, 2016; Reid and Gagné, 2016; Reid, GS2017-7, this volume).

Carbonate-hosted Pb-Zn mineralization in Manitoba

Several occurrences of sphalerite and galena mineralization have been reported in Paleozoic strata in Manitoba (Table GS2017-14-1, Figure GS2017-14-1). Gulf Minerals Canada Ltd. reported a single crystal of sphalerite in dolostone of the Stony Mountain Formation (drillcore 13-10-36-26W1; Assessment File 92116), representing the first documented occurrence of in situ carbonate-hosted base-metal mineralization in Manitoba.

McCabe (1980) noted "honey-coloured sphalerite" in drillcore M-06-80, which was identified by X-ray diffraction (XRD), however, the data was never published and is no longer available. To confirm the results, the drillcore was resampled. Microscope and X-ray fluorescence (XRF) analyses of the samples suggest that the "honey-coloured sphalerite" is in fact coarsely crystalline dolomite partially infilling vuggy porosity (Figure GS2017-14-3a). Small stringers of dark grey material, observed in cut sections of core under stereo microscope, may be very finely disseminated sphalerite mineralization, which could account for elevated Zn values obtained from this interval (Gale and Conley, 2000).

Drillcore M-05-00 was bored in the vicinity of drillcore M-06-80 to confirm the presence of the above-described "honey-coloured sphalerite" (Bezys, 2000). The core intersected black-jack sphalerite and pyrite in a vertical fracture and along a lamination surface in the inter-reefal facies of the upper member of the Winnipegosis Formation (Figure GS2017-14-3b). The XRD analysis also demonstrated the presence of minrecordite (zinc-carbonate) and stilleite (zinc-selenide; Table GS2017-14-1; Bamburak, 2007). Drillcore M-02-06, also completed to test for Pb-Zn mineralization in the vicinity of M-06-80 and M-05-00, intersected sphalerite on the surface of a slickenside in the Second Red Bed Member of the Dawson Bay Formation (Bamburak, 2006, 2007). Drillcore M-01-07, drilled north of this area on the western shore of Lake Winnipegosis (Figure GS2017-14-1), intersected probable hydrothermal dolomite within the Cedar Lake Formation (Bamburak, 2007); saddle dolomite was also identified in thin section from this zone (Rawluk, 2010; Table GS2017-14-1).

Prairie-type microdisseminated mineralization was noted by Fedikow et al. (2004) in the Mafeking area in high-calcium limestone quarries (Figure GS2017-14-1). Micrometre-sized precious- and base-metal sulphide aggregates were found to occur within altered and silicified inverted cone structures in the Upper Devonian Point Wilkins Member of the Souris River Formation.

Drillcore RP95-17

In 1995, Cominco Ltd. (Cominco) drilled six holes in the vicinity of Rabbit Point (Assessment File 94638) targeting the sub-Phanerozoic extension of the SBZ for base-metal potential in the Winnipegosis komatiite belt, which is interpreted to represent a Paleoproterozoic rift basin (Waterton et al., 2017). Previous to this program, Cominco had completed several drill and geophysical programs targeting the sub-Phanerozoic extension of the SBZ (Assessment files 94639, 94640, 94642, 94643, 94780, 94782), and continued working in this area until 1999 (Assessment files 94641, 94765, 94771, 94772). The MGS acquired some of the Cominco drillcore from the Rabbit Point programs, however, some of the intervals of Paleozoic strata were abandoned at drill sites or later discarded, after being logged by MGS geologists.

Drillholes RP95-17 and RP95-18 were drilled by Cominco in 1995, in the Kettle Hills area near the south end of Swan Lake

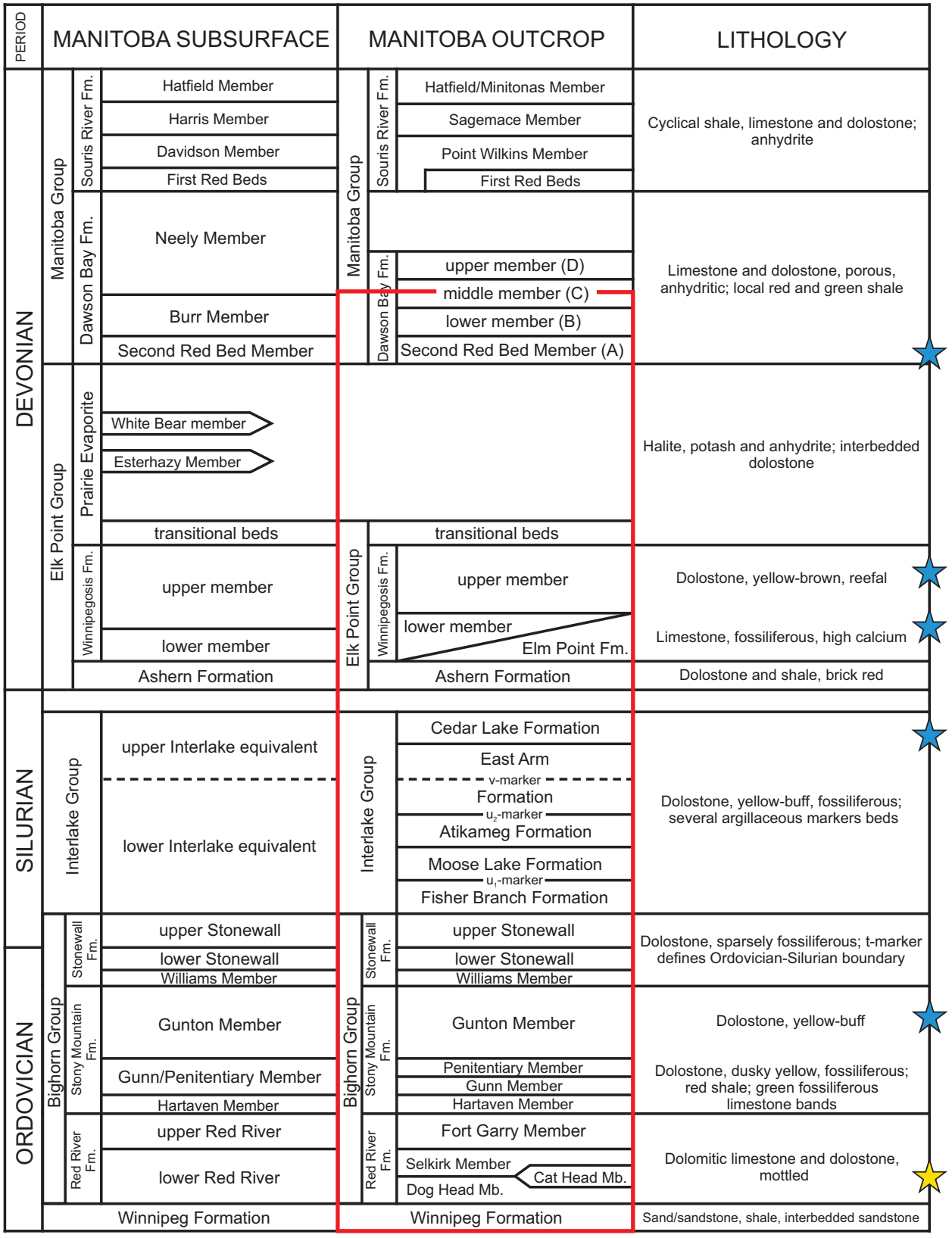

Figure GS2017-14-2: *Stratigraphy and general lithology of Ordovician to mid-Devonian strata in the Williston Basin, Manitoba. The stratigraphic units encountered in drillhole RP95-17 (Assessment File 94638, Manitoba Growth, Enterprise and Trade, Winnipeg) are outlined in red. Known occurrences of sphalerite and galena are indicated with blue and yellow stars, respectively.*

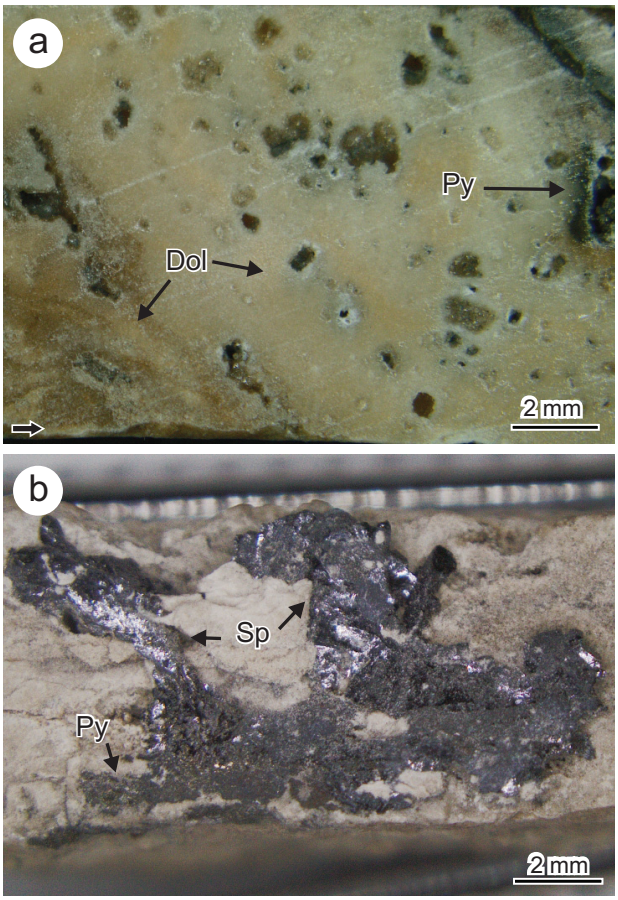

Figure GS2017-14-3: *Photographs of sphalerite occurrences in drillcore:* ***a)*** *'honey-coloured' dolomite with vuggy porosity; dark grey material associated with vugs is pyrite (core M-06-80, 112.90 m depth);* ***b)*** *sphalerite and pyrite occurring within a vertical fracture in laminated dolomudstone from the upper member, Winnipegosis Formation (core M-05-00, 114.20 m depth). Arrow indicates up direction in core. Abbreviations: Dol, dolomite; Py, pyrite; Sp, sphalerite.*

(Figure GS2017-14-1). Both drillholes targeted magnetic features along the sub-Phanerozoic section of the SBZ, and intersected sulphidic, graphitic, argillaceous metasedimentary rocks and peridotite-dunite intrusions (Assessment File 94638). The Phanerozoic section of drillcore RP95-17 was retained by MGS for future study, and is described below.

Stratigraphy

Drillcore RP95-17 provides a nearly complete section of the lower Paleozoic from the basal Ordovician Winnipeg Formation to the Devonian middle member of the Dawson Bay Formation. The section is mostly composed of dolostones and limestones, with subordinate sandstones and argillaceous/shaly units. A detailed description of the lithostratigraphy of RP95-17 is provided in Table GS2017-14-2. Drillhole RP95-17 was drilled to a true vertical depth (TVD) of 633.05 m (total measured depth 731.00 m), including 58.59 m (TVD) of Quaternary sediments and 321.57 m (TVD) of Paleozoic sedimentary rock. Refer to Assessment File 94638 for a detailed description of the Precambrian section of this core.

The Ordovician section of core RP95-17 comprises the siliciclastic Winnipeg Formation and a thick succession of dolomudstones and dolowackestones of the Red River, Stony Mountain and Stonewall formations (Table GS2017-14-2). The Winnipeg Formation is only represented by its upper unit in this part of the Williston Basin (Vigrass, 1971), and is reflected in the core as quartz arenites to wackes interbedded with arenaceous shale. The Lake Alma Member in the Red River Formation is represented by a restricted dolomudstone capped by an evaporitic dolomudstone equivalent to the Lake Alma anhydrite. The lack of anhydrite is most likely due to lateral facies variations across the Williston Basin and the proximity of the drillhole to the basinal edge, or may be related to postdepositional dissolution of primary evaporites and subsequent solution collapse. The Stony Mountain Formation is only represented by the upper Gunton Member; in northern portions of the Williston Basin the lower Hartaven, Gunn and Penitentiary members are not present.

The upper Stonewall Formation and Interlake Group contain a succession of dolomudstones separated by several argillaceous and arenaceous marker beds. The core box containing the v-marker bed in the East Arm Formation had been disturbed, so the exact depths of the bed are unknown. Breccia becomes more common upward through the Interlake Group, with the Cedar Lake Formation possessing multiple beds of chaotic and crackle breccia (Figure GS2017-14-4a, b). The basal portion of the Cedar Lake Formation is subdivided into two lower reefal units: the lowermost crinoidal reefal facies Cross Lake Member and the overlying stromatolitic reefal facies Chemahawin Member (Table GS2017-14-2). The upper contact of the Interlake Group is defined by a prominent hardground, representing a significant period of nondeposition and erosion.

The Devonian section of core RP95-17 consists of interbedded shales and dolostones/limestones that are interpreted to record one complete carbonate-evaporite cycle (Ashern-Winnipegosis-Prairie Evaporite) and the beginning of a second cycle (Dawson Bay Formation). Extensive brecciation occurred in the Ashern Formation, Winnipegosis Formation (Figure GS2017-14-4c), Prairie Evaporite and Dawson Bay Formation (GS2017-14-4d), which may be related to the dissolution of the Prairie Evaporite, karsting in the Interlake Group and other processes. The Prairie Evaporite is represented only by the conglomeratic to argillaceous transitional beds (Table GS2017-14-2), as dissolution in the subcrop belt has removed the evaporitic material from this formation. The Devonian section of core RP95-17 terminates in the middle member of the Dawson Bay Formation, and is overlain by Quaternary sediments.

Mineralization in RP95-17

The Paleozoic section of RP95-17 contains two occurrences of Pb-Zn mineralization. In the lower dolomudstone of the Red River Formation, aggregates (<0.65 mm) of galena were identified at 344.87 m (TVD) within the skeleton of a poorly

Table GS2017-14-2: Lithostratigraphy and general lithological descriptions of drillcore RP95-17; refer to Assessment File 94638 (Manitoba Growth, Enterprise and Trade, Winnipeg) for a detailed description of the Precambrian section. Abbreviations: MD, measured depth; TVD, true vertical depth.

MD (m)	TVD (m)	Thickness (m)		Description
0–64.65	0–58.59	58.59	Quaternary sediments	
64.65–89.82	58.59–81.4	22.81	Manitoba Group	
64.65–89.82	58.59–81.4	22.81	Dawson Bay Formation	
64.65–72.85	58.59–66.02	7.43	middle member (C)	
				Medium grey, argillaceous, lime mudstone–wackestone to argillaceous dolomudstone; bedded to laminated; fossiliferous, abundant echinoderms; somewhat brecciated; intercrystalline porosity, <2%; vugs and fractures partially or fully infilled by coarsely crystalline calcite; upper contact sharp, irregular
72.85–78.2	66.02–70.87	4.85	lower member (B)	
				Grey to yellowish-grey, argillaceous, lime mudstone–wackestone; some brecciation; massively bedded; fossiliferous, abundant brachiopods; intercrystalline and fracture porosity, <5%; upper contact sharp, irregular
78.2–89.82	70.87–81.4	10.53	Second Red Bed Member (A)	
				Red, grey and buff, variably calcareous dolostone and interbedded argillaceous dolomudstone; extensively brecciated, intraformational clasts contain multiple lithologies; bedded to laminated; finely disseminated pyrite-marcasite trace; upper contact sharp, directly overlain by shaly-clayey grey sediment
89.82–134.65	81.4–123.95	42.55	Elk Point Group	
89.82–90.62	81.4–83.42	2.02	Prairie Evaporite	
			transitional beds	
				Red, buff and grey, variably calcareous conglomerate to mudstone; intraclasts have multiple lithologies; brecciated; upper contact sharp and irregular
90.62–120.53	83.42–110.95	27.53	Winnipegosis Formation	
90.62–97.95	83.42–90.16	6.74	upper member	
				Grey and buff, lime mudstone to calcareous dolostone; argillaceous; well laminated, some bituminous laminations (varve-like); stylolitic; extensively brecciated; porosity 10–15%; inter-reefal facies; upper contact sharp
97.95–120.53	90.16–110.95	20.79	lower member	
				Buff to brownish-buff, calcareous dolomudstone to lime mudstone, grading upward into lime wackestone; argillaceous, wispy laminations common; massive to massively bedded also burrowed and mottled; vuggy and fracture porosity, 5–20%; some vugs and fractures partially or fully infilled by coarse calcite crystals; rare fossil fragments; rarely brecciated; subhedral to euhedral sphalerite crystals and chalcopyrite occurring on calcite-lined fracture from 109.95–110.28 m; upper contact sharp, marked by bituminous marker beds

Table GS2017-14-2 *(continued)*: Lithostratigraphy and general lithological descriptions of drillcore RP95-17; refer to Assessment File 94638 (Manitoba Growth, Enterprise and Trade, Winnipeg) for a detailed description of the Precambrian section. Abbreviations: MD, measured depth; TVD, true vertical depth.

MD (m)	TVD (m)	Thickness (m)			Description
120.53–134.66	110.95–123.95	13.00	Ashern Formation		
					Brown, red, green and grey, argillaceous, calcareous dolomudstone; massive to massively bedded; very permeable; finely disseminated pyrite-marcasite throughout, 1%; multiple brecciated intervals; coarsely crystalline calcite infilling vugs and fractures associated with brecciation; upper contact sharp
134.66–242.75	123.95–226.63	102.68	Interlake Group		
134.66–177.89	123.95–164.94	40.99	Cedar Lake Formation		
					Pinkish-, greyish- or brownish-buff, variably calcareous dolomudstone–boundstone; massive to bedded, uncommonly weakly laminated; variably argillaceous; interbeds of stromatoporoidal or stromatolitic intervals; uncommonly intraclastic to brecciated; rare vuggy and fracture porosity, <5%, permeable; 'raindrop' texture common throughout; upper contact sharp, hardground
176.6–177.55	163.74–164.62	0.88		Chemahawin Member	
					Buff, slightly calcareous doloboundstone; stromatolitic; vuggy porosity, 30%; upper contact gradational
177.55–177.89	164.62–164.94	0.32		Cross Lake Member	
					Pinkish-buff, slightly calcareous dolowackestone; bedded to massive; fossiliferous, abundant crinoidal material; finely disseminated pyrite-marcasite throughout, 1%; upper contact sharp, faint
177.89–204.10	164.94–189.24	24.30	East Arm Formation		
					Buff dolomudstone–boundstone; laminated to bedded to massive, uncommon brown, wispy, argillaceous laminations, few green clay laminations; possibly burrowed in places; few fossiliferous beds, stromatolitic and stromatoporoidal; vuggy and intercrystalline porosity in places, <5%; porcelaneous in places; finely disseminated pyrite-marcasite, 1%; upper contact sharp
195.4–199.75	181.17–185.21	4.04		v-marker bed	
					Buff, arenaceous (abundant fine- to medium-grained quartz sand), some intraformational clasts; 20 cm thick; sharp upper and lower contacts; core in this box was mixed, therefore exact depths are unknown
202.95–204.10	188.18–189.24	1.06		u_2-marker bed	
					Green-grey buff, somewhat calcareous dolomudstone; argillaceous and arenaceous, abundant green clay laminations and thin beds; abundant fine- to medium-grained rounded quartz grains; some beds of intraformational breccias; rarely vuggy, porosity <2%; finely disseminated pyrite-marcasite, in basal section of u_2-marker bed, 1%; upper contact sharp

Table GS2017-14-2 *(continued)*: Lithostratigraphy and general lithological descriptions of drillcore RP95-17; refer to Assessment File 94638 (Manitoba Growth, Enterprise and Trade, Winnipeg) for a detailed description of the Precambrian section. Abbreviations: MD, measured depth; TVD, true vertical depth.

MD (m)	TVD (m)	Thickness (m)		Description
204.1–215.4	189.24–199.72	10.48	Atikameg Formation	
				Buff, variably calcareous dolomudstone; occasionally stromatolitic; laminated to bedded to massive, wispy argillaceous laminations, sometimes with green clay; arenaceous; intercrystalline porosity, 1%; finely disseminated pyrite-marcasite, trace to 1%; upper contact sharp, marked with green clay
215.4–225.25	199.72–210.29	10.57	Moose Lake Formation	
				Buff dolomudstone; laminated to bedded, stromatolitic; argillaceous, wispy laminations sometimes with green clay; intercrystalline and vuggy porosity, 1%; raindrop texture; rarely fossiliferous; finely disseminated pyrite-marcasite, associated with fractures, 1%; upper contact sharp
223.85–225.25	208.99–210.29	1.30	u_1-marker bed	
				Bluish-greyish buff dolomudstone; laminated to bedded; arenaceous and argillaceous, fine- to medium-grained quartz sand; intercrystalline porosity, 1%; finely disseminated pyrite-marcasite, trace; upper contact gradational
225.25–242.75	210.29–226.63	16.34	Fisher Branch Formation	
				Buff, variably calcareous dolomudstone–wackestone; bedded to massive; argillaceous, rare wispy laminations; fossiliferous; chert nodules common; intercrystalline, vuggy and mouldic porosity, <2%; finely disseminated pyrite-marcasite, <1%; upper contact sharp
242.75–378.55	226.63–355.72	129.09	Bighorn Group	
242.75–265.7	226.63–248.06	21.43	Stonewall Formation	
242.75–255.5	226.63–238.53	11.90	upper Stonewall	
				Greyish-buff, slightly calcareous dolomudstone–wackestone; laminated to bedded, wispy argillaceous laminations; arenaceous, fine- to medium-grained quartz sand; fossiliferous, stromatolitic; mottled in places; vuggy to intercrystalline porosity, <2%; finely disseminated pyrite-marcasite, <1%; upper contact sharp
255.5–256.6	238.53–239.56	1.03	t-marker bed	
				Medium grey-blue dolomudstone; laminated to bedded, possible crossbedding or ripple marks; argillaceous; intercrystalline porosity, <1%; upper contact sharp, marked with argillaceous laminations
256.6–259.85	239.56–242.6	3.04	lower Stonewall	
				Blue-grey buff, dolomudstone; laminated to bedded to massive, occasional mottling; some brecciated beds (crackle breccia); rarely fossiliferous, echinoid fragments; wispy, argillaceous laminations common; intercrystalline and vuggy porosity, <2%; upper contact sharp

Table GS2017-14-2 *(continued)*: Lithostratigraphy and general lithological descriptions of drillcore RP95-17; refer to Assessment File 94638 (Manitoba Growth, Enterprise and Trade, Winnipeg) for a detailed description of the Precambrian section. Abbreviations: MD, measured depth; TVD, true vertical depth.

MD (m)	TVD (m)	Thickness (m)	Description
259.85–265.7	242.6–248.06	5.46	Williams Member
			Buff, variably calcareous dolomudstone–wackestone; argillaceous; vuggy and intercrystalline porosity, <2%; occasionally laminated; few intraformational conglomeratic beds; finely disseminated pyrite-marcasite, 1%; upper contact sharp
265.7–297.7	248.06–277.93	29.87	Stony Mountain Formation
265.7–297.7	248.06–277.93	29.87	Gunton Member
			Buff dolomudstone–wackestone; laminated to bedded, wispy argillaceous laminations; blue-grey mottling in places; nodular in places; chert nodules common throughout; vuggy and intercrystalline porosity, 2–5%; fossiliferous, echinoderms and rugose corals common; upper contact gradational
297.7–378.55	277.93–355.72	77.79	Red River Formation
297.7–320.4	277.93–299.13	21.19	upper Red River Formation
297.7–302	277.93–281.95	4.02	Redvers unit
			Blue-grey buff dolomudstone; laminated to mottled, crossbedded in places; argillaceous; core very rubbly in places, may be cherty; uncommon intraclastic beds; intercrystalline to vuggy porosity, <2%; upper contact gradational?
302–313.05	281.95–292.26	10.31	Coronach unit
			Brownish- to bluish-grey buff, slightly calcareous dolomudstone–wackestone; laminated to bedded to massive, wispy argillaceous laminations throughout; mottled and burrowed intervals; nodular in places; fossiliferous, echinoderm fragments; intercrystalline and vuggy porosity, <5%; upper contact sharp
313.05–320.4	292.26–299.13	6.87	Lake Alma Member
313.05–314.3	292.26–293.43	1.17	Lake Alma anhydrite equivalent
			Brownish-buff, slightly calcareous dolomudstone; laminated; argillaceous; some chert nodules; vuggy porosity, 30%; upper contact sharp and irregular
314.3–320.4	293.43–299.13	5.70	lower unit
			Buff dolomudstone–wackestone; laminated, sometimes massive; wispy argillaceous laminations common, often associated with burrows; rarely fossiliferous, echinoid fragments concentrated in beds; rare chert nodules; intercrystalline porosity, 1%; upper contact sharp
320.4–377.7	299.13–354.92	55.79	lower Red River Formation
			Buff dolomudstone; massively bedded, wispy argillaceous laminations; mottled and nodular; rarely fossiliferous, echinoid fragments and corals; chert nodules common; blue-grey mottling in places; galena occurs at 344.87 m, associated with a rugose coral; upper contact gradational

Table GS2017-14-2 *(continued)*: Lithostratigraphy and general lithological descriptions of drillcore RP95-17; refer to Assessment File 94638 (Manitoba Growth, Enterprise and Trade, Winnipeg) for a detailed description of the Precambrian section. Abbreviations: MD, measured depth; TVD, true vertical depth.

MD (m)	TVD (m)	Thickness (m)		Description
377.7–378.55	354.92–355.72	0.80	Hecla beds	
				Blue-grey buff dolomudstone; laminated to bedded, few wispy argillaceous laminations; arenaceous, abundant frosted quartz grains; vuggy to intercrystalline porosity, <5%; finely disseminated pyrite-marcasite throughout, locally concentrated (~30%) in some beds; upper contact sharp, marked by abundant sulphides
378.55–404.55	355.72–380.16	24.44	Winnipeg Formation	
378.55–404.55	355.72–380.16	24.44	upper unit	
				Light to medium grey, interbedded quartz arenite-wacke and arenaceous shale; massive to massively bedded, lenticular and flaser bedding, in places fissile; burrow-mottled in places; coarse- to very fine grained quartz sand, frosted, well rounded, well sorted; kaolinitic; hematitic; pyritic; upper contact sharp
404.55–731.00	380.16–633.05	252.89	Precambrian	
404.55–442.55	380.16–415.86	35.70		Regolith; weathered Precambrian rocks
442.55–731.00	415.86–633.05	217.19		Argillite, volcaniclastics, sulphides

preserved solitary rugose coral (Figure GS2017-14-5a). Under microscope one well-formed crystal face was observed with cubic cleavage and high reflectance (Figure GS2017-14-5b). The XRF analysis confirmed elevated levels of Pb above 3%.

Sphalerite was identified within a calcite-encrusted fracture in calcareous dolomudstone of the lower member of the Winnipegosis Formation at a depth of 109.95 to 110.28 m (TVD; Figure GS2017-14-5c). Several subhedral to euhedral crystals occur atop the medium- to coarsely-crystalline calcite lining of the fracture (Figure GS2017-14-5d). Trace amounts of chalcopyrite also occur in this section of core, formed on top of the calcite crystals lining this fracture. The sphalerite was originally reported as spinel in Assessment File 94638.

Evidence of MVT deposits in Manitoba

Many geological features common to MVT deposits (e.g., Paradis et al., 2007; Leach et al., 2010) are documented in the Williston Basin of Manitoba, as summarized in Table GS2017-14-3.

Modern understanding of MVT deposits suggests that the ores are sourced from high volumes of metal-rich, intrabasinal brines and require a tectonically driven fluid-flow event and fluid conduits to allow for deposition within host carbonates (Paradis et al., 2007; Leach et al., 2010). In most known MVT districts, orogenic events are thought to be the main driver of saline fluid flow leading to precipitation of Pb-Zn sulphides, however, the Manitoba portion of the Williston Basin was far removed from orogenic regions. McRitchie (1991) and Dietrich et al. (1997) presented evidence to suggest that the sub-Phanerozoic extension of the SBZ in Manitoba underwent movement through crustal flexure during the Paleozoic, which could have provided conduits for fluid flow via reactivation of basement faults. The SBZ coupled with evaporitic sequences in the Williston Basin, such as the Prairie Evaporite, could have been the source of metalliferous brines.

A number of other geological features in the Williston Basin further imply potential for carbonate-hosted Pb-Zn occurrences in Manitoba, including karsting, reefal structures and facies changes. These are all found within the Paleozoic strata of the Williston Basin and are known to be preferential locations for sulphide precipitation and development of MVT deposits (Paradis et al., 2007; Leach et al., 2010). Some of these structures can be correlated to faults within the SBZ, therefore favourable areas of emplacement could have been closely connected to fluid-flow conduits.

There are some features associated with the development of MVT deposits that have yet to be clearly identified in Manitoba. Typically, MVT deposits are located within 600 km of an orogenic belt and many were emplaced during the Late Devonian to Early Carboniferous and the Late Cretaceous to Early Paleocene during times of increased orogenic activity (Paradis et al., 2007; Leach et al., 2010). The Manitoba portion of the Williston Basin was far removed from the nearest orogenic belts, exceeding the 600 km distance. Some other type of event must be proposed to be the driving force of basinal fluid movement. Saddle dolomite has been identified in drillcore M-01-07

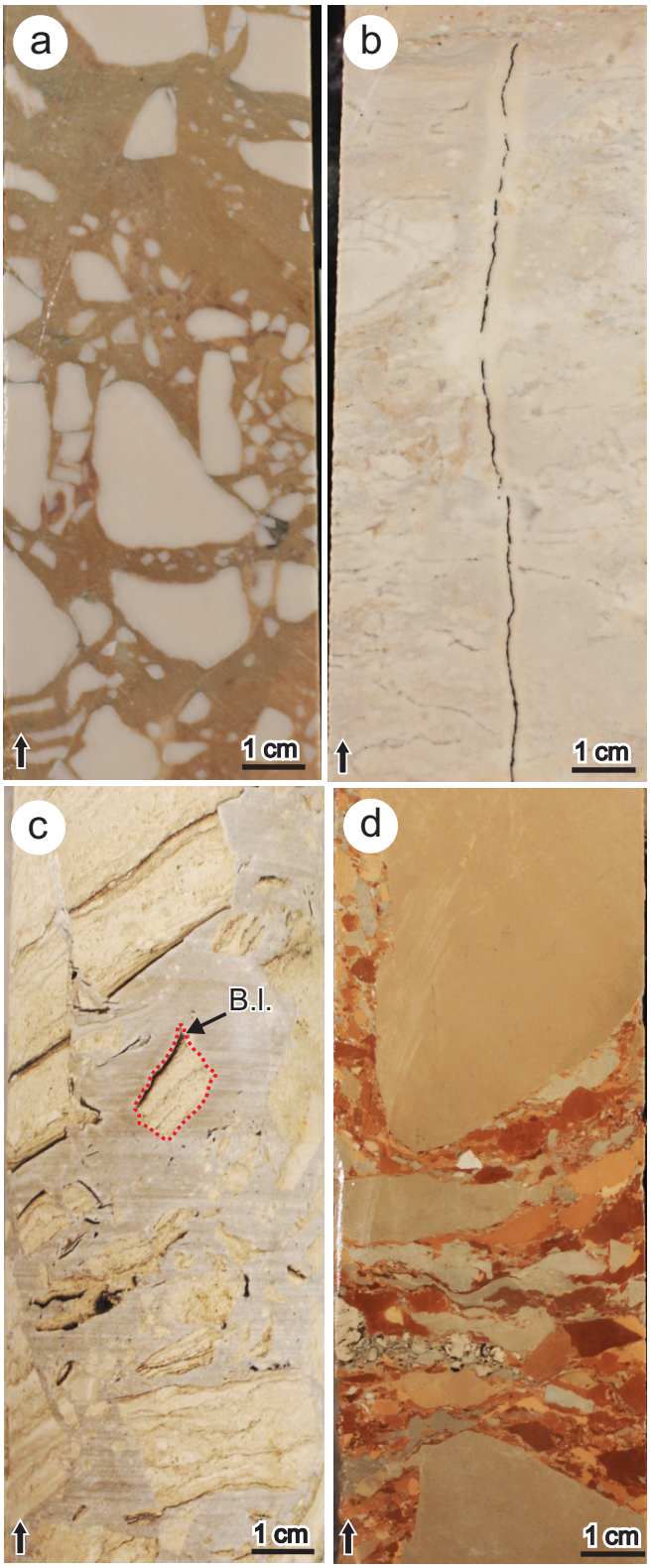

Figure GS2017-14-4: *Photographs of drillcore RP95-17 (Assessment File 94638, Winnipeg Growth, Enterprise and Trade, Winnipeg), showing* ***a)*** *chaotic breccia in the Cedar Lake Formation, at a depth of 134.4 m (true vertical depth [TVD]); buff dolomudstone clasts are embedded in a red argillaceous matrix;* ***b)*** *weakly brecciated dolomudstone in the Cedar Lake Formation, at a depth of 130.7 m (TVD); note the vertical fracture infilled with pyrite-marcasite;* ***c)*** *crackle to mosaic breccia in the inter-reefal facies upper member of the Winnipegosis Formation, at a depth of 89.37 m (TVD); note the clasts of bituminous laminated dolomudstone, red dotted line outlines a single clast;* ***d)*** *chaotic breccia in the Second Red Bed Member of the Dawson Bay Formation, at a depth of 76.45 m (TVD); clasts include several different lithologies. Abbreviation: B.l., bituminous laminations. Arrow indicates up direction in core.*

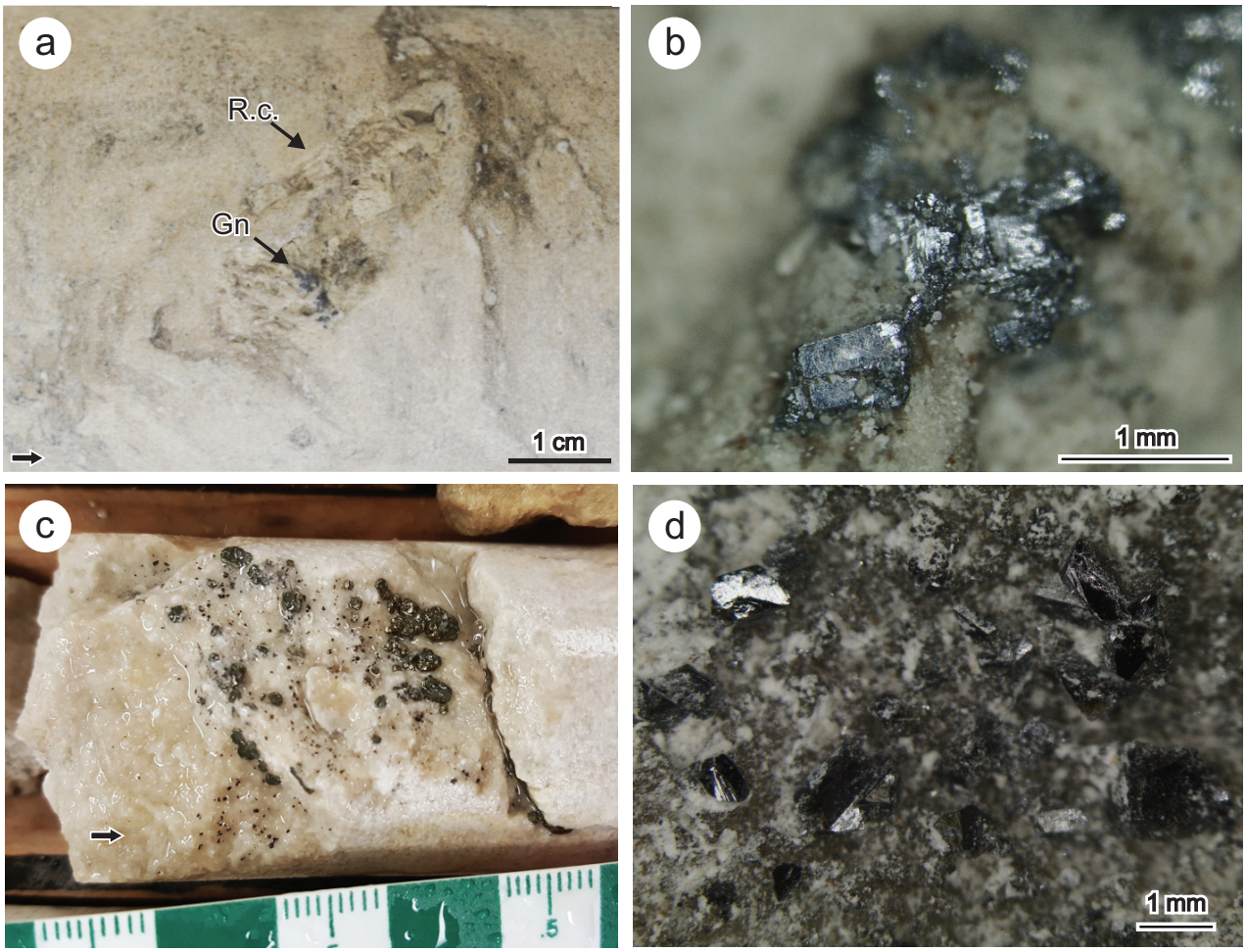

***Figure GS2017-14-5**: Lead and zinc mineralization in drillcore RP95-17 (Assessment File 94638, Winnipeg Growth, Enterprise and Trade, Winnipeg): **a)** photograph of galena (Gn) associated with a poorly preserved rugose coral (R.c.), from the Red River Formation at a depth of 344.85 to 344.90 m (true vertical depth [TVD]); **b)** photomicrograph of galena associated with a rugose coral from the Red River Formation, at a depth of 344.87 m (TVD); **c)** photograph of a subvertical fracture lined with calcite and sphalerite, in the lower member of the Winnipegosis Formation, at a depth of 109.95 to 110.28 m (TVD); **d)** photomicrograph of sphalerite on calcite crystals that line a subvertical fracture in the lower member of the Winnipegosis Formation, at a depth of 110.23 m (TVD). Arrow indicates up direction in core.*

(Rawluk, 2010), from an interval that may consist of hydrothermal dolomite. Hydrothermal alteration, and specifically saddle dolomite, is often associated with Pb-Zn mineralization in host carbonate rocks; in the Pine Point district, saddle dolomite is a gangue mineral that often encloses bodies of sulphide mineralization (Paradis et al., 2007). Further isotope and fluid inclusion work is required to confirm that hydrothermal processes have taken place in this and other cores.

Further work on known occurrences of carbonate-hosted Pb-Zn mineralization in Manitoba is required to demonstrate that these occurrences were formed from the same metalliferous brines. The X-ray diffraction (XRD) analysis of Pb-Zn mineralization in core RP95-17 will confirm the presence of sphalerite and galena. Isotopic analyses and fluid inclusion work may also be pursued to better understand the source fluid and compare it to other known occurrences of sphalerite and galena.

Economic considerations

Major occurrences of carbonate-hosted Pb-Zn mineralization have yet to be discovered in Manitoba. At this stage, however, a combination of features, including minor occurrences of galena and sphalerite, indicate that the potential for MVT deposits may exist in the Williston Basin. Given the tendency for such deposits to occur in district-scale clusters, the discovery of additional Pb-Zn occurrences in the Williston Basin could spur renewed interest in Manitoba's Interlake region.

The discovery of sphalerite and galena in previously logged core indicates that relogging the Paleozoic sections of drillcore from along and adjacent to the SBZ may be a cost-effective means of exploration for MVT deposits. Compiling geochemical data from industry and previously published and unpublished MGS programs, as well as modelling subsurface stratigraphy, may indicate areas of greater potential. There are still some

Table GS2017-14-3: Geological characteristics of Mississippi Valley–type deposits and districts, and possible equivalents in Manitoba.

General characteristics of Mississippi Valley–type deposits	Manitoba equivalent
Evidence of evaporite facies in regional carbonates[1]	Multiple evaporitic sequences in the Williston Basin: Prairie Evaporite, Hubbard Evaporite, Lake Alma anhydrite
Proximity to transtensional, wrench, strike-slip and fore bulge normal faults[1]	Evidence that the SBZ in southwestern Manitoba underwent movement through crustal flexure (McRitchie, 1991; Dietrich et al., 1997)
Presence of karstification[1,2]	Abundant karst development in Manitoba carbonates (Sweet et al., 1988); evidence of solution and collapse breccias (i.e., Dawson Bay Formation); major karst events occurred at the Cambrian-Ordovician and Silurian-Devonian boundaries, with minor karsting occurring in the Stonewall, Winnipegosis and Dawson Bay formations (McRitchie, 1991)
Widespread trace and minor occurrences of MVT mineralization and sulphides in carbonate rocks[1,2]	Wide distribution of minor lead-zinc mineralization; many documented occurrences of anomalous base-metal values in Paleozoic carbonates (i.e., Gale and Conley, 2000; Bamburak and Klyne, 2004; Fedikow et al., 2004; Assessment files 93877, 93878, Manitoba Growth, Enterprise and Trade, Winnipeg)
Presence of regional basal sandstone[1]	Ordovician Winnipeg Formation (and to a lesser degree the siliciclastic Cambrian Deadwood Formation) blankets the base of the Williston Basin
Presence of reef and barrier reef facies[1,2]	Devonian upper member Winnipegosis Formation contains reefal and inter-reefal facies, as well as massive reef complexes (Norris et al., 1982; Dietrich and Magnusson, 1998)
Presence of regional aquitards[1]	Multiple shale and argillaceous carbonate facies in Lower Paleozoic strata (i.e., Ashern Formation; Second Red Bed Member, Dawson Bay Formation; First Red Beds, Souris River Formation)
Rapid transition of basin sediments with basement contacts, and rapid facies changes in sedimentary strata[1]	Multiple sequences of shale to carbonate facies in Devonian strata; lateral facies variations across the Williston Basin (reefal to inter-reefal facies, Winnipegosis Formation)
Presence of hydrothermal dolomite[1,2]	Suspected hydrothermal dolomite and confirmed saddle dolomite in drill-core M-01-07 (Rawluk, 2010)
Deposits hosted in platform carbonate successions developed on the flanks of sedimentary basins[2]	Paleozoic strata of the Williston Basin are mostly composed of platformal carbonates; these strata are located at the edge of the much larger WCSB
Carbonate sequences that commonly overlie deformed and metamorphosed continental crustal rocks, and have some hydrological connection to basins affected by orogenic events[2]	Williston Basin overlies igneous and metamorphic Precambrian basement, specifically the SBZ shear zone; the Williston Basin is part of the larger WCSB, which is bordered to the west by the Cordilleran orogeny
Local geological features permitting upward migration of fluids[2]	Faults and fractures in the SBZ and overlying fractured Paleozoic strata may provide paths for fluid migration (McRitchie, 1991)

[1] Leach et al. (2010)
[2] Paradis et al. (2007)
Abbreviations: MVT, Mississippi Valley–type; SBZ, Superior boundary zone; WCSB, Western Canada Sedimentary Basin

stratigraphic inconsistencies within the lower Paleozoic strata of the Williston Basin, chiefly in the Silurian section; resolution of these issues through continued stratigraphic investigations will allow for industry to better develop targeted exploration programs for stratabound MVT deposits.

Acknowledgments

The authors thank D. Burk for bringing RP95-17 drillcore to their attention. C. Epp is thanked for his assistance in locating RP95-17, preparing it for viewing and preforming X-ray fluorescence analysis. Summer students M. Koziuk and G. Fouillard are thanked for their assistance in photographing and cutting core.

References

Bamburak, J.D. 2006: Manitoba Geological Survey's stratigraphic core-hole drilling program, 2006 (parts of NTS 62N16 and 63C1); *in* Report of Activities 2006, Manitoba Science, Technology, Energy and Mines, Manitoba Geological Survey, p. 246–252.

Bamburak, J.D. 2007: Manitoba Geological Survey's stratigraphic core-hole drilling program, 2007 (parts of NTS 62N1, 16, 63C1); *in* Report of Activities 2007, Manitoba Science, Technology, Energy and Mines, Manitoba Geological Survey, p. 166–174.

Bamburak, J.D. and Klyne, K. 2004: A possible new Mississippi Valley–type mineral occurrence near Pemmican Island in the north basin of Lake Winnipegosis, Manitoba (NTS 63B12 and 13, 63C9 and 16); *in* Report of Activities 2004, Manitoba Industry, Economic Development and Mines, Manitoba Geological Survey, p. 266–278.

Bamburak, J.D., Hosain, I.T. and Klyne, K. 2002: Phanerozoic solid-sulphide occurrence containing Devonian dolomite breccia clasts, Pemmican Island, Lake Winnipegosis (NTS 63B12NW), Manitoba; *in* Report of Activities 2002, Manitoba Industry, Trade and Mines, Manitoba Geological Survey, p. 131–143.

Bezys, R.K. 2000: Stratigraphic investigations and corehole drilling program, 2000; *in* Report of Activities 2000, Manitoba Industry, Trade and Mines, Manitoba Geological Survey, p. 196–201.

Bleeker, W. 1990: Evolution of the Thompson nickel belt and its nickel deposits, Manitoba, Canada; Ph.D. thesis, University of New Brunswick, Fredericton, New Brunswick, 400 p.

Dietrich, J.R. and Magnusson, D.H. 1998: Basement controls on Phanerozoic development of the Birdtail-Waskada salt dissolution zone, Williston Basin, southwestern Manitoba; *in* Eighth International Williston Basin Symposium, J.E. Christopher, C.F. Gilboy, D.F. Paterson and S.L. Bend (ed.), Saskatchewan Geological Society, Regina, Saskatchewan, October 19–21, 1998, Special Publication 13, p. 166–174.

Dietrich, J.R., Magnusson, D.H., Lyatsky, H.V. and Hajnal, Z. 1997: Basement-sedimentary cover relationships along the Churchill-Superior boundary zone, southwestern Manitoba (abstract); Manitoba Energy and Mines, Manitoba Mining and Minerals Convention '97, Winnipeg, Manitoba, November 20–22, 1997, Program, p. 33.

Fedikow, M.A.F., Bezys, R.K., Bamburak, J.D., Hosain, I.T. and Abercrombie, H.J. 2004: Prairie-type microdisseminated mineralization in the Dawson Bay area, west-central Manitoba (NTS 63C14 and 15); Manitoba Industry, Economic Development and Mines, Manitoba Geological Survey, Geoscientific Report GR2004-1, 76 p.

Gagné, S. 2016: Examination of exploration drillcore from the Reed Lake area, Flon Flon belt, west-central Manitoba (parts of NTS 63K7, 8, 9, 10); *in* Report of Activities 2016, Manitoba Growth, Enterprise and Trade, Manitoba Geological Survey, p. 63–73.

Gale, G.H. and Conley, G.G. 2000: Metal contents of selected Phanerozoic drill cores and the potential for carbonate-hosted Mississippi Valley–type deposits in Manitoba; Manitoba Industry, Trade and Mines, Manitoba Geological Survey, Open File Report OF2000-3, 126 p.

Genik, G.J. 1952: A regional study of the Winnipeg Formation; M.Sc. thesis, University of Manitoba, Winnipeg, Manitoba, 174 p.

Leach, D.L., Taylor, R.D., Fey, D.L., Diehl, S.F. and Saltus, R.W. 2010: A deposit model for Mississippi Valley–type lead-zinc ores, chapter A of mineral deposit models for resource assessment; United States Geological Survey, Scientific Investigations Report 2010-5070-A, 52 p.

McCabe, H.R. 1969: An occurrence of galena in float: Winnipeg area; *in* Summary of Geological Fieldwork, 1969, Manitoba Mines and Natural Resources, Mines Branch, Geological Survey of Manitoba, Geological Paper 69-4, p. 125.

McCabe, H.R. 1980: Stratigraphic mapping and core hole program, southwest Manitoba; *in* Report of Field Activities 1980, Manitoba Department of Energy and Mines, Mineral Resources Division, p. 70–73.

McRitchie, W.D. 1991: Caves in Manitoba's Interlake region; Speleological Society of Manitoba, Winnipeg, Manitoba, 150 p.

Nicolas, M.P.B., Matile, G.L.D., Keller, G.R. and Bamburak, J.D. 2010: Phanerozoic geology of southern Manitoba; Manitoba Innovation, Energy and Mines, Manitoba Geological Survey, Stratigraphic Map Series, Map 2010-1, Sheet B: Phanerozoic, scale 1:600 000.

Norris, A.W., Uyeno, T.T. and McCabe, H.R. 1982: Devonian rocks of the Lake Winnipegosis-Lake Manitoba outcrop belt, Manitoba; Manitoba Department of Energy and Mines, Mines Branch, Publication 77-1, 280 p.

Paradis, S., Hannigan, P. and Dewing, K. 2007: Mississippi Valley-type deposits; *in* Mineral Deposits of Canada: A Synthesis of Major Deposit-Types, District Metallogeny, the Evolution of Geological Provinces, and Exploration Methods, W.D. Goodfellow (ed.), Geological Association of Canada, Mineral Deposits Division, Special Publication No. 5, p. 185–203.

Rawluk, C. 2010: Sedimentology of Silurian Interlake Group dolostones near Duck Bay, west-central Manitoba; B.Sc. thesis, University of Manitoba, Winnipeg, Manitoba, 110 p.

Reid, K.D. and Gagné, S. 2016: Examination of exploration drillcore from the south Wekusko Lake area, eastern Flin Flon belt, north-central Manitoba (parts of NTS 63J5, 12, 63K8, 9); *in* Report of Activities 2016, Manitoba Growth, Enterprise and Trade, Manitoba Geological Survey, p. 74–86.

Sweet, G., Voitovici, P. and Ritchie, W.D. 1988: Karst investigations in Paleozoic carbonates of the Grand Rapids uplands and southern Interlake; *in* Report of Field Activities 1988, Manitoba Energy and Mines, Minerals Division, p. 143–156.

Vigrass, L.W. 1971: Depositional framework of the Winnipeg Formation in Manitoba and eastern Saskatchewan; *in* Geoscience Studies in Manitoba, A.C. Turnock (ed.), Geological Association of Canada, Special Paper 9, p. 225–234.

Waterton, P., Person, D.G., Kjarsgaard, B., Hulbert, L., Locock, A., Parman, S. and Davis, B. 2017: Age, origin and thermal evolution of the ultra-fresh ~1.9 Ga Winnipegosis komatiites, Manitoba, Canada; Lithos, v. 268–271, p. 114–130.

GS2017-15

Stratigraphy and geochemistry of the Cretaceous Boyne Member, Carlile Formation, in the Manitoba Potash Corporation core at 3-29-20-29W1, southwestern Manitoba (part of NTS 65K1)

by D.J. Shaw[1], M.P.B. Nicolas and N. Chow[1]

[1] Department of Geological Sciences, University of Manitoba, 125 Dysart Road, Winnipeg, MB R3T 2N2

In Brief:

- Boyne Member has potential for shallow, clean natural gas resources
- High TOC values (up to 11.18 wt. %) and low thermal maturity indicate an excellent biogenic gas source rock
- Stratigraphic and lithofacies mapping suggest potential for long-range continuity of the Babcock beds

Citation:
Shaw, D.J., Nicolas, M.P.B. and Chow, N. 2017: Stratigraphy and geochemistry of the Cretaceous Boyne Member, Carlile Formation, in the Manitoba Potash Corporation core at 3-29-20-29W1, southwestern Manitoba (parts of NTS 65K1); *in* Report of Activities 2017, Manitoba Growth, Enterprise and Trade, Manitoba Geological Survey, p. 173–182.

Summary

The Upper Cretaceous Boyne Member of the Carlile Formation, in the Manitoba Potash Corporation core at 3-29-20-29W1, was described and analyzed to provide the first subsurface description of this unit in Manitoba. The Boyne Member is a widely distributed mudstone horizon in southwestern Manitoba, with good potential for gas-bearing reservoirs, which could serve as a future, clean natural gas resource for the province. The stratigraphy, lithofacies analyses and organic geochemistry provide a basis for evaluating its economic potential.

Introduction

In 1986, Canamax Resources Inc. drilled a potash testhole, which is now owned by Manitoba Potash Corporation (MPC), as a pilot for the construction of a mine shaft for an underground potash mine located in L.S. 3, Sec. 9, Twp. 20, Rge. 29, W 1st Mer. (abbreviated 3-29-20-29W1). Continuous core was acquired during this drilling, with excellent recovery from 14.00 to 900.00 m vertical depth. The upper 420.00 m of this core includes the entire Cretaceous section, from the Swan River Formation to the Coulter Member of the Pierre Shale (Figure GS2017-15-1). Nicolas (2016) reported on the upper 360.00 m, with a focus on the Ashville Formation to Pierre Shale section, as part of the ongoing Shallow Unconventional Shale Gas (SUSG) Project (Nicolas and Bamburak, 2009). This core will be referred to herein as the MPC core.

Following this reconnaissance overview of the MPC core, Shaw (2017) completed a detailed stratigraphic and lithofacies analysis, and organic and inorganic geochemistry profiling of the Boyne Member of the Carlile Formation in the MPC core, as well as in an outcrop located along the Vermillion River. This report focuses only on portions of the core section examined by Shaw (2017), in particular those pertaining to the lithofacies analysis, mineralogy and organic geochemistry.

The Boyne Member of the MPC core was chosen for detailed study because

- it may be a target for unconventional shale gas exploration on the basis of production from this unit in other parts of the Williston Basin (Nicolas 2009); and
- siltstone beds present in the Boyne Member, the Babcock beds, are exposed in outcrop in southwestern Manitoba, but have yet to be correlated successfully into the subsurface (Nicolas et al., 2010).

These Babcock beds are suspected to be correlative to the Boyne sand, which is a productive shallow-gas reservoir in the Kamsack area of southwestern Saskatchewan (Nicolas et al., 2010).

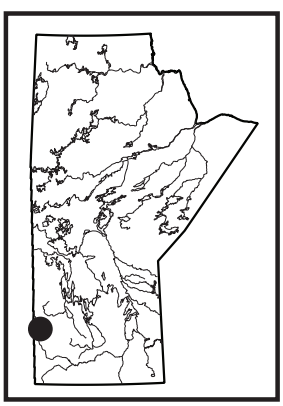

Stratigraphy and cyclothems

The Upper Cretaceous (Turonian to Santonian) Boyne Member of the Carlile Formation in southwestern Manitoba comprises mainly grey, variably calcareous mudstone. The Boyne Member is underlain by the Morden Member of the Carlile Formation, which is a black, non-calcareous mudstone. It is overlain by the black, non-calcareous mudstone of the Campanian Pembina Member or laterally discontinuous brown siltstone to mudstone of the Gammon Ferruginous Member of the Pierre Shale. The stratigraphic equivalent of the Boyne Member in other jurisdictions is a topic of considerable debate (e.g., McNeil and Caldwell, 1981; Christopher et al., 2006; Bamburak and Nicolas, 2009; Diaz and Velez, 2016). It is generally considered equivalent to the First White Speckled Shale in Alberta and the Niobrara Formation in southwestern Saskatchewan. The Babcock beds occur midway through the Boyne Member, near the top of the calcareous shale unit (Figure GS2017-15-1).

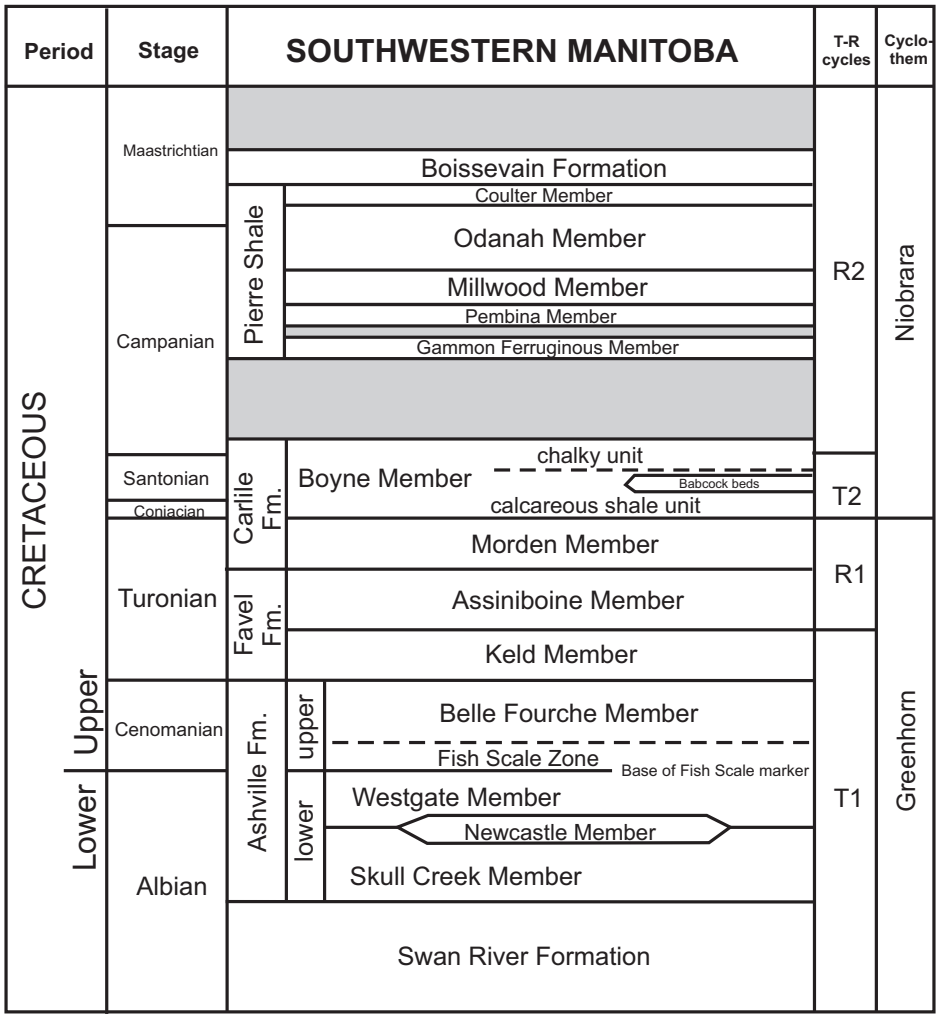

Figure GS2017-15-1: *Cretaceous stratigraphy of southwestern Manitoba, modified from Nicolas and Bamburak (2011), and the T-R cycles and cyclothems from McNeil and Caldwell (1981). Abbreviations: Fm., Formation; T-R, transgressive-regressive.*

The Cretaceous rocks of the Manitoba escarpment represent two major transgressive–regressive cycles: the earlier Greenhorn cyclothem and later Niobrara cyclothem (Figure GS2017-15-1; McNeil and Caldwell, 1981). The Greenhorn cyclothem reached its transgressive (T1 in Figure GS2017-15-1) peak in the early Turonian stage, corresponding to the deposition of the Keld Member of the Favel Formation, and its regressive (R1) trough in the middle to late Turonian stage, corresponding with the deposition of the Assiniboine and Morden members (Figure GS2017-15-1; McNeil and Caldwell, 1981). The transgressive (T2) cycle of the Niobrara cyclothem is represented overall by the Boyne Member and the transgressive peak corresponds to the deposition of the upper chalky unit. Within outcrops of the Boyne Member, there are up to four minor transgressive–regressive fluctuations reported by McNeil and Caldwell (1981), although they are difficult to identify and some cycles may be absent due to erosion or nondeposition. The resulting disconformities create difficulties in resolving stratigraphic correlations across the Williston Basin, as well as locally.

Lithofacies analysis

Detailed lithofacies analysis was conducted on the MPC core, despite its deteriorated condition (Shaw, 2017). Although the core recovery through this section was excellent, parts of the core were lost due to humidity causing them to expand out of their boxes as a result of poor storage conditions over decades. Extensive flaking and breaking of the dried-out core and prolific formation of tertiary gypsum crystal blooms on the surface have obscured features of the core. These conditions make it difficult to observe the lithology, textures and sedimentary structures. Using modern evaluation techniques specifically devised for mudrocks (Potter et al., 2005; Lazar et al., 2015), the lithology, textures and structures of the MPC core were described and interpreted. Figure GS2017-15-2 shows the detailed core log of the Boyne Member in the MPC core, for which the stratification, grading and clay content were determined using these techniques.

The variations in sedimentary structures and texture of the Boyne Member, consisting predominantly of grey, fine- to coarse-grained mudstone, were primarily used to distinguish

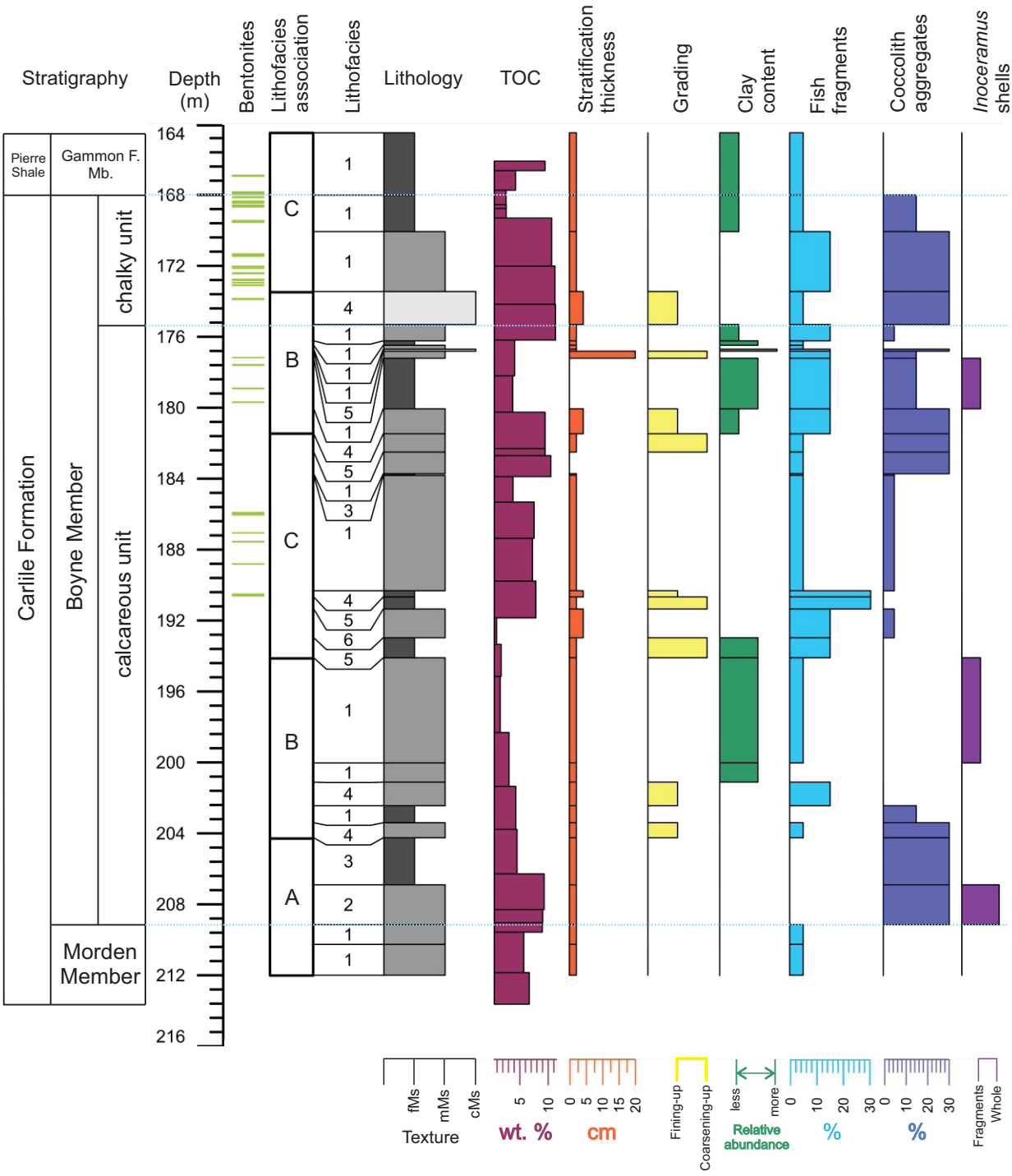

Figure GS2017-15-2: *Stratigraphic, lithological, textural and total organic carbon profile of the Cretaceous Boyne Member, Carlile Formation, in the core at 3-29-20-29W1, southwestern Manitoba. Depth track is true vertical depth, as measured in the core. Lithology-texture scale is based on Potter et al. (2005) and Lazar et al. (2015). Abbreviations: fMs, fine-grained mudstone; mMs, medium-grained mudstone; cMs, coarse-grained mudstone.*

the following seven lithofacies: 1) laminated mudstone; 2) medium-grained mudstone with fine-grained mudstone clasts; 3) fine-grained mudstone with medium-grained mudstone clasts; 4) fining-upward mudstone; 5) coarsening-upward mudstone; 6) burrowed mudstone; and 7) bentonite. A summary of these lithofacies is provided in Table GS2017-15-1.

These lithofacies are grouped on the basis of sedimentary structures, presence of *Inoceramus* and ichnofossils, and clay and total organic carbon (TOC) content into three lithofacies associations: A) outer shelf to upper slope deposits; B) upper slope to lower slope deposits; and C) lower slope to basin deposits (Figure GS2017-15-3).

Lithofacies association A: outer shelf to upper slope deposits

Lithofacies association A (LA-A) consists of laminated mudstone, medium-grained mudstone with fine-grained mudstone clasts and fine-grained mudstone with medium-grained mudstone clasts (lithofacies 1–3). It occurs in the MPC core from 204.25 to 212.00 m depth (Figure GS2017-15-1). This lithofacies

Table GS2017-15-1: Summary of lithofacies of the Boyne Member, Carlile Formation, in the MPC core at 3-29-20-29W1, southwestern Manitoba. Abbreviation: NA, not available.

Lithofacies		Thickness (m)	Lithology	Colour	Contacts	Sedimentary structures	Biological features
1	Laminated mudstone	0.11-6.5	Fine-grained mudstone; medium-grained mudstone; coarse-grained mudstone. Up to 15% silt grains, including up to 5% lithic clasts	Medium dark grey to very light grey	Lower and upper: sharp or gradational	Thick to thin laminations	None to few fish fragments. None to few coccolith aggregates. *Inoceramus* concentrated in 1 cm layers in some units (198.25, 179.45 m depth)
2	Medium-grained mudstone with fine-grained mudstone clasts	2.35	Medium-grained mudstone. Up to 15% silt grains	Brownish medium grey	Lower and upper: sharp	Medium laminations. Few clasts of fine mudstone (~1 mm wide, up to 1 cm long)	Few fish fragments. Few coccolith aggregates. *Inoceramus* throughout (3-7 mm, few)
3	Fine-grained mudstone with medium-grained mudstone clasts	0.1-2.65	Fine-grained mudstone	Medium to light grey	Lower: sharp; Upper: sharp or gradational	Medium laminations. Few clasts of medium mudstone (~2 mm wide, up to 1 cm long)	None to very sparse fish fragments
4	Fining-upward mudstone	0.35-1.83	Fine- to coarse-grained mudstone that show fining upward trends. Up to 15% silt grains (mostly lithic clasts)	Medium to light grey	Lower and upper: sharp or gradational	Medium laminations	Very sparse to few fish fragments. None to few coccolith aggregates.
5	Coarsening-upward mudstone	0.4-1.13	Fine- to coarse-grained mudstone that show coarsening upward trends. Up to 15% silt grains (up to 1/3 lithic clasts)	Medium light grey	Lower and upper: sharp or gradational	Medium laminations to very thin beds	Very sparse to few fish fragments. Sparse to few coccoliths
6	Burrowed mudstone	1.62	Medium-grained mudstone with up to 50% coarse mudstone throughout. Up to 10% silt grains	Light grey	Lower and upper: sharp	Medium to thick laminations	Sparse fish fragments. Very sparse coccolith aggregates. Burrows of *Planolites*, *Chondrites* and *Zoophycus* throughout section; highly burrow mottled at 192.48-192.62 m depth. Small gastropod at 191.85 m depth
7	Bentonite	0.005-0.13	Very fine clay	Pale yellow	Lower and upper: sharp	None	None

Abbreviations: TOC, total organic contents; NA, not available; UV, ultraviolet

Table GS2017-15-1 *(continued)*: Summary of lithofacies of the Boyne Member, Carlile Formation, in the MPC core at 3-29-20-29W1, southwestern Manitoba. Abbreviation: NA, not available.

Lithofacies		TOC (wt. %)	Other features	Depositional environment	Lithofacies association
1	Laminated mudstone	1.56-10.46	Calcareous concretion at 195.13-195.38 m depth. Crosscut by calcite-filled fracture (2.6 cm wide, dip 65°, sharp contacts). Scattered framboidal pyrite occurs as low as 200.03 m depth. Scattered manganese oxide occurs as low as 200.03 depth (appears to be replacing fish fragments)	Suspension settling under relatively low-energy conditions; *Inoceramus*-rich zones likely transported, possibly lag deposits	LA-A, -B, and -C
2	Medium-grained mudstone with fine-grained mudstone clasts	8.96-9.28	Strong petroliferous odour and streaming white cuts that fluoresced under UV light (209.15-208.90 m depth). Fracture dipping at 32° at 207.94-208.14 m depth	Erosion and bedload transport by turbulent bottom flows	LA-A
3	Fine-grained mudstone with medium-grained mudstone clasts	4.51	Vertical open fracture at 206.54-206.84 m depth. Gypsum nodules in fractures (up to 1 mm wide, 1 cm long, ovoid). Rare framboidal pyrite as low as 183.82 m depth	Erosion and bedload transport by turbulent bottom flows	LA-A
4	Fining-upward mudstone	4.96-11.28	Few to common, round white gypsum nodules (190.32-190.67 m depth, very fine sand sized). Some mud clasts present in coarse mud unit (173.45-175.31 m depth, closer to bottom, possible rip up clasts)	Low-energy turbidity currents	LA-B
5	Coarsening-upward mudstone	1.72-9.46	Scattered framboidal pyrite as low as 194.1 m depth	Low-energy deep marine; increasing energy conditions	LA-C
6	Burrowed mudstone	0.91	Rare pyrite (more cubic than framboidal)	Dysoxic, low-energy conditions that allowed biogenic reworking	LA-C
7	Bentonite	NA	Beds at 169.45-169.35 m and 168.58-168.51 m include glassy blue mineral (melanterite)	Periods of volcanic activity during deposition	LA-B and -C

Abbreviations: TOC, total organic contents; NA, not available; UV, ultraviolet

association has low clay content (Figure GS2017-15-2) and is distinguished by the presence of lithofacies 2 and 3, which have mudstone clasts. Whole *Inoceramus* shells are present within lithofacies 2 of LA-A.

LA-A is interpreted to have been deposited in the outer shelf to upper slope environment. The laminated mudstone and intact *Inoceramus* shells indicate generally low-energy conditions, likely below storm-wave base (Eriksson and Reczko, 1997; Potter et al., 2005). *Inoceramus* has also been shown to present the highest diversity in middle to outer shelf sediments (Thiede and Dinkelman, 2007). The clasts in lithofacies 2 and 3 may have been produced by episodic density currents that flowed along the shelf bottom into deeper water (Potter et al., 2005) and were triggered by storm events.

Lithofacies association B: upper to lower slope deposits

Lithofacies association B (LA-B) consists of laminated mudstone, fining-upward mudstone and bentonite beds (lithofacies 1, 4 and 7). It occurs from 173.45 to 181.47 m and 192.97 to

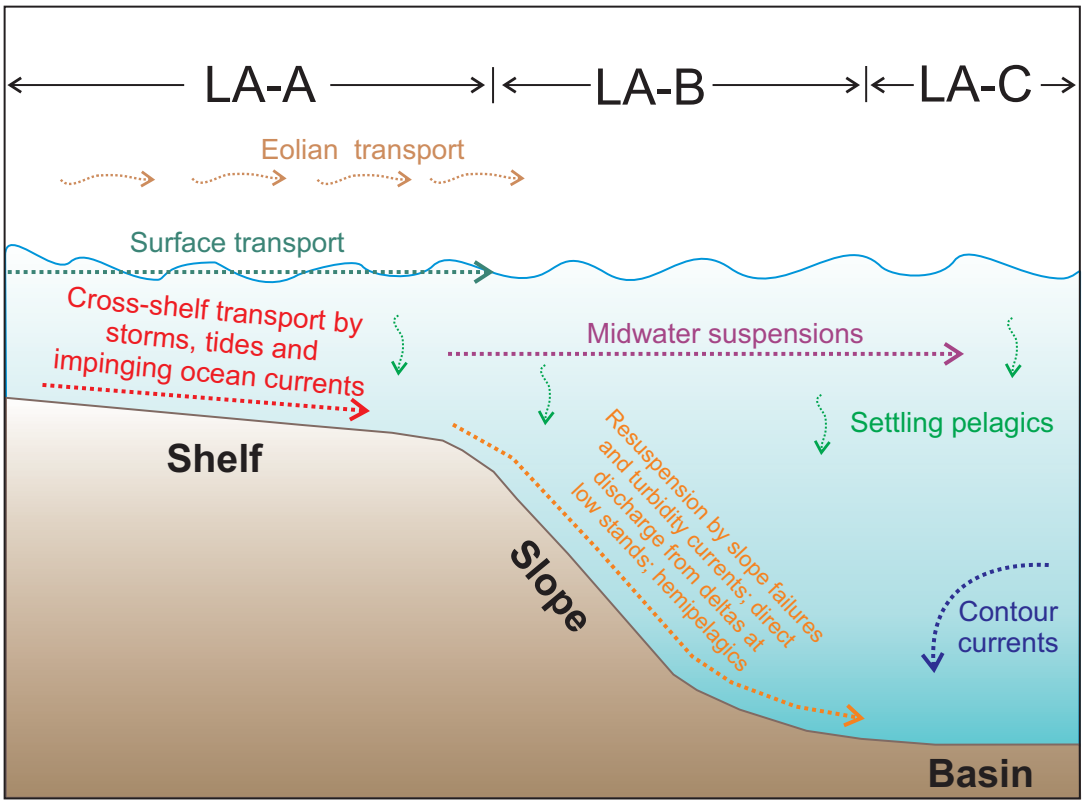

Figure GS2017-15-3: *Schematic interpretation of the lithofacies associations in the Boyne Member and the principal sediment transport on the shelf, slope and basin (modified from Stow, 1981). Abbreviations: LA-A, lithofacies association A; LA-B, lithofacies association B; LA-C, lithofacies association C.*

204.25 m depth in the MPC core (Figure GS2017-15-1). This lithofacies association is distinguished by the presence of lithofacies 4, comprising fining-upward units. *Inoceramus* fragments are present within lag deposits of lithofacies 1. In addition, LA-B has an overall high clay content (Figure GS2017-15-2).

LA-B is interpreted to have been deposited in the upper to lower slope environment. The laminated mudstone of lithofacies 1 again indicates low-energy conditions, but the fining-upward sequences in lithofacies 4 are interpreted to have been deposited by low-density turbidity currents, which commonly occur in slope settings (Potter et al., 2005; Lazar et al., 2015). Episodic storm events on muddy shelves re-suspended bottom-sediment–forming turbidity currents that flowed down the slope (Potter et al., 2005; Lazar et al., 2015).

The *Inoceramus*-rich lag deposits are interpreted to have been deposited during infrequent events of sediment winnowing by offshore-directed currents, induced by higher energy storm events (Konitzer et al., 2014). These currents likely reworked the shallow shelf and transported (simultaneously breaking up) the valve fragments off the shelf and deposited them onto the slope (Hosseininejad, 2016).

The high clay content of LA-B may be due to the resuspension and transport of shelf fines from storms, and the accumulation of these fines in a slope setting (Potter et al., 2005).

Lithofacies association C: lower slope to basin deposits

Lithofacies association C (LA-C) consists of laminated mudstone, coarsening-upward mudstone, burrowed mudstone and bentonite (lithofacies 1, 5, 6 and 7). It occurs from 164.00 to 173.45 m and 181.47 to 192.97 m depth in the MPC core (Figure GS2017-15-1). This lithofacies association is distinguished from the other associations by the presence of lithofacies 5 and 6, and has a low clay content.

LA-C represents the lowest energy conditions within the Boyne Member in the MPC core, as indicated by the occurrence of parallel laminations and lack of higher energy sedimentary structures in lithofacies 1, 5 and 6, as well as the abundance of burrows in lithofacies 6. The coarsening-upward trend of lithofacies 5 is interpreted as the result of increasing energy conditions, but the parallel laminations still suggest overall low-energy conditions. Collectively these interpretations suggest that deposition of LA-C took place in a lower slope or basinal setting (Potter et al., 2005).

Bentonites

Bentonite beds in the MPC core occur from 166.60 to 190.51 m depth and range in thickness from 1 to 13 cm (Figure GS2017-15-2). These grey-green to grey-yellow beds consist

mostly of swelling and nonswelling clay. Of the 100 bentonite beds identified between the upper Swan River Formation and Pierre Shale section of the MPC core (Nicolas, 2016), a total of 26 individual bentonite beds were recorded within the Boyne Member. The concentration of bentonite beds appearing in the middle of the Boyne Member forms the third largest Cretaceous volcanic-episode suite recorded in Manitoba and marks the resurgence of a very tectonically active western margin, resulting in large volcanic eruptions during the Laramide orogeny.

Cyclothems and lithofacies trends

The stacking pattern of lithofacies associations recognized in the Boyne Member in the MPC core (Figure GS2017-15-2) agrees well with the T-R cycles of McNeil and Caldwell (1981), and shows an overall retrogradational trend (LA-A to LA-C) stratigraphically upward. This trend is interpreted to represent an overall rise in relative sea level and corresponds with the overall transgression (T2) in the Niobrara cyclothem. The occurrence of LA-B at 173.45 to 181.47 m depth suggests a minor regression followed by a transgression. This last transgression is recorded in the chalky unit, which finding agrees with the interpretations of McNeil and Caldwell (1981).

Mineralogy

The mineralogical composition of the Boyne Member was evaluated using X-ray diffraction (XRD) analysis at the University of Manitoba crystallography laboratory on one or two samples from each lithofacies, where possible, in order to evaluate the bulk mineral phases present.

All of the Boyne Member samples have similar XRD patterns, indicating a high degree of commonality in their mineral composition. The dominant minerals are calcite, quartz and gypsum. Minor minerals include muscovite, hydronium jarosite, pyrite and clay minerals (possibly halloysite, illite, dickite and montmorillonite). A sample from a bentonite layer at a depth of 168.55 m in the MPC core contains a glassy blue mineral identified as melanterite.

Samples from lithofacies 4 (174.17 m depth) and 5 (182.31 m depth) were found to have very high calcite content. Samples from lithofacies 6 (192.90 m depth) were found to have very high quartz content. As expected, the calcite-rich samples were taken from calcareous intervals and the quartz-rich samples were from noncalcareous intervals. The sample from lithofacies 2 (209.00 m depth) has a very high gypsum content, which is attributed to gypsum blooms that formed as the core dried out in storage.

Organic geochemistry

Rock Eval® 6 pyrolysis was conducted at the Geological Survey of Canada (Calgary) organic geochemistry laboratory on 24 core samples to determine the source-rock potential of the Boyne Member. The samples were collected at 1–5 m intervals from the uppermost Morden Member, the entire Boyne Member and the lowermost Gammon Ferruginous Member. The Rock Eval results are presented in Table GS2017-15-2.

The temperature at which there is a maximum release of hydrocarbons from a gradually heated sample is measured as T_{max}. As such, values of T_{max} from Rock Eval pyrolysis increase linearly with the degree of maturation of a source rock and the thermal oil window is represented by T_{max} values that span from 435 to 470°C (Peters, 1986; Dellisanti et al., 2010). The T_{max} values for samples from the Boyne Member in the MPC core range from 393 to 422°C, indicating that the samples are thermally immature. Due to this immaturity, TOC and hydrogen index/oxygen index (HI:OI) ratio are the most useful parameters for evaluating source-rock potential in this study.

The TOC content is related to the quantity of organic matter (OM) in the rock and can be used to characterize source-rock richness (Peters, 1986). The TOC values in the MPC core range from 0.91 to 11.28 wt. %. Based on these results, the quantity of OM in the Boyne Member would seem to indicate 'very good' source-rock generative potential, as defined by Peters (1986). The TOC values fluctuate throughout the member and appear to be higher in specific intervals: 1) near the bottom of the member at ~208.00 m depth; 2) near the middle at ~183.00 m and ~190.00 m depth; and 3) at the top at ~172.00 m depth (Figure GS2017-15-2). The TOC values also appear to have a negative relationship with clay content. Fine mudstones generally have low TOC values, whereas medium to coarse mudstones have high TOC values.

The HI values range from 59 to 524 mg HC/g C_{org} and OI values range from 31 to 88 mg CO_2/g C_{org}. The modified van Krevelen diagram (HI versus OI) was used to distinguish the potential kerogen types (Figure GS2017-15-4); however, only a preliminary determination can be made because of the small sample set. Samples plot in the fields for Type II (oil prone) and Type III (gas prone) kerogen. The small cluster of values plotting closest to the Type II kerogen curve are from the bottom and middle intervals of high TOC values, as described above (occurring at depths of 209.07 m, 200.12 m, 190.80–188.75 m, 182.31 m and 174.17–169.85 m).

Boyne Member resource potential

Previous work done by the SUSG Project has shown that the Boyne Member in Manitoba has a high TOC content and is thermally immature (Nicolas and Bamburak, 2012). Boyne Member samples generally plot in the Type III (gas prone) field (Figure GS2017-15-3) and due to the thermal immaturity of the member, any gas present in the rocks was generated in situ by biogenic processes (Nicolas and Bamburak, 2012). The gas was produced by biodegradation of OM and is believed to have been rejuvenated with an inflow of meteoric water after the retreat of the Laurentide Ice Sheet (Nicolas and Grasby, 2009). As such, the production of gas in this area is typically accompanied by high water production (Nicolas, 2008).

Zones of medium to coarse mudstone (microporous rock) that contains high levels of organic carbon are good prospects for biogenic gas reservoirs (Nicolas, 2016). Higher quartz

Table GS2017-15-2: Rock Eval® 6 results of Upper Cretaceous units in the MPC core at 3-29-20-29W1, southwestern Manitoba. Table headers are: S1, milligrams of hydrocarbons that can be thermally distilled from one gram of rock; S2, milligrams of hydrocarbon generated by pyrolytic degradation of the kerogen from one gram of rock; S3, milligrams of CO_2 generated from a gram of rock when heated up to 390°C (mg/g); S3CO, milligrams of CO generated from a gram of rock when heated (mg/g); T_{max}, temperature at the point of maximum release of hydrocarbons during pyrolysis; TOC, total organic carbon; MINC, mineral carbon; HI, hydrogen index; OI, oxygen index; PC, pyrolyzed carbon; PI, production index; RC, residual carbon. Abbreviations: GF, Gammon Ferruginous; Mb., Member.

Sample number	Stratigraphic unit	Vertical depth m	S1 mg/L	S2 mg/L	S3 mg CO_2/g	S3CO mg CO/g	Tmax °C	TOC wt. %	MINC wt. %	HI	OI	PC %	RC %	PI
106-16-3384-166.1	GF Mb.	166.10	0.95	30.01	4.11	1.35	407	9.44	0.2	318	44	2.77	6.67	0.03
106-16-3384-167.16	GF Mb.	167.16	0.22	10.72	2.06	0.62	408	4.25	0.1	252	48	1.01	3.24	0.02
106-16-3384-168.31	Boyne Mb.	168.31	0.12	3.91	1.34	0.33	408	2.58	0.2	152	52	0.41	2.17	0.03
106-16-3384-168.77	Boyne Mb.	168.77	0.07	3.76	1.77	0.41	413	2.61	0.2	144	68	0.40	2.21	0.02
106-16-3384-169.85	Boyne Mb.	169.85	1.08	40.81	5.37	1.65	405	10.61	0.2	385	51	3.73	6.88	0.03
106-16-3384-174.17	Boyne Mb.	174.17	0.94	57.49	5.60	1.31	410	11.18	5.4	514	50	5.09	6.09	0.02
106-16-3384-178.2	Boyne Mb.	178.20	0.16	13.12	1.91	0.58	417	4.09	0.1	321	47	1.19	2.90	0.01
106-16-3384-182.31	Boyne Mb.	182.31	0.72	48.07	4.78	1.13	407	9.45	4.9	509	51	4.26	5.19	0.01
106-16-3384-183.1	Boyne Mb.	183.10	0.84	52.33	4.96	1.20	407	10.46	3.4	500	47	4.63	5.83	0.02
106-16-3384-184.67	Boyne Mb.	184.67	0.32	7.67	1.45	0.56	402	3.81	0.2	201	38	0.75	3.06	0.04
106-16-3384-185.97	Boyne Mb.	185.97	0.47	38.09	3.96	0.94	407	7.52	3.7	507	53	3.37	4.15	0.01
106-16-3384-188.75	Boyne Mb.	188.75	0.41	35.77	2.84	0.87	414	7.23	1.2	495	39	3.13	4.10	0.01
106-16-3384-190.8	Boyne Mb.	190.80	0.47	40.94	3.50	0.92	411	7.82	2.8	524	45	3.59	4.23	0.01
106-16-3384-192.9	Boyne Mb.	192.90	0.02	0.54	0.80	0.12	422	0.91	0.7	59	88	0.08	0.83	0.04
106-16-3384-193.79	Boyne Mb.	193.79	0.05	1.26	0.85	0.22	410	1.72	0.1	73	49	0.15	1.57	0.04
106-16-3384-196.51	Boyne Mb.	196.51	0.06	1.60	0.65	0.19	410	1.56	0.1	103	42	0.17	1.39	0.04
106-16-3384-200.12	Boyne Mb.	200.12	0.12	4.14	1.46	0.42	409	3.11	0.2	133	47	0.43	2.68	0.03
106-16-3384-202.58	Boyne Mb.	202.58	0.33	8.81	2.11	0.66	401	4.28	0.2	206	49	0.87	3.41	0.04
106-16-3384-204.97	Boyne Mb.	204.97	0.48	10.99	1.52	0.61	400	4.51	0.2	244	34	1.04	3.47	0.04
106-16-3384-207.59	Boyne Mb.	207.59	0.45	36.05	4.68	1.19	409	9.28	0.7	388	50	3.23	6.05	0.01
106-16-3384-209.0	Boyne Mb.	209.00	0.71	23.20	5.14	1.76	400	9.02	0.4	257	57	2.23	6.79	0.03
106-16-3384-209.07	Boyne Mb.	209.07	0.69	24.25	4.77	1.62	403	8.96	0.3	271	53	2.31	6.65	0.03
106-16-3384-210.07	Morden Mb.	210.07	0.40	11.42	1.77	1.23	393	5.69	0.5	201	31	1.09	4.60	0.03
106-16-3384-213.63	Morden Mb.	213.63	0.52	10.30	3.43	1.75	397	6.66	0.6	155	52	1.08	5.58	0.05

content in a reservoir is necessary to sustain sufficient permeability for gas extraction (Nicolas and Bamburak, 2012). Lower clay content, especially of non-swelling clay, is also preferred in a reservoir rock for gas extraction (Nicolas and Bamburak, 2012). Based on mudstone texture, TOC, quartz and clay content, two intervals in the MPC core are suggested to have the best biogenic gas potential: 185–190 m depth and 169–177 m depth. These sections have high TOC values, consistently higher silicate (likely quartz) and low clay contents, and consist of coarser mud. Another potential gas interval is located at 207–209 m. This interval meets all criteria, with the exception of lower silicate content (Shaw, 2017). Strong petroliferous odours and streaming white cuts that fluoresced in acetone under UV light were observed in samples from 203.90 m and 209.00 m depth. This observation further supports the gas potential of the proposed intervals.

Babcock beds

The Babcock beds, as described in Nicolas et al. (2010), are not clearly identifiable in this core. However, the stratigraphic positioning, variability in the lithology, texture and structure, and high TOC values of the interval between 177.21 and 173.45 m depth have similarities to those reported by Nicolas et al. (2010), suggesting this interval is a possible distal equivalent of the Babcock beds. In addition, this interval occurs within one of the potential gas horizons suggested above, which may also correspond with the gas-producing Boyne sand of the Kamsack reservoir in Saskatchewan. If these correlations are correct, then the Babcock beds and their equivalent distal facies, which potentially extend over a very large prospective area, may provide the key to the stratigraphic position–and targeting–of the best gas-bearing prospect in the Boyne Member.

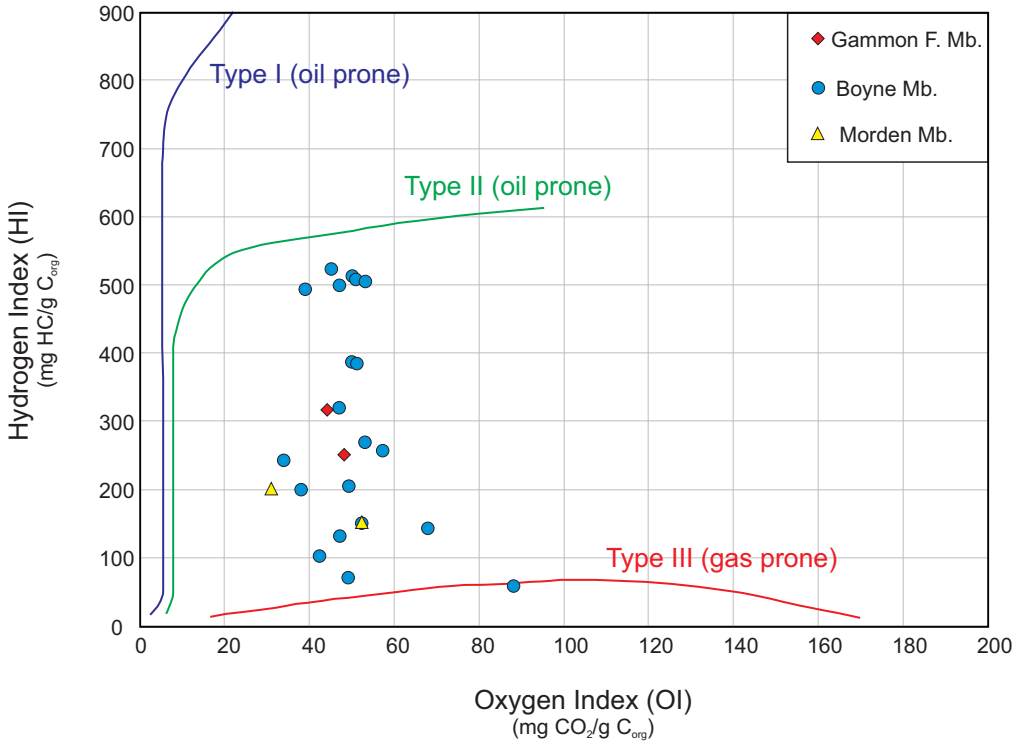

Figure GS2017-15-4: *Modified van Krevelan diagram of Rock Eval® 6 data from the MPC core at 3-29-20-29W1 from the Boyne Member, Carlile Formation, southwestern Manitoba. Abbreviations: F., Ferruginous; Mb., Member.*

Economic considerations

The goal of the SUSG Project is to provide energy exploration companies and investors with basic geoscience information in the risky, underexplored unconventional-gas play in southwestern Manitoba. This detailed evaluation of the Boyne Member offers a rare look into a thick section of this unit at 3-29-20-29W1, and provides important insight into the best horizon to target for potential natural gas production. Although further knowledge can still be gained from this core, this study provides the fundamental basis into this gas-bearing horizon from which to carry out further investigations.

Acknowledgments

The authors would like to acknowledge J. Bamburak (formerly Manitoba Geological Survey), and K. Lapenskie from the Manitoba Geological Survey (MGS) and M. Lennox for their assistance in the field; C. Epp from the MGS Midland Sample and Core Library for assistance with samples and core preparations; and M. Cooper and B. Elias from the Department of Geological Sciences of the University of Manitoba for their assistance with mineralogy and paleontology, respectively.

The authors would also like to thank H. Sanei and P. Webster from the Geological Survey of Canada, for their help with the organic geochemistry component of this project and their support through the hydrocarbon potential of Canadian oil shale program; and Manitoba Hydro (gas division), for their financial assistance.

References

Bamburak, J.D. and Nicolas, M.P.B. 2009: Revisions of the Cretaceous stratigraphic nomenclature of southwest Manitoba (parts of NTS 62F, G, H, J, K, N, O, 63 C, F); *in* Report of Activities 2009, Manitoba Innovation, Energy and Mines, Manitoba Geological Survey, p. 183–192.

Christopher, J.E., Yurkowski, M., Nicolas, M.P.B. and Bamburak, J.D. 2006: The Cenomanian–Santonian Colorado formations of eastern southern Saskatchewan and southwestern Manitoba; C. F. Gilboy and S.G. Whittaker (ed.), Saskatchewan and Northern Plains Oil & Gas Symposium 2006, Saskatchewan Geological Society Special Publication 19, p. 299–318.

Dellisanti, F., Pini, G. A. and Baudin, F. 2010: Use of T_{max} as a thermal maturity indicator in orogenic successions and comparison with clay mineral evolution; Clay Minerals, v. 45, p. 115–130.

Diaz, J.F. and Velez, M.I. 2016: New Insights on the lithostratigraphic nomenclature of the Carlile and Niobrara formations in southern Saskatchewan; *in* Summary of Investigations 2016, Saskatchewan Geological Survey, Saskatchewan Ministry of the Economy, Miscellaneous Report 2016-4.1, Paper A-2, vol. 1, p. 1–10.

Eriksson, P.G. and Reczko, B.F.F. 1997: Contourites associated with pelagic mudrocks and distal delta-fed turbidites in the Lower Proterozoic Timeball Hill Formation epeiric basin (Transvaal Supergroup), South Africa; Sedimentary Geology, v. 120, p. 319–335.

Hosseininejad, S.M. 2016: Organic, inorganic geochemistry and sedimentology of the Second White Specks Formation, eastern margin of the Western Interior Seaway, University of Calgary, Ph.D. thesis, 341 p.

Konitzer, S.F., Davies, S.J., Stephenson, M.H. and Leng, M. 2014: Depositional controls on mudstone lithofacies in a basinal setting: implications for the delivery of sedimentary organic matter; Journal of Sedimentary Research, v. 84, p. 198–214.

Lazar, R., Bohacs, K.M., Schieber, J., Macquaker, J. and Demko, T. 2015: Mudstone primer: lithofacies variations, diagnostic criteria, and sedimentologic-stratigraphic implications at lamina and bedset scale; Society for Sedimentary Geology, Tulsa, Oklahoma, v. 12, 200 p.

McNeil, D.H. and Caldwell, W.G.E. 1981: Cretaceous rocks and their foraminifera in the Manitoba Escarpment; Geological Association of Canada, Special Paper 21, 439 p.

Nicolas, M.P.B. 2008: Summary report on petroleum and stratigraphic investigations, southwestern Manitoba; *in* Report of Activities 2008, Manitoba Science, Technology, Energy and Mines, Manitoba Geological Survey, p. 171–179.

Nicolas, M.P.B. 2009: Williston Basin Project (Targeted Geoscience Initiative II): Summary report on Mesozoic stratigraphy, mapping and hydrocarbon assessment, southwestern Manitoba; Manitoba Science, Technology, Energy and Mines, Manitoba Geological Survey, Geoscientific Paper GP2009-1, 19 p.

Nicolas, M.P.B. 2016: Preliminary investigation from the Cretaceous section of the Manitoba Potash Corporation core at 3-29-20-29W1, southwestern Manitoba (NTS 65K1); *in* Report of Activities 2016, Manitoba Growth, Enterprise and Trade, Manitoba Geological Survey, p. 150–156.

Nicolas, M.P.B. and Bamburak, J.D. 2009: Geochemistry and mineralogy of Cretaceous shale, Manitoba (parts of NTS 62C, F, G, H, J, K, N): preliminary results; *in* Report of Activities 2009, Manitoba Science, Innovation, Energy and Mines, Manitoba Geological Survey, p. 165–174.

Nicolas, M.P.B. and Bamburak, J.D. 2011: Geochemistry and mineralogy of Cretaceous shale, southwestern Manitoba (parts of NTS 62F, G, J, K, N, 63C): phase 2 results; *in* Report of Activities 2011, Manitoba Innovation, Energy and Mines, Manitoba Geological Survey, p. 143–149.

Nicolas, M.P.B. and Bamburak, J.D. 2012: Update on the Shallow Unconventional Shale Gas Project, southwestern Manitoba (parts of NTS 62C, F, G, H, J, K, N, O, 63C); *in* Report of Activities 2012, Manitoba Innovation, Energy and Mines, Manitoba Geological Survey, p. 134–140.

Nicolas, M.P.B. and Grasby, S.E. 2009: Water and gas chemistry of Cretaceous shale aquifers and gas reservoirs of the Pembina Hills area, Manitoba (parts of NTS 62G); *in* Report of Activities 2009, Manitoba Innovation, Energy and Mines, Manitoba Geological Survey, p. 175–182.

Nicolas, M.P.B., Edmonds, S.T., Chow, N. and Bamburak, J.D. 2010: Shallow unconventional Cretaceous shale gas in southwestern Manitoba: an update (parts of NTS 62C, F, G, H, J, K, N); *in* Report of Activities 2010, Manitoba Innovation, Energy and Mines, Manitoba Geological Survey, p. 159–169.

Peters, K.E. 1986: Guidelines for evaluating petroleum source rock using programmed pyrolysis; American Association of Petroleum Geologist Bulletin, v. 70, no. 3, p. 318–329.

Potter, P.E., Maynard, J.B. and Depetris, P.J. 2005: Mud and mudstones: introduction and review; Springer-Verlag, Berlin, Heidelberg, Germany, 297 p.

Shaw, D. 2017: Stratigraphy, lithofacies analysis, and geochemistry of the Upper Cretaceous Boyne Member, Carlile Formation, southwestern Manitoba; University of Manitoba, B.Sc. thesis, Winnipeg, Manitoba, 124 p.

Stow, D. A.V. 1981: Laurentian fan: morphology, sediments, processes and growth patterns; America Association of Petroleum Geologist Bulletin, v. 65, p. 375–393.

Thiede, J. and Dinkelman, M.G. 2007: Occurrence of *Inoceramus* remains in Late Mesozoic pelagic and hemipelagic sediments; Deep Sea Drilling Program, v. 39, p. 899–910.

GS2017-16

Preliminary investigation of the potential for lithium in groundwater in sedimentary rocks in southwestern Manitoba

by M.P.B. Nicolas

In Brief:

- Salinities in Manitoba's complex groundwater aquifer system range from brines in deeper aquifers to freshwater in shallower aquifers
- Compiled archival water chemistry data indicate Li is rarely analysed
- The highest Li value (7.32 ppm) was obtained from the Souris Valley aquifer

Citation:
Nicolas, M.P.B. 2017: Preliminary investigation of the potential for lithium in groundwater in sedimentary rocks in southwestern Manitoba; *in* Report of Activities 2017, Manitoba Growth, Enterprise and Trade, Manitoba Geological Survey, p. 183–190.

Summary

Production of lithium (Li) from deep brines in continental sedimentary basins is the most common and cost-effective source of Li. Southern Manitoba has a complex groundwater aquifer system, with salinities ranging from brines in the deeper aquifers to freshwater in the shallower and eastern aquifers. Manitoba's oil and gas operations produce large quantities of these brines, which contain a wide range of trace elements. Although very limited preliminary results indicate the Li concentrations in Manitoba's brines are low, extrapolation of better, more comprehensive results from Saskatchewan suggests that there is potential for Li concentrations to be higher than currently recorded in Manitoba and that more work needs to be done to evaluate the deeper aquifers.

This project seeks to evaluate the current level of knowledge of Li concentration in the deep brines, as well as the freshwater aquifers, to develop a better understanding of the mineral potential of brines in southern Manitoba. This paper reviews archival Li data from the literature and well records.

Introduction

Brines are accumulations of saline groundwater that occur in continental sedimentary basins and can be a common source of dissolved trace metals, including Li. Metal extraction from these deep brines through evaporitic methods is currently the most common and economical way of extracting Li (Munk et al., 2016). Typically, this extraction is carried out by pumping the brines to the surface and metal concentration occurs by evaporation in a succession of artificial ponds, each subsequent one in the circuit having a greater Li concentration. Depending on the climate, but typically after a few months to about a year, a concentrate of 1 to 2% Li is further processed in a chemical plant to yield various end products, such as lithium carbonate and lithium metal (Bradley et al., 2013). When produced from brines, Li has an economical threshold of approximately 100 ppm from a maximum depth of 1 km (Munk et al., 2016), making that method much more cost-effective than extracting the Li from hard-rock sources (e.g., spodumene from Li-bearing pegmatite). However, all brine operations to date rely on hot, arid climates at the extraction site as a means to evaporate and concentrate the brines, which can be a lengthy process. Other technologies are being tested in order to reduce the amount of time typically needed in traditional evaporation ponds (i.e., from 18 months to 1 day; JWN Energy Group, 2017).

With the demand for Li increasing, particularly for use in batteries for hybrid cars and portable electronic devices (Munk et al., 2016), continental brines in untraditional climates are being looked at as possible sources and their production is only limited by the technology currently available to extract the elements. Most Li brines are associated with sodium chloride evaporite deposits, of which there is an abundance in the Williston Basin. Information on trace elements in brines in Manitoba is scarce and, with global demand increasing for Li, the Manitoba Geological Survey is addressing the growing need for this basic geoscience information. The objectives of this project are to 1) search available archival groundwater-chemistry databases and well files for trace elements, including Li, in the sedimentary rocks in southern Manitoba; and 2) collect and analyze new groundwater samples for trace elements, including Li, with the purpose of providing a better understanding of the mineral potential of brines in southern Manitoba. This paper reports on results of the archival data search.

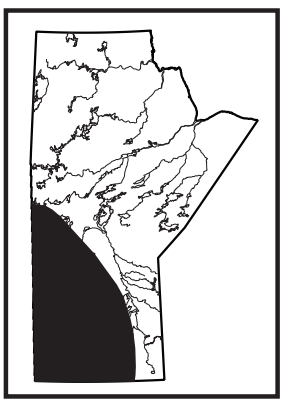

Regional setting

In Manitoba, the Williston Basin consists of Paleozoic, Mesozoic and Cenozoic strata that form a basinward, southwesterly-dipping wedge of carbonate, evaporite and clastic rocks (Nicolas, 2008; Nicolas and Barchyn, 2008). The Williston Basin is an intracontinental basin with potentially economic brines, as demonstrated by several groundwater aquifers hosted in sedimentary rocks with varying salinities and chemical signatures (Betcher et al., 1995; Grasby and Betcher, 2002; Palombi, 2008). This sedimentary package can range from a maximum thickness of approximately

2300 m in the extreme southwestern corner of the province to a few metres along its eastern outer edge (Nicolas and Barchyn, 2008). Within those strata are up to 16 separate regional aquifers, as defined by Palombi (2008), all with varying salinities (Figure GS2017-16-1). In the west, the Jurassic and Paleozoic aquifers are dominantly brines, with total dissolved solids (TDS) levels >35 000 mg/L, based on the classification system of Hem (1985); in the east, the Paleozoic aquifer, referred to as the carbonate-rock aquifer (Grasby and Betcher, 2002), is dominantly freshwater, with a TDS level <2000 mg/L. Narrow transition zones of saline to brackish water occur between these two end members; saline water has TDS levels between 10 000 and 35 000 mg/L, and TDS levels of brackish water range from 2000 to 10 000 mg/L (Hem, 1985). Figure GS2017-16-1 shows the variation in salinity from west to east.

The regional flow system is characterized by influx of freshwater from the topographic highs in the northwestern United States, at the western edge of the Western Canada Sedimentary

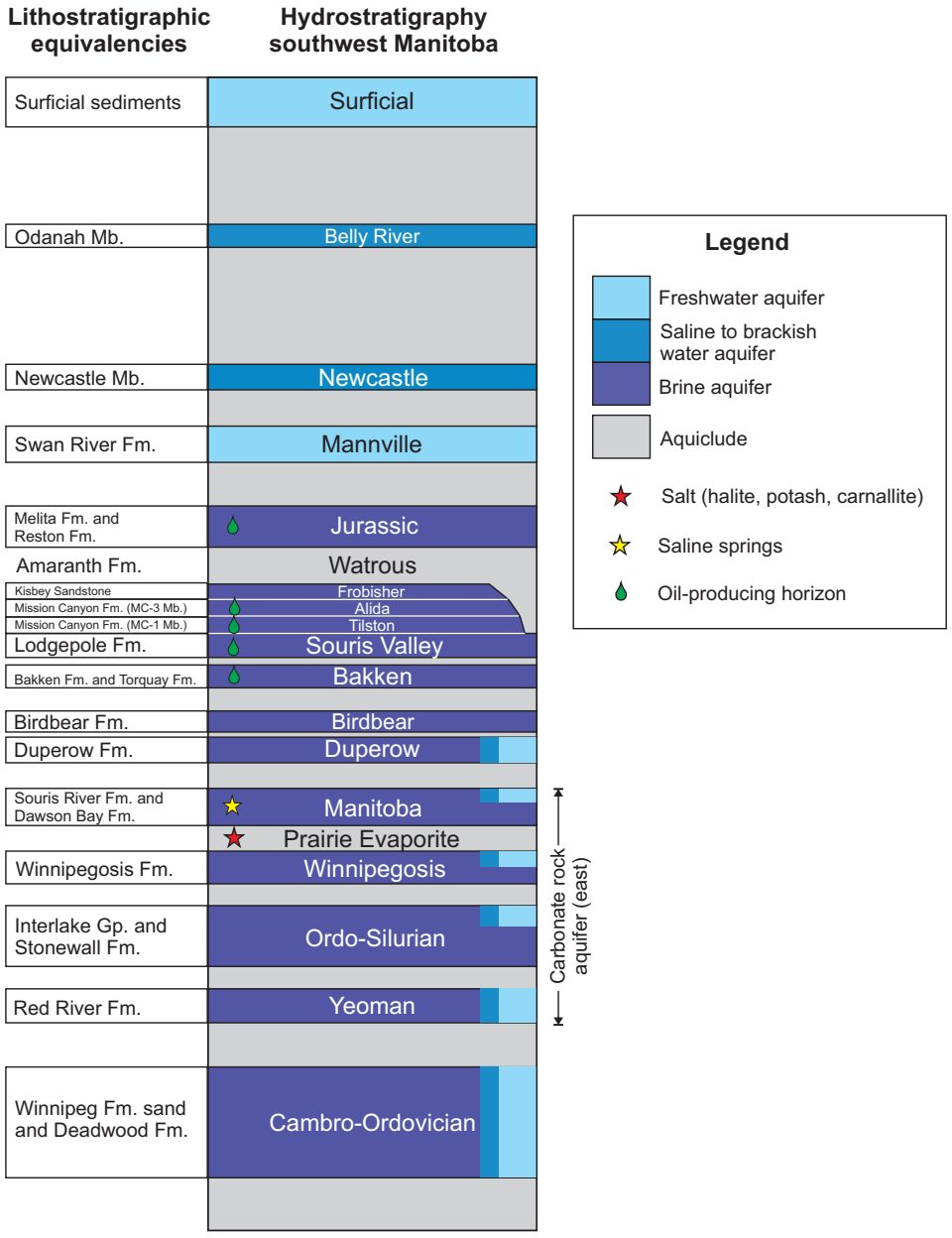

Figure GS2017-16-1: *Hydrostratigraphy of southwestern Manitoba, modified from Palombi (2008), with equivalent southwestern Manitoba lithostratigraphic units. Red star indicates formation consisting dominantly of raw salt dominated by halite, potash and carnallite. Yellow star indicates formation with saline springs at surface. Horizons with oil production in Manitoba are indicated. The carbonate-rock aquifer range is as defined by Grasby and Betcher (2002). Aquifer-salinity changes are indicated by colour gradients; full-height boxes indicate salinity changes occur east- and northward, half-height boxes indicate salinity changes occur northward only. Salinity ranges are based on the classification of Hem (1985), and the total dissolved solids mapping of Palombi and Rostron (2013). Abbreviations: Fm., Formation; Gp., Group; Mb., Member.*

Basin (WCSB), with a regional movement of formation water to the northeast resulting in a western regional-scale updip flow of saline water into Manitoba. In Manitoba, saline springs discharge along the eastern edge of the Williston Basin located in the eastern part of the WCSB (van Everdingen, 1971; Downey et al., 1987; Hannon, 1987; Plummer et al., 1990; Bachu and Hitchon, 1996; Grasby and Betcher, 2002). Within the Williston Basin, host to several thin evaporitic beds, the Devonian Prairie Evaporite is the thickest evaporitic unit, reaching up to 200 m in thickness (Fuzesy, 1984; Yang et al., 2009), as well as the most widespread. This unit consists dominantly of salt, including halite, potash and carnallite, with minor anhydrite and clay (Nicolas, 2015). The subsurface distribution of the Prairie Evaporite can be seen in Fuzesy (1984), Bezys and Conley (1998), TGI Williston Working Group (2008) and Nicolas (2015). The regional flow system provides less saline waters from the southwest, and as water driving forces push the waters deeper into the basin and to the northeast, they cause them to mix with in situ formation waters. These waters partially or completely dissolve the Prairie Evaporite in its path, further increasing the salinity of the groundwater. In the east, the regional flow trend is reversed along the eastern erosional edge of the basin in the Interlake and Sandilands regions, where freshwater flows from east to west (Figure GS2017-16-2; Simpson et al., 1987; Betcher et al., 1995). This eastern freshwater system is referred to as the carbonate-rock aquifer and consists of gently west-dipping, carbonate-dominated strata spanning from the Red River Formation up to the Souris River Formation, and includes minor shales and evaporites (Grasby and Betcher, 2002). A major hydrological divide separates these two regional groundwater-flow systems (Figure GS2017-16-2; Grasby and Betcher, 2002). Saline springs occur west of this divide, where deep basinal waters flow updip to the surface (Figure GS2017-16-2).

Salt water production from oil wells

The Williston Basin in southwestern Manitoba is host to oil, gas, potash and salt resources. Oil and gas extraction are the dominant resource extraction industry in this part of the province, with minor salt extraction through solution mining. Potash resources, although extensive, have yet to be extracted (Nicolas, 2015). Through all these extraction processes, a large volume of saltwater (mostly brine, but can include saline or brackish water) is produced that requires treatment before being disposed of at various stratigraphic levels in the subsurface. This saltwater waste contains dissolved trace elements that may be of economic value.

Water production associated with oil and gas extraction is normal, and requires treatment and disposal after separation at oil batteries. The economics of any given oil well is not only dependent on the market oil price, but also on the oil/water ratio of that well during its lifetime, with water production increasing over time. Wells with higher water production (usually mature, long-producing wells) are more expensive to operate due to the logistics and costs associated with saltwater disposal. The hydrogeochemistry of the saltwater is variable, depending on the source formation and location within the basin. In Manitoba, deeper formation water is brine, with decreasing salinity toward the outcrop edge of the formation. Based on the mapping by Palombi (2008), water in subcropping formations shows a slight decrease in salinity toward the formations' erosional edge (Figure GS2017-16-1), but mostly is classified as brine. If the brines have dissolved metals at a considerable concentration, then this could assist in the economics of marginal wells.

Southwestern Manitoba has thousands of producing oil wells, all of them producing saltwater along with oil. The current oil producing horizons in Manitoba span from the Devonian Torquay Formation up to the Jurassic Melita Formation (Figure GS2017-16-1). Much of the produced water is re-injected into the producing formation from which it was extracted to assist with enhanced oil recovery (EOR) operations, with the added benefit that the water is already chemically compatible with the reservoir. Saltwater from wells that produce water in excess of what is needed for EOR, or that is simply not required, needs to be disposed of, which is generally done by injecting it into other deep formations within an aquifer that will not adversely affect other local groundwater systems or extractive operations. This excess saltwater may contain economic concentrations of dissolved trace elements, including Li.

Despite the high number of oil wells, data on trace-element contents from produced saltwater are limited because petroleum companies do not require this information for their operations. Water analyses that are conducted by petroleum companies are most often restricted to basic water-analysis packages offered by analytical laboratories. As a result, water analyses in petroleum technical well files usually report only on these major ions: K, Na, Ca, Mg, Fe, Cl, HCO_3, SO_4 and CO_3. Other dissolved metals may be measured upon request from the company, such as Sr, Ba, Bo, and rarely Br and I, but overall trace-element analysis, either of the full suite or of selected elements, is not done.

Data sources and results

The oil industry, on occasion, collects water samples during drill-stem tests (DST) from producing wells, or at batteries, to conduct water analyses. These water analyses, along with any additional chemical analyses conducted, are submitted to the Government of Manitoba and stored in the database of Petroleum Technical Well files. In addition, there are two major regional groundwater studies that were conducted, each consisting of several sampling sites. Grasby et al. (1999) collected a total of 1156 water samples from various aquifers sourced from domestic wells and testholes, saline springs, oil wells and DST analyses. A large suite of elements were tested but Li concentrations were not reported by these authors. Ferguson et al. (2005) compiled groundwater chemistry data from various sources, including Grasby et al. (1999), but focused only on results from the Winnipeg Formation aquifer (Cambro-Ordovician). Ferguson et al. (2005) results comprised concentrations for Li, including previously unreported results from the study conducted by Grasby et al. (1999). Table GS2017-16-1 shows

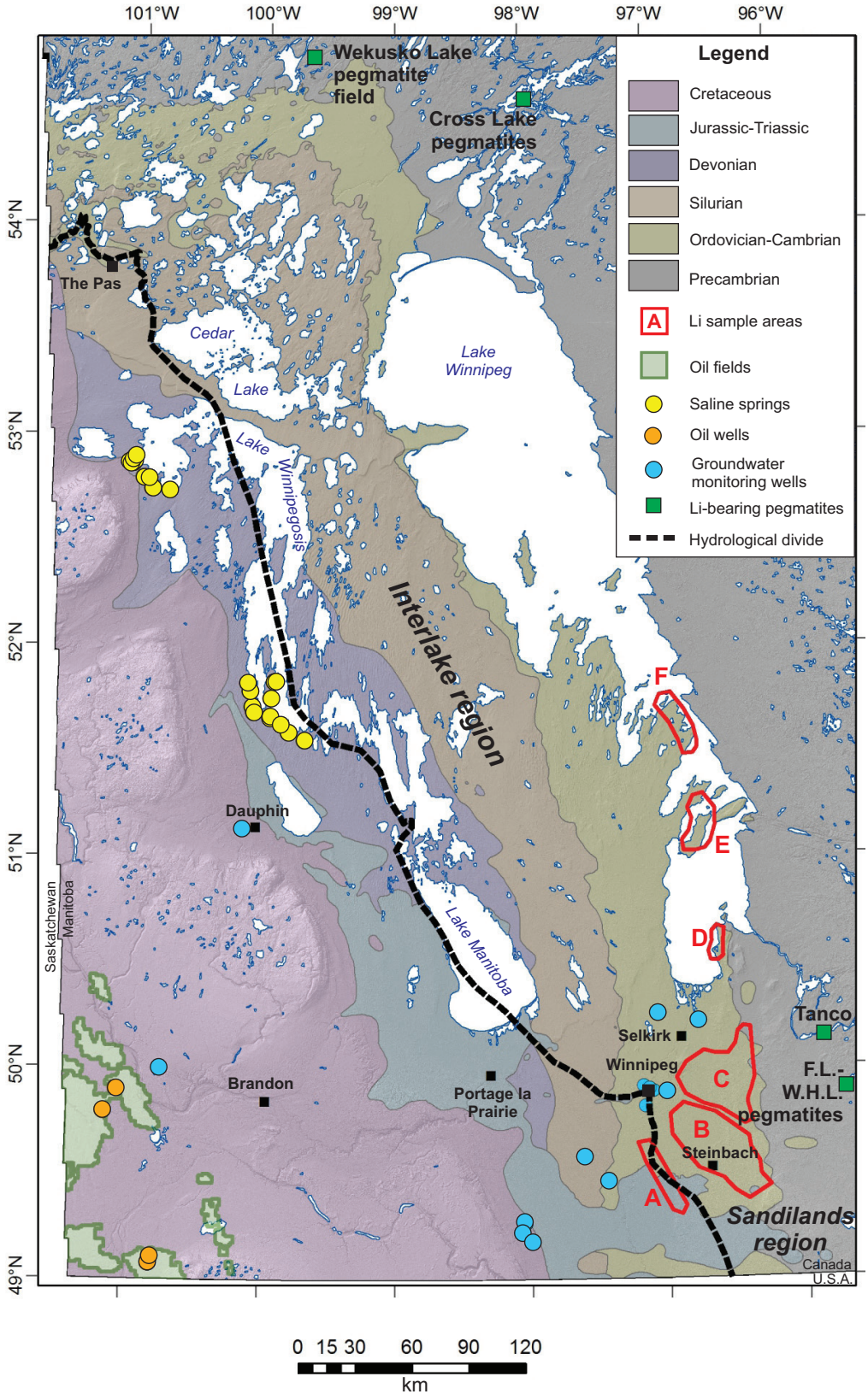

Figure GS2017-16-2: *Regional geological map with digital elevation model of southern Manitoba showing hydrological divide (follows the 2000 mg/L total dissolved solids contour) with the location of saline springs and freshwater recharge regions from Grasby and Betcher (2002); areas A through F group multiple water-sampling points (data from Ferguson et al., 2005); oil wells and groundwater-monitoring wells with Li analyses are shown. Digital elevation model from United States Geological Survey (2002). Abbreviation: F.L.–W.H.L., Falcon Lake–West Hawk Lake.*

Table GS2017-16-1: Lithium concentrations from selected Manitoba locations. All results are from groundwater analysis, except for the saltwater disposal well, which is measured from brine derived from a salt-solution operation. Licence numbers refer to the oil-well licence number. Water classification is based on Hem (1985). Areas A through F are as shown on Figure GS2017-16-2. Abbreviations: ABDP, abandoned producing well; Fm., Formation; Mb., Member; NA, not applicable; PTWF, Petroleum Technical Well File; SWD, saltwater disposal well; WSD, Water Stewardship Division.

Location	Well type	Stratigraphic unit or lithology	Depth (m)	Hydrostratigraphic unit	Water classification	Li (ppm)	Source
08-32-001-25W1 (licence 3311)	ABDP	Lower Amaranth Mb. (siltstone)	887.0-902.0	Jurassic aquifer	brine	3.970	PTWF
05-09-002-25W1 (licence 3492)	ABDP	Lower Amaranth Mb. (siltstone)	881.0-891.0	Jurassic aquifer	brine	0.258	PTWF
13-31-009-27W1 (licence 3138)	ABDP	Lodgepole Fm. (carbonate)	713.0-745.5	Souris Valley aquifer	brine	7.320	PTWF
03-12-011-27W1 (licence 4948)	SWD	Prairie Evaporite (salt)	1216.0-1299.0	Prairie Evaporite aquiclude	brine	< 1.800	PTWF
Area A	various	Winnipeg Fm.	NA	Cambro-Ordovician aquifer	saline and freshwater	0.000054-0.00115	Ferguson et al. (2005)
Area B	various	Winnipeg Fm.	NA	Cambro-Ordovician aquifer	freshwater	0.00001-0.170	Ferguson et al. (2005)
Area C	various	Winnipeg Fm.	NA	Cambro-Ordovician aquifer	brackish to freshwater	0.00003-0.300	Ferguson et al. (2005)
Area D	various	Winnipeg Fm.	NA	Cambro-Ordovician aquifer	freshwater	0.002-0.080	Ferguson et al. (2005)
Area E	various	Winnipeg Fm.	NA	Cambro-Ordovician aquifer	saline to freshwater	0.006-0.020	Ferguson et al. (2005)
Area F	various	Winnipeg Fm.	NA	Cambro-Ordovician aquifer	brackish to freshwater	0.005-0.190	Ferguson et al. (2005)
RIVER LOT UNKNOWN IN PARISH OF St. Boniface	observation	Winnipeg Fm. (sandstone)	172.935	Cambro-Ordovician aquifer	brine	3.440	WSD
RIVER LOT 0035 IN PARISH OF St. John	observation	Winnipeg Fm. (sandstone)	190.195	Cambro-Ordovician aquifer	brine	0.857	WSD
SW-4-11-4E	observation	carbonate	105.156	Carbonate rock aquifer	saline	0.780	WSD
NW-8-6-1E	observation	carbonate	36.576	Ordo-Silurian aquifer	saline	1.400	WSD
NW-13-7-2W	observation	carbonate	136.55	Ordo-Silurian aquifer	saline	0.488	WSD
NW-13-7-2W	observation	carbonate	136.55	Ordo-Silurian aquifer	saline	0.616	WSD
NE-1-15-3E	observation	sandstone	147.523	Cambro-Ordovician aquifer	saline	2.000	WSD
NE-30-14-6E	test well	sandstone	89.611	Cambro-Ordovician aquifer	saline	3.230	WSD
SW-6-3-4W	observation	sandstone	86.563	Jurassic aquifer	saline	1.560	WSD
SW-6-3-4W	observation	sandstone	86.563	Jurassic aquifer	saline	1.330	WSD
SW-6-3-4W	observation	sandstone	86.563	Jurassic aquifer	saline	1.280	WSD
SW-6-3-4W	observation	sandstone	86.563	Jurassic aquifer	saline	1.200	WSD
SW-22-3-5W	observation	sandstone	96.926	Jurassic aquifer	saline	0.949	WSD
SW-22-3-5W	observation	sandstone	96.926	Jurassic aquifer	saline	1.470	WSD
SW-22-3-5W	observation	sandstone	96.926	Jurassic aquifer	saline	1.030	WSD
NW-35-3-5W	observation	sandstone	71.628	Jurassic aquifer	saline	0.761	WSD
NW-35-3-5W	observation	sandstone	71.628	Jurassic aquifer	saline	1.380	WSD
NW-35-3-5W	observation	sandstone	71.628	Jurassic aquifer	saline	1.140	WSD
RIVER LOT 0035 IN PARISH OF St. John	production	carbonate	NA	Carbonate rock aquifer	brine	3.840	WSD
NW-8-12-24W	observation	shale	27.45	Belly River aquifer?	saline	1.180	WSD
SE-12-25-20W	production	shale	39.65	Belly River aquifer?	saline	0.706	WSD
RIVER LOT 0015 IN PARISH OF St. Vital	test well	Winnipeg Fm. (sandstone)	158.6	Cambro-Ordovician aquifer	saline	0.958	WSD

the range in Li concentrations reported in Ferguson et al. (2005) grouped by geographic area (also shown in Figure GS2017-16-2). Another source of water-chemistry data is from groundwater monitoring and test wells from the internal database GWDrill managed by the Water Stewardship Division of Manitoba Sustainable Development (Table GS2017-16-1; Manitoba Water Stewardship, 2007). Although restricted to shallower (<200 m) aquifers, it provides information on different aquifers and complements data collected by Grasby et al. (1999) and Ferguson et al. (2005).

The search through the Petroleum Technical Well files returned only four well records with Li concentrations reported (Table GS2017-16-1). Due to the high number of well records, a strategic search was conducted focusing on 1) wells with chemical analyses indexed in the well files; 2) wells with water analyses indexed in the well files that are either water-source wells or saltwater-disposal wells (abandoned or active); and 3) random sampling of producing or abandoned dry wells. Of the four well records, only three represent samples from the groundwater itself, and the fourth is from brine from a salt-solution operation in the Prairie Evaporite.

Comparison to brines in Saskatchewan

Saskatchewan extracts oil from deeper horizons than that produced in Manitoba, allowing for a wider range of aquifers to be easily tested at the oil-well sites. As a result, the deep aquifers in the Saskatchewan portion of the Willison Basin have undergone more testing for trace-metals concentrations, including Li. Rostron et al. (2002) report on the Saskatchewan Brine Sampling Program, which collected formation water from several deep aquifers. Follow-up work was conducted by Jensen (2011, 2012, 2016). Rostron et al. (2002) reported Li values from southeastern Saskatchewan as high as 112 ppm from the Yeoman aquifer, 108 and 83.7 ppm from the Duperow aquifer, whereas Jensen (2012, 2016) reported subeconomic Li values, the highest being 59.0 ppm, from the Birdbear aquifer and 63 ppm from the Winnipegosis aquifer.

Discussion

The concentration of Li in Manitoba's groundwater is variable, with values from brines in the oil wells ranging from 0.258 to 7.320 ppm; values from freshwater to brackish water wells ranging from 0.00001 to 0.300 ppm; and values from shallow saline waters to brines in monitoring wells ranging from 0.488 to 3.840 ppm (Table GS2017-16-1). Despite the small number of results from deep brines, Li concentrations in Manitoba's groundwater are low, with overall higher concentrations in the deep Jurassic and Paleozoic brines of southwestern Manitoba's oil region. Shallower brines and saline waters measured from the groundwater monitoring wells have slightly lower values for Li, compared with the brines derived from deep oil wells (Table GS2017-16-1). Freshwater-dominated Cambro-Ordovician aquifers along the eastern erosional edge of the Williston Basin have extremely low Li concentrations, likely just within detection limits.

The Li values in Table GS2017-16-1, regardless of the source, do not meet the economic threshold used for current evaporitic extraction methods (Munk et al., 2006), notwithstanding the fact that the climate in Manitoba is not suitable for open-air evaporation ponds. Although Li extraction from the brines is generally more promising than extraction from the freshwater in Manitoba's groundwater column, extracting this element can only be considered with the help of new low-cost, efficient technologies that would be capable of treating the brine on site, such as at oil batteries and saltwater source or disposal sites. Such technologies are currently being developed by MGX Mineral Inc., where a new low-energy design, rapid-recovery process is being tested with promising results (MGX Minerals Inc., 2017). This type of technology could also be used in Manitoba if it can be developed for application in commercial-scale operations.

Given that Saskatchewan reports higher Li concentrations in deeper horizons than those tested in Manitoba and the regional groundwater flow is to the east and northeast (Figure GS2017-16-2), there is the possibility that higher Li concentrations can also be found in Manitoba. More testing would need to be done to verify this hypothesis but given the current oil production, testing would be limited to the restricted oil column currently in production and the deeper horizons (e.g., Red River and Duperow formations) could not be tested, unless wells deeper than those reaching the current oil-producing horizons were drilled.

Lithium concentrations in the Cambro-Ordovician freshwater aquifer, despite being low, are quite variable. Of all the samples in Ferguson et al. (2005), area C shows the highest Li values (Figure GS2017-16-02). Based on the regional groundwater flow for this region (from east to west), the source of Li may be from the weathering of proximal Precambrian rocks underlying the samples sites or from the eastern highlands, which have known hard-rock Li occurrences, such as the Cat Lake–Winnipeg River pegmatite field (including the highly Li-enriched Tanco pegmatite; Černý et al., 1981) and the pegmatites of the Falcon Lake–West Hawk Lake area (Bannatyne, 1985). It is uncertain if the overlying carbonate-rock aquifer would present similar Li ranges, but it nevertheless warrants testing. In the northern extension of the aquifers, Li occurrences in the Wekusko Lake pegmatite field (Černý et al., 1981; Martins et al., GS2017-5, this volume) and Cross Lake pegmatite swarm (Bannatyne, 1985) may also provide a suitable source for enrichment.

Future work

In the next phase of the project, brine samples from existing oil-well operations, as well as from the saline springs, will be collected to analyze them for a range of trace elements and evaluate their mineral potential.

Economic considerations

Saltwater production and disposal from oil wells is a constant issue for the petroleum industry and is one of the dominant reasons for marginal well abandonment. The mineral

potential of these brines may serve as an excellent economic opportunity for the operators to improve their profits and extend the life of marginal oil wells, taking advantage of the array of infrastructure already in place for these operations.

Acknowledgments

The author would like to thank T. Martins of the Manitoba Geological Survey for her support and guidance throughout this project, and P. Fulton-Regula from the Manitoba Petroleum Branch for her assistance in searching the well file database. The author would like to gratefully acknowledge G. Phipps of Manitoba Sustainable Development, Water Stewardship Division for water data and his critical review of this paper.

References

Bachu, S. and Hitchon, B. 1996: Regional-scale flow of formation waters in the Williston Basin; American Association of Petroleum Geologist Bulletin, v. 80, p. 248–264.

Bannatyne, B.B. 1985: Industrial minerals in rare-element pegmatites of Manitoba; Manitoba Energy and Mines, Mineral Resources Division, Economic Geology Report ER84-1, 96 p.

Betcher, R., Grove, G. and Pupp, C. 1995: Groundwater in Manitoba, hydrogeology, quality concerns, management; National Hydrology Research Institute Contribution CS-93017, Environment Canada.

Bezys, R.K. and Conley, G.G. 1999: Manitoba Stratigraphic Database and the Manitoba stratigraphic map series; Manitoba Energy and Mines, Geological Services, Open File Report OF98-7, 1 CD-ROM.

Bradley, D.B., Munk, L.A., Jochens, H., Hynek, S.A. and Labay, K. 2013: A preliminary deposit model for lithium brines; U.S. Geological Survey Open File Report 2013-1006, 6 p.

Černý, P., Trueman, D.L., Ziehlke, D.V., Goad, B.E. and Paul, J. 1981: The Cat Lake–Winnipeg River and the Wekusko Lake pegmatite fields, Manitoba; Manitoba Energy and Mines, Mineral Resources Division, Economic Geology Report ER80-1, 216 p.

Downey, J.S., Busby, J.F. and Dinwiddie, G.A. 1987: Regional aquifers and petroleum in the Williston Basin region of the United States; *in* Willison Basin: Anatomy of a Cratonic Oil Province, J.A. Peterson, D.M. Kent, S.B. Anderson, R.H. Pilatske and M.W. Longman (ed.), Rocky Mountain Associations of Geologists, p. 299–312.

Ferguson, G., Betcher, R.N. and Grasby, S.E. 2005: Water chemistry of the Winnipeg Formation in Manitoba; Geological Survey of Canada, Open File 4933, 37 p.

Fuzesy, A. 1984: Potash in western Canada; *in* The Geology of Industrial Minerals in Canada, G. R. Guillet and W. Martin (ed.), Canadian Institute of Mining and Metallurgy, Special Volume, vol. 29, p. 188–194.

Grasby, S.E. and Betcher, R.N. 2002: Regional hydrogeochemistry of the carbonate rock aquifer, southern Manitoba; Canadian Journal of Earth Sciences, v. 39, p. 1053–1063.

Grasby, S.E., Betcher, R.N. and McDougall, W.J. 1999: Water quality of the carbonate rock aquifer, southern Manitoba; Geological Survey of Canada, Open File 3725, 166 p.

Hannon, N. 1987: Subsurface water flow patterns in the Canadian sector of the Williston Basin; *in* Williston Basin: Anatomy of a Cratonic Oil Province, J.A. Peterson, D.M. Kent, S.B. Anderson, R.H. Pilatske and M.W. Longman (ed.), Rocky Mountain Associations of Geologists, p. 313–322.

Hem, J.D. 1985: Study and interpretation of the chemical characteristics of natural water; U.S. Geological Survey, Water Supply Paper 2254, 264 p.

Jensen, G.K.S. 2011: Investigating the mineral potential of brines in southeastern Saskatchewan; *in* Summary of Investigations 2011, Volume 2, Saskatchewan Geological Survey, Saskatchewan Ministry of Economy, Miscellaneous Report 2016-4.1, Paper A-3, p. 3.

Jensen, G.K.S. 2012: Initial results of a Brine Sampling Project: investigating the mineral potential of brines in southeastern Saskatchewan; *in* Summary of Investigations 2012, Volume 1, Saskatchewan Geological Survey, Saskatchewan Ministry of Economy, Miscellaneous Report 2012-4.1, Paper A-8, p. 8.

Jensen, G.K.S. 2016: Results from the 2016 field season for the Brine Sampling Project: investigating the mineral potential of brines in Saskatchewan; *in* Summary of Investigations 2016, Volume 1, Saskatchewan Geological Survey, Saskatchewan Ministry of Economy, Miscellaneous Report 2016-4.1, Paper A-3, p. 7.

JWN Energy Group 2017: MGX Minerals extracts first lithium from oilsands wastewater; JWN Energy Group, January 5, 2017, URL <http://www.jwnenergy.com/article/2017/1/mgx-minerals-extracts-first-lithium-oilsands-wastewater/> [September 2017].

Manitoba Water Stewardship 2007: GWDrill: a database of water well logs and groundwater chemistry of the province of Manitoba, Groundwater Management Section, Manitoba Water Stewardship, Winnipeg, Manitoba.

MGX Minerals Inc. 2017: Unlocking North America's lithium brine potential; MGX Minerals Inc., URL <https://www.mgxminerals.com/assets/lithium.html> [September 2017].

Munk, L.A., Hynek, S.A., Bradley, D.C., Boutt, D., Labay, K. and Jochens, H. 2016: Lithium brines: a global perspective; Review in Economic Geology, v. 18, p. 339–365.

Nicolas, M.P.B. 2008: Williston Basin Project (Targeted Geoscience Initiative II): results of the biostratigraphic sampling program, southwestern Manitoba (NTS 62F, 62G4, 62K3); Manitoba Science, Technology, Energy and Mines, Manitoba Geological Survey, Geoscientific Paper GP2008-1, 28 p.

Nicolas, M.P.B. 2015: Potash deposits in the Devonian Prairie Evaporite, southwestern Manitoba; *in* Report of Activities 2015, Manitoba Mineral Resources, Manitoba Geological Survey, p. 97–105.

Nicolas, M.P.B. and Barchyn, D. 2008: Williston Basin Project (Targeted Geoscience Initiative II): summary report on Paleozoic stratigraphy, mapping and hydrocarbon assessment, southwestern Manitoba; Manitoba Science, Technology, Energy and Mines, Manitoba Geological Survey, Geoscientific Paper GP2008-2, 21 p.

Palombi, D.D. 2008: Regional hydrogeological characterization of the northeastern margin in the Williston Basin; M.Sc. thesis, University of Alberta, Edmonton, Alberta, 196 p.

Palombi, D. and Rostron, B.J. 2013: Regional hydrogeological characterization of the northeastern margin of the Williston Basin; Manitoba Innovation, Energy and Mines, Manitoba Geological Survey, Open File OF2011-3, set of 55 1:3 000 000 scale maps.

Plummer, L.N., Busby, J.F., Lee, R.W. and Hanshaw, B.B. 1990: Geochemical modeling of the Madison aquifer in parts of Montana, Wyoming, and South Dakota; Water Resources Branch Research, v. 26, p. 1981–2014.

Rostron, B.J., Kelley, L.I., Kreis, L.K. and Holmden, C. 2002: Economic potential of formation brines: interim results from the Saskatchewan Brine Sampling Program; *in* Summary of Investigations 2002, Volume 2, Saskatchewan Geological Survey, Saskatchewan Industry Resources, Misc. Rep. 2002-2.4, Paper C-1, p. 29.

Simpson, F., McCabe, H.R. and Barchyn, D. 1987: Subsurface disposal of wastes in Manitoba - Part I: Current status and potential subsurface disposal of fluid industrial wastes in Manitoba; Manitoba Energy and Mines, Geological Services, Geological Paper GP83-1.

TGI Williston Working Group 2008: Devonian Prairie Evaporite: structure contour; Manitoba Science, Technology, Energy and Mines, Manitoba Geological Survey, Stratigraphic Map Series SM2008-DPE-S, Digital web release, scale 1:1 000 000, URL <http://www.gov.mb.ca/stem/mrd/geo/willistontgi/mapfiles/pdfs/044_dev_prairie_evap_str.pdf>. [October 2017]

United States Geological Survey 2002: Shuttle Radar Topography Mission, digital elevation model, Manitoba; United States Geological Survey, URL <ftp://edcsgs9.cr.usgs.gov/pub/data/srtm/>, portions of files N48W88W.hgt.zip through N60W102.hgt.zip, 1.5 Mb (variable), 90 m cell, zipped hgt format [March 2003].

van Everdingen, R.O. 1971: Subsurface-water composition in southern Manitoba reflecting discharge of saline subsurface waters and subsurface solution of evaporites; *in* Geoscience Studies in Manitoba, A.C. Turnock (ed.), Geological Association of Canada, Special Paper 9, p. 343–352.

Yang, C., Jensen, G. and Berenyi, J. 2009: The stratigraphic framework of the potash-rich members of the Middle Devonian Upper Prairie Evaporite Formation, Saskatchewan; *in* Summary of Investigations 2009, Volume 1, Saskatchewan Geological Survey, Saskatchewan Ministry of Energy and Resources, Misc. Rep. 2009-4.1, Paper A-4, p. 1–28.

GS2017-17

Till sampling and ice-flow mapping between Leaf Rapids, Lynn Lake and Kinoosao, northwestern Manitoba (parts of NTS 64B12, 64C9, 11, 12, 14–16, 64F3, 4)

by M.S. Gauthier and T.J. Hodder

In Brief:

- Purpose is to better-inform drift prospecting efforts in the Lynn Lake area
- Collected new till samples for analyses of till composition and kimberlite-indicator-minerals (KIM)
- Six phases of paleo-ice flow are reconstructed

Citation:
Gauthier, M.S. and Hodder, T.J. 2017: Till sampling and ice-flow mapping between Leaf Rapids, Lynn Lake and Kinoosao, northwestern Manitoba (parts of NTS 64B12, 64C9, 11, 12, 14–16, 64F3, 4); *in* Report of Activities 2017, Manitoba Growth, Enterprise and Trade, Manitoba Geological Survey, p. 191–204.

Summary

Quaternary geology fieldwork, including till sampling and ice-flow–indicator mapping, was conducted for 10 days in June 2017 along the road between Kinoosao (Saskatchewan), Lynn Lake and Leaf Rapids in northwestern Manitoba. Regional-scale (2.5–4 km spacing) till sampling was conducted along Provincial roads 391, 394 and 396 for characterization of the till composition. A total of 48 till samples (22.7 L each) were collected for kimberlite-indicator-mineral analysis. Additional 3 kg till samples were collected for trace-element geochemistry (<63 µm size-fraction) and clast lithology (2–30 mm size-fraction) analysis. Digitization of previous till-geochemistry sample results in the area is ongoing.

Paleo–ice-flow indicators were documented at 22 stations, and at least six ice-flow phases are recognized. Southerly paleo-ice flow (170–214°) is the dominant ice-flow phase. The till-sampling road-transect is aligned roughly perpendicular to this ice-flow orientation. Remnants of older ice-flow phases to the northwest, southwest and southeast were mapped, as were younger spatially restricted ice-flow phases to the southeast and southwest.

Esker ridges are the dominant glacial landforms, and a veneer of till drapes bedrock in most of the area. Preliminary results indicate the dominant till is a brown noncalcareous sand to silty sand till. Following the retreat of ice, shallow waters of glacial Lake Agassiz inundated the region. Wave-washing affected the till and bedrock highs between 330 and 435 m asl. Sand veneers were deposited between 280 and 435 m asl, and clay of variable thickness was deposited below 340 m asl.

From a mineral exploration point of view, results of this study will assist in evaluating the regional-scale diamond potential, and guide drift prospecting efforts in the Lynn Lake area.

Introduction

The Manitoba Geology Survey (MGS) conducted 10 days of road-based fieldwork in June 2017, along roads between Kinoosao, Lynn Lake and Leaf Rapids. A total of 109 stations were visited to log and sample exposed glacial sediments (till) and/or document the paleo–ice-flow history. The goals of this project were to

- conduct regional-scale (one sample every 2.5–4 km) kimberlite-indicator-mineral (KIM) sampling of till to assess the diamond potential of the study area along a transect roughly perpendicular to the dominant ice-flow orientation;
- conduct paleo–ice-flow mapping to assist reconstructions of the glacial dynamics of this area of Manitoba, which in turn guides drift exploration studies; and
- compile, digitize and update existing surficial mapping and till-geochemistry data (Figure GS2017-17-1).

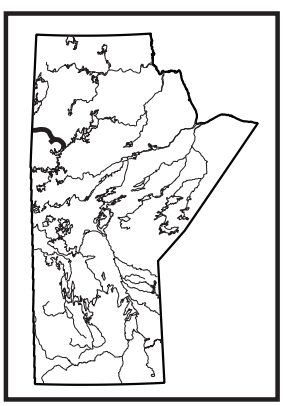

Physiography

The study area is located in the northwestern part of Manitoba, northwest of Leaf Rapids along road access to the Saskatchewan boundary (Figure GS2017-17-1). Elevation varies mainly from 250 m asl (above sea level) in the east to 450 m asl in the west. Local relief is generally 5 to 30 m. Drift cover is generally thin, though up to 50 m of drift has been intersected in drillholes within the region. The area is part of the extensive discontinuous permafrost zone (Sladen, 2011), and permafrost was encountered beneath organic deposits at most sites.

The study area is characterized by moderately drained coniferous forests, underlain by both mineral and organic soils (Land Resource Group - Manitoba, 2003). Well drained silty sand soils on upland sites are dominated by closed stands of medium to tall black spruce, jack pine, trembling aspen, balsam poplar and some paper birch. On sandier upland sites, more open stands of jack pine are common. The vegetation on bedrock exposures is sparse, and limited to areas where pockets

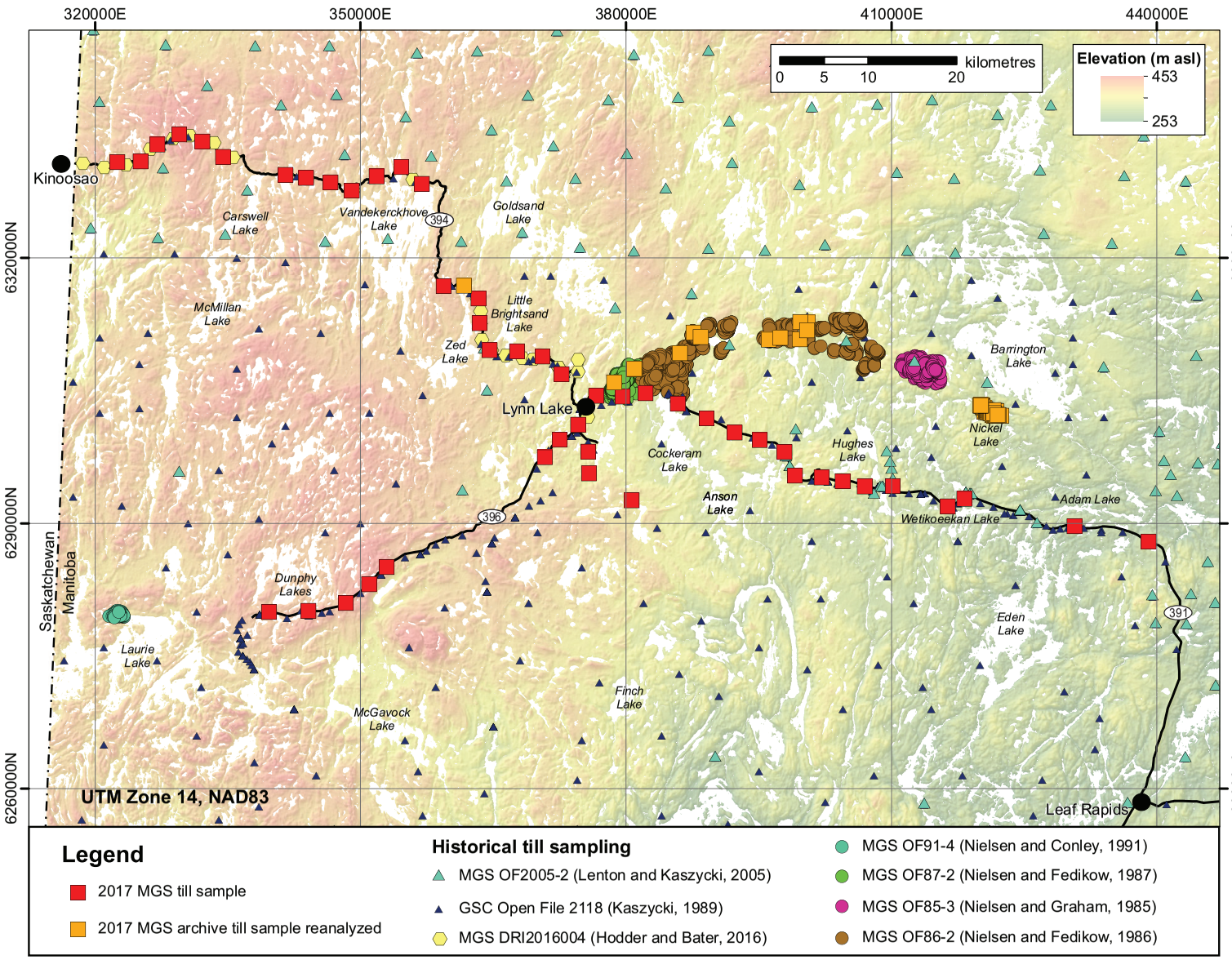

Figure GS2017-17-1: *The 2017 till sample sites and historical sample sites in the study area. Background hillshade was generated using a Canadian Digital Surface Model (Natural Resources Canada, 2012). Abbreviations: GSC, Geological Survey of Canada; MGS, Manitoba Geological Survey.*

of soil are present. Closed to open stands of black spruce, with Labrador tea and ground cover of mixed sphagnum moss and feathermoss, form the dominant vegetation on poorly drained mineral soils. On bog peatlands, the black spruce is more stunted and open, and in places is mixed with small quantities of tamarack.

Bedrock geology and diamond prospectivity

The study area is largely underlain by rocks belonging to the Lynn Lake greenstone belt, namely supracrustal rocks of the Wasekwan group (Gilbert et al., 1980), along with younger molasse-type sedimentary rocks of the Sickle group (Norman, 1934). These supracrustal rocks are intruded by granitoid plutons of different ages (Gilbert et al., 1980; Baldwin et al., 1987; Beaumont-Smith et al., 2006).

The diamond potential of the Lynn Lake area of Manitoba is unknown. There are currently no public KIM data available for the Lynn Lake region (Keller et al., 2004), hence this study will provide the first regional-scale insight into diamond potential from an indicator-mineral perspective. Results from the Lynn Lake area will be compared to recent KIM results in the Southern Indian Lake area (Hodder, 2017).

To the west, the Sask craton is known to host the Cretaceous Fort à la Corne diamondiferous kimberlites (Leckie et al., 1997). In addition, recent diamondiferous kimberlites have been discovered within the Sask craton at the Pikoo project (Armstrong and Kupsch, 2016), which is located approximately 100 km west of Flin Flon, Manitoba. The presence of Archean to earliest Proterozoic rocks in the west-central area of Southern Indian Lake, as well as the ubiquitous presence of zircons of Archean age in volcaniclastic rocks of the Southern Indian domain, suggests the potential existence for cratonic basement to the Trans-Hudson orogeny rocks in the area (Kremer et al., 2009). This may be analogous to the Archean crust of the Sask craton that is thought to underlie regions in east-central Saskatchewan. Ages consistent with that of the Sask craton were also observed in the Lynn Lake area in rocks from the Sickle group (Beaumont-Smith et al., 2006).

Surficial geology

Surficial geology between Kinoosao, Lynn Lake and Leaf Rapids (parts of NTS 64B12, 64C9, 11, 12, 14–16, 64F3, 4; Figure GS2017-17-2) has been mapped at a reconnaissance scale by DiLabio et al. (1986, 1:125 000 scale) and Kaszycki and Way Nee (1989a, 1:125 000 scale), and re-released as regional "A" series maps (Kaszycki and Way Nee, 1990a, b, 1:250 000 scale). The NTS map sheets 64C14 (Lynn Lake) and 15 (Cockeram Lake) were mapped in more detail, and produced as 1:50 000 scale black and white maps (O'Donnell, 1976a, b). A biophysical land classification has been published for a small portion of the study area (Land Resource Group - Manitoba, 2003). Most of the above mapping is not considered accurate enough for a detailed till-sampling program, but provides a guideline toward the regional surficial materials.

Till sample analyses

More information about the surficial geology of the field area can be gleaned from till-composition surveys conducted across the region. This includes a regional northwestern Manitoba study (Kaszycki, 1989), which included sampling and analyzing the <2 µm (clay) and <63 µm (silt and clay) size-fractions of till by standard atomic absorption spectroscopy (AAS) and instrumental neutron activation analysis (INAA), respectively. A report including this data was later released digitally (Kaszycki et al., 2008).

In 2003, MGS reanalyzed the <0.177 mm size-fraction of till samples from different locations that included sites between Lynn Lake and Kinoosao along PR 394 (Hodder, 2016). These samples were submitted for near-total digestion (four acid) followed by analysis with inductively coupled plasma–emission spectrometry (ICP-ES) and inductively coupled plasma–mass spectrometry (ICP-MS), as well as INAA. In 2005, MGS also reanalyzed the <0.177 mm size-fraction of a subset of till samples from the northwestern Manitoba project (Lenton and Kaszycki, 2005). These samples were submitted for near-total digestion followed by analysis with ICP-ES and ICP-MS (ultra-trace 3), as well as INAA. For unknown reasons, only a few of those samples were actually within NTS areas 64C14, 15 or 16.

Detailed till-geochemistry sampling projects were undertaken at targeted sites (Figure GS2017-17-1). These include studies at Farley Lake (NTS 64C16; Nielsen and Graham, 1985), between Minton and Nickel lakes (NTS 64C15 and 16; Nielsen and Fedikow, 1986), the Dot Lake to MacLellan mine area (NTS 64C15; Nielsen and Fedikow, 1987) and Laurie Lake area (Nielsen and Conley, 1991). All four studies analyzed the <2 µm (clay) size-fraction of till using standard AAS. Forty-seven samples from the Nickel Lake area have been pulled from archive and are currently being reanalyzed using modern analytical techniques to determine till-composition in this region.

Gold

Heavy mineral separates were analyzed for gold in three of the detailed till-geochemistry studies (Nielsen and Graham, 1985; Nielsen and Fedikow, 1986, 1987), and in the regional study (Kaszycki, 1989). The separates were concentrated from the 'fine sand fraction', which likely translates to between 0.125 and 0.25 mm on the Wentworth grain-size scale (Wentworth, 1922). Processing and grain counts for visible gold were carried out by Overburden Drilling Management Limited (Nepean, Ontario).

Methods

Road-based fieldwork was undertaken over 10 days in June 2017, based out of Lynn Lake (Figure GS2017-17-2). A total of 109 field sites were visited to ground-truth the surficial geology mapping, collect till samples and identify ice-flow indicators.

The surficial material at each field station was investigated by means of a hand-dug shovel hole and/or a Dutch auger (1.2 m long). Till samples were collected from the C-horizon

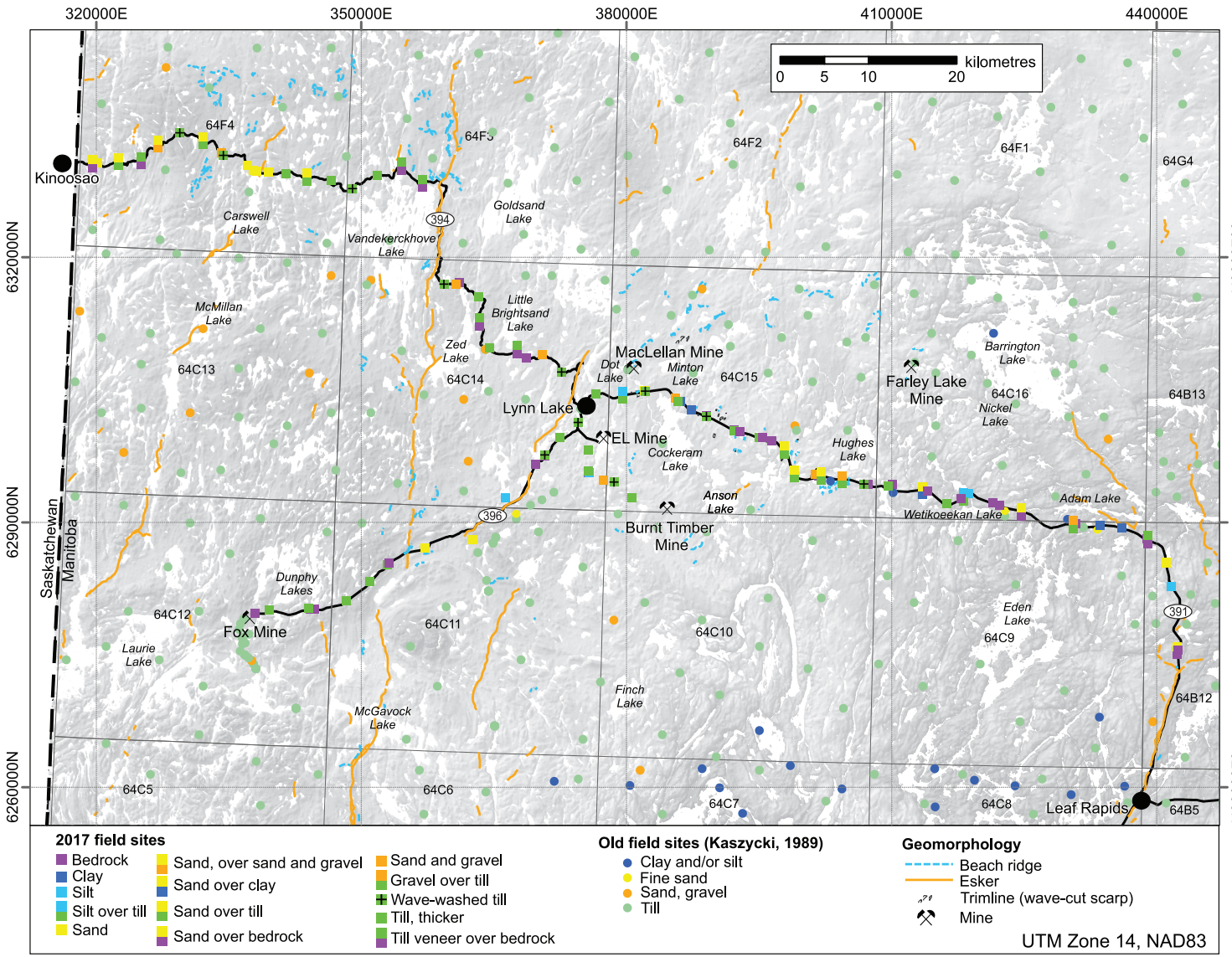

Figure GS2017-17-2: *Field sites visited during the 2017 field season, classified by surficial material. Field site data from Kaszycki (1989) is also shown, though the reader is cautioned that the upper first metre of sediment was not recorded at all locations; hence organic material, if present at surface, is not depicted and may be quite thick in places. Eskers, beach ridges and trimlines are digitized from existing surficial maps, orthophotos and light detection and ranging (LiDAR) imagery.*

soil, except where thin till draped bedrock and only the B horizon was present, or in poorly drained areas where the soil was gleyed. Permafrost was encountered at numerous sites during the late June fieldwork, which hampered till sampling at depth. Additionally, a surprising number of reforested (~70 years ago) sites, which were disturbed by the original road-building activities, were present along the road between Lynn Lake and Leaf Rapids. In these areas, careful attention was required when sampling and efforts were made to walk farther into the bush to find undisturbed till. Finally, it must be noted that previous work in this area (Kaszycki, 1989; Kaszycki et al., 2008) portrayed the majority of till sampled as surface samples. However, many of the samples were situated at depths of >1 m and sampled with the aid of borrow pits and backhoe trenches. Hence, any further till sampling in the area must take into consideration previous sample depth as part of the sample design plan.

A total of 48 till samples, in 22.73 L pails, were collected for KIM analyses. Blind KIM samples were submitted to the De Beers Group of Companies (De Beers) to be analyzed through in-kind support. The KIM sample locations were withheld from De Beers, to allow equal opportunity for follow-up by all interested parties when the data is publicly released at a later date. Additional 3 kg till samples were collected for trace-element geochemistry (<63 µm size-fraction) and clast lithology (2–30 mm size-fraction) analysis.

The orientations of striations, grooves, chattermarks and roches moutonnées were measured at 22 sites and are contained in Data Repository Item DRI2017003[1] (Gauthier and Hodder, 2017).

Results

Surficial geology

Organics

Organic, treed bog peatlands are common on very poorly drained surfaces in the study area, and are usually underlain by permafrost. Organic cover is commonly thin (5–30 cm) where it overlies topographic highs, and thicker in low-lying areas or where the underlying surficial material is finer textured (Figure GS2017-17-3a). According to 1:250 000 scale mapping, organic deposits are thickest within NTS areas 64C14 and 15 (Kaszycki and Way Nee, 1990b).

Glaciofluvial

Ice-contact sediments

Esker ridges are the dominant glaciofluvial landform in the region. Four major esker systems cross the project area (Figure GS2017-17-2). Three eskers are used as road stretches—from the Lynn Lake airport south along PR 396, north of Leaf Rapids along PR 391 and along the east side of Vandekerckhove Lake. These eskers are a mix of ridged and hummocky landforms that can be up to 20 m high. Smaller (1–5 m high) and shorter esker ridges are scattered throughout the study area. At the few sites visited, these esker segments consisted of massive to weakly stratified fine- to coarse-grained sand with 5 to 15% subrounded to rounded granule- to cobble-sized clasts.

Glaciolacustrine sediments

The entire study area was inundated by glacial Lake Agassiz (Dredge, 1983), resulting in washing and erosion of the topographic highs and the deposition of clayey and silty glaciolacustrine sediments in the lows. Lake limits in the area, defined by beach ridges, trimlines, washed till and sand blankets, are between 440 and 340 m asl. This means that the lake levels lowered progressively throughout the study area after deglaciation.

Washed till

At sites between 435 and 330 m asl, till has been wave-washed. This means that fines have been removed from the upper 0.1 to 0.4 m of the till, and the concentration of fines increases with depth (Figure GS2017-17-4a, b). In some areas, wave-washing has left a lag of boulder- and cobble-sized clasts at surface (Figure GS2017-17-3b). Wave-washed till is preferentially situated on topographic highs, and may be more extensive than noted in Figure GS2017-17-2. Future analyses of till-sample grain-size distribution will help to determine the extent of wave-washing.

Sand and gravel beach deposits

A veneer (0.3–0.7 m) of poor- to well-sorted gravelly sand was found at seven sites throughout the study area, between 405 and 300 m asl (Figure GS2017-17-2). These sites are either beach ridges or areas where extensive wave-washing has created beach gravel (Figure GS2017-17-4c) that overlies till. Beach ridges are situated at 400–390 m asl between Kinoosao and Zed Lake, 370 m asl at MacLellan mine, and 345–330 m asl at Hughes Lake (Figure GS2017-17-5). Beach ridges have been mapped across the study area (DiLabio et al., 1986; Kaszycki and Way Nee, 1989a), but are likely far more extensive than depicted on Figure GS2017-17-2. For example, the beach ridges at Hughes Lake depicted on Figure GS2017-17-5 are small (0.2–0.7 km) features that are visible on light detection and ranging (LiDAR) imagery but likely hidden by forest cover on aerial photographs.

Sand

Moderate- to well-sorted sand (Figure GS2017-17-4d) and/or gravelly sand was found at surface between 435 and 280 m asl. In some areas, the landscape underlain by sand

[1] MGS Data Repository Item DRI2017003, containing the data or other information sources used to compile this report, is available online to download free of charge at http://www2.gov.mb.ca/itm-cat/web/freedownloads.html, or on request from minesinfo@gov.mb.ca or Mineral Resources Library, Manitoba Growth, Enterprise and Trade, 360–1395 Ellice Avenue, Winnipeg, Manitoba R3G 3P2, Canada.

Figure GS2017-17-3: *Examples of forested landscapes in the Lynn Lake area include* ***a)*** *organic bog peatlands with stunted spruce trees and sphagnum moss that overlies clay at 338 m asl,* ***b)*** *open spruce forest with wave-washed till surfaces resulting in cobble and boulder lags at 368 m asl,* ***c)*** *flat, well-drained, jack pine forest that overlies sand,* ***d)*** *moderately drained spruce forest that overlies till,* ***e)*** *recently burnt spruce forest exposes a till-derived boulder field that contains subrounded to subangular clasts of different lithologies, and* ***f)*** *open, unforested, bedrock-derived boulder field that contains subangular to angular clasts of the same lithology.*

Figure GS2017-17-4: *Examples of various sediment types encountered during fieldwork include* ***a)*** *washed till that has a sandy texture,* ***b)*** *unwashed till that has a silty sandy texture,* ***c)*** *poorly sorted beach gravel derived from till,* ***d)*** *moderately sorted fine- to medium-grained sand,* ***e)*** *massive clay sampled by an auger, and* ***f)*** *interbedded silt (dark) and sand (light).*

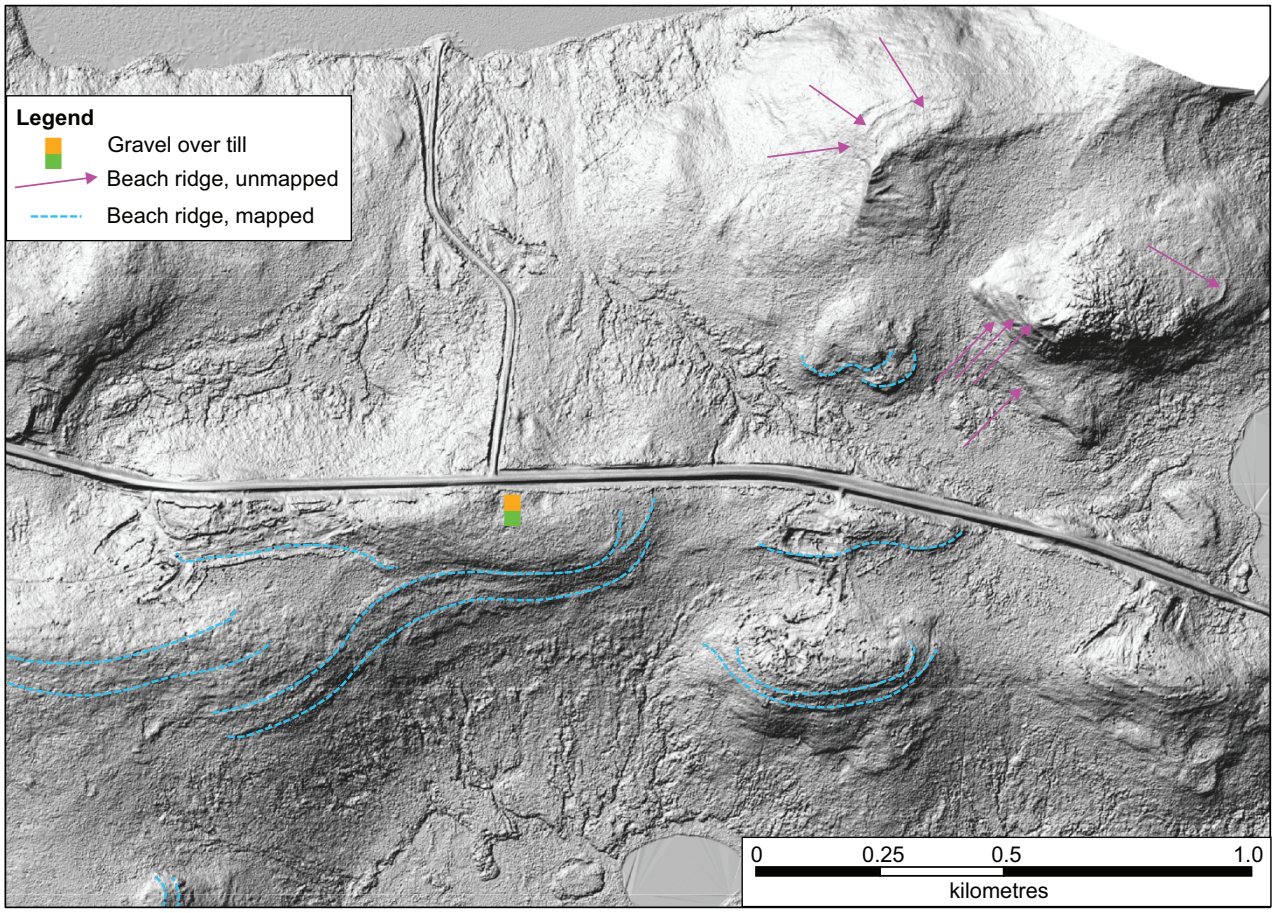

Figure GS2017-17-5: *Beach ridges surround most topographic highs in the area of Hughes Lake, and 0.3 m of gravel overlying till was dug from the topographic high at 344 m asl. The pink arrows point to some unmapped beach ridges, so the reader can more easily see these features. Background image is generated from light detection and ranging (LiDAR) data (imagery provided by Stantec Consulting Manitoba, 2017).*

is flat, well-drained and covered by jack pine forests (Figure GS2017-17-3c). Sand thickness was generally between 0.3 and 0.9 m overlying till, though at one site southeast of Adam Lake greater than 1.7 m of sand was mapped at 302 m asl. At another site southeast of Hughes Lake, sand overlies clay at 306 m asl.

Silt and clay

Dense, compact, milk-chocolate brown, generally massive silty clay to clay (Figure GS2017-17-4e) was encountered between Lynn Lake and Adam Lake (Figure GS2017-17-2), and is common at surface within NTS areas 64C7 and 8 (Kaszycki et al., 2008). This deepwater glaciolacustrine sediment was mapped between elevations of 340 and 270 m asl.

Less dense, brown, sandy silt was encountered at three sites in the study area, between 380 and 335 m asl. At one site along PR 396, silt was interbedded with sand (Figure GS2017-17-4f).

In some places, glaciolacustrine sedimentation occurred while the underlying till was still soft, resulting in flame structures from sediment loading (Figure GS2017-17-6). The thickness of these sediments is unpredictable at any one site, but generally varies from 0.3 to >2 m. It should be noted that glaciolacustrine sediments are probably more widespread than mapped by either this study or earlier studies, as these studies were targeting till sites for sampling purposes.

Till

Diamict, interpreted as till, was sampled at 48 sites in the study area (Figure GS2017-17-1). The matrix can be sandy, silty-sandy or sandy-silty, and the till typically contains 10 to 15% granule- to pebble-sized clasts (Figure GS2017-17-4a, b). Cobble- and boulder-sized clasts are rare, but present (Figure GS2017-17-3b, d, e). Till colours, determined by using the Munsell (Munsell Color–X-Rite, Incorporated, 2015) classification on wet till matrices, include light olive brown (47%), light to dark yellowish–brown (29%), gleyed grey (11%), grey brown (11%) and dark brown (2%). Colour distribution is random and not controlled by spatial patterns, with the exception of gleyed grey till, which was found in vegetated, wet lows. Preliminary field testing with 10% HCl acid suggests the till is noncalcareous, with the exception of one field station near Wetikoeekan Lake (Figure GS2017-17-2). Previous fieldwork (Kaszycki, 1989)

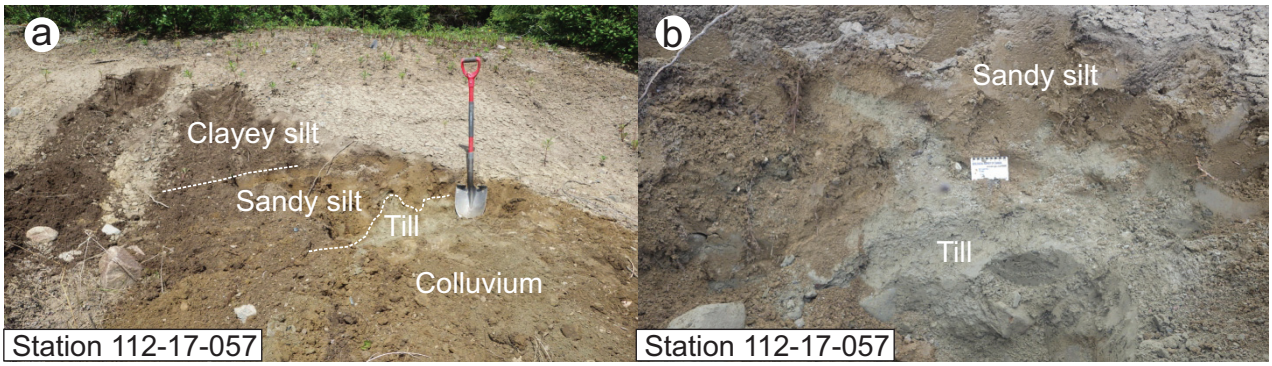

Figure GS2017-17-6: *Glaciolacustrine sedimentation at site 112-17-057 consists of dark brown clayey silt that drapes light brown sandy silt, overlying beige till* ***(a)****. A closer view of the glaciolacustrine-till contact shows water-escape structures* ***(b)****, which means that the till was still soft and water-saturated when glaciolacustrine sediments were deposited.*

suggests that patchy calcareous till is present at Wetikoeekan Lake, and becomes more predominant east of the community of South Indian Lake (Trommelen and McMartin, 2017).

Till is present at surface beneath most treed (spruce and/or jack pine), moderate- to well-drained, upland areas (Figure GS2017-17-3d) in the study area. Permafrost is usually present at depth near the crest of these uplands, and near the surface (20–30 cm) at the toe slopes. In some areas, the till forms crag-and-tail or drumlinoid ridges (0.13–2.1 km long with a mean length of 0.7 km) that trend between 195 and 210°. Throughout most of the study area, till is generally thin and drapes bedrock-controlled topography. Where till is thick, and permafrost is close to surface, rare vegetated permafrost mud boils are present in spruce bogs. Additionally, where till is thick but vegetation cover is thin, permafrost can form till-derived boulder fields (Figure GS2017-17-3e).

Bedrock

Bedrock outcrops are common throughout the study area (Figure GS2017-17-2), especially near the crest of most topographic rises. Along the roads, the majority of these bedrock surfaces are polished and striated, and the outcrops tend to form roches moutonnées that trend southward. In the forest, where vegetation cover is absent, permafrost can form bedrock-derived boulder fields (Figure GS2017-17-3f). These are distinguishable from till-derived boulder fields, because bedrock-derived boulder fields contain more angular clasts and are composed of only the local bedrock lithologies.

Ice flow

New ice-flow measurements were obtained from striations, grooves, chattermarks, crescentic gouges and fractures, and roches moutonnées at 22 field sites in the study area, and were combined with measurements from previous mapping in the area (Figure GS2017-17-7; Gauthier and Hodder, 2017).

Northwesterly ice-flow indicators were documented at just one road-cut along PR 391. At this site (Figure GS2017-17-8a, b), there are large outcrops with abundantly striated, steeply dipping, north-northeast–facing slopes. The shape of the outcrops (stoss and lee relationships), as well as plucking, confirm that ice flowed to the northwest between 308 and 314°. The steeply dipping faces were protected from the dominant southerly ice flow in the area, perhaps by a cover of till ('vanished protector', Veillette and Roy, 1995; Trommelen and Ross, 2011), as only the top and upper portions of the outcrops were later striated toward 174 and 180°.

Southwesterly ice-flow indicators were documented at four sites in 2017. At two sites, crescentic gouges were measured at or near the top of outcrops, trending toward 244 and 260°, where they were crosscut by striations trending toward 158 and 188°, respectively (Figure GS2017-17-8c). At the other two sites, striations trending toward 235 and 254° on east-southeast–sloping outcrop faces were crosscut by striations trending toward 174, 198 and 210° near the tops of the outcrops.

Southwesterly ice-flow indicators were also documented just east of Leaf Rapids (Kaszycki and Way Nee, 1989b; Figure GS2017-17-7). At this site, an ice-flow indicator toward 257° was recorded as being younger than another indicator toward 212°.

Southeasterly ice-flow indicators were documented at seven sites in 2017 (Figure GS2017-17-7). At site 112-17-060, three crescentic gouges on a southwest-sloping greenstone bedrock outcrop trend toward 100°. These crescentic gouges are crosscut near the top of the outcrop by fine, abundant striations that trend between 155 and 160°. On other outcrops at this site, there are a few low-lying spots that preserve fine striations between 205 and 208° (Figure GS2017-17-8d), which have been protected from the younger 160° flow. At three other sites, crescentic gouges or striations that trend between 125 and 150° are the only ice-flow indicators at that site, or are crosscut by other striations that trend toward 184 and 200° (Figure GS2017-17-8e). At three additional sites, fine striations that trend toward 158 and 172° dominate the surface of their respective outcrops (Figure GS2017-17-8f).

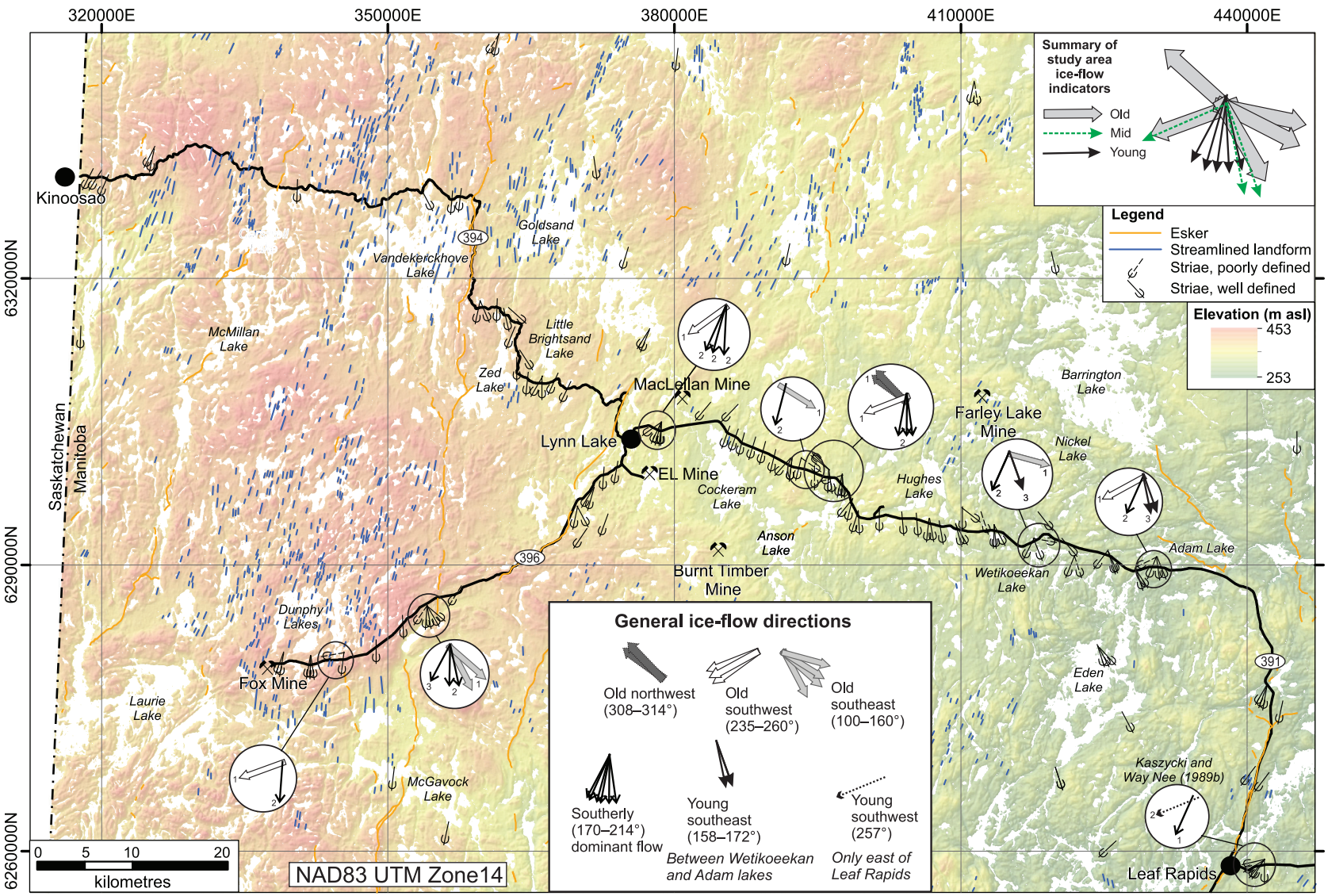

Figure GS2017-17-7: *Historical and recent field-based ice-flow–indicator data in the study area. Larger circles are a summary of the relative ages (1=oldest) and trends of ice-flow indicators for a single site or sites in close proximity to each other. The generalized ice-flow directions provide a key for differentiating between old and young ice flows of similar orientation. Background hillshade was generated using a Canadian Digital Surface Model (Natural Resources Canada, 2012).*

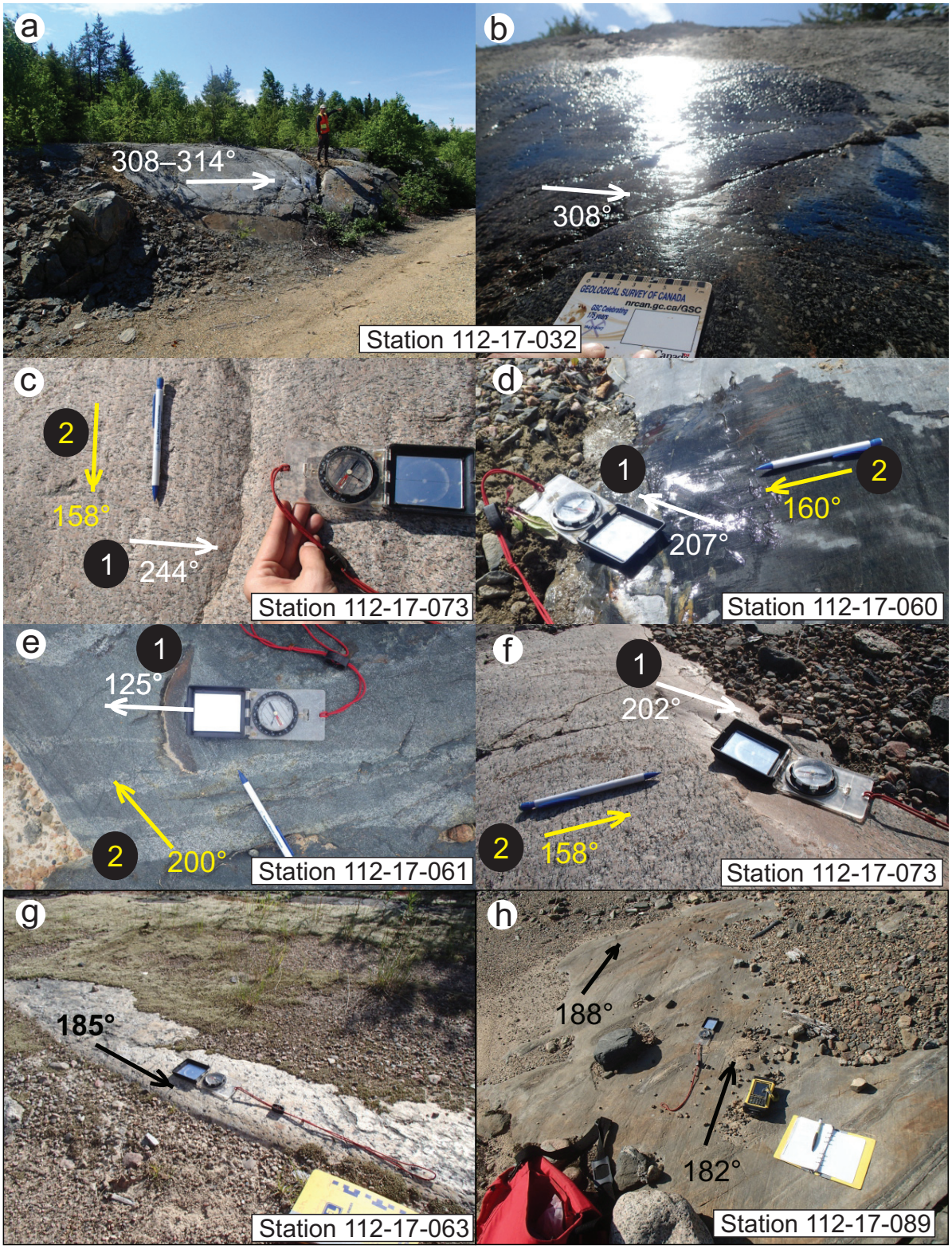

Figure GS2017-17-8: *Examples of ice-flow indicators in the study area include* ***a)*** *large roches moutonnées that trend northwest,* ***b)*** *abundant, fine striations toward 308° on the same outcrops; direction is interpreted from the shape and plucking relationships on the larger outcrop,* ***c)*** *a crescentic gouge toward 244° that is crosscut by striations toward 158°,* ***d)*** *fine striations toward 207° are protected in a low-lying area from younger fine striations toward 160°,* ***e)*** *a crescentic gouge toward 125° that is crosscut by striations toward 200°,* ***f)*** *striations toward 202° on a sloping face are protected from fine striations toward 158° on the top surface,* ***g)*** *abundant striations toward 185° on a low-lying bedrock outcrop,* ***h)*** *deep striations toward 182 and 188° on a low-lying, nearly flat, bedrock outcrop.*

Southerly ice-flow indicators were documented at most sites in 2017 (Figure GS2017-17-7), and are the most common trend of indicators mapped during previous work. The roches moutonnées, crescentic gouges and striations measured in 2017 trend between 170 and 214°. Southerly ice-flow indicators crosscut other indicators to the northwest, southwest and southeast (Figure GS2017-17-8e), and are crosscut by striations that trend toward the southeast (Figure GS2017-17-8d, f) in the area between Wetikoeekan and Adam lakes. Southerly striations dominate most outcrops and can be found on all surface slopes (Figure GS2017-17-8g, h).

Ice-flow history

Ice-flow measurements yielded at least six phases of ice flow in the study area. Northwest-, southwest- and southeast-trending ice-flow indicators are rare and probably old. Old southwesterly ice flow is regionally extensive (Dredge et al., 1986; Campbell, 2001, 2002; Smith, 2006; Smith and Kaczowka, 2007; Trommelen, 2011, 2013a, 2015a; Campbell et al., 2012) and is correlated to the pre-Late Wisconsinan. Old east-southeast ice flow is also regionally extensive (Dredge et al., 1986; Campbell, 2001, 2002; Smith, 2006; Smith and Kaczowka, 2007; Trommelen, 2011, 2015a, b; Campbell et al., 2012), though an age has not been assigned. Old northwesterly ice flow (270–300°) has been mapped in the Southern Indian Lake area (Hodder, 2015, 2016), approximately 145 km northeast of Leaf Rapids, as well as in parts of northeastern Manitoba (Campbell et al., 2012; Trommelen, 2015a). No relationships were documented in the field area between old southwesterly, southeasterly or northwesterly ice-flow indicators. Fieldwork within the Southern Indian Lake area (Hodder, 2015, 2016; Trommelen, 2015b), suggests that southeasterly ice flow is older than southwesterly ice flow. The relationships with old northwesterly ice flow remain uncertain, mainly because these ice-flow indicators are rare.

Dominant ice flow in the Lynn Lake area was to the south, between 170 and 214°. Southerly ice flow is regionally extensive across northern Manitoba, and is likely Wisconsinan in age. Most streamlined landforms in the region were also formed during this major southerly ice-flow phase. Young southeasterly ice flow (158–172°) crosscuts the southerly flows between Wetikoeekan and Adam lakes, and may relate to deposition of the Adam Lake esker ridge during late deglaciation (Figure GS2017-17-7). Young southwesterly ice flow (257°) crosscuts the southerly flows just east of Leaf Rapids, and is also documented further east along the road to South Indian Lake and at Karsakuwigamak Lake (Kaszycki and Way Nee, 1989b). This young southwest- to northwest-trending (260–280°) ice flow was also mapped near Thompson and Split Lake (McClenaghan et al., 2009; McMartin et al., 2010; Trommelen, 2013b), where it is correlated with late deglacial ice flow related to ice flowing from Hudson Bay.

Future work

Ongoing surficial geological analysis focuses on tracing lithological indicators from known bedrock source areas, using clast counts and the major- and trace-element geochemical composition of the collected till samples. Kimberlite-indicator-mineral analysis is also ongoing. Results of these analyses will

- identify favourable geochemical or mineralogical indicators within till to aid mineral exploration;
- establish compositional till characteristics and aid investigation of subglacial transport processes and distances;
- develop a framework to assist drift prospecting practises in the Kinoosao to Leaf Rapids corridor; and
- provide the first KIM results from the Kinoosao to Leaf Rapids corridor, to compare with those sampled at Southern Indian Lake and elsewhere.

Economic considerations

A thorough understanding of surficial geology is essential for drift prospecting in Manitoba's northern region. Till-sample analysis is commonly used in drift-covered regions to help determine the source area for mineralized erratics and boulder trains, as well as to narrow in on lake sediment sample results (Geological Survey of Canada, 1985; Schmitt, 1989). Interpretation of till composition depends on exactly what material was sampled, as well as detailed attention to the potential for palimpsest dispersal patterns in areas that have been modified by more than one ice advance and transport direction.

Forthcoming results will provide new constraints to drift exploration in the study area, applicable to exploration for a variety of commodity types, including gold and diamonds. Kimberlite-indicator-mineral analysis of till in the Lynn Lake area will provide the first insight into the diamond potential of the region from an indicator-mineral perspective. The outcomes of these studies are geared toward providing mineral exploration geologists with an up-to-date surficial geology knowledge base and the adequate tools to more accurately locate exploration targets in Manitoba's north.

Acknowledgments

The authors thank N. Clark (University of Manitoba) for providing capable and enthusiastic field assistance. The De Beers Group of Companies is thanked for their continued analytical support for Quaternary projects at the MGS by providing kimberlite-indicator-mineral processing. Thanks also go to N. Brandson, E. Anderson and C. Epp from the MGS for logistical support throughout the project.

References

Armstrong, K. and Kupsch, B. 2016: Pikoo diamond project – 2016 exploration update; Saskatchewan Geological Survey, Saskatchewan Ministry of the Economy, Open House 2016, Saskatoon, Saskatchewan, November 28–30, 2016, PowerPoint® presentation, 20 p., URL <http://publications.gov.sk.ca/documents/310/96863-6_Kupsch_Pikoo%202016%20Sask%20Geological%20Open%20House.pdf> [October 2017].

Baldwin, D.A., Syme, E.C., Zwanzig, H.V., Gordon, T.M., Hunt, A. and Stevens, R.D. 1987: U-Pb zircon ages from the Lynn Lake and Rusty Lake metavolcanic belts, Manitoba: two ages of Proterozoic magmatism; Canadian Journal of Earth Sciences, v. 24, p. 1053–1063.

Beaumont-Smith, C.J., Machado, N. and Peck, D.C. 2006: New uranium-lead geochronology results from the Lynn Lake greenstone belt, Manitoba (NTS 64C11–16); Manitoba Science, Technology, Energy and Mines, Manitoba Geological Survey, Geoscientific Paper, GP2006-1, 11 p.

Campbell, J.E. 2001: Phelps Lake project: highlights of the Quaternary investigations in the Bonokoski Lake area (NTS 64M NW); *in* Summary of Investigations 2001, Volume 2, Saskatchewan Geological Survey, Saskatchewan Energy and Mines, Miscellaneous Report 2001-4.2, p. 19–27.

Campbell, J.E. 2002: Phelps Lake project: highlights of the Quaternary investigations in the Keseechewun Lake area (NTS 64M-9,-10,-15 and -16); *in* Summary of Investigations 2002, Volume 2, Saskatchewan Geological Survey, Saskatchewan Industry and Resources, Miscellaneous Report 2002-4.2, 16 p.

Campbell, J.E., Trommelen, M.S., McCurdy, M.W., Böhm, C.O. and Ross, M. 2012: Till composition and ice-flow indicator data, Great Island–Caribou Lake area (parts of NTS 54L, 54M, 64I and 64P), northeast Manitoba; Geological Survey of Canada, Open File 6967 and Manitoba Innovation, Energy and Mines, Manitoba Geological Survey, Open File 2011-4, 26 p., 1 CD-ROM.

DiLabio, R.N.W., Kaszycki, C.A., Way Nee, V.J. and Nielsen, E. 1986: Surficial geology, Granville Lake, Manitoba; Geological Survey of Canada, Open File 1258, scale 1:125 000.

Dredge, L.A. 1983: Character and development of northern Lake Agassiz and its relation to Keewatin and Hudsonian ice regimes; *in* Glacial Lake Agassiz, J.T. Teller and L. Clayton (ed.), Geological Association of Canada, Special Paper 26, p. 117–131.

Dredge, L.A., Nixon, F.M. and Richardson, R.J.H. 1986: Quaternary geology and geomorphology of northwestern Manitoba; Geological Survey of Canada, Memoir 418, 38 p.

Gauthier, M.S. and Hodder, T.J. 2017: Field-based ice-flow–indicator data, Kinoosao–Lynn Lake–Leaf Rapids, northwestern Manitoba (parts of NTS 64B12, 64C9, 11, 12, 14–16, 64F3, 4); Manitoba Growth, Enterprise and Trade, Manitoba Geological Survey, Data Repository Item DRI2017003, Microsoft® Excel® file.

Geological Survey of Canada 1985: Regional lake sediment and water geochemical reconnaissance data, Manitoba; Geological Survey of Canada, Open File 1288, 130 p.

Gilbert, H.P., Syme, E.C. and Zwanzig, H.V. 1980: Geology of the metavolcanic and volcaniclastic metasedimentary rocks in the Lynn Lake area; Manitoba Energy and Mines, Mineral Resources Division, Geological Paper 80-1, 118 p.

Hodder, T.J. 2015: Ice-flow mapping and till sampling in the northern area of Southern Indian Lake, north-central Manitoba (parts of NTS64G7-10); *in* Report of Activities 2015, Manitoba Mineral Resources, Manitoba Geological Survey, p. 124–130.

Hodder, T.J. 2016: Till sampling and ice-flow mapping in the central area of Southern Indian Lake, north-central Manitoba (parts of NTS 64G1, 2, 7–10, 64B15); *in* Report of Activities 2016, Manitoba Growth, Enterprise and Trade, Manitoba Geological Survey, p. 196–202.

Hodder, T.J. 2017: Kimberlite-indicator-mineral results derived from glacial sediments (till) in the Southern Indian Lake area of north-central Manitoba (parts of NTS 64B15, 64G1, 2, 7, 8); Manitoba Growth, Enterprise and Trade, Manitoba Geological Survey, Open File OF2017-2, 6 p.

Hodder, T.J. and Bater, C.W. 2016: Till-matrix (<177 µm) geochemistry analytical results from the Lynn Lake (parts of NTS 64C14, 64F3, 4), Southern Indian Lake (parts of NTS 64G8, 9), Churchill River (parts of NTS 64F14, 64K3, 6, 11) and Fisher Branch (NTS 62P) areas, Manitoba; Manitoba Growth, Enterprise and Trade, Manitoba Geological Survey, Data Repository Item DRI2016004, Microsoft® Excel® file.

Kaszycki, C.A. 1989: Surficial geology and till composition, northwestern Manitoba; Geological Survey of Canada, Open File 2118, 50 p.

Kaszycki, C.A. and Way Nee, V.J. 1989a: Surficial geology, Brochet, Manitoba; Geological Survey of Canada, Open File 1331, scale 1:125 000.

Kaszycki, C.A. and Way Nee, V.J. 1989b: Surficial geology, Uhlman Lake, Manitoba (64B); Geological Survey of Canada, Open File 2019, scale 1:125 000.

Kaszycki, C.A. and Way Nee, V.J. 1990a: Surficial geology, Brochet, Manitoba; Geological Survey of Canada, Map 1760A, scale 1:250 000.

Kaszycki, C.A. and Way Nee, V.J. 1990b: Surficial geology, Granville Lake, Manitoba; Geological Survey of Canada, Map 1759A, scale 1:250 000.

Kaszycki, C.A., Dredge, L.A. and Groom, H. 2008: Surficial geology and glacial history, Lynn Lake - Leaf Rapids area, Manitoba; Geological Survey of Canada, Open File 5873, 105 p.

Keller, G.R., Bogdan, D.J. and Matile, G.L.D. 2004: Manitoba kimberlite indicator mineral database (version 3.0); Manitoba Industry, Economic Development and Mines, Manitoba Geological Survey, Open File Report OF2004-25, Microsoft® Access 2000 database, URL <http://www.manitoba.ca/iem/info/libmin/OF2004-25.zip> [September 2017].

Kremer, P.D., Rayner, N. and Corkery, M.T. 2009: New results from geological mapping in the west-central and northeastern portions of Southern Indian Lake, Manitoba (parts of NTS 64G1, 2, 8, 64H4, 5); *in* Report of Activities 2009, Manitoba Innovation, Energy and Mines, Manitoba Geological Survey, p. 94–107.

Land Resource Group - Manitoba 2003: Biophysical land classification of the Ulhman Lake (64B) and Granville Lake (64 C - SE 1/8) map areas; prepared by Agriculture and Agri-Food Canada, Semiarid Prairie Agricultural Research Centre, Research Branch, Land Resource Group - Manitoba for Manitoba Hydro, Information Bulletin 2003-5, 50 p.

Leckie, D.A., Kjarsgaard, B.A., Bloch, J., McIntyre, D., McNeil, D., Stasiuk, L. and Heaman, L. 1997: Emplacement and reworking of Cretaceous, diamond-bearing, crater facies kimberlite in central Saskatchewan, Canada; Geological Society of America, Bulletin 109, p. 1000–1020.

Lenton, P.G. and Kaszycki, C.A. 2005: Till geochemistry in northwestern Manitoba (NTS 63N, 64B, 64F and 64G and parts of 63K, 63O, 64A and 64C); Manitoba Industry, Economic Development and Mines, Manitoba Geological Survey, Open File Report OF2005-2, 1 CD-ROM.

McClenaghan, M.B., Matile, G.L.D., Layton-Matthews, D. and Pyne, M. 2009: Till geochemical signatures of magmatic Ni-Cu deposits and regional till geochemistry, Thompson Nickel belt, Manitoba; Geological Survey of Canada, Open File 6005, 121 p.

McMartin, I., Campbell, J.E., Dredge, L.A. and Robertson, L. 2010: A digital compilation of ice-flow indicators for central Manitoba and Saskatchewan: datasets, digital scalable maps and 1:500 000 scale generalized map; Geological Survey of Canada, Open File 6405, 1 DVD-ROM.

Munsell Color–X-Rite, Incorporated 2015: Munsell Soil Color Book; Pantone LLC, Carlstadt, New Jersey, 42 p.

Natural Resources Canada 2012: Canadian Digital Surface Model; Natural Resources Canada, URL <http://geogratis.gc.ca/api/en/nrcan-rncan/ess-sst/34F13DB8-434B-4A37-AE38-03643433FBBB.html> [September 2016].

Nielsen, E. and Conley, G.G. 1991: Glacial dispersion and till geochemistry around the Lar Cu-Zn deposit, Lynn Lake greenstone belt; Manitoba Energy and Mines, Geological Services, Open File Report OF91-4, 45 p.

Nielsen, E. and Fedikow, M.A.F. 1986: Till geochemistry of the Minton Lake-Nickel Lake area (Agassiz Metallotect), Lynn Lake, Manitoba; Manitoba Energy and Mines, Geological Services, Open File Report OF86-2, 36 p.

Nielsen, E. and Fedikow, M.A.F. 1987: Glacial dispersal of trace elements in Wisconsinan till in the Dot Lake-MacLellan mine area, Manitoba; Manitoba Energy and Mines, Geological Services, Open File Report OF87-2, 73 p.

Nielsen, E. and Graham, D.C. 1985: Preliminary results of till petrographical and till geochemical studies at Farley Lake; Manitoba Energy and Mines, Geological Services, Open File Report OF85-3, 62 p.

Norman, G.W.H. 1934: Granville Lake district, northern Manitoba; *in* Summary Report 1933, Part C, Geological Survey of Canada, p. 23–41, Map 301A, scale 1:253 440.

O'Donnell, N.D. 1976a: Quaternary geology of the Cockeram Lake area; Manitoba Mines, Resources and Environmental Management, Mineral Resources Division, Preliminary Map 1976P-2, scale 1:50 000.

O'Donnell, N.D. 1976b: Quaternary geology of the Lynn Lake area, NTS 64C/14; Manitoba Mines, Resources and Environmental Management, Mineral Resources Division, Preliminary Map 1976P-1, scale 1:50 000.

Schmitt, H.R. 1989: Geochemical results and interpretations of a lake sediment and water survey in the Lynn Lake - Leaf Rapids region, northern Manitoba; Geological Survey of Canada, Open File 1959, 80 p.

Sladen, W.E. 2011: Permafrost; Geological Survey of Canada, Open File 6724, 1 sheet.

Smith, J.S. 2006: Northeast Wollaston Lake project: Quaternary investigations of the Cochrane River (NTS map sheets 64L-10,-11,-14 and -15) and Charcoal Lake (NTS map sheets 64L-9 and -16) areas; *in* Summary of Investigations 2006, Volume 2, Saskatchewan Geological Survey, Saskatchewan Industry and Resources, Miscellaneous Report 2006-4.2, Paper A-6, 15 p.

Smith, J.S. and Kaczowka, A. 2007: Northeast Wollaston Lake project: Quaternary investigations in the Wellbelove Bay - Ross Channel - Rabbabou Bay area, northeast Wollaston Lake, Saskatchewan (parts of NTS 64L/06, 07, 10 and 11); *in* Summary of Investigations 2007, Volume 2, Saskatchewan Geological Survey, Saskatchewan Ministry of Energy and Resources, Miscellaneous Report 2007-4.2, Paper A-4, 24 p.

Trommelen, M.S. 2011: Far North Geomapping Initiative: Quaternary geology of the Snyder-Grevstad lakes area, far northwestern Manitoba (parts of NTS 64N5); *in* Report of Activities 2011, Manitoba Innovation, Energy and Mines, Manitoba Geological Survey, p. 18–28.

Trommelen, M.S. 2013a: Preliminary Quaternary geology in the Gillam area, northeastern Manitoba (parts of NTS 54D5-9, 11, 54C12); *in* Report of Activities 2013, Manitoba Mineral Resources, Manitoba Geological Survey, p. 169–182.

Trommelen, M.S. 2013b: Quaternary geology between Gauer Lake and Wishart Lake, north-central Manitoba (NTS 64H4, 5, 12, 13, parts of 64G1, 8); *in* Report of Activities 2013, Manitoba Mineral Resources, Manitoba Geological Survey, p. 156–168.

Trommelen, M.S. 2015a: Surficial geology, till composition, stratigraphy and ice-flow indicator data, Seal River–North Knife River area, Manitoba (parts of NTS 54L, M, 64I, P); Manitoba Mineral Resources, Manitoba Geological Survey, Geoscientific Paper GP2013-2, 27 p. plus 11 appendices.

Trommelen, M.S. 2015b: Till composition and glacial history, Gauer Lake – Wishart Lake, Manitoba (NTS 64H4, 5, 12, 13); Manitoba Mineral Resources, Manitoba Geological Survey, Geoscientific Paper GP2014-1, 32 p. plus 14 appendices.

Trommelen, M.S. and McMartin, I. 2017: Manitoba carbonate dispersal analyses in till; Manitoba Mineral Resources, Manitoba Geological Survey, URL <http://www.manitoba.ca/iem/geo/surficial/carbonate.html> [September 2017].

Trommelen, M.S. and Ross, M. 2011: Far North Geomapping Initiative: palimpsest bedrock macroforms and other complex ice-flow indicators near Churchill, northern Manitoba (part of NTS 54L16); *in* Report of Activities 2011, Manitoba Innovation, Energy and Mines, Manitoba Geological Survey, p. 29–35.

Veillette, J.J. and Roy, M. 1995: The spectacular cross-striated outcrops of James Bay, Quebec; *in* Current Research 1995-C, Geological Survey of Canada, p. 243–248.

Wentworth, C.K. 1922: A scale of grade and class terms for clastic sediments; The Journal of Geology, v. 30, p. 377–392.

GS2017-18

Quaternary stratigraphy and till sampling in the Kaskattama highland region, northeastern Manitoba (parts of NTS 53N, O, 54B, C): year two

by T.J. Hodder

In Brief:

- Follow-up to prospective KIM and till geochemistry results from 2016
- Collection of new till samples and stratigraphic data
- Clast fabrics conducted to help reconstruct the paleo-ice flow history

Citation:
Hodder, T.J. 2017: Quaternary stratigraphy and till sampling in the Kaskattama highland region, northeastern Manitoba (parts of NTS 53N, O, 54B, C): year two; *in* Report of Activities 2017, Manitoba Growth, Enterprise and Trade, Manitoba Geological Survey, p. 205–214.

Summary

The 2017 field season in the Kaskattama highland region follows up on intriguing results from 2016 fieldwork in the area, including elevated kimberlite-indicator-mineral (KIM) concentrations, elevated till-matrix geochemistry values in multiple commodities and an elevated clast-lithology signature of undifferentiated greenstone and greywacke clasts. The goals of the 2017 field season were to collect additional surficial till samples to tighten the sampling grid, sample additional stratigraphic sections and gather accompanying ice-flow information. All of the above work will assist with drift prospecting and ice-flow reconstruction in the area.

Sixty-two till samples collected in 2017 will be processed for till-matrix (<63 µm size-fraction) geochemistry and clast-lithology (2–30 mm size-fraction) analysis. At 34 till sample sites, an additional 11.4 L of till was collected, which will be analyzed for kimberlite-indicator minerals. Clast-fabric measurements were conducted at 17 stratigraphic till-sample sites to determine the ice-flow direction during deposition of the till. In addition to fieldwork, 15 till samples were collected from an archived drillcore, from a hole drilled on the Kaskattama highland, and these samples will also be processed for till-matrix (<63 µm size-fraction) geochemistry and clast-lithology (2–30 mm size-fraction) analysis.

Introduction

In July 2017, the Manitoba Geological Survey (MGS) conducted Quaternary fieldwork in the Kaskattama highland region of northeastern Manitoba (parts of NTS 53N, O, 54B, C; Figure GS2017-18-1). This work builds upon observations and analytical results from the 2016 field season (Hodder and Kelley, 2016, 2017). The purpose of this study is to document the till composition and Quaternary stratigraphy in this remote region, as well as provide baseline values for drift exploration. This study is also part of a renewed evaluation of the Quaternary stratigraphy in the Hudson Bay Lowland region of Manitoba (Trommelen, 2013; Trommelen et al., 2014; Kelley et al., 2015).

The goals and rationale of the 2017 field season were to

- conduct additional kimberlite-indicator-mineral (KIM) sampling to follow up on elevated KIM results from the 2016 till samples; the highest single sample-count recovered in 2016 was 17 KIMs (Hodder and Kelley, 2017), and average recovery from 2016 samples was more than double the mean amount of KIMs recovered in the prospective Knee Lake area (approximately 250 km southwest of the study area; Anderson, 2017);
- follow-up on unexpected elevated till-matrix geochemistry values of Au, Cu, Fe, Ni, Zn and Cr returned in 2016 samples, including a gold grain recovered from a KIM sample;
- document the sediments present at Quaternary sections, sample till and conduct clast-fabric measurements to determine the ice-flow direction during deposition of sampled till, which in turn guides drift exploration studies; and
- conduct additional surficial till sampling to establish compositional variations observed between streamlined-landform flowsets in the study area, including following up on elevated concentrations of undifferentiated greenstone and greywacke clasts identified in some 2016 till samples (Hodder et al., 2017b).

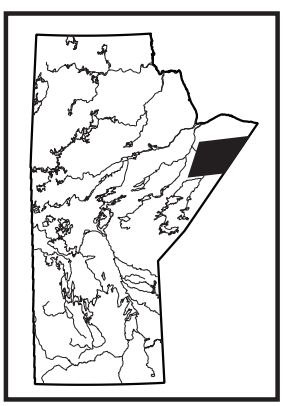

Previous work

The Kaskattama highland region is largely unexplored, primarily due to remoteness. Diamond exploration within the study area has taken place primarily through airborne geophysical surveys. A single drillhole was completed on the northwest side of the highland, the drillhole is Foran Mining Kaskattama Kimberlite No. 1 and referred to as KK1 (Figure GS2017-18-1; Nicolas and Armstrong, GS2017-12, this volume; Assessment File 74223, Manitoba Growth, Enterprise and Trade,

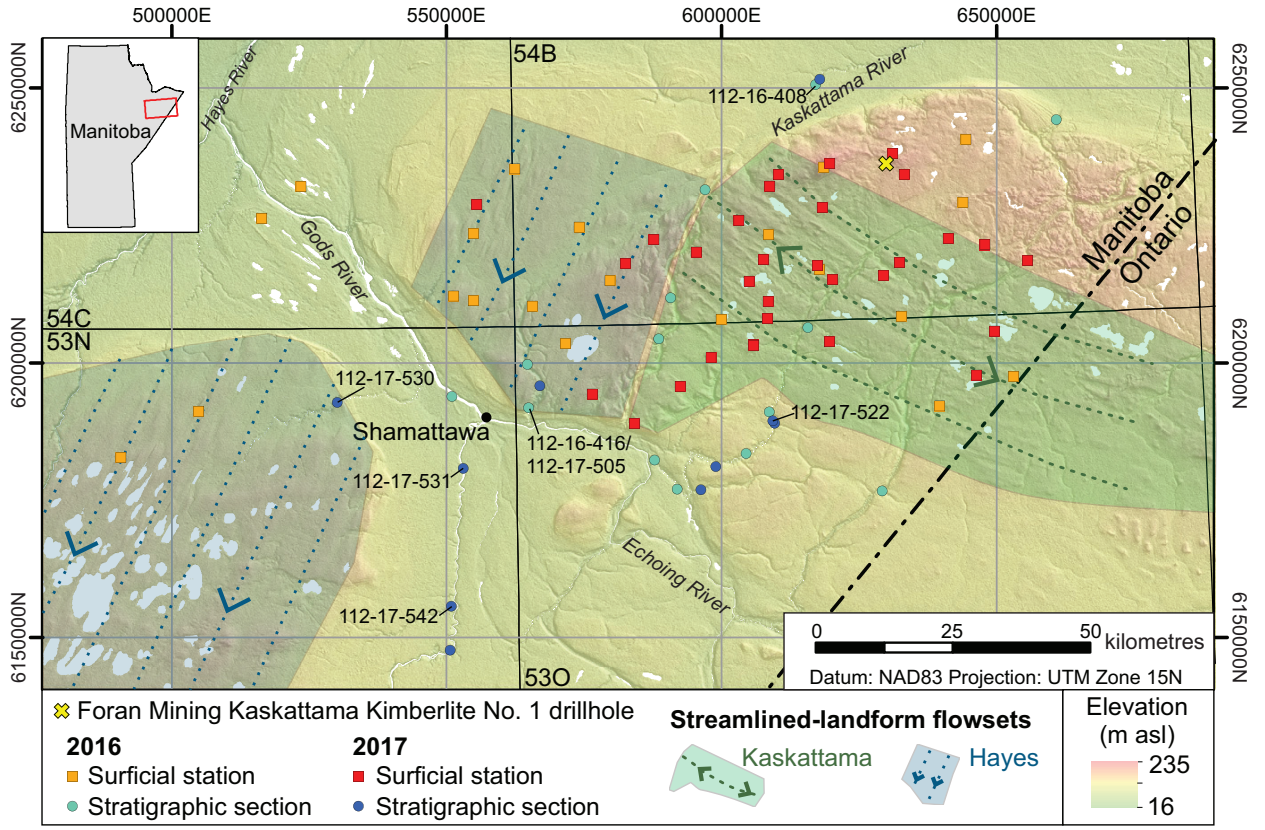

Figure GS2017-18-1: *Stations visited during the 2016 and 2017 field seasons, Kaskattama highland region, northeastern Manitoba. Sections discussed within the text are noted. Background hillshade image was generated using Canadian Digital Surface Model (Natural Resources Canada, 2012).*

Winnipeg). This drillhole intersected 223 m of inferred Quaternary sediments.

General knowledge of the Quaternary stratigraphy in northeastern Manitoba comes from descriptions of river-cut sections along the Hayes, Gods, Kaskattama and Echoing rivers, and the Nelson, Angling, Fox, Stupart and Pennycutaway rivers to the west of the study area (B.G. Craig, H. Gwyn and B.C. McDonald, unpublished notes, 1967; Netterville, 1974; Dredge and Nielsen, 1985; Dredge et al., 1990; Nielsen, 2002; Nielsen and Fedikow, 2002; Hodder et al., 2017a). Thick stratigraphic sections expose a long glacial history, including deposition from two or three different glacial and interglacial events (e.g., Dredge and McMartin, 2011). Observations of Quaternary stratigraphy in the Kaskattama highland region has been limited to reconnaissance-scale, mostly unpublished, observations from the Geological Survey of Canada's Operation Winisk (B.G. Craig, H. Gwyn and B.C. McDonald, unpublished notes, 1967), which included river traverses and helicopter-supported fieldwork across the Hudson Bay Lowland region in Quebec, Ontario and Manitoba (McDonald, 1968).

Greenstone, greywacke and the potential for a buried Precambrian inlier

In 2016, elevated concentrations of undifferentiated greenstone and greywacke clasts were identified in some till samples (Hodder et al., 2017b). The Kaskattama region is underlain by Paleozoic carbonate (Nicolas and Young, 2014), and hence the presence of these clast lithologies was unexpected. Additional geophysical surveys, sampling and drilling is required to confirm the suspicion that these undifferentiated greenstone and greywacke clasts are sourced locally, from a buried inlier of the Precambrian shield—much like the Sutton ridge in Ontario (Stott et al., 2010).

Regional setting

The Kaskattama highland in northeastern Manitoba, a prominent topographic high within the Hudson Platform, rises 130 m above the flat-lying Hudson Bay Lowland terrain, reaching a maximum elevation of 235 m asl. The Gods River is the main drainage channel flowing northwestward toward a confluence with the Hayes River, which drains northeastward into Hudson Bay. The Kaskattama River drains northeastward to Hudson Bay with the headwaters situated on the Kaskattama highland.

Geomorphology

Two streamlined-landform flowsets, defined as discrete assemblages of subglacial streamlined landforms based on their similar direction and the degree of internal consistency

(Kleman and Borgstrom, 1996; Clark et al., 2000; Greenwood and Clark, 2009), are present in the geomorphic record of the study area (Figure GS2017-18-1). Firstly, the curvilinear Kaskattama flowset overlies the Kaskattama highland. There is evidence for both northwest- and southeast-trending ice flow in the regional record, and the trend of this flowset is uncertain. Secondly, the Hayes flowset is a large, radiating, southwest-trending flowset, which starts in the study area and extends to the southwest. The Hayes flowset is part of the large deglacial Hayes lobe (Dredge and Cowan, 1989), which was approximately 320 km long and 270 km wide.

Bedrock geology

Regionally, the area is underlain by Paleozoic carbonate sedimentary rocks of the Hudson Bay Basin (Nicolas and Young, 2014), with Precambrian crystalline rocks mapped in the southwestern portion of the study area (Manitoba Department of Mines, Natural Resources and Environment, 1979). Bedrock is hidden beneath thick Quaternary sediments throughout the study area. Outcrops of Paleozoic bedrock were only observed along the base of the Gods River, northwest and south of the First Nation community of Shamattawa.

Methods

Helicopter-supported fieldwork was undertaken in July 2017. A total of 43 stations were visited to document both the Quaternary stratigraphy along natural sections and sediments present at surficial stations. Surficial till samples were collected from C-horizon material in mud boils (e.g., Figure GS2017-18-2a) or from hand-dug pits (e.g, Figure GS2017-18-2b). Mud boils are the preferred till-sampling sites, as these permafrost features bring unweathered till to the surface (McMartin and McClenaghan, 2001). Whenever possible, sample pits were dug in the crests of streamlined landforms (e.g., Figure GS2017-18-2c, d) to avoid postglacial sediments typically deposited at lower elevations around these landforms. Till encountered at natural exposures was sampled at 2–4 m intervals, depending on changes in stratigraphy and restrictions on the weight of samples being hauled out.

Sixty-two new till samples, each weighing 2–3 kg, were collected from C-horizon tills, bringing the total number of till samples to 119 for this study (Figure GS2017-18-3). The new till samples were split for archival purposes at the MGS Midland Sample and Core Library and then submitted for processing, till-matrix geochemistry (<63 µm size-fraction) and clast-lithology (2–30 mm size-fraction) analyses. At 34 till sample sites, an additional 11.4 L of till was collected for KIM analysis, which brings the total to 64 KIM samples for this study. Blind KIM samples were submitted to the De Beers Group of Companies (De Beers) to be analyzed through in-kind support. The KIM sample locations were withheld from De Beers, to allow equal opportunity for follow-up by all interested parties when the data (with sample locations) are publicly released at a later date. The KIM results from the 2016 field season have been released (Hodder and Kelley, 2017b) and the sample locations are depicted on Figure GS2017-18-3.

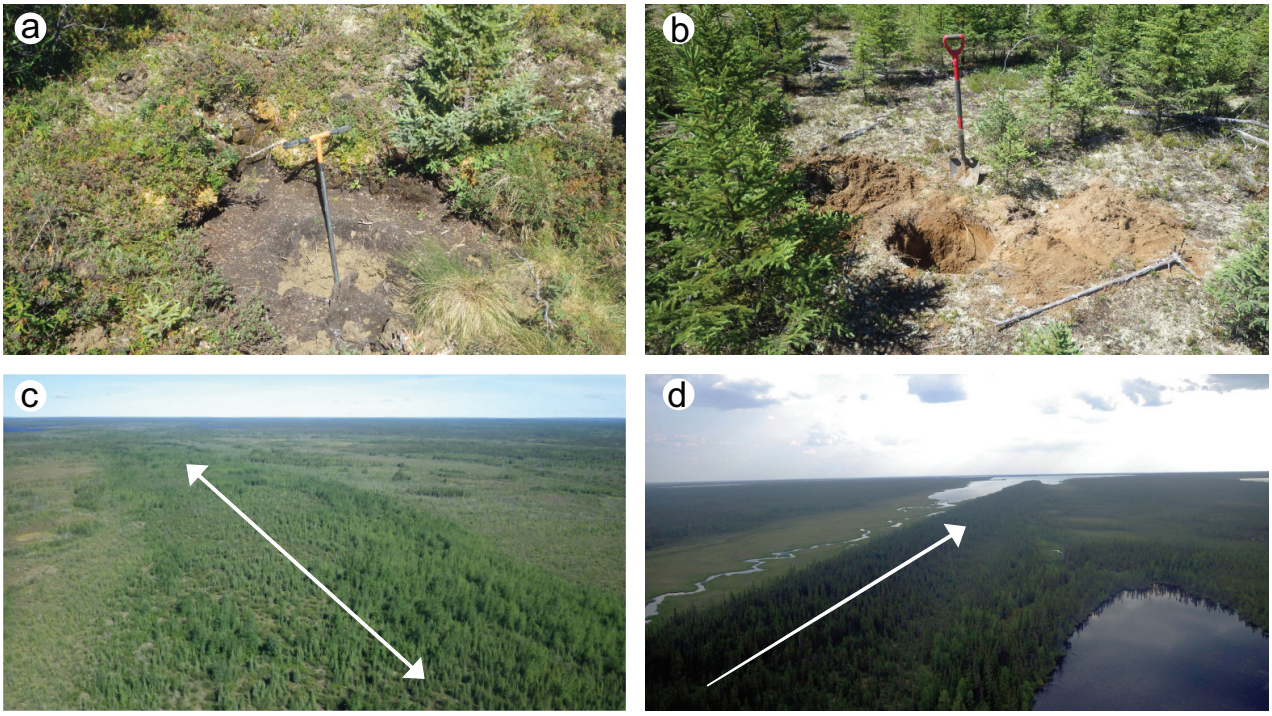

Figure GS2017-18-2: *Geomorphic expressions of till sampled in the study area:* ***a)*** *example of a vegetated, inactive, permafrost mud boil, which provides easy access to unweathered surficial till;* ***b)*** *example of a hand-dug pit used to sample surficial till where mud boils don't occur;* ***c)*** *northwest-southeast–oriented drumlin within the Kaskattama flowset;* ***d)*** *southwest-trending drumlin within the Hayes flowset.*

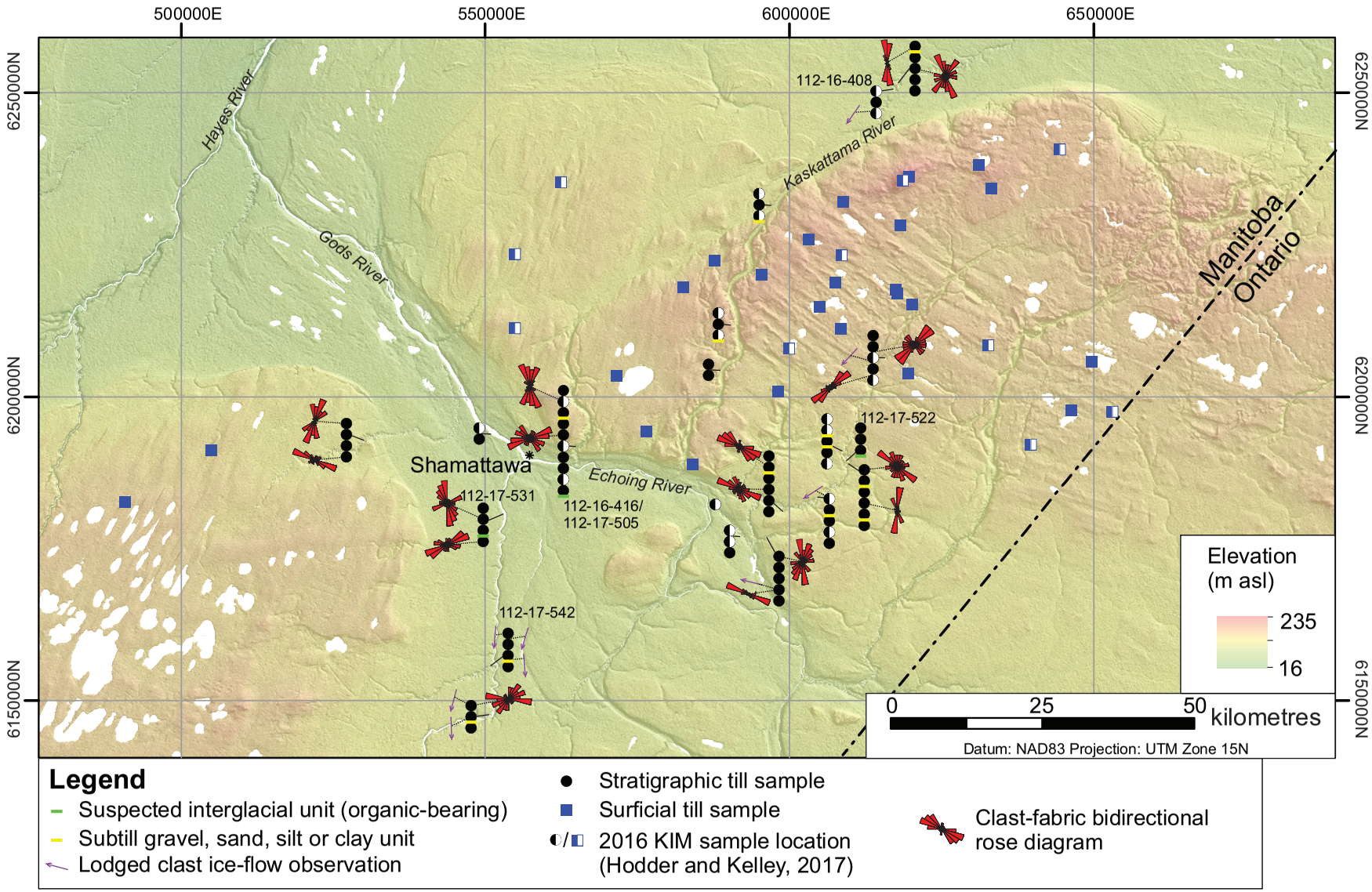

Figure GS2017-18-3: *Sites of surface and subsurface till samples collected in the Kaskattama highland region, northeastern Manitoba. Stratigraphic bidirectional ice-flow data, determined by measurements of clast fabrics and/or lodged striated clasts, are depicted. The 2016 kimberlite-indicator-mineral (KIM) sample sites are displayed. Background hillshade image was generated using Canadian Digital Surface Model (Natural Resources Canada, 2012).*

Ice-flow data was obtained from studied sections by measuring the long-axes orientation, or fabric, of clasts within till. It has been proven that certain shapes of clasts, defined as a particular arrangement of the a-axis (longest), b-axis (middle) and c-axis (shortest), will deposit parallel to the direction of stress that the overriding glacier puts on the till (Holmes, 1941). Clast fabric measurements were conducted at 17 sample sites. Sites were chosen based on uniformity of till and the absence of sand lenses or discontinuous bedding. At each site, a horizontal step was excavated at least 20 cm into the section face. Clasts were then carefully excavated and measured from within a 'box' consisting of three vertical faces of different orientations, over a maximum distance of 30 by 30 by 30 cm. Measurements were taken of the length of all axes, the a-axis orientation and the dip of the a-axis. At each site, the orientations of 30 rod, tabular-rectangle or wedge-shaped, elongate (a:b ratio of ≥1.5) clasts were recorded. Lodged clasts with parallel striae on their upper surface—considered to be a good indicator of ice flow—were observed at nine stratigraphic depths (Figure GS2017-18-3) and examples are presented in Figure GS2017-18-4.

In addition to fieldwork conducted, the KK1 drillcore (Figure GS2017-18-1) was pulled from the MGS archive and re-examined. The till that was present from 82–167 m depth was split and sampled at 5–8 m intervals, resulting in 15 till samples. These till samples will be processed for till-matrix (<63 µm size-fraction) geochemistry and clast-lithology (2–30 mm size-fraction) analysis.

Preliminary results

Ice flow

In 2017, clast fabric measurements were conducted at seven new sections and two sections initially visited in 2016 (Figure GS2017-18-3). When interpreting clast fabrics, it is commonly assumed that ice-flow direction was the opposite direction of that to which the clasts dip/plunge (Mark, 1974; Kjaer and Kruger, 1998). However, several studies, including MGS unpublished studies within the Hudson Bay Lowland, have since noted that only 40 to 60% of till fabrics dip up-ice, whereas the remainder dip down-ice (Andrews and Smith, 1970; Saarnisto and Peltoniemi, 1984; Larsen and Piotrowski, 2003). Additionally, till fabrics can have low dips, meaning that a preferred dip direction is not specified (Drake, 1974; Catto, 1998). As such, preliminary fabric data is displayed on bidirectional rose diagrams in Figure GS2017-18-3. Regional ice-flow interpretations give no indication that ice has flowed to the north, northeast or east, and hence an orientation of flow could be assigned to those clast fabrics that trend south, southwest or west. The regional ice-flow history neither precludes nor prefers ice flow to the northwest or southeast and thus assigning a trend to these clast fabrics is difficult. The data and further results, such as Schmidt equal-area stereonets and eigenvalue and eigenvector statistics, will be published in a forthcoming paper. Interpretations may be somewhat revised once till-composition data has been analyzed.

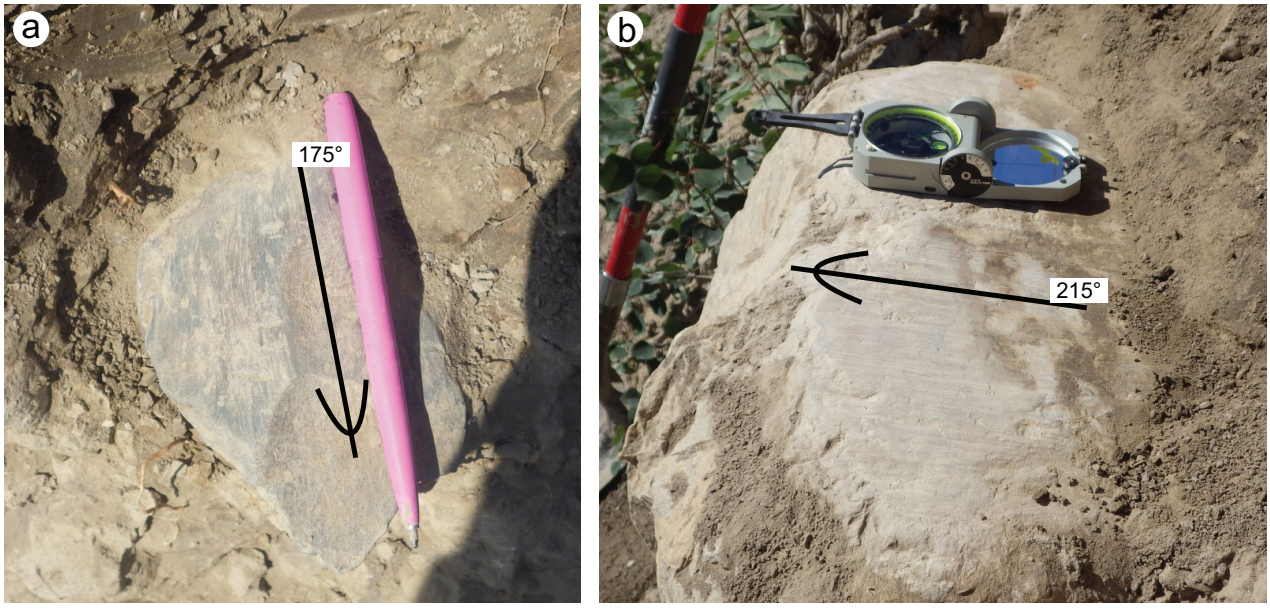

Figure GS2017-18-4: *Examples of lodged striated clasts that can be used to interpret ice-flow direction:* ***a)*** *lodged bullet-shaped cobble with parallel striae on its upper surface indicating ice flow toward 175° at a depth of 14.6 m at section 112-17-542;* ***b)*** *lodged boulder with parallel striae on its upper surface indicating ice flow toward 215° at a depth of 11.0 m at section 112-16-408.*

Regional ice-flow interpretations, including along portions of the Gods and Hayes rivers (depicted on Figure GS2017-18-3), can be found in Hodder et al. (2017a). That study releases data collected in 2001 and 2002, and also provides an analyses of the till composition.

The Hayes and Kaskattama flowsets do not overlap and therefore relative ages cannot be directly inferred from cross-cutting relationships of streamlined landforms. However, based on regional reconstructions it is anticipated that the Kaskattama flowset preceded the Hayes flowset, which is suspected to have been the last major ice-flow phase in this region (Dredge and Cowan, 1989).

Quaternary stratigraphy

The Quaternary stratigraphy was documented at nine sections along active river-cuts during the 2017 field season.

Section 112-17-542 (Figure GS2017-18-5) is an example of a section described during the 2017 field season. Section 112-17-542 is located 36.5 km south of Shamattawa along the Gods River (Figure GS2017-18-1) and exposes three diamict units recognizable in the field. The upper diamict is soft and olive brown (Munsell colour 2.5Y 4/3; Munsell Color–X-Rite, Incorporated, 2015), and is separated from the middle diamict by a boulder pavement (Figure GS2017-18-5c). The middle diamict is dense, blocky, dark greyish–brown (Munsell colour 2.5Y 4/2), and has a sharp, undulating lower contact with a 0.3 m thick, partially cemented sand and sandy gravel unit (Figure GS2017-18-5d). The lower diamict is greyish brown (Munsell colour 2.5Y 5/2) and is noticeably denser than the upper and middle diamicts. All three diamicts are interpreted as tills, because they are massive and contain striated clasts of various lithologies.

A striated clast within the upper till at 7.5 m depth indicates deposition by south-trending (185°) ice flow. A striated clast at the boulder pavement indicates deposition by south-southwest–trending (197°) ice flow. Collectively, these observations suggest deposition by ice flowing to the south. Near the lower contact of the middle till, a clast with parallel striation on its upper surface (Figure GS2017-18-4a) indicates ice flow toward 175°. Till-composition data is needed to confirm whether the upper and middle tills have the same composition, and hence were both deposited during southerly ice flow. If the composition is different, it would indicate slightly different (south-southwest versus south-southeast) ice-flow direction during deposition of the till units.

Suspected interglacial sediments

Subsurface organic-bearing sequences have been noted in the study area by previous workers, and interpreted to be of interglacial age (Dredge and Nielsen, 1985). Although organic-bearing sequences are rare, they are often correlated with the more abundant oxidized sand and gravel found below or between till units in exposed sections (Dredge et al., 1990; Dredge and Nixon, 1992; Dredge and McMartin, 2011). Deposits found in Manitoba, such as the Nelson River sediments (Nielsen et al., 1986; Nielsen and Fedikow, 2002) and the Gods River sediments (Netterville, 1974), may be correlative to the better studied Missinaibi Formation found in Ontario and Quebec (Wyatt, 1990; Thorleifson et al., 1993; Dalton et al., 2016).

Subsurface organic-bearing sequences are rare, and were observed at only three sections (Figures GS2017-18-3, 6). These subsurface units can consist of multiple beds (Figure GS2017-18-6a, b) or a single, laterally discontinuous bed (Figure GS2017-18-6c). There may be scattered pieces of wood and/or shell fragments, or organic-rich lenses within a sediment unit (Figure GS2017-18-6). One of these sections, section 112-17-522, is known as the “Echoing River” section (Dredge and Nielsen, 1985; Dredge et al., 1990; Dredge and McMartin, 2011) despite its location on an unnamed tributary. At this site, Dredge and McMartin (2011) suggested that the lower black clay is possibly marine, as it contains foraminifera in addition to elevated quantities of boron and vanadium. The upper sediments of this sequence are interpreted as having been deposited within terrestrial or shallow freshwater environments, as they consist of silt, marl and peat with infinite ^{14}C-age gastropods and spruce twigs (samples GSC-892 and GSC-4444HP, Dredge et al., 1990). The ages of all of these subtill organic-bearing units are unknown. However, they are currently being further characterized from a paleoenvironmental perspective using isotopic and deoxyribose nucleic acid (DNA) methods undertaken at the University of Colorado (Boulder, Colorado) and University at Buffalo (Buffalo, New York).

Inorganic subsurface beds of sorted sediments, situated below or within till units and termed ‘subtill sorted units’, were encountered at 50% (10 out of 20) of the sections where till outcrops (Figure GS2017-18-3). These include massive to bedded layers of sand, sand and gravel, silt and/or clay, devoid of organics, that typically have sharp upper and lower contacts. Subtill sorted units vary from 0.1 to >3.0 m thick. These inorganic subtill sorted units may have been deposited during an interglacial or interstadial period. Alternatively, they may be subglacial units that record decoupling at the ice-bed interface or the presence of subglacial lakes.

Future work

Future work will continue to focus on interpreting till-matrix geochemistry, clast-lithology and KIM analytical results. Ice-flow data and stratigraphic observations will be combined with till-composition results to provide a more thorough understanding of the Quaternary history of the study area and to assist drift prospecting practises in the region.

This work, in conjunction with studies conducted on the Nelson River and reinterpretation of earlier work along the Hayes and Gods rivers, will be used to aid ongoing efforts to reconstruct the glacial stratigraphy of the Hudson Bay Lowland. Additional characterization of subtill organic-bearing sediments is being conducted by S. Crump (University of Colorado) and E. Thomas (University at Buffalo).

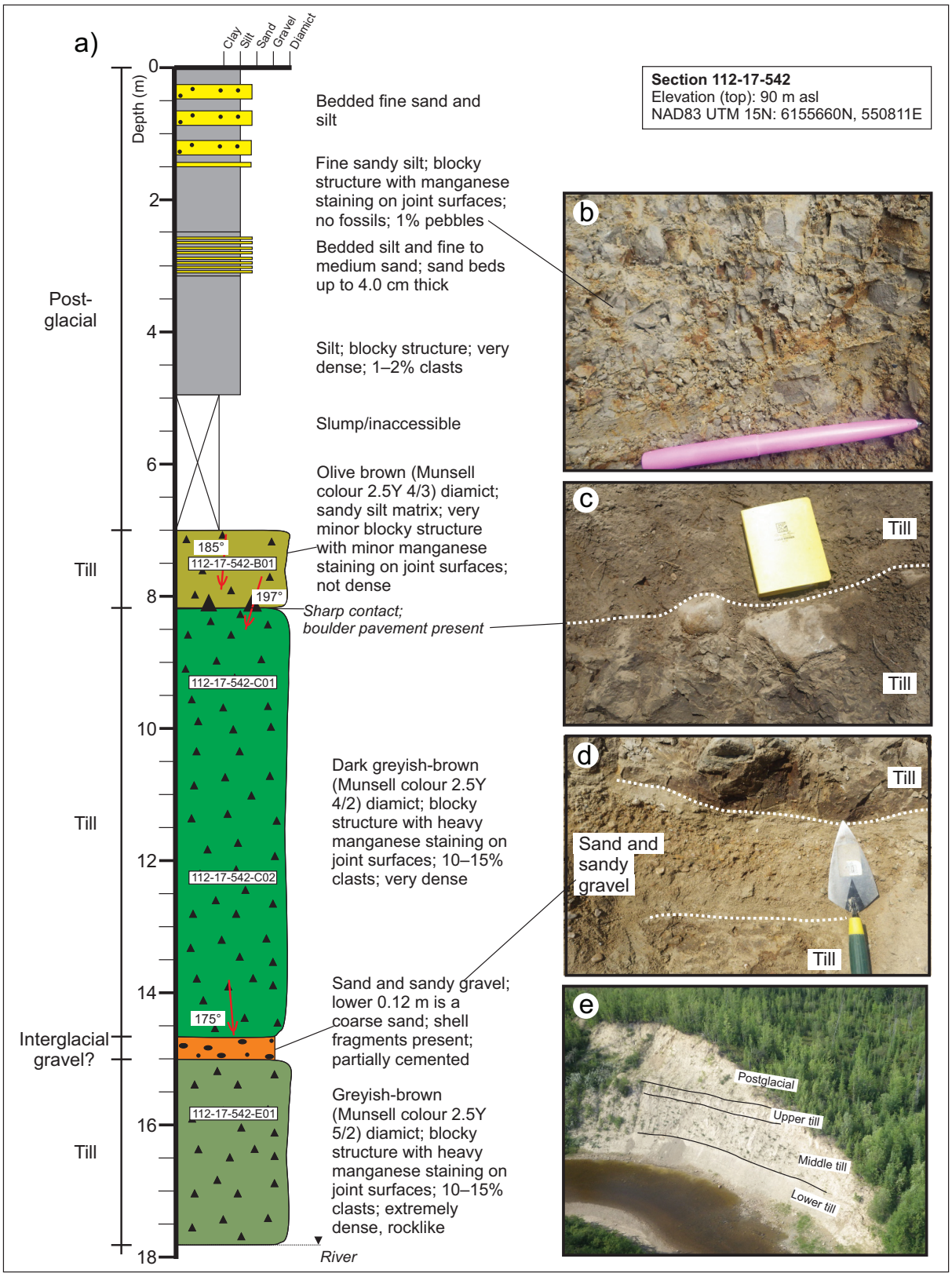

Figure GS2017-18-5: *Example of a stratigraphic section described and sampled during the 2017 field season.* ***a)*** *Stratigraphy at section 112-17-542. Till-sample numbers are labelled within the white boxes. Munsell colour was determined using Munsell Color–X-Rite, Incorporated (2015). Locations of lodged, striated clasts are indicated by red arrows and azimuths measured are indicated.* ***b)*** *Blocky, postglacial, fine sandy silt.* ***c)*** *Boulder pavement contact between the upper and middle till.* ***d)*** *Upper and lower contact of the subtill sand and sandy gravel unit.* ***e)*** *Oblique aerial view of section 112-17-542.*

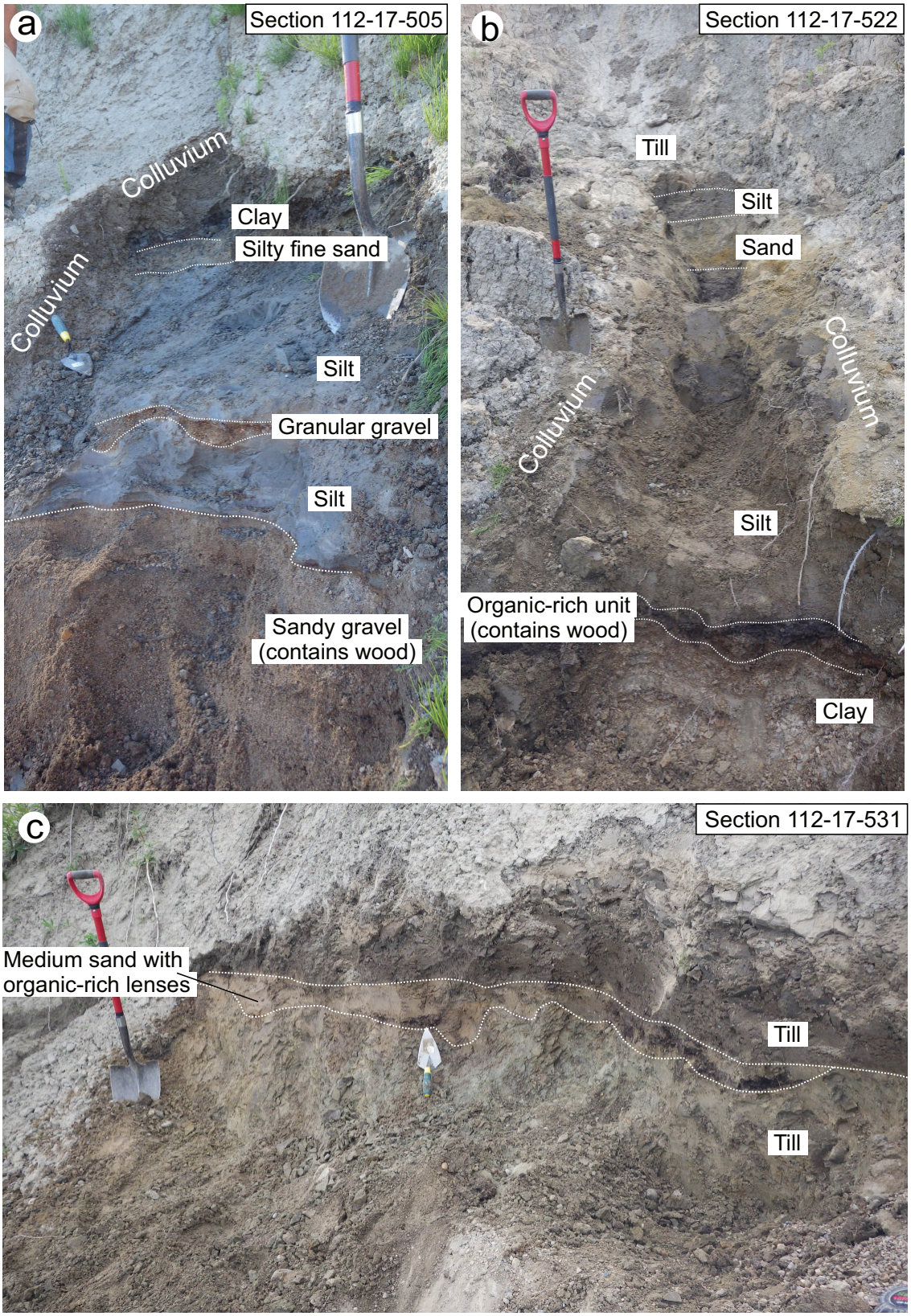

Figure GS2017-18-6: *Examples of subsurface organic-bearing sediments observed in the Kaskattama highland region:* ***a)*** *subtill inorganic- and organic-bearing sediments at 31.0–31.2 m depth at section 112-17-505;* ***b)*** *subtill inorganic- and organic-bearing sediments at 6.0–8.5 m depth at section 112-17-522;* ***c)*** *laterally discontinuous bed of thin subtill organic-bearing sediments at 11.8 m depth at section 112-17-531.*

Economic considerations

The Kaskattama highland region is a largely unexplored region of northeastern Manitoba. This study, started in 2016, is documenting the Quaternary stratigraphy and till composition in the region. The KIM grains recovered during the 2016 field season have hinted at the diamond potential of the region, and 2017 results will provide additional data. Elevated till-matrix geochemistry values in elements of economic interest have been documented and additional sampling conducted during the 2017 field season followed-up on these areas. Till-composition data coupled with ice-flow data will provide insight into potential glacial dispersal patterns in the Kaskattama highland area.

Acknowledgments

C. Böhm is thanked for his enthusiastic field assistance and insightful discussions throughout the field season. Prairie Helicopters Inc., and in particular pilot K. Dunthorne, are thanked for providing excellent air support during both field seasons of this study. The De Beers Group of Companies is thanked for their continued analytical support for Quaternary initiatives at the Manitoba Geological Survey by providing kimberlite-indicator-mineral processing. H. Thorleifson from the Minnesota Geological Survey is thanked for discussions regarding the Quaternary stratigraphy in the Hudson Bay Lowland region. Thanks also go to N. Brandson, E. Anderson and C. Epp from the Manitoba Geological Survey for logistical support throughout the field season. M. Gauthier and M. Nicolas are thanked for thoughtful reviews of this contribution.

References

Anderson, S.D. 2017: Preliminary geology of the diamond occurrence at southern Knee Lake, Oxford Lake–Knee Lake greenstone belt, Manitoba (NTS 53L15); Manitoba Growth, Enterprise and Trade, Manitoba Geological Survey, Open File OF2017-3, 27 p.

Andrews, J.T. and Smith, D.I. 1970: Statistical analysis of till fabric: methodology, local and regional variability (with particular reference to the north Yorkshire till cliffs); Quaternary Journal of the Geological Society, v. 125, p. 503–542.

Catto, N.R. 1998: Comparative study of striations and basal till clast fabrics, Malpeque-Bedeque region, Prince Edward Island, Canada; Boreas, v. 27, p. 259–274.

Clark, C.D., Knight, J. and Gray, J.T. 2000: Geomorphological reconstruction of the Labrador Sector of the Laurentide Ice Sheet; Quaternary Science Reviews, v. 19, p. 1343–1366.

Dalton, A.S., Finkelstein, S.A., Barnett, P.J. and Forman, S.L. 2016: Constraining the Late Pleistocene history of the Laurentide Ice Sheet by dating the Missinaibi Formation, Hudson Bay Lowlands, Canada; Quaternary Science Reviews, v. 146, p. 288–299.

Drake, L.D. 1974: Till fabric control by clast shape; Geological Society of America Bulletin, v. 85, p. 247–250.

Dredge, L.A. and Cowan, W.R. 1989: Quaternary geology of the southwestern Canadian Shield; *in* Quaternary Geology of Canada and Greenland, R.J. Fulton (ed.), Geological Survey of Canada, Geology of Canada Series, no. 1, p. 214–248.

Dredge, L.A. and McMartin, I. 2011: Glacial stratigraphy of northern and central Manitoba; Geological Survey of Canada, Bulletin 600, 27 p.

Dredge, L.A. and Nielsen, E. 1985: Glacial and interglacial deposits in the Hudson Bay Lowlands: a summary of sites in Manitoba; *in* Current Research, Geological Survey of Canada, Paper 85-1A, p. 247–257.

Dredge, L.A. and Nixon, F.M. 1992: Glacial and environmental geology of northeastern Manitoba; Geological Survey of Canada, Memoir 432, 80 p.

Dredge, L.A., Morgan, A.V. and Nielsen, E. 1990: Sangamon and pre-Sangamon interglaciations in the Hudson Bay Lowlands of Manitoba; Geographie physique et Quaternaire, v. 44, no. 3, p. 319–336.

Greenwood, S.L. and Clark, C.D. 2009: Reconstructing the last Irish Ice Sheet 1: changing flow geometries and ice flow dynamics deciphered from the glacial landform record; Quaternary Science Reviews, v. 28, p. 3085–3100.

Hodder, T.J. and Kelley, S.E. 2016: Quaternary stratigraphy and till sampling in the Kaskattama highland region, northeastern Manitoba (parts of NTS 53N, O, 54B, C); *in* Report of Activities 2016, Manitoba Growth, Enterprise and Trade, Manitoba Geological Survey, p. 187–195.

Hodder, T.J. and Kelley, S.E. 2017: Kimberlite-indicator-mineral results derived from glacial sediments (till) in the Kaskattama highland area of northeast Manitoba (parts of NTS 53N, O, 54B, C); Manitoba Growth, Enterprise and Trade, Manitoba Geological Survey, Open File OF2017-1, 6 p. plus two appendices.

Hodder, T. J., Gauthier, M.S. and Nielsen, E. 2017: Quaternary stratigraphy and till composition along the Hayes, Gods, Nelson, Fox, Stupart, Yakaw, Angling and Pennycutaway rivers, northeast Manitoba (parts of NTS 53N, 54C, 54D, 54F); Manitoba Growth, Enterprise and Trade, Manitoba Geological Survey, Open File OF2017-4, 20 p.

Hodder, T.J., Kelley, S.E., Trommelen, M.S., Ross, M. and Rinne, M.L. 2017b: The Kaskattama highland: till composition and indications of a new Precambrian inlier in the Hudson Bay Lowland?; Geological Association of Canada–Mineralogical Association of Canada, Joint Annual Meeting, Kingston, Ontario, May 14–17, 2017, poster presentation.

Holmes, C.D. 1941: Till fabric; Bulletin of the Geological Society of America, v. 52, p. 1299–1354.

Kelley, S.E., Hodder, T.J., Wang, Y., Trommelen, M.S. and Ross, M. 2015: Preliminary Quaternary geology in the Gillam area, northeastern Manitoba – year 3 (parts of NTS 54D5–9, 11, 54C12); *in* Report of Activities 2015, Manitoba Mineral Resources, Manitoba Geological Survey, p. 131–139.

Kjaer, K.H. and Kruger, J. 1998: Does clast size influence fabric strength?; Journal of Sedimentary Research, v. 68, p. 746–749.

Kleman, J. and Borgstrom, I. 1996: Reconstruction of palaeo-ice sheets: the use of geomorphological data; Earth Surface Processes and Landforms, v. 21, p. 893–909.

Larsen, N.K. and Piotrowski, J.A. 2003: Fabric pattern in a basal till sucession and its significance for reconstructing subglacial processes; Journal of Sedimentary Research, v. 73, no. 5, p. 727–734.

Manitoba Department of Mines, Natural Resources and Environment 1979: Geological map of Manitoba; Manitoba Department of Mines, Natural Resources and Environment, Mineral Resources Division, Geological Report 79-2, scale 1:1 000 000.

Mark, D.M. 1974: On the interpretation of till fabrics; Geology, v. 2, no. 2, p. 101–104.

McDonald, B.C. 1968: Glacial and interglacial stratigraphy, Hudson Bay Lowland; *in* Earth Science Symposium on Hudson Bay, P.J. Hood (ed.), Geological Survey of Canada, Paper 68-83, p. 78–99.

McMartin, I. and McClenaghan, M.B. 2001: Till geochemistry and sampling techniques in glaciated shield terrain: a review; *in* Drift Exploration in Glaciated Terrain, M.B. McClenaghan, P.T. Bobrowsky, G.E.M. Hall and S.J. Cook (ed.), Geological Society, Special Publication, no. 185, p. 19–43.

Munsell Color–X-Rite, Incorporated 2015: Munsell Soil Color Book; Pantone LLC, Carlstadt, New Jersey, 42 p.

Natural Resources Canada 2012: Canadian Digital Surface Model; Natural Resources Canada, URL <http://geogratis.gc.ca/api/en/nrcan-rncan/ess-sst/34f13db8-434b-4a37-ae38-03643433fbbb.html> [September 2015].

Netterville, J.A. 1974: Quaternary stratigraphy of the lower Gods River region, Hudson Bay lowlands, Manitoba; M.Sc. thesis, The University of Calgary, Calgary, Alberta, 79 p.

Nicolas, M.P.B. and Young, G.A. 2014: Reconnaissance field mapping of Paleozoic rocks along the Churchill River and Churchill coastal area, northeastern Manitoba (parts of NTS 54E, L, K); *in* Report of Activities 2014, Manitoba Mineral Resources, Manitoba Geological Survey, p. 148–160.

Nielsen, E. 2002: Quaternary stratigraphy and ice-flow history along the lower Nelson, Hayes, Gods and Pennycutaway rivers and implications for diamond exploration in northeastern Manitoba; *in* Report of Activities 2002, Manitoba Industry, Trade and Mines, Manitoba Geological Survey, p. 209–215.

Nielsen, E. and Fedikow, M.A.F. 2002: Kimberlite indicator-mineral surveys, lower Hayes River; Manitoba Industry, Trade and Mines, Manitoba Geological Survey, Geological Paper GP2002-1, 39 p.

Nielsen, E., Morgan, A.V., Morgan, A., Mott, R.J., Rutter, N.W. and Causse, C. 1986: Stratigraphy, paleoecology and glacial history of the Gillam area, Manitoba; Canadian Journal of Earth Sciences, v. 23, p. 1641–1661.

Saarnisto, M. and Peltoniemi, H. 1984: Glacial stratigraphy and compositional properties of till in Kainuu, eastern Finalnd; Fennia, v. 162, p. 163–199.

Stott, G.M., Buse, S., Davis, D.W. and Hamilton, M.A. 2010: The Sutton inliers – a Paleoproterozoic succession in the Hudson Bay Lowland; *in* Summary of Fieldwork and Other Activities 2010, Ontario Geological Survey, Open File Report 6260, p. 19-1–19-14.

Thorleifson, L.H., Wyatt, P.H. and Warman, T.A. 1993: Quaternary stratigraphy of the Severn and Winisk drainage basins, northern Ontario; Geological Survey of Canada, Bulletin 442, 65 p.

Trommelen, M.S. 2013: Preliminary Quaternary geology in the Gillam area, northeastern Manitoba (parts of NTS 54D5–9, 11, 54C12); *in* Report of Activities 2013, Manitoba Mineral Resources, Manitoba Geological Survey, p. 169–182.

Trommelen, M.S., Wang, Y. and Ross, M. 2014: Preliminary Quaternary geology in the Gillam area, northeastern Manitoba (parts of NTS 54D5–11, 54C12) – year two; *in* Report of Activities 2014, Manitoba Mineral Resources, Manitoba Geological Survey, p. 187–195.

Wyatt, P.H. 1990: Amino acid evidence indicating two or more ages of pre-Holocene nonglacial deposits in Hudson Bay Lowland, northern Ontario; Geographie physique et Quaternaire, v. 44, no. 3, p. 389–393.

PUBLICATIONS

Data Repository Items

DRI2017001

Biogeochemistry data from a vegetation orientation survey in the area of the Tanco pegmatite, Bernic Lake, southeastern Manitoba (NTS 52L6)

by M.A.F. Fedikow, C.E. Dunn, T. Martins and S.K.Y. Lee

Microsoft® Excel® file supplements:
Fedikow, M.A.F. and Dunn, C.E. 1990: Anomalous trace element concentrations in vegetation from the area of the Tanco pegmatite, Bernic Lake, Manitoba (NTS 52L/6); *in* Report of Activities 1990, Manitoba Energy and Mines, Minerals Division, p. 100–104.

Fedikow, M.A.F. and Dunn, C.E. 1991: A vegetation geochemical survey in the vicinity of the Tanco pegmatite, Bernic Lake area, southeastern Manitoba (NTS 52L/6); *in* Report of Activities 1991, Manitoba Energy and Mines, Minerals Division, p. 105.

Fedikow, M.A.F. and Dunn, C.E. 1992: Vegetation geochemical surveys in the area of the Tanco Pegmatite - a regional assessment of geochemical haloes (NTS 52L/6); *in* Report of Activities 1992, Manitoba Energy and Mines, Minerals Division, p. 114.

DRI2017002

Carbon and oxygen stable-isotope results from Paleozoic cores and outcrops from the Hudson Bay Basin, northeastern Manitoba (NTS 54B7, 54C10, 54G1, parts of 54E, K, L)

By M.P.B. Nicolas

Microsoft® Excel® file supplements:
Nicolas, M.P.B. and Armstrong, D.K. 2017: Update on Paleozoic stratigraphic correlations in the Hudson Bay Lowland, northeastern Manitoba and northern Ontario; *in* Report of Activities 2017, Manitoba Growth, Enterprise and Trade, Manitoba Geological Survey, p. 133–147.

DRI2017003

Field-based ice-flow–indicator data, Kinoosao–Lynn Lake–Leaf Rapids, northwestern Manitoba (parts of NTS 64B12, 64C9, 11, 12, 14–16, 64F3, 4)

By M.S. Gauthier and T.J. Hodder

Microsoft® Excel® file supplements:
Gauthier, M.S. and Hodder, T.J. 2017: Till sampling and ice-flow mapping between Leaf Rapids, Lynn Lake and Kinoosao, northwestern Manitoba (parts of NTS 64B12, 64C9, 11, 12, 14–16, 64F3, 4); *in* Report of Activities 2017, Manitoba Growth, Enterprise and Trade, Manitoba Geological Survey, p. 191–204.

DRI2017004

Whole-rock and mineral geochemistry as exploration tools for rare-element pegmatite in Manitoba: examples from the Cat Lake–Winnipeg River and Wekusko Lake pegmatite fields (parts of NTS 52L6, 63J13)

By T. Martins and R.L. Linnen

Microsoft® Excel® file supplements:
Martins, T., Linnen, R.L., Fedikow, M.A.F. and Singh, J. 2017: Whole-rock and mineral geochemistry as exploration tools for rare-element pegmatite in Manitoba: examples from the Cat Lake–Winnipeg River and Wekusko Lake pegmatite fields (parts of NTS 52L6, 63J13); *in* Report of Activities 2017, Manitoba Growth, Enterprise and Trade, Manitoba Geological Survey, p. 42–51.

DRI2017005

Stable C and O isotope and major- and trace-element data, with calcite-dolomite equilibration geothermometry, for genetically diverse carbonate rocks in the Pikwitonei granulite domain and Split Lake block (parts of NTS 63P11, 12, 64A1)

By J.A. Macdonald, A.R. Chakhmouradian, C.G. Couëslan and E.P. Reguir

Microsoft® Excel® file supplements:
Macdonald, J.A., Chakhmouradian, A.R., Couëslan, C.G. and Reguir, E.P. 2017: Discriminative study of genetically diverse carbonate rocks in the northwestern Pikwitonei granulite domain and Split Lake block, central Manitoba (parts of NTS 63P11, 12, 64A1); *in* Report of Activities 2017, Manitoba Growth, Enterprise and Trade, Manitoba Geological Survey, p. 30–41.

DRI2017006

MB GeoTours of southern Manitoba

By J.D. Bamburak, J.M.Pacey, and K. Lapenskie

Microsoft® Excel® file

Open Files

OF2017-1

Kimberlite-indicator-mineral results derived from glacial sediments (till) in the Kaskattama

by T.J. Hodder and S.E. Kelley

OF2017-2

Kimberlite-indicator-mineral results derived from glacial sediments (till) in the Southern Indian Lake area of north-central Manitoba (parts of NTS 64B15, 64G1, 2, 7, 8)

by T.J. Hodder

OF2017-3

Preliminary geology of the diamond occurrence at southern Knee Lake, Oxford Lake–Knee Lake greenstone belt, Manitoba (NTS 53L15)

by S.D. Anderson

OF2017-4

Quaternary stratigraphy and till composition along the Hayes, Gods, Nelson, Fox, Stupart, Yakaw, Angling and Pennycutaway rivers, northeast Manitoba (parts of NTS 53N, 54C, 54D, 54F)

by T.J. Hodder, M.S. Gauthier and E. Nielsen

Preliminary Maps

PMAP2017-1

Geology of the exposed basement in the Reed Lake area, Flin Flon belt, west-central Manitoba (parts of NTS 63K9, 10, 15, 16)

by S. Gagné, E.C. Syme, S.D. Anderson and A.H. Bailes (scale 1:30 000)

PMAP2017-2

Sub-Phanerozoic geology of the Reed Lake area, Flin Flon belt, west-central Manitoba (parts of NTS 63K7, 8, 9, 10)

by S. Gagné (scale 1:30 000)

PMAP2017-3

Bedrock geology of the Wasekwan Lake area, Lynn Lake greenstone belt, northwestern Manitoba (parts of NTS 64C10, 15)

by X.M. Yang and C.J. Beaumont-Smith (scale 1:20 000)

Brown, J.A., Martins, T. and Černý, P. 2017: The Tanco pegmatite at Bernic Lake, Manitoba, XVII: mineralogy and geochemistry of alkali feldspars; Canadian Mineralogist, v. 55, p. 483–500.

Craven, J.A., Ferguson, I.J., Nicolas, M.P.B., Zaprozan, T., Hodder, T., Roberts, B.R. and Clarke, N. 2017: Report of activities for the ground geophysical survey across the Kaskattama highland, Manitoba: GEM-2 Hudson-Ungava Project; Geological Survey of Canada, Open File OF8321, 30 p.

Dragovic, B., Guevara, V., Caddick, M., Couëslan, C. and Baxter, E. 2017: Punctuated HT/UHT metamorphism during prolonged Archean orogenesis in the Pikwitonei Granulite Domain revealed by garnet petrochronology; 19th European Geoscience Union General Assembly (EGU 2017), Vienna, Austria, April 23–28, 2017, Program with Abstracts, v. 19, p. 11430.

Hahn, K.E., Armstrong, D.K., Turner, E.C. and Nicolas, M.P.B. 2016: Toward a sequence stratigraphic framework for the Ordovician Hudson Bay and Moose River basins, northern Ontario; *in* Summary of Field Work and Other Activities 2016; Ontario Geological Survey, Open File Report 6323, p. 28-1–28-10.

Hahn, K.E., Turner, E.C., Armstrong, D.K. and Nicolas, M.P.B. 2017: Late Ordovician chemostratigraphy of the Hudson Bay and Moose River basins; Geological Association of Canada-Mineralogical Association of Canada, Joint Annual Meeting, Kingston, Ontario, May 14–17, 2017, poster presentation; URL < http://gac.esd.mun.ca/GAC_2017/search_abs/sub_program.asp?sess=98&form=13&abs_no=382> [October 2017].

Hodder, T.J., Kelley, S.E., Trommelen, M.S., Ross, M. and Rinne, M.L. 2017: The Kaskattama highland: till composition and indications of a new Precambrian inlier in the Hudson Bay Lowland?; Geological Association of Canada-Mineralogical Association of Canada, Joint Annual Meeting, Kingston, Ontario, May 14–17, 2017, poster presentation.

Lavoie, D., Nicolas, M.P.B., Armstrong, D.K., Ardakani, O.H., Jiang, C., Reyes, J., Dhillon, R.S., Savard, M.M., Pinet, N., Brake, V.I., Duchesne, M.J., Beauchemin, M. and Tolszczuk-Leclerc, S. 2017: Report of Activities for the 2017 GEM-2 Hudson Bay-Ungava project: stratigraphy, source rock, and RADARSAT-2 research, Nunavut, Manitoba, and Ontario; Geological Survey of Canada, Open File OF8319, 18 p.

Martins, T., Kressall, R., Medici, L. and Chakhmouradian A.R. 2017: Cancrinite–vishnevite solid solution from Cinder Lake (Manitoba, Canada): crystal chemistry and implications for alkaline igneous rocks; Mineralogical Magazine, v. 81(5), p. 1261–1277.

Scoates, J.S., Scoates, J.R.F., Wall, C.J., Friedman, R.M. and Couëslan, C.G. 2017: Direct dating of ultra-mafic sills and mafic intrusions associated with Ni-sulfide mineralization in the Thompson nickel belt, Manitoba, Canada; Economic Geology, v. 112, p. 675–692.

Trommelen, M.S., Kelley, S.E., Hodder, T.J., Wang, Y. and Ross, M. 2017: Till compositional inheritance and overprinting in the Hudson Bay Lowland and across onto the Precambrian Shield; Geological Association of Canada-Mineralogical Association of Canada, Joint Annual Meeting, Kingston, Ontario, May 14–17, 2017, oral presentation.

Yang, X.M. 2017: Book review on Peter C Lightfoot: Nickel sulfide ores and impact melts: Origin of the Sudbury Igneous Complex; Mineralium Deposita, v. 52(1), p. 135–136.

Yang, X.M. 2017: Estimation of crystallization pressure of granite intrusions; Lithos, v. 286, p. 324–329.

Yang, X.M. 2017: Paleo-Asian oceanic slab under the North China craton revealed by carbonatites derived from subducted limestones: Comment; Geology, v. 45(5), p. e413, doi: 10.1130/G39005C.1

MANITOBA RESOURCE DEVELOPMENT AND GEOLOGICAL SURVEY CONTACTS

Position	Personnel	E-mail	Phone	Areas of interest / expertise
Director	Chris Beaumont-Smith	chris.beaumont@gov.mb.ca	204-945-6505	
MINERAL DEPOSITS SECTION				
Chief Geologist	Scott Anderson	scott.anderson@gov.mb.ca	204-945-6561	Superior and Hearne cratons / orogenic gold deposits
Geologist	Simon Gagné	simon.gagne@gov.mb.ca	204-945-8430	Flin Flon belt / volcanogenic massive sulphide and orogenic gold deposits
Geologist	Kyle Reid	kyle.reid@gov.mb.ca	204-945-7255	Trans-Hudson orogen / volcanogenic massive sulphide and uranium deposits
Geologist	Marc Rinne	marc.rinne@gov.mb.ca	204-945-6554	Superior craton and Fox River belt / magmatic nickel, volcanogenic massive sulphide and intrusion-related deposits
Geologist	Eric Yang	eric.yang@gov.mb.ca	204-945-6555	Superior craton and Trans-Hudson orogen / intrusion-related and magmatic nickel deposits
PRECAMBRIAN GEOSCIENCE SECTION				
Chief Geologist	Christian Böhm	christian.bohm@gov.mb.ca	204-945-6549	Superior and Hearne cratons / geoscience collaborations, land-use planning
Geologist	Chris Couëslan	chris.coueslan@gov.mb.ca	204-945-6548	Superior craton and Thompson nickel belt / high-grade gneiss terranes
Geologist	Tânia Martins	tania.martins@gov.mb.ca	204-945-0661	Trans-Hudson orogen and Superior craton / intrusion-related rare metal deposits
SEDIMENTARY GEOSCIENCE SECTION				
Chief Geologist	Michelle Nicolas	michelle.nicolas@gov.mb.ca	204-945-6571	Williston and Hudson Bay basins / petroleum geology and Phanerozoic stratigraphy
Geologist	Michelle Gauthier	michelle.gauthier@gov.mb.ca	204-945-6552	Quaternary geology, surficial mapping
Geologist	Tyler Hodder	tyler.hodder@gov.mb.ca	204-945-6540	Quaternary geology, surficial mapping, sand and gravel aggregate resources
Geologist	Kathryn Lapenskie	kathryn.lapenskie@gov.mb.ca	204-945-8968	Industrial and specialty minerals, crushed stone aggregate resources, sedimentary geology
GEOSCIENCE INFORMATION SECTION				
Manager	Paul Lenton	paul.lenton@gov.mb.ca	204-945-6553	Geological data management and analysis
GIS Specialist	Len Chackowsky	len.chackowsky@gov.mb.ca	204-945-8204	GIS geologist
GIS Specialist	Greg Keller	greg.keller@gov.mb.ca	204-945-6744	Surficial and 3-D geological mapping
GIS Specialist	Sharon Lee	sharon.lee@gov.mb.ca	204-945-6562	GIS geologist
Cartographer	Bonnie Lenton	bonnie.lenton@gov.mb.ca	204-945-0637	
GIS Specialist	Mark Pacey	mark.pacey@gov.mb.ca	204-945-4624	GIS; Internet Map Server
Cartographer	Mark Timcoe	mark.timcoe@gov.mb.ca	204-945-6590	
MIDLAND LABORATORY AND ROCK STORAGE FACILITY				
Technician	Colin Epp	colin.epp@gov.mb.ca	204-945-6550	Sample storage and preparation
Field Support Manager	Neill Brandson	neill.brandson@gov.mb.ca	204-793-3831	
Storekeeper	Eric Anderson	eric.anderson@gov.mb.ca	204-792-4933	
CORPORATE SERVICES SECTION				
Marketing and Communications				
A/Manager	Craig Steffano	craig.steffano@gov.mb.ca	204-945-0726	Information production and distribution; publications; website
Mineral Resources Library	Tomaz Booth	tomaz.booth@gov.mb.ca	204-945-6569	Library; publication sales
Outreach	Susan Michaels	susan.michaels@gov.mb.ca	204-945-6584	Mineral education; Indigenous outreach
Administrative Secretary	Candace Regan	candace.regan@gov.mb.ca	204-945-1119	
Marketing Coordinator	Mark Zaluski	mark.zaluski@gov.mb.ca	204-945-6288	
Corporate Policy and Planning Coordinator	Bryan Spencer	bryan.spencer@gov.mb.ca	204-945-5325	
Finance and Administration				
Manager	Diana Savage	diana.savage@gov.mb.ca	204-945-6558	
Accounts Clerk	Jennifer Chartrand	jennifer.chartrand@gov.mb.ca	204-945-8405	
A/Accounts Clerk	Jacqueline Gervais	jacqueline.gervais@gov.mb.ca	204-945-6577	
Accounts Clerk	Kelly Heglin	kelly.heglin@gov.mb.ca	204-945-6500	

Manitoba Growth, Enterprise and Trade
Resource Development Division
360-1395 Ellice Avenue
Winnipeg, Manitoba R3G 3P2
Tel: 204-945-1119
Toll free: 1-800-223-5215
Fax: 204-945-8427
Email: minesinfo@gov.mb.ca

manitoba.ca/minerals

Printed in Canada